

Meteorological and Tidal Forcing of Loch Linnhe, a Scottish Sea-loch.

Lorna A. Taylor

Submitted for

Degree of Doctor of Philosophy,
Department of Statistics and Modelling Science,
University of Strathclyde.

September 1997

©The copyright of this thesis belongs to the author under the terms of the United Kingdom Copyright Acts as qualified by the University of Strathclyde Regulation 3.49. Due acknowledgement must always be made of the use of any material contained in, or derived from, this thesis.

Acknowledgements

I would like to thank my supervisor Bill Gurney for his advice and help with the research, as well as the various sources of funding. I am also grateful to Dr. Mike Heath of the Marine Laboratory of Aberdeen for the wide range of data I have used in the course of this work and without which it would not have been possible. I am grateful to the University of Strathclyde and the European Union for the funding which has enabled this work and Bill Gurney for locating the funding. Many thanks also to the computer manager Ian Thurlbeck for all his help and assistance.

Finally I would like to thank my friends and family for their friendship, help, support and of course patience.

Abstract

The aim of this work was to examine the impact of meteorological and tidal forcing on Loch Linnhe, a Scottish sea-loch. In 1991 the Marine Laboratory of Aberdeen undertook a programme of pelagic ecosystem monitoring in Loch Linnhe. This generated an extensive dataset, including a substantial spatial component, which enabled this work to take place.

In Part 1, hydrodynamics and physical conditions in fjords are considered globally, along with the effect of the physical conditions on the biota. The nature of the data available and Loch Linnhe are also described.

In Part 2, the data are analysed. Much of the work done involved visualisation of the data and the examination of the resulting spatial patterns. The interpolation and visualisation of the data are discussed. For the Loch Linnhe data, a conservative interpolation method is more suitable as it generates fewer boundary effects. The vertical and horizontal structure of Loch Linnhe is investigated and related to the meteorological and tidal conditions existing at the time. From this it was found that Loch Linnhe experiences extensive tidal mixing, frequent deep water renewal events on spring tides and the surface structure is strongly influenced by the lunar tidal cycle and wind forcing. The degree of turbulent mixing in Loch Linnhe probably exceeds that of other Scottish sea-lochs. Unfortunately the temporal resolution of the data does not allow for the effects of the physical conditions on the biota to be assessed.

In Part 3, an existing ecosystem was applied to Loch Linnhe and developed. These developments were used in particular to examine the effects of meteorological and tidal forcing, which were identified in Part 2, on the biota. It is shown that the high gelatinous carnivore biomass in Loch Linnhe maintained a low herbivore biomass throughout 1991, thus the control of the phytoplankton biomass was largely through tidal and wind effects rather than predation. This does not imply that the physical processes in Loch Linnhe are more important than in other Scottish sea-lochs, but that without control by zooplankton of phytoplankton the importance of physical factors becomes apparent.

Part 4 is an overview and discussion of the thesis where Loch Linnhe is compared with fjords globally in its conditions and behaviour.

Contents

I	Introduction	1
1	Fjords	2
1.1	Introduction	2
1.2	Fjord Processes	3
1.2.1	Classification	4
1.2.2	River Discharge and Stratification	5
1.2.3	Two Layer Circulation	5
1.2.4	Upper and Lower Prodelta	6
1.2.5	Flushing and Deep Water Renewal	8
1.2.6	Mixing Processes and Bathymetry	10
1.3	Nutrients and Primary Production	12
1.3.1	Euphotic Zone	12
1.3.2	Spring Bloom	12
1.3.3	Phytoplankton Species Succession	13
1.3.4	Nutrients and Regeneration	14
1.4	Fjord Research	16
1.4.1	Deep Water Renewal	16
1.4.2	Mixing Processes and Bathymetry	18
1.4.3	Physical Influences on Plankton	20
1.5	Horizontal Heterogeneity In Fjords	24
1.5.1	Physical Sources of Heterogeneity	24
1.5.2	Biological Processes	27

1.5.3	External Controls	28
1.5.4	Spatial Scales	30
1.5.5	Temporal Continuity	31
1.6	Understanding Heterogeneity	31
1.6.1	Data Collection	31
1.7	Modelling fjords	32
1.7.1	Estuarine Circulation	32
1.7.2	Exchange	33
1.7.3	Mixing	35
1.8	Thesis Outline	36
2	Loch Linnhe	38
2.1	Introduction	38
2.2	Loch Linnhe	38
2.3	Loch Linnhe Dataset	42
2.3.1	Vertically resolved data	42
2.3.2	Surface Layer Dataset	43
2.3.3	Table of Data - including axial, surface and sample site data	45
2.3.4	Instrumentation	45
2.3.5	Jellyfish	45
2.4	Hydrodynamic Parameters	48
2.4.1	Flushing Rate: Inner Basin	48
2.5	External Driving Functions	49
2.5.1	Freshwater Input	49
2.5.2	Tide	49
2.5.3	Meteorological Data	51
2.6	Physical Features of Loch Linnhe	54
2.6.1	Inner Basin	54

II	Data Analysis	57
3	Seasonal Trends in the Data Sets	58
3.1	Introduction	58
3.2	Vertical Data	58
3.2.1	Thermistor Chain	58
3.2.2	Sample Site Data	60
3.2.3	Axial Cruise Data	73
3.3	Horizontal Data	77
3.3.1	Salinity	77
3.3.2	Temperature	78
3.3.3	Chlorophyll	78
3.3.4	Zooplankton	79
3.3.5	Beam Attenuation	79
3.3.6	Relationship between variables	80
3.4	Conclusions	85
4	Interpolation and Analysis	86
4.1	Introduction	86
4.2	Data Visualisation	86
4.3	Predicting Pycnocline Depth	95
4.3.1	Inner Basin	96
4.3.2	Lynn of Morvern	99
4.3.3	Outer Basin	100
4.4	Turbidity	101
4.5	Conclusions	103
5	Vertical Processes	104
5.1	Introduction	104
5.2	Inner Basin: Physical Structure	104
5.2.1	Stratification Index	105

5.2.2	Tidal Cycle	106
5.2.3	Physical Influences on Vertical Structure	108
5.2.4	Deep Water Renewal	115
5.2.5	Bathymetry	124
5.3	Inner Basin: Biotic Structure	125
5.3.1	Chlorophyll <i>a</i> in the Water Column	125
5.3.2	Influence of Physical Structure	125
5.3.3	External Factors	133
5.4	Outer Basin: Physical Structure	134
5.4.1	Stratification Index	134
5.4.2	Tidal Cycle	135
5.4.3	Physical Influences on Vertical Structure	138
5.4.4	Deep Water Renewal	141
5.4.5	Bathymetry	150
5.5	Outer Basin: Biotic Structure	153
5.5.1	Chlorophyll <i>a</i> in the Water Column	153
5.5.2	Influence of Physical Structure	156
5.6	Conclusions	156
6	Horizontal Heterogeneity	160
6.1	Introduction	160
6.2	Inner Basin: Physical Structure	160
6.2.1	River Discharge	161
6.2.2	Fronts	161
6.2.3	Corran	161
6.2.4	Bathymetry	162
6.2.5	Wind	162
6.3	Outer Basin: Physical Structure	168
6.3.1	Corran Outflow	168
6.3.2	Fronts	169

6.3.3	Wind	170
6.4	Inner Basin: Biological Heterogeneity	176
6.4.1	Zooplankton	179
6.5	Outer Basin: Biological Heterogeneity	180
6.5.1	Phytoplankton	180
6.5.2	Zooplankton	181
6.6	Influence of Adjoining Water Bodies	182
6.6.1	Lynn of Lorne	182
6.6.2	Influence on Outer Basin	185
6.7	Conclusions	188

III Ecosystem Modelling 191

7 Ecosystem Modelling 192

7.1	Introduction	192
7.2	Sea-loch Model	193
7.2.1	Physical System	194
7.2.2	Biological System	194
7.2.3	Nutrient Cycling	195
7.2.4	Implementation	195
7.3	Application to Loch Linnhe Inner Basin	196
7.3.1	System Specific Parameters and Driving Functions	196
7.3.2	Results	199
7.3.3	Model Sensitivity	200
7.4	Changes to Zooplankton and Carnivores	203
7.5	The Role of the Physical Regime	207
7.5.1	Model Sensitivity	208
7.5.2	Lunar Tidal Cycle	209
7.5.3	River Discharge	211

7.6	Strategic Modelling of Wind and Tidal Forcing	213
7.6.1	Tidal Mixing	213
7.6.2	Wind Forcing	215
7.7	Hydrodynamic Events	218
7.7.1	Wind Forcing	218
7.7.2	Tidal Mixing	221
7.7.3	Deep Water Renewal	222
7.8	Further Developments	223
7.8.1	Physical	223
7.8.2	Biological	225
7.9	Discussion	227
7.9.1	Physical Forcing	227
7.9.2	Other Factors	228
7.9.3	Carnivores	229
7.9.4	Sea-lochs and Fjords	230

IV Overview and Discussion 232

8 Overview and Discussion 233

8.1	Summary	233
8.2	Discussion	235
8.2.1	Data Analysis and Comparison with Other Fjords	235
8.2.2	Ecosystem Modelling	239
8.2.3	Data Collection	241
8.3	Future Work	243

V	Bibliography	244
VI	Appendices	257
A	Surface data	258
A.1	Introduction	258
A.2	Inner Basin	260
A.3	Outer Basin	274
A.4	Firth of Lorne	288
B	Axial Data	301
B.1	Inner Basin	301
B.2	Outer Basin	307
C	Loch Model	327
C.1	The Loch Model	327
C.2	Parameters and driving functions	331

Part I

Introduction

Chapter 1

Fjords

1.1 Introduction

Fjords are a class of estuary and occupy a large proportion of the global coastal zone. They are found within coastal regions once dominated by Quarternary ice sheets - mountainous coastal zones north of 43° N and south of 42° S. Typically fjords are narrow, long, steep sided inlets which are often branched and sinuous but may be straight if following a geological fault line. The shape is often determined by the geological structure of the region. There is generally at least one submarine sill and typical glacial features such as corries and hanging valleys are common features of fjord valleys. As with estuaries - fjords are immature estuaries - the predominant source of freshwater input is at the head, with subsidiary river input along the length. Fjord valley rivers often have high sediment transport capacity and fjords are sites of net sediment accumulation, with the level of sedimentation being affected by wind, waves and climate. Sills, one of the principal differences between fjords and other estuaries affect water structure, circulation, sediment transport and biological life. They control exchange with the sea and are a source of energy through the generation of internal waves.

Fjords may be:

1. completely or nearly ice filled, eg. Greenland and Baffin Island
2. contain floating glaciers eg. Alaska and Chile
3. have glaciers in the catchment region eg. British Columbia and Northern Norway
4. have no or very little permanent icefield eg. Scotland, Canadian islands and Southern Norway

Fjords are changing environments, those with a substantial ice field are still being formed while sedimentary processes within and at the mouth are changing the nature of others.

The shoreline of fjords, in general, is lowly populated and the land of poor quality. Human use of fjords, however, is increasing due to aquaculture - fin and shellfish farming - especially in the northern hemisphere. Intensive cultivation of fish results in large quantities of organic and inorganic waste, such as uneaten food, faecal and excretory material, being produced continuously at a single site. Wu (1975) estimated that 85% phosphorus, 80-88% carbon and 52-95% of nitrogen input into fish farms, as feed, may be lost into the environment through the processes covered above. This has the potential to cause an excessive build up of nutrients (known as eutrophication) and has been linked with blooms of toxic dinoflagellates.

Many studies have been, and are being, done on the effect of aquaculture on marine environments, including Gowen and Bradbury (1987) and Gowen et al. (1992). The hydrodynamic conditions of the site are important in the long term effect of fish farms, with dispersal of waste matter being particularly important. The positioning of fishfarms in some countries, including Canada, Norway and Scotland, is based on known physical information on the fjords and the ecological criteria required in a selection of countries are described in Levings et al. (1995). The impact of fish farming has been found to depend on species, method of culture, stocking density, feed type and hydrography.

Fjords may be considered to be semi-enclosed coastal bodies which connect with the sea. They are ideal for marine data collection as the inputs, outputs and internal gradients are easily measured. The wide variety of marine environments which fjords encompass and the variety of habitats found within them, enables research done on fjords to be applied to other marine environments where data collection is more problematic.

1.2 Fjord Processes

The physical structure and processes in fjords have been studied for more than a century. Early study of Scandinavian fjords, including those by Ekman (Farmer and Freeland 1983) led to an understanding of circulation. Initial studies took place almost solely in Norway, with research into British Columbian and Washington State fjords commencing after a research programme on Alberni Inlet by Tully in 1949. Most research into fjords is still carried out on Norwegian and Canadian fjords. Canada has the longest coastline in the world, partly due to it having more fjords than the rest of the world combined (Syvitski et al. 1987).

The vertical structure of marine environments, has in general been of more interest as there is more variability vertically than horizontally. The vertical structure of fjords is very important in controlling nutrient circulation and therefore productivity, as stratification may be very strong with little transport between the layers. In a fjord, the surface water may be of very low salinity with the deep water salinity equivalent to that of the coastal sea.

1.2.1 Classification

Traditionally fjords were classified by their surface layer dynamics. The three principal categories below are based on vertical profiles of density (σ), which may be considered to represent the degree of stratification and mixing - from active to passive (fig. 1.1).

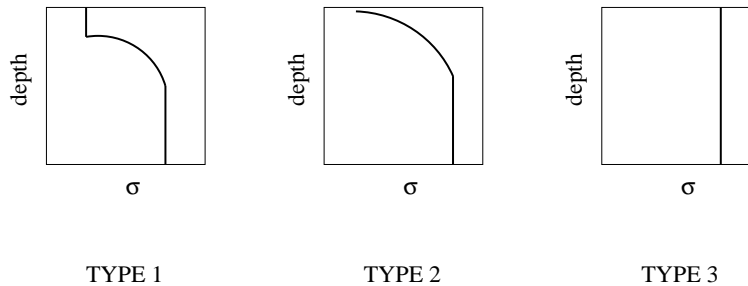


Figure 1.1: Classification of fjords, after Pickard (1961)

This descriptive categorisation is very much a generalisation, as at different times of the year a fjord may belong to a different classification and at a given time the structure may vary over the fjord. Type 1 and 2 may be considered to be active as river discharge has created surface circulation. Type 3 is passive being closely linked to and being very similar to the adjacent sea and may be considered to be an embayment of the coastal sea.

Fjords typically become less active with a deeper sill, which allows more tidal mixing, and a wider sill. Along its length, a fjord may also become less active further away from the head as the surface layer is mixed into the water column, reducing the degree of stratification. Other factors which influence mixing also lead to the vertical homogenisation of a fjord - such as a lessening of river discharge, high tidal amplitude and increased wind velocity.

With type 1 fjords the salinity and density of the surface layer is relatively homogeneous, with a sharp change in salinity and density at the pycnocline. The surface layer velocity is thus relatively uniform with a much weaker compensatory flow below. While with type 2 fjords the gradual increase in salinity and density throughout the water column means the velocity increases continuously away from the surface (Pedersen 1978).

An alternative classification method by Hansen and Rattray (1966), is based on two tidally averaged parameters representing circulation and stratification. The ratio of surface to bottom salinity difference to mean surface to bottom salinity is plotted against the ratio of net surface circulation velocity to cross-sectionally averaged net river discharge velocity.

1.2.2 River Discharge and Stratification

The circulation of the surface layer of a fjord is thought to be principally controlled by the level of stratification maintained by freshwater discharge. There is a balance between the stabilising effect of the river output and the destabilising mixing energy. The reliance on river discharge for stratification means that it often varies seasonally. In regions with glaciated catchment regions, such as British Columbia, fjords experience a peak in river discharge throughout the summer (the summer freshet), with very low winter river discharge levels, as precipitation principally falls then as snow. In Scottish sea-lochs there is a much closer link between precipitation and river discharge as more precipitation falls as rain and winter snow is more transient than in glaciated regions.

River discharge is principally concentrated at the head of a loch and generates a freshwater plume which is considered to consist of two zones, the upper and lower prodeltas. The upper prodelta is in the immediate vicinity of the river mouth and the energy of the river discharge controls the spreading and mixing of the surface plume. In the lower prodelta, other sources such as tidal currents, wind, shoreline morphology and the earth's rotation control the transport and mixing processes. Five principal sources of kinetic energy in fjords were defined by Farmer and Freeland (1983): wind stress, tidal interactions with topography, surface cooling and sea ice formation, kinetic energy at fronts and double diffusion instabilities in deep water.

1.2.3 Two Layer Circulation

Estuarine circulation (fig. 1.2) is driven by the horizontal pressure gradient between the low density surface freshwater and the higher density deeper basin water. River discharge generates a hydraulic head near the river mouth, from where the discharge flows towards the sea driven by the buoyancy of the freshwater. This flow may be considered to be 'downhill' and the gradient calculated from the level (geopotential) surface and the free (actual) surface. Farmer and Freeland (1983) calculated it to be approximately 1 cm/10 km. As the surface layer flows out to sea, it accelerates and entrains water into its outflow. The shear - between the two layers moving in opposing directions, surface flowing seaward and deeper water landward - generates an exchange of water parcels. There is a downward movement of brackish water parcels and a corresponding upward one of saline water parcels. The turbulence in the surface layer is generated by river flow instabilities and friction between the two layers - the more turbulence there is, the more mixing between the two layers. Along the loch there is a balance between the acceleration of the outward flowing surface water and the more saline water being entrained behind to produce a relatively constant surface layer thickness. Entrainment is the transport of fluid from a less to more turbulent region and means that as water moves up into the seaward flowing layer a compensating flow of seawater is drawn in to the loch at depth.

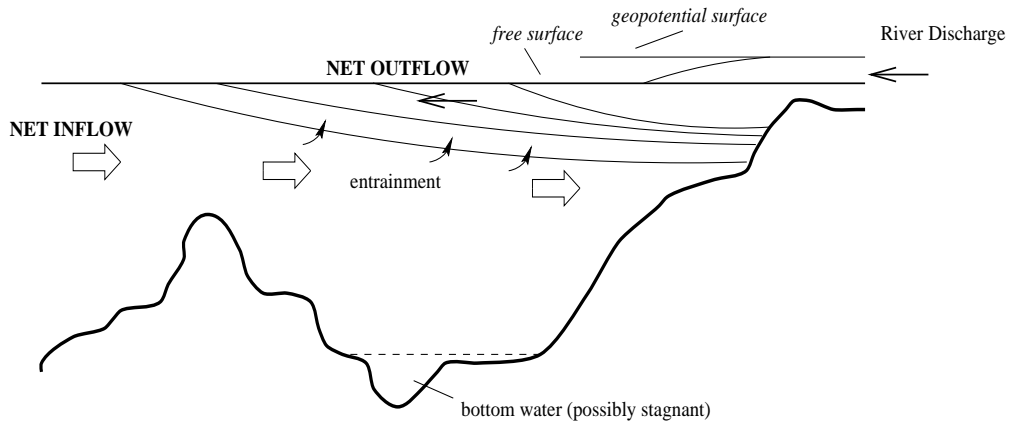


Figure 1.2: Two layer fjord circulation, after Syvitski *et al.*, (1987).

The Richardson Number (R_{fE}) is used as an indicator of stratification and is a ratio between the stabilising effect of density stratification and destabilising effect of velocity shear. Generally $R_{fE} = (\text{freshwater buoyancy}/\text{width of river mouth}) \times \text{mixing power of tides}$. It can also be considered as an estimate of the likelihood that internal waves become unstable and break into turbulence. If density stratification is strong (high Richardson No.) then waves on the interface between the surface and intermediate layers tend to be damped out.

1.2.4 Upper and Lower Prodelta

River flow into the head of a fjord is often turbulent (as fjords have steeply sloping sides,) catchment areas may be extensive, they are in regions of high precipitation and many fjords are in regions where river discharge is concentrated in one season. This means that the surface layer is well mixed near the river mouth but it is frequently surrounded by a brackish layer.

The river plume spreads laterally to a width determined by narrow channels further down the fjord, such as Corran in the inner basin of Loch Linnhe. There are extreme cases where the channel to the sea is so narrow that the mixing energy of the surface flow has little effect on the deeper water and the river mouth can effectively be considered to be the sill of the fjord, as the change in salinity of the river plume as it flows down the fjord is negligible. The deceleration of the surface flow is a function of lateral mixing of the river discharge and movement of the surrounding brackish water into and out of the discharge. The more the plume spreads out and mixes with the loch water, the more speed it loses.

The surface layer in the upper prodelta is relatively homogeneous, of low salinity, subject to transverse gradients and dominated by the instabilities of the river flow. Its extent is highly variable depending largely on river flow.

The circulation of the lower prodelta is influenced by a much wider range of factors such as wind, tidal currents, the Coriolis force, centrifugal acceleration

and topographically induced vorticity shedding. The surface plume may migrate laterally from shore to shore, the stratification may vary along the loch and it will become more saline, seaward and downward.

Coriolis Force

The Coriolis force is the geostrophic result of the earth's rotation in curving the path of a freely moving parcel of water (Mann and Lazier 1991). If the width of a fjord exceeds its Rossby radius of deformation (r') then a significant deflection of water may be expected (Huppert 1980).

$$r' = \frac{u}{f} \quad (1.1)$$

where u is the current velocity and f the Coriolis parameter:

$$f = 2\Omega \sin \phi \quad (1.2)$$

where Ω = angular velocity of the Earth about its axis and ϕ = latitude.

Surface Layer Thickness and Velocity

The thickness of the surface layer is a function of the discharge dynamics (flow velocity and width of river mouth), wind mixing and fjord morphology. Though thickness is largely a function of discharge, strong upinlet winds may be correlated with high river discharge - storm precipitation - which will further increase the surface layer thickness.

Wind is influential by generating surface waves and increasing the vertical exchange between affected layers by increasing turbulence. Upinlet winds can generate a subsurface seaward flowing jet (Mann and Lazier 1991) and if prolonged cause the surface layer to pile up at the head of the loch. Downinlet winds may increase the thickness and velocity of the seaward flowing surface layer and if prolonged may remove it entirely.

In fjords the effect of the tide is considered to be mainly that of a standing wave and its influence decreases below sill level. Tidal oscillations can however, effect the velocity and thickness of the surface layer, particularly in the vicinity of the river mouth with the potential for the tide to be influential, increasing at times of lower discharge.

Solar radiation also plays a role in the thickness and more importantly stability of the surface layer. During the summer, heating stabilises the surface and can be important in the formation of the pycnocline during periods of low river discharge. The shallower the surface layer is, the lower the volume of water it contains and

the more it is liable to warm by surface heating. While, in winter, cooling of the surface water and its subsequent rise in density leads to thermohaline convection, when the surface layer is mixed down through the water column.

1.2.5 Flushing and Deep Water Renewal

Traditionally, fjord research concentrated on the dynamically more active surface layer, however, circulation below the main pycnocline is important. Without deep water renewal the bottom water of the fjord may stagnate and become anoxic while the surface layer may become deficient in nutrients. It is generally believed that flushing and deep water renewal are necessary for overall renewal of the biogeochemical environment.

Geostrophic Currents

In the sea and particularly fjords, the sea surface is not horizontal. Freshwater discharge causes the sea level to be higher at the head of a fjord as can upinlet winds. This produces an uneven pressure on a horizontal seabed. Just as wind blows from high to low pressure, water flows to even out lateral pressure differences - this flow is called a horizontal pressure gradient force. If the Coriolis force acting on moving water is balanced by a horizontal pressure gradient force, then the current is in geostrophic equilibrium and is a geostrophic current, in which the water moves at right angles to the horizontal pressure gradient.

Barotropic and Baroclinic Conditions

Ideally, within the sea the surfaces of equal pressure (isobaric surfaces) are parallel to the sea surface, which is the uppermost isobaric surface. Where ocean waters are relatively homogeneous, density increases with depth because of the compression of the overlying water. If isobaric surfaces are parallel with the surface and planes of constant density (isopycnal surfaces) they are described as being barotropic. In barotropic conditions, the variation of pressure over a horizontal plane at depth is determined solely by the slope of the sea surface.

Variability in seawater density affects the pressure acting on a horizontal plane at depth. Where there are lateral variations in density, isopycnal surfaces are not parallel with the sea surface, but intersect the isobaric surfaces and the two slope in opposite directions, producing baroclinic conditions. Baroclinic conditions are found in regions of stratification and are particularly strong in regions of fast current flow.

The isobaric and isopycnal surfaces in barotropic flow are parallel to the surface and the slopes remain constant at all depths. This produces a horizontal pressure gradient which remains constant with depth, therefore, so does the geostrophic

current.

For baroclinic flow, although the isobaric surfaces remain parallel to the surface at shallow depth, with increasing depth, the gradient decreases due to the unequal mean density of the water column over the region. As the depth increases the isobaric surfaces tend to the horizontal which decreases the horizontal pressure gradient and in turn the geostrophic current. In sufficiently deep water the horizontal geostrophic current will reach zero.

Renewal Processes

Deep water renewal occurs when the water seaward of a sill (either coastal water or that of a more seaward fjord basin) is denser than the fjord basin water and there is an adequate supply of sill water to the basin. Then a density current attempts to replace the basin water. There are many conditions controlling this but it is essential for the sill water to be more dense than the basin water.

Sill depth affects the provision of an adequate supply of renewing water. In a deep silled fjord with the baroclinic flow causing renewal, the barotropic component (from wind, tides and meteorological events) may be insufficient to reverse the baroclinic flow over the sill and as long as the density condition is satisfied renewal will take place. With varying barotropic flow the baroclinic flow may also vary and the degree of inflow will also vary. With shallower sills, especially those in narrow channels, the baroclinic flow may be hydraulically controlled allowing the barotropic flow to be more influential. The shallower a sill is, the more likely barotropic flow is to stop inflowing water if it is directed out of the fjord and augment it if directed in. This can lead to a pulsing of water across shallow sills. Although shallow sills may be expected to have less frequent and smaller renewal events, Stigebrandt (1977) found that augmentation by barotropic flow can increase the carrying capacity of a sill to more than that of a solely baroclinic one.

The frequency of renewal is variable and may be due to tides, wind and other meteorological effects which are capable of generating barotropic currents, such as a lowering of atmospheric pressure. Tides are generally considered to be the most influential (Gade and Edwards 1980) and can drive renewal semi-diurnally, diurnally and with the lunar tidal cycle.

Renewing water is denser than the resident basin water and it sinks to the bottom as a turbulent density current. The primary forces acting on it are gravity, a pressure gradient due to the changing thickness of the inflowing plume, bottom friction and a force due to the acceleration of the water being entrained (Gade and Edwards 1980). If a plume starts slowly, gravity will dominate and it will accelerate, however, if the velocity is initially high, the increased entrainment of the basin water will slow it down. As the plume moves deeper into the basin, mixing will decrease its density while the density of the surrounding water increases - this may cause partial renewal.

Renewal is considered to be partial when fjord water up to the sill is not entirely replaced. This may be due to the renewal being over too short a time period or the intruding water being insufficiently dense to replace the existing bottom water. If the inflowing water does not reach the seabed it will fill up the basin from the lowest point it reaches. Partial renewal still has the potential to affect deeper water through turbulence and an inflowing plume with sufficient velocity is capable of attaining a depth greater than its density should allow.

1.2.6 Mixing Processes and Bathymetry

Gade and Edwards (1980) considered mixing energy in fjords to be derived from two primary sources - tides and wind.

Tides

Within fjords most of the tidal energy is reflected to give a standing wave with a small progressive component and the sea level moves up and down synchronously. Tidal energy is converted to turbulence by boundary mixing, tidal jets and plumes and the breaking of internal waves. Shallow sills and narrows which constrict the flow of water, often concentrate tidal currents into turbulent jets and plumes which interact with the main fjord water mass. Long sills are able to convert tidal currents to tidal streams, where the water column is well mixed from the surface to the seabed, with clearly defined boundary flow. Tidal streams follow and are influenced by local bathymetry - narrow channels have been found to produce eddies, whirlpools and upwelling. The slope of the seabed is able to increase entrainment and upwelling (Syvitski et al. 1987). Other influential external forces are friction, the Coriolis force, river discharge, winds, inertia and momentum. The velocity along the floor and sides of a fjord tends to be diminished by friction, but in cases of strong stratification, flood currents may be stronger closer to the seafloor than further up the water column.

Tidal energy can play an important role in contributing energy and therefore heterogeneity and life to a fjord. On the flood tide, energy is imported into the system and on the ebb, exported at rates proportional to (water speed)³ (Edwards and Sharples 1986). In general tides flood faster than they ebb, with the result that, over the entire tidal cycle, there is a net input of energy into the system, with much of this energy being lost due to friction. At Corran, the maximum flood current is 4.9 m.sec⁻¹ while the ebb maximum is only 3.6 m.sec⁻¹.

Wind

The wind on the surface sets up a stress modifying flow which causes the water to flow in the same direction as the wind. The water flow is modified by the Coriolis effect with the water just below the surface flowing slightly to the right

(in the northern hemisphere,) and moving progressively further to the right with increasing depth. This forms an Ekman spiral over the Ekman depth - the depth of water affected by the wind. Over the Ekman depth, the water flows at a mean angle of 90° to the right of the wind direction. Coastal longshore winds can result in surface waters flowing offshore - Ekman drift - with a compensatory upwelling of deep water along the coast - coastal upwelling (fig. 1.3). During coastal upwelling the deep cooler water does not necessarily outcrop on the surface, however it may penetrate a fjord, affecting salinity, temperature and nutrients within the basin.

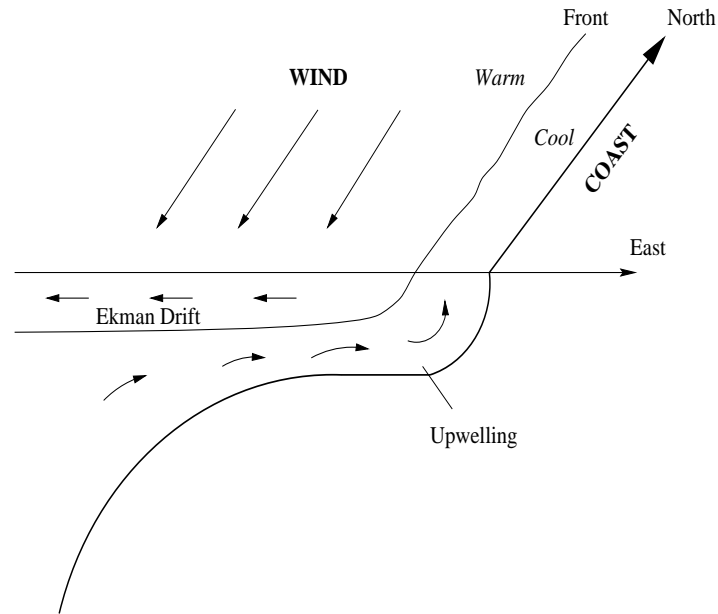


Figure 1.3: Coastal upwelling, after Mann and Lazier (1991).

Wind stress on the surface is transmitted down through the water column as a result of internal friction. If the water column is well stratified, there is very little frictional coupling, particularly at abrupt changes in density, and the energy and momentum from the wind is transmitted only to the surface layer. Fjords are often highly stratified environments, due to river discharge, with a shallow surface layer. In such conditions, the power of the wind over the surface layer is greater than it would be over a deeper mixed layer (Mann and Lazier 1991).

Secondary sources for turbulence include the breaking of waves on the surface, rough flow over the seabed but principally the breaking of internal waves on the interface between the surface and intermediate layers (Farmer and Freeland 1983). Internal waves can be generated on the interface by surface wind, variability of atmospheric pressure and tidal interaction with sills and the bottom bathymetry.

Internal Waves

Tidal mixing may cause tidal currents after interacting with fjord bathymetry. In turn, this can lead to turbulence, mixing the lower layers of the water column,

and if sufficiently strong the entire water column. If tidal mixing is less strong and the water column stratified, then internal waves may form along gradients in the water column such as the thermocline or halocline. The interaction of tidal flow and obstacles, such as the edge of a shelf may also generate internal waves, which decay away from the obstacle due to shear within them. An alternative source of internal waves is a result of the displacement of the pycnocline. If the pycnocline is displaced vertically a restoring force returns it to its equilibrium position - this can lead to oscillations and the propagation of waves along the pycnocline.

Internal waves along the pycnocline mean that the depth of the surface layer varies along the wavelength of the internal wave. Above the pycnocline, water flows from the peak regions to the trough regions which causes the water to converge behind crests and diverge behind troughs. These convergent and divergent regions exist to the surface but their strength diminishes away from the pycnocline. The surface wave is 180° out of phase with the internal wave and its amplitude is smaller. On the surface, these regions can be identified by the accumulation of organic matter in the convergent zones. Below the pycnocline the convergent and divergent zones are half a wavelength behind the those above.

1.3 Nutrients and Primary Production

1.3.1 Euphotic Zone

Phytoplankton require light and nutrients to grow and survive. The layer in which this is possible, is known as the euphotic zone or compensation depth. The compensation depth, is the depth at which plant respiration during 24 hours consumes the organic material made by photosynthesis in that time (Tett and Edwards 1984). The depth of the euphotic zone may also be defined by the depth at which a fixed percentage, defined as being between 0.1% and 1.0% by Rees et al. (1995) of surface irradiance reaches.

Tett and Edwards (1984) defined critical depth to be the depth at which between the sea surface and that depth, the sum of 24 hours gross photosynthesis is equivalent to the sum of 24 hours plant respiration.

1.3.2 Spring Bloom

With negligible grazing, phytoplankton blooms occur when the water is sufficiently stabilised to ensure phytoplankton cells are not persistently advected out of the euphotic zone. In coastal seas and estuaries this stabilisation is produced by increasing insolation and warming of the surface water. Fjords are capable of blooming earlier as the high river discharge (which may be due to spring snow melt) stabilises the surface water. Variability in the year to year initiation of

the spring bloom may be due to varying cloud cover, turbidity, river discharge and processes which counteract stabilisation such as wind driven vertical mixing (Townsend et al. 1994) and tidal mixing. Townsend et al. (1994) also found that the spring bloom may commence before surface warming if stratified due to runoff, or before stratification if the wind speed is sufficiently low.

Evolution of the bloom then depends on the continuation of solar radiation, availability of dissolved inorganic nutrients, turbidity (including self shading) and losses of phytoplankton biomass from respiration, grazing and sedimentation, (Townsend et al. 1994). Termination may occur with nutrient depletion if the water column continues to be strongly stratified, self shading by the phytoplankton or increasing grazing by herbivores. With weaker stratification, surface nutrients are more likely to be renewed but large cells are more likely to sink out of the euphotic zone (Syvitski et al. 1987).

The timing of the bloom may have a continuing effect on productivity throughout the year (Syvitski et al. 1987; Townsend et al. 1994). Townsend et al. (1994) found that with a sufficiently early bloom, such as found with river discharge driven stratification, then the water temperature may be low enough to inhibit the metabolic rates of herbivores, or occur before there is a substantial population of herbivores (Syvitski et al. 1987). Herbivores are thought to lower their consumption in cold water - as a over wintering strategy - when there is a low food supply. Townsend et al. (1994) found that with early density driven stratification, there was less grazing of the phytoplankton and more sank to the benthos, increasing benthic productivity. This was in water of $< 2^{\circ}\text{C}$.

1.3.3 Phytoplankton Species Succession

During the spring bloom there is often one dominant and some subsidiary diatom species (Syvitski et al. 1987) and the composition may vary between different years or inlets in the immediate vicinity. The diatom *Skeletonema costatum* is often the predominant species in poorly stratified waters (Syvitski et al. 1987) as it forms long chains which are able to retain their position in the water column where individual diatoms would sink (Braarud 1976). *Skeletonema costatum* is widely found in an extensive range of marine conditions, as it has a wide temperature range tolerance, can survive in exceptionally low salinities, has a low light requirement and high maximum growth rate (Braarud 1976). For these reasons it often dominates the first bloom and is common in fjords where conditions may be highly variable both in space and time.

Later in the year, stratification may strengthen as the surface warms and if there is a summer freshet, river discharge increases and nutrient concentration levels fall as the phytoplankton deplete the euphotic zone. Flagellates may then dominate the phytoplankton biomass (Syvitski et al. 1987; Haigh et al. 1992). Heterotrophic dinoflagellates are of a similar size and growth rate to diatoms and are also found to occur at or just after the Spring bloom peak (Tiselius 1992).

Flagellates are smaller, have a higher nutrient uptake efficiency at low ambient nutrient concentrations and maintain their position in the water column due to their shape rather than the diatoms' need for turbulence within the euphotic zone (Syvitski et al. 1987). This enables them to remain in the euphotic zone in conditions of lower turbulence, such as with lower wind speeds during the summer. Later in the year there may be a further transition to domination by *Chaetoceros sp.* or a return to diatoms as turbidity and turbulence increase. Tett (1973) found in the Lynn of Lorne that species diversity increased from the spring bloom, reaching a peak in August and September in 1970 and in June of 1971.

1.3.4 Nutrients and Regeneration

Phytoplankton require light and nutrients for growth and reproduction. Energy from the sun decreases exponentially with depth through the water column (Mann and Lazier 1991) and this loss of energy can be enhanced by particulate matter in the water such as phytoplankton, or organic matter from river discharge or tidal stirring.

In the absence of turbulence, the euphotic zone may become depleted of nutrients and productivity decline. In many fjord systems, growth has been found to be limited by the availability of nutrients (La Roche 1983). Such conditions prompted the belief that nutrient regeneration and transport of nutrients to the euphotic zone is an important process controlling primary productivity in fjords.

Nutrients are regenerated by the sedimentation and decomposition of organic matter from the euphotic zone to the benthos (Baker et al. 1985; Mann and Lazier 1991) - with the vertical flux of phytoplankton being part of this process. With no turbulence, transfer of nutrients from the nutrient rich benthos to the depleted surface layer is by molecular diffusion. Turbulent mixing, upwelling and deep water renewal all contribute to bringing nutrients up into the euphotic zone. While wind driven turbulence and during the winter thermohaline convection, generate downward mixing and the deepening of the surface mixed layer. As the turbulence moves deeper, it moves into the zone of higher nutrients, bringing nutrient rich water up to the euphotic zone. At the same time however, phytoplankton may be pushed below the euphotic zone (Mann and Lazier 1991). Deepening the surface layer, recirculates nutrients but makes it slower to warm from irradiance as there is more water to heat.

Nutrients are lost from the surface layer by uptake by phytoplankton, sedimentation of phytoplankton and the consumption of phytoplankton by zooplankton. Gain of nutrients is from vertical diffusion and excretion by zooplankton. Excretion and respiration by zooplankton have been hypothesised to be the most important sources of water column nutrient regeneration in coastal waters (La Roche 1983). The sinking of phytoplankton cells also affects the vertical distribution of biomass, production, species succession and seasonal growth cycles (Bienfang et al. 1982).

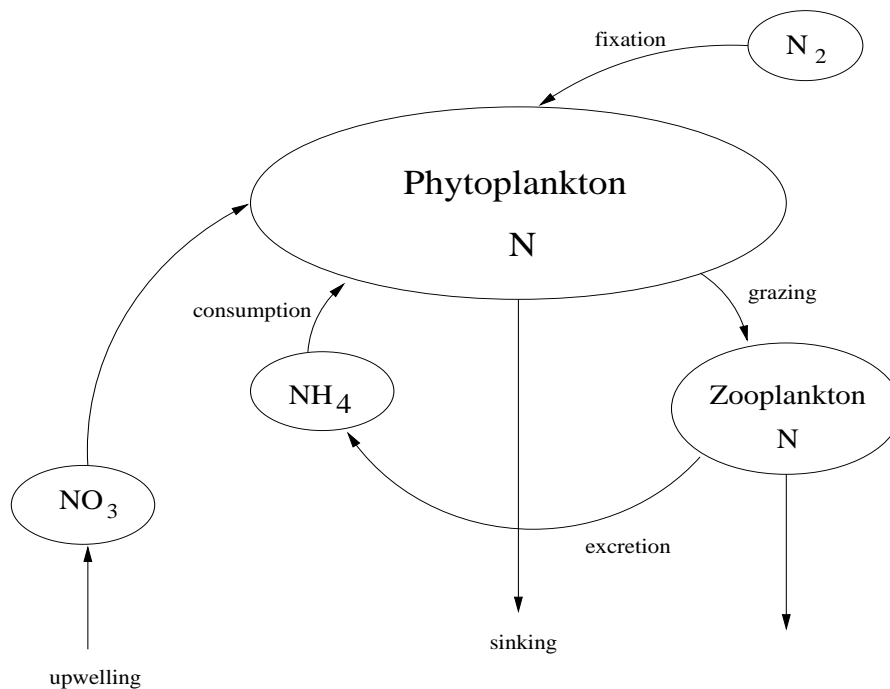


Figure 1.4: Diagram of nitrogen circulation within the surface layer, after Dugdale and Goering, (1967).

There are two principal hypotheses on the causes of subsurface chlorophyll maxima in cases where they have not formed due to fronts or internal waves - one is physically based and the other biologically (Mann and Lazier 1991). The physical explanation is that at the surface, phytoplankton are exposed to more light and grow faster, depleting the available nutrients more rapidly and then sinking. Deeper cells, will grow more slowly, generating a subsurface maximum after the surface layer has sedimented, this process may continue through the euphotic zone, generating deeper and deeper maxima (Mann and Lazier 1991). The biologically driven hypothesis is that cells sink from the surface, and then cease sinking upon reaching higher nutrient concentrations (Mann and Lazier 1991). The sinking rate of *Skeletonema costatum* has been found to decrease upon reaching deeper, darker water with a higher nutrient concentration (Steele and Yentsch 1960). Bienfang et al. (1983) also found that in lower light conditions alone, diatoms sink at a slower rate.

Nutrient depletion is often believed to be a contributory factor in the sedimentation of phytoplankton, especially diatoms. The physical condition of phytoplankton affects their buoyancy as it is regulated by physiological mechanisms, which are coupled to growth and photosynthetic processes (Bienfang et al. 1982). For *Skeletonema costatum*, Bienfang et al. (1982) found that in conditions of nitrate and phosphate depletion, the sinking rate decreased, only with silicate depletion did the sinking rate increase. In the first two cases, the mean cell volume and length of chain did not change, so the change in sinking rate was not due to size. In the silicate deplete case, *Skeletonema costatum* decreased its chain length which may have lessened its potential to sink. This suggests that *Skeletonema*

costatum may be able to change the chain structure to maximise its buoyancy.

Nitrogen is generally considered to be the most important nutrient for phytoplankton growth. Its principal source however, may vary according to the prevailing conditions and the relative importance of nitrate and ammonium to nitrogen assimilation in coastal waters is not fully understood (Dortch 1990). Ammonium (NH_4) is the first end product of degradation of organic material, it is also a direct excretory product of some zooplankton (Ward et al. 1984). NH_4 is converted to NO_2 then to NO_3 . In low light conditions and high NH_4 concentrations uptake of NH_4 , by phytoplankton, exceeds that of NO_3 (Dortch 1990) conversely in conditions of high NO_3 and low NH_4 , NO_3 is preferred. In Loch Linnhe. Rees et al. (1995) measured preferential assimilation of ammonium, however, >50% of production was driven by nitrate assimilation and only during the summer was ammonium an important source of nitrogen.

1.4 Fjord Research

Fjords are complex environments and there is a great deal of variability between fjords in climate and topography, both of which have the potential to influence the processes taking place. While events in fjords can be understood and explained, prediction is more problematic. The interaction of the many variables within a fjord, produces a range of responses to the same conditions. One of the most important features in fjordic circulation, deep water renewal, is particularly variable in its timing in different fjords.

1.4.1 Deep Water Renewal

Deep water renewal is an important feature of a fjord and the time scale of renewal processes plays a large role in the environment and productivity within the fjord. While the semi-diurnal and lunar tidal cycles are in general acknowledged to be important in the timing of renewal processes, in different fjords the relationship varies.

Gade and Edwards (1980) considered the depth of the sill relative to the pycnocline to be important in determining the timing of renewal. Spring tides increase the water supply facilitating renewal, but the increased mixing energy at sills during spring tides may reduce the density at the sill and prevent renewal. De Young and Pond (1988) found that the increases in mixing energy during spring tides prevented renewal in Indian Arm, with renewal events all occurring during neap tides when the density of water at the sill reached its maximum. Indian Arm is separated from coastal waters by a long region of sills and narrows. By comparison, in Puget Sound, Lavelle et al. (1991) found flood tidal heights greater than 3.5m (which only occur close to spring tides) to be essential for renewal to take place. Edwards et al. (1980) found that for Loch Eil which has a very shallow

sill - 6 m (Edwards and Sharples 1986) - renewal is frequent and occurs regularly during spring tides.

Over most of the west coast of Scotland tidal ranges are large and stagnation of the bottom water is not in general a problem in Scottish sea-lochs. In Scotland, only in Loch Kanaird and Loch Etive has O_2 saturation been measured to fall below 50% (Syvitski et al. 1987).

A build up of higher density water outside the most seaward sill may be due to external forces such as coastal upwelling or the wind field advecting the coastal sea. Exchange at internal sills is however dominated by processes within the fjord basins (Gillibrand and Turrell 1995). Internal forces affecting the density balance across the sill, include the effect of wind on the circulation and the relationship between river discharge and the density of entrained water.

Wind causes baroclinic flow which may import water into the basin, but it can also change the surface level causing barotropic flow which may augment or diminish flow. It is not possible to say from the wind direction which effect it will have on renewal. In Howe Sound, Bell (1973) found renewal was assisted by down channel winds. Gillibrand and Turrell (1995) found that in the innermost Loch Sunart basin, downinlet winds, by enhancing estuarine circulation in the more seaward basin, (removing low salinity water and entraining high salinity water) caused renewal. Changing coastal longshore wind has also been shown to affect the inflow rate (Gade and Edwards 1980).

The influence of river discharge on renewal is also variable. Freshwater discharge may drive barotropic and baroclinic currents at the sill, preventing or enabling renewal. Inflowing water, if it mixes with lower salinity water at the sill may lose enough density for the renewal event to cease, but if the water column is sufficiently stratified, dilution of inflowing water is minimal. In such a situation, renewal may be promoted as the river discharge may enhance estuarine circulation, accelerating the baroclinic currents and therefore the supply of renewing water. As the supply increases however, it reaches a maximum, after which increasing barotropic outflow decreases the supply, until with sufficient runoff there is no further inflow (Bell 1973). Long sills may generate mixing which prevents baroclinic flow. In regions where mixing at the sill is a frequent occurrence, such as with shallow or long sills and narrow channels, and sufficient to prevent renewal, renewal events will tend to occur during periods of low runoff. Edwards and Edelsten (1977) found that for Loch Etive, low river discharge was essential for renewal to take place as the outflowing surface layer mixes with the deeper water lowering salinity. Loch Etive has the highest ratio of river input to tidal flow of a Scottish fjord (Edwards and Sharples 1986) due to its very large catchment area in a region of high precipitation and renewal events are infrequent. The sill is long and shallow, - 4 km long and 10 m deep (Edwards and Edelsten 1977) and tidal range low, - 2 m (Hydrographic Department 1977b). High river discharge was also found to prevent exchange in Indian Arm (de Young and Pond 1988) which also has a long sill. In Loch Ailort where river discharge is considerably less than for Loch Etive, Gillibrand et al. (1996) found renewal occurred

on average every 8 weeks. In Loch Sunart, the ratio of river input to tidal flow is relatively low for Scotland and Gillibrand and Turrell (1995) found renewal there to be frequent and enhanced by low river discharge.

Watts (1994) studying the inner basin during the Spring bloom in 1991 and 1992, found deep water renewal in the Inner Basin of Loch Linnhe to be linked to wind driven upwelling seaward of Corran and spring tides. In 1992 there was also a temperature inversion throughout the water column preceding a renewal event.

1.4.2 Mixing Processes and Bathymetry

As with deep water renewal, the sill is an important component in determining the mixing regime.

Tide

Griffin and LeBlond (1990) found the lunar tidal cycle to be the most important component in modulating the export of freshwater from the Strait of Georgia-Juan de Fuca Strait system. During neap tides there is less mixing at sills and narrows, producing a less saline surface layer than during spring tides. Downinlet wind events, coinciding with a period of low energy, were found to enhance outflow but outwith neaps had no effect.

Farmer and Osborn (1976) found that internal tides were generated on internal slopes in Alberni Inlet, of the type shown by Rattray (1960) for the open coast, as well as at sills.

Stratification is a ubiquitous feature of fjords and often an important control in the growth of phytoplankton - in particular the timing of the spring bloom. Freshwater runoff and to a lesser degree heating of the surface layer by solar irradiation are the main determinants in strengthening the degree of stratification. In a variety of coastal shelf seas and estuarine systems there is a fine balance between the water column being predominantly stratified or briefly becoming more homogeneously mixed. These transient states of homogeneity or weaker stratification may be prompted by increased tidal mixing during spring tides (Sharples et al. 1994). Goodrich (1988) found in three east coast U.S.A. estuaries that short term fluctuations, where the strength of stratification declined, were associated with peaks in wind mixing energy. Sharples et al. (1994) also found that stratification was related to semi-diurnal tides, increasing on the ebb tide and decreasing on the flood. If water is sufficiently shallow, winds may have the energy to mix the entire water column but in deeper water only the surface layer will be affected. In the Gulf of Maine, Balch (1981) found the surface temperature to be affected by the tidal range, with a sharp decrease in temperature during or after the peak spring tide and in tributaries of Chesapeake Bay, Haas (1977) found stratification and mixing to be closely correlated with the lunar tidal cycle, with the height of high tide being more influential than the tidal range.

The breakdown in stratification caused by an increase in mixing energy, either periodically (spring tides) or episodically (wind mixing), is a mechanism which enables the replenishment of the surface layer with nutrients and the bottom water with O₂.

Tidal flow through narrows, may cause choking where the flow is restricted and barotropic flow dominates. Such processes lead to increased turbulent mixing.

Wind

Coastal upwelling can have a dramatic effect on the salinity, temperature and nutrients in a fjord (Holbrook et al. 1980). Inlets in Nova Scotia, Canada, have been found to experience substantial changes in salinity, temperature and nutrient concentration after coastal upwelling (Syvitski et al. 1987) as have west Norwegian fjords (Wassman and Aadnesen 1984) and Bantry Bay on the south-west coast of Ireland (Edwards et al. 1996). In Jøsenfjord, west Norway, the mean circulation of the intermediate layer was found to be strongly influenced by the offshore wind conditions by Svendsen (1977). Coastal upwelling leads to the intermediate layer flowing upinlet and coastal downwelling causes the intermediate layer to flow out. In St Georges Bay, Nova Scotia, cross axial wind stress near the mouth of the bay was found by Drinkwater (1994) to generate Ekman drift with a compensating flow in the lower layer.

Within a fjord, axial winds are generally considered the most influential (Cokelet 1992). Upinlet winds may lead to a pile up of the brackish surface layer at the head of the basin (Svendsen and Thompson 1978) with the depth of the surface layer more than doubling within in a few hours of the commencement of upinlet winds as found by Farmer and Osborn (1976) at the head of Alberni Inlet, British Columbia.

Winds do not, however, only affect the surface layer, flow at the surface may induce compensatory deeper flow. Cokelet (1992) found a link between wind and saltwater intrusions into Puget Sound. The lessening or removal of upinlet wind stress allowed ponded water to flow out of the surface layer and a corresponding influx of coastal, more saline water was drawn into the sub-pycnocline layer of the fjord. Within St Georges Bay, surface wind stress produced upwind currents in deep water which were topographically steered (Drinkwater 1994). Pickard and Rodgers (1959) conducted one of the earliest studies of wind in a fjord and found wind to be highly influential in the circulation of Knight Inlet, BC. Pickard and Rodgers (1959) found that in a shallow region (70–80m) in light wind conditions there was a two layer circulation pattern but upinlet winds caused three layer flow, with the surface and deep water flowing upinlet. Light or upinlet winds produced a similar pattern in a deeper, 350m, section of Knight Inlet, but downinlet winds generated four layer flow, with 0–40m flowing out, 40–100m flowing in, 100–250m flowing out and the bottom water flowing in. Gade (1970) found that within a few hours after the start of upinlet winds in Vestfjord a three layer circulation pattern formed with inflow on the surface and at depth, with outflow between.

In Knight Inlet, Pickard and Rodgers (1959) discovered that wind stress was only able to push the surface layer to the head of the inlet for a limited length of time before the pressure was too great and outflow recommenced. In other fjords this has not necessarily been found.

1.4.3 Physical Influences on Plankton

The productivity of fjords and coastal seas is strongly influenced by circulation (Winter et al. 1975) and vertical structure (Jones and Gowen 1990; Gowen and Stewart 1995; Mann and Lazier 1991). In Puget Sound, Winter et al. (1975) found that phytoplankton growth was affected by vertical advection and turbulence and rapid wind induced horizontal advection. Estuarine circulation has been found to be of importance by entraining nutrients into the euphotic zone, and recirculating phytoplankton cells which had sunk into deeper water - but were still viable - into the surface layer (Winter et al. 1975; Braarud 1976).

Productivity may be increased wherever there is an influx of nutrients into the euphotic zone (Syvitski et al. 1987) this may be through entrainment or localised tidal or wind induced turbulence. In a generally well stratified region, any areas of reduced stability may have higher nutrient concentrations and be more productive. These regions are generally at shallow sills, islands and frontal regions where there is enhanced vertical turbulence.

River Discharge

River input, if nutrient rich, will increase productivity but if of lower nutrient concentration than the fjord water or of high light attenuation due to humic content, will suppress growth (Syvitski et al. 1987; Mann and Lazier 1991). High river discharge enhances estuarine flow, entraining more water to the surface and upwelling more nutrients. It also stabilises the water column which may enhance productivity or limit it if the surface layer is depleted of nutrients. In fjords river input driven stratification is often the source of bursts of productivity, both in spring (Haigh et al. 1992) and autumn (Sakshaug and Mykkestad 1973). Regions of lower salinity may also affect species diversity as fewer types of phytoplankton will grow in low salinity water (Tett 1973).

While river discharge is capable of increasing productivity, fjords are situated in infertile regions and the nutrient content of river discharge will generally be low, as may the transparency. Increases in productivity due to river discharge will therefore be predominantly a result of river discharge driven stratification. Rees et al. (1995) considered suspended sediment to be the main contribution to vertical attenuation in Loch Linnhe, and found the euphotic zone as estimated by the 0.3% irradiance depth to deepen away from the head of the system where the principal input of freshwater is.

Fronts

Fronts occur for various reasons and are found at the conjunction of stratified and unstratified water. The time scale over which they exist may vary from being relatively permanent on continental shelves, to more transient in estuaries and fjords. At the mouth of an inlet such as a fjord, the frontal zone is generally considered to be maintained by the changing water velocity (Parsons et al. 1983). The tidal cycle is therefore an important component in determining its position and magnitude. Fronts are not necessarily found at the mouth of fjords. There is no front at the mouth of Jervis Inlet, BC (Parsons et al. 1984) which has a deep sill with little effect on water movement.

It has been hypothesised that during spring tides, or periods of greater mixing energy, the front is pushed further into the stratified region, bringing nutrients into the surface of a possibly nutrient deficient region. Then during neap tides, the front retreats to its former position and the water close to the front, which had been tidally mixed, is once more stratified and there may be a burst of growth (Mann and Lazier 1991; Holligan 1981) - cross frontal transport. On the surface, there is an accumulation of organic matter which often coincides with chlorophyll surface maxima and fronts are generally regions of high productivity. In the mixed region, diatoms such as *Skeletonema costatum* dominate and during the summer, there is often a dinoflagellate population along the thermocline extending to the surface at the front (Mann and Lazier 1991; Holligan 1981). Nutrients in the stratified region are augmented by cross frontal transport. Simpson and Bowers (1981) however, showed that a water column retains its state, whether stratified or mixed, with the result that frontal displacement from the spring-neap tidal cycle is small.

Parsons et al. (1983) found in Saanich Inlet, British Columbia that maximum chlorophyll density at the front coincided with the most stable period - neap tides - and the lowest density with spring tides. Despite the front being the most productive region of the fjord, zooplankton and gelatinous zooplankton biomasses were lower there, than within the more stable environment of the fjord (Parsons et al. 1983). Parsons et al. (1983) considered that in this case, the higher productivity at the front was driven by the increase in available nutrient rather than from phytoplankton cells being advected to the surface.

Internal Waves

Internal waves are also capable of increasing or maintaining productivity. The passage of internal waves along gradients transports nutrients and provides sufficient mixing to maintain the position of flagellates in the water column (Mann and Lazier 1991). Convergent zones on the surface, generated by internal waves, are a source of high productivity and buoyant organisms such as phytoplankton may be transported there (Mann and Lazier 1991) generating lines of productivity along the loch.

Stratification

Margalef (1978) suggested that species succession of phytoplankton is controlled by light levels and turbulence. In environments where vertical mixing exceeds horizontal, succession is governed by a species ability to grow within a turbulent euphotic zone. The spatial pattern of the water column structure is thus able to determine spatial variation, in phytoplankton growth and species composition, where it exists on a timescale comparable to phytoplankton growth (Jones and Gowen 1990; Gowen and Stewart 1995). As mentioned in 3.3.2 above, diatoms and dinoflagellates exist in conditions of different light and mixing. Jones and Gowen (1990) considering the Sound of Jura, Scilly Isles and the Loch Linnhe system (including the Lynn and Firth of Lorne,) found that in conditions of extreme stratification, dinoflagellates almost totally dominated, with > 75 % dinoflagellates. Even in conditions of low illumination and high stratification dinoflagellates were predominant. In conditions of intense stratification, diatoms sink out of the surface layer and the nutrient depletion which often accompanies stratification is commonly believed to enhance sedimentation (Jones and Gowen 1990).

In fjords, intense stratification may be interspersed by periods of high mixing which, if existing for a sufficient period of time, may alter the species composition. In the more stable environment of a coastal sea, Gowen and Stewart (1995) were able to identify physically distinct, tidally generated regions characterised by different phytoplankton populations.

Lunar Tidal Cycle

Just as seasonal phytoplankton community changes are associated with the seasonally changing hydrographic regime, variability in vertical structure over the lunar tidal cycle may cause changes in species composition (Balch 1981; Roden and Raine 1994) and abundance (Cloern 1991).

Off the west coast of Ireland, Roden and Raine (1994) found that chlorophyll concentrations (considering diatoms and dinoflagellates) on the shallower side of an escarpment, were related to tidal range. In the Gulf of Maine, Balch (1981) found surface diatom blooms to be associated with major spring tides, while dinoflagellate abundances increased with minor spring and neap tides; the greater mixing energy advects deep, cool, high nutrient, high chlorophyll water to the surface. The inverse relationship was, however, found in South San Francisco Bay by Cloern (1991). There the chlorophyll density ranged from 2-4 mg Chl m⁻³ to 20-40 mg Chl m⁻³ over the lunar tidal cycle, with the greater stability during neap tides enabling the phytoplankton biomass to increase. Differences between the regions may partly be a result of differing dominant species; in South San Francisco Bay, dinoflagellates are a more important part of the population than for the other two regions.

Turbulence, due to flow of water across the sill, brings bottom water to the surface on both sides of the sill and this mixing may increase the supply of nutrients to the surface productive region. With greater tidal ranges this effect is enhanced.

Semi-diurnal Tidal Cycle

The interaction of tidal flow and coastal features has been found to affect the distribution of many forms of marine life from phytoplankton to benthic invertebrates (Alldredge and Hamner 1980). Alldredge and Hamner (1980) found zooplankton density increased linearly with current speed in the lee of a promontory during flood tide, with densities reaching 40 times those of the nearby channel.

Wind

As mentioned previously, wind induced turbulence can increase the depth of the surface mixed layer, increasing the nutrient concentration of the surface layer, but at the same time phytoplankton may spend more of their time below the euphotic zone (Erga and Heimdal 1984). Such conditions may also affect the species composition, as flagellates are more able to maintain their position within the water column than diatoms.

When diatoms cells collide, if sticky enough they may form a doublet (Tiselius 1992). Collisions are known to increase at higher levels of mixing, such as with wind driven turbulence (Tiselius 1992), aggregates form and large aggregates may sink rapidly from the surface mixed layer. After a gale with winds exceeding 15 ms^{-1} , Tiselius (1992) found that the cell concentration of small diatoms fell from 4000-7500 to 30-40 cells ml^{-1} within a week. In the Santa Barbara Channel, Alldredge and Gotschalk (1989) found that flocculation of a bloom could occur within 24 hours and that the coagulation and sinking were not due to nutrient depletion. Riebesell (1991) found that different species flocculated separately and that flocculation species succession closely followed the bloom succession pattern.

The exchange of intermediate layer water caused by wind induced coastal processes may also influence plankton. Coastal water may be rich in nutrients, which if advected into the basin can increase phytoplankton density (Erga and Heimdal 1984). Influx of deeper water, however, may be accompanied by outflow of surface water with phytoplankton biomass being advected out of the fjord. Reigstad and Wassman (1996) found that surface phytoplankton levels fell due to the surface population being advected out of the fjord by downfjord wind stress, however, the accompanying intermediate inflow of nutrient rich coastal water, when entrained to the surface enabled a subsequent bloom to develop. Species composition may also be affected by horizontal water exchange as coastal species may be advected into the fjord (Erga and Heimdal 1984).

Kaartvedt and Svendsen (1995) found in Sandsfjorden that zooplankton position may be wind influenced. Intermediate water exchange, whether due to coastal

or fjord processes may advect zooplankton into a basin. In Sansfjorden, coastal processes were found to be more important in the distribution of zooplankton, than even large quantities of river discharge.

1.5 Horizontal Heterogeneity In Fjords

Horizontal heterogeneity in marine and aquatic environments has been observed for a long time. It was originally assumed that plankton drift passively (hence the name,) producing homogeneous or random distributions in lakes. In lakes, Ricker (1937), believed that there was little difference between single samples at random sites and replicate samples at one. Berzins (1958) found that patchy distributions were generated in lakes and that different species formed different patterns (Patalas and Salki 1993). The importance of physical and biological factors in producing the heterogeneity has since been recognised. The phytoplankton population is dependent on growth and grazing rates and physical factors, with the balance of these factors determining the success of the population. Biological oceanographers generally consider the physical characteristics of the marine environment to be primarily responsible for pattern generation in biological communities, with the capacity for pattern formation from biological interactions being considered to be of much less importance (Steele et al. 1993). Spatial dependence and heterogeneity are not the same. While spatial dependence often causes horizontal heterogeneity, heterogeneity may not depend on spatial position. In understanding mechanisms it is necessary to identify the cases of spatial dependence, either directly or through another factor. Analysis and study of heterogeneity may consider ‘measured heterogeneity’ or ‘functional heterogeneity’. ‘Measured’ focuses on identification of scales of heterogeneity without considering generating mechanisms. ‘Functional heterogeneity’ is the variation over space in relation to structural heterogeneity in the environment (Pinel-Alloul 1995). It takes into account environmental variability and its effect on populations.

Horizontal variability in the surface layer is unlikely to be solely due to the effects of lateral turbulent diffusion in that layer and vertical variability plays an important role in both physical and biological heterogeneity (Steele et al. 1993). Horizontal heterogeneity of the surface cannot be separated fully from vertical heterogeneity and processes and some interest in patchiness and horizontal variability has in fact been derived from the study of enclosed water column ecosystems such as by Gamble et al. (1977).

1.5.1 Physical Sources of Heterogeneity

“the major determinants of spatial and temporal variation in biological populations and processes are usually considered to be imposed by corresponding patterns in the physical system, especially variations in temperature, salinity, light and nutrients.” Steele et al. (1993)

Heterogeneity in the marine environment may be created through physical processes which cause variability in temperature and salinity. This in turn influences nutrients and the ability of phytoplankton to grow. The effect of events is also variable - conditions which promote the growth of phytoplankton may also reduce it. It is the balance, extent, timing and time scale of physical conditions which ultimately leads to the resulting spatial environment. Physical forcing does not only affect large scale patterns, physical variability is also considered to be the dominant cause of horizontal variations on scales of less than 1 m (Steele et al. 1993).

Topography

The topography of a fjord has the potential to be a key factor in generating the hydrodynamic environment.

The sill increases the influence of air temperature on fjord water and the smaller the tidal range the greater this influence will be. Fjords typically have a greater temperature range than the coastal sea water, warmer in summer and colder in winter with the widest temperature range being found in the shallower, furthest inland part of the loch. Large amounts of freshwater runoff will override warming of the water and can lead to rapid cooling of the surface layer (Milne 1972).

In many fjords, such as Lochs Linnhe, Etive, Creran and Leven, there are one or more sills within the main loch system. This increases mixing of the near surface layers but may increase bottom water stagnation, nutrient depletion of surface layers and O₂ deficiency of deep water in internal basins. They can lead to the basins being largely independent of each other, particularly if the basin at the head of the loch is large - creating differences throughout the system. Conversely, if the mixing rates are high, small high energy basins may have no separate identity (Edwards and Sharples 1986).

Irregularities of the seabed may influence circulation within the fjord, leading to variability in the surface layer. These resulting surface irregularities may not be noticeable in water immediately adjacent to the seafloor features generating them. Such circulatory features have the potential to influence biological processes directly and indirectly. A sudden shallowing of the seafloor may generate turbulence and upwelling, bringing nutrient rich water up to the euphotic zone creating an area of increased phytoplankton density. Various factors combined determine the ability of such features to affect the surface layer. In deep water, there may not be sufficient energy to affect the entire water column, depending on the speed of the bottom currents but deep water renewal or spring tides may induce faster than usual currents in deep water.

Deep water renewal is essential to the ecology of fjords and the frequency with which they occur is fundamental to productivity, growth and survival of all fjordic populations. Advective mixing between the surface and intermediate layers is necessary to maintain productivity as diffusive mixing and sedimentation are

insufficient alone. Aeolian forces are also important as they promote deep water renewal and turbulent mixing.

Tidal flow may induce transient mixing plumes near coastal features such as promontories and spits, (Alldredge and Hamner 1980; St John and Pond 1992). St John and Pond (1992) found a mixing plume which commenced during ebb tides, increased nitrate concentrations from 0.20 to 2.80 $\mu\text{g atoms l}^{-1}$ and almost doubled phosphate concentrations. Entrainment of water by such events may produce a region of enhanced primary productivity.

Stratification

Islands in stratified regions may produce zones of intensified vertical mixing, generally tidally induced. This mixing increases the supply of nutrients to the euphotic zone (Simpson et al. 1982). Around the Scilly Isles in the Celtic Sea, Simpson et al. (1982) found that only in the immediate vicinity of the islands, was the maximum chlorophyll density at the surface. In the more stratified areas away from the islands, the chlorophyll maximum was at 12–18 m. They suggest that three layer circulation, as observed by Hachey (1934), is induced by the tidal stirring around an island, which causes nutrient rich water to be forced out along the pycnocline away from the island.

River Discharge

It was suggested by Solórzano and Grantham (1975), that the patchiness of chlorophyll in Lochs Creran and Etive reflects the relationship between saline fjord water and the less saline river discharge, as well as other factors affecting the surface circulation of the loch such as topographically induced turbulence.

Biotic Interactions

Physical events such as upwelling and deep water renewal, along with fronts and a stratified water column can all affect the position, heterogeneity, size and composition of the biological population. Gelatinous zooplankton are known to aggregate at fronts and Schneider and Bajdik (1992) found scyphomedusae - predominantly *Aurelia aurita* - to have aggregated in lines along convergent zones set up by Langmuir circulation. In fjords the effects of physical variability have the potential to be particularly strong as there is less continuity than in the open sea or even freshwater lochs. Unlike the oceans there are far more edge effects. A ‘typical’ fjord has a high aspect ratio - one of the qualifying criteria for inclusion in Edwards and Sharples (1986) was a sufficiently high aspect ratio. This potentially creates strong edge effects such as shore avoidance by zooplankton or enhanced phytoplankton productivity in shallower and warmer water around the shore. There is also a large amount of horizontal variation along the length of the

fjord. The freshwater input is localised causing brackish water at the head of the system to coastal/ocean water at the mouth; strong stratification in areas of high runoff to well mixed regions at the sills and more coastal areas. These factors are particularly important as non-polar fjords are in areas of high precipitation. The principal source of nutrient input may be from river discharge or in other regions, from the sea. There are sills and constricted channels which lead to deep water renewal, surface plumes and turbulent regions. The steep sides provide a channel for the wind either up or down the loch, increasing wind driven turbulence and preventing or increasing the flow of the surface layer.

1.5.2 Biological Processes

Biological processes are also important in creating variability and attempts have been made to study the pattern generating abilities of biological factors alone. The area chosen for FLEX (Fladen Experiment) was studied as it is relatively hydrodynamically uniform (Solow and Steele 1995). On a much smaller scale, enclosure experiments (Gamble et al. 1977; Andersen et al. 1987; Andersen and Nival 1989) consider an environment free from all but small scale horizontal movement. These have shown that horizontal dispersion and mixing are not essential for persistence - at least not over periods of less than 60 days (Steele 1978). Gamble et al. (1977) found that over the period of the experiment, the enclosures, which had started identically within sampling error, became qualitatively and quantitatively different - showing that predators can influence lower trophic levels.

In general, increasing life span and size indicates a movement up the trophic web and there is a corresponding increase in independence from water movement. Only phytoplankton can be considered to be largely passive in their behaviour. Zooplankton are able to migrate vertically, though horizontal movement is limited. Invertebrates and pelagic fish are able migrate vertically, horizontally and are more independent of turbulence and mixing processes, being able to swim against them or utilise them (Steele 1978).

The food chain creates inter-trophic interactions with influence moving both up and down the trophic web. Phytoplankton can influence the position and aggregation of herbivores such as copepods (Tiselius 1992) by their presence and low densities of phytoplankton will lead to vertical migration of zooplankton in a search for food. Predation by invertebrates and fish can also cause zooplankton to aggregate, while aggregation of zooplankton affects invertebrate and fish predation rates.

Patchiness of zooplankton affects their behaviour. Folt and Schulze (1993) found that as density increased, grazing of individuals decreased and hypothesised that this may be connected to predator avoidance, as some species of copepods are carnivorous and predation avoidance in copepods reduces grazing. A patchiness index rise from 1.1 to 8.8, led to a reduction by 83% in predation (Folt and

Schulze 1993). Aggregation in zooplankton has also been linked to reproduction, Colebrook (1960) found reproducing crustaceans were more likely to be found in patches, and invertebrate predation avoidance (Pinel-Alloul and Pont 1991). As large zooplankton are less heterogeneously distributed, the competition for food in dense patches may outweigh benefits of protection from predation, to which they are less at risk than small zooplankton.

Kolasa and Rollo (1991) hypothesised that patchiness in natural habitats is often nested and it has been suggested (Pinel-Alloul and Pont 1991; Haury et al. 1978) that zooplankton spatial heterogeneity, for marine and freshwater species, occurs on hierarchical spatial scales. The originating environmental forces (physical, chemical and biological) which determine the heterogeneity form a continuum of scales which are spatially and temporally coupled. The exception to this is diel vertical migration (Haury et al. 1978) which occurs on a variety of spatial scales. The importance of biotic processes in patch formation tends to increase inversely with the scale of the patch.

Variable sedimentation of phytoplankton from the surface layer may also be an important factor in generating horizontal inhomogeneity in biomass during the Spring bloom (Smetacek et al. 1978). Sedimentation is caused by a variety of factors - nutrients, coagulation due to turbulence, wind and tide.

1.5.3 External Controls

The wind potentially plays a large role in the surface heterogeneity of a fjordic system. Most work in this area has been done on the fjords of Norway and the Pacific Northwest, where many of the conditions are different from Scottish sea-lochs.

In Alberni Inlet, BC, Farmer and Osborn (1976) found that the surface layer during strong upinlet winds could thicken, in a few hours, to more than twice its original depth. The build up of water by ponding decreased along the length of the loch whereas with downinlet winds the surface layer was of even depth.

In Howe Sound, BC, Buckley and Pond (1976) studied the circulation of the surface layer using drogues tracked by radar. They found that of the tide, wind, freshwater runoff, entrainment and friction with the water below, the main determinant of the surface circulation was wind. River discharge caused horizontal shear which diminished rapidly away from the river mouth, but all other effects were negligible. The density of the surface layer was almost homogeneous and friction between the surface layer and deeper water almost negligible enabling the wind energy on the surface to spread throughout the surface layer.

All these studies were done on systems with a strong density structure and shallow surface layer. In Howe Sound the salinity of the surface at the sill was only 4 PSU compared to 29 PSU at 20 m indicating very low entrainment and turbulent exchange. The surface layers for Alberni Inlet and Jøsenfjord were estimated to

be 2/3 m. The sill of Howe Sound is 70 m deep and for Jøsenfjord 90 m so tidally induced mixing is unlikely to affect the surface layer. Also the maximum tidal range for Jøsenfjord is < 50 cm. The strong gradient between the surface layer and the deeper water leads to frictional coupling being negligible. The effect of the wind in systems with a more mixed water column is going to be less as there will be more entrainment and it will require more wind energy to force a deeper less ‘disconnected’ surface layer.

The wind is also able to influence the surface layer less directly. Cushman-Roisin et al. (1994) found in Posdangfjord, Norway that longitudinal winds were able to cause upwelling and downwelling within the fjord, creating a salinity gradient across the basin. The process, in sufficiently wide fjords, is identical to that of coastal upwelling. In coastal regions, longshore winds generate Ekman drift offshore, (with a mean direction of 90° to the wind, over the depth of the Ekman spiral.) If sufficiently strong and prolonged this will cause deeper, more saline, water to be upwelled along the coast. Seabed bathymetry can also affect upwelling - submarine ridges have been shown to produce favourable conditions for upwelling (Mann and Lazier 1991).

In broad fjords, where the width exceeds the baroclinic radius of deformation, corresponding to its stratification (R), the Coriolis effect generates upwelling and downwelling along each side and each side behaves as a separate coastal ocean.

$$R = \frac{\sqrt{\frac{g'H_1H_2}{H}}}{f} \quad (1.3)$$

where, f is the Coriolis parameter

$$f = 2\Omega \sin \phi \quad (1.4)$$

and g' , reduced gravity

$$g' = g \frac{(\rho_2 - \rho_1)}{\rho_2} \quad (1.5)$$

H = depth of the fjord, H_1 = depth of the surface layer, $H_2 = H - H_1$, ρ_1 = density of the surface layer, ρ_2 = density of the deeper water, Ω = angular velocity of the Earth about its axis and ϕ = latitude.

The wind blowing down the fjord, if strong enough will generate Ekman drift to the right (in the northern hemisphere,) perpendicular to the wind direction. As the surface layer flows across the basin, deeper water is upwelled along the left coast. This upwelling does not necessarily outcrop on the surface, but in a suitable fjord and with sufficiently strong winds, for a sufficient time period, outcropping of more saline and warmer water may occur. The narrower a fjord is the stronger the wind needs to be.

In narrower fjords the surface layer may be forced out of the basin generating

a pattern of higher salinity at the head than the mouth (Farmer and Freeland 1983).

1.5.4 Spatial Scales

Lower trophic levels, as they have shorter life spans and are less mobile, form patches on smaller scales (Steele 1978). Steele (1978) proposed that a few kilometres is the maximum scale at which phytoplankton can maintain patch structure in a horizontally turbulent environment, while zooplankton are able to aggregate in patches of tens of kilometres.

In marine systems, abiotic forces generate larger patches than biotic factors (Pinel-Alloul 1995). Large scale hydrodynamic processes generating ocean surface circulation have been found to be capable of forming patches of 10^4 km (McGowan 1971). In coastal regions upwelling and eddies can form patches of 10^2 kilometres. Biotic processes such as phytoplankton-herbivore interactions, aggregation and migration are only able to generate patches on scales of less than 10^4 m (Pinel-Alloul 1995) and even then, these processes can be overridden by microscale turbulence and larger hydrodynamic events.

Omori and Hamner (1982) suggest five time dependent attributes of aggregations: period length, frequency, wave form, threshold and amplitude; three spatial attributes: area, volume and shape in quantifying heterogeneity of populations. They also consider the orientation of animals within a patch and their density to be important in assessment of heterogeneity.

Patalas and Salki (1993) studied the heterogeneity of surface copepods in a variety of sizes of freshwater Canadian lakes. Their premise was, as vertical and horizontal mixing and advection of water by wind is related to the size of a lake, therefore the horizontal distribution of zooplankton may also be expected to be a function of lake size. They found that as the wind fetch of the lake increased, so did the tendency for deeper mixing, until it reached a plateau. A fetch of > 25 km was found to not increase the extent of vertical or horizontal mixing. The tendency to form isolated water masses does however increase. As lake size increases these physical regions were more strongly defined and less likely to be disturbed by wind mixing. Despite the increasing fetch and potential for mixing the resulting patch size remained constant. The overall effect of this is that there was less mixing in the small and large lakes, than in the mid-sized ones. Small lakes were more homogeneous but as size increases so does the tendency for the copepod density to be greatest in the shallower and warmer water inshore. Embayments, in particular, were found to increase heterogeneity. At all lake sizes, where total numbers of copepods appeared relatively homogeneous, individual species were less so.

1.5.5 Temporal Continuity

Temporal continuity in marine environments can create problems in the collection, analysis and understanding of processes. An apparent spatial difference may be entirely due to temporal variation in productivity or grazing. Cycles may commence at different times at different locations. The different starting times may be due to a physical factor which could be transient or permanent, or the current growth rate may be different due to different physical conditions. When monitoring a single site, changes in density may not be due to an evolution of processes, but with the advection of water masses, or the voluntary movement of organisms.

Also of interest is the stability of patches. This may vary between species and conditions. Herbivores are known to aggregate during the day, presumably as a defence against predation, dispersing at night to feed. In a freshwater lake, Tessier (1983), found *Holopedium gibberum* (a cladoceran) formed a single cohesive patch of tens of metres, which remained intact over the summer. This was despite diurnal vertical migration and with no relationship to wind speed or direction. Over the same period, *Daphnia catawba* was far less aggregated despite the biomass exceeding that of the cladoceran for much of the time.

1.6 Understanding Heterogeneity

1.6.1 Data Collection

When sampling any ecosystem the various time scales of the different components must be taken into account. The time scale of processes, compared to the sampling time, is also of importance. In the marine environment a further problem is created as dispersion and water movement mean that a proper time series is virtually impossible to obtain. Measurements at a single site are affected by processes and populations passing by, and sampling along a transect may involve populations passing along or through it. In particular, instantaneous horizontal measurements are limited to satellite images which are limited in the depth information can be obtained from, they are also affected by cloud cover and require validation. Henderson and Steele (1993) considered satellite data to be inappropriate for scales of less than 30km, without supplementary *in situ* data.

Species further up the trophic web become more difficult to sample as they are more mobile; copepods vertically migrate diurnally, medusae migrate horizontally and vertically according to circulatory patterns (Schneider and Bajdik 1992) and the sun's position (Hamner et al. 1994) as well as in search for food.

Sampling a heterogeneous population can produce uncharacteristic results, generating a mean value significantly greater or less than the true value. Classical sampling design and analysis assumes an independent selection of samples but

in a patchy environment the population density is spatially correlated. Spatial autocorrelation should, whenever possible, be taken into account when sampling heterogeneous populations. If the spatial structure is known, then optimisation may be carried out, allocating sampling by stratifying the samples to minimise the variance of the estimate and structure dependent bias. This, however, is only possible with a known and stable structure, marine environments tend to be more mobile and prior structure unlikely to be known. When the structure is of interest, the time scales of sampling frequency is more important. The heterogeneity of species may also vary according to the time of day or seasonally (Omori and Hamner 1982) with some species aggregating during the day to avoid predation and becoming less heterogeneous overnight when feeding, as predation is less of a threat then. This may produce a relatively stable biomass with large seasonal or hourly changes in density. Medusae such as *Mastigias sp.* may be simultaneously random and aggregated (Omori and Hamner 1982) and within the aggregation, denser regions may be formed by the medusae stacking closely.

Conventional zooplankton sampling, horizontally and vertically integrating, is time and labour intensive and limited in resolving fine and large scale patches. Pinel-Alloul (1995) described three new technologies which have been introduced in the past two decades: acoustic, optical plankton counter (OPC) and video systems. Acoustic systems were originally able to map abundance, aggregation and spatial distribution. More recent developments, using multiple frequencies, have enabled them to detect different sized organisms and their abundance. The OPC permits large scale continuous sampling of zooplankton size and distribution and coupled with a fluorometer and CTD the possible biotic and abiotic processes generating the patches may also be monitored. Video systems can be used to detect abundances and monitor behaviour. The OPC is more suitable for smaller (< 4 mm) zooplankton which the other systems are unable to detect. Of the three methods, taxonomic information can only be obtained from video but visibility is often a problem.

1.7 Modelling fjords

The early recognition of fjord circulation meant that fjord modelling initially concentrated on estuarine circulation.

1.7.1 Estuarine Circulation

Circulation within a fjord is the result of the mixing between river discharge and coastal water. Circulatory models represent river input, mixing within the fjord, flow of surface water out of the system and compensatory inflow of coastal water. Intermediate water exchange is not considered, nor is the Coriolis effect (fjords are in general considered sufficiently narrow for it to be negligible) and a tidal average used. The modelling depends on the representation of turbidity and the

outer boundary of the coastal sea or an outer basin. Two principal types of model exist: layered models in which there is a clearly defined pycnocline over which mixing occurs rapidly and those with a continuous density distribution. The former are simpler and more commonly used. Layered models consist of vertically homogeneous layers and a sharp pycnocline. Though a pycnocline may consist of a steadily varying density over several metres, the assumption of a sharp density gradient is applicable to many fjords and with mixing occurring primarily within rather than between layers, individual layers may be relatively homogeneous. The lower layer of a two layer model is deep and varies little, with velocity and the horizontal gradient being considered negligible, the resulting problem is that of entrainment into the surface layer (Farmer and Freeland 1983).

Stommel (1951) developed a two layer model representing fjord estuarine circulation with Stommel and Farmer (1952) including changes in width along the fjord. Further knowledge of exchange mechanisms enabled Long (1975) to extend the model of Stommel and Farmer (1952) to include more detailed entrainment, where the thickness of the brackish layer is determined by the interfacial Froude number, the drag ratio and the interfacial density difference. For a fjord of constant width, the solution can be analytically obtained, but varying width requires a numerical solution. The solution of the original dynamic circulation model and its subsequent developments is dependent on the boundary condition at the fjord mouth (Gade and Edwards 1980; Farmer and Freeland 1983) which controls the surface layer properties. Conditions at the mouth of a fjord are, however, difficult to measure and identify. Such models are more applicable to deep fjords with low levels of tidal forcing (Farmer and Freeland 1983).

Hodgins (1979) considered unsteady fjord circulation, with tide, river discharge and wind inputs, along with baroclinic and topographical effects in a model of Albern Inlet. The finite difference model enabled the time steps to be independent of the spatial grid. Stigebrandt (1981) considered that two layer flow, while correct for very wide, in comparison with the mouth, and possibly in narrow well stratified fjords, was not applicable for all fjords as recirculation of the surface layer occurs. Stigebrandt (1981) developed a model of recirculation of the surface layer, otherwise the deep water entrained to the surface immediately flows out, with the salinity further into the fjord being unaffected.

1.7.2 Exchange

Exchange between a fjord and the coastal sea (or outer fjord basins) is a defining characteristic of a fjord and an important influence on productivity.

Deep Water Renewal

The timing between renewal events partly depends on the level of mixing within the basin. The density of deep water gradually decreases due to it interacting

with the lower density water above through mixing processes generated by tides, surface wind stress, thermohaline convection etc. The other salient feature being the presence of sufficiently dense water. The modelling of these features has involved simple techniques, Welander (1974) used a one-dimensional deterministic exchange model and Gade (1973) a stochastic model with the external density condition varying.

As shown in **1.2.5** mixing at the sill is important in determining whether renewal will take place - whether mixing is insufficient to inhibit baroclinic flow. Gade and Edwards (1980) suggested that the relative depth of the sill and pycnocline may partly control the time of renewal: sills shallower than the deepest pycnocline being more likely to renew in winter, with deeper silled fjords renewing in summer.

In a hydraulic model of deep water renewal in Indian Arm, de Young and Pond (1988) predict deep water renewal at neap tides as the surface layer is dynamically weak and baroclinic flow is prevented by mixing at spring tides. This enables the density to reach its maximum at neap tides and renewal to occur then.

Lavelle et al. (1991) describes a laterally averaged hydrodynamic model of intrusions into Puget Sound, a shallow silled fjord. Their aim was to investigate deep water renewal and the resulting circulation. They developed a 2 dimensional, time dependent (daily simulation), vertical model with baroclinic intrusion. The model includes river discharge, tidal currents and wind forcing. Increases in the salinity gradient, such as by wind forcing, increase renewal. With extreme river discharge however, increased mixing suppresses baroclinic flow.

In a 3-dimensional baroclinic numerical model of the Central Strait of Georgia described by Marinone and Pond (1996), deep water renewal is predicted at neap tides. The renewal occurs over a sill at which only at extreme neap tides did LeBlond et al. (1991) find two-layer flow occurred, allowing water to flow into the basin.

Tides

Barotropic tide can be an important source of energy within a fjord and may even drive the surface circulation. An important consideration in modelling tidal processes is the loss of tidal energy through friction and topographic features. The principal loss of energy is through internal wave drag at a sill (Farmer and Freeland 1983).

Linear barotropic response in fjords is simple, and ignoring the Coriolis effect the tide may be treated as a plane wave (Farmer and Freeland 1983). Numerical models are required for width and depth changing rapidly and changes in the direction of the channel (Jamart and Winter 1978). Jamart and Winter (1980) further developed a 2-dimensional finite element modal analysis model of barotropic flow.

Linear barotropic models do not include the internal response over the sill. Non-

linearity will be more important in fjords with shallow sills and large tidal ranges, ie. where the tidal response is more important, linear models are less useful. Modelling of the non-linear response of tidal flow through narrows has been considered as purely frictional by Glenne and Simensen (1963) or frictionless by McClimans (1978). Stigebrandt (1980) considered both frictional and gradient effects.

Internal tides in fjords may be generated along slopes such as towards the head of a basin or at the sill. Both situations have been modelled. The first has been considered by Rattray (1960) and Stigebrandt (1980) modelled the generation of internal tides at a sill.

Coastal Processes

Exchange is often linked with coastal shelf processes. Klinck et al. (1981) developed a linear, 2 layer, numerical model of a fjord driven by the continental shelf environment, which is driven by wind forcing. As the model is linear, the sill appears to be unimportant but with a non-linear model, the importance of the sill would be expected to increase. The model also does not include river discharge and there is no mixing, therefore it is more applicable to fjords with a deep sill and low river input. Edwards et al. (1996) developed a simple, hydrostatic equilibrium, 2 layer model of wind driven flow to study the effect of coastal winds on upwelling and downwelling. Any model considering the coastal sea has the additional complication of the Coriolis effect being more important, as is the fjord mouth boundary condition (Farmer and Freeland 1983).

1.7.3 Mixing

In the previous two sections, mixing within a fjord is an inherent problem as it includes entrainment and the effects of mixing on baroclinic renewal. The main sources of mixing are wind and tides.

Wind

Wind often flows along the the length of a fjord, being funneled by the steep sides. Onshore breezes are also often common, with the strength of onshore breezes often being greater than of land-sea flow even during the night (Syvitski et al. 1987). The narrowness of fjords means that most modelling does not take account of the Coriolis effect. Ponding has been modelled by Farmer and Osborn (1976), Svendsen and Thompson (1978) and Hodgins (1979). Cushman-Roisin et al. (1994) considered the Coriolis effect to be of importance in fjords and modelled the effect of axial winds in different widths and depths of a two layer fjord. They found conditions underwhich coastal upwelling could occur and could outcrop in fjords, which is determined by its width, stratification and the wind

impulse. Considering interfacial shear stress, Buch (1981) analytically modelled the impact of wind stress on mixing across the pycnocline.

Tides and Sills

Cushman-Roisin et al. (1989) modelled the spatial distribution of internal waves in a stratified fluid, without time periodicity. The two dimensional finite difference representation was further developed by Tverberg et al. (1991) and applied to a Norwegian fjord.

Griffin and LeBlond (1990) examined the impact of the lunar tidal cycle and wind forcing on mixing in the Strait of Juan de Fuca. A representation of the balance between buoyancy input and mixing was constructed by using an estimate of the interfacial Froude number of the tide ebbing through Boundary Pass. Hibiya and LeBlond (1993) then developed a model of the effect of the lunar tidal cycle on mixing within a fjord. Flow was modelled as a two dimensional vertical plane, with mixing varying in a fortnightly cycle. The model does not consider the Coriolis effect or the semi-diurnal tidal cycle. Localised mixing generates internal waves, propagating landward and seaward. During spring tides, a considerable fraction of the inflowing deep water is upwelled to the surface, in the mixing region, and flows seaward. Only during weak tidal currents is deep water able to flow landward. LeBlond et al. (1994) developed a predictive two-layer box model of the Juan de Fuca Strait which includes river discharge, tidal mixing and wind forcing. The model concentrated on mixing and entrainment at the two sills encountered by outflow into the Strait. Parameters were fitted to six years of data and surface salinity predicted for the subsequent twelve.

Simpson and Rippeth (1993) initially developed a box model of the Clyde Sea with turbulent mixing caused by wind and the barotropic tide. This overestimated the strength of stratification, with renewal and internal tides being found necessary to replicate the degree of mixing found. Internal tides were particularly important and found to be the dominant form of mixing in the summer.

1.8 Thesis Outline

In this chapter fjords have been shown to be complex marine environments in which interaction between meteorological conditions, the lunar tidal cycle and the topography, plays a significant role in determining the individual fjord environment. It has also been shown that the complexity of these relationships means that the response to external conditions of a individual fjord cannot necessarily be predicted. The degree of mixing is a potentially important feature and is controlled by many factors including sill depth, tidal range and stratification.

The aim of this thesis is to develop an understanding of the effects of meteorological and tidal forcing on Loch Linnhe, a Scottish sea-loch. The response of

the sea-loch to conditions is also compared with other fjords - within Scotland and globally - and the key features of Loch Linnhe identified. Scottish sea-lochs are different to most of the fjords generally studied. They are smaller than most Norwegian and North American fjords - in depth, volume and surface area, with other differences including the seasonal pattern of river discharge, depth of sill and tidal range. The influence of the physical regime in Loch Linnhe on primary and secondary productivity is also examined. Fjord research has tended to concentrate on the hydrodynamics or the biology without the interaction of the physical regime on productivity considered. The main exception to this is in frontal zones. There is potential for hydrodynamics to control the biological behaviour within fjords but with the variety of physical regimes, this will be variable in its extent and nature. By developing an understanding of how the physical conditions in Loch Linnhe affect productivity, it is possible to further consider the differences between it and other basins and speculate as to the biological role of the dynamics in other sea-lochs.

In the following chapter I shall introduce a complex spatial dataset collected in Loch Linnhe in 1991. The data was primarily collected in order to derive a nutrient budget but the spatial nature of it provides an opportunity to look at the hydrodynamic processes within Loch Linnhe. The extent of the dataset available allows a more thorough evaluation of the influence of meteorological events and the tidal cycle than possible in many other systems. Generally one physical feature has been concentrated on in the collection of data in fjords. Part 2 encompasses analysis of the data, including the spatial structure of the surface layer and its relationship with meteorological and tidal forcing. The temporal resolution of the data unfortunately limits understanding of the effect of the physical regime on productivity. While hypotheses can be made, the data with which to test them is limited. In Part 3, an existing ecosystem box model is applied to the Loch Linnhe data and modifications carried out. In particular the influence of the vertical and horizontal features identified in Part 2 is further examined. This has enabled the testing of hypotheses of how the basin behaves and furthered understanding of the physical regime and its effect on the biology in Loch Linnhe.

Chapter 2

Loch Linnhe

2.1 Introduction

Throughout 1991, the Scottish Office Agriculture and Fisheries Department - SOAFD - Marine Laboratory of Aberdeen conducted a programme of pelagic ecosystem monitoring in Loch Linnhe. The primary aim of the experimental programme was to evaluate nutrient and carbon budgets, with Dr. M. Heath as the lead scientist.

The project collected a unique dataset for a Scottish sea-loch. An extensive part of the monitoring was on the horizontal variability of physical conditions, nutrients and primary and secondary producers. The dataset provides an opportunity for the relationships between physical, chemical and biological variables in fjords to be explored, hopefully leading to a greater understanding of these processes both in fjords and other marine environments. It also provides an opportunity to study the spatial variation along the length of the sea-loch from river mouth to coastal sea. The resolution of horizontal scales was as low as 144 m, with 0.2 m being the vertical minimum. Surveys were carried out monthly, with replicate horizontal surveys in April, July and October. Three fixed moorings were also deployed throughout the year.

2.2 Loch Linnhe

Loch Linnhe is the principal section of the largest sea-loch system on the west coast of Scotland. The system also includes Lochs Eil, Leven, Creran, Etive, and O'Choire. Loch Linnhe itself consists of an Inner Basin (IB) and Outer Basin (OB) - which includes the Lynn of Morvern - and the Lynn of Lorne.

Loch Eil flows into Loch Linnhe at the head of the IB across a very shallow, 8 m sill. The IB and OB are separated at Corran Narrows by a shallow sill, with a maximum depth of 18 m, mean depth 9 m and width of 290 m at HW and 270 m

at LW (Edwards and Sharples 1986). The maximum current speed across the sill is 4.9 knots and the mean spring tidal range is 3.7 m (Hydrographic Department 1977a). The Lynn of Lorne is separated from the OB by a shallow sill at Appin and the limestone island of Lismore, with the southern end connected to the Firth of Lorne. There is no sill between the Lynn of Morvern and the Sound of Mull but there is one between the southern end of Lismore and Mull with a depth of approximately 25 m. Either side of this, the seabed drops to 200 m and overfalls and tide rips have been noted in this area (Connor 1990). Loch Leven flows into the northern end of the OB and Loch Creran and Etive are on the east side of the Lynn of Lorne which is considerably shallower than other areas of the Loch Linnhe system. Narrow, shallow channels link Creran and Etive to the Lynn of Lorne.

The IB is 15 km long and 1 km wide. From Corran to Mull, the distance is 45 km and the width of the OB approximately 6 km. The OB alone is longer and wider than most Scottish sea-lochs. Along the length of Loch Linnhe, from the head of the IB to the Firth of Lorne the water changes from being brackish river water to a coastal sea with strong currents. This change in habitat means that along its length, from Loch Eil through Loch Linnhe to the Firth of Lorne, there is an increase in species diversity as the environment changes (Connor 1990). Over the

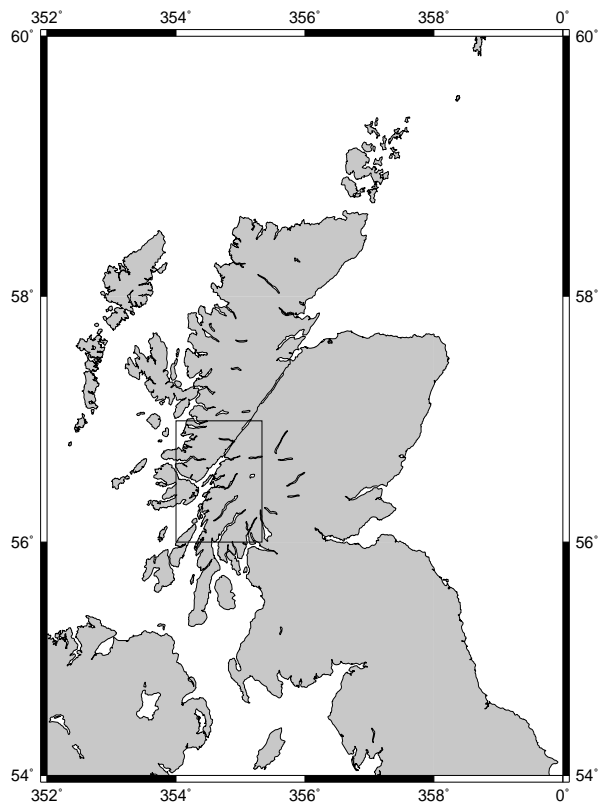


Figure 2.1: Scotland with fig. 2.2 (the Loch Linnhe system) inset.

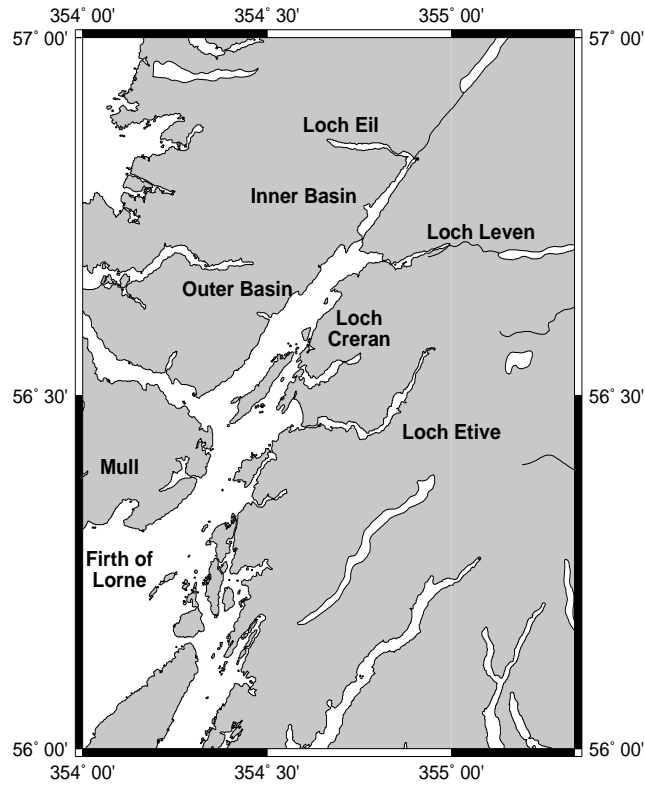


Figure 2.2: Loch Linnhe sea-loch system

Loch Linnhe system there is a wide variety of habitats - brackish water to coastal sea, weak to strong wave action, tidal streams, sheltered or exposed to wind.

The principal source of freshwater input is from the Rivers Lochy and Nevis which flow into the head of the inner basin. The coastal sea at the mouth of Loch Linnhe is the Firth of Lorne which consists of 75% Irish Sea/Clyde water and 25% Atlantic water (MacKay 1986). The quantity of river discharge from the Loch Linnhe system, means that the surface of the Firth of Lorne is less saline than the rest of the Inner Hebridean water (Ellett and Edwards 1983). The low density surface water in this region has also been found to flow to the north (Ellett and Edwards 1983).

The IB is a typical deep U shaped fjord with steeply sloping sides and a maximum depth of 152 m. The OB is much wider, with more embayments and though mostly deeper than 50 m is in general shallower than the IB. The southern part of the Lynn of Morvern is deeper, reaching depths of more than 200 m and there is in general a shallowing towards the north.

The position of Mull at the mouth, means that the loch is protected from the wave action of the Atlantic, however the axis of Loch Linnhe lies along the direction of the prevailing wind. With the steeply sloping fjord sides, the winds are channeled

upinlet increasing wave action and wind driven mixing. In comparison, the lochs flowing into Loch Linnhe are all sheltered from most of the wind and wave action.

Table 2.1: Catchment area, volume, depth and surface area data for the Loch Linnhe system. Sources are A: Highland River Purification Board, B: Edwards and Sharples (1986) and C: Dr. M. Heath.

		source
Catchment area of the River Lochy and Nevis	1328.8 km ²	A
Catchment area of Loch Eil and the Inner Basin	1820 km ²	C
Catchment area of Loch Leven and the OB	609.5 km ²	C
Catchment area of Loch Leven	338 km ²	B
Surface Area Inner Basin	18.642x10 ⁶ m ²	C
Surface Area Outer Basin	156.098x10 ⁶ m ²	C
Median Depth Inner Basin	37.95982 m	C
Median Depth Outer Basin	33.41803 m	C
Mean Depth Inner Basin	59.58534 m	C
Mean Depth Outer Basin	52.15954 m	C
Volume Inner Basin	1110.79x10 ⁶ m ³	C
Volume Outer Basin	8142x10 ⁶ m ³	C
Volume Loch Eil and Inner Basin	1345x10 ⁶ m ³	C
Volume Loch Leven and Outer Basin	8268.7x10 ⁶ m ³	B & C

In common with many other fjords (Syvitski et al. 1987) Loch Linnhe is associated with a geological fault. This makes it straight, whereas other long Scottish sea-lochs typically change direction along their length. It lies along the southern end of the Great Glen faultline which starts at Inverness and consists of a chain of lochs - Loch Ness, Loch Oich and Loch Lochy joined by the Caledonian Canal. The surrounding region is mountainous, including the highest peak in the British Isles, Ben Nevis, and lowly populated. The population is centred around Fort William at the head of IB and Oban on the Firth of Lorne. Most of the population is on the east coast and despite the low population there is more coastal development than around most Scottish sea-lochs. There is very little agricultural land use, with forestry and hill farming dominant. The water flowing into the head of the IB is controlled by the aluminium smelter in Fort William, as is that into Loch Leven by the Kinlochleven smelter. In 1991, use by fishfarms was low.

2.3 Loch Linnhe Dataset

2.3.1 Vertically resolved data

Axial cruises were made to assess the vertical inhomogeneities. They involved a sampling vehicle being towed in a cyclic zigzag path, along the axis of the loch, from the surface to within 10m of the seabed. Measurements were made of physical quantities (pressure, sounding, salinity, temperature, light intensity and transmissivity), nutrient concentrations (nitrate, ammonium and oxygen) and biological quantities (chlorophyll fluorescence and zooplankton particle counts.)

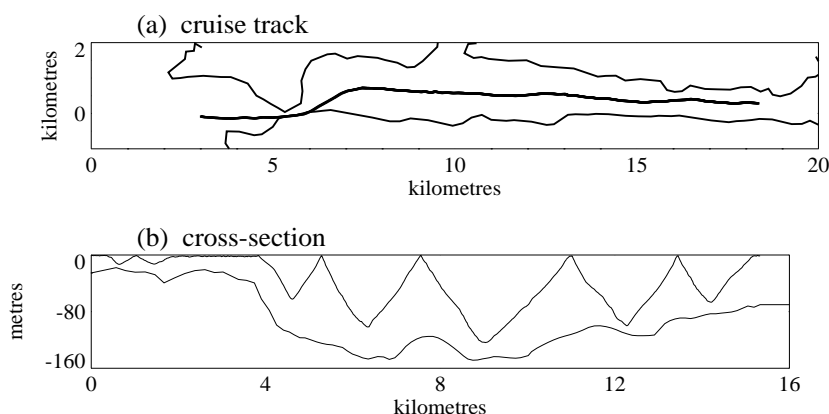


Figure 2.3: Typical axial cruise of the Inner Basin (13 July) with (a) showing the axial track and (b) indicating the surface to seabed oscillations. The coastlines used in the following plots of Loch Linnhe are based on digitised coastline data courtesy of M. Heath and in the axial plots the loch bathymetry was determined from the sounding data from the axial cruises.

The undulating sampler ascended/descended at a rate of 0.2ms^{-1} with data collected every 5 seconds. An additional dataset of salinity and temperature was collected every second, the equivalent of every 0.2 metre. Zooplankton counts were integrated over 1 minute intervals and nitrate and ammonium over 2 minute intervals. Most quantities are of a resolution of 1 metre with zooplankton at 12 metres and nitrate and ammonium at 24 m intervals. Every second zooplankton sample was frozen for species identification, the rest being used to give dry weights. The ship's position was determined by GPS.

Three sets of instrumentation were deployed throughout the year and indicated in fig. 2.4. The most northerly was in the inner basin close to Corran Narrows, another in the northern end of the outer basin and the third in the Lynn of Morvern close to Lismore. The IB and LoM moorings included a thermistor chain buoyed from the surface with measurements at 2, 4, 6, 10, 15, 20, 25, 30, 40, 50 and 60 metres. At all moorings, other instrumentation was fixed to the bottom. All moorings also had current meters at a variety of depths. On each monthly cruise, readings were collected from the fixed moorings and further

highly resolved measurements (less than 1m) were made of the vertical distributions of salinity, temperature, chlorophyll, transmissivity, dissolved oxygen and light intensity, with less detailed information on nutrients. Additionally, vertical distribution samples were carried out at a site in the Firth of Lorne.

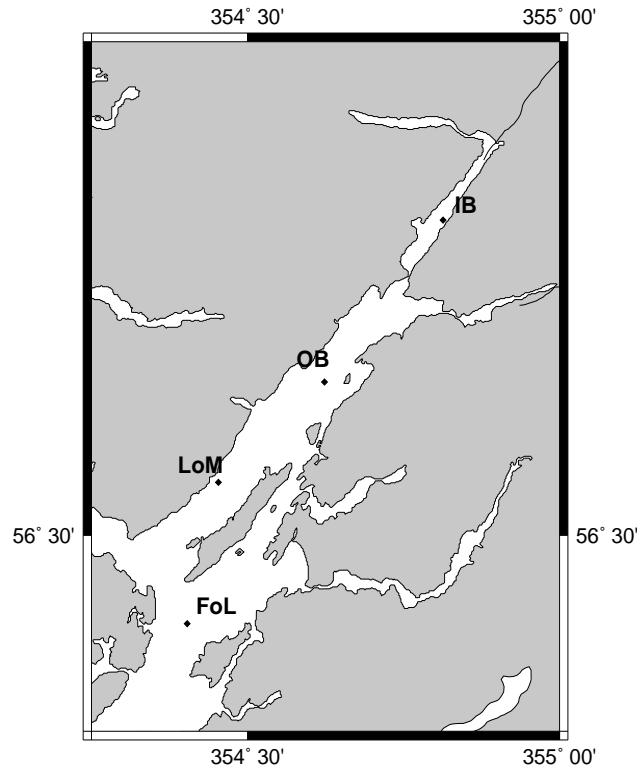


Figure 2.4: Loch Linnhe sample sites, indicated by IB - inner basin, OB - outer basin, LoM - Lynn of Morvern and FoL - Firth of Lorne. There were also fixed moorings at the IB, OB and LoM and thermistor chains at the IB and LoM.

2.3.2 Surface Layer Dataset

During each monthly survey (except December) the survey vessel followed a zigzag course from shore to shore, from the head of Loch Linnhe to the Firth of Lorne, south of Kerrera. Along side it, a tow fish flew approximately 4 metres below the surface. The instrumentation measured physical parameters (temperature, salinity and turbidity), chlorophyll fluorescence and size resolved particle counts. Sea water was also collected from an intake on the tow fish and pumped back to the ship to be fed into a continuous flow analyser measuring nitrate concentration. A series of additional nutrient (including silicate, phosphate, ammonium and DON) tests were also made. During January and August no chlorophyll samples

or transmissivity measurements were taken. On 25 April and 14 August, the OB cruises included the Lynn of Lorne.

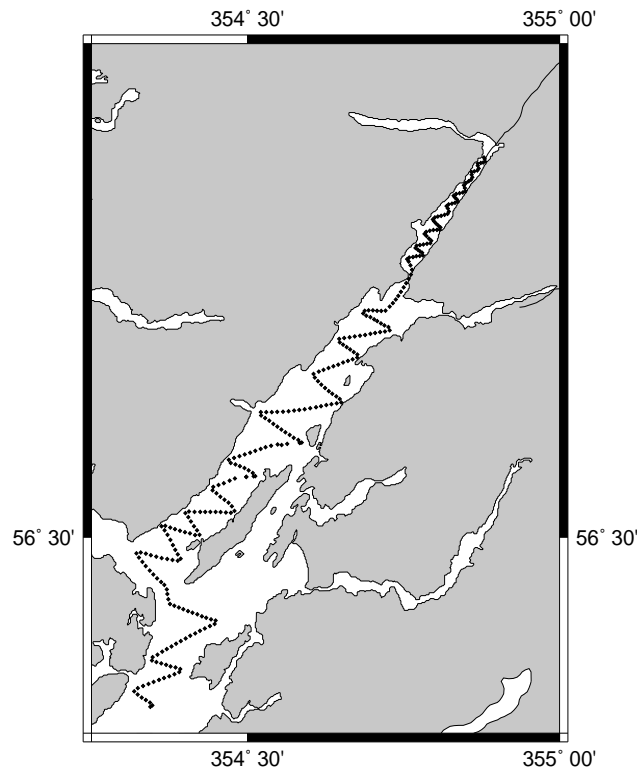


Figure 2.5: Typical Surface Cruise Track - 9 October 1991. On this day the cruise was from north to south but south to north cruises were also carried out.

The physical parameters and chlorophyll were measured approximately every minute and the zooplankton were integrated over 4 minute intervals. Nitrate analysis was digitised every minute and time shifted to allow for the time delay in the analysis and pumping, while the ancillary nutrient measurements were made every 20 minutes. Within the confines of the IB the ship's speed was 2.4 ms^{-1} , while in the OB and Firth of Lorne it increased to 4 ms^{-1} . For the IB the physical parameters, nitrate and chlorophyll readings were spaced approximately 144 m apart along the zigzagging cruise track, with the zooplankton counts 576 m apart and the additional nutrient data at a resolution of around 2880 metres. Elsewhere the respective distances were 240 m, 960 m and 4800 m, with the total cruise track length being approximately 120 km.

2.3.3 Table of Data - including axial, surface and sample site data

The following table describes the full set of axial, surface and sample site data collected in 1991. The reference to each set of data consists of two capital letters denoting the type of data (A - axial, S - surface, P - sample) and the area it was collected in (I - inner basin, O - outer basin, F - Firth of Lorne, in the outer basin O denotes the northern site and L that in the Lynn of Morvern.) Surface cruises covered all areas on the same day and are represented in the table by S*, where the * may be replaced by I, O or F. The only exception to this was 10 October when the Firth of Lorne was not covered in the cruise.

The subscripts indicate the month and where multiple samples were made the number of the data collection within that month. Months are indicated as follows: j - January, f - February, m - March, a - April, my - May, jn - June, jl - July, ag - August, s - September, o - October, n - November, d - December. The third outer basin axial cruise in August is thus denoted by AO_{ag3}.

The sample site data consists of two data sets of differing resolution. These are indicated in the table by superscripts with *s* and *c* representing high and low resolution respectively.

2.3.4 Instrumentation

ARIES: an Autosampling and Recording Instrumental Environmental Sampler was developed by scientists at the SOAFD Marine Laboratory in Aberdeen and was used during the Loch Linnhe project in the collection of the surface and axial cruise data. *ARIES* incorporates a water sampling unit, plankton sampling unit and oceanographic sensor unit and enables high resolution concurrent sampling throughout the water column from a moving ship. In understanding and modelling relationships between physical, chemical and biological variables the simultaneous collection of data is advantageous, as is collection at the same frequency. This is particularly important at fronts and regions of high mixing where the environment is heterogeneous and unstable. From the description of scales of data collection in 2.3.1 & 2.3.2 it can be seen that physical variables can be measured at a finer resolution than measurements from water bottle sampling. A full description of *ARIES* may be found in Dunn, Hall, Heath, Mitchell and Ritchie (1993).

2.3.5 Jellyfish

Large species of gelatinous zooplankton were collected vertically in nets from the surface to within 10m of the seabed, with the predominant species being *Aurelia aurita*. The diameter was measured and converted to volume by assuming the volume of a jellyfish to be equivalent to that of half a hemisphere.

Table 2.2: The data collected in the Loch Linnhe program from January to June 1991.

date		axial		surface	sample			
		IB	OB		IB	OB	LoM	FoL
Jan	19		AO _{j1}					
	20		AO _{j2}			PO _{j^{sc}}		
	21							PF _{j^s}
	22						PL _{j^{sc}}	
	23			S* _j	PI _{j^{sc}}			
	14		AO _{j3}					
Feb	23						PL _{f1^{sc}}	
	24	AI _f	AO _{f1}					
	25							PF _{f^s}
	26		AO _{f2}				PL _{f2^{sc}}	
	27			S* _f	PI _{f^{sc}}			
	28					PO _{f^s}		
Mar	22				PI _{m1^{sc}}			
	23					PO _{m1^s}	PL _{m1^{sc}}	
	24		AO _{m1}				PL _{m2^s}	
	25	AI _m	AO _{m2}		PI _{m2^{sc}}			
	26			S* _m				PF _{m^s}
	27		AO _{m3}			PO _{m2^c}		
April	20	AI _a	AO _{a1}		PI _{a1^s}		PL _{a1^{sc}}	
	21					PO _{a1^s}		
	22		AO _{a2}			PO _{a2^{sc}}		
	23			S* _{a1}				PF _{a^s}
	24				PI _{a2^{sc}}		PL _{a2^s}	
	25			S* _{a2}				
May	17				PI _{my1^s}		PL _{my1^{sc}}	
	18	AI _{my}	AO _{my1}		PI _{my2^c}			
	19		AO _{my2}				PL _{my2^{sc}}	
	20		AO _{my3}			PO _{my^{sc}}		
	21			S* _{my}				PF _{my^s}
	22				PI _{my3^{sc}}		PL _{my3^{sc}}	
	23						PL _{my4^{sc}}	
June	14				PI _{jn1^s}		PL _{jn1^s}	
	15	AI _{jn1}	AO _{jn1}		PI _{jn2^{sc}}			
	16		AO _{jn2}				PL _{jn2^{sc}}	
	17		AO _{jn3}			PO _{jn^{sc}}		
	18			S* _{jn}				PF _{jn^s}
	19				PI _{jn3^{sc}}			
	20	AI _{jn2}						

Table 2.3: The data collected in the Loch Linnhe program from July to December, 1991.

date		axial		surface	sample			
		IB	OB		IB	OB	LoM	FoL
July	12				PI_{jl1}^{sc}		PL_{jl1}^{sc}	
	13	AI_{jl}	AO_{jl1}					
	14		AO_{jl2}				PL_{jl2}^{sc}	
	15		AO_{jl3}			PO_{jl}^{sc}	PL_{jl3}^s	
	16			S^*_{jl1}	PI_{jl2}^c			PF_{jl}^s
	17				PI_{jl3}^{sc}			
	18			S^*_{jl2}				
Aug	9				PI_{ag1}^{sc}		PL_{ag1}^{sc}	
	10	AI_{ag1}			PI_{ag2}^s			
	11		AO_{ag1}			PO_{ag1}^s	PL_{ag2}^{sc}	
	12		AO_{ag2}			PO_{ag2}^{sc}		
	13							PF_{ag}^s
	14			S^*_{ag}				
	15	AI_{ag2}			PI_{ag3}^{sc}			
Sept	6					PO_{s1}^{sc}	PL_{s1}^s	
	7	AI_{s1}	AO_{s1}		PI_{s1}^{sc}			
	8		AO_{s2}			PO_{s2}^{sc}	PL_{s2}^{sc}	
	9		AO_{s3}					PF_s^s
	10					PL_{s3}^{sc}		
	11			S^*_s	PI_{s2}^{sc}		PL_{s4}^{sc}	
	12						PL_{s5}^{sc}	
Oct	4						PL_{o1}^{sc}	
	5		AO_{o1}		PI_{o1}^{sc}			
	6		AO_{o2}			PO_{o1}^{sc}	PL_{o2}^{sc}	
	7					PO_{o2}^{sc}		
	8							PF_o^s
	9			S^*_{o1}	PI_{o2}^{sc}			
	10			S^*_{o2}				
Nov	8						PL_{n1}^{sc}	
	9				PI_{n1}^{sc}	PO_{n1}^{sc}		
	10	AI_n			PI_{n2}^{sc}			
	11		AO_{n1}					
	12							
	13		AO_{n2}				PL_{n2}^{sc}	
	14				S^*_n		PL_{n3}^{sc}	
Dec	14				PI_d^{sc}			
	15		AO_{d1}			PO_d^{sc}	PL_{d1}^s	
	16		AO_{d2}				PL_{d2}^{sc}	

2.4 Hydrodynamic Parameters

Information on hydrodynamic parameters for the inner basin was obtained from Edwards and Sharples (1986), with additional information on tidal ranges, current speeds and topography from Admiralty charts (Hydrographic Department 1977a; Hydrographic Department 1977b).

Moving up the west coast of Scotland towards Skye, the tidal range and spring-neap variation increase, diminishing once more after Skye (Ellett and Edwards 1983). Within the Loch Linnhe system, the tidal range increases inland with the maxima at Corran, where 3.7m and 1.4m are the spring and neap ranges respectively, before decreasing by Corpach at the head of the IB (Hydrographic Department 1977a).

Current speeds are affected greatly by the shallow sills. To the north-west of the Lismore-Mull sill, flooding spring tides reach 3.0ms^{-1} (Hydrographic Department 1977b) while the equivalent measurement at Corran is 4.9ms^{-1} (Hydrographic Department 1977a). For ebb tides the equivalent values are 1.8ms^{-1} and 3.6ms^{-1} (Hydrographic Department 1977a; Hydrographic Department 1977b).

2.4.1 Flushing Rate: Inner Basin

A simple approximation of the time for the volume of tidal inflow to equal the volume of the loch basin may be calculated as follows;

$$\frac{\text{volume of system}}{\text{volume of water entering system}} = \text{tidal cycles}$$

Average tidal range at Corran	2.65m
Surface Area of IB and Loch Eil	$34.1 \times 10^6 \text{m}^2$
Volume of IB and Loch Eil	$1345 \times 10^6 \text{m}^3$
Volume of water for average tidal range	$2.65 \times 34.1 \times 10^6 = 9.04 \times 10^7 \text{m}^3$

$$\frac{1345 \times 10^6}{9.04 \times 10^7} = 15 \text{ tidal cycles}$$

With the large tidal range and relatively small volume of Loch Linnhe and Loch Eil, the flushing rate for both basins is only 7-8 days. This calculation is very much a simplification, particularly as the volume of water entering the system varies considerably over the tidal cycle and the accuracy of the total volume measurement is debatable.

2.5 External Driving Functions

Other sources of data relevant to the behaviour of Loch Linnhe were collected by the Oban Meteorological Station and the Highland River Purification Board. These are incident irradiation, precipitation and wind speed and direction from Oban Meteorological Station with daily flow and nitrate concentrations of the Rivers Lochy and Nevis, from the Highland River Purification Board. MLA provided the precipitation and river data, with irradiance, wind and temperature being provided by the Glasgow Met. Office.

2.5.1 Freshwater Input

Both precipitation and runoff are highly seasonal. Runoff from the Rivers Lochy and Nevis has a correlation of 0.6175 with the precipitation of the previous day. While snowfall may lessen the direct input of precipitation into the loch, the main summer/winter difference is due to the ground being drier during periods of lower precipitation and higher irradiance. The ground, much of which is peat, then has a greater ability to absorb rainfall.

Nitrogen input from the rivers resembles smoothed river discharge. During the winter, humic content of the river is greater than in the summer - both from leaf fall and the erosion of the river banks during extreme flows.

Over the course of 1991, the volume of river discharge into Loch Eil and Linnhe was 285.5% of the low water volume of the two basins combined. Freshwater input from runoff is much more important in the IB than in the OB, as despite having a smaller volume and surface area the catchment area is larger and includes the major sources of freshwater into Loch Linnhe. The greater freshwater input means that proportionally far more brackish water flows into the surface layer of the IB than the OB, leading to different environments.

2.5.2 Tide

There is a semi-diurnal tidal cycle at Oban. The pattern in fig. 2.8 is a prediction and not representative of the true pattern of tidal height for 1991 which is influenced by factors such as wind and freshwater discharge.

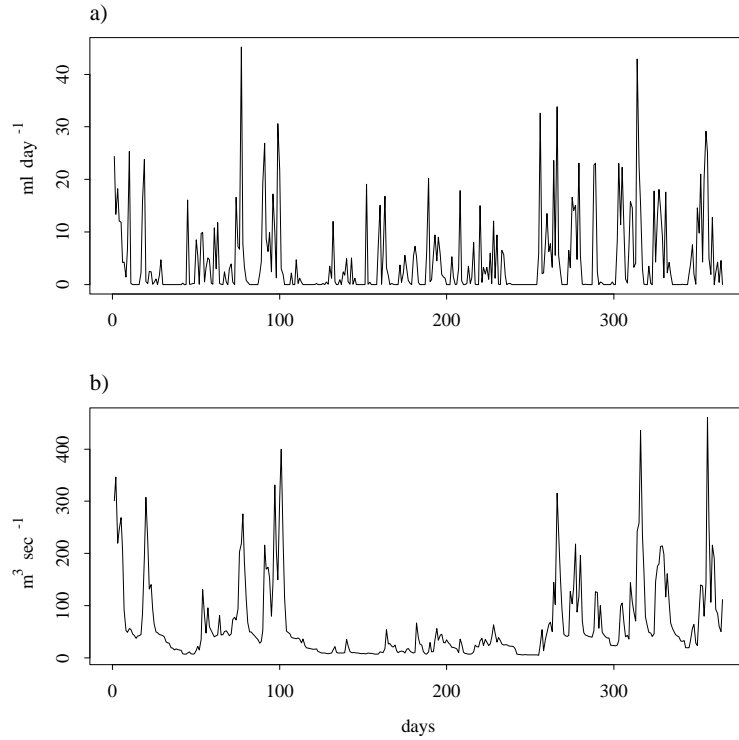


Figure 2.6: (a) precipitation at Oban and (b) daily mean flow of Rivers Lochy and Nevis ($\text{m}^3 \text{sec}^{-1}$). Sources: (a) Met. Office and (b) Highland River Purification Board.

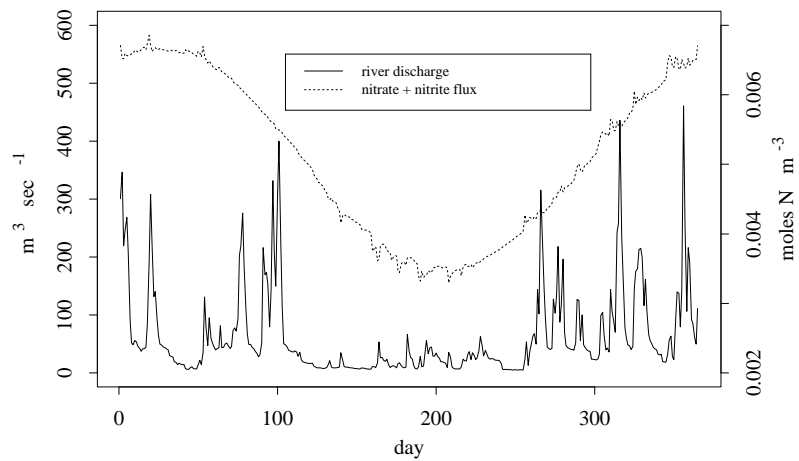


Figure 2.7: Daily nitrogen input from the Rivers Lochy and Nevis plotted with river discharge. Source: Highland River Purification Board.

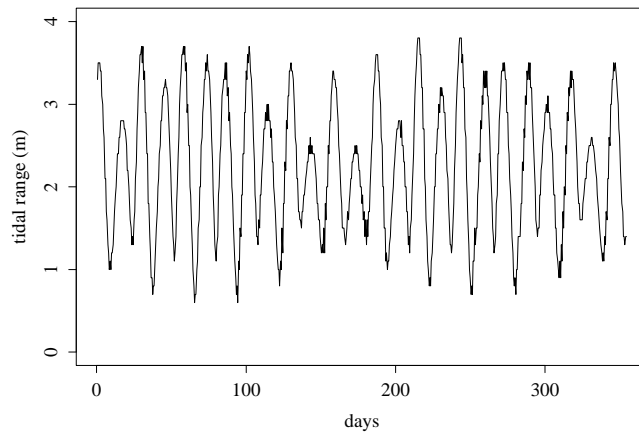


Figure 2.8: Predicted tidal ranges at Oban for 1991. Source: Admiralty Tide Tables.

2.5.3 Meteorological Data

Irradiance

Irradiance in 1991 was low, particularly in the early part of the year when values were lower than for 1978, which Tyler (1983) described as having low irradiance levels.

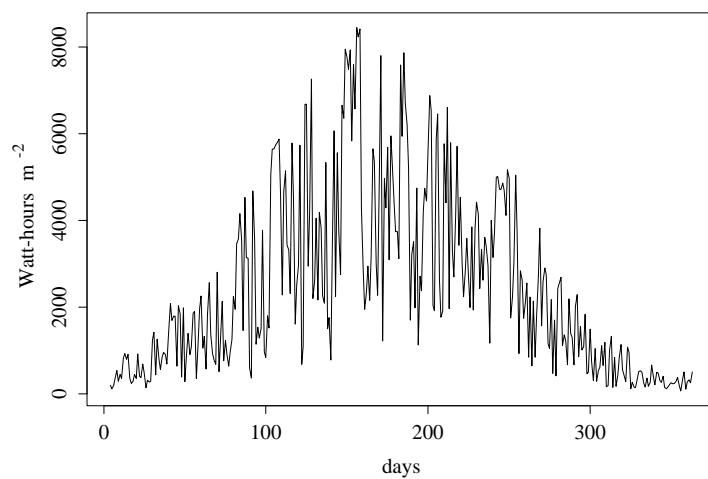


Figure 2.9: Irradiance at Oban in 1991. Source: Met. Office.

Wind

The daily mean wind speed and direction were both highly variable. From fig. 2.11 it can be seen that the prevailing wind direction was southwesterly ($\sim 225^\circ$), which corresponds to upinlet winds in Loch Linnhe - the axis of the inner and outer basins lies on $\sim 222^\circ$. 24.5% of mean hourly wind direction measurements lay between 200° and 250° in 1991 with only 9.3% in the opposing downinlet direction. The sides of the loch may protect it from cross axial winds.

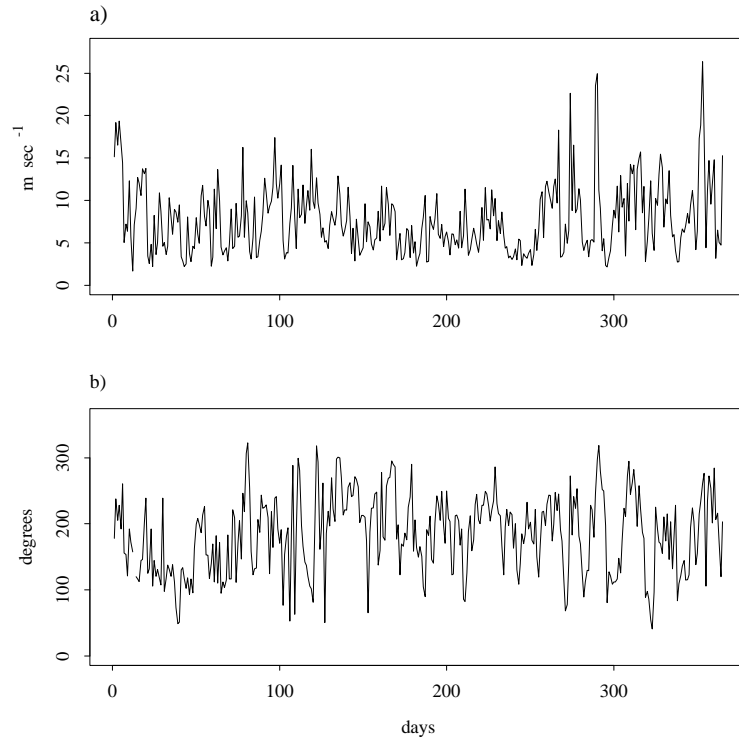


Figure 2.10: (a) daily mean wind speed m sec^{-1} and (b) daily mean wind direction. Source: Met. Office.

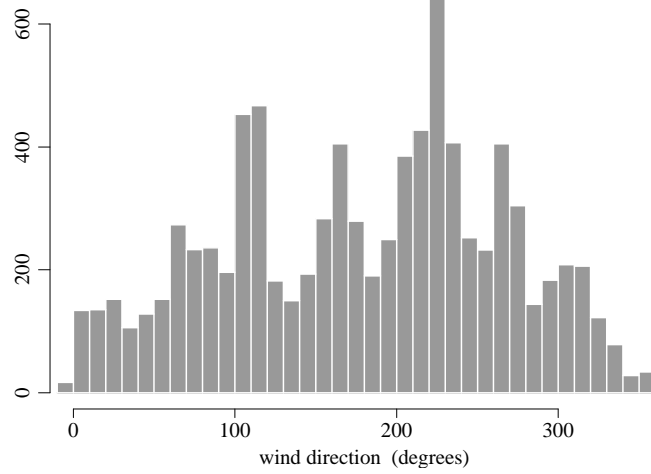


Figure 2.11: Frequency distribution of hourly wind direction measurements at Oban. Source: Met. Office.

2.6 Physical Features of Loch Linnhe

To conclude this chapter I am going to consider the topographical features of Loch Linnhe which are of most hydrodynamic interest or may induce spatial heterogeneity.

2.6.1 Inner Basin

The sill at Corran Narrows would be expected to be very important in determining the hydrodynamical behaviour of the inner basin, as the channel is very narrow and shallow. The combination of the narrows and the large tidal range in this region produce fast currents. The sill is known to generate internal waves producing seiching currents (Overnell and Young 1995) and the steady slope within the outer basin up to Corran (fig. 2.12) may generate internal waves of the type described by Rattray (1960).

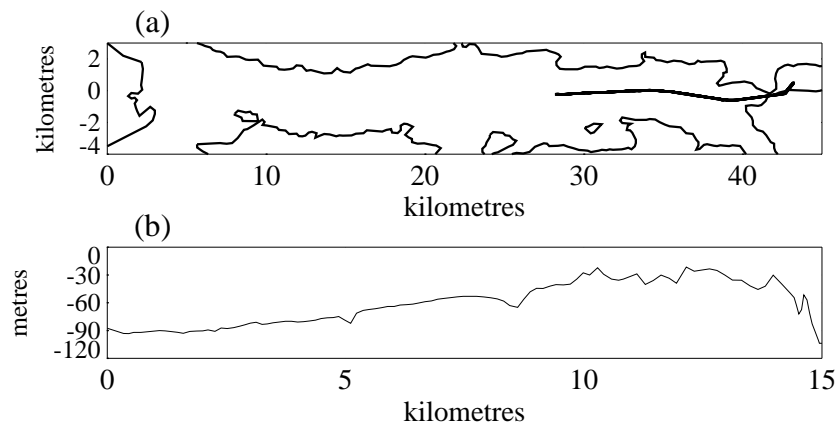


Figure 2.12: Corran and the northern end of the Outer Basin of Loch Linnhe: (a) map of Outer Basin showing position of the seabed transect (b) through the narrows at Corran and along the gently sloping loch-floor in the north of the outer basin

The bathymetry of the inner basin is in general regular, with only one embayment, Inverscaddle Bay, and apart from a slight bump along the axis (at ~ 9 km in fig. 2.13), the seabed is relatively smooth. Such an irregularity in the seabed may lead to upwelling (Syvitski et al. 1987) or interrupt the flow of renewing water.

Overnell and Young (1995) found axial currents to predominate with very small lateral currents - the surface layer flows up the loch on the flood tide and the bottom water down, with slack water between 30 and 60m. The current at 110m reached a maximum speed of $40\text{cm}\cdot\text{sec}^{-1}$ on 0.6% of tides and exceeded $25\text{cm}\cdot\text{sec}^{-1}$ on 11% of tides. Despite the importance of the tidal cycle in generating these strong currents, it does not fully explain them. Overnell and Young (1995) found extremely high river discharge to have an effect, and hypothesised



Figure 2.13: Bathymetry of the Inner Basin: (a) map of Inner Basin showing position of the seabed transect (b) along the axis of the inner basin and through the Corran Narrows

that other meteorological factors were of potential importance. Deep water renewal presumably has the potential to cause strong internal currents and Watts (1994) considered deep water renewal in the inner basin of Loch Linnhe to be linked to spring tides and wind driven upwelling seaward of the sill. It was suggested by Watts (1994) that during spring tides, flow through Corran is not continuous, but restricted to pulses on both the ebb and flood. Such an effect would enhance mixing in the Corran region.

Edwards and Sharples (1986), calculated the mixing depth of the inner basin and Loch Eil to be 10 m from tidal energy alone - by considering the morphology of the sills and currents speeds. As the prevailing wind direction is upinlet for the inner basin and wind is known to increase mixing of the surface layer of estuaries (Goodrich 1988) and fjords, the potential for the wind to enhance the mixing rate is high.

The catchment area of Loch Linnhe experiences high rainfall with a strong seasonal pattern. Much of the precipitation occurs in relation to frontal systems from the Atlantic which predominantly have southwesterly winds. The prevailing wind direction is upinlet with the principal input of freshwater runoff at the head of the loch. As most of the runoff flows into the head of the IB, stratification would be expected to be stronger there than elsewhere, with this possibly being diminished by turbulence generated by Corran Narrows. These meteorological conditions may also lead to ponding at the head of the inner basin.

Outer Basin

In the outer basin, the sill, which lies between the southern end of Lismore and Mull, has a less immediate effect than Corran, as the inflowing water initially flows into the Sound of Mull before branching off into the Lynn of Morvern. The

sill is however shallow, rising to between 20 to 30m and the maximum current speed is 3.0 knots (Hydrographic Department 1977b). A potentially important topographical feature is the sudden shallowing of the seabed, by over 100 m in less than 3 km, along the axis of the loch, alongside Lismore. This would seem to be capable of inducing a front between the outflowing ‘loch water’ and upwelled ‘coastal water’, it may also generate internal waves. Along Lismore there is also an west-east gradient, with a deep channel along the west shallowing across the loch towards Lismore, generating a difference of as much as 60m in approximately 4 km.

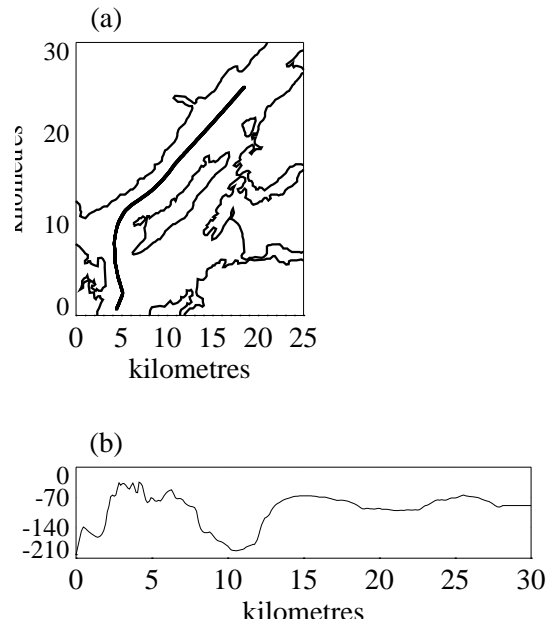


Figure 2.14: Bathymetry of southern section of Outer Basin and Lynn of Morvern: map (a) shows the position of the seabed transect (b). The sill between Mull and Lismore is centred at 5 km

In the outer basin there is a group of small islands to the north of Lismore and larger isolated islands which may enhance productivity locally. There are also embayments which may provide sheltered, shallower and warmer regions, enhancing productivity.

The OB has very little river runoff and freshwater induced stratification will be far less important than in the inner basin. As with the IB, the OB lies in the direction of the prevailing wind. It is, however, much broader and cross channel effects more likely.

Part II

Data Analysis

Chapter 3

Seasonal Trends in the Data Sets

3.1 Introduction

In this chapter the seasonal patterns of 1991 are summarised over the entire range of data available. Initially the vertical data is considered which encompasses the fixed moorings, sample sites and axial tows and then the horizontal surface data. Information on the method of interpolation for the colour plots is included in Chapter 4.

3.2 Vertical Data

3.2.1 Thermistor Chain

Thermistor chain data was collected between 24 February to 3 October at the inner basin mooring and from 20 January to 4 October at the Lynn of Morvern mooring. Comparing the sites, for 82.8% of the days (with measurements at both moorings) the surface (2m) in the Lynn of Morvern was warmer than the inner basin. The mean in the LoM was 10.66°C compared to 10.06°C in the IB and the maximum temperature in the LoM was almost 1°C greater than for the IB (14.80°C compared to 13.83°C .) As the LoM experiences more tidal mixing and less river discharge, there was less vertical variation (fig. 3.2) than in the IB and the surface layer was deeper.

In the IB, from 6-8 m to the seabed attained approximately the same maximum, and to a lesser extent minimum temperatures, while in the LoM this was demonstrated more clearly for 20 m down, indicating a much shallower thermocline in the IB. The temperature changes in deep water in the IB were more marked than those for the LoM, and the deep water of the IB was more variable than the intermediate layer. This pattern may have been generated by deep water exchange producing greater variation along the seabed than in the intermediate

zone, also Overnell and Young (1995) reported surface and deep water flow with an intermediate low energy zone for the inner basin.

The LoM warmed sooner at the start of the year and cooled later at the end, as it does not experience the direct river input of the IB, fig. 3.1. River discharge did not rise to the higher winter levels until soon after the surface layer had started to cool in both basins, and the warming of the surface layer commenced before the river discharge lessened. The 2 moorings reflect similar patterns of warming and cooling but the more mixed nature of the LoM means that the fluctuations in surface temperature are less rapid than in the IB, fig. 3.1. During the period between the initial deployment of the thermistor chain and the end of April/start of May the thermocline was weak, with frequent temperature inversions. This pattern reoccurred from the start of September with the increase in freshwater runoff and the fall in daily irradiance levels.

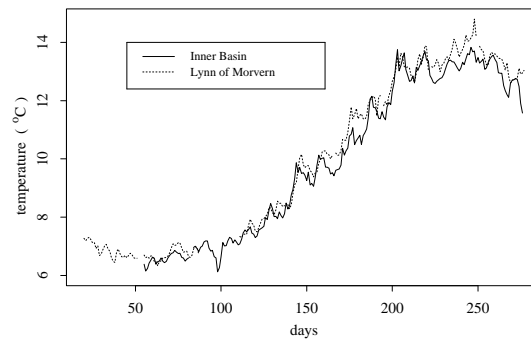


Figure 3.1: Thermistor chain data collected at 2m, at the inner basin (IB) and Lynn of Morvern (LoM) moorings.

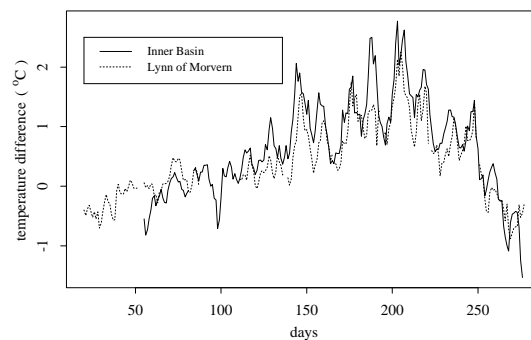


Figure 3.2: Temperature difference between 2m and 60m, at the IB and LoM thermistor chains.

The surface pattern of rapid cooling and warming was dampened with increasing depth in both basins. The temperature between the basins was closely linked, with the correlation between the IB and the LoM at each depth being the greatest on the same day, except at 2 m where the LoM correlates most highly with the previous day in the IB.

3.2.2 Sample Site Data

Temperature

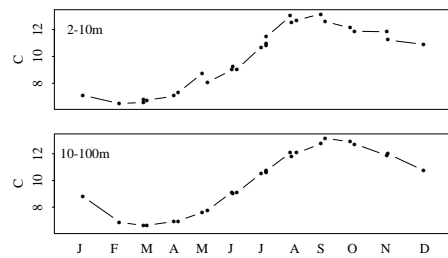


Figure 3.3: Inner basin sample site temperature data, a) the surface 10m and b) the rest of the water column.

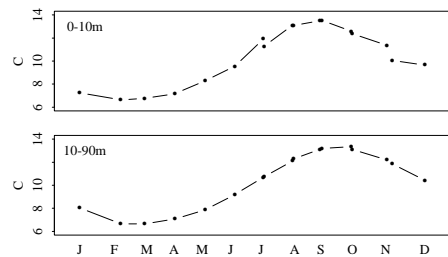


Figure 3.4: Outer basin sample site temperature data, mean for a) the surface 10m and b) the rest of the water column.

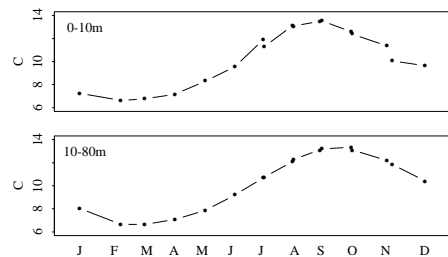


Figure 3.5: Lynn of Morvern sample site temperature data, mean for a) the surface 10m and b) the rest of the water column.

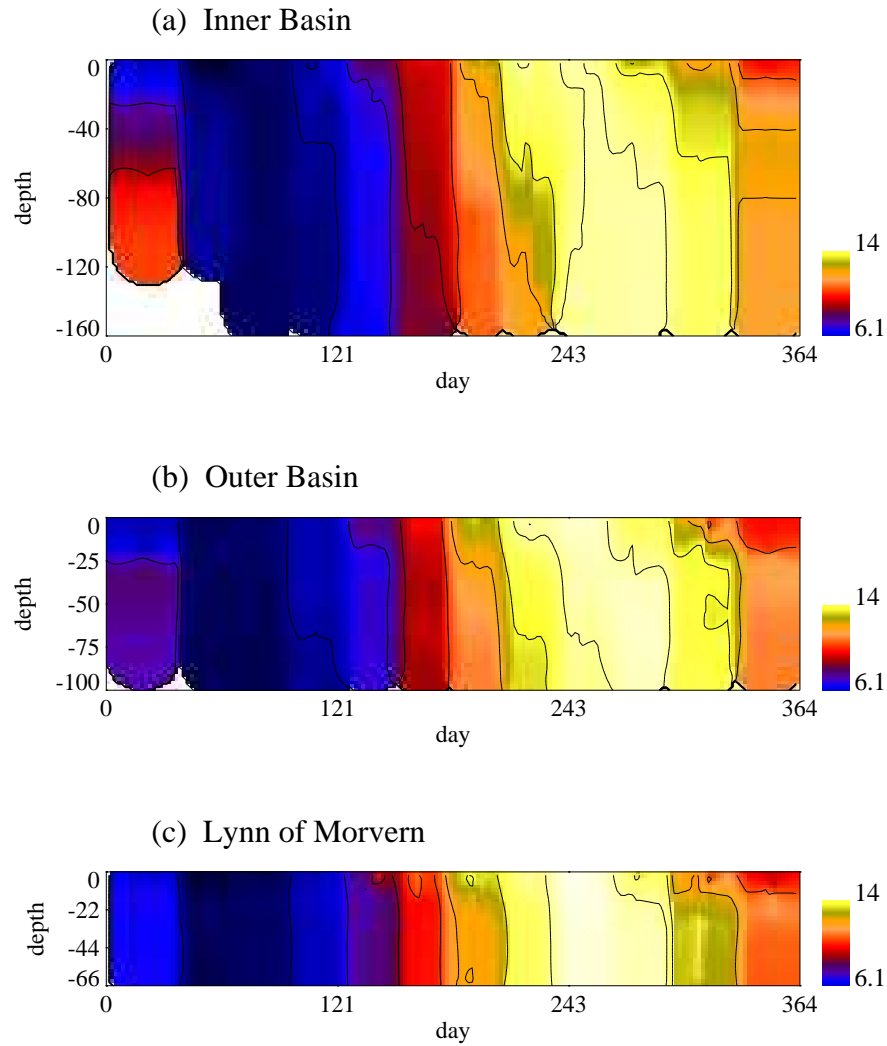


Figure 3.6: Interpolated sample site temperature data for (a) IB, (b) OB and (c) LoM. Contour intervals are 1°C apart.

From January to December there was a change from the deepest water being the warmest through to the water column being uniformly cool; then from May the surface layer warmed with this spreading through to all depths before the surface cooled and the maximum was again subsurface in December. The greatest thermal variability was in winter. The concurrence in temperature between the seabed temperatures for the IB and OB moorings shows a degree of exchange between the basins, namely deep water renewal. The only months where they do not appear to have been closely linked were January and late July/early August, which may indicate that no renewal occurred in July. Between 10 and 15 August, there was a warming of the deep IB water which once more raised it to a level similar to that in the OB.

Moving from the inner basin to the Lynn of Morvern there was less thermal variability between the surface and the seabed, often less than 1°C difference over the water column in the LoM, fig. 3.6. Seaward, mixing is greater and surface heating is transported down through the water column more rapidly. At all sites the surface can be seen to warm and cool before the deeper water with this effect greatest in the IB. In the IB, between August and September, the deep water (<120m) warmed before intermediate depths - this may have been due to an intrusion of water from the outer basin

The time series plots for each sample site show a similar pattern and time scale at each site, with the maximum being attained in September and the minimum in February.

Salinity

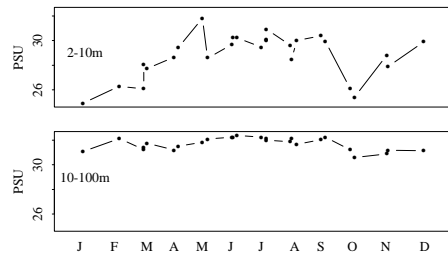


Figure 3.7: Inner basin sample site salinity data, a) the surface 10m and b) the rest of the water column.

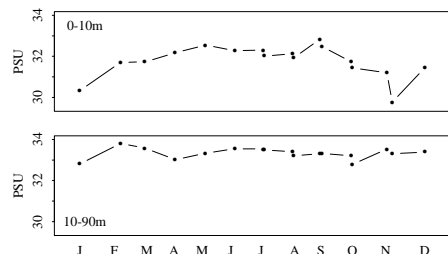


Figure 3.8: Outer basin sample site salinity data, mean for a) the surface 10m and b) the rest of the water column.

Deep water salinity did not vary much through the year, < 1 PSU throughout the outer basin and < 2 PSU in the IB. River discharge typically only affected the surface salinity in the IB but after very high levels of river discharge in March, the salinity as far as the seabed (at 160m) was affected. As most of the river input into the basins flows directly into the IB, the surface salinity there falls to much lower levels than south of Corran (hence the different scale in the colour plots fig. 3.10.) Despite the IB mooring being sited almost two thirds down the basin, the surface salinity still fell as low as 17 PSU in January.

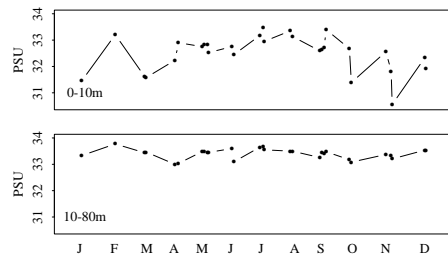


Figure 3.9: Lynn of Morvern sample site salinity data, mean for a) the surface 10m and b) the rest of the water column.

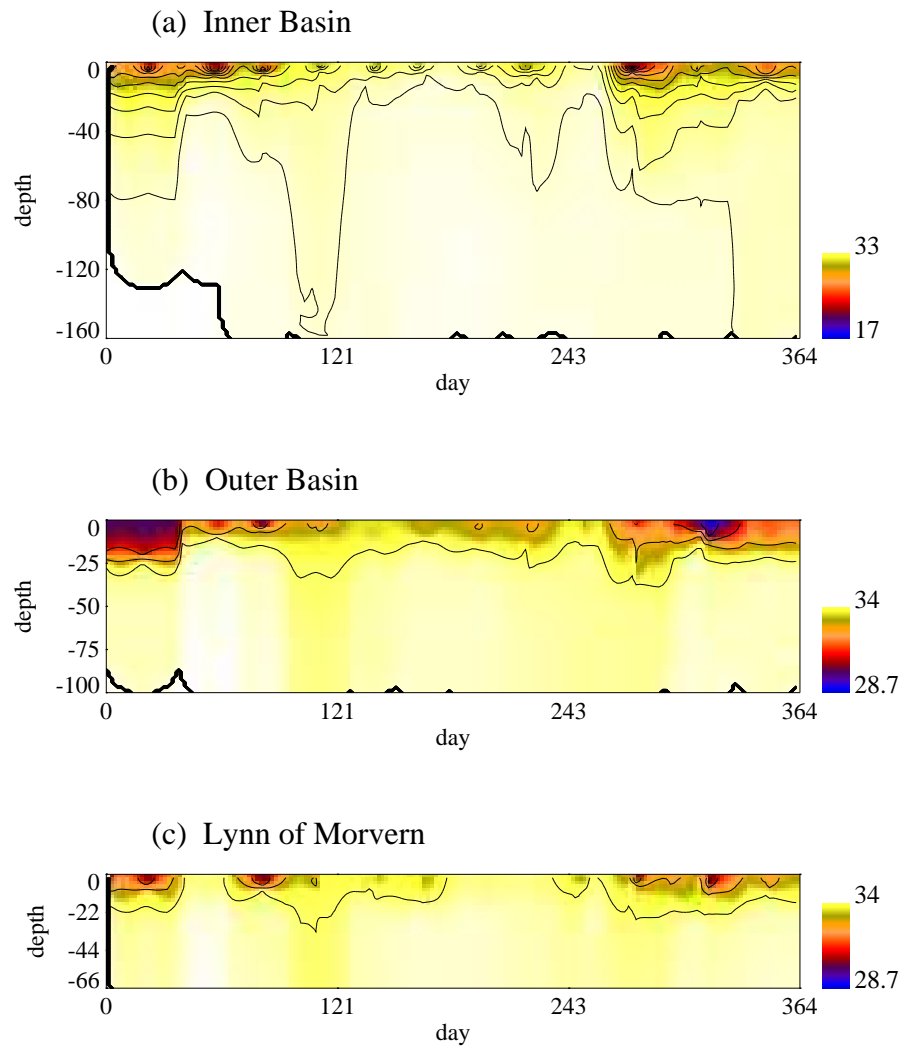


Figure 3.10: Interpolated sample site salinity data for (a) IB, (b) OB and (c) LoM. Contour intervals are 1 PSU apart. Note - the IB scale is different.

At the OB mooring the effect of river discharge outwith the surface 30m was less significant and less still in the LoM where the salinity of the water column at times varied by < 1 PSU. The extreme river flow in March, however, also affected the salinity as far as the LoM, but the effect was less dramatic. Passage of the outflowing water through Corran may contribute to homogenising the water column and the further the surface layer flows the more deep water will be entrained into it, increasing the salinity.

Despite the high river discharge in March affecting the water column down to 30m as far as the LoM and affecting the entire depth of the IB, it did not generate unusually low surface salinities. This suggests that the water column was well mixed at this time - possibly from strong winds. At other times, such as January, October and November, surface salinities were much lower but the effect was confined to a shallower surface region. The mean salinities for surface and deep water were also not particularly low at this time, figs. 3.7, 3.8 & 3.9.

Chlorophyll

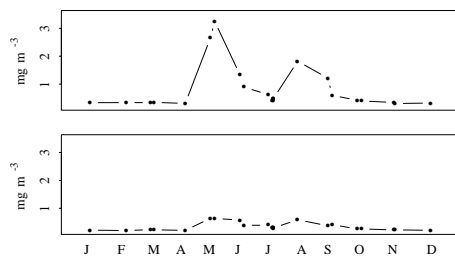


Figure 3.11: Inner basin sample site chlorophyll data, a) the surface 10m and b) the rest of the water column.

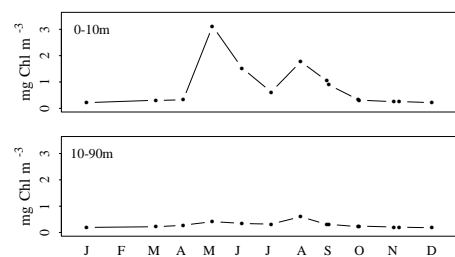


Figure 3.12: Outer basin sample site chlorophyll data, mean for a) the surface 10m and b) the rest of the water column.

Throughout Loch Linnhe, the chlorophyll density was low and the spring bloom late - at the end of May/beginning of June, with a further smaller bloom in August. The timing was not due to a lack of irradiance, as the Lynn of Lorne, which is adjacent bloomed in April with a significantly higher chlorophyll density

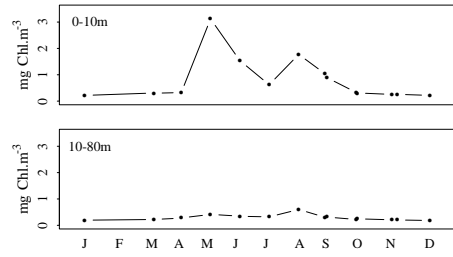


Figure 3.13: Lynn of Morvern sample site chlorophyll data, mean for a) the surface 10m and b) the rest of the water column.

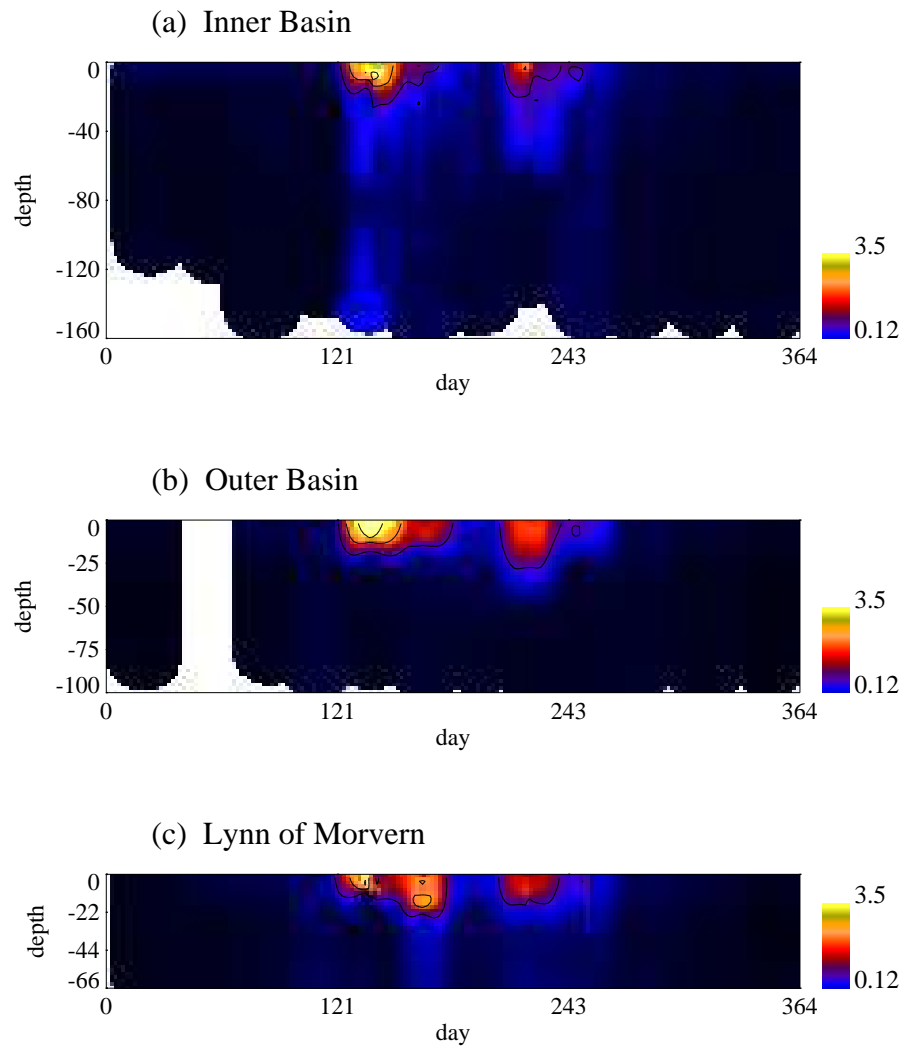


Figure 3.14: Interpolated sample site chlorophyll data for (a) IB, (b) OB and (c) LoM. Contour intervals are $1.0 \text{ mg Chl m}^{-3}$ apart.

than found at any time in Loch Linnhe. Very heavy river discharge in March and April may have contributed to the later bloom by increasing attenuation at the surface. Overnell and Young (1995) found high levels of river discharge and turbidity to be associated in the inner basin.

In the IB, sedimentation had commenced by 18 May (fig. 3.14) but to a much lesser degree at the other sites. In May 1991, Overnell and Young (1995) found sedimentation rates in the IB to be high before the surface had bloomed and hypothesised that chlorophyll had been advected into the basin during deep water exchange. With the temporal resolution available, the OB and LoM blooms seem to have been longer, though in May (fig. 3.13) the LoM sample site mean surface density fell by $> 50\%$ over 6 days. Such measurements are affected by the advection of phytoplankton as well as sedimentation from the surface.

Beam Attenuation

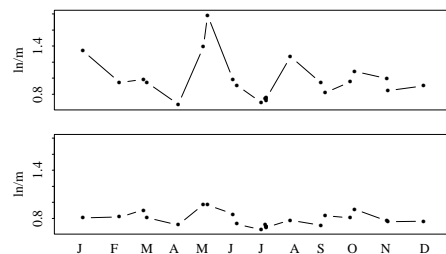


Figure 3.15: Inner basin sample site beam attenuation data, a) the surface 10m and b) the rest of the water column.

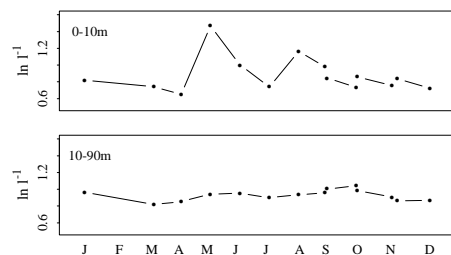


Figure 3.16: Outer basin sample site beam attenuation data, a) the surface 10m and b) the rest of the water column.

Surface beam attenuation was related to chlorophyll during the summer and to high river discharge in January, fig. 3.18(a). The highest values measured, however, were in proximity with the seabed and caused by tidal currents interacting with the bathymetry. Overnell and Young (1995) found that sedimentation rates throughout the IB water column were affected by the height of the predicted tide and to a lesser extent by extreme levels of river discharge. In the IB in particular,

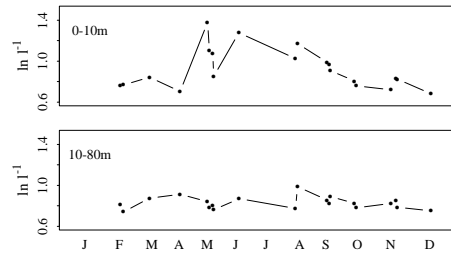


Figure 3.17: Lynn of Morvern sample site beam attenuation data, a) the surface 10m and b) the rest of the water column.

the turbidity can be seen to extend for almost 80m from the seabed in March and October - the May values may have been influenced by sedimenting chlorophyll, fig. 3.18(a). If resuspension is predominantly due to deep water currents then deep water renewal will also increase beam attenuation at the seabed and further up in the water column.

Seabed turbidity was particularly high and consistent at the OB site which may be due to the loch shallowing towards Corran at this point. Internal waves may be generated by the interaction of the slope and tidal currents, increasing turbidity in this region.

In general the LoM values were lower than elsewhere, the position of the mooring to the side of the loch may affect the speed of deep water currents, or the benthos may be rockier as the region is exposed to more tidal flow. The neighbouring island, Lismore, is limestone which may also be influential. The rapid increase in deep water turbidity, at the LoM mooring, between 12 and 14 July may have been caused by an increase in current speed with there was a predicted tidal maxima on the 13th.

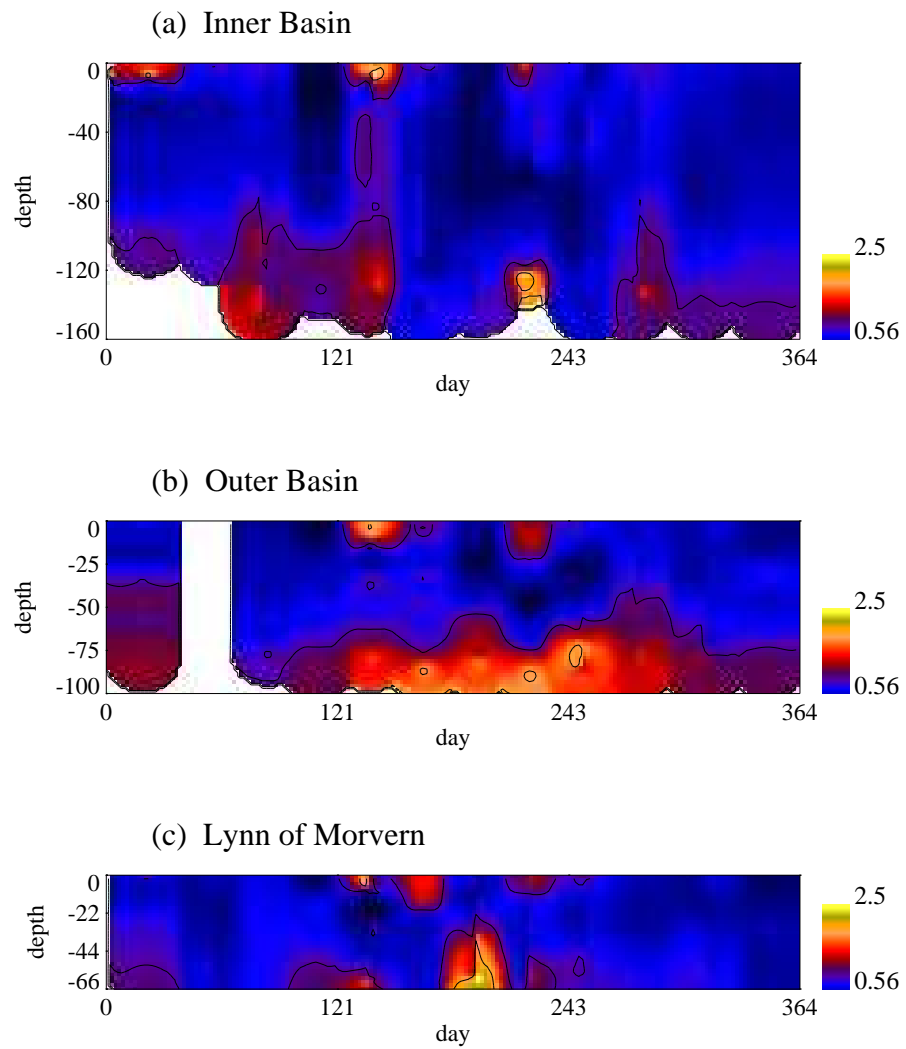


Figure 3.18: Interpolated sample site beam attenuation data for (a) IB, (b) OB and (c) LoM. Contour intervals are 0.5 \ln/m apart.

Nutrients

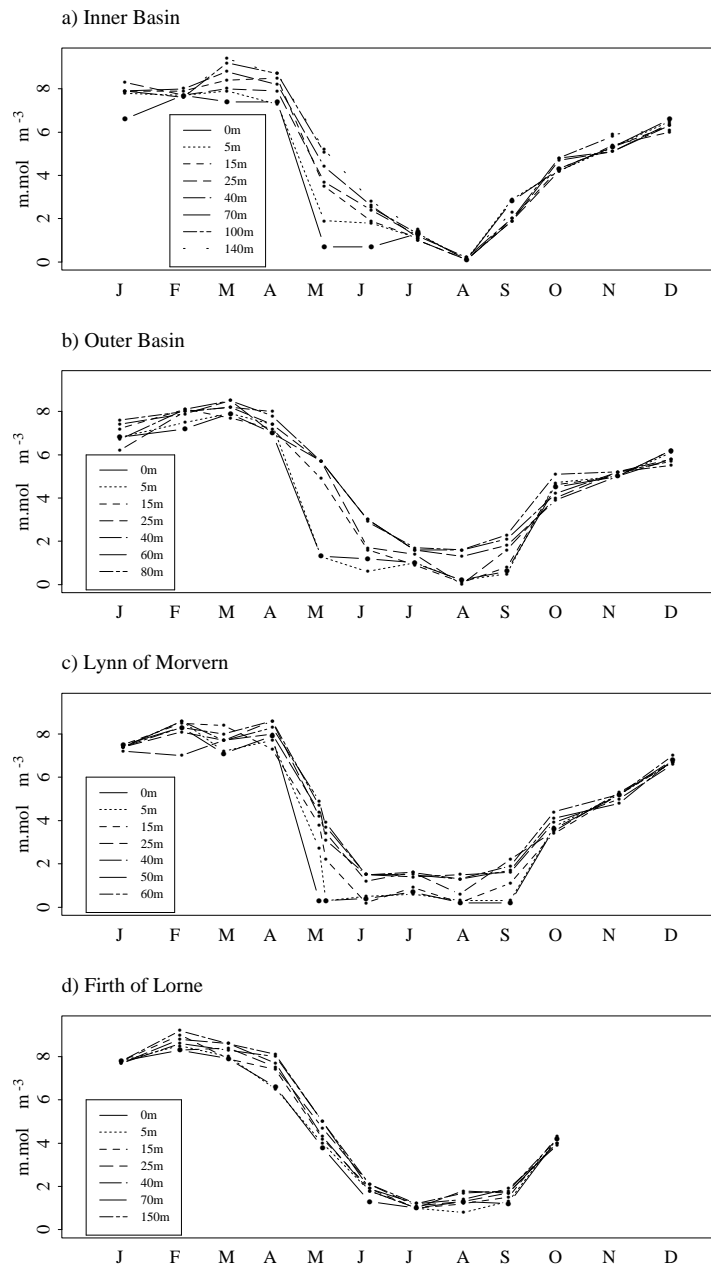


Figure 3.19: Nitrate concentrations at the sample sites in a) Inner Basin, b) Outer Basin, c) Lynn of Morvern and d) Firth of Lorne.

At all depths, at all sample sites, the maximum nitrate values were found during the months preceding the spring bloom - February, March or April - with the maximum in deeper water being attained later. Vertical variation everywhere was greatest during the spring bloom. The overall pattern is typical of a spring bloom with an increase in nutrients in autumn.

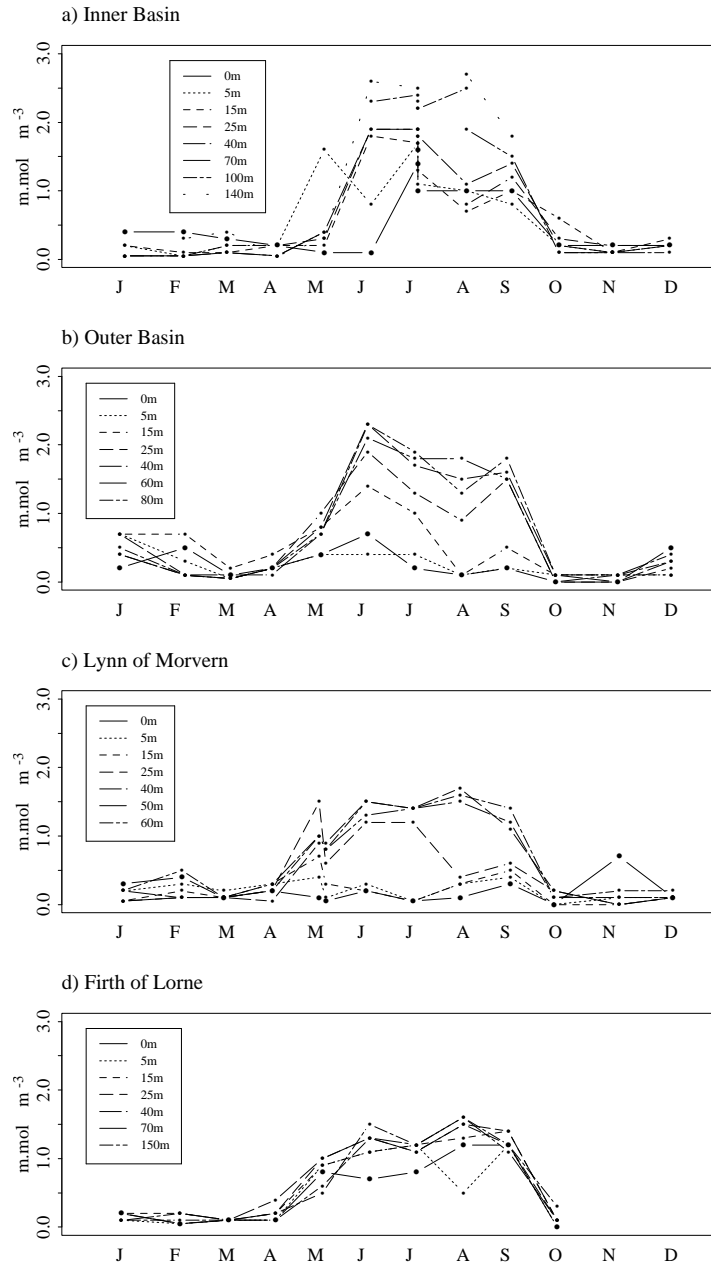


Figure 3.20: Ammonium concentrations at the sample sites in a) Inner Basin, b) Outer Basin, c) Lynn of Morvern and d) Firth of Lorne.

In the IB (fig. 3.19a) there was a rapid decline in nitrate concentration between 24 April and 22 May, with the extent of the decrease in nitrate, decreasing with depth. At the surface, there was a fall from 7.4 to 0.7 m mol m^{-3} while at 140m the fall was from 8.7 to 5.2 m mol m^{-3} . By 17 July the surface nitrate concentration rose slightly (corresponding with a fall in surface chlorophyll) and the distribution throughout the water column was relatively homogeneous - values ranged from 1 to 1.5 m mol m^{-3} . The minimum at all depths was attained on 15

August. Concentrations increased from then, remaining homogeneous throughout the water column. Ammonium concentrations also indicate a late bloom with low levels at most depths until June, when there was a rise in concentration except at the surface, which increased in July. Maximum NH_4 concentrations were in deep water during the summer and from October onward the ammonium concentration at all depths was low. Overnell et al. (1995) considered benthic remineralisation to be unimportant in the inner basin, with most remineralisation occurring in the water column during resuspension. The homogeneous, low nitrate concentration in the IB in comparison with the relatively high ammonium concentrations may indicate low rates of remineralisation. The internal waves and resuspension reported by Overnell and Young (1995) may give rise to the homogeneity.

The deeper surface at the OB mooring (fig. 3.19b) is indicated by the similar pattern at 0 and 5m. As for the IB, the spring decrease in DIN was between 21 April and 20 May but less than in the IB - this is partly explained by the deeper surface layer. As for the IB, the minimum was in August, however in September the nitrate concentration was still low at the surface, indicating that phytoplankton growth persisted later there. Only the surface 25m of the OB became depleted of nitrate, with the concentration between 40m and 80m never falling below 1.3 m mol m^{-3} . The depth of the surface depleted layer can also be seen to change, nitrate levels at 25m in August were similar to those in shallower water, but by September had increased to levels closer to those of deeper water as the euphotic zone shallowed. In the surface 5m, NH_4 concentrations never exceeded 1 m mol.m^{-3} and from August onward the concentration at 15m was also $< 1 \text{ m mol.m}^{-3}$. At all other depths concentrations were lower than in the IB.

The spring bloom caused a sharp decline in nitrate concentrations at the LoM mooring, fig. 3.19c. The two measurements in May, 19th and 23rd, illustrate the dramatic change that may occur in a short period. The surface concentration fell from 7.9 to 0.3 m mol m^{-3} from 21 April to 19 May with no further change by the 23rd. At all other depths, however, there was a decline between 19 and 23 May, with a fall of 2.4 m mol m^{-3} at 5m and 1.6 m mol m^{-3} at 60m. There is evidence of a further bloom in August. As for the OB, nitrate concentrations increased in deep water sooner and surface concentrations remained low through to September. At both the OB and LoM sites deep water exchange with the FoL may replenish nutrients. As with the OB, the surface 5m at the LoM mooring remained low in NH_4 throughout the year.

The Firth of Lorne, due to the greater extent of mixing never displayed the extreme behaviour of the more sheltered sea-loch and there was little difference in the yearly cycle at the surface and at 60m, with a minimum at all depths from June to September. The first indication of the spring bloom was in April, which then progressed further up the loch where May was the first indication of the bloom. Nutrient depletion was not a problem in 1991 and phytoplankton growth may be considered to have been light limited.

Gelatinous Zooplankton

The gelatinous zooplankton collected were of large species and predominantly *Aurelia aurita* (L.) which have been found to be very abundant in Scottish coastal waters and other North Sea coastal regions (Hay et al. 1990). In most regions, *A. aurita* and other scyphomedusae, only survive for one season, strobilating in the spring and reproducing and dying, or being washed seaward, in late summer/autumn. In the Baltic and North Sea, there is evidence of considerable interannual variability in abundance and size (Hay et al. 1990; Schneider and Behrends 1994). From the change in diameter and abundance of medusae between years in the western Baltic, Schneider and Behrends (1994) believe the population to be density dependent - with small, food limited, medusae during years of high population and larger medusae in years of low population. If such a relationship occurs in the Loch Linnhe population, the volume alone may cause problems in estimating feeding and excretion rates.

The medusa data available is the volume.m⁻³, which was calculated by assuming the volume of a medusa to be equivalent to that of half a hemisphere:

$$V = 0.131 \times (\text{diameter cm})^3. \quad (3.1)$$

As jellyfish predominantly consist of water, their volume is generally equated with wet weight (Bámstedt 1990). Typical volume/wet weight measurements from the literature include:

$$V = 0.095 \times (\text{diameter cm})^{2.701} \quad (3.2)$$

from Bámstedt (1990);

$$V = 0.07 \times (\text{diameter cm})^{2.8} \quad (3.3)$$

from Hay et al. (1990) and

$$V = 0.09 \times (\text{diameter cm})^{2.75} \quad (3.4)$$

from Schneider and Behrends (1994).

Compared to equations 3.2 to 3.4, 3.1 considerably overestimates the volume of the population and the figures for Loch Linnhe data would be expected to exceed the actual volume of the medusa measured. If the volume is calculated by eqn. 3.3, then for a 1.4cm diameter *A. aurita*, considering the medusa to be half a hemisphere predicts double the volume, for medusae of diameter 10.7cm the volume is overpredicted by a factor of three. In order to calculate the carbon content, I used conversion values from Lucas and Williams (1994): dry weight being 3.8% wet weight and carbon to be 4% of dry weight. As the volume may be an overestimate, 4% was chosen as it is the minimum of the range measured by Lucas and Williams (1994) of 4-15%.

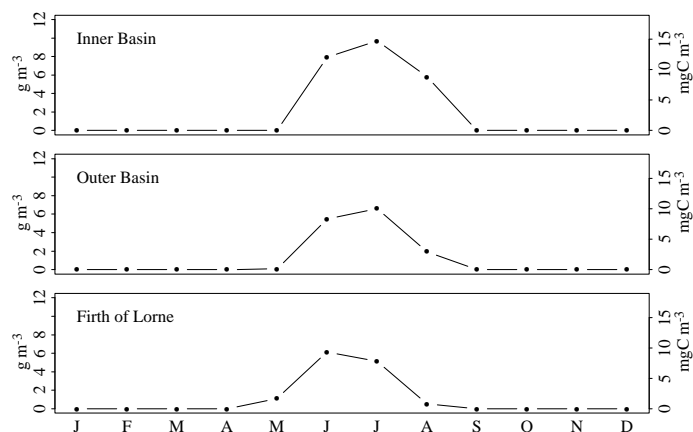


Figure 3.21: Medusa wet weight g m^{-3} and biomass, mg.C m^{-3} , depth averaged from surface to 10m from seabed - assuming an average diameter of approximately 10.7cm.

In 1991, in all areas, the first catches of medusae occurred in May and the last in August. In May the FoL population was considerably larger than elsewhere, with the IB density being the greatest for the rest of the summer. The data either indicates a process of the young medusae being washed into the system from coastal water or strobilation - which is temperature dependent (Möller 1980) - occurring later inland as the deep water takes slightly longer to heat there. That the IB density remained the highest until no population was measured, indicates that the medusae predominantly died within the basin, rather than being washed out to sea.

Medusa carbon densities measured elsewhere include a yearly maxima of 30.2 mgC.m^{-3} in Southampton Water in May 1990 with 27.6 mgC.m^{-3} in June 1991 from Lucas (1994) and during the summer of 1992 the carbon density in the Kiel Bight was estimated to be 50 mgC.m^{-3} (Schneider and Behrends 1994). A 10.7cm diameter *A. aurita* is not large for Scottish coastal water and this diameter was used to keep the volume estimate conservative. While the density of medusae in Loch Linnhe in 1991 was large, with the change in volume calculation, in comparison with other areas it was not excessively so.

3.2.3 Axial Cruise Data

Considering the mean conditions throughout the basins, rather than the single site sample site data, produces smoother plots but the overall pattern is similar. The main differences are in the chlorophyll plots where the horizontal heterogeneity of the phytoplankton highlights the difference between single site and multiple samples.

Salinity

In both basins the surface 10m was considerably more variable than deeper water and the pattern of deep water salinity was not related to that of the surface. The seasonal cycle of salinity over the year displays a similar pattern between the surface layer of each basin and between the deeper water of the basins. The inner basin was more variable than the outer basin and of lower salinity. In February the mean salinity in the inner basin was more than 6 PSU lower than that in the outer basin.

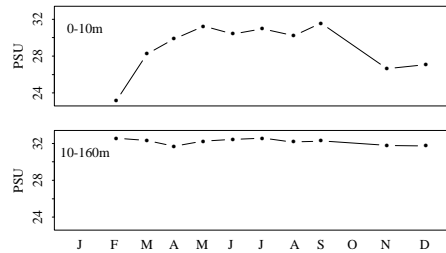


Figure 3.22: Volume averaged seasonal salinity in the Inner Basin.

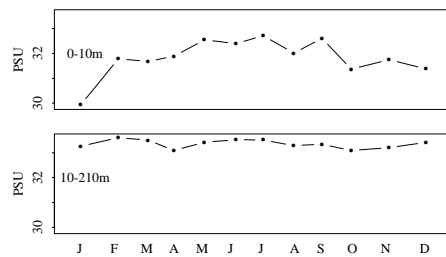


Figure 3.23: Volume averaged seasonal salinity in the Outer Basin.

Temperature

As with the sample sites, the maximum surface and deep water temperature for both basins occurred in September with the minimum in March - except for the IB surface which attained its minimum in February - the turbulent mixing which lowered the salinity at the sample site seabed in March, may also have brought deeper warmer water to the surface.

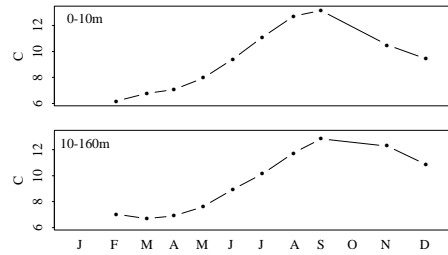


Figure 3.24: Volume averaged seasonal temperature in the Inner Basin.

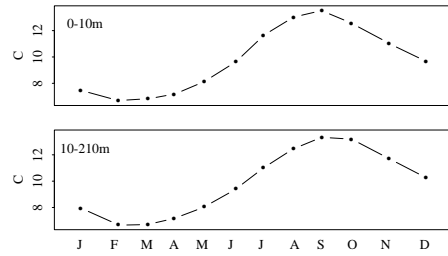


Figure 3.25: Volume averaged seasonal temperature in the Outer Basin.

Chlorophyll

Though the IB axial spring bloom peak was much smaller than that of the sample site, by considering the entire basin it can be seen that the June density was also high. Similarly, in the outer basin, the mean of the entire basin is smoother than that of individual sites, in particular the rapid changes over a short time span would not be present.

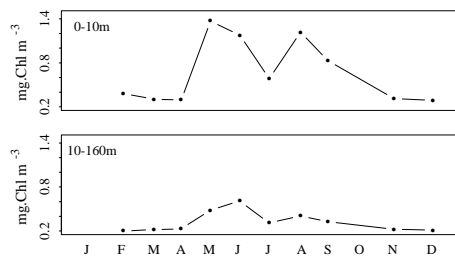


Figure 3.26: Volume averaged seasonal chlorophyll in the Inner Basin for the surface 10m and the rest of the water column.

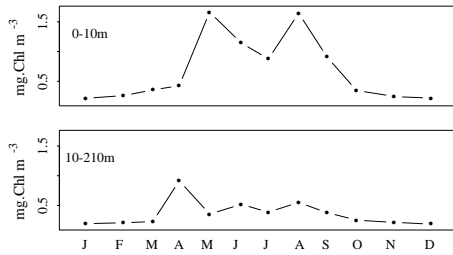


Figure 3.27: Volume averaged seasonal chlorophyll in the Outer Basin.

Zooplankton

The mesozooplankton population peaked in May throughout the loch system, with the highest density in the inner basin, and fell most rapidly in the outer basin before increasing again in the late summer/early autumn with a lower second bloom. The increase in zooplankton can be seen starting in the FoL and moving inland. In March and April, the FoL population was higher than that in the outer basin, which in turn was greater than that in the inner. It has been claimed that the increase in gelatinous zooplankton biomass follows that of copepods (a principal component of their diet) (Möller 1980) and the successive movement of mesozooplankton and then medusae further up the loch system would agree with this.

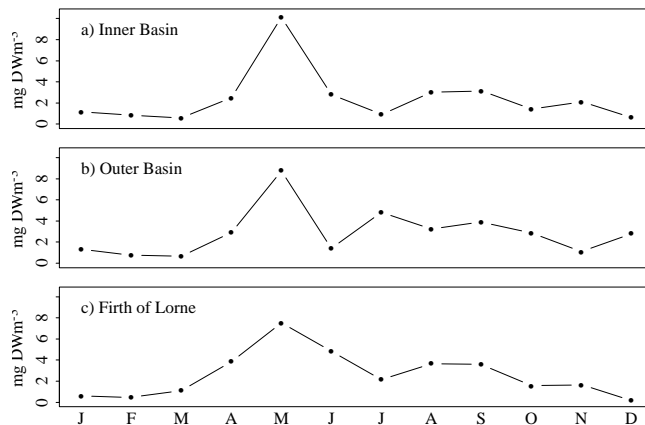


Figure 3.28: Mesozooplankton dry weights from the axial cruises for the a) Inner Basin, b) Outer Basin and Lynn of Morvern and c) Firth of Lorne.

3.3 Horizontal Data

The mean surface cruise values provide little information not available from the sample site data but the data collection at approximately 4m highlights the influence of river discharge on the inner basin.

3.3.1 Salinity

The greater variability of salinity in the IB can also be seen in fig. 3.29, of the mean salinity over the surface cruises. In the IB, the mean surface salinity fell to levels of < 20 PSU. As the OB does not have a large source of freshwater input the salinity varied over a considerably smaller range and the coastal sea mean salinity remained > 30 PSU throughout the year. Maximum salinities were attained during periods of low river discharge, with the effect of the river input diminishing seaward.

After very high river flow, surface salinity values as low as 12 PSU and 8 PSU were measured in the IB during the January and November cruises respectively. Salinity levels in the OB were less affected by these events, but still attained values as low as 23 PSU in January and 25 PSU in November.

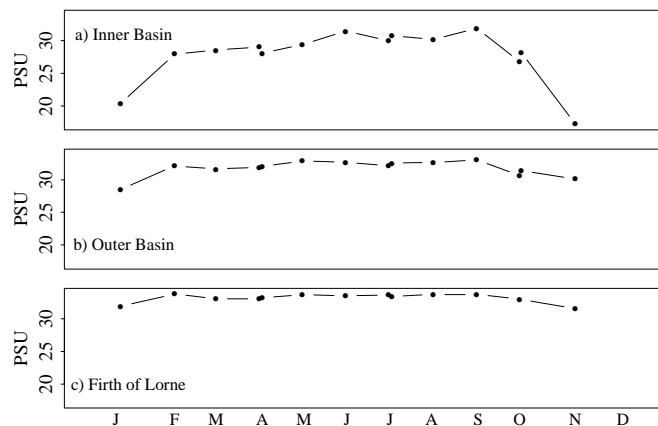


Figure 3.29: Mean salinity from the surface cruise data for a) Inner Basin, b) Outer Basin and Lynn of Morvern and d) Firth of Lorne.

From the surface plots in Appendix A it can be seen that the pattern of surface salinity in both basins was highly variable. In the inner basin the most saline regions may be in the south (as expected,) the north (despite being closest to the river input) or the middle. In the outer basin, there were often prominent bands of constant salinity across, along and diagonally within the basin. These patterns do not correspond with the predicted semi-diurnal tidal cycle or with the lunar tidal cycle. Being the source of the freshwater input for the two basins,

the salinity range in the inner basin typically exceeded 2 PSU, with that of the outer basin being much less.

3.3.2 Temperature

After the minima in February, surface temperature warmed gradually through the year, with the warmest month being September. Freshwater runoff affects the surface temperature and this effect can be seen in January and November. After very high river discharge, parcels of colder water are in the surface layer creating a wide range of temperature over the inner basin, 1.7°C and 3.4°C in January and November respectively. For most of the rest of the year temperature varied by less than 1°C in the inner basin. In the larger OB, temperature generally varied by less than 1.5°C from Corran to Mull. As with salinity, the effects of runoff on temperature in the outer basin were considerably less than for the inner. Cooling from the maxima in September to November was rapid. The minimum temperature fell by more than 1°C for each month, and the maxima on 14 November was less than the minima on 10 October.

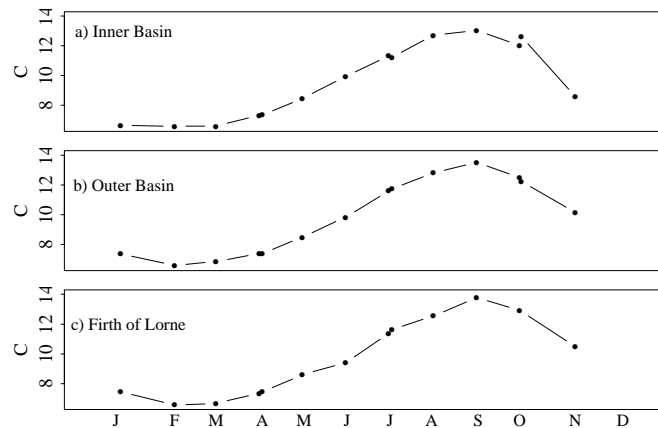


Figure 3.30: Mean temperature from the surface cruise data for a) Inner Basin, b) Outer Basin and Lynn of Morvern and d) Firth of Lorne.

3.3.3 Chlorophyll

Considering the entire surface layer of the loch, there was an increase in chlorophyll density between 23 and 25 April in each area. From a 23% rise in the IB, to 69.97% and 35.13% in the OB and FoL respectively. The bloom had already commenced in the FoL by this time and there had been a slight increase in chlorophyll density in the OB. In both the FoL and the OB the peak of the spring bloom probably lay between 25 April and 21 May, as by the May cruise the chlorophyll density was diminishing, more so in the FoL than the OB.

The other month with a replicate cruise which covered the entire system was July. Between 16 and 18 July there was very little change in the IB, (a fall of 1.2%) while the OB density increased by 79% and the FoL density decreased by 74.8%. These values, which are the mean of a large area, would be expected to have a much smoother temporal pattern than individual sites. As these show relatively large changes in density over short time periods, there is presumably a great deal of change in chlorophyll density at individual sites over short time intervals.

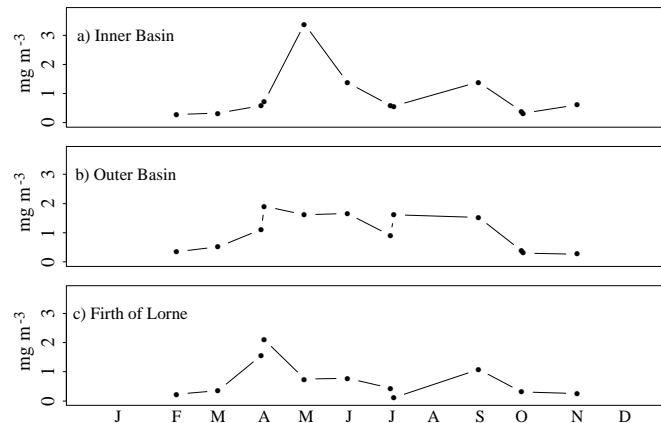


Figure 3.31: Mean chlorophyll from the surface cruise data for a) Inner Basin, b) Outer Basin and Lynn of Morvern and c) Firth of Lorne.

3.3.4 Zooplankton

The zooplankton surface data does not provide a monthly sequence for the year as there is no data for March and from May to August, when, from the axial data the peak density would have been. Of the months available, the September density was highest. Sampling of zooplankton at a single depth may only be considered representative at that time, as within a few hours, diurnal migration may drastically alter the density at a particular depth.

3.3.5 Beam Attenuation

Times of maximum turbidity vary between the basins. In the IB, very high levels of river discharge generated the yearly maximum in November, whereas in other basins, maximum turbidity was associated with chlorophyll, peaking in May and June in the OB and FoL respectively. Turbidity was lowest before the spring bloom, which may indicate that the high turbidity levels of the loch contribute to low productivity and the late bloom.

For most of the year the Sound of Mull was more turbid than the main body of the outer basin. In the northern end of the basin, beam attenuation was slightly higher, which was probably due to the outflow of water from Corran, both from

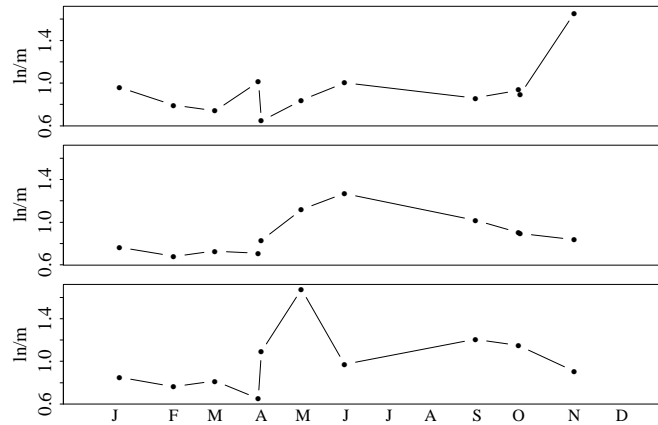


Figure 3.32: Mean beam attenuation from the surface cruise data for a) Inner Basin, b) Outer Basin and Lynn of Morvern and c) Firth of Lorne.

the turbulence generated, as the loch is less than 40m deep for 5km and the higher turbidity of the water.

3.3.6 Relationship between variables

Salinity and Temperature

In the IB, surface temperature and salinity (fig. 3.33) tended to correlate - positively and negatively. During winter - September to February - the correlation was positive, with predominantly negative relationships from March to August. For some dates, 2 regions of water can be identified, including 25 April, 21 May, 14 August and 11 September. On 11 September, the relationship was positive in both regions. In April and May, however, at lower salinity levels the correlation was positive and negative in more saline water. Such situations may have been caused by entrainment behind rapid outflow or ponding.

During the summer months, high salinity is associated with a more mixed water column where warming of the surface water is lessened by its mixing with deeper cooler water. Lower salinity water lies close to the surface of more stratified regions where the surface is warmer, as it is consistently exposed to insolation, being isolated from deeper water. Thus during the summer, surface river discharge is warmer, while in winter the runoff is cold, as there is insufficient insolation to warm it and deeper water is warmer, producing negative and positive correlations respectively.

In the OB (fig. 3.34), relationships between temperature and salinity are less clear than for the IB. From September to January, salinity and temperature were positively correlated but within the OB there were no negative correlations as explicit as those for the IB. The Lynn of Lorne on 25 April displayed a strong negative relationship. The OB was more likely to contain more than one water

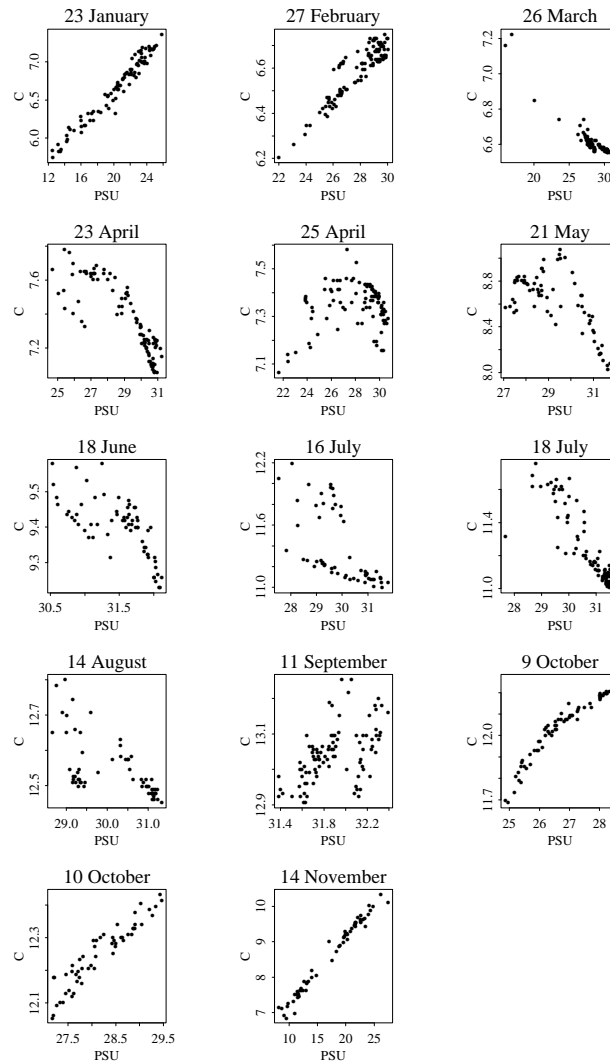


Figure 3.33: Scatter plots of the Inner Basin surface salinity and temperature data.

mass, as may be expected with its position between the less saline IB and the Firth of Lorne. For 25 April until 14 August it can be seen in the surface plots (Appendix A) that there was a mixture - with the northern end of the basin being positively correlated and the seaward end negatively.

Temperature and Chlorophyll

In the inner basin, during the winter - October to February - temperature and chlorophyll were negatively correlated. fig. 3.35. At this time, entrained water would have been the warmest, but the lowest in chlorophyll. From March to July, chlorophyll was associated with warmer water with a weaker relationship than that during winter. During the summer, a stable, shallow surface layer will be

warmer than more mixed water and with available nutrients, will tend to be more productive.

In the outer basin (fig. 3.36), correlations again were lower, particularly during the summer, but the overall pattern similar. Of the positive correlations, that of the Lynn of Lorne was again stronger than those for the outer basin. This may be as it is smaller more stable area containing a single region of water.

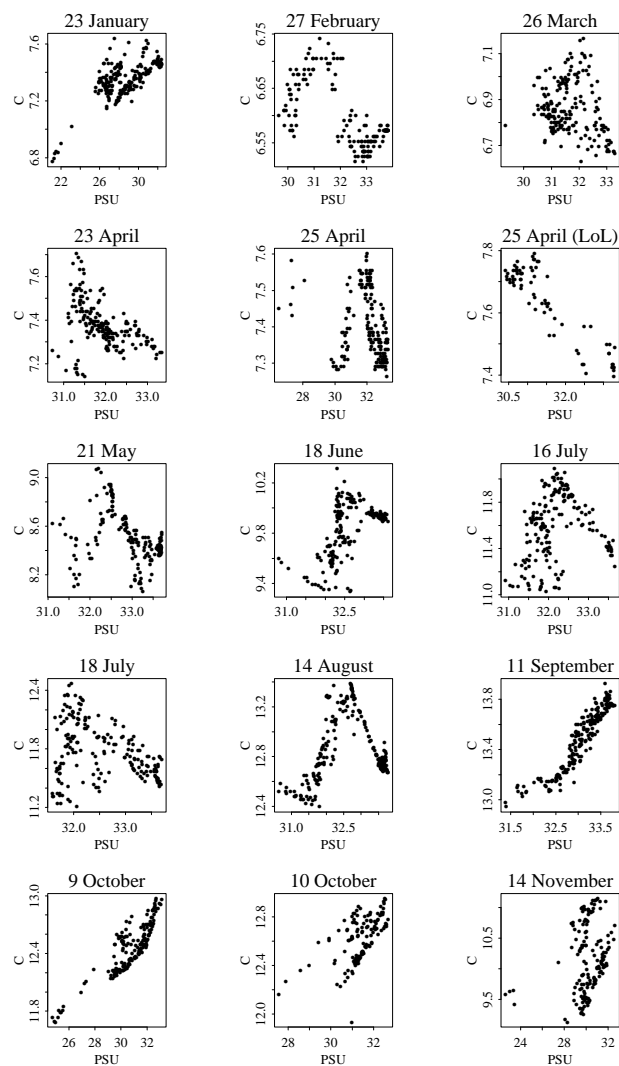


Figure 3.34: Scatter plots of the Outer Basin surface salinity and temperature data .

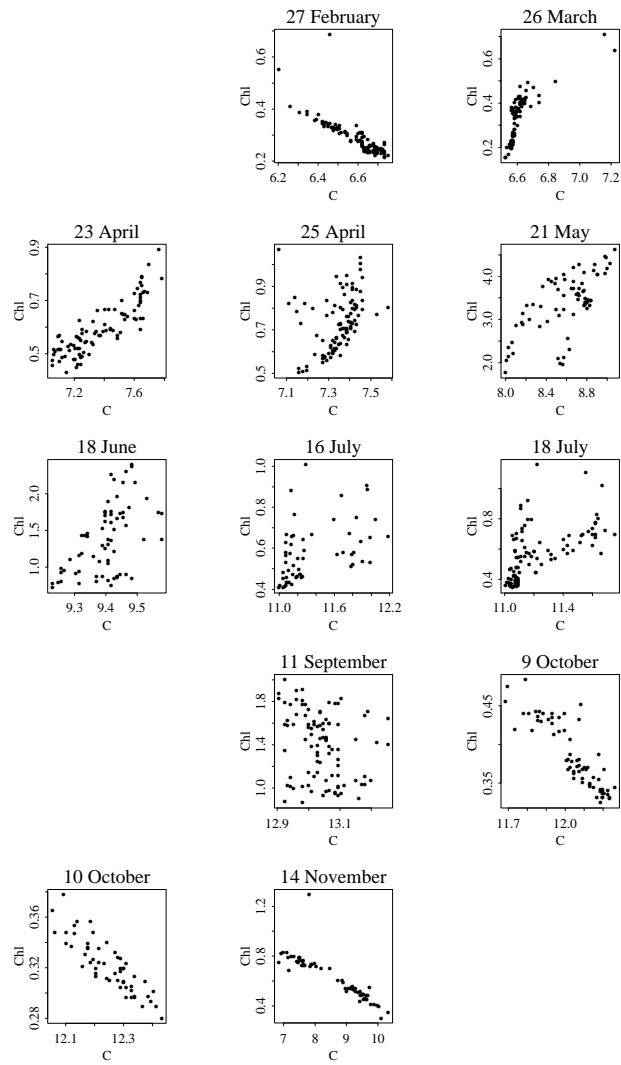


Figure 3.35: Scatter plots of the Inner Basin surface temperature and chlorophyll data .

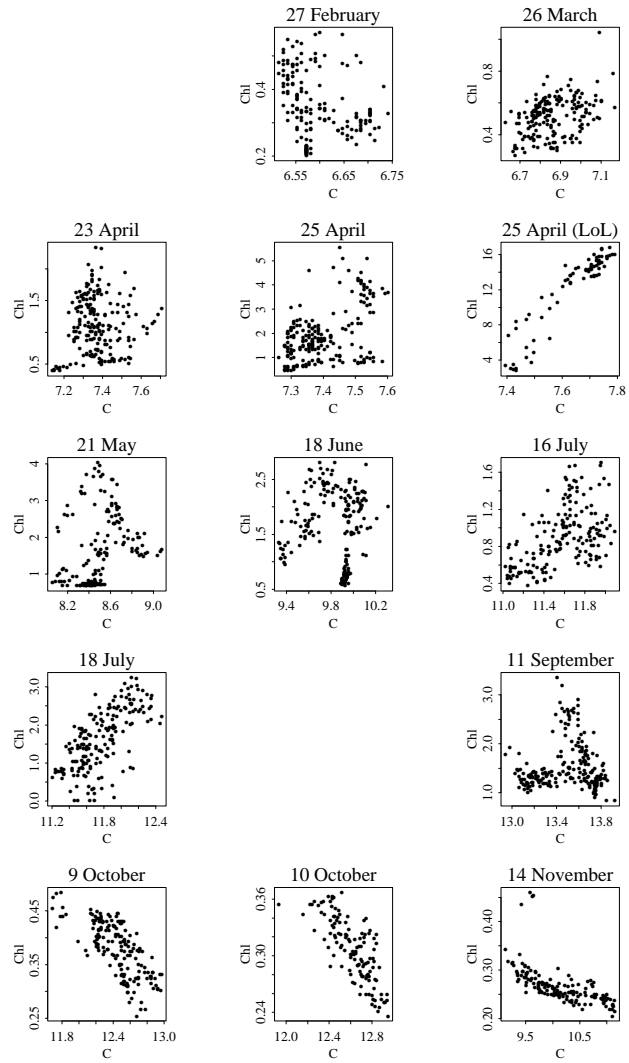


Figure 3.36: Scatter plots of the Outer Basin surface temperature and chlorophyll data .

3.4 Conclusions

Spatially averaging the axial data to provide seasonal cycles for Loch Linnhe, provides no more information than sample sites. The temporal resolution of the data collection also means that there is very little information about the timing, duration and size of the spring bloom and subsequent blooms. What we do learn from the averaged axial data, as it is smoother than that for the sample sites, is that the water column varies along the basins and that spatial variability should be considered. The horizontal relationships between variables, particularly in the OB where there appears to have been more than one body of water (at least in the surface layer) for a substantial part of the year and the variability of the surface layer structure, shown in Appendix A, would suggest that the mechanisms causing horizontal variability are of interest.

Information on stratification and nutrients can be derived from this chapter. The IB is more stratified and has a shallower surface layer than the OB. The IB water column, in general, and the surface layer in particular is more variable than that of the OB. This is due to most of the river input into Loch Linnhe flowing into the head of the IB. More importantly, exchange between the outer and inner basins appears to have been frequent, occurring most months according to the concurrence of the deep water temperature. In 1991 the spring bloom was late and productivity low for both phytoplankton and zooplankton throughout Loch Linnhe. Nutrient depletion was not, however a problem so the high level of turbidity may have contributed. Productivity in the Firth of Lorne, the coastal sea of Loch Linnhe, was also low leading to low levels of phytoplankton being advected into the basin. The density of *Aurelia aurita* was high, possibly from strong links with the sea. This would have contributed to the low zooplankton population along with the low prey densities. The progression of growth of phytoplankton, then mesozooplankton, then gelatinous zooplankton can be seen to move up the loch system from the Firth of Lorne to the IB - from the area least affected by freshwater discharge to that most.

Chapter 4

Interpolation and Analysis

4.1 Introduction

As shown in Chapters 2 and 3, the dataset collected in 1991 is large and contains a substantial spatial component. When basin averages are taken, however (as in Chapter 3,) little information is provided which could not have been derived from sample site and mooring data. In order to consider the spatial aspect of the data, visualisation is an important tool which requires the interpolation of the data over a regular grid with the type of gridding algorithm being the first consideration.

Statistical analysis of spatial data, requires a very large dataset as it is not independently distributed. The ungridded dataset is too small and analysis of the interpolated data is affected by the algorithm applied. For these reasons spatial statistics have not been applied to the data and the temporal resolution also does not allow for time series analysis.

For the model, turbidity and the relative importance of self-shading by phytoplankton are calculated. The principal statistical causes of seasonal variability in turbidity and pycnocline depth are also of interest and the seasonal cycles are replicated using simple statistical models.

4.2 Data Visualisation

Visualisation of 2-dimensional data, such as the surface and axial cruises, requires the generation of a uniform grid from the observed data. The initial stage was to determine an appropriate interpolation method. I considered in detail GTGRID, an optional software application for PV-Wave Command Language, which allows a choice of gridding methods and SGRID a gridding application available within STAMS.

GTGRID initially estimates locally, within a defined radius, using the known values and then extends the estimated area using the estimated values. The resulting surface may then be smoothed. I considered the ‘cluster’ and ‘weighted’ options, but found no difference in the generated grid. ‘Cluster’ is recommended for noisy or closely spaced data as it ignores excessive gradients by averaging. GTGRID applies gradient methods, these assume that a parameter increasing (or decreasing) will continue to do so. This can create problems with edge effects and with sparse, noisy data. The variability of a dataset has the potential to be increased as values outside the bounds of the data may be produced. Gradients in biological systems may of course continue and as there is, by definition, no information outside the region of data collection, it is very difficult evaluate interpolation in this area.

SGRID applies a weighted average, also within a defined radius, and the weighting may also be determined. Weighted averages are far more conservative - the value of a point is found by taking a (variable) weighted average of all data points within a predetermined radius. Beyond the range of the data, the value remains the same as the last point and values cannot be generated outwith the range of the data. Both methods allow for the interpolation to be restricted to a defined region, enabling the coastline (or seabed) to limit the interpolation.

I compared the performance of the gridding methods over 3 sets of IB surface cruise data:

- ln(mesozooplankton) - 10 October
- salinity - 14 November
- salinity - 11 September

These examples were chosen as the zooplankton data was collected at a lower resolution than the other surface data and November and September represent the widest and narrowest ranges of salinity values. The two methods were compared over three radii. The GTGRID radius is defined as a given percentage of the grid points in the x and y directions away from the node being estimated, whereas the SGRID radius is defined by distance from the estimated node. Thus with a non-square grid of 15km horizontally by 2.5km, with the number of grid points scaled to distance, a GTGRID radius of 10% is equivalent to a SGRID radius of 1.5km horizontally and 0.25km vertically. As the radii cannot be equivalent on a non-square grid, I compared the methods by horizontal radii, using 10% (1.5km), 15% (2.25km) and 20% (3km) on a grid of 210 points horizontally and 35 vertically.

Table 4.1 illustrates the removal, by smoothing, of extreme values generated by GTGRID. With a radius of 15%, the data range fell by 13.76% of its presmoothed value, after 20 smoothing operations, however, the range still exceeded that of the observed data. From tables 4.1 & 4.2 it can be seen that in all cases, GTGRID output exceeded the range of the observed values, while SGRID remained within

the range and on four of six occasions equaled boundary values. The greatest GTGRID error was for the noisiest dataset - November - where with a radius of 20% the maximum value was 41.8% greater than the maximum observed value. With the less variable September data at 20% the maximum only exceeded the observed max. by 0.25%. With noisy data, increasing the radius increased error, however, with smoother data the reverse was true.

The interpolated data may be viewed as contour or colour plots.

Table 4.1: The ranges of $\ln(\text{zooplankton})$ values produced by the gridding methods.

		minimum	maximum
Observed Data		5.24296	6.83674
GTGRID not smoothed	10%	5.01967	6.94836
	15%	5.02041	7.00473
	20%	5.02188	7.02589
GTGRID smoothed	10%	5.11451	6.92426
	15%	5.23322	6.94458
	20%	5.23303	6.96378
SGRID	1.5km	5.24296	6.83674
	2.25km	5.24296	6.83674
	3km	5.24296	6.83674

Table 4.2: The ranges of salinity values for November and September produced by the gridding methods.

		November		September	
		minimum	maximum	minimum	maximum
Observed Data		8.201	26.135	31.383	32.395
GTGRID smoothed	10%	7.27	31.434	31.13	32.587
	15%	7.37	36.151	31.13	32.494
	20%	7.47	37.052	31.13	32.475
SGRID	1.5km	8.201	25.655	31.383	32.382
	2.25km	8.201	25.655	31.383	32.382
	3km	8.201	25.655	31.383	32.382

The zooplankton contour plots display similar patterns despite the gridding method, but because of the different regions covered by the radius, SGRID was more likely to produce across loch bands, with GTGRID more likely to generate along loch bands. From the salinity plots the tendency for edge effects to be produced by the gradient method can be seen, particularly for November when the gradients were steeper.

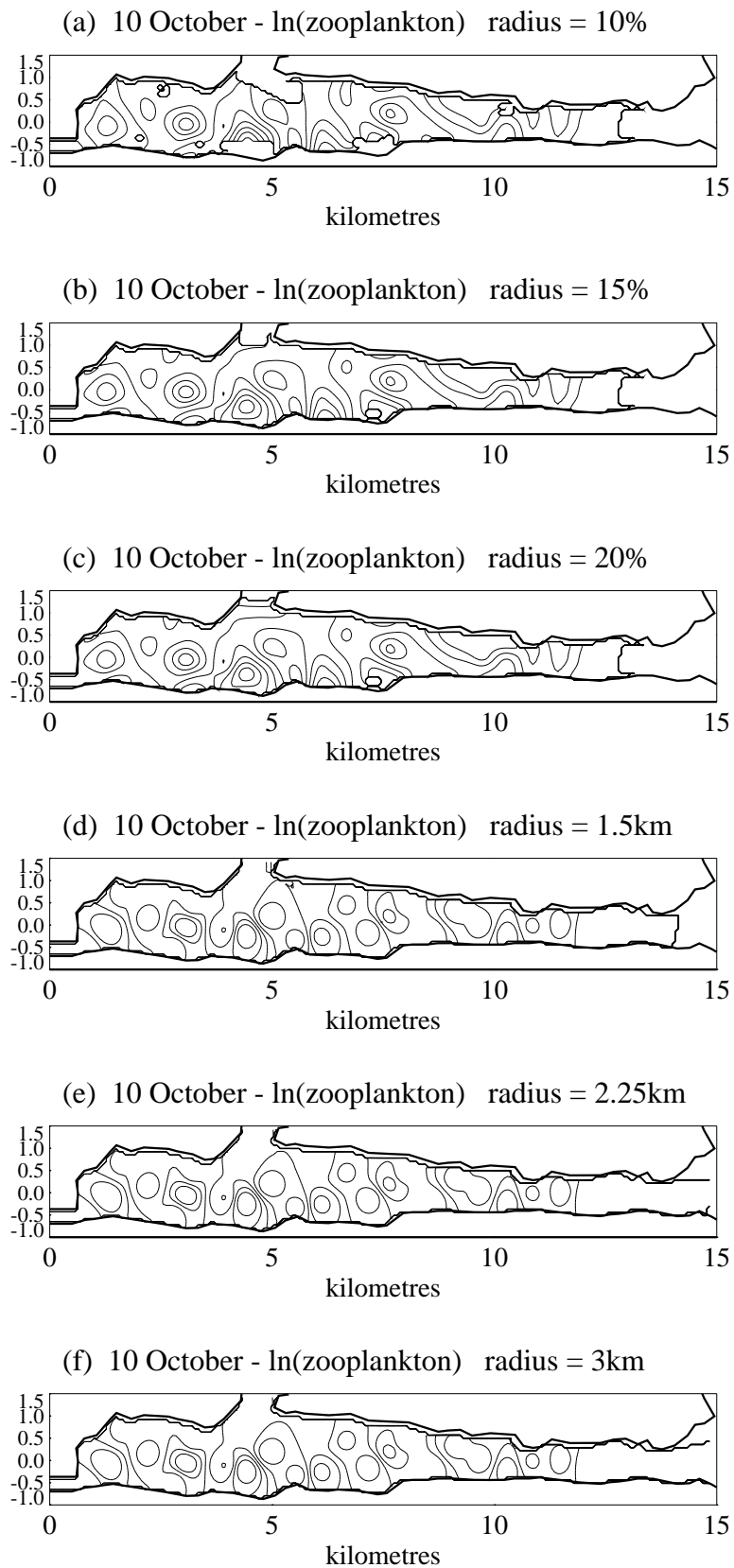


Figure 4.1: Contour plots of gridded zooplankton data, (a)-(c) gridded using GTGRID and smoothed and (d)-(e) gridded with SGRID.

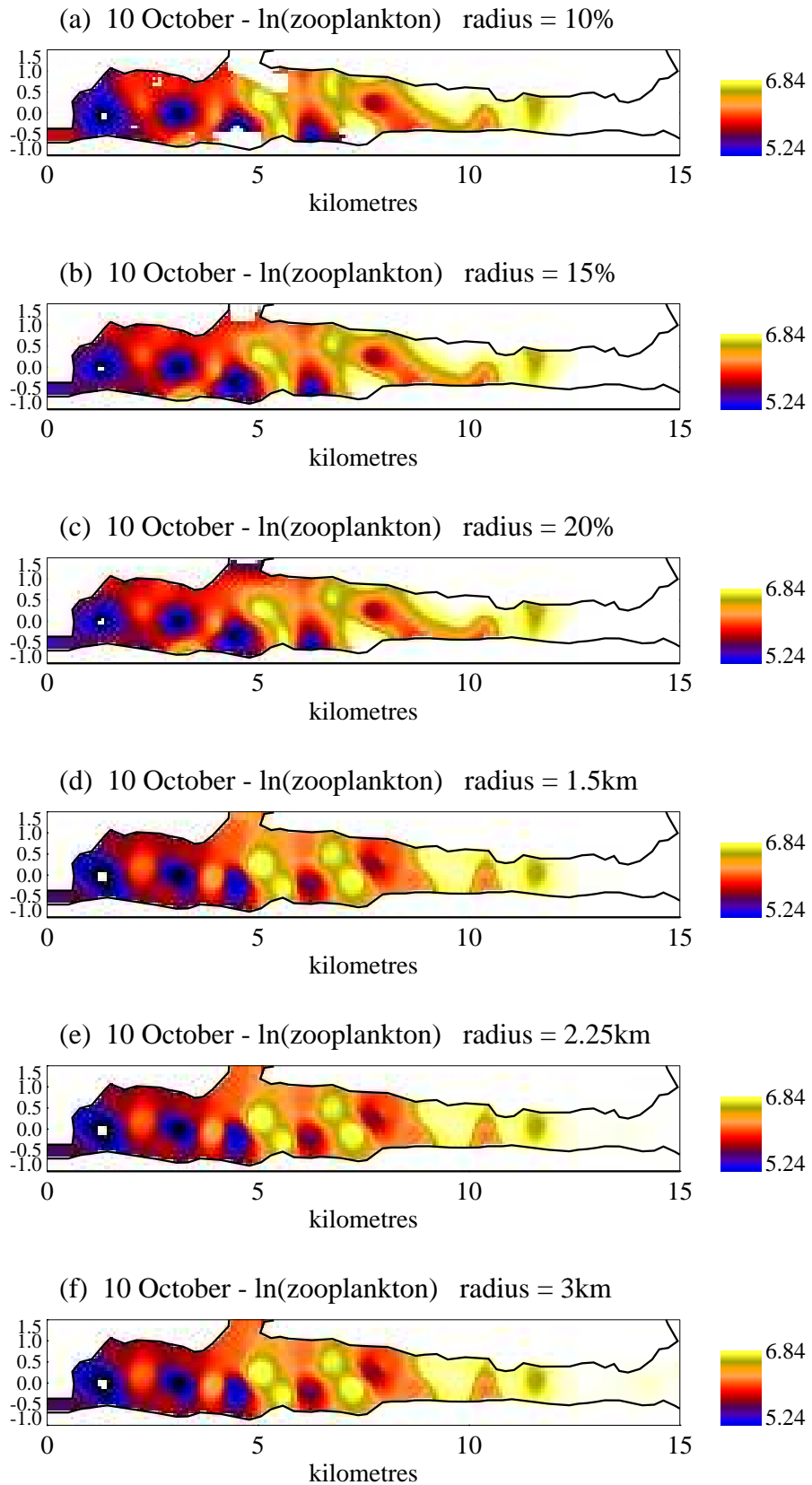


Figure 4.2: The colour plots corresponding to fig. 4.1.

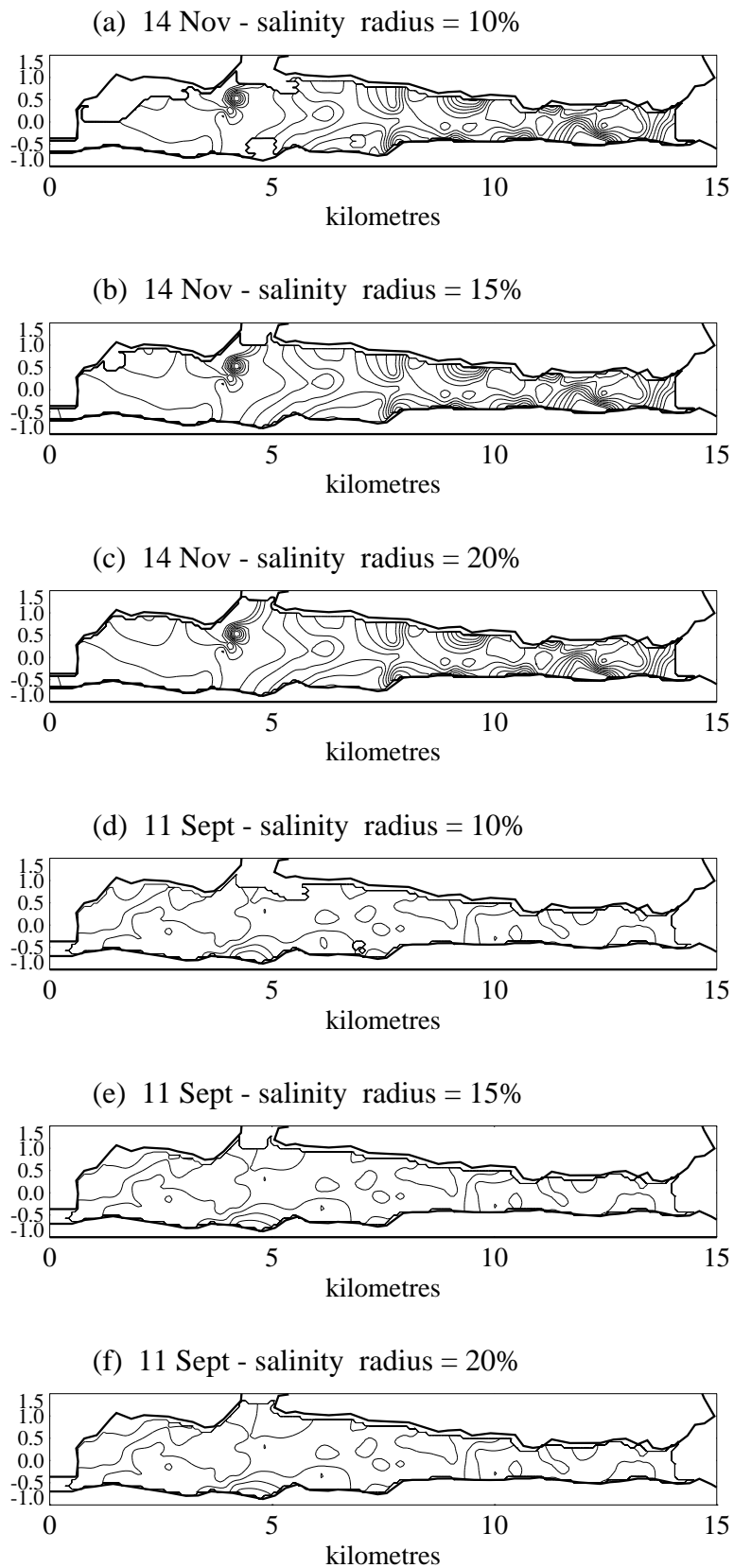


Figure 4.3: Contour plots of salinity data gridded with GTGRID, (a)-(c) 14 November and (d)-(e) 11 September.

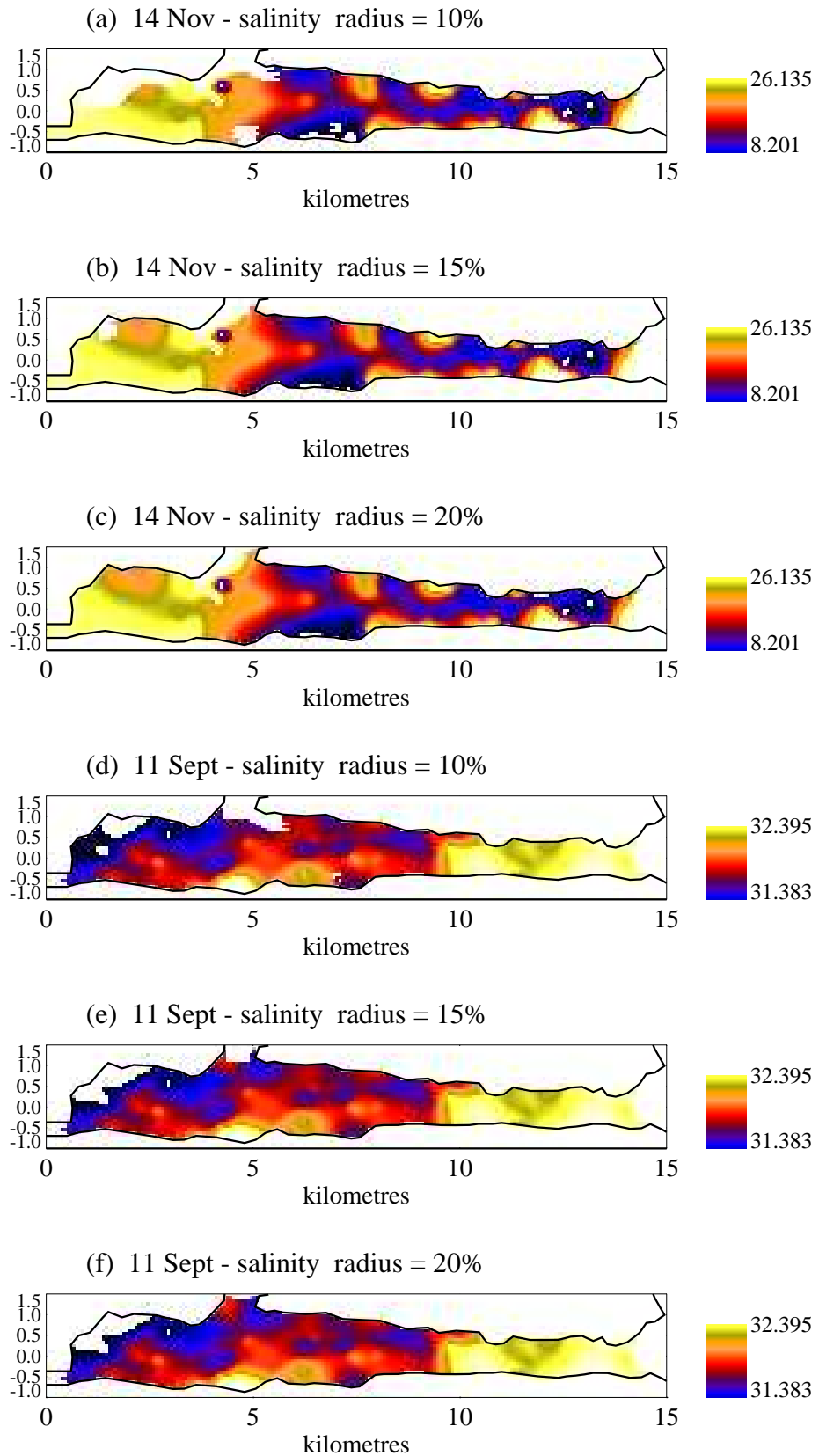


Figure 4.4: The colour plots corresponding to fig. 4.3.

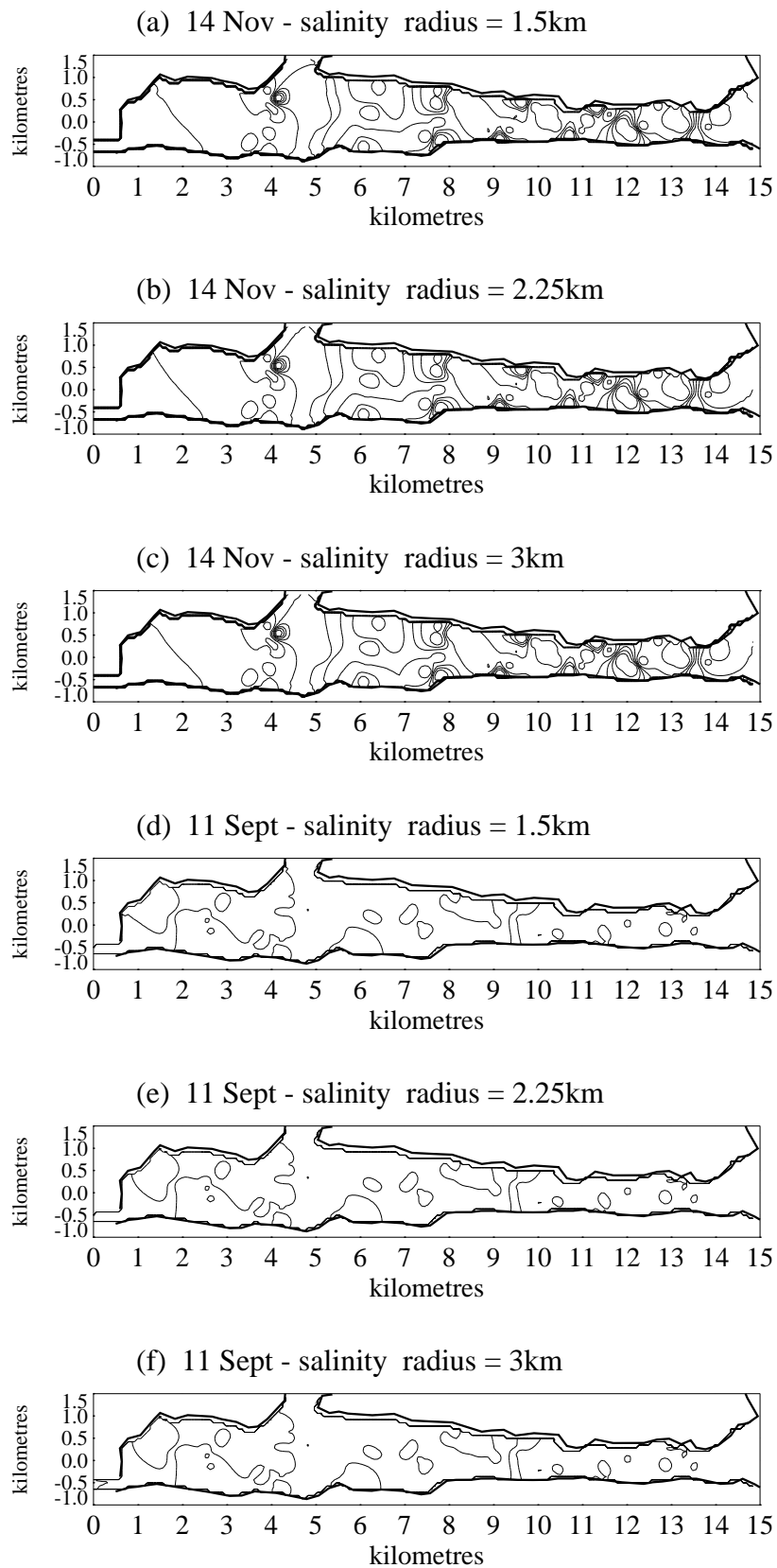


Figure 4.5: Contour plots of salinity data gridded with SGRID, (a)-(c) 14 November and (d)-(e) 11 September.

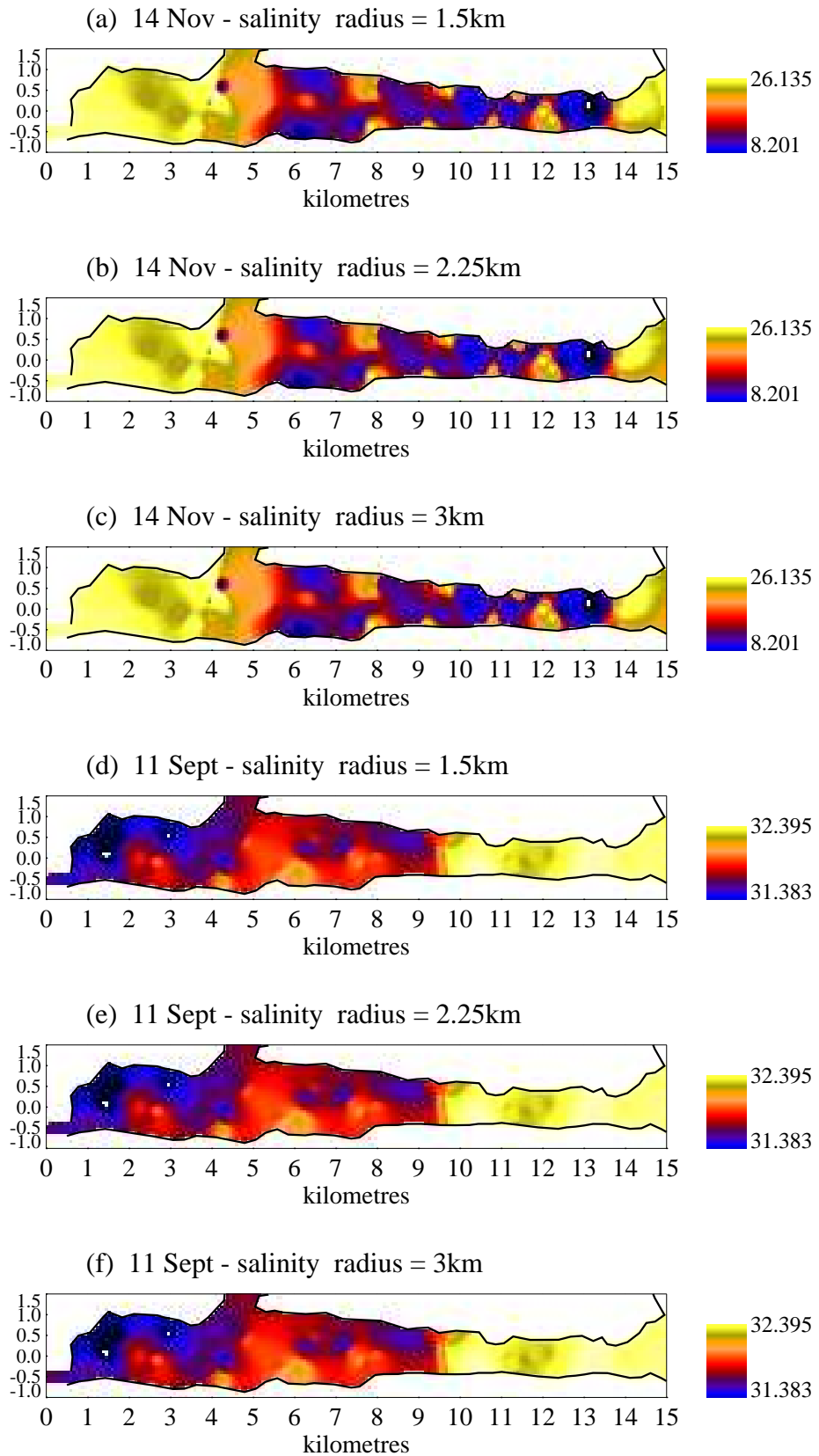


Figure 4.6: The colour plots corresponding to fig. 4.5.

The axial data being more highly resolved along the cruise track and with vertical gradients tending to be steeper than horizontal, provides more problems - particularly as there is often a single vertical gradient. GTGRID creates steep gradients, generates values beyond the range of the data, has pronounced edge effects with values increasing or decreasing sharply towards the edges and has more problems with the contrast between the close vertical spacing of the data compared to the wide horizontal spacing. With SGRID (unless a very finely resolved grid is generated) the close spacing of data points leads to the loss of extreme observed values through averaging, with a resulting narrowing of the range of values. With both methods the patchy distribution of chlorophyll was particularly problematic.

Despite there being problems with both methods, I chose to use SGRID as the more conservative of the two. Though SGRID may not generate values over the entire range of observed values, it always encompassed most of the range ($> 95\%$ in all the above cases) and never exceeded it.

The grid dimensions and radii were chosen to maximise visual information within a 'reasonable' time. The radius was chosen to be sufficient to provide coverage of the loch surface with the usual data spacing, breaks in the cruise track would not necessarily be gridded over. With SGRID the gradient of the weighting may also be defined and was set at $(1/\text{distance})^3$ to lessen the impact of points further away.

4.3 Predicting Pycnocline Depth

A statistical representation of changes in pycnocline depth has the potential to be a useful tool in modelling the annual cycle of Loch Linnhe. The identification of the key elements controlling the depth of the surface layer and an indication of their relative importance is of interest alone. It is possible that the timescale of the data collection does not enable the influence of the changes in surface layer depth to be apparent in the biological data, however, by varying the pycnocline depth in the model, biological information may be derived. The aim is to be able to run a yearly model of pycnocline depth, driven by daily time series. While a mechanistic approach to modelling the pycnocline depth would be preferred, there is insufficient information. This exercise is initially only relevant to Loch Linnhe, which is unusual with respect to other Scottish sea-lochs in both its size, depth and orientation and the dataset is not substantial enough to generate a conclusive result for Loch Linnhe, let alone be applied to other systems.

The models were derived by regressing possible forcing functions against pycnocline depths estimated from the sample site data. With a process as complex as changes in surface layer depth, regression analysis is limited as so many factors - and combinations of events - may be of importance; including changes (e.g. prolonged period of wind from the SW switching to the east) and length of time a phenomenon has occurred for (e.g. long period of high irradiance) rather than

simple daily values. The range of the explanatory variables also varied considerably more over the entire year than over the days pycnocline depths are available for.

Parameters investigated as being possible influencing factors were:

- daily mean wind speed
- $|222^\circ - \text{daily mean wind direction}|$
- freshwater discharge
- precipitation
- irradiance
- air temperature
- lunar tidal cycle

Wind, precipitation, irradiance, air temperature and tidal cycle were taken from values for Oban. The axis of the IB and OB of Loch Linnhe lies along 222° , hence the wind direction being centred around this value. Freshwater discharge was taken to be daily flow of the Rivers Lochy and Nevis. The lunar tidal cycle was estimated by the maximum predicted tidal range of the day or the maximum predicted tidal height. As I am only interested in a daily value the semi-diurnal tidal cycle was ignored.

4.3.1 Inner Basin

The analysis commenced with pycnocline depths estimated from the highest resolution sample site data, which encompasses 23 days, with two measurements on two days. As the annual cycle produced from this generates outlying values on some days with extreme weather conditions, a further dataset was then constructed using the lower resolution sample site data (which added 2 days) and thermistor chain data. The low resolution of the thermistor chain depth profile, especially as the pycnocline in the IB moved over a relatively small range, decreases the reliability of this dataset. It is also uncertain whether the pycnocline and the thermocline coincided on these days, as for a temperature greater than 5°C , a change in temperature of 1°C has a comparable effect on density as a change in salinity of 0.1 PSU (Open University 1989) - therefore in Scottish sea-lochs, the density distribution is primarily determined by salinity. The thermistor chain values used were mainly from days around extreme weather events in order to cover a wider parameter range, and those days where the thermocline appeared to be more clearly defined. A further regression model was obtained from this data.

The most significant parameters from each of the models were combined to create a compromise between the two models. The greater accuracy of the high resolution data would be expected to generate a better model, explaining more of the variance. The limited number of days however means that the parameters do not cover a great enough annual range and any prediction using the model would be unreliable over much of the parameter range. Using the expanded dataset, the parameters cover much more of the annual range for 1991, though the lack of thermistor chain data for the winter months prevents values being obtainable for the highest river discharge and wind speed values.

From the high resolution dataset (*odat*) the most suitable regression model is:

$$\begin{aligned} Pycnocline\ Depth = \beta_0 + \beta_1(MW_{-1})^3 + \beta_2 \ln |222^\circ - MD| \\ + \beta_3 \ln |222^\circ - MD_{-2}| \end{aligned} \quad (4.1)$$

The 'best' model from all the data (*adat*) is:

$$\begin{aligned} Pycnocline\ Depth = \beta_0 + \beta_1 I_{-3} + \beta_2 \ln |222^\circ - MD| \\ + \beta_3(MW_{-1})^3 + \beta_4(RD_{-3})^2 \end{aligned} \quad (4.2)$$

Where,

MW - daily mean wind speed
MD - daily mean wind direction
I - irradiance
RD - freshwater discharge

Subscripts indicate the number of days previously of the parameter, e.g *RD*₋₃ is freshwater discharge 3 days ago.

The best compromise between the two models is:

$$\begin{aligned} Pycnocline\ Depth = \beta_0 + \beta_1 \ln |222^\circ - MD| + \beta_2 I_{-3} \\ + \beta_3(MW_{-1})^3 + \beta_4(RD_{-3})^2 \end{aligned} \quad (4.3)$$

For *odat* the full model is:

$$\begin{aligned} Pycnocline\ Depth = 7.5183 - 0.8763 \times \ln |222^\circ - MD| \\ - 0.0003 \times I_{-3} + 0.0030 \times (MW_{-1})^3 \\ - 3.28 \times 10^{-5} \times (RD_{-3})^2 \end{aligned} \quad (4.4)$$

$$R^2 = 64.74\% \quad p\text{-value} = 0.0001377$$

The corresponding model for *adat* is:

$$\begin{aligned} Pycnocline\ Depth = 10.0074 - 0.7777 \times \ln |222^\circ - MD| \\ - 0.0006 \times I_{-3} + 0.0017 \times (MW_{-1})^3 \\ - 4.77 \times 10^{-5} \times (RD_{-3})^2 \end{aligned} \quad (4.5)$$

$$R^2 = 56.23\% \quad p - \text{value} = 9.326 \times 10^{-15}$$

These models compare well with the initial models, where the multiple R^2 for the high resolution dataset was 69.9% along with a p-value of 6.042×10^{-6} , and the corresponding figures for the entire dataset were 59.62% and 1.887×10^{-15} .

The parameters found in this analysis in general agree with those which are shown in Chapters 5 and 6 to be important in the vertical structure of the loch. The time lag for river discharge to be influential may be partly due to the mooring being sited towards the southern end of the basin and the greater importance of irradiance for *adat* may be related to it being obtained partly from thermocline data.

Wind speed is known to increase mixing in the surface layer and in fjords where there is limited access for cross axial winds, the direction would also be expected to be important. As the direction of the axis of Loch Linnhe coincides with the prevailing wind, the influence of the wind direction on Loch Linnhe may be greater than in other Scottish fjords. It is interesting that the analysis should find (mean wind speed)³ to be the best representation of wind speed as the power (P) of air (or a fluid) is proportional to its velocity (v) cubed:

$$P(v) = E(v)/t = 0.5 \times \rho \times A \times v^3 \quad (4.6)$$

Where,

ρ - density
 E - energy
 A - area
 t - time

With river discharge however, using $(RD_{-3})^3$ instead of $(RD_{-3})^2$, the *adat* model is slightly better and for *odat* slightly worse, with the change in R^2 in both cases being less than 1%.

The annual cycles of pycnocline depths for 1991, from the above models are illustrated in figs. 4.7 & 4.8. The high resolution model, in particular, still produces some very deep values. These are primarily generated by high wind speeds which affect both models.

The days with the most extreme values for both wind speed and river discharge are not encompassed by the available pycnocline depth data. These parameters are the most variable and by using powers this further increases their outlying values. The reduced models with $(MW_{-1})^2$ and RD_{-3} generate more stable annual cycles and perform well compared to the original models with R^2 's of 60.68% and 53.96% for *odat* and *adat* respectively. For generating pycnocline depths within the loch model, eqn 4.7 is more conservative as the influence of extreme values of wind speed and river discharge is lessened.

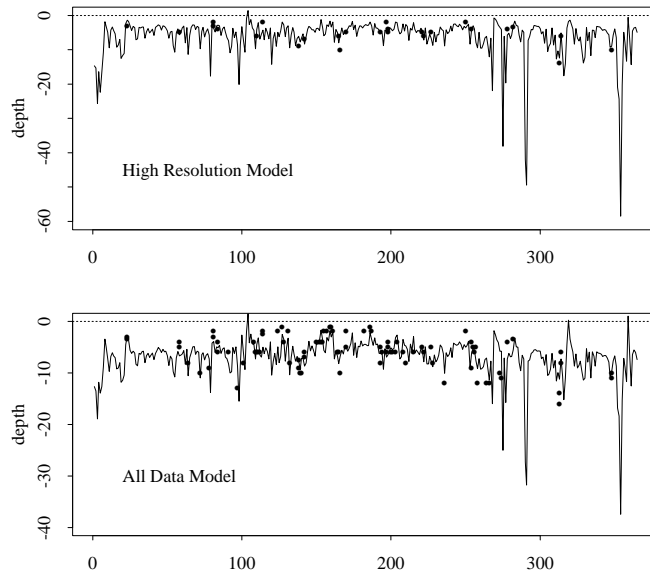


Figure 4.7: The annual patterns of pycnocline depths generated by the full regression models, the points represent the observed values of the predicted variable.

$$\begin{aligned}
 \text{Pycnocline Depth} = & \beta_0 + \beta_1 \ln |222^\circ - MD| + \beta_2 I_{-3} \\
 & + \beta_3 (MW_{-1})^2 + \beta_4 RD_{-3}
 \end{aligned}
 \tag{4.7}$$

4.3.2 Lynn of Morvern

A similar technique was applied to the Lynn of Morvern data but models explained very little of the variation and were extremely sensitive to changes in the dataset. Small changes to the dataset generated large changes in the significant variables. A variety of reasons may contribute towards this. Stratification in the LoM is weaker than in the IB making estimation of pycnocline depth less reliable, it also moves over a much greater range than in the IB. This generates a noisier estimate of pycnocline depth and would be expected to contain significantly more error than for the IB, creating more problems in the regression analysis. The closer proximity of the LoM to the Sound of Mull may also introduce more factors in determining the surface layer depth such as the semi-diurnal tidal cycle and coastal upwelling. Wind direction may also be more complicated, with wind being channeled from the Sound of Mull, Firth of Lorne and down Loch Linnhe, while Mull may provide some protection from the prevailing wind which affects the IB. In Chapter 6, it is hypothesised that Ekman drift may be occurring in the LoM which would also be expected to affect surface layer depth.

4.3.3 Outer Basin

There was no thermistor chain at the outer basin mooring and only 17 days of sample site data. Analysis did however produce some interesting results. Precipitation rather than river discharge is a very important component of the model, with the precipitation of the previous day explaining 55.96% of the variation compared to the river discharge of 3 days prior being the important variable in the IB. With wind speed, it is the wind speed on that day which is included in the model, rather than the previous day's. The pycnocline depth in the OB may respond more quickly to meteorological forcing as it is less stratified.

$$\begin{aligned} Pycnocline\ Depth = 20.5500 + 0.0341 \times (P_{-1})^2 - 0.1248 \times |222^\circ - MD| \\ - 0.0041 \times MW^3 \quad (4.8) \end{aligned}$$

$$R^2 = 82.88\% \quad p - value = 5.328 \times 10^{-6}$$

Unlike the IB, inclusion of the lunar tidal cycle improves the model performance, with the adjusted R^2 increasing from 79.45% to 83.09% with tidal range being included in the model. Though the improvement is small, it reflects the closer proximity of the OB mooring to the sea.

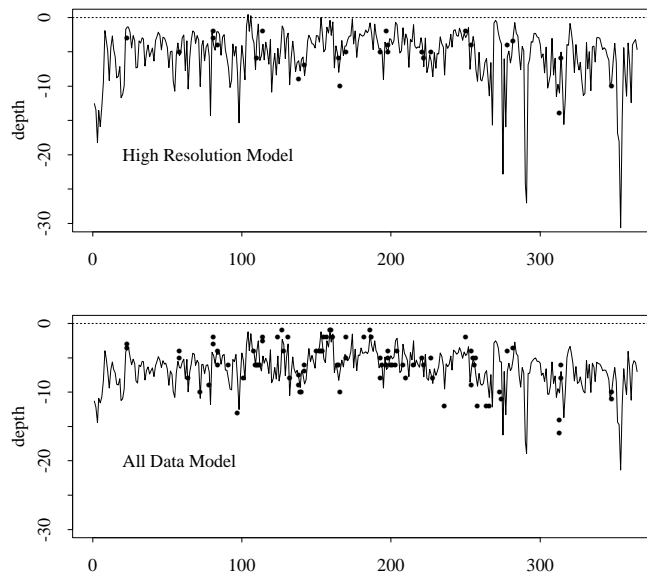


Figure 4.8: The annual patterns of pycnocline depths generated by the reduced model.

$$Pycnocline\ Depth = 26.4758 + 0.0333 \times (P_{-1})^2 - 0.01136 \times |222^\circ - MD| - 0.0037 \times MW^3 - 2.4668 \times T_{-3} \quad (4.9)$$

$$R^2 = 86.85\% \quad p - value = 4.824 \times 10^{-6}$$

Where,

P: precipitation T: tidal range

The resulting annual cycle cannot be considered representative of the changes in pycnocline depth in the outer basin as the 17 days of data encompass a limited range of the explanatory variables.

4.4 Turbidity

Measurements of downwelling irradiance at the three sample sites within the loch were used to calculate the attenuation coefficient K at each site. The natural logarithm of irradiance was linearly regressed against depth (m) with the surface 10m being considered - as the loch is turbid, beam attenuation measurements were limited to the surface.

$$\ln(light) = \beta_o + \beta_1 \times depth \quad (4.10)$$

Where β_1 is K .

The relationship between K and chlorophyll was then ascertained from linear regression of K on mean chlorophyll, (mg m^{-2}) for the surface 10m, to calculate K_o , the background attenuation.

$$K = \beta_o + \beta_1 \times chlorophyll \quad (4.11)$$

Where β_1 is ρ .

$$K_o = K - \rho \times chlorophyll \quad (4.12)$$

At the IB mooring, there is no significant relationship between K and chlorophyll when the entire year is considered. Only using the summer months, May to September, of low river discharge, a value of $\rho = 0.0832$ is found, with chlorophyll accounting for 82% of the variability in attenuation. Tyler (1983) by discounting extreme values after heavy rainfall, calculated $\rho=0.0236$ considering the entire year (though the removed values were from winter.) At the OB mooring, using

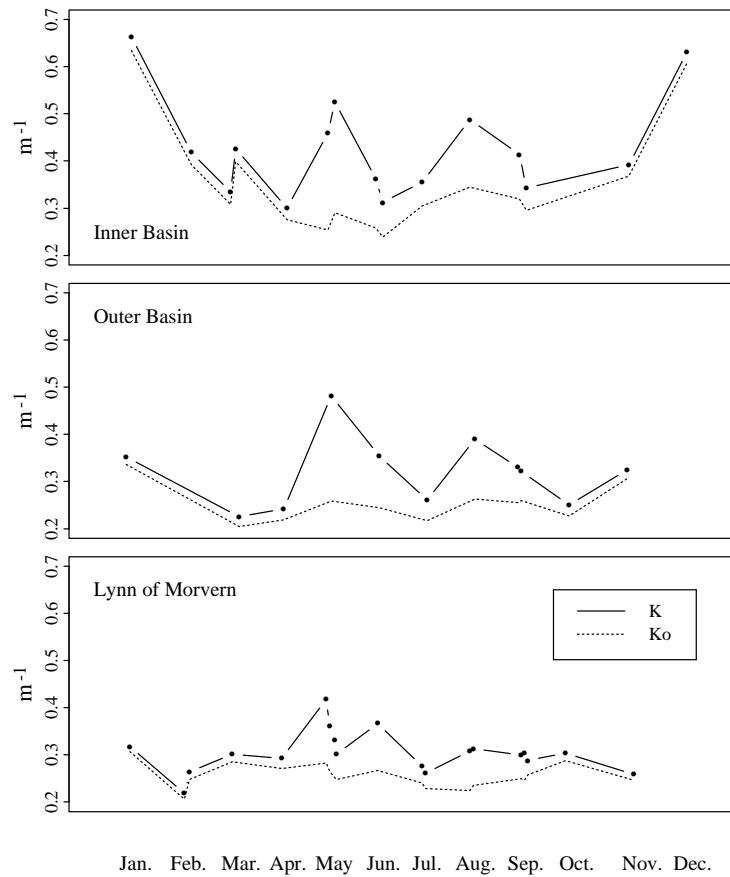


Figure 4.9: The attenuation coefficient (K) and background attenuation (Ko) at the three sample sites.

data from the entire year, chlorophyll accounted for 72.66% of variability in K and $\rho = 0.0713$ and at the LoM site, $\rho = 0.0526$ with chlorophyll producing 69.2% of variation.

Overnell and Young (1995) found turbidity in the inner basin to be principally due to the spring-neap tidal cycle (5.2.2) with extreme river discharge also being influential. From regression I found the most important influences on background attenuation to be maximum tidal height 2 days previously and $(RD_{-1})^2$ which account for 84% of the variability between them. If the February value is ignored, it was the only datapoint collected after heavy river discharge, less variability is explained and the importance of river discharge falls but the contribution of the tidal cycle remains similar.

4.5 Conclusions

The most appropriate interpolation algorithm for the spatial data is the more conservative. This maintains all predicted output within the range of the observed data and does not generate large peaks and troughs or obvious edge effects. Though both perform similarly for smoother datasets, GTGRID created problems for more heterogeneous data and in particular the vertical data which often has a strong gradient between the seabed and surface.

Regression analysis identified important components of the causes of pycnocline depth in the inner basin and the outer basin. For the Lynn of Morvern no clear results were obtained. The applicability of these results elsewhere is unclear, in particular the relative importance of each factor. An initial problem is the estimation of the depth of the surface layer from the vertical profile measurements. In the LoM, the less defined surface layer probably contributed to the problems in identifying the causes of the surface layer depth, as the regression models were very sensitive to small changes in the predicted variable. The orientation of Loch Linnhe may increase the importance of wind in determining pycnocline depth, compared to other sea-lochs such as Loch Etive which are more sheltered from the prevailing wind. In Loch Etive, however, river discharge may play a greater role as the volume of river discharge into the head of the loch is greater. The closer proximity to the sea may increase the importance of the lunar tidal cycle for surface layer depth in the OB.

Linear regression revealed river discharge, when particularly high and the lunar tidal cycle to be the most important components of turbidity in the IB, which agrees with the findings of Overnell and Young (1995). That tidal mixing affects beam attenuation at the surface despite the basin being 150m deep, illustrates the extent of mixing and resuspension in Loch Linnhe being generated by the lunar tidal cycle.

Despite statistical analysis being limited by the spatial and temporal resolution of the data collection, it is possible to ascertain that the wind - speed and direction, river discharge and lunar tidal cycle all play important roles in determining conditions within the loch.

Chapter 5

Vertical Processes

5.1 Introduction

In this chapter the vertical processes, their causes and the effect of the hydrodynamics on the biological life of Loch Linnhe are considered. As shown in Chapter 1, a wide variety of behavioural responses are found in fjords to wind, tides and topography and in Chapter 4 wind and river discharge were shown to be influential in Loch Linnhe. I would like to ascertain the effects of meteorological and tidal forcing on Loch Linnhe, the differences and similarities between Loch Linnhe and other fjord systems and possibly identify some of the causes of these relationships. Initially the physical, then the biological structure of the inner basin are considered, then similarly for the outer basin. The entire collection of interpolated axial data is contained in Appendix B.

5.2 Inner Basin: Physical Structure

The physical structure of fjords may be considered to be largely determined by the depth of the surface layer and the vertical density gradient. In Loch Linnhe there is little evidence of the existence of a boundary lower than that between the surface and intermediate layers. I consider there to be surface, intermediate and benthic layers, the last being the water in direct contact with the seabed.

An important step in understanding temporal variation is understanding the controlling mixing processes at different times. In Loch Linnhe we have a variety of data sources to reconstruct the vertical structure from.

5.2.1 Stratification Index

The vertical density gradient varies between fjords and seasonally within a fjord. The level of stratification, at the Inner Basin sample site, was calculated using the vertically averaged potential energy anomaly, φ , as described by Simpson et al. (1982). φ (Jm^{-3}), is the energy requirement per unit volume to bring about complete vertical mixing, thus indicating the degree of stratification. The temperature and salinity data from the high resolution samples (with < 1 m between each sample) were converted to produce the vertical density (σ_t) distribution. From this φ was calculated using equation (5.1):

$$\varphi = \frac{1}{h} \int_{-h}^0 (\bar{\rho} - \rho).g.z.dz \quad (5.1)$$

where

$$\bar{\rho} = \frac{1}{h} \int_{-h}^0 \rho.dz \quad (5.2)$$

h is the water column depth (m), ρ is the density of seawater (kg m^{-3}) at depth z and g is the acceleration due to gravity (m s^{-2}).

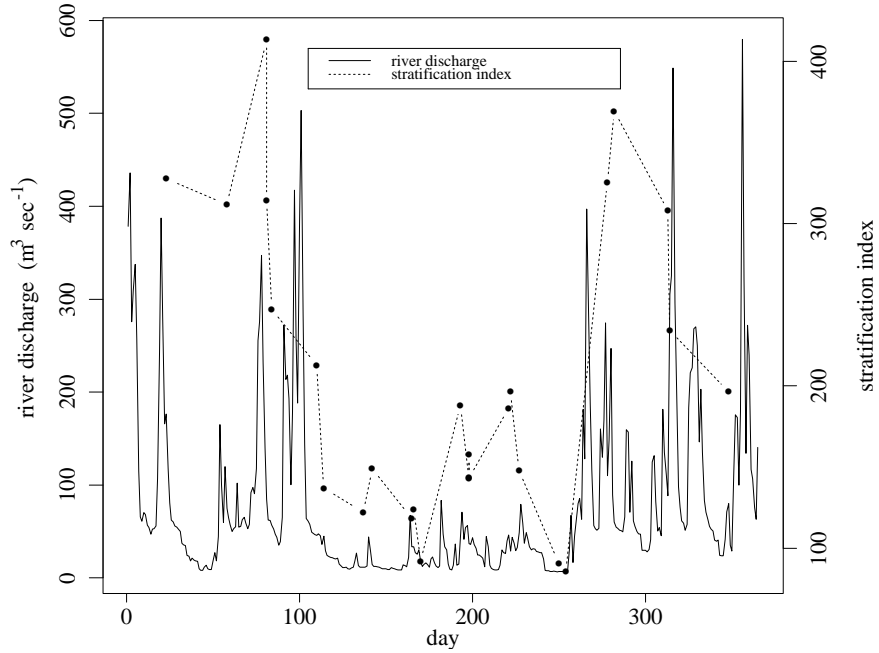


Figure 5.1: Inner basin stratification index (φ) and river discharge

In the IB, φ was calculated between 2-100 m in order to encompass as many of the vertical density distributions as possible. Throughout the year the inner

basin was well stratified, generally exceeding 100 Jm^{-3} , despite the sample site being in the southern, presumably more mixed region of the inner basin. The degree of stratification (fig. 5.1) was considerably lower during the summer - May to September - than the winter months. Regression analysis suggests that river discharge was the dominant control of stratification, with 73.25% of variation explained by the quantity of river discharge two days before the data collection, and 82% explained by $\sqrt{(\text{sum of the three previous days' river flow})}$, which agrees with the influence of river discharge on surface layer depth. During the months of lower river discharge, this influence lessens, with $< 40\%$ of the variation being explained by river discharge and the lunar tidal cycle contributing more.

If the temporal resolution of the vertical density gradient was greater, solar radiation may be influential in strengthening the stratification of the immediate surface and more frequent collection of data may also increase the importance of the lunar tidal cycle in the mixing of the water column.

The maximum values calculated by Jones and Gowen (1990) - for an area encompassing the head of Loch Eil to the Firth of Lorne, in July 1983 - are in accordance with those for the IB in 1991. In comparison with fjords in the Pacific North West and Norway, however, Loch Linnhe is less stratified, such as Jøsenfjord where the surface layer was found to be approximately 2m deep by Svendsen and Thompson (1978) and Albern Inlet which has a 3m deep brackish layer (Farmer and Osborn 1976). Smaller tidal ranges and higher river discharge levels contribute to the greater degree of stratification in these regions and may be an important difference between other fjord regions and Scottish sea-lochs.

5.2.2 Tidal Cycle

In the Strait of Georgia-Juan de Fuca Strait system Griffin and LeBlond (1990) found the lunar tidal cycle to an important source of mixing, as it is in many other estuaries, (Balch 1981; Haas 1977; Goodrich 1988; Sharples et al. 1994). The lunar cycle is also an important source of turbulent mixing in the inner basin, with its importance probably being enhanced by the passage of tidal currents through Corran Narrows. Balch (1981) found the surface layer temperature of Chesapeake Bay to be controlled by the lunar tidal cycle with the increased mixing at spring tides causing the temperature to drop. A similar effect is true for the IB. In fig. 5.2 the loss of thermal stratification at (predicted) spring tides can be seen, with greater homogenisation clearly taking place on those spring tides with a greater tidal range. The seasonal pattern of the tidal range (fig. 2.8) would suggest that in early spring and late summer - when the tidal range was particularly high - the loch will be more homogeneous, particularly during periods of low river discharge. This could influence the timing of the spring bloom by delaying the onset of a stable water column or may shorten the duration of blooms.

Spectral analysis, of water temperature at 2m, identifies periodicity at approximately 14 and 28 days - similar to that of the tidal range, but the time series is

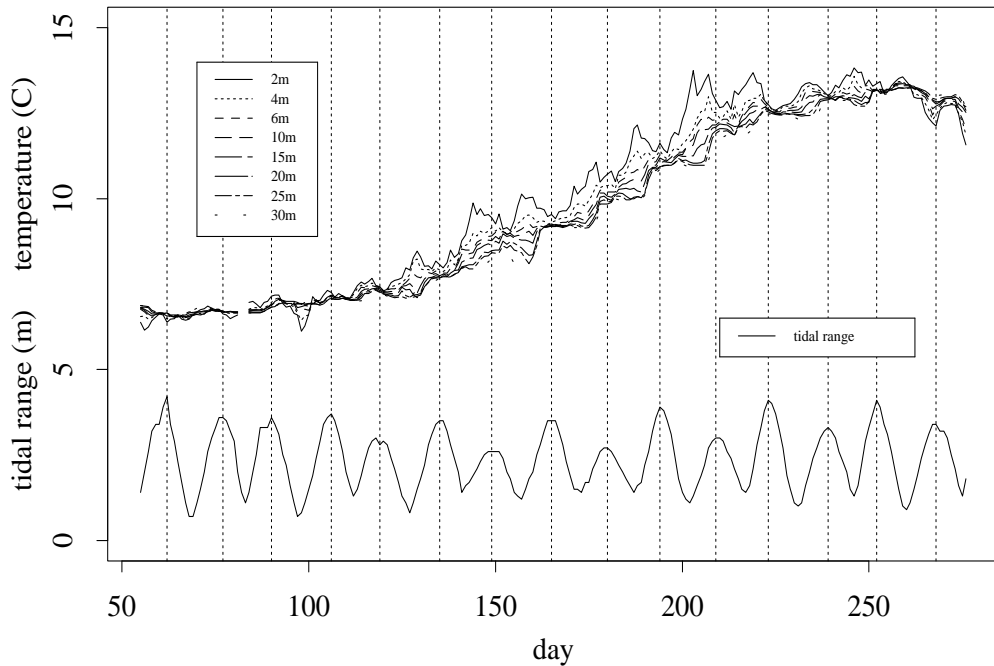


Figure 5.2: Predicted tidal range at Oban and the Inner Basin thermistor chain data from 2m to 30m

too short for results to be conclusive.

Seabed turbidity

In the inner basin of Loch Linnhe, Overnell and Young (1995) report a strong relationship between predicted tidal amplitude and current speed at 115m, the seabed being at 120m. At the same site, they also found sedimentation at 110m to be a function of tidal amplitude and the freshwater content of the loch, with increased sedimentation during spring tides. Only when the predicted spring tides were small did sedimentation vary little over the tidal cycle. A strong correlation was also found between beam attenuation and current speed at 110m, (*Allen and Simpson* from Overnell and Young (1995)), but there was a lot of scatter in the relationship between current speed and tidal amplitude. Stanley et al. (1981) considered spring tides to be an important source of resuspension in Loch Eil and Edwards et al. (1980) found sedimentation (including resuspension) increased tenfold between neaps and springs in Loch Eil.

In fig. 5.3 there is an example of increasing beam attenuation, especially in deep

water, with increasing tidal amplitude. This type of pattern is found at other times of the year, but the summer results may be confounded by phytoplankton sedimentation. Sedimentation of phytoplankton may increase with tidal mixing if the surface mixed layer extends below the euphotic zone or stratification declines. The phytoplankton cells may spend too much time in conditions of insufficient light to grow and sink increasing the beam attenuation close to the seabed.

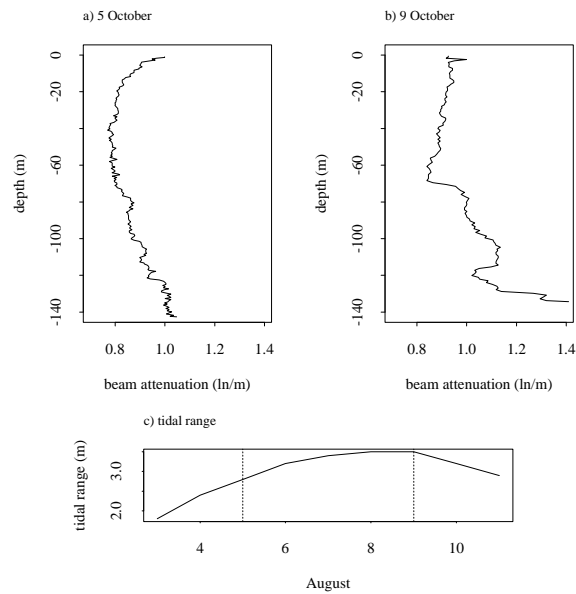


Figure 5.3: Beam attenuation (ln/m) at the Inner Basin sample site on a) 5 October, b) 9 October and c) tidal range over the period.

5.2.3 Physical Influences on Vertical Structure

In this section the effect of river discharge and wind on the vertical structure shall be considered. The effect of meteorological conditions on the structure of Loch Linnhe may be increased by the topography as the axis of the loch is relatively straight and lies in the direction of the prevailing wind. This may cause wind to be channeled along the loch. Precipitation may also be important as the catchment area for the Inner Basin alone is 1820 km² (Edwards and Sharples 1986) and encompasses some of the highest land and rainfalls in the UK. Also, most of the freshwater input is concentrated into the head of the inner basin.

River Discharge

River discharge in Loch Linnhe, as we saw above in relation to the stratification index (fig. 5.1) is, as with many other fjords highly influential on the physical structure.

In March there was a period of very heavy river discharge (fig. 5.4a), with upinlet winds (the cause of ponding) (fig. 5.4c), coinciding with the peak inflow rate on 19 March. The stratification index on 22 March fell from 413.6 J m^{-3} at 06 00 to 314.3 J m^{-3} at 14 55 - a 33% fall in 9 hours - with a subsequent drop to 247.3 J m^{-3} by 25 March (fig. 5.1) when the wind moved to the west. The river discharge led to a drop in surface temperature of 0.25°C in three days (fig. 5.5) which gradually increased as the river input diminished.

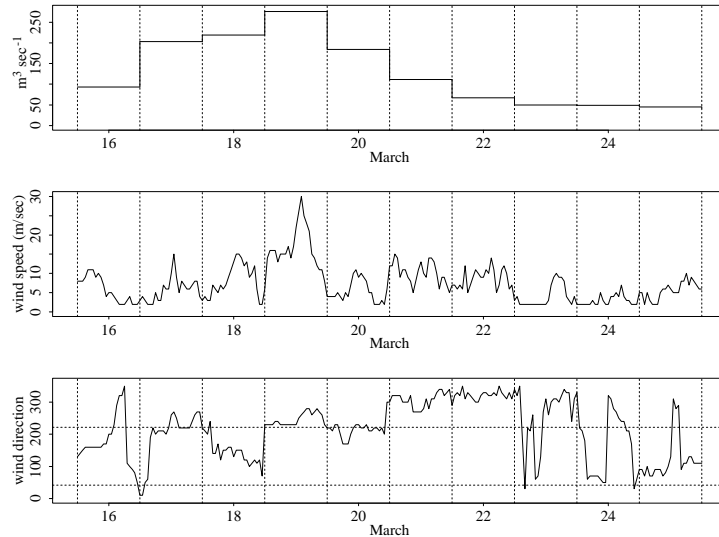


Figure 5.4: Meteorological data from 16 to 25 March for a) river discharge, b) wind speed and c) wind direction. The horizontal lines in (c) indicate upinlet winds at 222° and downinlet winds at 42° .

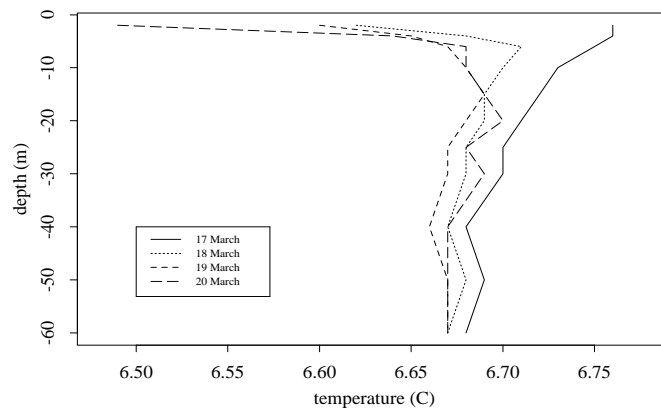


Figure 5.5: Inner Basin thermistor chain data from 17 March to 20 March

From the axial data of the inner basin on 25 March (fig. 5.6) it can be seen that the surface salinity was still very low - 20 PSU is the lowest recorded value

for 1991 from the axial data. There was a shallow surface layer and strong stratification, indicating very little mixing with the water below. Higher levels of river discharge, by increasing the speed of the outflowing surface layer increase the amount of water entrained behind. From 16-25 March, the wind had for periods been downinlet, which may have enhanced estuarine circulation (especially with a low tidal range) and increased entrainment further still.

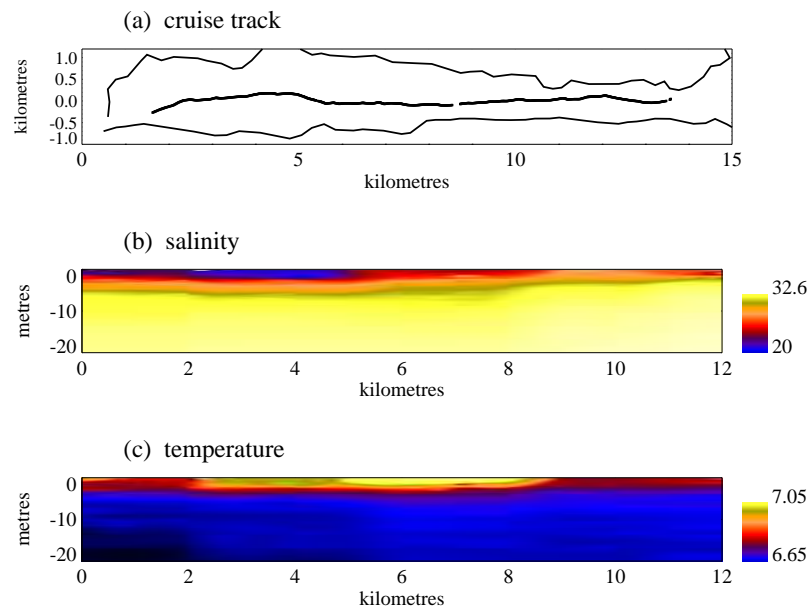


Figure 5.6: Interpolated axial plots showing the effect of river discharge into the head of the inner basin on 25 March on a) salinity (PSU) and b) temperature (C). The corresponding scales for each plot are located to the right.

Wind - ponding

As shown in 1.4.2 and 1.5.3 ponding of the surface layer is often found in fjords. Ponding occurred at the head of the inner basin on 18 May after upinlet winds commenced on the 17th, on 15 June after two days of upinlet winds, 13 July after upinlet winds began on the 12th (with a short period on the 11th) and in August. River discharge in June and July may have accentuated the degree of ponding. By generating a clearly defined shallow surface layer, which mixes little with the water below, ponding enables the surface layer to warm faster and further stratification which in turn has the potential to affect productivity.

On 18 May (fig. 5.8) there was a deepening of the surface layer at the head of the loch, where it was more than twice as deep as the surface layer further down the

basin. This deepening enabled the surface layer to warm deeper than elsewhere, fig. 5.8c. From fig. 5.7 it can be seen that this ponding occurred after only one day of upinlet wind, and a period of relatively low river discharge. For Alberni Inlet Farmer and Osborn (1976) recorded a the doubling of the surface layer depth within a few hours of the commencement of upinlet winds.

There is no evidence of the build up of ponding eventually flowing seaward - despite upinlet winds continuing, - as found in Alberni Inlet by Pickard and Rodgers (1959). There was however, only one month where data collection covered a prolonged period of upinlet wind (August) and then river discharge was low which will have reduced the build up of water. The lower level of stratification and river discharge in Loch Linnhe will also contribute, even with ponding there will be more exchange with deeper water than in more stratified basins such as Alberni Inlet.

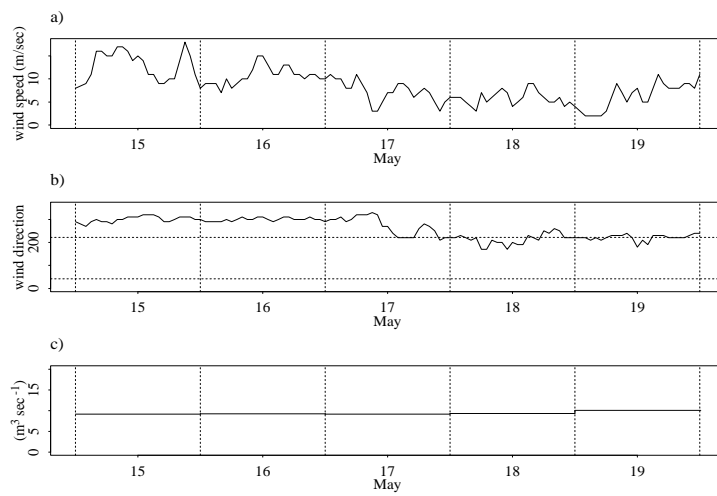


Figure 5.7: Meteorological conditions from 15 to 19 May, (a) wind speed, (b) wind direction and (c) river discharge.

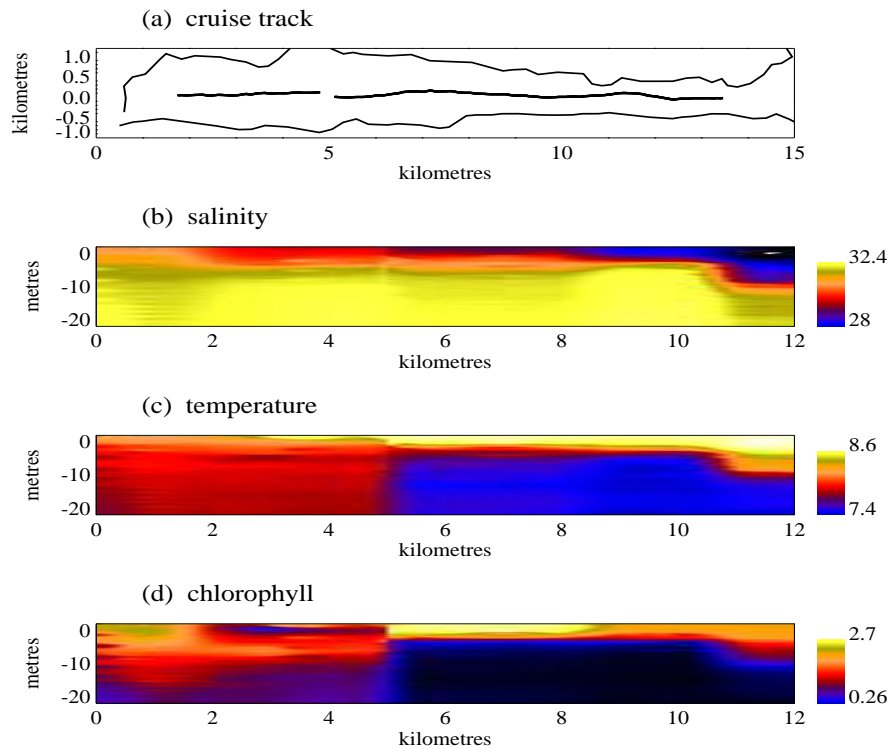


Figure 5.8: Ponding at the head of the inner basin on 18 May. Axial plots of (b) salinity (PSU), (c) temperature ($^{\circ}\text{C}$) and (d) chlorophyll (mg m^{-2}) with (a) a plan of the cruise track.

Wind - release of ponding

Between 2 and 8 April (days 92 to 98) there was a rapid fall in the temperature of the surface layer by $\sim 1^{\circ}\text{C}$ over six days and a subsequent temperature inversion, fig. 5.9. This was followed by the temperature rising again to a similar level in four days, fig. 5.10. Over this period there had been heavy river discharge which continued over the rewarming of the surface layer, fig. 5.10(c). Wind speed was also high, but continued to be so as the water warmed, fig. 5.10(a). From 31 March to 3 April the wind was upinlet (fig. 5.10b) and there were spring tides, fig. 5.10(c). I believe that in this time, water was ponded at the head of the basin, then as the wind changed direction it was released, flooding down the basin rapidly cooling the surface of the southern section of the inner basin. Spring tides may also have prevented water from flowing out of the basin. It can be seen in fig. 5.10(b) that even as the surface temperature was falling, when the wind was upinlet there was a slight rise in temperature on 5 April (day 95).

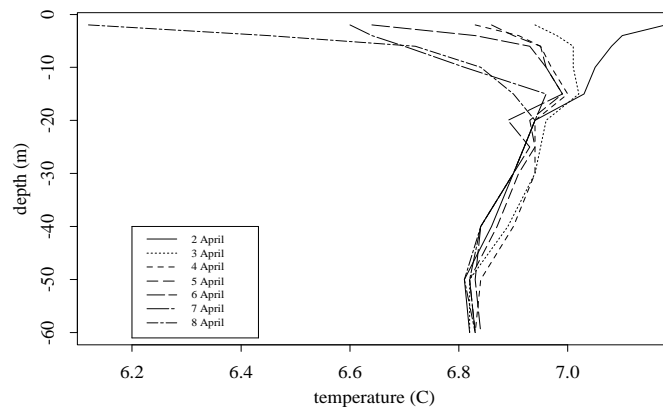


Figure 5.9: Inner Basin thermistor chain data from 2 to 8 April.

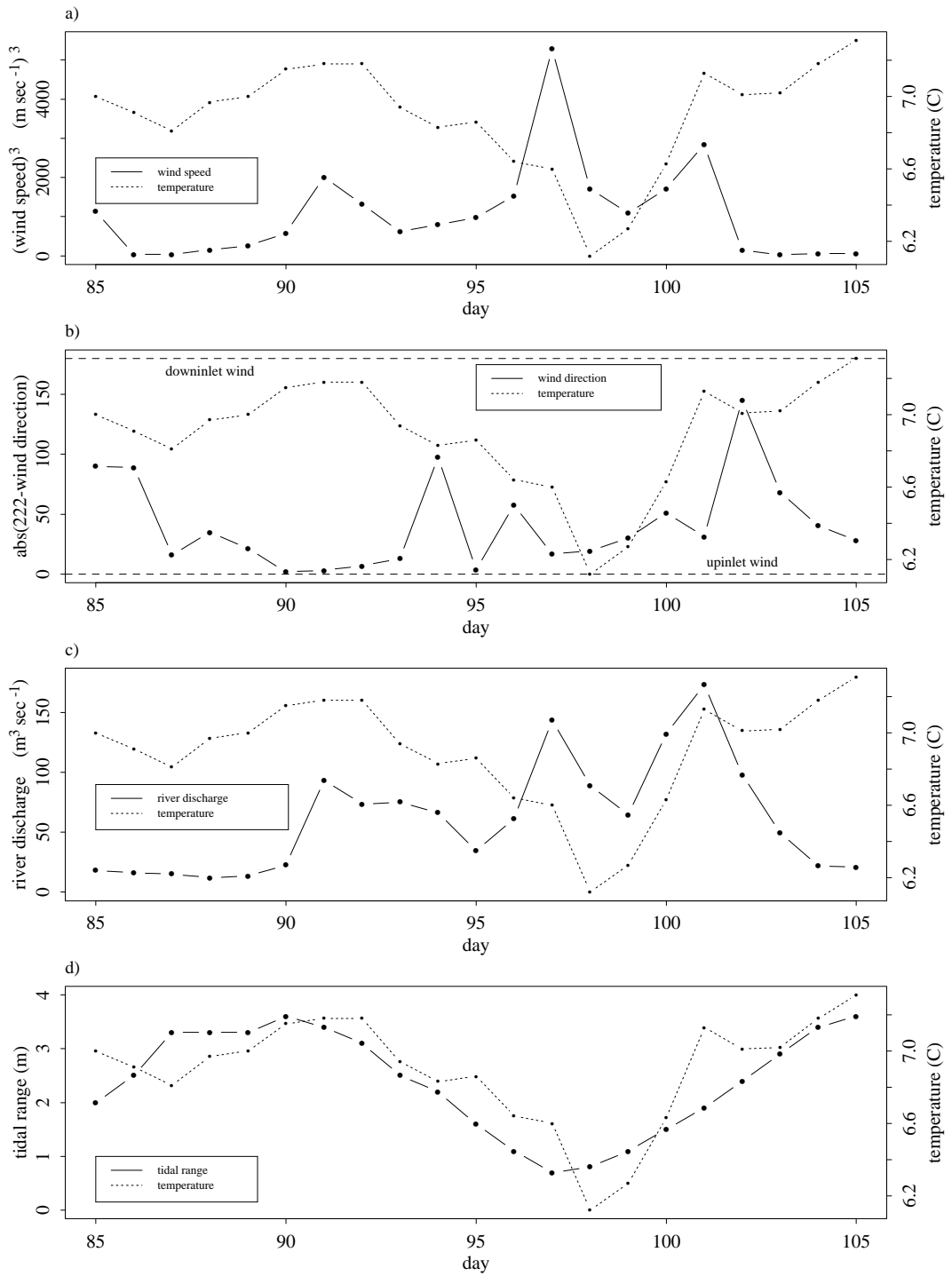


Figure 5.10: 2m thermistor chain data from 26 March to 15 April with a) (mean daily wind speed)³, b) |222 - wind direction|, c) freshwater input and d) predicted tidal range.

5.2.4 Deep Water Renewal

Deep water renewal is an aspect of fjord hydrodynamics which is particularly variable in its response to conditions such as the tidal cycle, wind and river discharge. In the inner basin of Loch Linnhe I found evidence of possible renewal events in April, May, August, September and October.

April

On 20 April there was an area of higher temperature and higher density water in the southern part of the inner basin. The warmer water was also deeper in the south than further north, dissolved O₂ slightly greater and there was more chlorophyll *a* in the water column. In an internal fjord basin, dissolved oxygen will not necessarily increase substantially after a renewal event as the water in the external basin may also be low in O₂.

The predicted maximum tidal range before the 20th was on 16 April, which may have prompted renewal. The abundance of chlorophyll outwith the surface layer, in the south of the basin, suggests that the cells may have been advected into the inner basin from the outer basin. There is no evidence from the data available of a bloom on the surface before May and Overnell and Young (1995) found no evidence of the spring bloom until the start of June, so it is unlikely that the cells could have sunk from the surface.

May

There was a contrast in May between the stratified northern section of the inner basin which was affected by ponding and the well mixed southern section where renewal may have taken place. Axial plots of the surface 20m (fig. 5.8) illustrate the contrasting levels of stratification over the basin at that time.

On 17 May (fig. 5.11) there was a well defined pycnocline and the salinity of the surface layer was relatively homogeneous. Thermally, there existed two separate layers of relatively uniform temperature. By 22 May the water column was more mixed and was warmer at most depths, indicating an influx of water. Over this period, there were spring tides, with a maximum predicted tidal range on 15/16 May and low river discharge. The warming of the surface 60m over this period is illustrated in fig. 5.12.

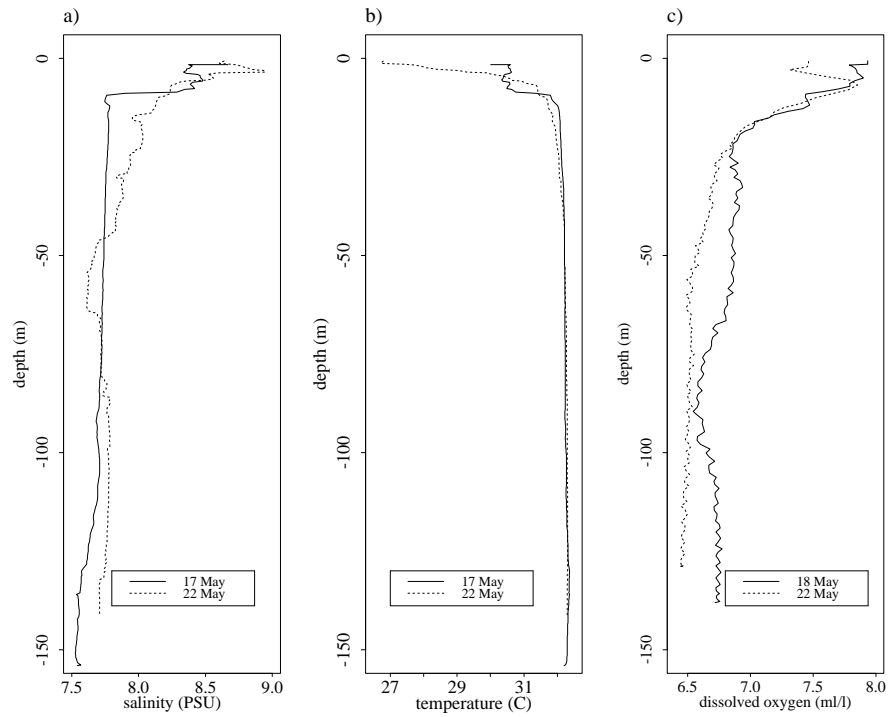


Figure 5.11: Inner Basin sample site data of (a) salinity (PSU), (b) temperature ($^{\circ}\text{C}$) and (c) dissolved O_2 (ml/l) over the May renewal period.

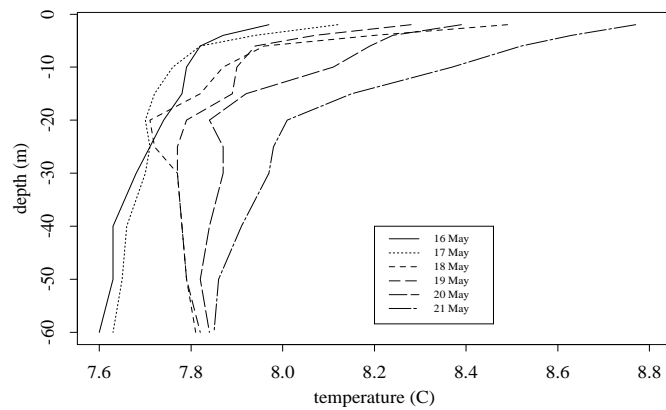


Figure 5.12: Thermistor chain data over the May renewal period indicating a rise in temperature at all depths.

August

On 10 August, (page 118) the water in the southern section of the inner basin was clearly warmer than that further north, a similar distribution pattern can be seen in chlorophyll *a*. By 15 August, (page 119) the basin was considerably more uniform horizontally, as the intruding water had spread throughout the basin.

At the sample site the water column had warmed below 30m by as much as 0.5 °C over this time, with the surface cooling. From the thermistor chain data in fig. 5.13, it can be seen that from the 9th to the 10th, the surface had cooled while deeper water had warmed.

During this period there had been ponding in the inner and outer basin which inhibits estuarine circulation, would be expected to lessen upwelling at the head of the outer basin and decrease the likelihood or strength of a renewal event. Renewal, may again be linked to spring tides, as a predicted tidal range maxima was on 11 August.

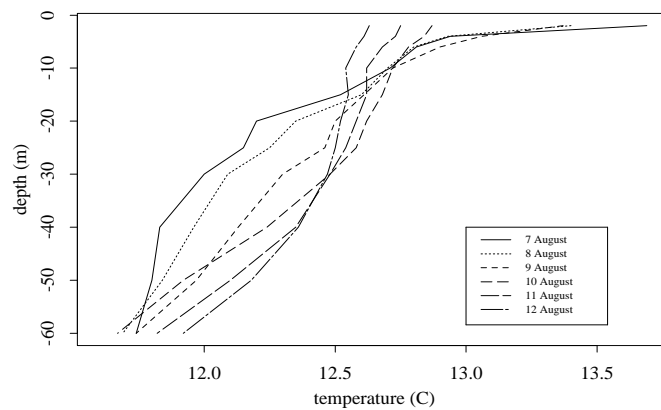


Figure 5.13: Thermistor chain data over the August renewal period, indicating the deep water warming while the surface cooled.

September

On 7 September (page 121) there was a region of considerably warmer water near the sill in the inner basin, which corresponded with higher levels of dissolved O₂. By 8 September (page 122) the intruding water had spread further into the inner basin. In fig. 5.14, a change in temperature below 50m can be seen from 5 to 6 September, with a further increase in temperature below 20m of as much as 0.5°C from the 6th to 7th - suggesting that the renewal event commenced between the 5th and 6th.

The axial plots (page 121) of temperature and dissolved oxygen on 7 September show regions where renewing water reached further into the basin these may relate to the differential current speeds of water flowing into the inner basin reported by Overnell and Young (1995).

The sample site data (fig. 5.15) shows a continuing rise in salinity, temperature and dissolved O₂ between 7 and 11 September over most depths. The exceptions are below 120m and above 20m, where values on 7 September were greater than on the 11th. The deeper water may have been relatively unchanged if the renewal was partial or its initial change after the renewal may have occurred by the 7th, as suggested by the temperature profile with the subsequent fall being due to mixing.

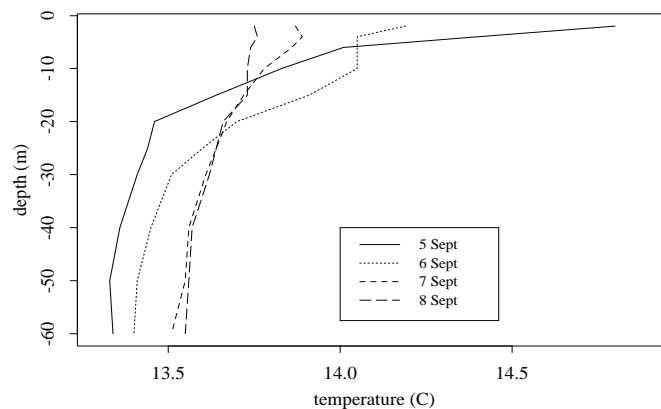


Figure 5.14: Inner basin thermistor chain data from 5 to 9 September, showing the increase in temperature starting deep and moving up the water column.

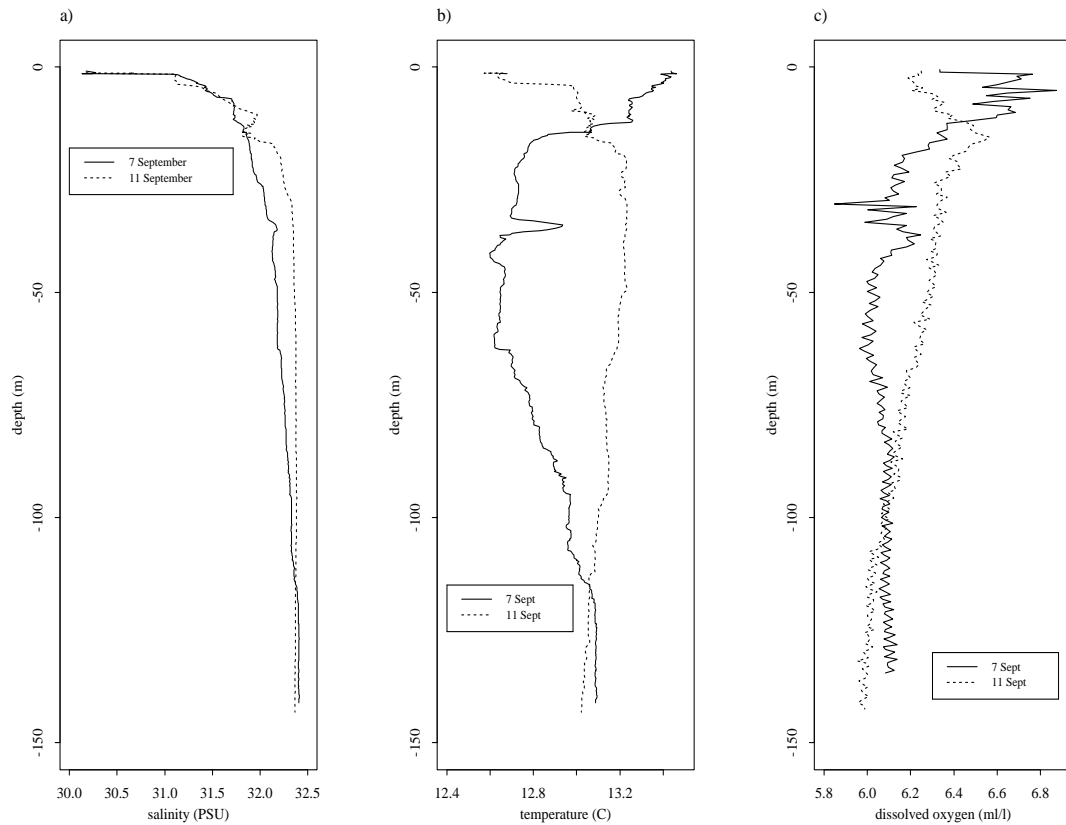


Figure 5.15: Sample site data for (a) salinity, (b) temperature and (c) dissolved O₂ on 7 and 11 September, illustrating the influx of more saline, warmer water into the IB.

October

No axial cruises were made of the inner basin during October and there is no thermistor chain data for this time, however, from the surface cruises on 9 and 10 October there was an increase in salinity of 5.2 ‰ over 24 hours, with a corresponding increase in nitrate of 6.3 ‰. This coincided with a spring tide - one of the largest of the year, being close to an equinox - and may indicate renewal. The interpolated sample site data (fig. 3.6) indicates that the temperature of inner and outer basin deep water in October was of a comparable level, which often indicates the occurrence of deep water exchange.

Conclusions

The unifying factor in all these months is that the renewal events occurred around spring tides. As with other fjords where renewal takes place with larger tidal ranges, e.g. Puget Sound (Lavelle et al. 1991), the sill into the IB is shallow.

This also agrees with Edwards et al. (1980) who found that Loch Eil renewed regularly at spring tides. The wind direction with these renewal events was variable, though with upinlet winds the river discharge was lower than for those months with downinlet winds.

Other months for which there is data for the spring tide period are June and July. From the sample site temperature data for the IB and OB moorings (figs. 3.3 & 3.4) at the end of June the deep water temperature difference between the sample sites was slightly greater than normal, with the difference increasing until renewal in August. For both of these months renewal if it occurred was partial and the July event particularly weak. In June, from PI_{jn1} and PI_{jn2} the salinity increased above 100m overnight which may have been a result of a partial renewal event. A weak intrusion may also have little effect at the sample site. In these months, there was either no renewal or, it was weaker than in the other months. Factors which may account for this are the spring tide being lower, and possibly the combination of upinlet winds and river discharge. The only month with river discharge greater than $40 \text{ m}^3\text{sec}^{-1}$ in which renewal may have occurred was October when the wind was downinlet and there is insufficient evidence for this event to be confirmed. With higher levels of river discharge, downinlet winds may be required to enhance estuarine circulation as mixing may be too great with upinlet winds.

In other Scottish sea-lochs low river discharge has been found to facilitate renewal: in Loch Sunart by Gillibrand and Turrell (1995) and in Loch Etive by Edwards and Edelsten (1977). With deep water renewal being less likely to occur in the IB with high river discharge, this is as mixing at shallow sills reduces the density of the intruding water thereby preventing baroclinic flow. With stronger estuarine circulation, such as with downinlet winds, the baroclinic flow may be sufficient for renewal to take place.

5.2.5 Bathymetry

As the deep water current speeds in the inner basin of Loch Linnhe are fast (Overnell and Young 1995), discontinuities in the seabed have the potential to be influential in generating turbulence and upwelling (Syvitski et al. 1987). Renewal has the potential to produce fast flowing currents, particularly where the sill to lochfloor distance is large - as it is in the IB - though with partial renewal there will only be interaction with the sides. In the inner basin there is a bump in the seabed, at $\sim 8\text{km}$ on page 118 (fig (a)), which appears to affect the flow of water along the bottom of the basin, particularly after renewal when the current speed is greater.

From page 118, on 10 August the effect of this rise in the seabed on the inflowing water can be seen. The surface layer is deeper above this region and the warmer water is deeper. On 15 August (page 119) this effect was less pronounced.

5.3 Inner Basin: Biotic Structure

The physical processes discussed above such as deep water renewal, fronts and upwelling would be expected to affect the biotic structure, as may river discharge, wind and the lunar tidal cycle. The monthly data collection, however, makes it difficult for the timing and extent of biological processes to be evaluated and the influence of the physical regime assessed.

5.3.1 Chlorophyll *a* in the Water Column

Measurement of phytoplankton does not indicate the viability of cells. This creates a problem in differentiating between a productive subsurface maxima and a non-viable sinking population below the euphotic zone.

5.3.2 Influence of Physical Structure

Temperature Gradient

The vertical temperature distribution is highly influential on the distribution of phytoplankton within the water column. In May, phytoplankton density was closely coupled to the vertical temperature distribution. Between 18 and 22 May (fig. 5.16) the change in temperature distribution produced a corresponding change in the distribution of phytoplankton.

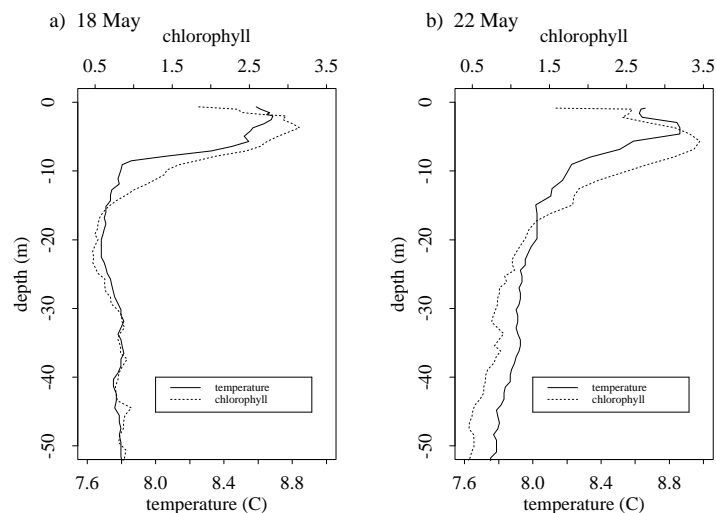


Figure 5.16: Sample site data of chlorophyll *a* and temperature on a) 18 and b) 22 May

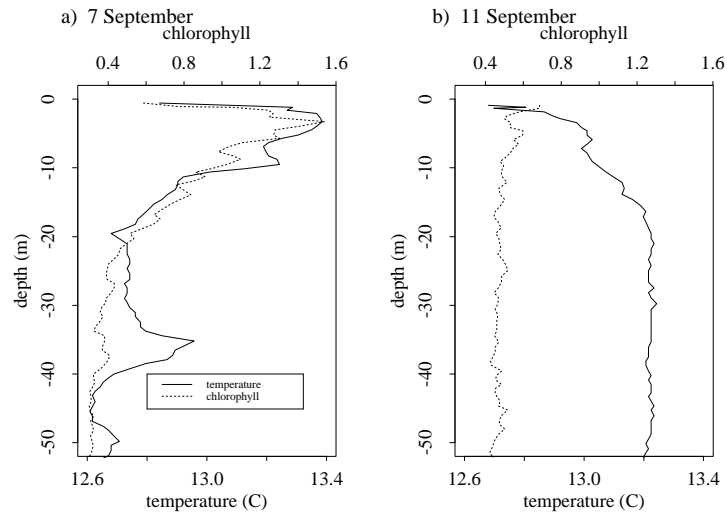


Figure 5.17: Sample site data of chlorophyll *a* and temperature on a) 7 and b) 11 September

In September, cooling of the surface layer was accompanied by a fall in the chlorophyll concentration, fig. 5.17. This may have been due to increased mixing deepening the surface layer and decreasing stratification - the stratification was already very low for the inner basin, fig. 5.1. Deepening of the surface mixed layer may cause phytoplankton to spend too much time out of the euphotic zone, leading to sedimentation and less stratification may increase sinking from the surface layer.

The depth of the surface layer and its degree of stratification indicate closely the position of phytoplankton within the water column. The 18 May axial plots (fig. 5.8) show how in the ponded northern region (< 10km along the cruise track) the chlorophyll extended down to the pycnocline, double the depth it existed at in the rest of the stratified region.

On 13 July, the pattern of high concentration chlorophyll followed the varying depth of the surface layer, with the influence of the thermocline particularly strong, fig. 5.18(c) and (d). Where the thermocline fell to more than twice the depth further south, through a combination of ponding and river discharge, the highest chlorophyll values and the warmest water were found. Towards the front of the surface plume, chlorophyll was also found along the thermocline.

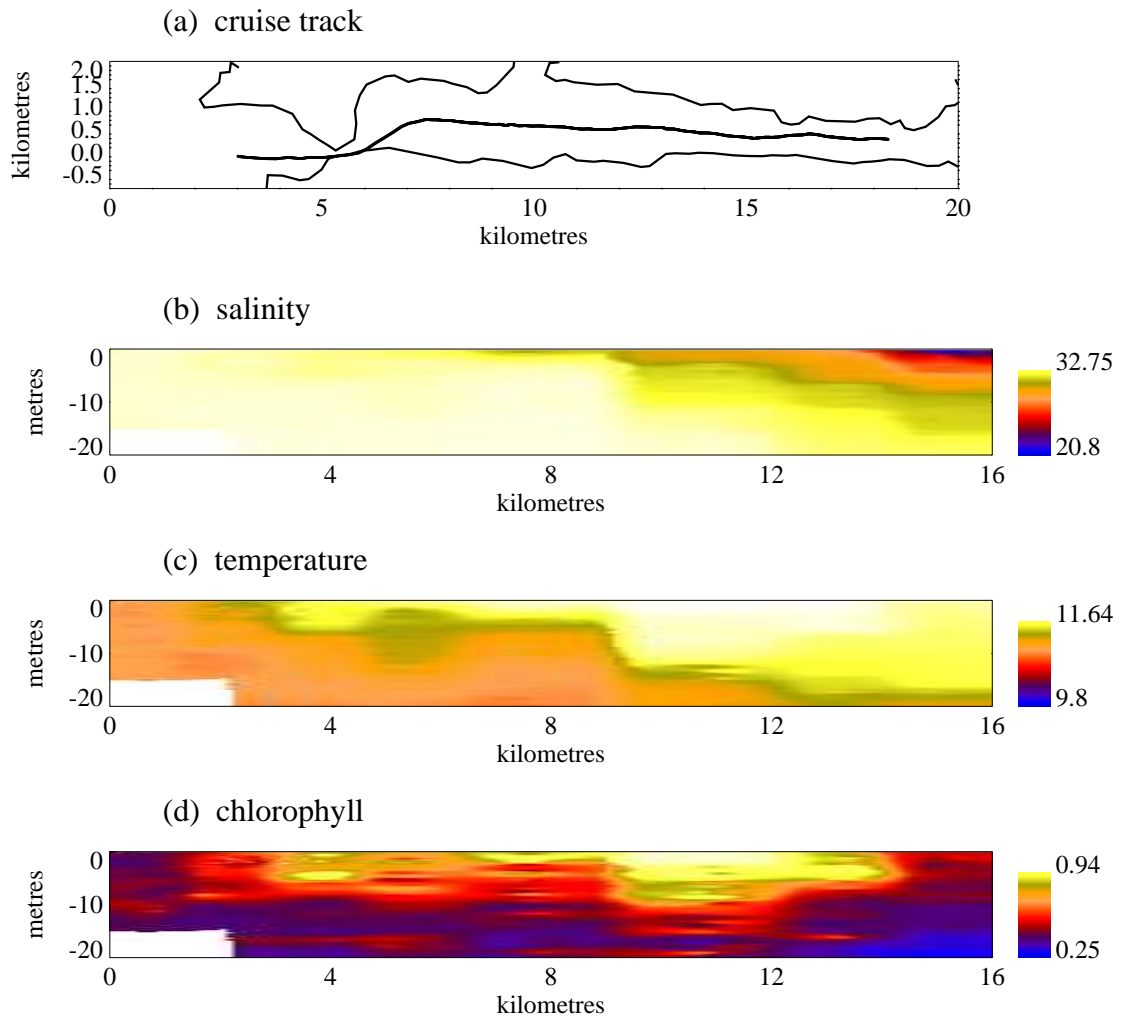


Figure 5.18: Gridded axial data on 13 July

Deep Water Renewal

Deep water renewal close to 16 May caused an influx of warmer chlorophyll *a* carrying water. This can be seen from vertical profiles on 18 May (fig. 5.19(a)) by 22 May (fig. 5.19(b)) those cells not advected into the euphotic zone will have sedimented out of the water column.

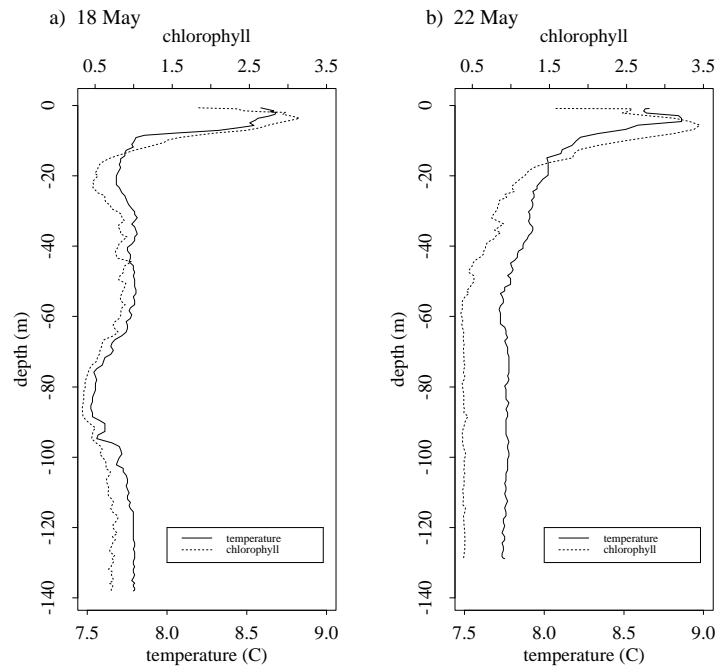


Figure 5.19: Sample site data of chlorophyll *a* and temperature on a) 18 and b) 22 May

The axial plot of chlorophyll *a* on 18 May (fig. 5.8) shows that in the southern mixed section of the IB, chlorophyll concentration was much greater in deeper water than further north in the stratified section of the loch. Thermally the water column was well mixed, with chlorophyll being found over a greater range of depths. Overnell and Young (1995) found that sedimentation at 110m was greater than at 20m before the bloom had started in May 1991 and hypothesised that the cells were transported into an intermediate depth in the inner basin from the outer basin.

The axial data on 10 August (page 118) also shows an influx of chlorophyll with the renewing water. In September however (fig. 5.20) there was no corresponding influx of chlorophyll cells with the warmer water as the chlorophyll density was greater in the Inner Basin than the north of the Outer Basin.

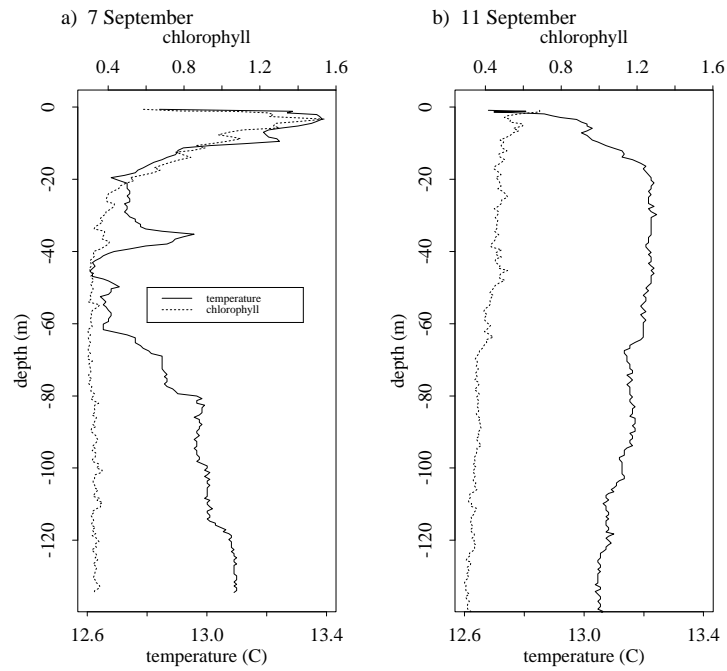


Figure 5.20: Sample site data of chlorophyll *a* and temperature on a) 7 and b) 11 September

Bathymetry

During deep water renewal in August, the chlorophyll *a* concentration was closely related to temperature (page 118.) Above this bump, the chlorophyll concentration was greater, deeper and the pattern was still present on 15 August (page 119.)

On 15 June (fig. 5.21) chlorophyll *a* was found throughout the water column but in the south of the basin the concentration was lower. Upwelling in the south of the basin due to the bathymetry may have been sufficient to maintain the phytoplankton population. While in the northern, more stratified region, the surface layer may have been depleted of nutrients, causing the phytoplankton to sink out of the surface layer. In June the upwelled water would have been of greater nitrogen concentration than the surface water, as the nitrogen concentration was $0.7 \text{ mg.atm.m}^{-3}$ on the surface compared to $2.8 \text{ mg.atm.m}^{-3}$ at 140m.

Other factors causing the sedimentation may have been the spring tide, though one of the lowest of the year, or the wind. Overnell and Young (1995) recorded rapid sedimentation in the IB.

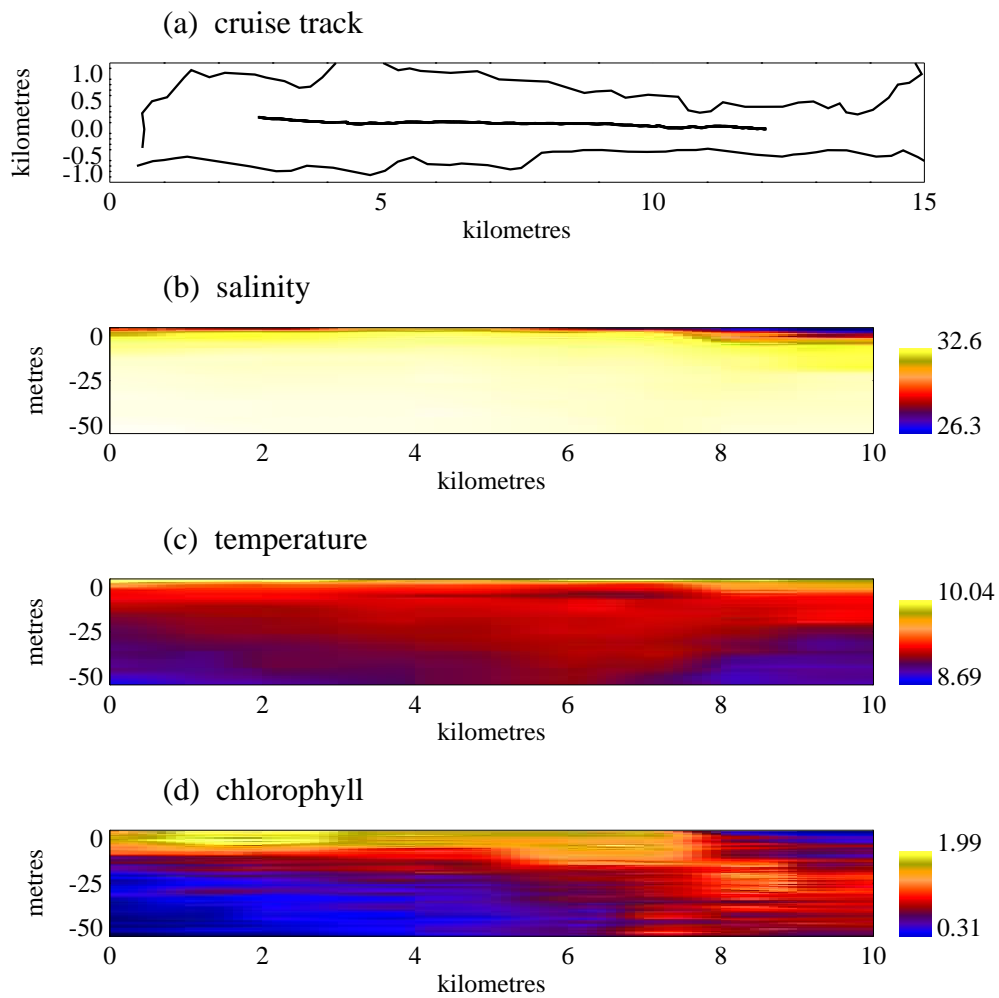


Figure 5.21: Sinking of chlorophyll in the inner basin on 15 June. Axial plots of (b) salinity (PSU), (c) temperature ($^{\circ}\text{C}$) and (d) chlorophyll with (a) a plan of the cruise track.

Fronts

In the inner basin there was often a discontinuity where the low salinity outflowing surface layer met the resident fjord water and a chlorophyll maxima was often present at this front.

In fig. 5.8 of the surface 20m on 18 May there was a maxima at the surface on the boundary between the two regions, while in the more mixed south the maxima was subsurface. On 15 August, there was ponding in the inner basin (fig. 5.22), producing a clearly defined low salinity (27 PSU) surface layer, at the head of which was a patch of higher density chlorophyll. The wind had been upinlet since the 8th, enabling the surface to warm and the degree of stratification may have restricted mixing with deeper water - keeping the phytoplankton within the euphotic zone. The maxima is just to the north of a possible site of upwelling, which may have contributed to the supply of nutrients to the surface layer and also may have influenced the position of the front.

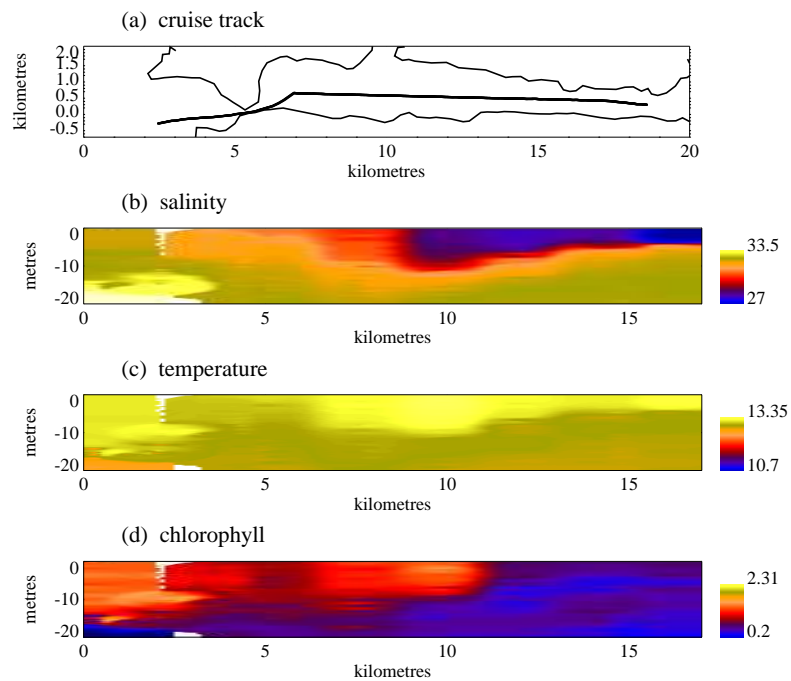


Figure 5.22: Gridded axial data on 15 August.

On 7 September (fig. 5.23) chlorophyll was again associated with the head of a front, but the maxima was subsurface and along the pycnocline, with a similar situation on the 8th (fig. 5.24) except that the chlorophyll extended into shallower water as the pycnocline was shallower.

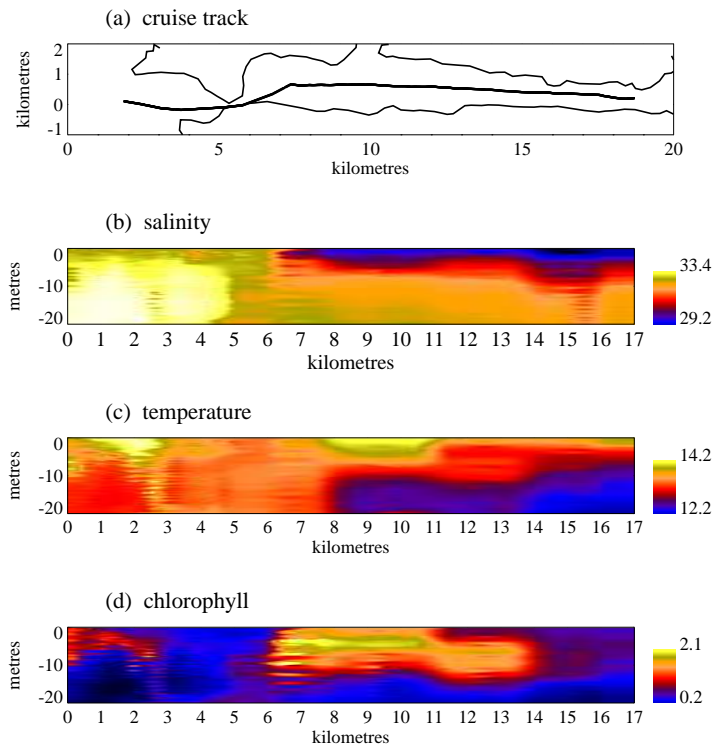


Figure 5.23: Gridded axial data on 7 September

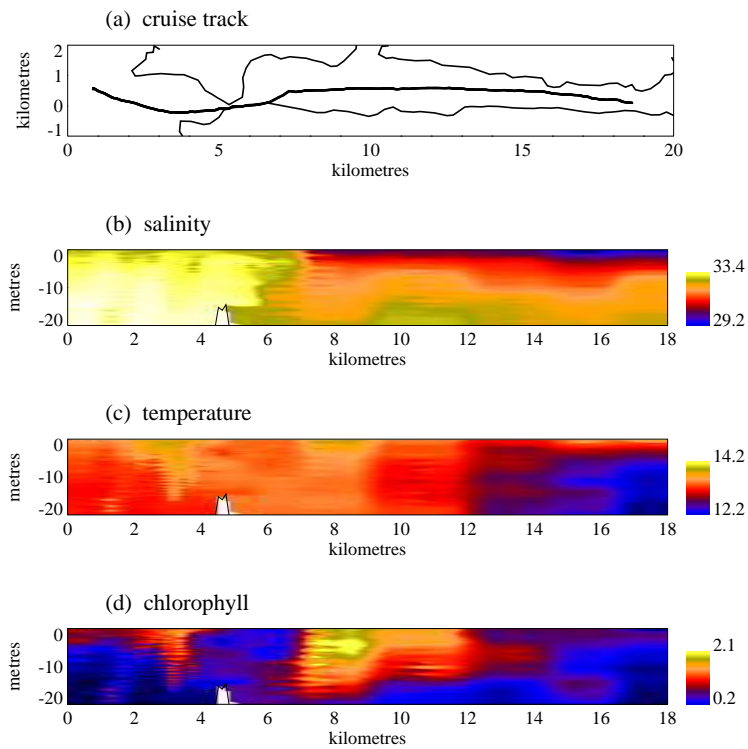


Figure 5.24: Gridded axial data on 8 September

5.3.3 External Factors

Lunar Tidal Cycle

Overnell and Young (1995) found sedimentation within the IB to be related to the lunar tidal cycle, with increased sedimentation at spring tides but the effect reduced with less spring-neap variation. The substantial mixing that occurs during spring tides in the IB would be expected to affect the phytoplankton population - even if only short term - but the temporal resolution of the data does not allow this to be examined.

The ability of mixing to affect the biology may depend on the timescale of mixing and stabilisation. Tidal mixing may induce rapid sedimentation accompanied by nutrient input into the surface layer. This may then lead to another bloom upon stabilisation, generating cycles of growth followed by decay. The time for stabilisation to occur in such a situation may determine productivity. During the most productive months of 1991 - May and June - the tidal range was lower, so the surface layer would be expected to be more stable than in other months. That phytoplankton density was at its highest during these months may have been in part due to the relatively low level of tidal mixing.

Wind

The vertical plots with sedimentation most obvious are those for June and July, when the wind was upinlet. There is however, no evidence that the sinking was influenced by the wind, as the tidal range was near its maxima at the time of the data collection and tidal mixing also drives sedimentation. There are sub-pycnocline peaks of chlorophyll within the water column in June and July which may indicate sinking or a viable population. The low density of phytoplankton within the IB makes coagulation an unimportant effect.

River Discharge

The river input into Loch Linnhe is low in nutrients and will not increase phytoplankton density by inputting nutrients into the system. River discharge, is however an important factor maintaining stratification and the vertical temperature gradient. Extreme discharge however, increases turbidity which by limiting light will decrease growth.

5.4 Outer Basin: Physical Structure

In this section the hydrographical features of the outer basin are studied and compared with those of the inner basin. Unlike the inner basin, axial cruises of the outer basin rarely covered the entire length. More cruises were however made and on more more days, though comparison between sequential days is not often possible as different sections of the loch were sampled.

5.4.1 Stratification Index

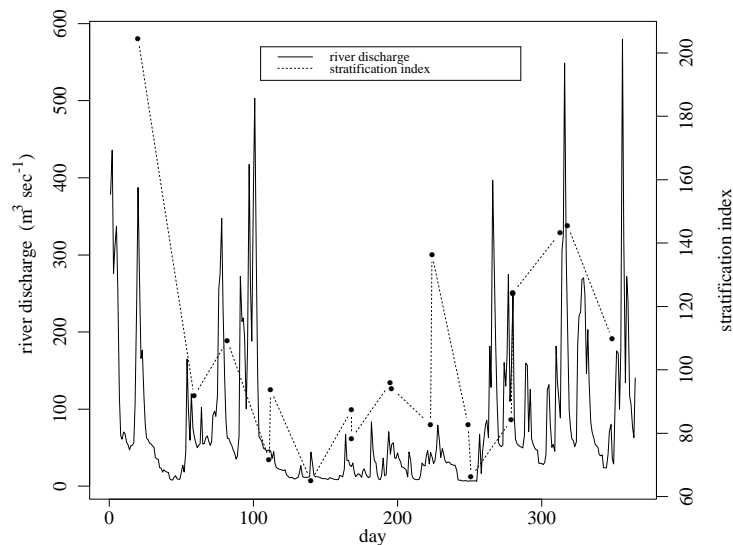


Figure 5.25: Stratification index (φ) and river discharge at the Outer Basin mooring.

At the outer basin mooring the stratification index φ was calculated from data covering 2 to 60m. Stratification at this site was considerably less than for the inner basin (fig. 5.25) with a maximum of approximately half the inner basin maximum. Regression analysis suggests that wind speed is of importance as well as river discharge in maintaining stratification here. It is to be expected that the relationship between river discharge and stratification is more complex than for the inner basin, as the effect of river discharge on stratification will be affected by ponding in the time it takes to reach the outer basin. The degree to which it is mixed into deeper water will also be affected by other factors such as wind and the spring neap tidal cycle. While all these factors will affect the inner basin, the greater distance to the outer basin sample site from the principal sources of river input and the passage of the outflowing water through Corran Narrows will increase the homogeneity of the water column and complicate the relationships between stratification and its causes. The fetch at the outer basin mooring is also greater than for the inner basin and may increase the relative

importance of the wind in affecting stratification. The available dataset from which stratification may be calculated, includes less than twenty days of the year and cannot be expected to give a complete picture of the mechanisms involved and the importance of wind speed, suggests that wind direction may also be important, given the shape and orientation of the loch.

At the Lynn of Morvern mooring the stratification index was calculated from 2 to 40m, fig. 5.26. There was even less stratification than at the outer basin mooring, being approximately quarter that of the IB. Mean stratification at the inner basin was 205.36 with a variance of 8791.73, compared to 57.49 and 634.84 respectively in the Lynn of Morvern. Moving seaward there was also less winter/summer variation, as indicated by the variances above: 100-400 Jm^{-3} in the IB, 70-200 Jm^{-3} and 20-105 Jm^{-3} in the LoM. In the inner basin the stratification was mainly caused by the river discharge 2 days previously and in the Lynn of Morvern three days previously.

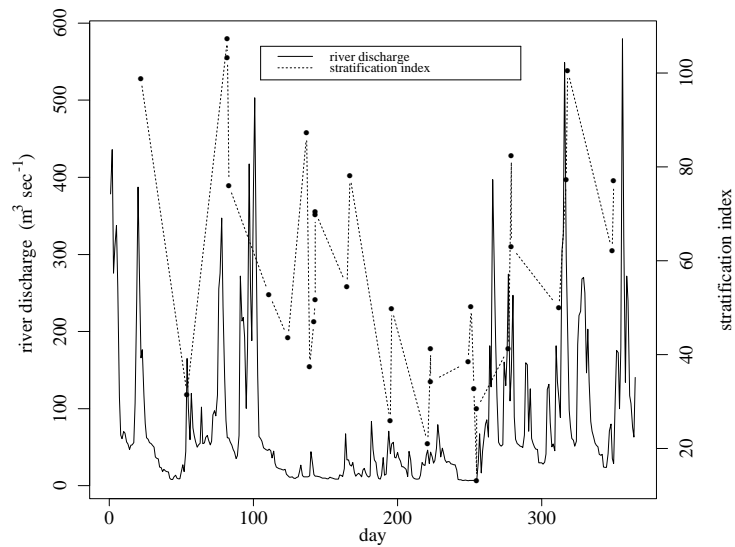


Figure 5.26: Stratification index (φ) and river discharge at the Lynn of Morvern mooring.

5.4.2 Tidal Cycle

In comparison with the inner basin there was a greater delay, at the Lynn of Morvern thermistor chain, for the surface layer to cool after predicted spring tides, fig. 5.27. Considering the difference between 2 m and 30 m at both moorings, mixing in the Lynn of Morvern occurred approximately one day after the Inner Basin.

At the shallowest point on the thermistor chains (2m), the Inner Basin and Lynn of Morvern the greatest correlation was for one day's lag from the Inner Basin

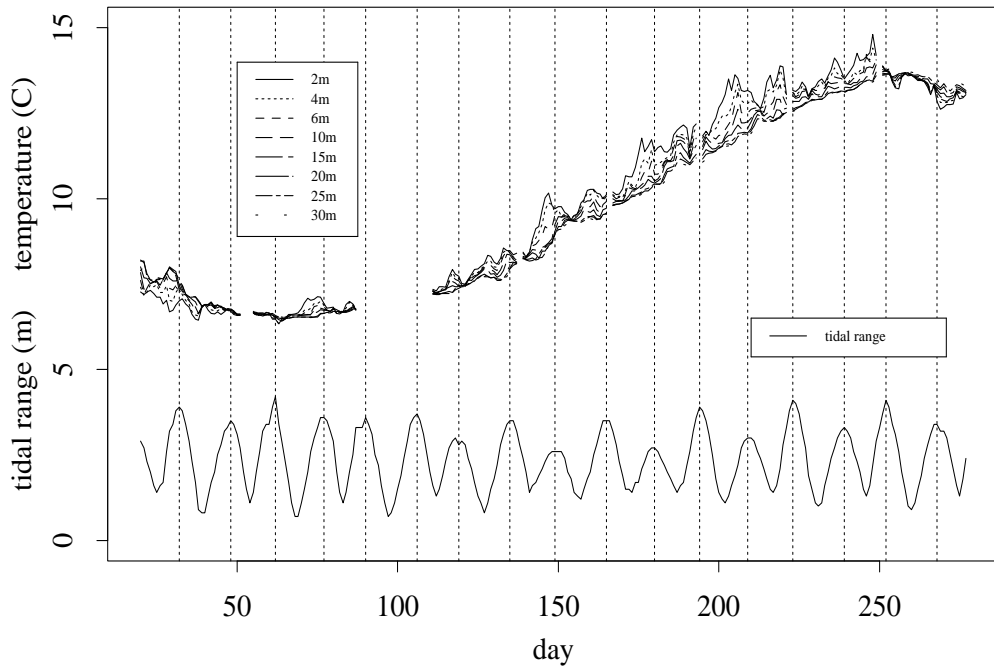


Figure 5.27: Tidal range at Oban and Lynn of Morvern thermistor chain data from 2m to 30m

to the Lynn of Morvern (0.9936), with the correlation slowly falling with greater lags - it is still 0.9833 for a lag of 5 days. At all other depths, 4m to 60m the greatest correlation was with the same day.

Seabed turbidity

As for the inner basin, beam attenuation close to the seabed increased with greater predicted tidal range. Examples below are of 12 & 14 July (fig. 5.28) and 9 & 11 August (fig. 5.29) both at the Lynn of Morvern sample site. Despite primary production occurring at both of these times, sedimentation of chlorophyll from the surface layer does not appear to have had much effect on deep water turbidity. The chlorophyll plots (figs. 5.30(a)-(d)) show that chlorophyll in the water column had fallen over both periods shown, but there was little at depth and no increase between the days and resuspension caused by the interaction of tidal currents with the loch floor seems to have been the primary source of the turbidity.

There are also signs of increased beam attenuation with greater tidal range at

the outer basin mooring in October, in September, however, the relationship did not hold. Seabed turbidity was also present at neap tides, such as on 22 April when the tidal range was at a minima, fig. 5.51.

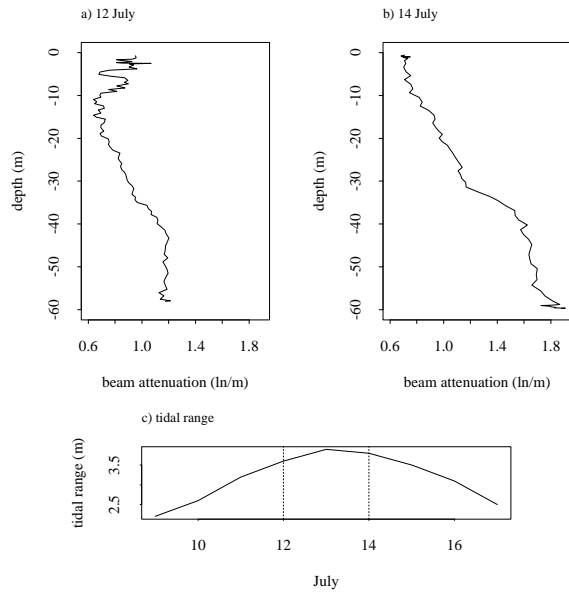


Figure 5.28: Beam attenuation (ln/m) at the Lynn of Morvern sample site on a) 12 July, b) 14 July and c) tidal range over the period.

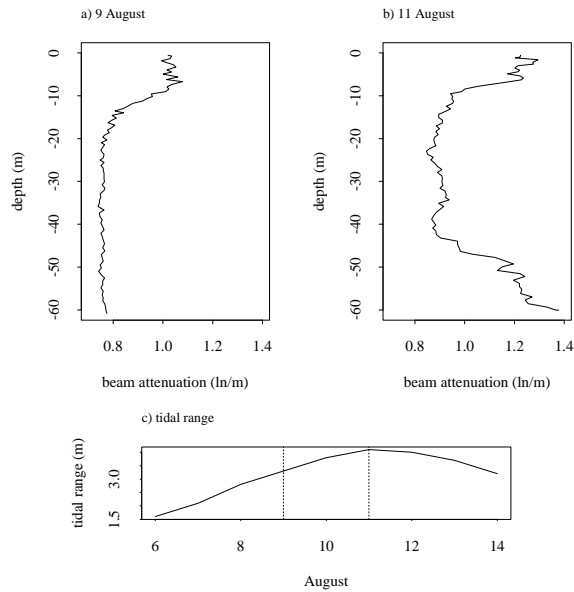


Figure 5.29: Beam attenuation (ln/m) at the Lynn of Morvern sample site on a) 9 August, b) 11 August and c) tidal range over the period.

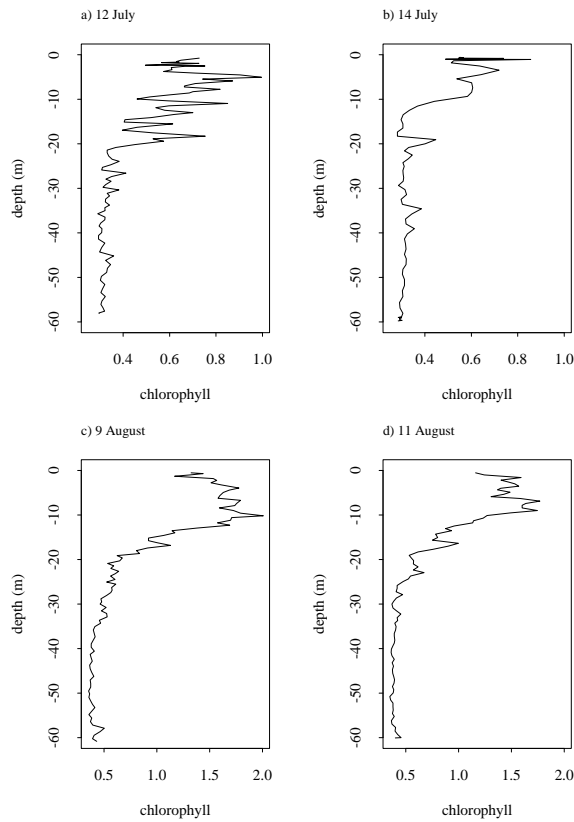


Figure 5.30: Chlorophyll (ml/l) at the Lynn of Morvern sample site on a) 12 July, b) 14 July, c) 9 August and d) 11 August.

5.4.3 Physical Influences on Vertical Structure

As shown by the level of stratification, river discharge is less influential in the outer than the inner basin. With the vertical density gradient being weaker, the physical structure and changes in it are less clear than for the inner basin.

River Discharge

River discharge would be expected to have less impact on the structure of the outer than inner basin, as it will be partially mixed into the near surface fjord water by the time it reaches the outer basin. The effect of river input into the head of the inner basin was however, discernible in the outer basin when the discharge had been particularly high.

In January the river discharge was very high, (fig. 5.31) with a maximum, over the time scale considered here, of $307 \text{ m}^3 \text{ sec}^{-1}$, compared to a yearly mean of $62.8 \text{ m}^3 \text{ sec}^{-1}$. On 19 January, there was a clearly defined surface layer (fig. 5.32) with a gradient sloping down towards the north. By the 20th, (fig. 5.33) the

salinity had fallen by >1 PSU - considering the overlapping sections of the cruise tracks - between 17 00 on the 19th and 19 00 on the 20th.

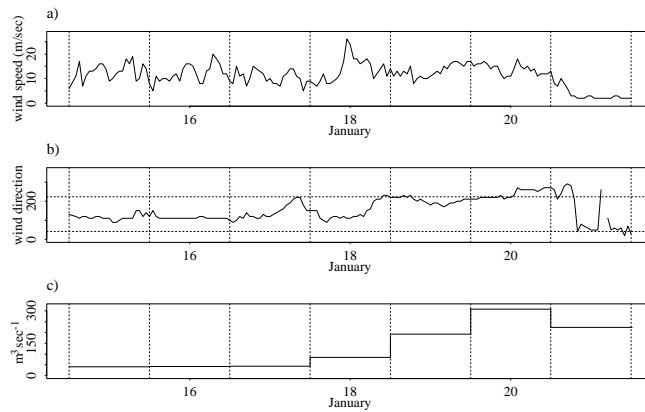


Figure 5.31: Meteorological data from 15 to 21 January, a) wind speed (m/s^{-1}), b) wind direction and c) river discharge (m^3s^{-1} .)

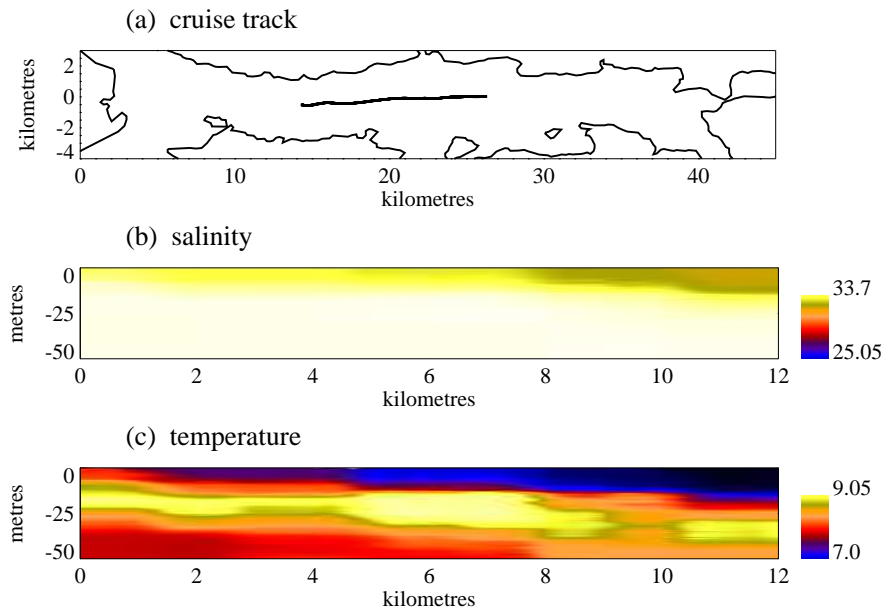


Figure 5.32: Axial plots showing the effect of river discharge on the upper 50m of the outer basin on 19 January.

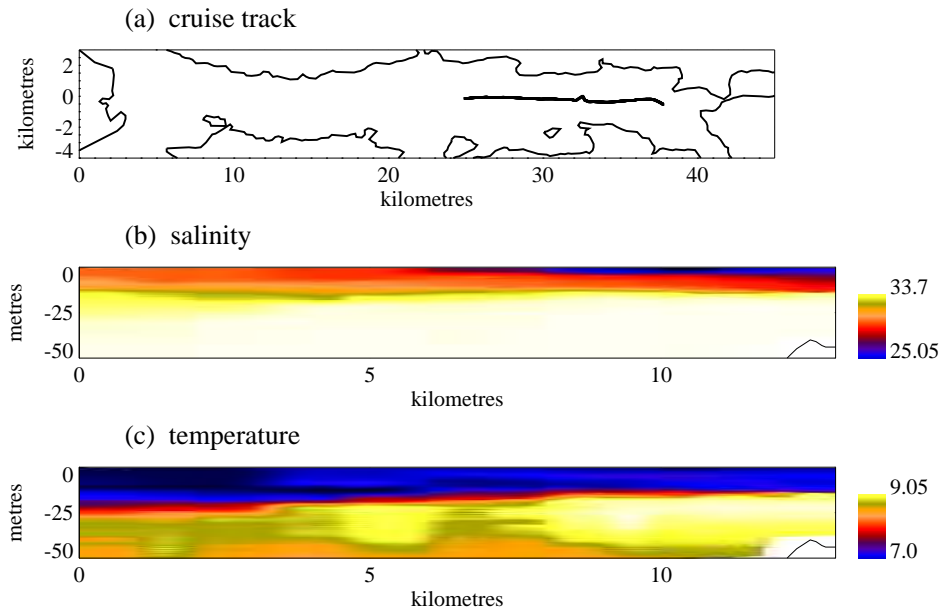


Figure 5.33: The effect of increasing river discharge on the upper 50m of the outer basin on 20 January.

The high freshwater input in January increased turbidity. In the inner basin on the 23rd, the beam attenuation maximum was 2.43 ln.m^{-1} at 5.13m and in the Lynn of Morvern on the 22nd, 1.3 ln.m^{-1} at 1m. In March, as for the inner basin there were signs of the influence of river discharge in the outer basin, with a vertical change in salinity of 4 PSU in 6m, approximately half way along the outer basin. The stratification index was also the highest of the year in the Lynn of Morvern.

Wind - ponding

The change in the vertical structure of the outer basin with ponding was less pronounced than for the inner basin. The lower level of stratification and deeper surface layer will have contributed to this, as may turbulent mixing caused by Corran. There is some evidence of ponding in May as there was for the inner basin, but the clearest example is August. On 11 August, there was a build up of lower salinity water at the head of the outer basin (fig. 5.34) with a deepening of the surface layer towards the north. There was also ponding in the inner basin at this time, as there had been upinlet winds since 8 August.

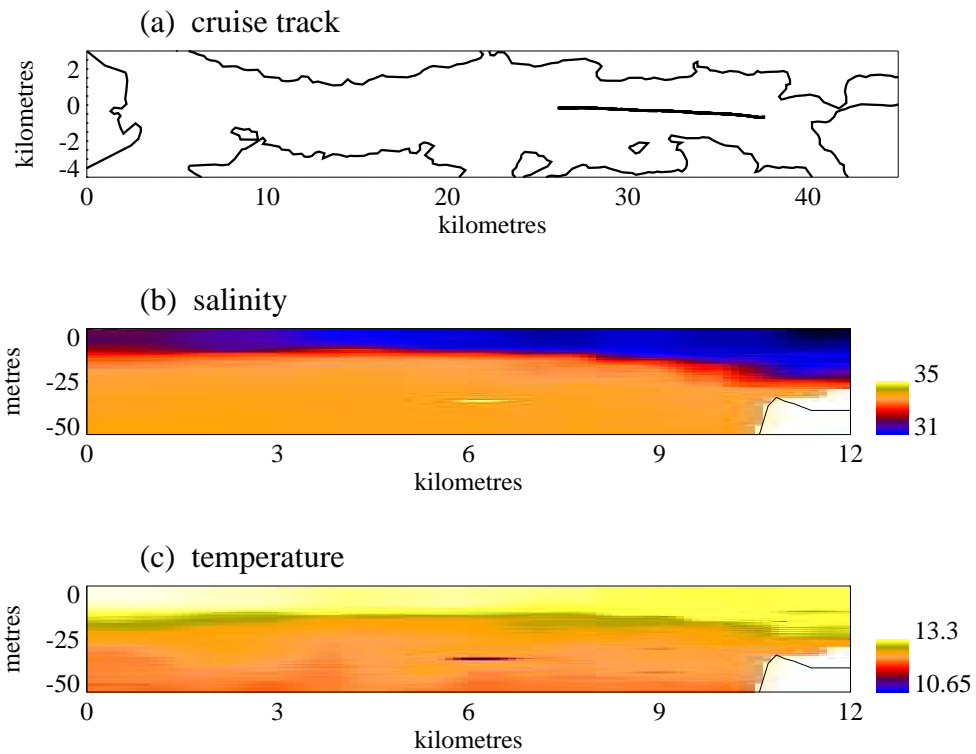


Figure 5.34: Axial plots of ponding in the Outer Basin on 11 August.

5.4.4 Deep Water Renewal

As for the inner basin, renewal in the outer basin was associated with spring tides and as expected of an external basin occurred more frequently - or at least stronger on partial renewal.

May

In fig. 5.35 of 19 May, warmer water can be seen intruding into the outer basin and there is turbulence on the loch floor stirring sediment, indicated by the beam attenuation. The water column below 15m warmed between 17 and 19 May (fig. 5.36(a)) and salinity increased over most of the water column (fig. 5.36(b)).

June

The data for 16 June (fig. 5.38) depicts a similar pattern to that of May, but the inflowing water also had a higher dissolved O_2 content. At the Lynn of Morvern sample site, the water column warmed below 20m from 14 to 16 June (fig. 5.39) but salinity over this time fell (fig. 5.37). The degree of stratification also declined (fig. 5.26) so in June the warming may just be due to mixing rather than a weak intrusion of coastal water.

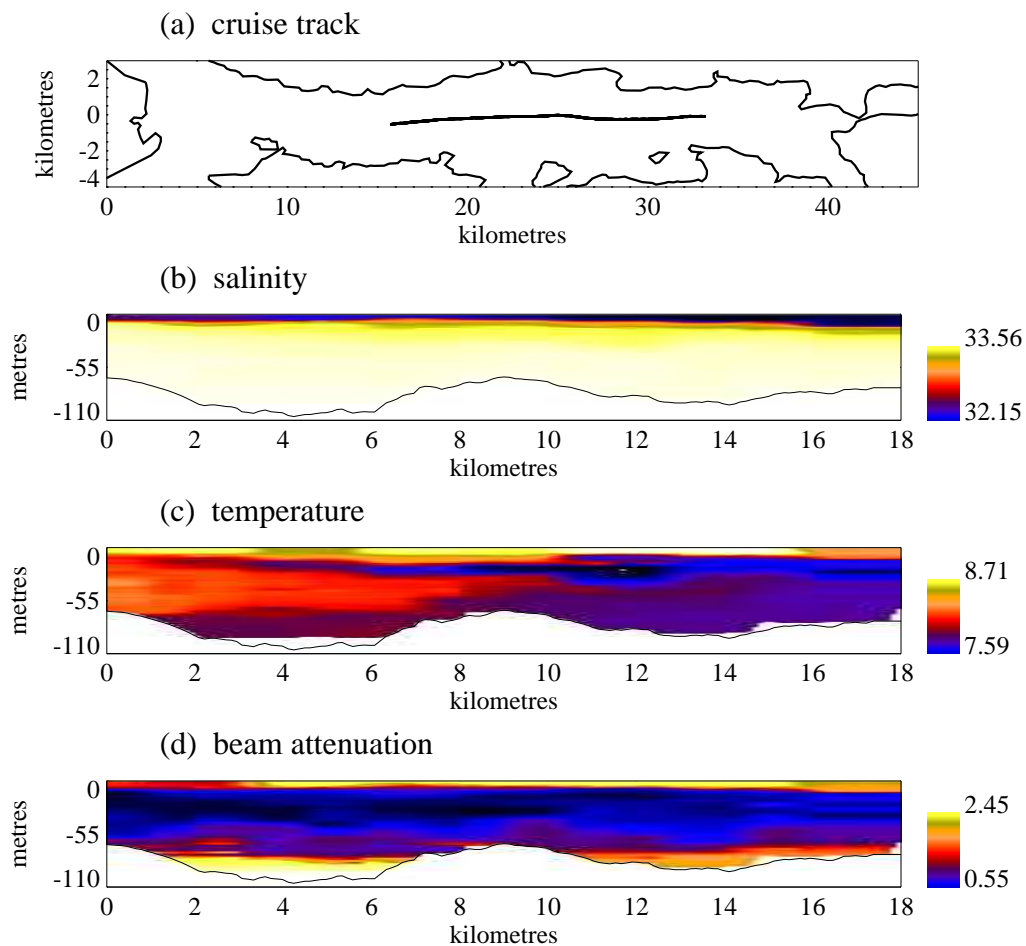


Figure 5.35: Axial plots of renewal in the Outer Basin on 19 May - warm water intruding in (c).

19 May and 16 June were just after maximum predicted tidal ranges, with the maximum in May on the 15th and the maximum in June on 14, 15 and 16th. The predicted spring tidal ranges for May and June are among the lowest of the year, so if the tidal cycle is one of the more important conditions, renewal in the outer basin of Loch Linnhe would be expected to be frequent as it is able to occur even at low tidal amplitudes.

In both the 19 May and 16 June temperature plots there is a tongue of colder water intruding into the warmer southern water, centred about ~ 20 -30m. In the inner basin Overnell and Young (1995) found that the inflowing tide flowed along the surface, with deep water flowing out and slack situated between 30 and 60m. If a similar situation exists in the OB, then the inflowing tide is accompanied by renewal this may produce inflow at the surface and at the depth at which renewal is taking place, with a compensating outflow between. Such a regime, may produce the images in fig. 5.35(c) and fig. 5.38(c). In May, renewal was

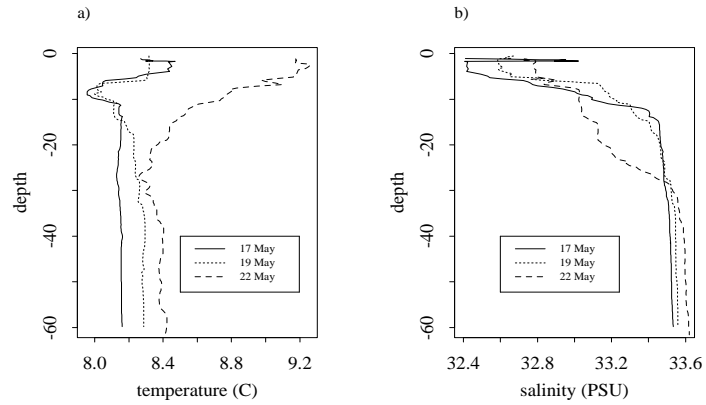


Figure 5.36: Lynn of Morvern sample site data on 17, 19 and 22 May of a) temperature and b) salinity.

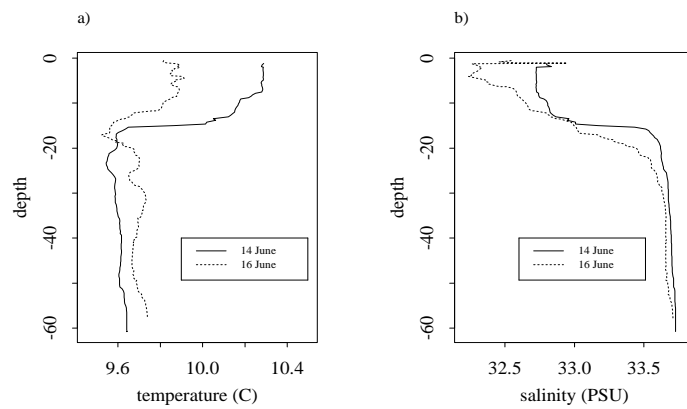


Figure 5.37: Sample site data of 14 and 16 June of a) temperature and b) salinity.

accompanied by ponding which by restricting surface outflow will increase the likelihood of subsurface outflow.

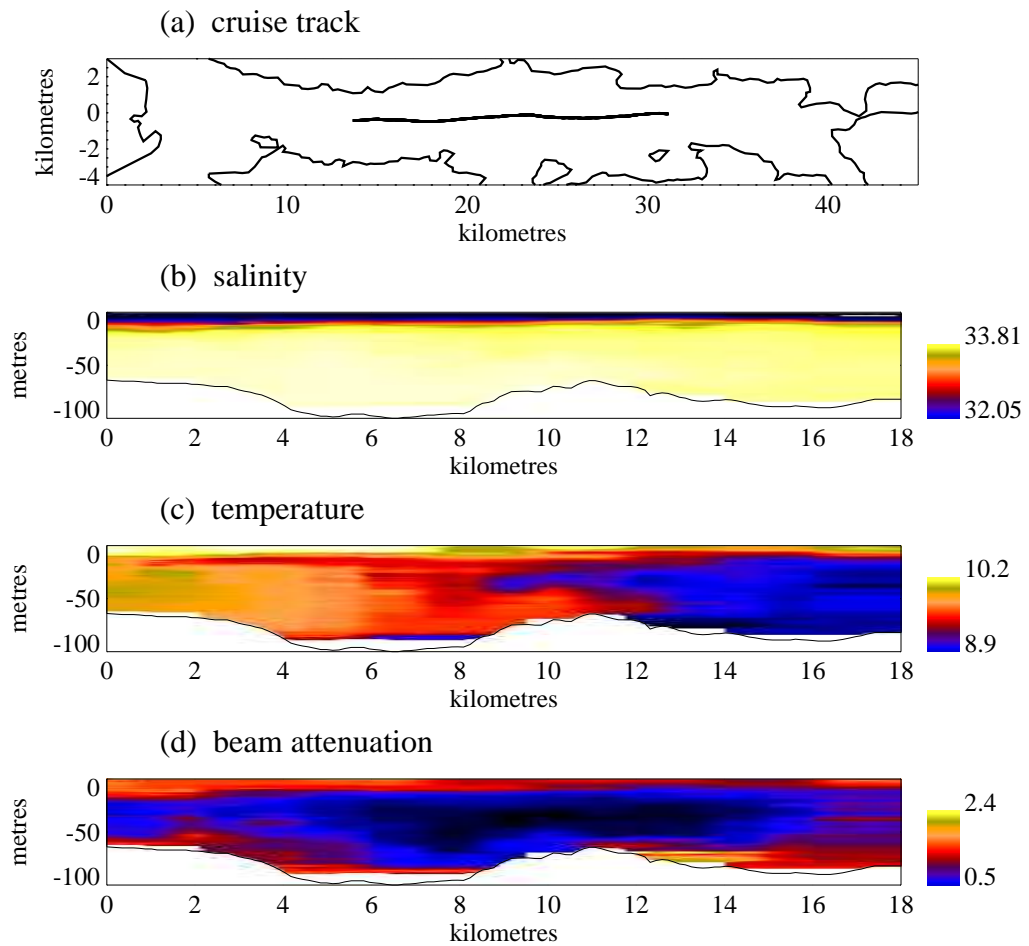


Figure 5.38: Axial plots of renewal in the Outer Basin on 16 June.

July

The axial cruise of 14 July, shows a region of warmer water intruding into the outer basin. There was a predicted maximum spring tide on 13 July and thermistor chain data also shows the water column warming below 15m from 10 to 16 July. There were upinlet winds during this period which may have caused ponding and river discharge was high - for the summer - exceeding $307 \text{ m}^3\text{s}^{-1}$ from 12 July on, though it was lower before the 12th.

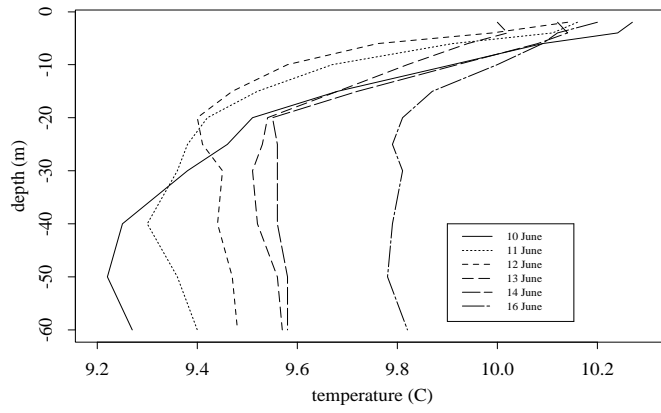


Figure 5.39: Lynn of Morvern thermistor chain data from 10 to 16 June.

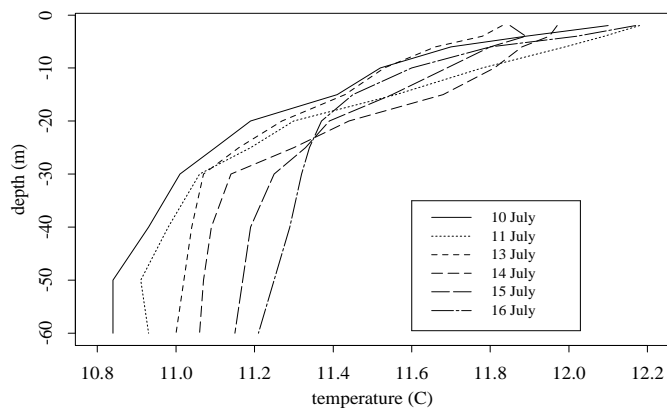


Figure 5.40: Lynn of Morvern thermistor chain data from 10 to 16 July.

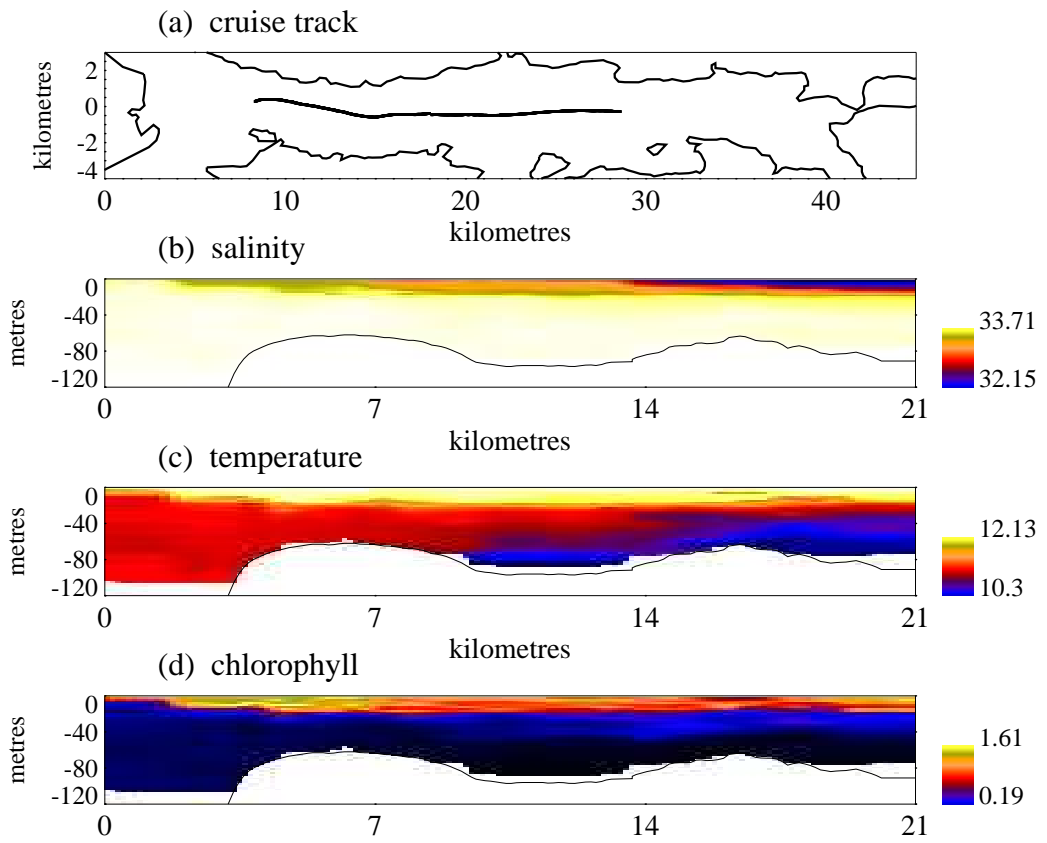


Figure 5.41: Axial cruise of 15 July.

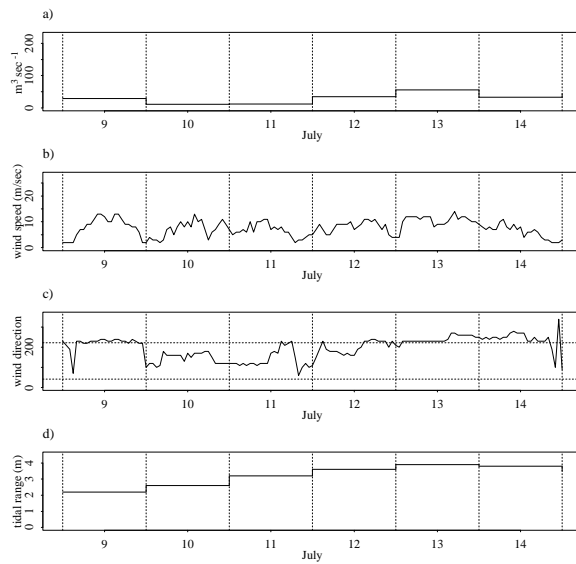


Figure 5.42: From 9 to 14 July, a) river discharge, b) wind speed, c) wind direction and d) tidal range.

September

The spring tidal range in September was particularly high with a maximum range of 4.1m on 9 September. From the axial cruise of 8 September (fig. 5.43) the southern section can be seen to be more saline and warmer and the thermistor chain (fig. 5.44) also shows a warming of the deep water. The Firth of Lorne - the coastal sea of Loch Linnhe - is warmer than the loch throughout the year. Fjords often have cooler winters and warmer summers than the coastal sea (Milne 1972) but many fjords flow into the Firth of Lorne and its depth is similar to that of the Lynn of Morvern.

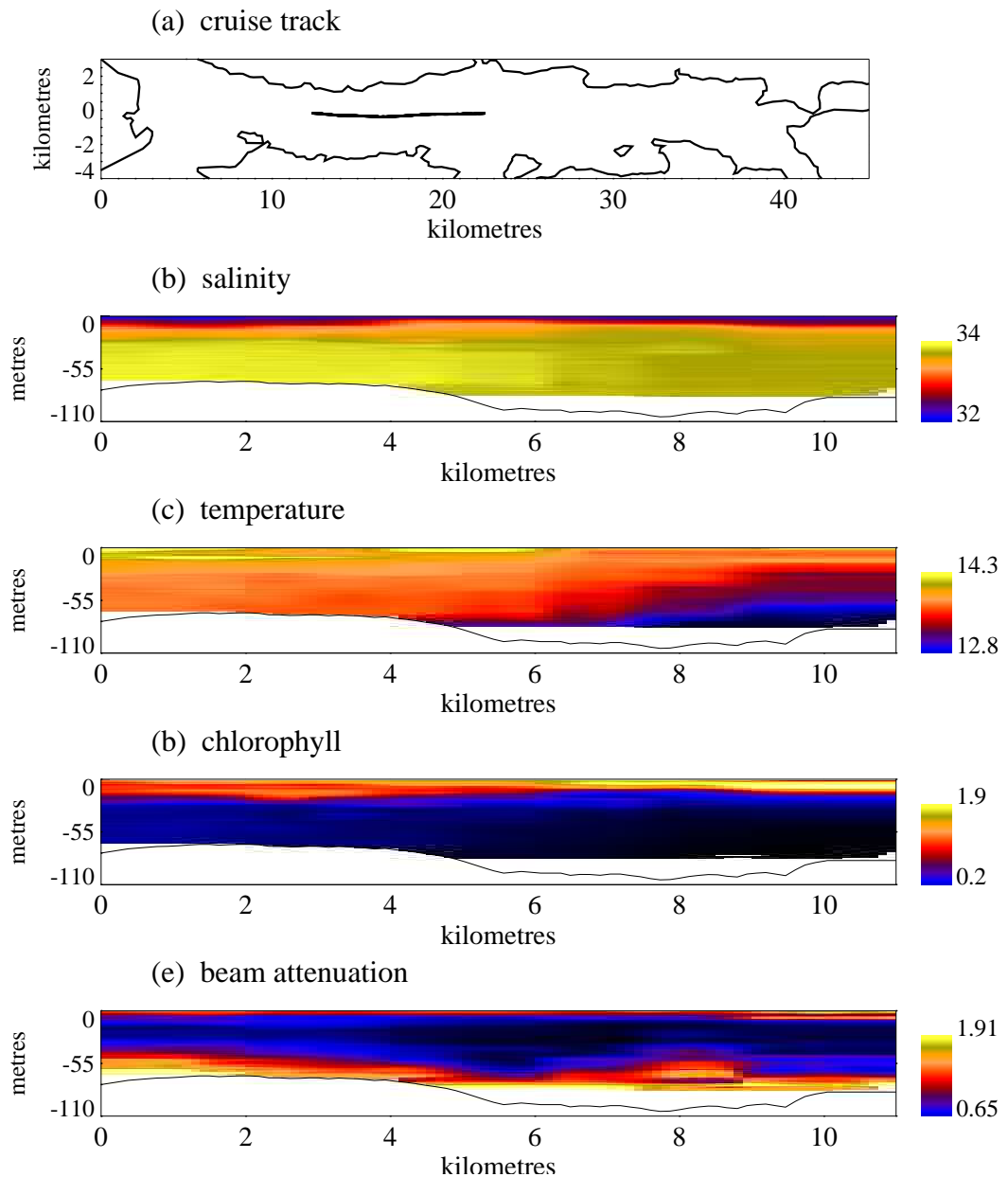


Figure 5.43: Deep water renewal into the outer basin on 8 September.

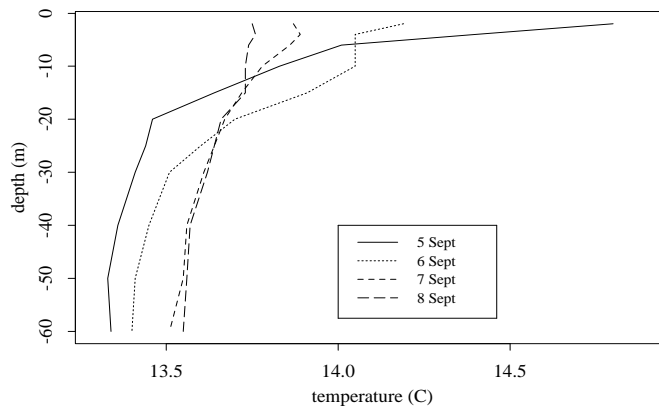


Figure 5.44: Lynn of Morvern thermistor chain data from 5 to 8 September.

October

From the axial data of 5 October (fig. 5.45) there was a slight increase in chlorophyll and decrease in temperature in the southern section of the outer basin. Between 4 and 6 October, however, there was no sign of an influx of coastal water at the LoM sample site and no thermistor chain data was measured for the period. The sample site was positioned close to the western shore which may not experience renewal immediately if the intrusion goes up the centre of the basin spreading laterally.

6 October was two days before the maximum spring tide, the predicted range of which was 3.5m. Renewal in October may have happened later, when the tidal range was greater - in Puget Sound Lavelle et al. (1991) estimated the minimum tidal height for renewal to take place to be 3.5m. The September renewal may have been able to commence before the maximum was reached because of the greater tidal range or considerably lower river discharge. River discharge did not exceed $7 \text{ m}^3\text{s}^{-1}$ from 30 August to 12 September, whereas it was greater than $80 \text{ m}^3\text{s}^{-1}$ from 1 to 7 October, with a maximum of $218 \text{ m}^3\text{s}^{-1}$ on 4 October. Wind conditions in September were light and variable in direction, but in October the wind was predominantly upinlet and much stronger. Upinlet winds and high freshwater input are both adverse conditions for renewal in the inner basin and may also be in the outer.

Conclusions

Comparing the timing of renewal events in the two basins, the outer basin would be expected to renew more frequently (Syvitski et al. 1987). River discharge, except for extreme values would be expected to be of considerably less importance

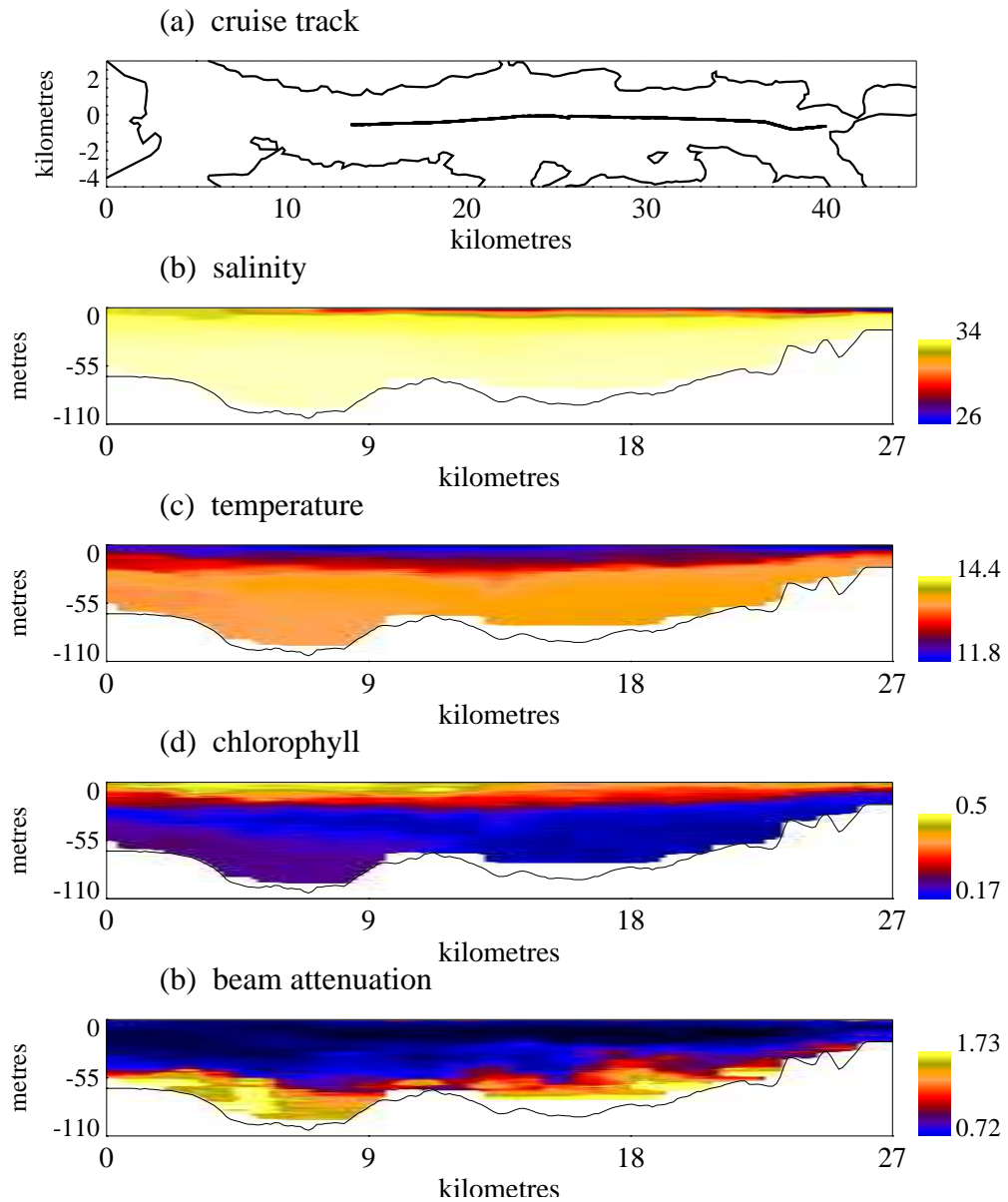


Figure 5.45: Axial cruise of 5 October.

than in the inner basin as its role in maintaining stratification is less and by the Lynn of Morvern it is generally mixed into the water column. In May, river discharge was very low ($< 10 \text{ m}^3 \cdot \text{sec}^{-1}$) which may have aided the renewal since the tidal range was relatively low (maximum of 3.5m.)

The position of Loch Linnhe makes it difficult to check the importance of coastal upwelling and there are insufficient examples of the timing and extent of renewal events in the outer basin to identify any factors of importance other than the tidal range. It can however be hypothesised to behave similarly to the IB.

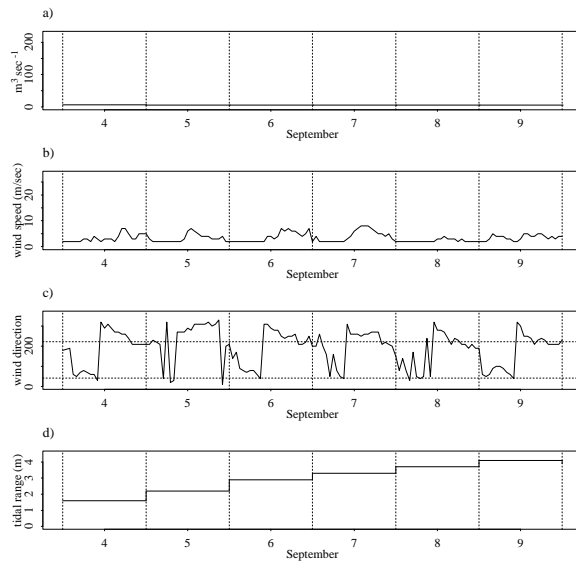


Figure 5.46: From 5 to 9 September, a) river discharge, b) wind speed, c) wind direction and d) tidal range.

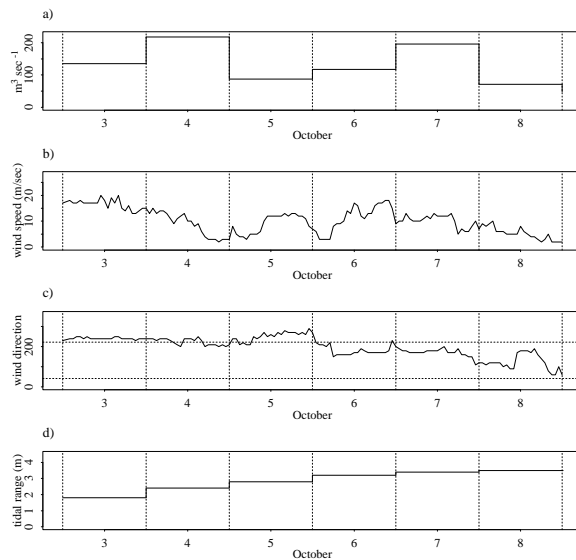


Figure 5.47: From 3 to 7 October, a) river discharge, b) wind speed, c) wind direction and d) tidal range.

5.4.5 Bathymetry

Fronts often occur at the mouth of a fjord (Parsons et al. 1983) with the position and magnitude being determined by the water velocity. A principal factor in controlling the position of the front in the Lynn of Morvern is the tidal cycle. During spring tides the front was further into the basin, being located around the region where the seabed shelves up at the southern end of Lismore. While during

neap tides, it was closer to the sill between Lismore and Mull. Other factors such as the direction of axial winds and the freshwater content of the loch, which influence the speed of outflow, were also of importance.

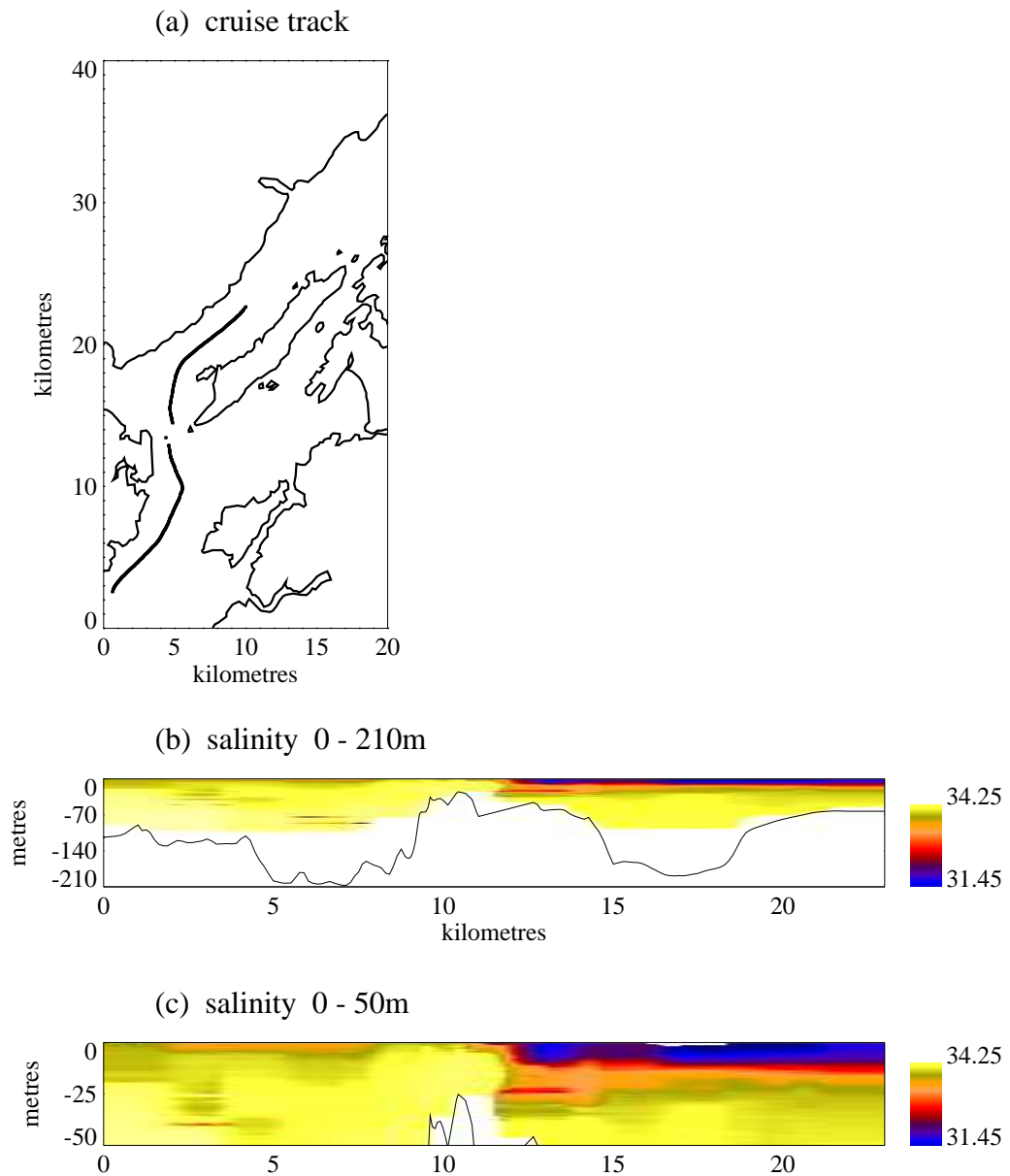


Figure 5.48: Axial plot of the front at the mouth of the Lynn of Morvern on 27 March .

On 27 March there were neap tides and the front was close to the sill between Lismore and Mull (fig. 5.48.) Other factors may have contributed in pushing the sill south, such as the heavy river discharge and periods of downinlet winds.

On 12 August there were spring tides and the front was close to the start of the Outer Basin shelf (fig. 5.49.) Upinlet winds will have contributed to this effect - there was ponding in both basins preceding this date - by lessening surface outflow.

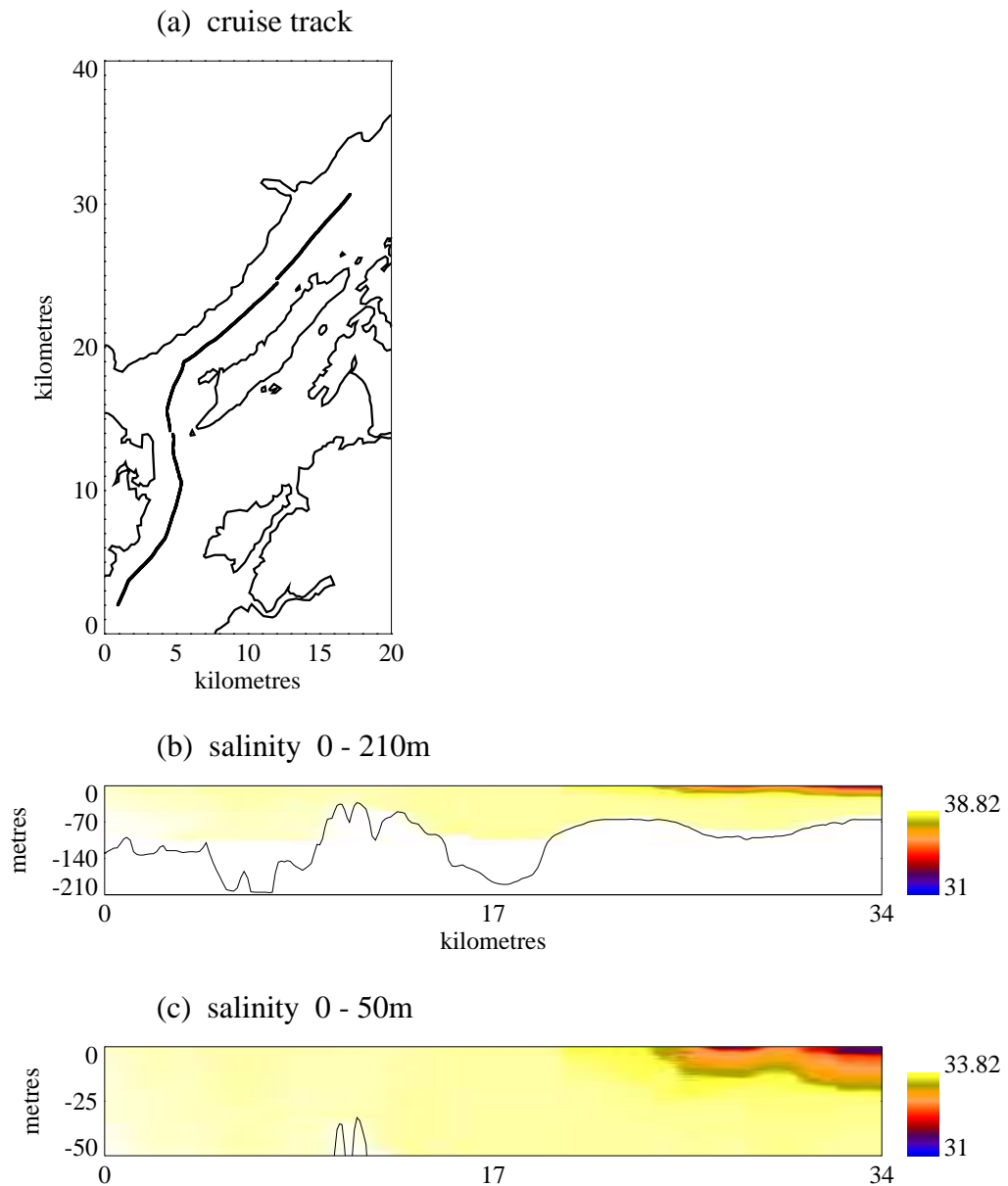


Figure 5.49: Axial plot of the front at the mouth of the Lynn of Morvern on 12 August.

This general behaviour is visible in other months, with the influence of meteorological conditions playing a role in the final position, such as on 14 July when upinlet winds and spring tides pushed the front further north while on 6 October, despite the spring tides the downinlet winds pushed the front southwards.

The influence of the spring-neap tidal cycle on the position of the front may also be influenced by the flow of water through the Sound of Mull. Water flowing from the Firth of Lorne over the sill between Lismore and Mull either flows up Loch Linnhe or round Mull into the Sound of Mull. Similarly, water flows from the Sound of Mull into the Firth of Lorne. The relative position of the front in this region will be affected by the strengths of these conflicting flows. Other

contributing factors are axial winds, river discharge and stratification. The semi-diurnal tidal cycle may also be of importance but there is insufficient evidence to examine this.

5.5 Outer Basin: Biotic Structure

5.5.1 Chlorophyll *a* in the Water Column

As for the IB, the vertical structure of chlorophyll in the OB changed rapidly. fig. 5.50 shows the change in the vertical structure at the LoM sample site over 7 days in May.

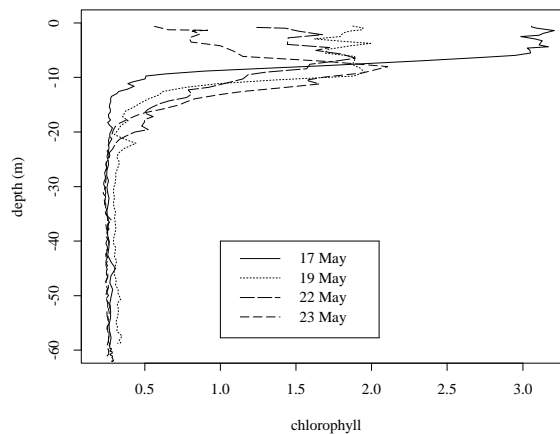


Figure 5.50: Changing vertical structure of chlorophyll *a*, in May at the Lynn of Morvern mooring.

On 22 April there was an extensive region of chlorophyll on the seabed (fig. 5.51) in the centre of the outer basin. This may have entered the loch in water from the Firth of Lorne or the Lynn of Lorne. It is highly unlikely that the chlorophyll could have sedimented from the surface layer of the outer basin, as there is no evidence of a large phytoplankton bloom on the surface before this date. The most likely source is the Lynn of Lorne, water from which may enter Loch Linnhe through the channel between the north of Lismore and the mainland. The chlorophyll density in the northern part of the Lynn of Lorne on 25 April was as high as 16.8 mg m^{-3} , which is significantly greater than any measured value over 1991 in Loch Linnhe or the FoL. The possible link between Loch Linnhe and the Lynn of Lorne, especially in regard to chlorophyll is discussed further in the following chapter on horizontal heterogeneity.

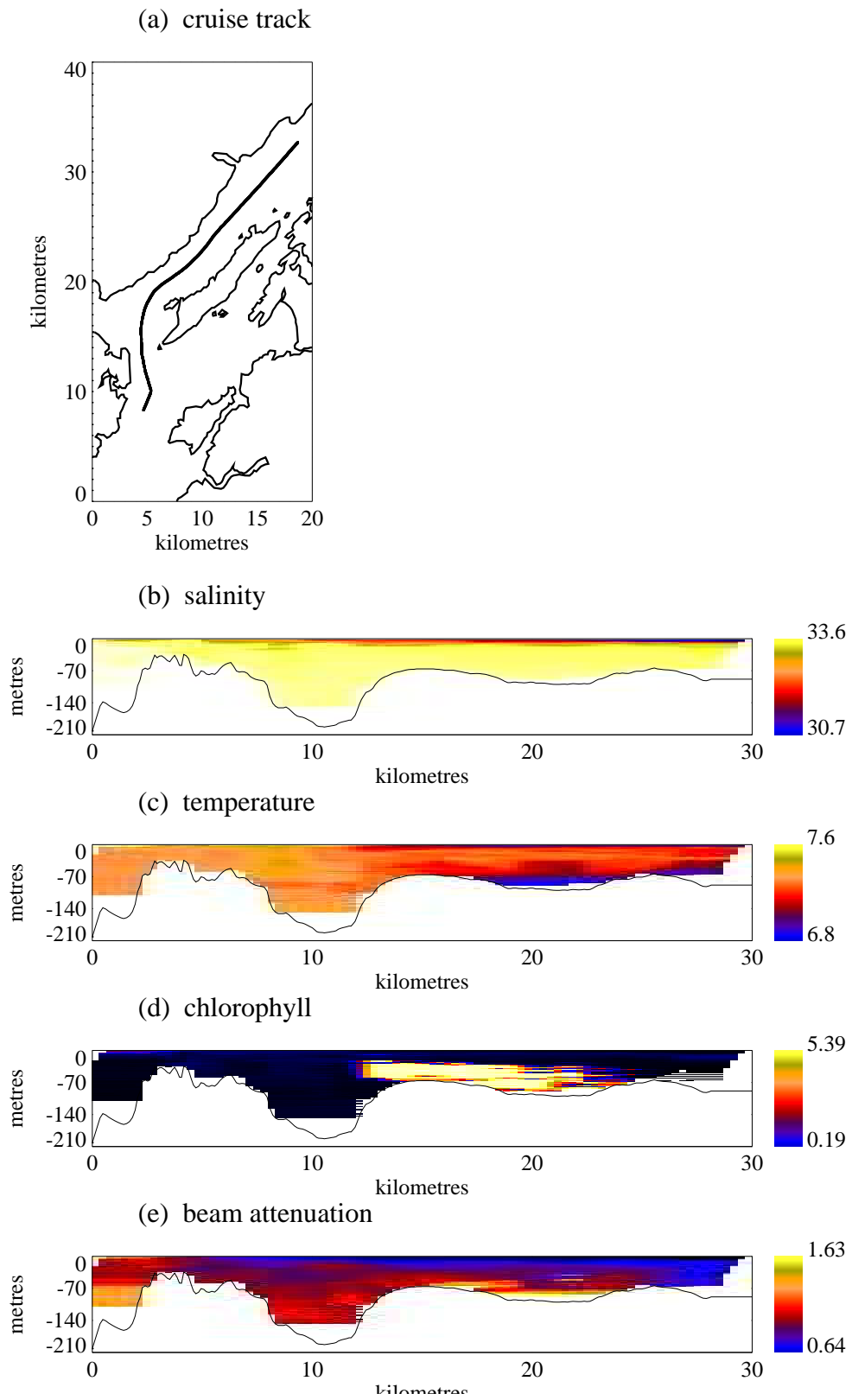


Figure 5.51: Axial plot the Outer Basin on 22 April, with a high density of chlorophyll in deep water.

Subsurface Chlorophyll

Moving seaward, the species composition of Loch Linnhe may diversify, as the influence of river discharge decreases and water temperature and salinity are more stable. Tett (1973) found the species diversity of the Lynn of Lorne to be greater than Loch Etive. Unlike the inner basin, in the outer basin there was often a subsurface maximum of chlorophyll density, which may reflect the presence of a greater variety of species. Contact with the Lynn of Lorne may influence species composition as Loch Creran, which flows into the northern end of the Lynn of Lorne, was found by Lewis (1988) to be dominated by dinoflagellates during the late summer and early autumn. Dodge (1995) considered the density of *Lingulodinium machaerophorum* in Loch Creran to be unusual for a Scottish sea-loch but similar to that for Norwegian fjords.

For 15, 16 and 17 June the chlorophyll maximum was predominantly subsurface, throughout the outer basin. In May and August, however, chlorophyll was confined to the surface. If the position of chlorophyll was due to a change in species composition, then the relatively low spring tides in June may have allowed dinoflagellates to be dominant.

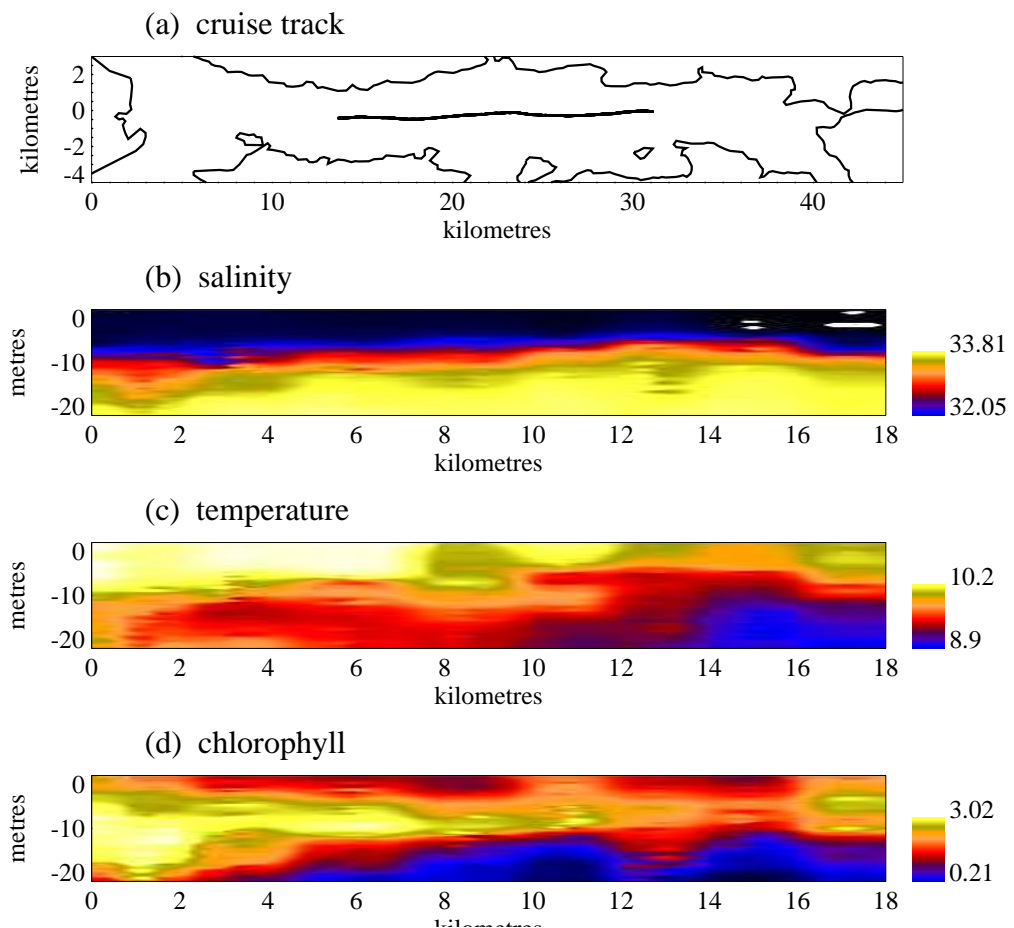


Figure 5.52: Axial plot of 16 June, indicating a deep water chlorophyll maxima.

5.5.2 Influence of Physical Structure

Deep Water Renewal

Deep water renewal appears to be of less importance in the import of chlorophyll than in the IB. This may be as the Firth of Lorne was not particularly productive. The Lynn of Lorne, however, the head of which is half way along the outer basin, may be a source of chlorophyll and this is dealt with further in the following chapter.

The 7 September axial cruise shows the surface chlorophyll to go deeper than further north, but have a lower maximum, and the chlorophyll also appears to be sinking throughout the water column. This may be due to there being more turbulent mixing in the south, which causes the chlorophyll to sink out of the surface. For 5 October, the chlorophyll density near the seabed in the south was higher than the water above - except for the surface layer. This may also be a result of there being more mixing close to spring tides. Thermohaline convection may also play a role in mixing at this time as the surface layer was being cooled by river discharge and was cooler than the water below.

Fronts

Parsons et al. (1983) found that the chlorophyll density at the front in Saanich Inlet varied according to the lunar tidal cycle. While the productivity of the Lynn of Morvern front can be seen from the axial data, the temporal resolution of the data does not allow for the assessment of tidal effects on productivity.

5.6 Conclusions

The primary aim of this analysis was to identify the ways in which meteorological and tidal forcing within Loch Linnhe affected the hydrodynamics and to ascertain the resulting effect on the biota. From the vertical data, notably that from the axial cruises, Loch Linnhe has been shown to be highly susceptible to meteorological and tidal forcing. This is interesting, not only in the degree of response to external forces but also in the range of hydrodynamic features that have been identified for a single loch system.

Over the entire water column, the lunar tidal cycle is particularly influential. In both basins, spring tides lead to vertical homogenisation of the water column, along with resuspension and sedimentation. The strength of tidal mixing throughout Loch Linnhe may also account for the lack of a lower boundary. While mixing is expected to be greater with wider tidal ranges and vertical homogeneity following spring tides has been shown for estuaries, this extent of mixing is unusual for a fjord. The weaker stratification of Loch Linnhe, in comparison with

the fjords of North America and Southern Norway (those tending to be represented in literature,) along with the shallower sills and greater tidal range will increase the importance of tidal mixing. This will also be true of other Scottish sea-lochs. Tidal mixing in the inner basin would be expected to be stronger than for most basins as the tidal range is high, and the entrance into the basin shallow and narrow generating fast flows into the basin and possibly tidal choking. Unfortunately, the frequency of data collection does not enable the effects of the fortnightly periods of homogenisation and restratification on the biota of the loch to be identified. The effect of which would be largely determined by the time taken for the re-establishment of stratification. The greater freshwater content of the inner basin over the outer basin will allow stratification to build up quicker, despite the more extensive tidal mixing. The timescale of the lunar tidal cycle can affect the establishment of a phytoplankton bloom. In South San Francisco Bay (Cloern 1991) and the Gulf of Maine (Balch 1981) variations in tidal mixing were found to affect species composition and the overall biomass over the lunar tidal cycle.

The orientation of Loch Linnhe - along with the linear alignment of the basins - makes it particularly vulnerable to the wind, thus ponding has the potential to be a frequent event. From the periods of data collection alone, there were four clear ponding events in the inner basin in 1991. While inner basin ponding could be established within 24 hours, the weaker stratification of the outer basin - through the surface layer having a lower freshwater content and being deeper, along with the turbulent mixing from Corran - means that the response time of the outer basin is longer. Ponding will affect primary production both in the stratification and stabilisation of the surface which permits rapid warming and in the subsequent outflow of the surface and entrainment, on the relaxation of the wind stress. As with the tidal mixing described above, this may produce a boom and bust type situation, with rapid growth being stopped by the surface layer flowing rapidly out of the basin, rather than by turbulent mixing. The orientation of Loch Linnhe and river input being predominantly into the head of the loch will increase its susceptibility to ponding but the relatively weak stratification and strong tidal mixing will lessen it, in comparison with other basins.

Deep water renewal is frequent in both basins, particularly in the outer basin. In both basins renewal is very clearly linked with spring tides. The strength of individual renewal events, along with evidence of the outer basin renewing more frequently, indicates that the amount of river discharge is also influential. In other studies of renewal in fjords, fjords with shallow sills tend to renew in periods with high tidal ranges. Shallow sills have also been linked with high river discharge preventing renewal. In Scottish sea-lochs, sills are typically shallow and tidal ranges high, so spring tide driven renewal will be expected to dominate in many Scottish sea-lochs. Lochs Fyne and Striven are exceptions to this with deep sills, low tidal ranges and low freshwater input. This does not however mean that renewal can necessarily be considered frequent for all Scottish sea-lochs, as with greater freshwater discharge baroclinic flow will be prevented. In October, inner basin renewal may have occurred despite heavy river discharge, but the data is

not conclusive. Downinlet wind may have enhanced estuarine flow enough for the mixing at Corran to be insufficient for the prevention of renewal. In more stratified basins, heavy river discharge may enhance estuarine circulation enough on its own for renewal to be able to take place. The relationships are complex, in Loch Etive, the very shallow long sill along with high river discharge makes renewal an infrequent event, presumably because of the extent of mixing at the sill. The substantial mixing taking place around spring tides in the inner basin, by contributing to the mixing of the freshwater deeper into the water column may also play a role in the prevention of the event - furthering the preference for low river discharge. In other regions with greater stratification of the surface layer, heavy river discharge is less problematic as with a deeper sill and stronger stratification, the surface layer is not mixed down through the water column. In such a situation, however, renewal may be more frequent with neap tides.

The injection of nutrient rich water with deep water renewal does not increase the phytoplankton biomass in Loch Linnhe. In more stratified fjords renewal has the potential to break down the stratification bringing nutrient rich water up into the depleted surface layer. Throughout Loch Linnhe, the surface layer is never depleted of nutrients and there is no evidence of renewal increasing productivity. As renewal is driven by spring tides, they are more likely to be periods of low growth as turbulent mixing is greater. In May, the transport of chlorophyll cells from the head of the outer basin into the inner basin during the renewal event did increase the chlorophyll density but only through advection of the cells. Increased productivity at the head of the outer basin at this time, being the result of stabilisation through ponding.

The amount of information which can be derived from the biological data is limited. Loch Linnhe experiences frequent mixing, with a continually changing regime of stratification and tidal mixing. Since ponding is able to increase production, productivity may be hindered by the lack of stability due to the continual transition from vertical homogeneity to stratification and back again. The continual seaward flow of the surface layer is also prevented by ponding. In the inner basin, there are times when the tidal range exceeds the depth of the surface layer. This extensive exchange with the sea produces high levels of surface layer outflow and entrainment. The typically short residence time of water in the surface layer will contribute to the low productivity as on the spatial scales within the loch system, phytoplankton behave as passive tracers. Net growth cannot take place if the rate and depth of mixing mean that the phytoplankton are carried out of the surface layer before it can multiply. The prevention of outflow with ponding by increasing the residence time will increase growth.

As spring and summer is the most important time for phytoplankton growth, an important difference between mainland North American and Norwegian fjords is in the seasonal pattern of river discharge. More northern fjords often receive most of their river input from snow melt in spring and ice melt in summer. In Scottish sea-lochs however, river discharge is strongly related to precipitation and spring and summer is the time of low river input. The relationship between

hydrodynamics and productivity will be different between fjords experiencing a summer freshet and strong summer stratification and those with low summer river discharge with resulting low stratification. The less stratified fjord may also experience considerably more tidal mixing because of its smaller size, greater tidal range and smaller entrance. The lack of river discharge will therefore also increase the overall importance of tidal mixing. This will increase the importance of features such as ponding to primary productivity within Loch Linnhe, in comparison to more stratified fjords elsewhere. Less turbid Scottish sea-lochs may experience a stratification driven bloom following high precipitation in the Spring, but the turbidity in Loch Linnhe prevents the bloom commencing until later.

A key feature of Loch Linnhe is that it is a very active environment, many other fjords are typically strongly stratified with short periods of rapid turnover during renewal. This may in part answer the question posed in Chapter 3 of the reason for low primary and secondary production. Tidal mixing undoubtedly contributes to this, by increasing turbidity, causing sedimentation of phytoplankton and through turbulent mixing prevent the strengthening of stratification. In Part 3, through the application of an ecosystem model to Loch Linnhe, the aim is to try to understand why productivity is low and gauge the importance of the active hydrodynamic environment on production.

Chapter 6

Horizontal Heterogeneity

6.1 Introduction

Horizontal variability in fjords, both physical and biological, is generated by the change in conditions from river mouth to coastal sea and the influence of topographical features such as sills and shelves - typical glacial features - on circulation. Horizontal structure may be controlled by processes and events covered in Chapter 5, other processes confined to the surface layer, meteorological forcing and the relationship with other water bodies. In this chapter, an understanding of the horizontal structure is developed along with the identification of some of the meteorological, tidal and structural influences. A full catalogue of the interpolated surface data is available in Appendix A.

6.2 Inner Basin: Physical Structure

The inner basin is a more ‘typical’ fjord than the outer basin, its aspect ratio is higher and the sides more regular. The topography makes the funneling of winds along its length more likely than in the outer basin but will also provide more protection from cross-axial winds. The narrows at Corran may provide some shelter for the south-west corner of the basin and the embayment on the western shore, Inverscaddle Bay, may provide a source of interference from cross-axial winds.

With most of the freshwater input flowing into the northern end of the basin, the influence of river discharge will be greater in the north with turbulent mixing and tidal choking being more influential at Corran in the south. The localisation of the freshwater input creates a wide range of surface salinities which enables the effects of wind forcing to be more clearly seen. They can, however, be masked by extremely heavy rainfall. This freshwater runoff also increases the level of stratification in the north, making it more sensitive to wind forcing than the

more mixed southern region.

As shown in Chapter 5, the surface layer of the inner basin is relatively thin and strongly stratified - both of which increase the susceptibility of the surface layer to wind forcing. As the prevailing wind direction is upinlet, and storm events are generally associated with weather systems from the Atlantic - consisting of upinlet winds and heavy precipitation - ponding of the surface layer, which in Chapter 5 was shown to occur, may be frequent.

6.2.1 River Discharge

The effect of river discharge, in particular the freshwater plume, is not immediately apparent in the surface data. This is probably due to the depth of data collection, at approximately 4m it will tend to be below the surface plume. During periods of high river discharge such as in January and November, the northern end was more turbid than the rest of the basin. River discharge, however, is an important factor in driving stratification - generating a lower salinity and warmer northern end to the basin. Entrainment, which is enhanced by heavy river discharge, often produced a more saline landward end of the basin.

6.2.2 Fronts

From the axial data, a front was present in the inner basin on 19 May (fig. 5.8.) Horizontally on 21 May (fig. 6.1 (c) & (d)) there was a sharp north-south difference at the surface, of low salinity and high temperature in the north, characteristic of stratified water, and high salinity and low temperature in the south, typical of more mixed conditions. Stratification in the north had confined the river discharge to the surface layer where it had warmed through solar radiation and turbulence in the south had mixed the less saline surface down into the water column bringing up cooler water from below.

6.2.3 Corran

Flow through Corran is visible for many months and surface layer turbidity was greater there. Dependence on factors such as semi-diurnal tidal cycle, lunar tidal cycle, depth of the surface layer and the degree of stratification on mixing here is not clear. The depth of data collection, will also play an important role in a plume being visible in the data. Turbidity throughout the basin, however, has already been linked with the lunar tidal cycle.

From 23 to 25 April, salinity in the south fell as the temperature and chlorophyll increased. The cruises were conducted at comparable depths and positions in the semi-diurnal tidal cycle. The tidal range however, increased between these cruises, which may have increased mixing and turbidity in this region. Estuarine

circulation on 25 April may also have been greater than on the 23rd, as the wind had moved away from being upinlet. If tidal choking is important, as suggested by Watts (1994), then the lunar tidal cycle especially would affect turbulence in this region.

6.2.4 Bathymetry

A possible influence of the bathymetry on upwelling was discussed in 5.2.5. Such an effect may not, however, outcrop on the surface. In some months there is a salinity/temperature boundary in the vicinity of the rise in the seabed which may be due to the bathymetry, but it also may identify the range of turbulence generated by Corran.

On 27 February, 18 July and 9 October the surface plots suggest that entrainment may have occurred to the north of the rise in the seabed. The water to the north of it was of; higher salinity, warmer in February and October and cooler in July. Beam attenuation was also lower there at the start of the entrainment in February and July. On 18 June (fig. 6.20) the surface plots suggest that there was upwelling in this region.

6.2.5 Wind

There is evidence of ponding, the release of ponding and the surface layer being forced down the loch. The high aspect ratio of the inner basin seems to protect it from all but axial winds, to which the response time is rapid. The influence of cross-axial winds cannot be discounted, but there is no evidence of it in the available data.

Ponding

There is horizontal evidence of ponding on: 23 April, 21 May and 14 August. In May and August, there had been a prolonged period of upinlet wind, but on 23 April it was only on the day. The freshwater driven stratification on 23 April will have increased the susceptibility of the surface layer to wind forcing.

Surface layer plots of salinity (fig. 6.1) show horizontal banding with lower salinity water in the northern end, progressively becoming more saline seaward. The strong stratification and stability, generated by ponding, allowed the surface layer to warm rapidly, as with the strong density gradient, mixing between the surface and deeper water was minimal.

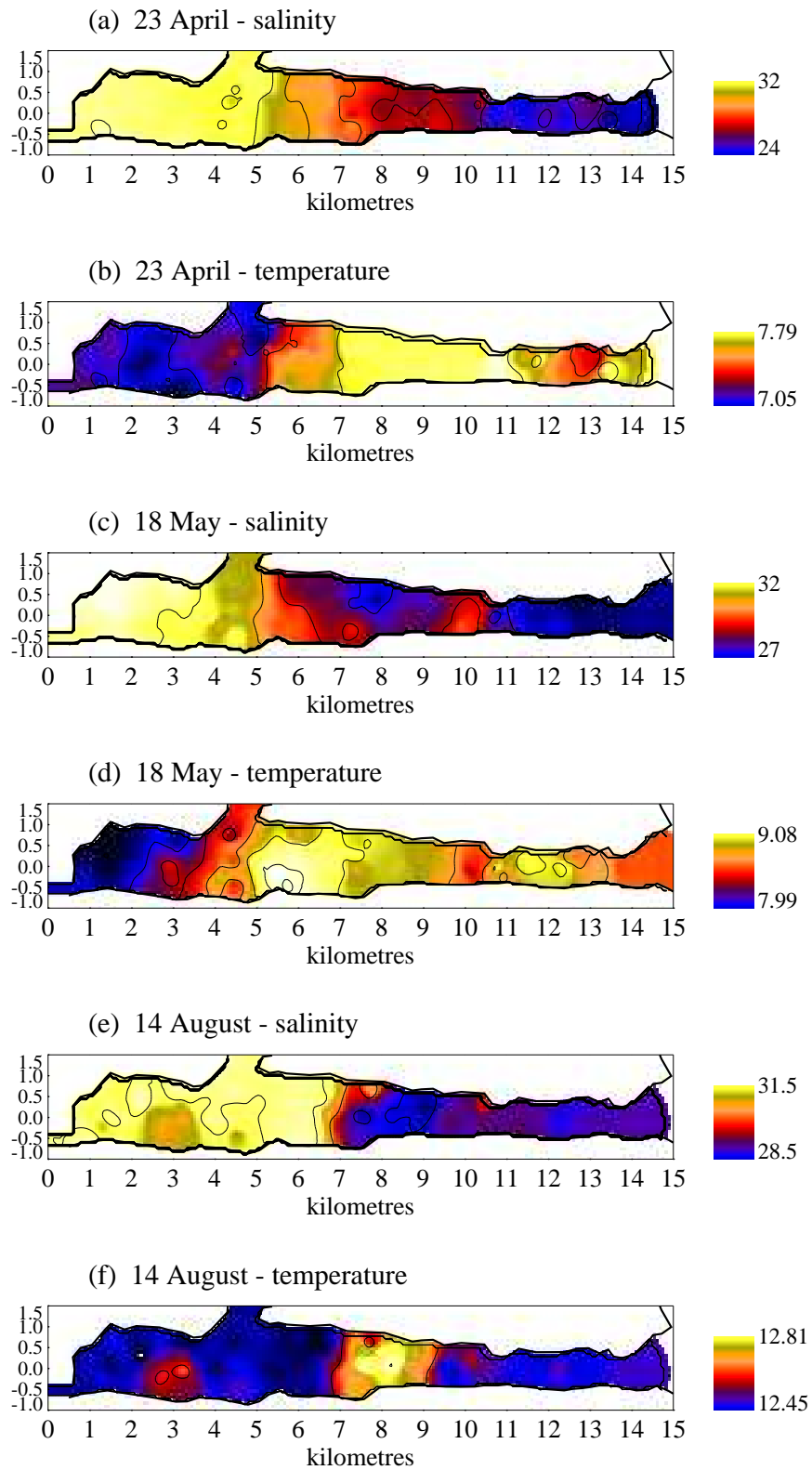


Figure 6.1: Inner Basin interpolated surface cruise plots of salinity (PSU) for (a) 23 April, (c) 21 May and (e) 14 August and temperature (C) for (b) 23 April, (d) 21 May and (f) 14 August. Prior to these cruises the wind had been upinlet, causing ponding.

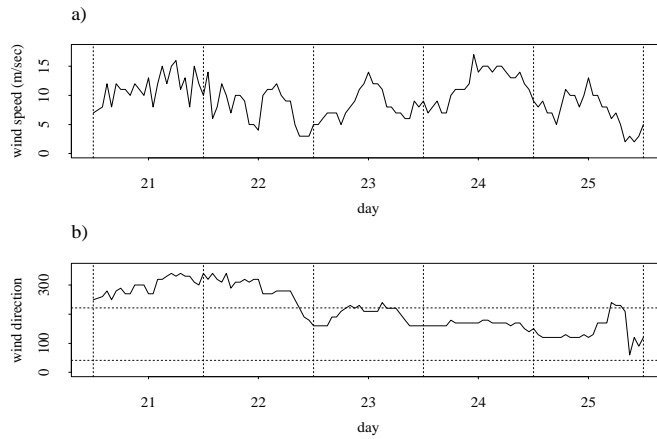


Figure 6.2: (a) wind speed and (b) wind direction from midnight 20th to midnight 25 April, the dashed horizontal lines on indicate upinlet (222°) and downinlet (42°) winds.

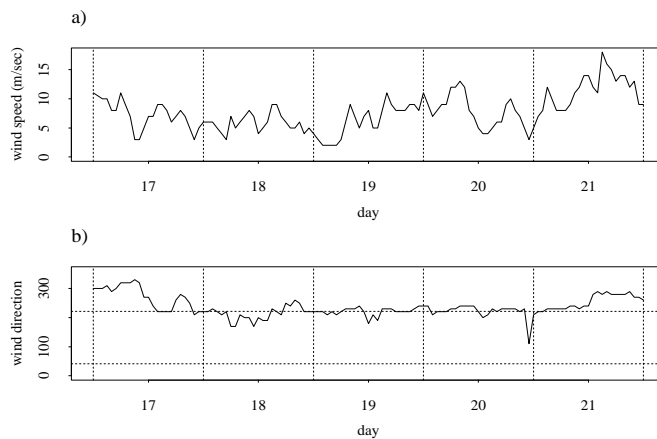


Figure 6.3: (a) wind speed and (b) wind direction from midnight 16th to midnight 21 May.

Release of Ponding

Before 16 July, there had been a period of upinlet winds (fig. 6.6). Overnight between the 14th and 15th the wind had been downinlet, before changing to up again. If the surface layer ponded before the 14th (evidence from other occasions suggests that it would have,) upon the change in wind direction the ponding will have been released and blown down the loch, before outflow was curtailed once more. As the surface layer was forced down the loch, a compensating flow of deeper, more saline water will have been entrained into the surface behind

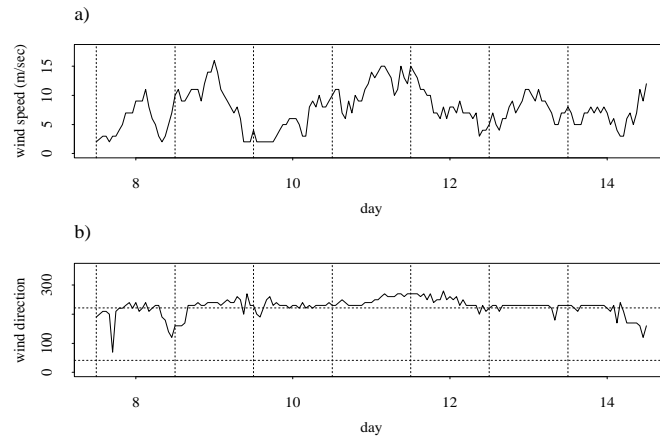


Figure 6.4: (a) wind speed and (b) wind direction from midnight 7th to midnight 14 August.

it. Such a pattern of events would generate the surface structure of 16 July (fig. 6.5a.) Residence times in the basin during July, as calculated by Officer and Kester (1991), change between 12 to 17 July from being relatively long, for Loch Linnhe, to the shortest of the year. This also supports the premise of ponding followed by outflow. By 18 July, the wind was no longer from the south-west and the ponded surface layer had been allowed to flow out of the inner basin entraining more saline water up behind it (fig. 6.5b.)

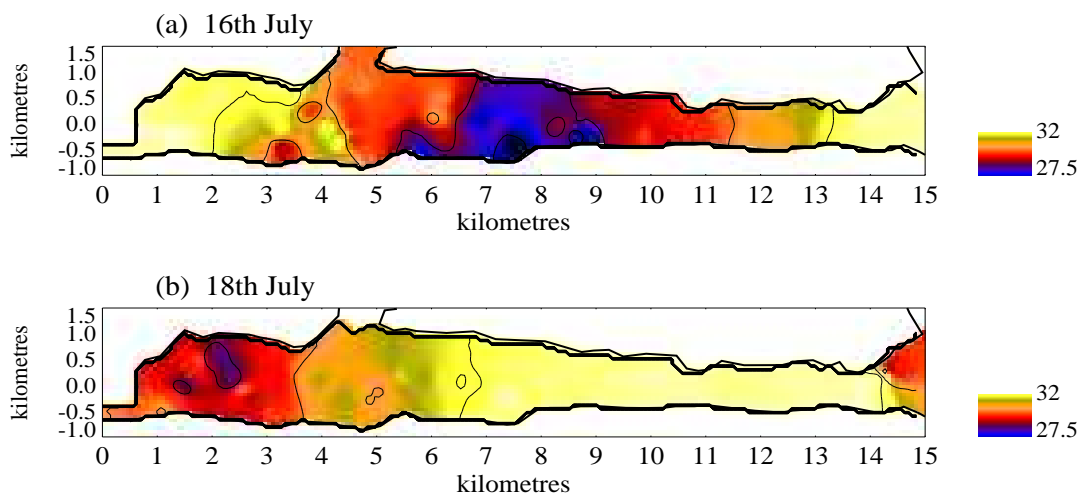


Figure 6.5: Inner Basin surface cruise plots of salinity (PSU) for (a) 16 July and (b) 18 July.

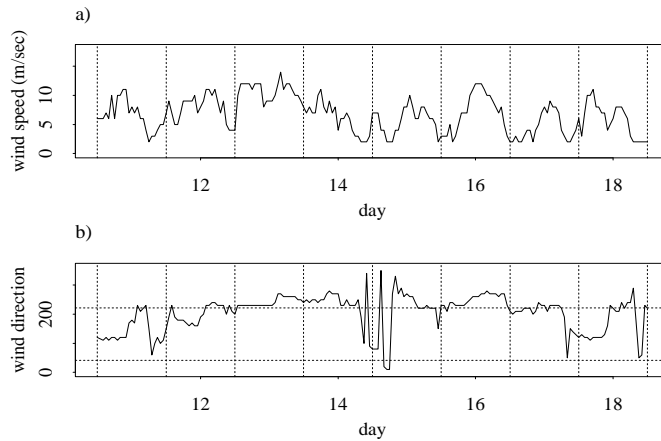


Figure 6.6: (a) wind speed and (b) wind direction from midnight 10th to midnight 18 July.

Downinlet wind

Wind direction, during the September and October cruises, was predominantly downinlet (figs. 6.7 & 6.9.)

The September cruise took place after a period of low river discharge, $< 10 \text{ m}^3 \text{ sec}^{-1}$. Downinlet winds increased the flow of the surface layer out of the inner basin, which in turn enhanced estuarine circulation and increased entrainment, as depicted in fig. 6.8(a).

On 7 October river discharge was heavy ($200 \text{ m}^3 \text{ sec}^{-1}$). Without any opposing wind, the surface layer would have flowed rapidly out of the basin, as the velocity of the surface layer is related to the velocity of river discharge. Downinlet winds on the 9th augmented the seaward velocity of the surface flow, further increasing the entrainment of deep water. In fig. 6.8(b), the higher salinity entrained water starts just north of the rise in the seabed. As high river input continued, though at a reduced rate, river discharge lowered the salinity of the entrained water in the north of the basin. Flooding spring tides may have reduced the outflow from the inner basin, causing the surface layer to be held in the south of the basin, until it could flow out on the ebb (fig. 6.8(b).) By 10 October, though a similar structure existed to that on the 9th, it was smoother (fig. 6.8(c)) and the lowest salinity water had left the basin. Part of this effect may be explained by the deeper collection of data on 10 October.

The radii of deformation for the inner basin in September and October indicate that the basin will generally be too narrow and stratified for coastal upwelling (see 1.5.3) to take place. With the greater vertical density gradient in October, due to high river discharge, the radii of deformation were more than twice the width of the basin.

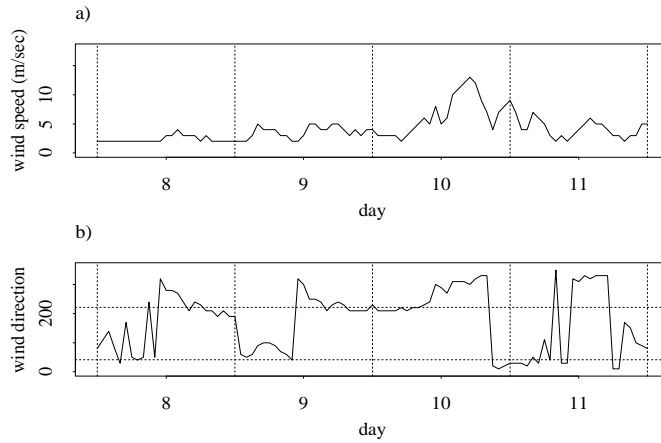


Figure 6.7: (a) wind speed and (b) wind direction from midnight 7th to midnight 11 September.

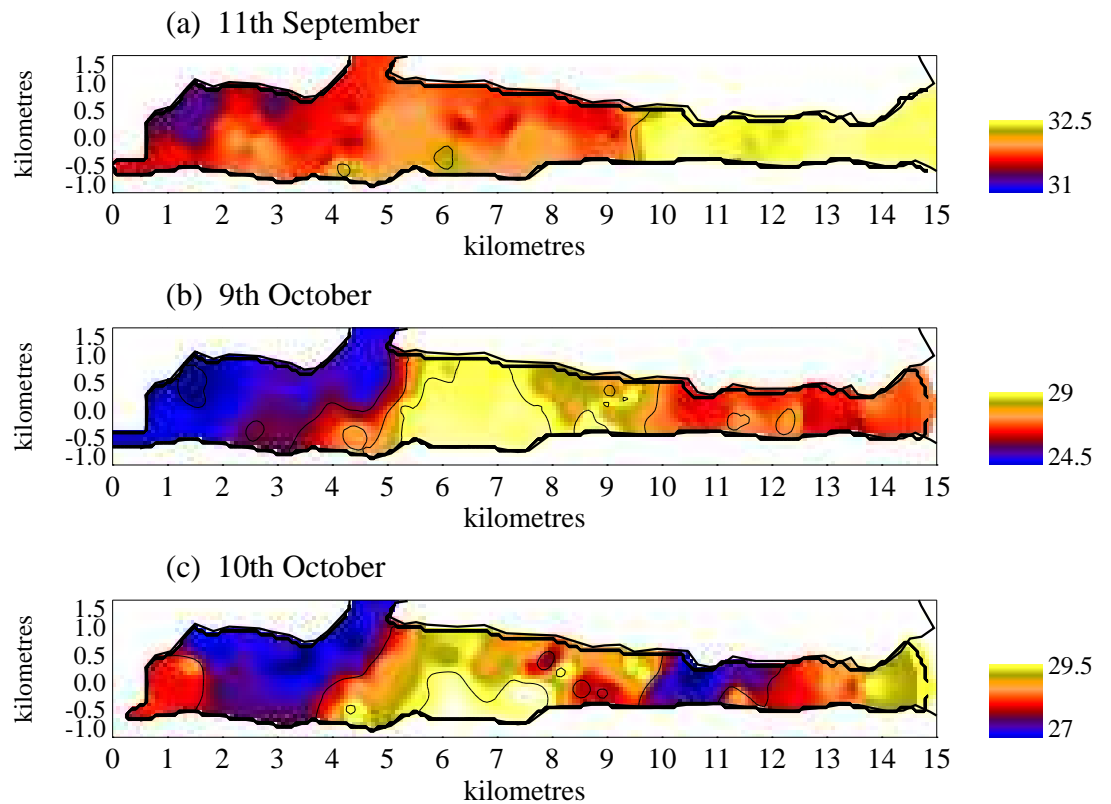


Figure 6.8: Inner Basin surface cruise plots of salinity (PSU) for (a) 11 September, (b) 9 October and (c) 10 October. Prior to these cruises the wind had been downinlet.

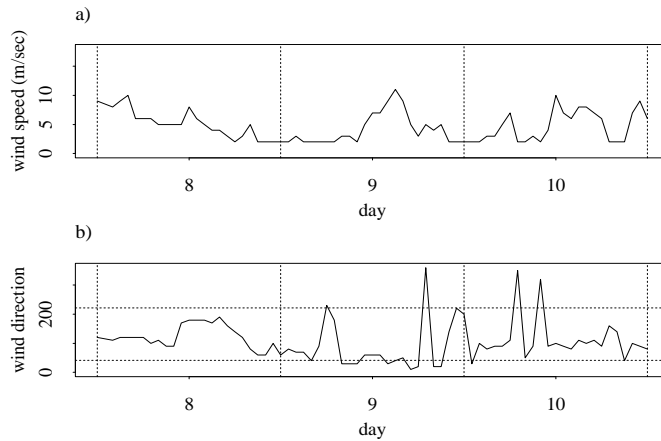


Figure 6.9: (a) wind speed and (b) wind direction from midnight 7th to midnight 10 October.

6.3 Outer Basin: Physical Structure

The more open aspect of the outer basin will increase the range of influence wind will have on the dynamics of the surface layer. Mull may partly shelter the south of the basin from the wind, but this effect will be localised. Loch A'Choire, on the western shore of the outer basin may also channel winds across the basin.

The lower degree of stratification and the deeper surface layer in the outer basin may lessen the effect of wind forcing and increase the response time of the surface layer, requiring more prolonged and stronger winds to create similar effects. The greater length of the basin, however, by increasing the fetch will increase the impact of the prevailing wind. The front between Loch Linnhe and the coastal sea will also affect the horizontal structure. It may be a more productive region - fronts in fjords have been found to be more productive than the rest of the basin. As with the vertical data, there is insufficient data to determine the importance of the tidal cycle on productivity at the frontal region.

6.3.1 Corran Outflow

Unlike the inner basin, salinity in the outer basin always increased seaward. The northern end was always less saline, cooler - except for November, and more turbid than the rest of the basin. The constricted flow through Corran will generate mixing throughout a substantial part of the water column and internal waves formed by the interaction of the tide and the sloping seabed at the northern end of the basin, will also be a source of mixing and turbidity.

6.3.2 Fronts

From the horizontal data, the front in the outer basin moves between the Lynn of Morvern and the sill between Lismore and Mull.

Tidal range again appears to be the most important factor in determining the position of the front - along with river discharge and wind direction. With the increasing tidal range between 23 to 25 April, there was a corresponding inland movement of the front. Those cruises with the greatest tidal ranges tended to have the most inland fronts but the influence of wind direction also was of importance. In May and August, after periods of upinlet winds the front was particularly far north. Whereas in September and October - periods of downinlet winds - despite similar tidal ranges, the front was further south. The higher river discharge of October compared to September, pushed the front even further south.

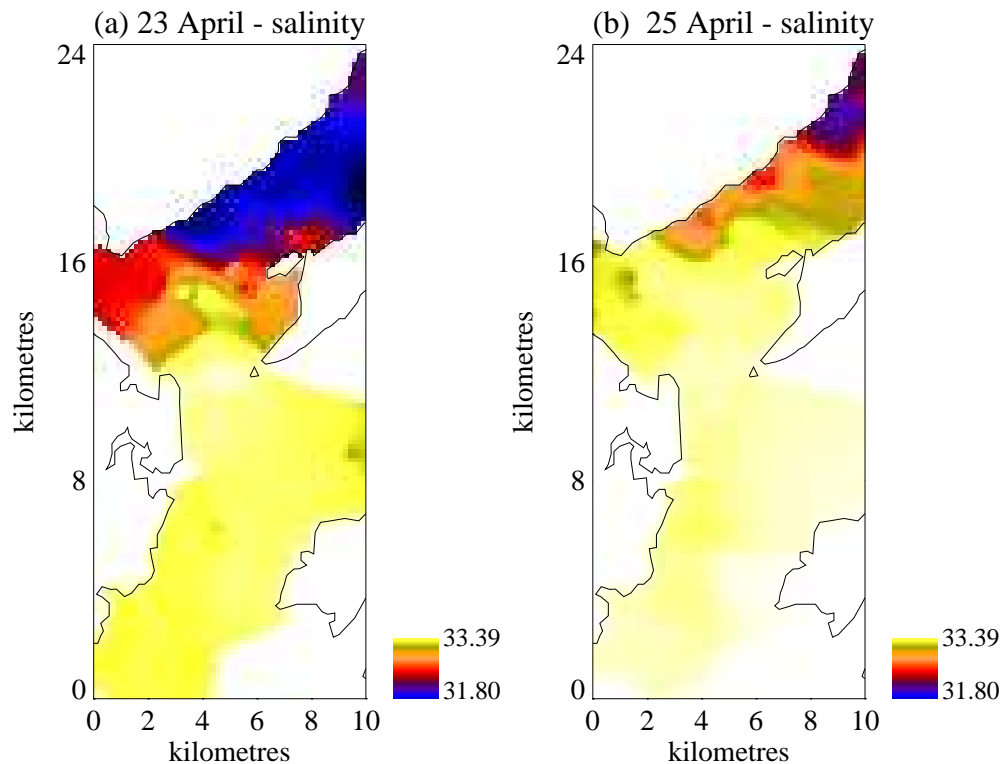


Figure 6.10: The front between fjord water and the coastal sea as it moves inland with increasing tidal range on (a) 23 and (b) 25 April.

River discharge, unless extremely high appears to have little effect alone. Despite river discharge exceeding $100 \text{ m}^3 \cdot \text{sec}^{-1}$ and being on a similar level to that in October, with a high tidal range the front on 27 February was one of the most northerly. In March however, the extremely high river discharge ($> 250 \text{ m}^3 \cdot \text{sec}^{-1}$) had pushed the front across the sill into the Forth of Lorne.

The front often did not lie straight across the fjord but intruded further up the east coast - along Lismore, as it did on 18 June, 18 July and 14 August. This may be related to the flow of water around the end of Lismore or the presence of

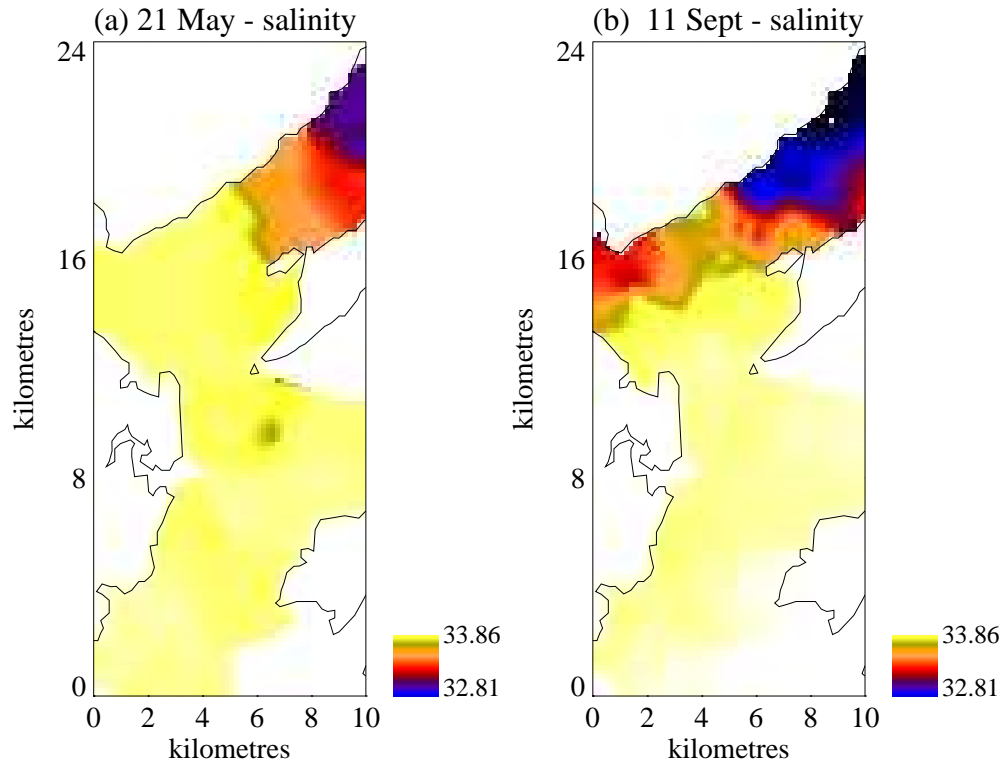


Figure 6.11: The front between fjord water and the coastal sea with similar tidal range but opposing wind direction on (a) 21 May and (b) 11 September.

Bernera Island, on the west coast of Lismore - both may increase turbulence and cause a turbulent plume to form with flooding tides. The bathymetry may also be influential, as across the basin, the seabed slopes up to Lismore making the east considerably shallower than the west.

6.3.3 Wind

Wind played a considerable role in the structure of the surface layer of the outer basin, with different wind directions producing different surface salinity patterns. Unlike the inner basin where only axial winds were of consequence, cross-axial winds were also influential in the outer basin. The lower aspect ratio and greater size of the basin will make it more susceptible to non-axial winds.

Upinlet Wind

Only on 21 May and 14 August (figs. 6.3 & 6.4) had there been a preceding period of continual upinlet (south-westerly) winds. The surface layers in these plots (fig. 6.12) consist of bands of salinity and temperature across the basin with salinity decreasing towards Corran, as outflow was being prevented. The brief period of upinlet wind before 23 April, appears to have been insufficient

to generate ponding in the outer basin, unlike the more stratified inner basin, indicating a longer response time.

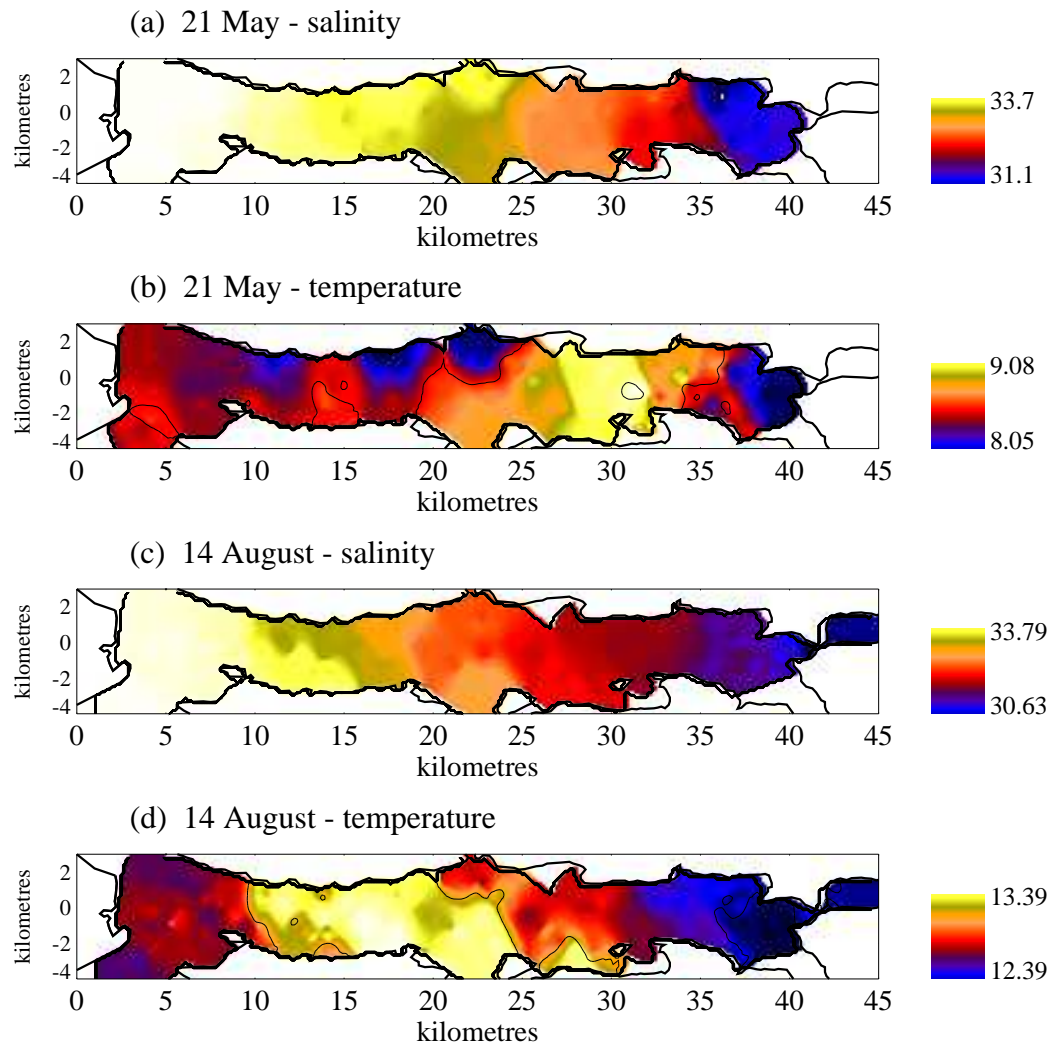


Figure 6.12: Ponding on 21 May and 14 August with the effect on (a) & (c) salinity (PSU) and (b) & (d) temperature (C).

Release of Ponding

In November, there was entrainment in the upper section of the basin. There may have been ponding prior to this, which on relaxation of the upinlet wind stress led to enhanced estuarine circulation, or it may be entirely due to extreme river discharge enhancing estuarine circulation. November was the only month in which the water temperature in the north was greater than in the south.

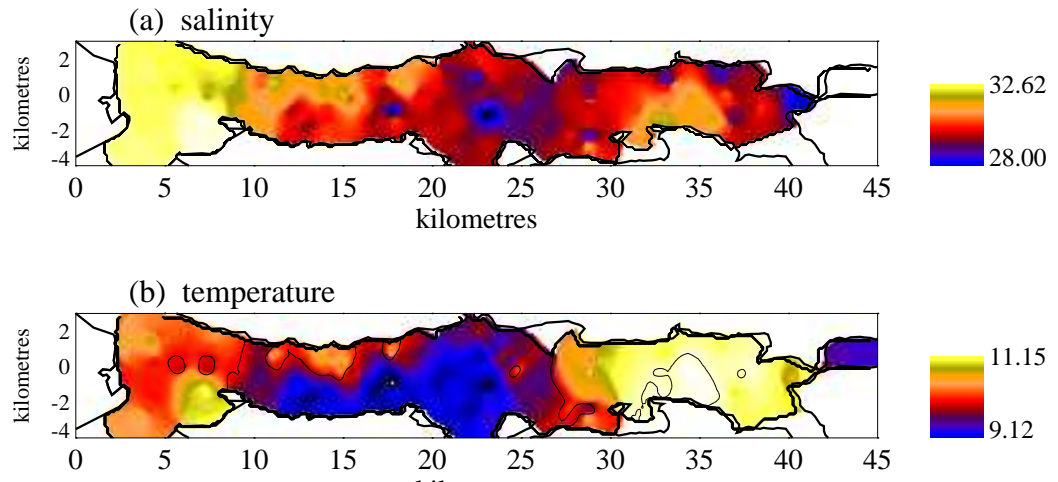


Figure 6.13: 14 November, (a) salinity (PSU) and (b) temperature (C).

Cross Axial Wind

With a change in wind direction from easterly to southerly, the outflowing surface layer was pushed towards the north-west corner of the outer basin - generating diagonal bands, with the lower salinity water extending further down the west than the east coast. This wind pattern was found on 27 February, 25 April and 18 July (figs. 6.14, 6.2 & 6.6.)

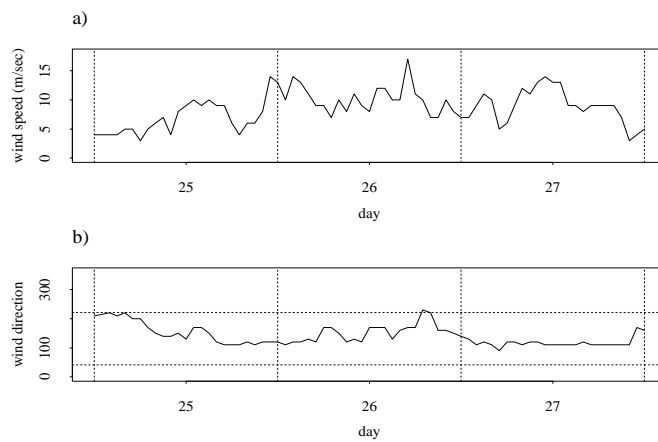


Figure 6.14: (a) wind speed and (b) wind direction from midnight 24th to midnight 27 February.

In February and April the wind had been predominantly from the south-east for the preceding two days and the changes in direction had been gradual. In July the wind had only been from the south-east overnight and prior to that had been upinlet; however river discharge was low, the pycnocline less than 10 m deep and the water column was strongly stratified. Under these conditions the surface layer would be expected to be more responsive to wind forcing. South-easterly winds

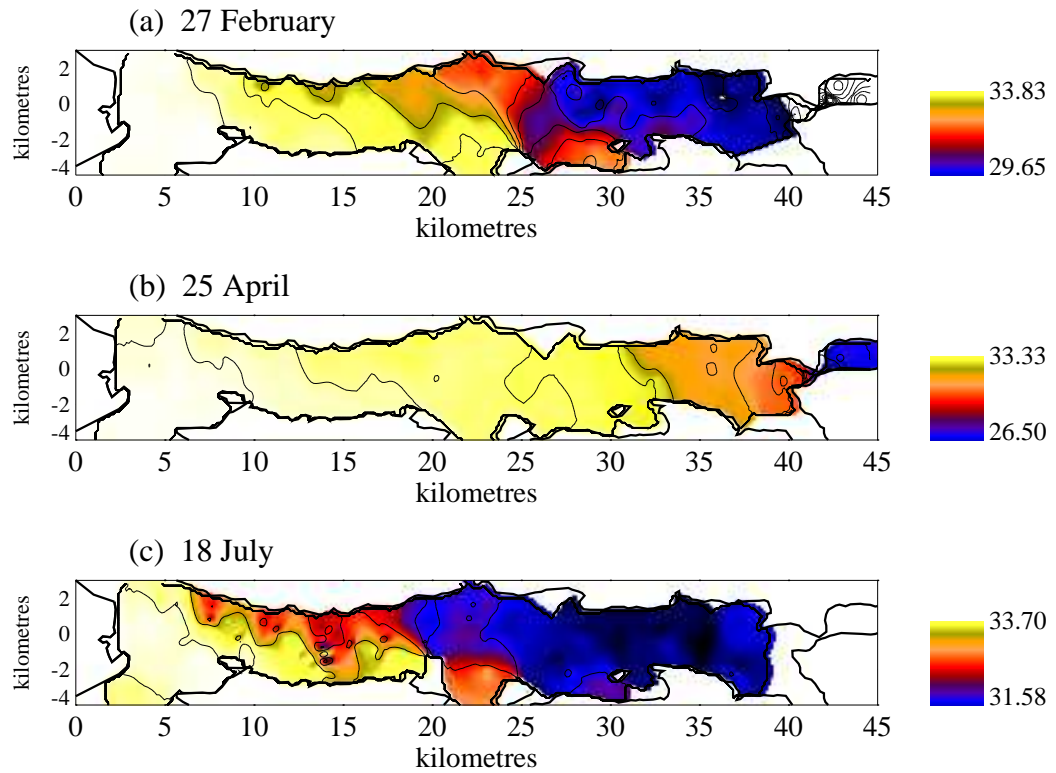


Figure 6.15: The effect of south-easterly wind on the salinity of the surface layer on (a) 27 February, (b) 25 April and (c) 18 July.

may affect the Firth of Lorne and by forcing the water into Loch Linnhe through the Lismore/Mull sill contribute to the diagonal banding with water flooding into Loch Linnhe propagating a surface plume at the end of Lismore and around Bernera (the island on the south west coast of Lismore.)

Downinlet Wind

On 11 September and 9 and 10 October, the wind was predominantly downinlet (from the north-east) generating a surface pattern of high salinity and high temperature water along the east coast, with lower salinity and temperature along the west (fig. 6.16.) This pattern corresponds to the expected outcome of upwelling and downwelling generated by longitudinal winds in a broad fjord, as modelled by Cushman-Roisin et al. (1994). The baroclinic radii of deformation (BRD) for both months supports this hypothesis but unfortunately there is insufficient hydrodynamical data to test it. On 10 and 12 September, at the Lynn of Morvern mooring, the BRD was 2.06 km and 0.94 km respectively. The latter being well within the width of the basin which is 4.1 km in the narrow LoM section. With stronger stratification in October, the BRD was 2.5 km on 6 October, but with decreasing river discharge, increasing tidal range and the changing wind direction this would have decreased by 9 October when the data collection took place. Other factors facilitating this circulatory pattern could be the bathymetry of the

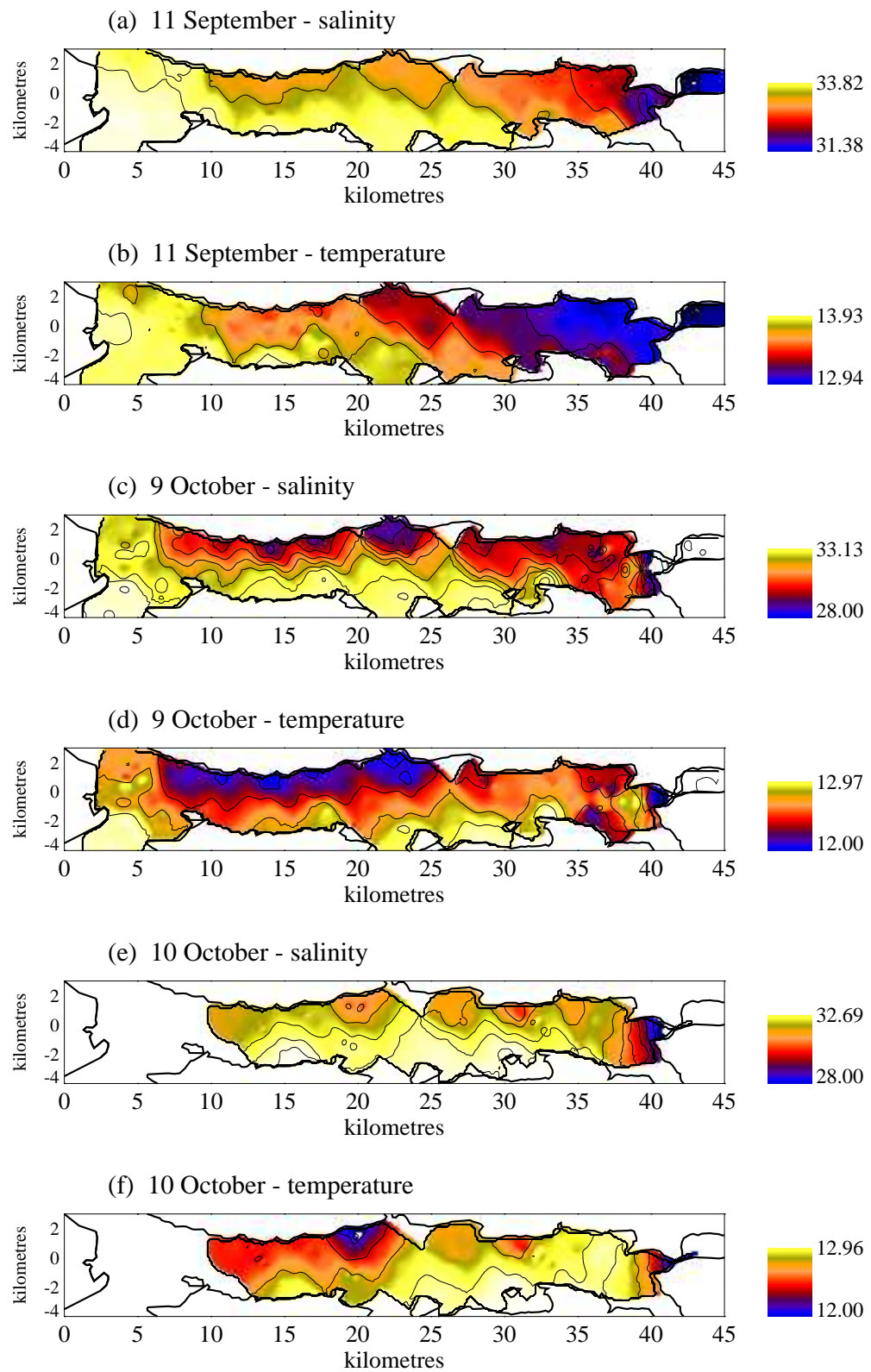


Figure 6.16: Outer Basin surface cruise plots of salinity (PSU) and temperature (C) for (a) & (b) 11 September, (c) & (d) 9 October and (e) & (f) 10 October. The banding pattern of salinity and temperature was generated by Ekman drift across the basin, accompanied by upwelling outcropping on the surface.

outer basin or wind channeling. In the southern part of the outer basin the basin shallows towards the east coast which may enhance upwelling and warming of the water - or the shallowing may enhance the upwelling generated by Ekman drift enabling the deeper water to outcrop on the surface more easily.

Wind was also downinlet on 26 March and the surface data (fig. 6.17) does display higher salinity in the east, particularly in the northern half of the basin.

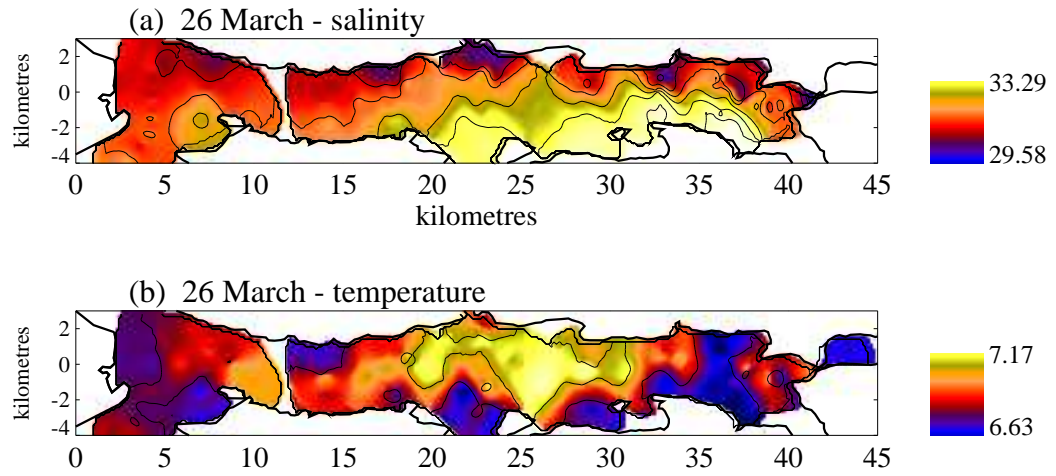


Figure 6.17: Outer basin surface plot on 26 March, after down-inlet wind, (a) salinity (PSU) and (b) temperature (C).

For more than seven days, approximately one week before the March cruise, the runoff had been very high, but had since fallen (fig. 5.4.) The high freshwater inflow was accompanied by northerly winds which would have allowed the brackish surface layer to flow out of the loch, hence the most seaward part of the surface layer being the least saline (fig. 6.17.) Further north, upwelling may have been taking place, the BRD on 23 March was 2.6 km at the OB mooring and 2.9 km in the LoM. By 26 March the more stratified low salinity water in the south of the basin would have a higher BRD than the water further north which may account for signs of upwelling in the north but not south.

6.4 Inner Basin: Biological Heterogeneity

Physical features such as stratification, upwelling, deep water renewal, forcing of the surface layer and fronts have the potential to affect the distribution of phytoplankton and zooplankton in the surface layer.

Stratification

The northern end of the inner basin was generally lower in chlorophyll than closer to Corran. This may be connected with the transport of phytoplankton cells from the outer basin as described by Overnell and Young (1995) in May, or river discharge being low in nutrients, salinity and temperature.

In April, chlorophyll levels were higher in the north (fig. 6.18) as river driven stratification, along with ponding on 23 April generated a warm stable region for phytoplankton to grow in. At the start of the year, in low irradiance conditions, such conditions would be expected to be more important than during the summer. The boundary between the northern stratified region and the more mixed south was also an important zone of productivity, as was shown in Chapter 5.

Deep Water Renewal

On 21 May, after a renewal event between 17 and 19 May, there was a bloom in the southern part of the basin. Despite many of the chlorophyll cells associated with the renewal event sedimenting to the seabed without reaching the surface, as found by Overnell and Young (1995), some may have been upwelled causing a surface bloom.

Bathymetry

Upwelling at the rise in seabed may have caused low chlorophyll in the centre of the basin on 18 June. From the salinity and temperature plots (fig. 6.20,) upwelling may have occurred and the chlorophyll density in this region was lower, as would be expected of deep water entrained to the surface. There were similar conditions on 25 April and 18 July, with a similar effect on the chlorophyll. As nutrient depletion was not a problem in Loch Linnhe, the advection of water higher in nutrients to the surface did not enhance productivity and from July onwards, there was little difference in DIN content throughout the water column anyway.

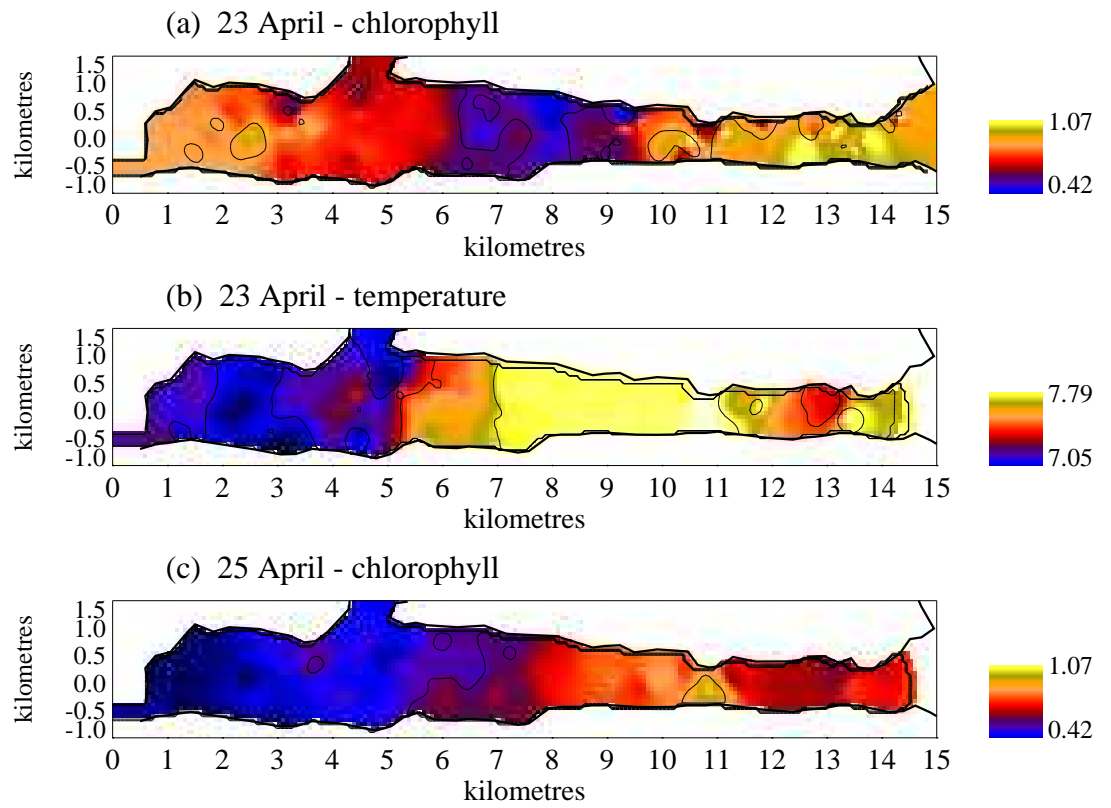


Figure 6.18: Inner Basin surface cruise plots of chlorophyll ($\text{mg}\cdot\text{m}^{-3}$) for (a) 23 April and (c) 25 April with (b) temperature (C) on 23 April.

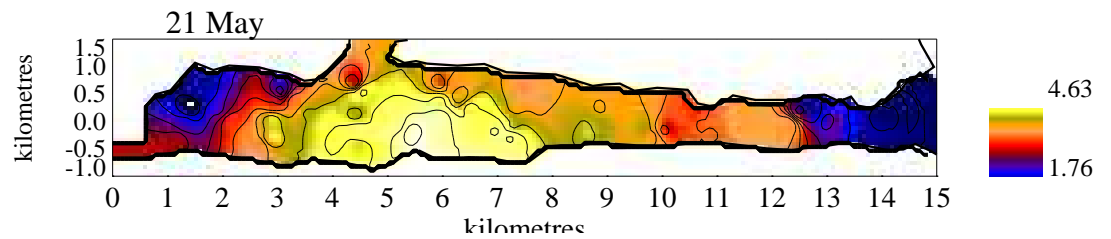


Figure 6.19: Inner Basin surface cruise plots of chlorophyll ($\text{mg}\cdot\text{m}^{-3}$) on 21 May.

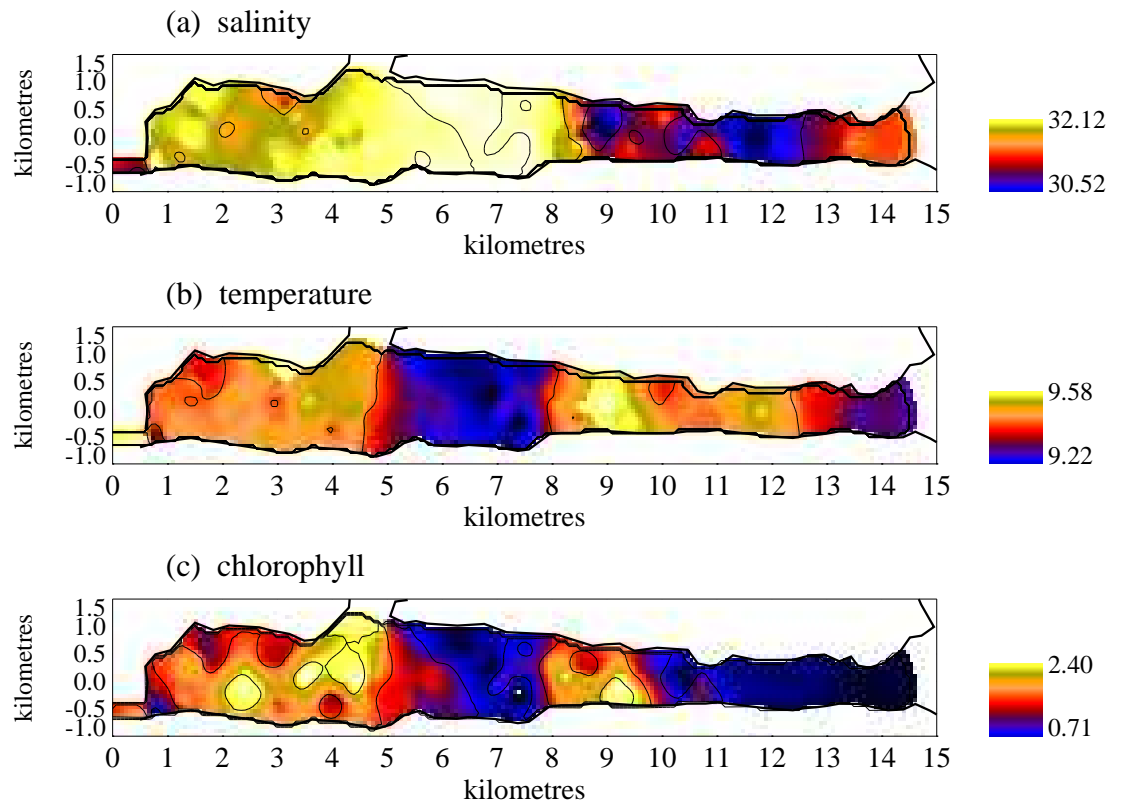


Figure 6.20: Inner Basin surface cruise plots on 18 June of (a) salinity (PSU), (b) temperature (C) and (c) chlorophyll (mg.m^{-3}).

Wind

As the wind controls the movement of surface layer, it also has the potential to affect the position, productivity and survival of chlorophyll patches.

During the downinlet winds in September and October, the surface layer and the phytoplankton contained in it were pushed down the loch, with a compensating entrainment of water behind. The entrained water was particularly low in chlorophyll content as can be seen from the October plots (fig. 6.21.) The region of high salinity entrained water in the centre of the basin was lower in chlorophyll than the less saline water further south. It is not possible to ascertain whether the cells were being advected, or whether the predominance of entrained water in the north lowered the chlorophyll content of the surface.

During ponding in May, the chlorophyll patch (see fig. 6.19) was closely related to the warmer water at the seaward end of the ponded region (fig. 6.1(d)). This may be from a combination of the water being able to warm in the stable ponded region creating a suitable environment, along with the transport of cells into the

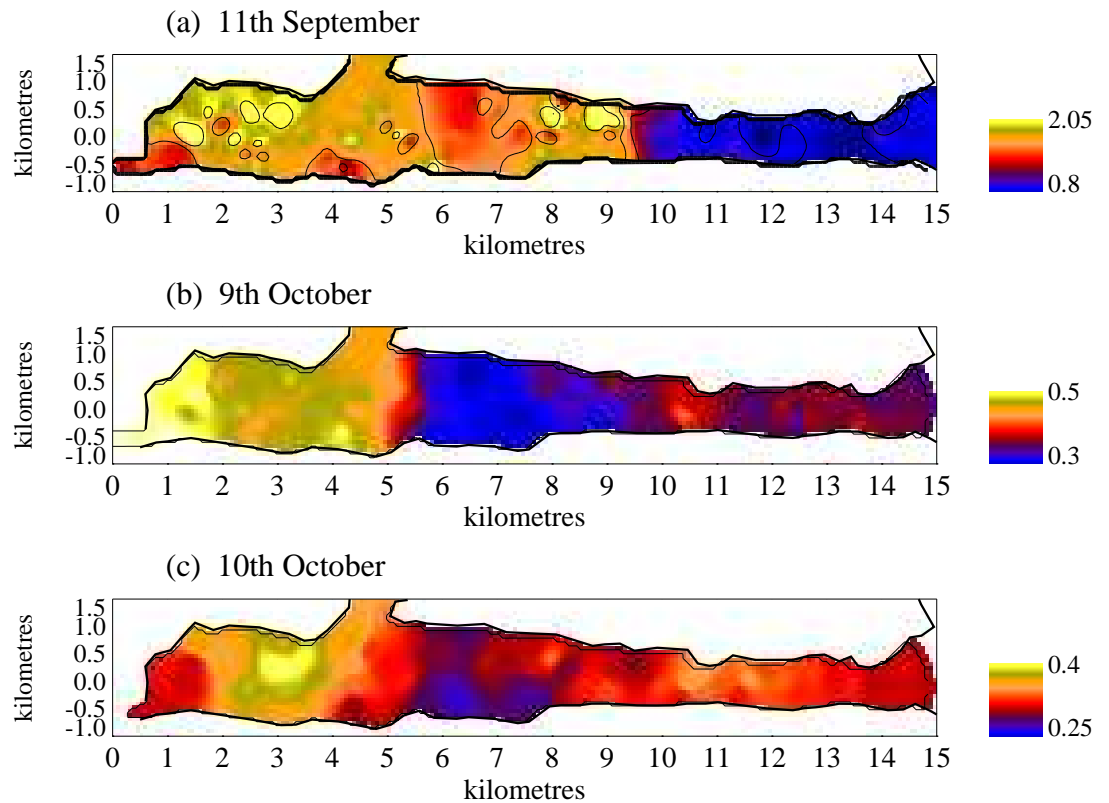


Figure 6.21: Inner Basin surface cruise plots of chlorophyll ($\text{mg}\cdot\text{m}^{-3}$) for (a) 11 September, (b) 9 October and (c) 10 October. Prior to these cruises the wind had been blowing down the loch.

basin during renewal and upwelled to the surface in this area.

6.4.1 Zooplankton

There are problems in the interpretation of zooplankton data collected horizontally as they are to a certain extent able to determine their depth in the water column and undertake diurnal vertical migration. Zooplankton, in general were not spatially associated with phytoplankton, but followed a similar surface pattern to temperature - inverse to the relationship of phytoplankton and temperature. During periods of strong entrainment, such as in September and October, they appear to have been advected to the surface. Regions of higher density also tended to occur in mixed as opposed to stratified regions, which again suggests advection to the surface. On 23 and 25 April, they were distributed inversely with chlorophyll, with phytoplankton in the stratified north and zooplankton in the mixed south. Only on 18 July did zooplankton follow a similar pattern to phytoplankton.

6.5 Outer Basin: Biological Heterogeneity

6.5.1 Phytoplankton

May uniquely had the highest density of chlorophyll at the northern end of the loch (fig. 6.22.) Ponding may have generated a shallow, warm productive surface layer or the cells may have been advected there by the wind.

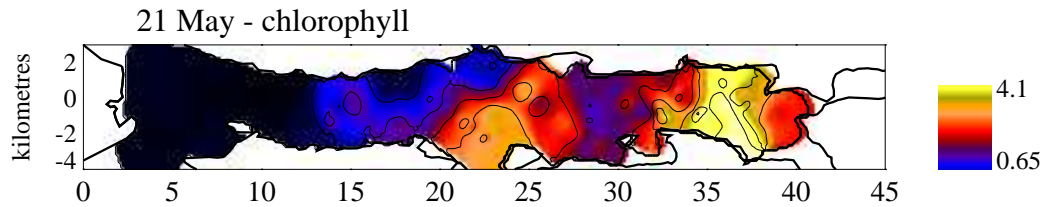


Figure 6.22: The influence of upinlet wind on chlorophyll in the outer basin on 21 May.

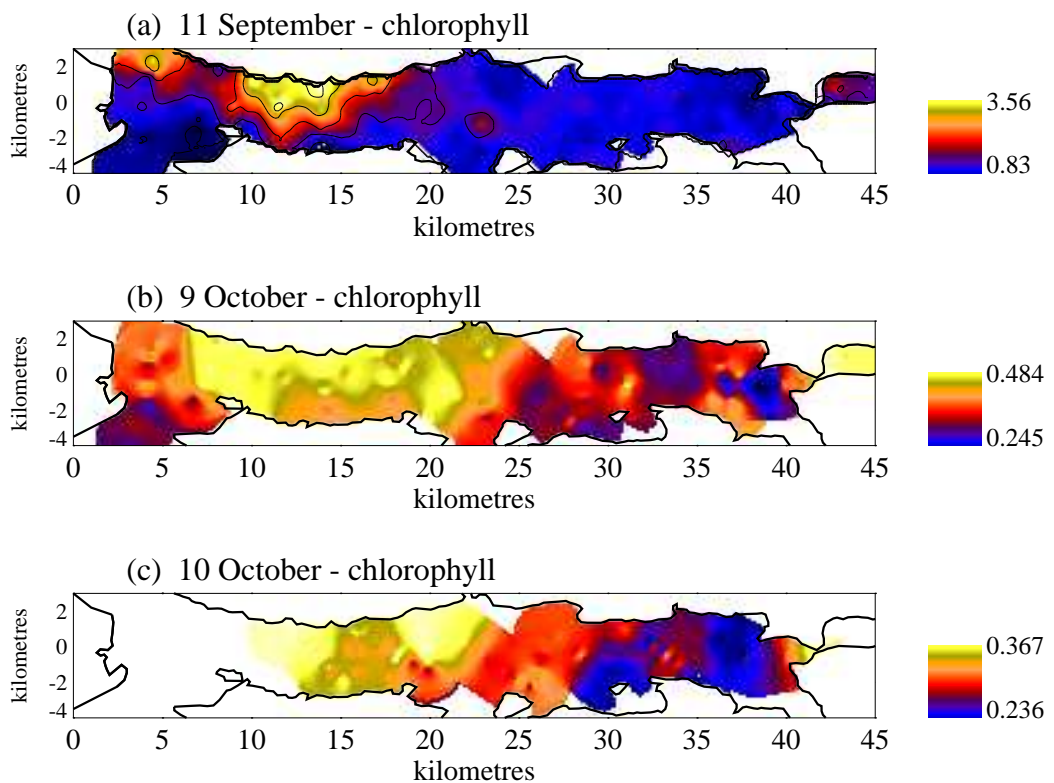


Figure 6.23: The influence of downinlet wind on chlorophyll density in (a) 11 September, (b) 9 October and (c) 10 October.

With the downinlet winds on 11 September and 9 & 10 October, the surface chlorophyll maximum was in the southern part of the loch (fig. 6.23.) On 11 September phytoplankton were predominantly along the west coast further south, supporting the hypothesis of upwelling on the east, as upwelled water would be lower in chlorophyll.

The Lismore/Mull front is a boundary between the stratified and relatively productive fjord and the mixed and less productive Firth of Lorne. At the depth of data collection, the front was not in general, more productive than the rest of the basin. Only for 25 April is there evidence of a peak in productivity there.

6.5.2 Zooplankton

Unlike the inner basin, in the outer basin zooplankton were often associated with chlorophyll - including 25 April, 21 May, 18 July and 11 September - and the effect of mixing and entrainment on their position was less important. Experiencing less river input, being less stratified and less responsive to meteorological forcing will mean that estuarine circulation and entrainment in the outer basin will be weaker than the inner. Hydrodynamic processes being the predominant control over the distribution of zooplankton will therefore occur less often. In October, however, zooplankton appear to have been entrained to the surface.

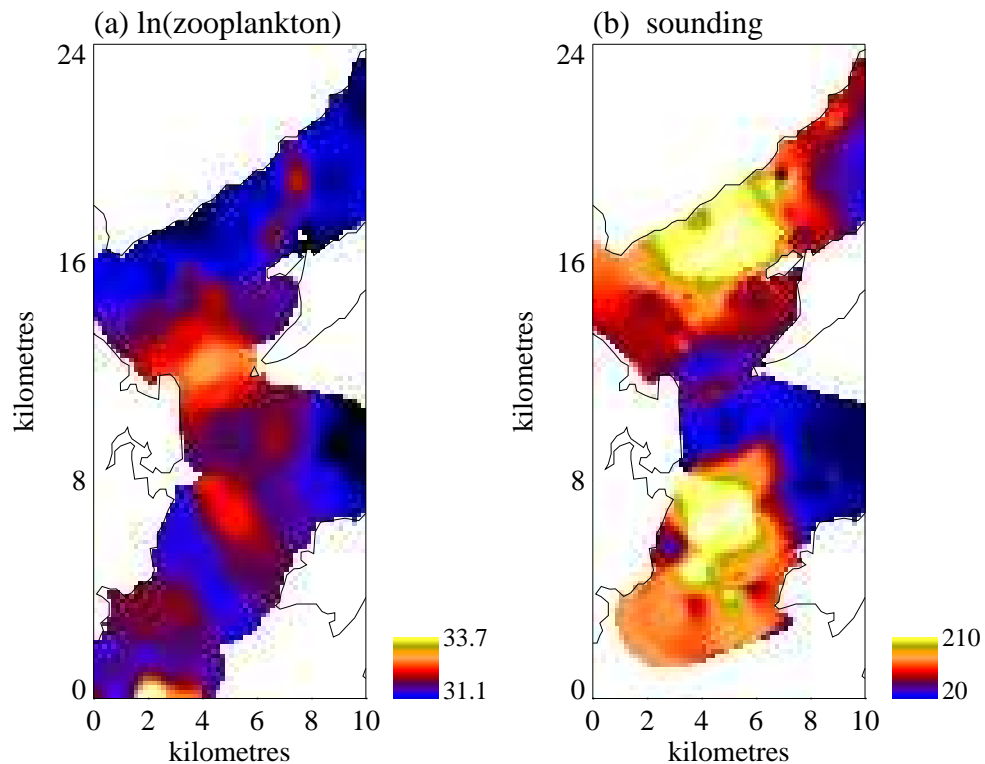


Figure 6.24: The influence of rapid changes of depth on the surface pattern of mesozooplankton density on 23 January, (a) $\ln(\text{mesozooplankton})$ ($\ln(\text{mgDW}\cdot\text{m}^{-3})$) and (b) sounding (m).

On 23 January, the position of zooplankton in the south, may have been influenced by the depth of the water column and the effect of that on the circulation. There was a peak at the Lismore/Mull sill, the shelf at the south of the outer basin and the shelf in the Firth of Lorne - all of these are at rapid changes in bathymetry (fig. 6.24.) It may be that at lower temperatures when the metabolic rate of mesozooplankton is low and chlorophyll densities low, the position of chlorophyll is relatively unimportant for the zooplankton and hydrodynamics dominate.

6.6 Influence of Adjoining Water Bodies

Adjacent water bodies would be expected to be of some influence on the heterogeneity of Loch Linnhe. Loch Eil to the west of the head of the inner basin will be an additional source of low salinity water. The outer basin has more adjoining basins: Loch Leven at the north of the outer basin, the Lynn of Lorne which connects at the northern end of Lismore, the Sound of Mull and Firth of Lorne. The Sound of Mull may be more productive than the outer basin as there are signs of higher chlorophyll density at the edge of the Sound of Mull on 23 April, 18 July and 11 September. The difference however is small. The Firth of Lorne, close to Loch Linnhe is not more productive than the sea-loch. There is surface data available for the Lynn of Lorne on 25 April and 15 August, but unfortunately, no chlorophyll or light data is available from the August survey. From the 25 April cruise, it can be seen that the Lynn of Lorne was considerably more productive than Loch Linnhe and in this section I shall discuss the possibility of it influencing the heterogeneity of chlorophyll in the outer basin.

6.6.1 Lynn of Lorne

The Lynn of Lorne (LoL) is separated from the Lynn of Morvern by Lismore and connects approximately half way up the OB through a narrow, high energy, rocky channel at Appin. The LoL as it has no prominent seaward sill is more closely linked to the Firth of Lorne than the LoM is. It is also much shallower, with much of the seabed lying between 30 and 50 m, compared to the LoM which reaches 200 m and is mostly deeper than 60 m. The LoL also has a greater freshwater input as Loch Creran flows into the northern end, while most of the OB freshwater comes from the IB.

In April, the LoL was considerably more productive than the LoM or the coastal sea as can be seen in table 6.1. On 25 April, the mean chlorophyll density in the Lynn of Lorne was significantly greater than for any other region sampled. The mean density was also greater than any single sample for Loch Linnhe or the Firth of Lorne in 1991. The salinity was slightly less and the temperature slightly higher in the LoL than the LoM. The lower salinity may have been due to freshwater runoff from Loch Creran which as well as lowering the salinity may also have increased stratification allowing more surface warming and increasing

Table 6.1: Comparison of the physical and biological properties of the Firth of Lorne (FoL), Lynn of Morvern (LoM) and Lynn of Lorne (LoL) on the 25 April 1991.

	FoL	LoM	LoL
Salinity (PSU)	33.25	32.7	31.5
Temperature ($^{\circ}\text{C}$)	7.43	7.34	7.64
Chlorophyll ($\text{mg}\cdot\text{m}^{-3}$)	1.99	1.75	12.2
Beam Attenuation ($\text{uW}\cdot\text{cm}^2$)	1.08	0.86	1.76
Zooplankton ($\text{mgDW}\cdot\text{m}^{-3}$)	793.77	614.57	1654.31

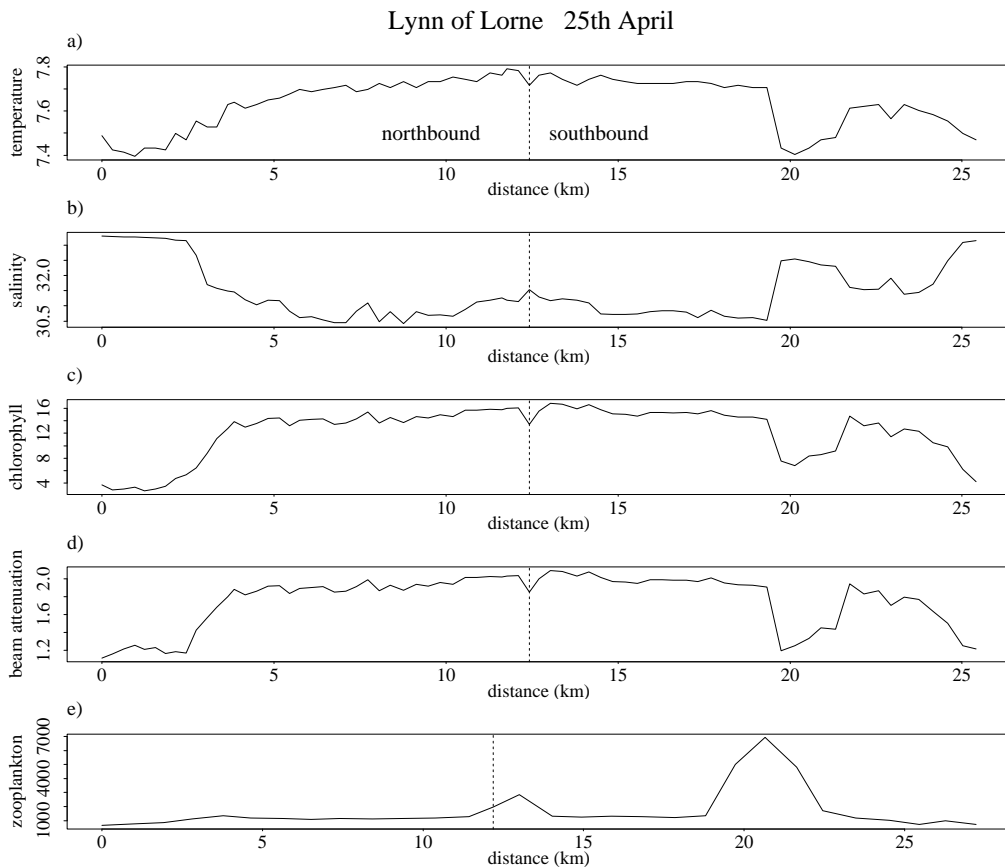


Figure 6.25: Surface cruise data for the Lynn of Lorne on the 25 April 1991. The central vertical line indicates the change in direction of the research vessel.

the temperature. The \log_{10} light level in the LoL was $1.76 \text{ uW}\cdot\text{cm}^2$ compared to $0.86 \text{ uW}\cdot\text{cm}^2$ despite the chlorophyll density being almost seven times greater. This would suggest that the greater chlorophyll density may be partly due to the euphotic zone being deeper and higher light levels will also prompt earlier and faster growth. Tidal stirring in the Lynn of Lorne is probably lower than elsewhere in this region as there is no sill. This will contribute to the lower turbidity and will also allow stronger stratification. These differences may also

produce a difference in phytoplankton species composition between the Lynn of Lorne and Loch Linnhe.

There was a strong horizontal gradient in the LoL. Heading north, the temperature increased and the salinity decreased sharply (figs. 6.25 & 6.26.) Where the salinity decreased, the increase in chlorophyll density was almost as fast.

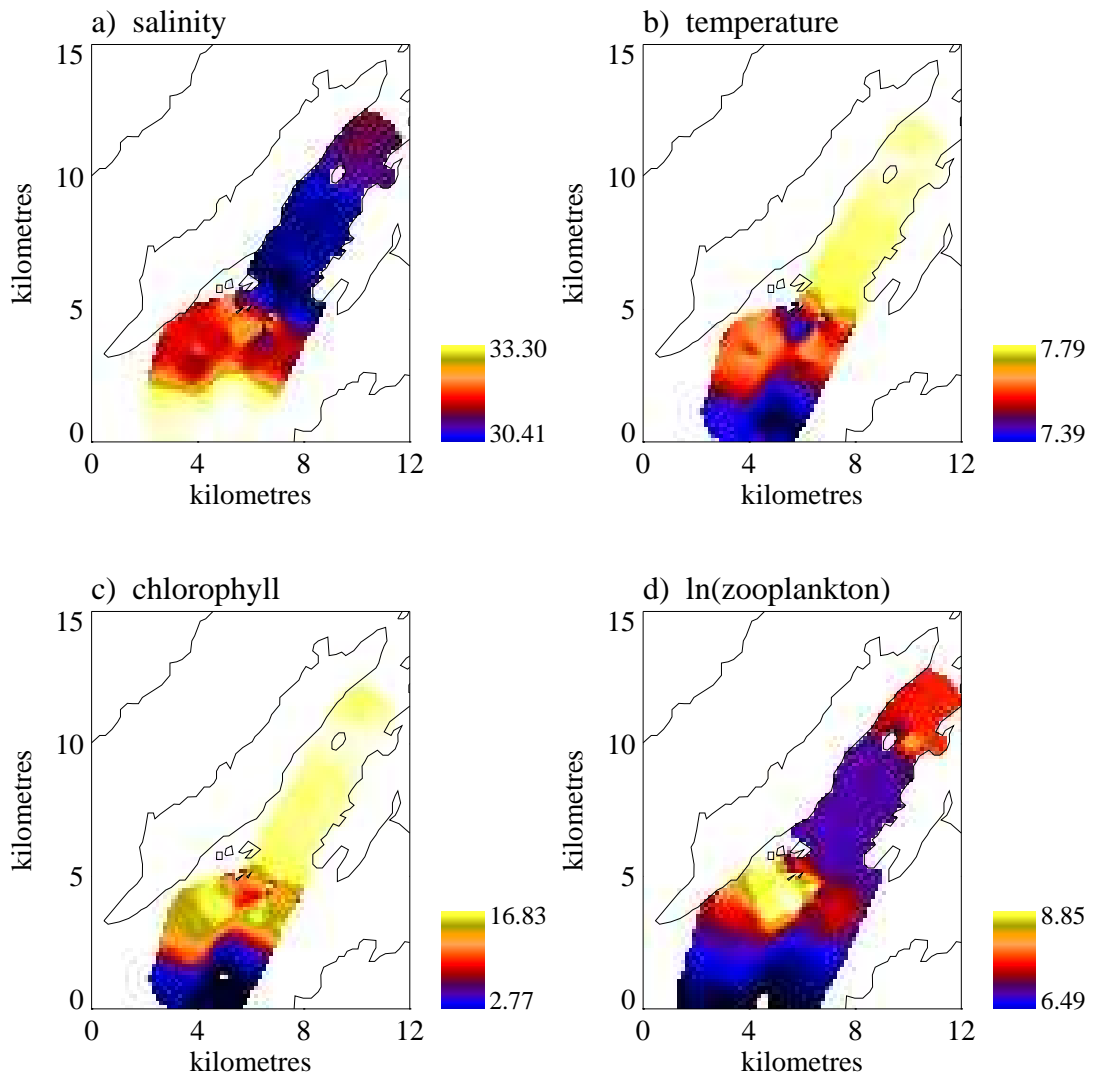


Figure 6.26: Interpolated surface of the data in fig. 6.25

The correlations between temperature, salinity, chlorophyll and attenuation were high; small deviations in the overall pattern were replicated through all the measured variables. The increase in salinity at the turning point was due to the boat turning and the instrumentation depth changing. Zooplankton density in general also increased up the bay, but there was also a large patch of considerably higher

density about the islands. Tidal stirring around islands, in otherwise stratified regions, has been found to generate subsurface chlorophyll maxima (Simpson et al. 1982) with the maximum in surrounding waters being at the surface. If this is the case in the Lynn of Lorne, chlorophyll may not be present in the data due to the depth of the data collection, but may be the cause of the accumulation of zooplankton in the vicinity of the islands.

For August, chlorophyll density and beam attenuation data are not available. The nitrate concentration in both the LoL and LoM decreased up the loch. In the LoM however, these concentrations fell to zero, while the LoL was not fully depleted, though its highest concentrations were not as high as those in the LoM. The physical parameters, salinity and temperature, were similar in August, which may have been a result of low river discharge over the summer months.

6.6.2 Influence on Outer Basin

During the spring and summer months of enhanced chlorophyll density, the area of the outer basin close to the northern end of the LoL appears to have been a region of consistently high phytoplankton biomass, relative to the rest of the basin. I believe the LoL is an important source of phytoplankton cells for the outer basin of Loch Linnhe. The region of the OB immediately adjacent to the LoL is however relatively shallow with several islands and may be naturally more productive without the LoL's influence.

For both the surface and axial cruises the end of April was the most productive time. In particular there was a large increase in mean phytoplankton density between 23 and 25 April as illustrated in fig. 6.27.

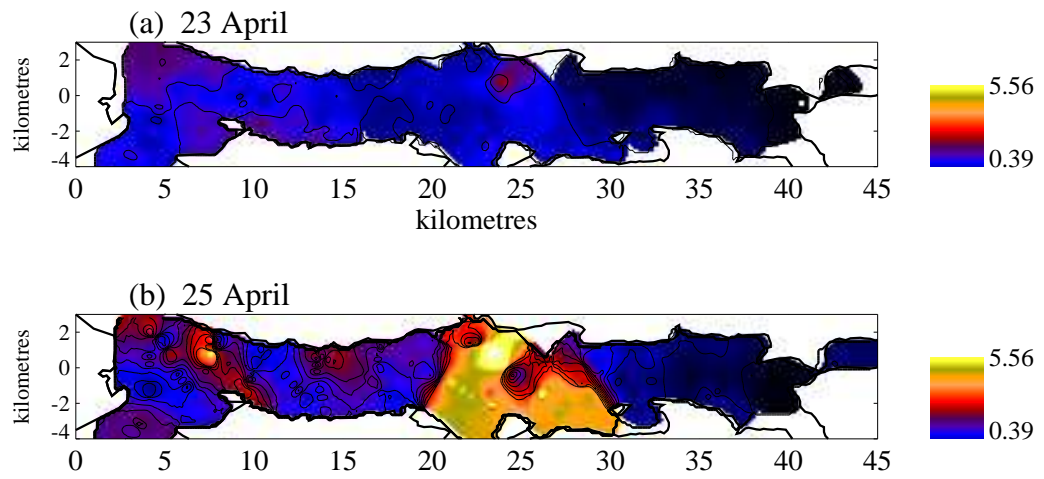


Figure 6.27: Outer Basin surface cruise plots of chlorophyll ($\text{mg}\cdot\text{m}^{-3}$) on (a) 23 and (b) 25 April

In fig. 6.27(b) of 25 April, there is a clearly defined region of enhanced chlorophyll density stretching across the loch starting from the northern end of Lismore. On

the 23 April, (fig. 6.27(a)), the ‘hot spot’ of the cruise on the 25 was present and was spreading out. Otherwise the southern end of the LoM and the Sound of Mull were more productive than most of the northern section. There was a band of high chlorophyll density spreading up the western coast of Lismore. This may be because the bloom was initiated from the LoL but this is also the shallower side of the loch $\sim 30\text{m}$, instead of 100m which may have enhanced productivity there.

Axial data from 22 April, see fig. 5.51, showed an aggregation of chlorophyll cells on the seabed of the outer basin, adjacent to the northern end of Lismore. Some of these cells may have been upwelled to the surface generating the bloom on 25 April.

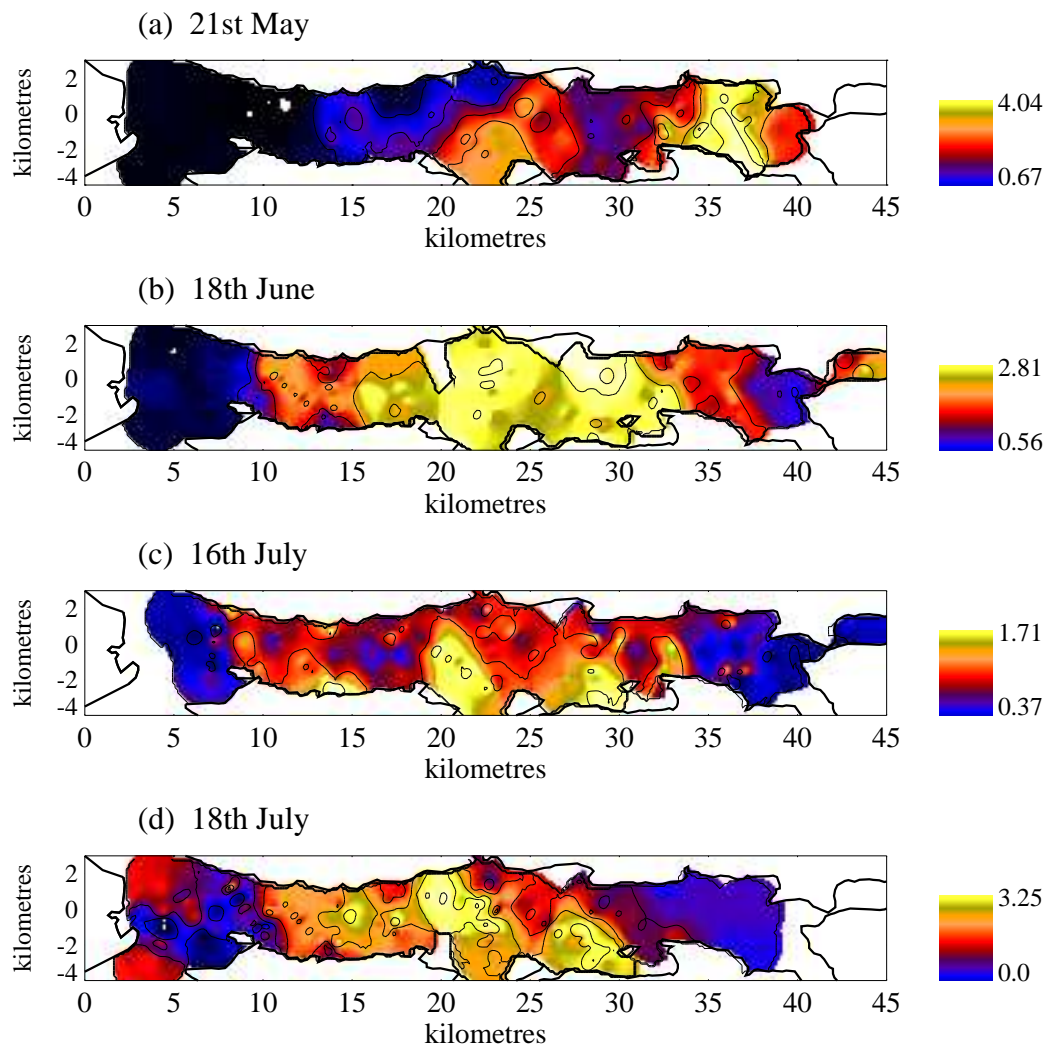


Figure 6.28: Outer Basin surface cruise plots of chlorophyll ($\text{mg}\cdot\text{m}^{-3}$) for (a) 21 May, (b) 18 June, (c) 16 July and (d) 18 July.

Again on 21 May (fig. 6.28a) there was an area of high chlorophyll density around the northern end of Lismore and Shuna, the island to the north of Lismore. The

highest density at this time was however in the north, this was after a prolonged period of upinlet winds. The chlorophyll seems to have been advected north with the surface water. By 18 June (fig. 6.28b) the pattern was less patchy and the patch boundaries less clearly defined than before, but the large region of higher chlorophyll density was close to Appin and spread north and south of there. On 16 and 18 July (figs. 6.28c & d) the peak was again close to Appin, particularly so on the 16th but it had moved further west by the 18th. With the downinlet winds in September and October, most of the chlorophyll was south of Appin (fig. 6.23.)

Mesozooplankton may also be advected into Loch Linnhe from the LoL. On 25 April, 21 May and 18 July, higher mesozooplankton densities were associated with the region around Appin. The similarities between chlorophyll and zooplankton in the outer basin may partly be due to them being in the same water mass as they are advected into the basin.

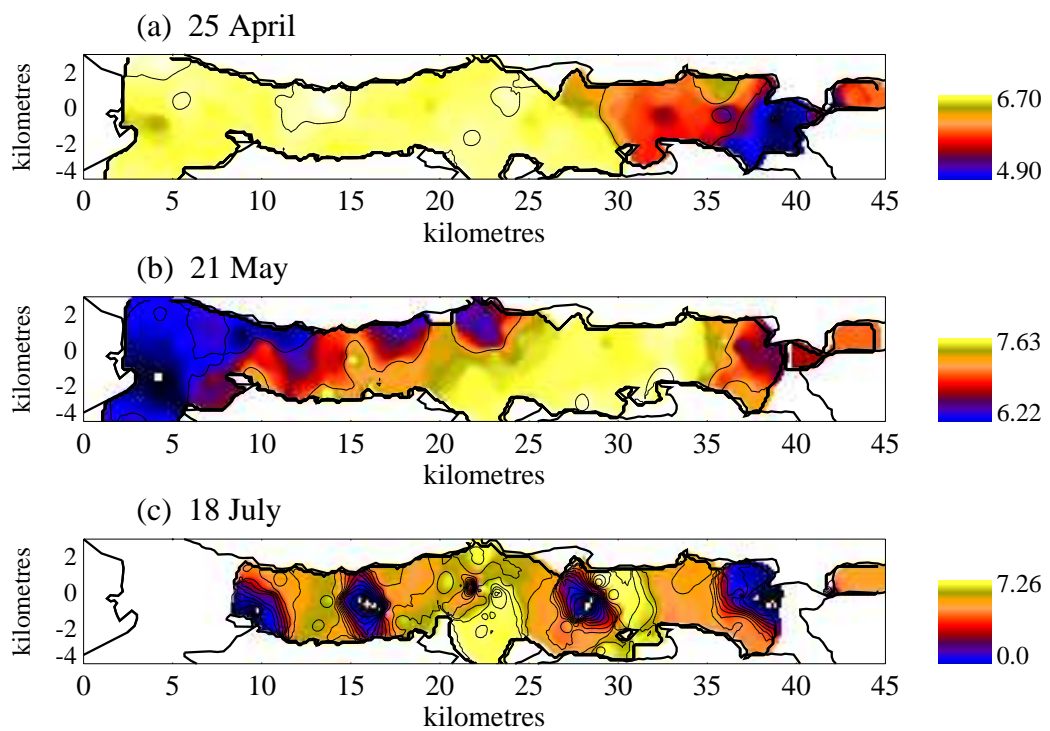


Figure 6.29: Outer Basin surface cruise plots of mesozooplankton ($\ln(\text{mgDW} \cdot \text{m}^{-3})$) for (a) 25 April, (b) 21 May and (c) 18 July.

6.7 Conclusions

While the vertical data emphasised the importance of the lunar tidal cycle on Loch Linnhe, the surface data highlights the importance of the wind on the surface structure of both basins. The wide range of information derived was only made possible by the horizontal collection of data. Such information, makes it possible to identify the key features of interest which may be concentrated on in further sampling programmes, collecting more specific information such as with current meters.

The main wind induced feature apparent in the vertical data, was ponding, but the surface data unveils the importance of other wind directions on the loch. The ponding described previously in Chapter 5 shows up clearly in the surface data - particularly for the inner basin in April, May and August. The response of the surface layer to upinlet wind stress is strongly affected by the amount of river discharge and the strength of stratification in the basin. Heavier river discharge in April along with stronger stratification enabled ponding to be established more quickly than in the other months. The lower freshwater content of the surface layer in the outer basin also meant that it responded more slowly to upinlet wind stress and that ponding was less frequent and weaker there.

In Knight Inlet, Pickard and Rodgers (1959) found that after a period of upinlet winds, the pressure gradient built up and the surface layer eventually flowed against the wind. There are no signs of such an event in Loch Linnhe despite upinlet winds for over two weeks. The weaker stratification in Loch Linnhe, lesser river input and greater tidal mixing will reduce the physical extent of ponding and limit the degree to which water can pile up at the head of the basin. In the outer basin, this will be even less, as the head of the basin experiences turbulent mixing from Corran and the freshwater input mixed into the water column.

As for the vertical data, the horizontal data provides evidence of strong water movement, particularly within the inner basin. The surface layer of the inner basin often displays a pattern of higher salinity water in the north than the more seaward water. This is due to the amount of entrainment which can take place in the basin with enhanced estuarine circulation, such as after the relaxation of upinlet wind stress when the ponded water is able to flood out of the basin and with downinlet winds. In the larger and less stratified outer basin, the north is always less saline.

While downinlet wind stress increases the seaward flow in the inner basin, the effect in the outer basin is considerably more interesting. Coastal upwelling takes place within the outer basin as it is broad, the surface layer is deep and weakly stratified and while deep for a Scottish sea-loch, the basin is shallow for a fjord. This has previously only been shown for a northern Norwegian fjord by Cushman-Roisin et al. (1994). The sea-bed at this point may further enable the cross basin flow to outcrop at (4-5m) the depth of data collection, if not on the surface, as it slopes up towards the east - the side of outcropping. Within Scotland, many

sea-lochs would be too narrow and stratified for cross basin upwelling, except under extreme circumstances and globally many fjords will be too stratified and have too shallow a surface layer. The position of Loch Linnhe at the southern end of the Great Glen also makes it more exposed to downinlet winds than many other fjords and sea-lochs.

The outer basin also differs from the inner in that it is affected by cross-axial winds - this will be aided by its width and more open aspect - while there is only evidence of axial winds forcing the surface of the inner basin. Cross-axial winds are in general considered to be less important, but Scottish sea-lochs and those in Ireland are surrounded by less mountainous terrain which may leave them open to forcing by cross-axial winds.

Tidal information on the surface is limited, as within the regions where tidal flow would be expected to be most influential, the strong currents prevented a constant depth of data collection being maintained. The principal effect of the tidal forcing of the surface is the position of the front at the mouth of the Lynn of Morvern. The spatial data collection allows for the movement of the front over the year to be monitored. Within fjords, studies of the front have concentrated on the productivity of it at different stages of the tidal cycle. In Loch Linnhe, there is evidence of the front moving by over 6 kilometres, with the position being primarily determined by the lunar tidal cycle, as would be expected. Wind and to a lesser extent river discharge were also influential. The sensitivity of the front to river discharge is particularly interesting, as it is over 50km from the main source of freshwater input and the surface layer experiences a considerable amount of turbulent mixing in its passage downinlet. The tidal ranges in the area, along with the current speeds will also influence the extent to which the front moves and this may be an unusual case - as on either side of the 25-30m deep sill between Lismore and Mull, the seafloor falls to 200m deep.

The surface data on phytoplankton does not appear to be particularly patchy. Denman and Platt (1975) amongst others, have shown that on scales of 10m to several kilometres physical processes dominate phytoplankton heterogeneity. The continually changing environment in Loch Linnhe with fortnightly loss of vertical structure, rapid outflow and entrainment may not provide a stable enough environment for the formation of patches. When ponding has occurred, there is evidence that it encouraged productivity, however, the subsequent outflow of the surface water (rich in chlorophyll,) accompanied by the entrainment of water poor in chlorophyll may then decrease productivity again. In Chapter 3 it was shown that chlorophyll was associated with warmer water. The strong coherence between the spatial variability of temperature and chlorophyll indicates that the phytoplankton distribution is determined by the hydrodynamic forcing of the loch with the phytoplankton as a passive tracer. Considering the structure of the basin, much of the temperature variability at the surface is determined by estuarine circulation, with ponding allowing it to warm and during the summer, entrainment cooling the surface. The spatial structure and productivity of phytoplankton in the inner basin may be largely determined by short term stability

and estuarine circulation - both restricted and enhanced. The modelling in Part 3 will enable the examination of such questions.

The surface plots of zooplankton, demonstrate the importance of water movement in the inner basin. Only on one day were the zooplankton spatially associated with their prey, on all others being predominantly in regions of entrainment and upwelling - which were particularly low in phytoplankton. In the outer basin, where the water movements were less influential, the zooplankton were in general spatially associated with the phytoplankton. Only in January and October (times of low chlorophyll) did the influence of hydrodynamics dominate. Along with the weaker water movements within the basin, the presence of more than one region of water would promote the association of zooplankton with their prey.

An important source of water exchange for the outer basin is highlighted by the surface data. It supports the hypothesis that exchange with the Lynn of Lorne is an important source of phytoplankton for the outer basin of Loch Linnhe and as a source of phytoplankton it may also be a source of zooplankton.

The evidence so far suggests that both basins experience too much tidally induced mixing and turbulence to be highly productive - the tidal mixing destroys stratification and causes sedimentation and resuspension - increasing turbidity. A substantial part of the primary productivity of the outer basin is through the input of chlorophyll rich water from the productive Lynn of Lorne into the outer basin. The most productive period for the inner basin was also at least partly influenced by the input of water from the north of the outer basin. Since tidal mixing and exchange are so important, the low productivity of the adjoining coastal sea - the Firth of Lorne - means that exchange with the sea is a poor source of phytoplankton. In comparison, Lochs Etive and Creran which are in close proximity to Loch Linnhe experience higher productivity, but flow into the shallow, productive Lynn of Lorne. The extent of exchange with the Firth of Lorne may also cause the high jellyfish density, but there is no data with which to compare this with other sea-lochs.

Part III

Ecosystem Modelling

Chapter 7

Ecosystem Modelling

7.1 Introduction

With the increasing use of sea-lochs and the surrounding land, it is becoming more important that we are able to understand and evaluate the impact of human activities. In order to do this, we first need to understand how an ecosystem functions without interference. This involves developing an understanding of the relationship between primary producers and their environment and how they utilise the available light and nutrients. Furthermore, it is necessary to understand the interaction of primary and secondary producers and the impact of carnivores. Ecosystem models are a useful tool in enabling the evaluation of such mechanisms and relationships.

With different methods of ecosystem modelling, a range of detail and realism is encompassed. A model may represent a realistic system or concentrate on a specific aspect. With complex simulation models representing a real system such as those by Nixon and Kremer (1977), Aksnes and Lie (1990), Skogen et al. (1995), Tamsalu and Myrberg (1995) and Tamsalu and Ennet (1995) there is conflict between reality and mathematical tractability. Ecosystem models containing detailed, realistic representations of the physical and biological dynamics are not suitable for mathematical analysis, tend to be difficult to parameterise and the run time of the numerical models often too long to permit extensive investigation. Existing datasets also tend to be insufficiently spatially and temporally resolved to allow parameterisation and testing. When specific aspects of an ecosystem are considered alone, as in Steele and Frost (1977), Woods and Onken (1982), Tett et al. (1986), Tett (1987), Fasham et al. (1990), Taylor and Stephens (1993) and Woods and Barkman (1994) with everything else taken to be external parameters, information about underlying mechanisms is revealed, but the effect of, or on, the whole system cannot be considered. They also are highly reliant on the choice of boundary conditions. Woods and Onken (1982) applied a Lagrangian technique opposed to the usual Eulerian as used by Tett (1987). Another method is to create an enclosed ecosystem and model the behaviour within it such as described

in Andersen et al. (1987) and Andersen and Nival (1989). This maximises the accuracy of parameterisation and testing, however no information is provided on spatial heterogeneity, interaction with the benthos and transport mechanisms.

In this chapter I shall apply an existing sea-loch ecosystem model, which was originally developed in Ross et al (1993) and Ross et al (1994), to the inner basin of Loch Linnhe; assess the initial results and modify the model. The model was initially developed for Loch Linnhe and was used to determine the programme of data collection. It has been applied to Lochs Etive, Creran and Ardbhair and Killary Harbour in Ross et al (1993) and Ross et al (1994) but has not previously been tested on Loch Linnhe.

The application of the model to the inner basin enables the impact of meteorological and tidal forcing on the biota to be assessed. In Part 2 the analyses suggested that the lunar tidal cycle and wind plays an important role in mixing and entrainment in Loch Linnhe. In particular, as the temporal resolution of the data did not allow for the effects of the physical regime on the biota to be identified, the application of the model will allow the effect of the physical features on productivity to be studied and the importance of these features evaluated.

The model was initially applied in its basic form with only the basin specific hydrographic constants changed, before the varying physical conditions of Loch Linnhe were considered. The main features highlighted in Part 2 were the turbulent mixing driven by the lunar tidal cycle, which was accompanied by increasing turbidity and sedimentation; downinlet wind accompanied by strong entrainment and upinlet wind causing ponding with subsequent outflow, which again increased entrainment.

7.2 Sea-loch Model

The aim of the sea-loch model developed in Ross et al (1993) was to construct a dynamic model which would be simple enough for its mechanisms to be understood and be investigated computationally. Full descriptions of the development of the loch model are to be found in Ross et al (1993) and Ross et al (1994).

The testing and parameterisation of an ecosystem model are restricted by the limits of existing datasets, which are required for testing the model, and the data available is limited by the physical ability of collection on small spatial and temporal scales and the sampling cost. As there is typically insufficient data to test more finely resolved output, the loch model uses spatially and temporally averaged information to predict an average seasonal cycle.

The food web consists of phytoplankton, herbivorous zooplankton and carnivores - which only consume the zooplankton. There is no species subdivision and a typical species was chosen from each classification for parameterisation. Primary production is limited by nitrogen - with phosphorus and silicon ignored - while zooplankton and carnivores are limited by carbon.

Initial findings from the model were that persistence within a sea-loch is largely determined by the balance of nutrient import and export; with primary production being determined by irradiance, temperature and higher trophic levels.

7.2.1 Physical System

Within the model, hydrodynamic behaviour is greatly simplified. Water fluxes, which are often large compared to the volume of the surface layer, are represented by daily average flows. The vertical structure is described by a pycnocline and lower boundary, with **S** the surface layer above the pycnocline, **I** below the pycnocline and **J** between the lower boundary and the benthos. As mixing within layers is considered to be greater than between, each layer is vertically and horizontally (for spatial simplicity) well mixed - this also allows for the resolution of available data. Tidal flow into **I** is partly entrained into **S** and the volume entrained, in addition to the volume of river discharge, flows into the sea from the surface layer. The remaining volume of tidal inflow, flows into the sea from **I**. There is also turbulent diffusion between the layers which consists of exchanges of equivalent volume.

The initial formulation of the model included **S**, **I** and **J** but with an additional layer **B** which was the interface between the benthos and the bottom layer. As Ross et al (1993) found that **S** & **I** are weakly influenced by nutrient cycling from **J** - as exchange with the sea or seaward basin is more important for nutrient exchange - **B** and **J** were combined with no change in the model results.

7.2.2 Biological System

The typical species chosen for parameterisation were the diatom *Skeletonema costatum*, copepod *Acartia clausi* and ctenophore *Pleurobrachia pileus*. *Pleurobrachia pileus* was originally employed as data for the parameterisation of *A. aurita*, the predominant gelatinous carnivore in Scottish sea-lochs, was scarce.

Phytoplankton in **S** and **I** are modelled separately, coupled by physical processes but existing predominantly within **S**. Those within **I** are still considered viable and may be advected into **S**, while cells which sink below **I** sediment to the seabed. Single populations of zooplankton and carnivores are modelled, as they have more control over their position and are considered to spend a fixed fraction of time in each layer.

Phytoplankton are input into the system with tidal inflow at a rate determined by the phytoplankton density in the coastal sea. Zooplankton and carnivore inflow, however are determined by seasonal immigration rates. Phytoplankton are swept out of the system by tidal outflow, with a retention factor - as the chlorophyll maxima are often subsurface - causing fewer to be advected out whereas zooplankton and carnivores cannot be swept out of the basin.

Phytoplankton carbon fixation is modelled by irradiance or the N:C ratio with nutrient and light limitation being represented by Droop quota and Michaelis-Menten respectively. The uptake of carbon by zooplankton and carnivores is represented by Michaelis-Menten with the assimilation efficiency fixed.

Applications of the initial Ross et al (1993) model showed irradiance to be very important which led to more a more detailed description of light limitation and self shading. Within **S** and **I** surface irradiance decreases exponentially at a rate (κ) determined by a linear combination (eqn. 4.12) of the background attenuation (κ_o) and a phytoplankton self shading term (ρ). Uptake of nitrogen is determined over the light and nutrient limited regions separately, with the lowest rate being used.

The zooplankton representation was altered in two ways between Ross et al (1993) and Ross et al (1994) to introduce aggregation and increase egg production. Zooplankton were changed to aggregate within the region of higher phytoplankton density, rather than spend a fixed time in each layer. To reduce the number of zooplankton at the end of the year and introduce overwintering, zooplankton were changed to excrete more biomass and produce more eggs with increasing temperature. For Loch Linnhe, I have returned to the original formulation with zooplankton spending a fixed amount of time in each layer as with the strong movements of water there is no evidence of zooplankton accumulating with phytoplankton in the inner basin of Loch Linnhe.

7.2.3 Nutrient Cycling

As an aim of the model was to investigate the importance of nutrients and nutrient flux in sea-lochs, the exchange of DIN across boundaries is modelled with separate **S** and **I** DIN. As Pearson (1970) showed that for Loch Linnhe the organic nutrient component in contact with the bottom layer is 3-4 times greater than for the **S** & **I** only one DON population is considered.

Phytoplankton uptake DIN from **S** and **I** and excrete DON, which changes back to DIN at a fixed rate. Zooplankton graze on **S** and **I** phytoplankton and excrete DIN into **S** and **I** according to the ratio of time spent in each layer, with carnivores grazing on zooplankton and excreting DIN.

7.2.4 Implementation

The model is described by ordinary differential equations which are integrated using a fourth order Runge Kutta algorithm with a step size which varies between 0.01 and 1.0 day⁻¹. The model is run to obtain an annual cycle independent of the initial conditions.

The loch is primarily described in the model by layer depths and volumes. In addition, basin and year specific seasonally varying driving functions are input of

irradiance, river discharge from the catchment area, nutrient content of the river discharge, sea (or adjoining basin) phytoplankton, basin temperature and DIN and DON of the sea or adjoining basin.

The fit of the model is measured using the normalised mean absolute error (E_{abs}) which is calculated for each state variable and an average taken over all. The noisy nature of the data does however mean that the E_{abs} can be misleading and fitting by eye a useful technique.

$$E_{abs} = \frac{\sum_{i=1}^n |P_i(x) - O_i(x)|}{\sum_{i=1}^n O_i(x)} \quad (7.1)$$

Where P is the predicted value and O the observed.

7.3 Application to Loch Linnhe Inner Basin

The sea-loch model was initially developed to determine the collection of data most appropriate to enable the understanding of the nutrient budget and fluxes within a sea-loch and was used to determine the collection of data within the Loch Linnhe system. Another aim of the model was to be able to represent a sea-loch with a limited number of system specific inputs, as it was hypothesised that the differences in seasonal cycles between lochs is primarily due to their hydrographic rather than biological differences. The hydrographic features considered in the model are basin volume, layer depths, mean tidal exchange, tidal upwelling and turbulent mixing between the surface and intermediate layers. As the model is being applied to a sea-loch basin which does not flow directly into the sea, the boundary driving functions were taken from the northern end of the outer basin.

7.3.1 System Specific Parameters and Driving Functions

For the initial runs, the only biological parameter changed for Loch Linnhe was ρ , the contribution of phytoplankton to the attenuation coefficient. The value previously used was $0.0012 \text{ m}^2(\text{mg C})^{-1}$ which was calculated for Loch Creran by Tyler (1983). I used ρ of $0.00416 \text{ m}^2(\text{mg C})^{-1}$ as calculated in section 4.4 along with κ_o . The regression described in Tyler (1983), from which the previous values of ρ and κ_o were derived, did not include all the available days as those with high attenuation due to river discharge were not included. The Loch Linnhe values were calculated using all the available data. As there was no evidence of a lower boundary in the inner basin during 1991, γ_I was taken to be 140m. Tidal upwelling (β) and turbulent mixing (T_{IS}) were kept the same as for the Scottish sea-lochs modelled previously.

Table 7.1: Hydrographic parameters for the inner basin of Loch Linnhe. VER - volume exchange rate and d'less - dimensionless.

	Description		Units
γ_S	mean depth of surface layer	10	m
γ_I	mean depth of intermediate layer	140	m
V_S	volume of S	1	d'less
V_I/V_S	volume of I / V_S	5.50885	d'less
V_J/V_S	volume of J / V_S	0.0037	d'less
β	proportion of tide entrained into S	0.25	d'less
T_E	VER for tide into I/ V_S	0.475	day ⁻¹
T_{IS}	VER for mixing between I and S / V_S	0.05	day ⁻¹
κ_o	background attenuation coefficient	0.3525	m ⁻¹

Table 7.2: Driving Functions for the Inner Basin of Loch Linnhe for 1991. The sea values are taken from the northern end of the outer basin.

	Description		Units
$C_{PE}(t)$	phytoplankton C conc in sea	fig. 7.1	mg C m ⁻³
$N_{PE}(t)$	phytoplankton N conc in sea	$0.15 \times C_{PE}$	mg N m ⁻³
$D_E(t)$	DON conc in sea	fig. 7.1	mg N m ⁻³
D_R	DON conc in runoff	0.075	mg N m ⁻³
$F_E(t)$	DIN conc in sea	fig. 7.1	mg N m ⁻³
$F_R(t)$	DIN conc in runoff	fig. 7.1	mg N m ⁻³
$I_C(t)$	immigration rate of carnivores	fig. 7.1	mg C day ⁻¹
$I_Z(t)$	immigration rate of zooplankton	fig. 7.1	mg C day ⁻¹
$L_S(t)$	incident irradiance at surface	fig. 7.1	μ Einst m ² sec ⁻¹
$\theta(t)$	basin temperature	fig. 7.1	°C

In fig. 7.1, sea chlorophyll, the driving function for phytoplankton, has a higher autumn than spring peak. In comparison with the datasets in Chapter 3 this is most likely an artefact of the timing of the data collection. The sea chlorophyll density is also much lower than for that used in modelling Lochs Creran and Etive, both of which flow into the more productive Lynn of Lorne (see Chapter 6.) The other main difference from the driving functions of Ross et al (1994) is that the nutrient content of the river water is lower but river input is considerably less important than exchange with the sea. Unlike the other basins, measured values are available for nutrient boundary conditions in Loch Linnhe.

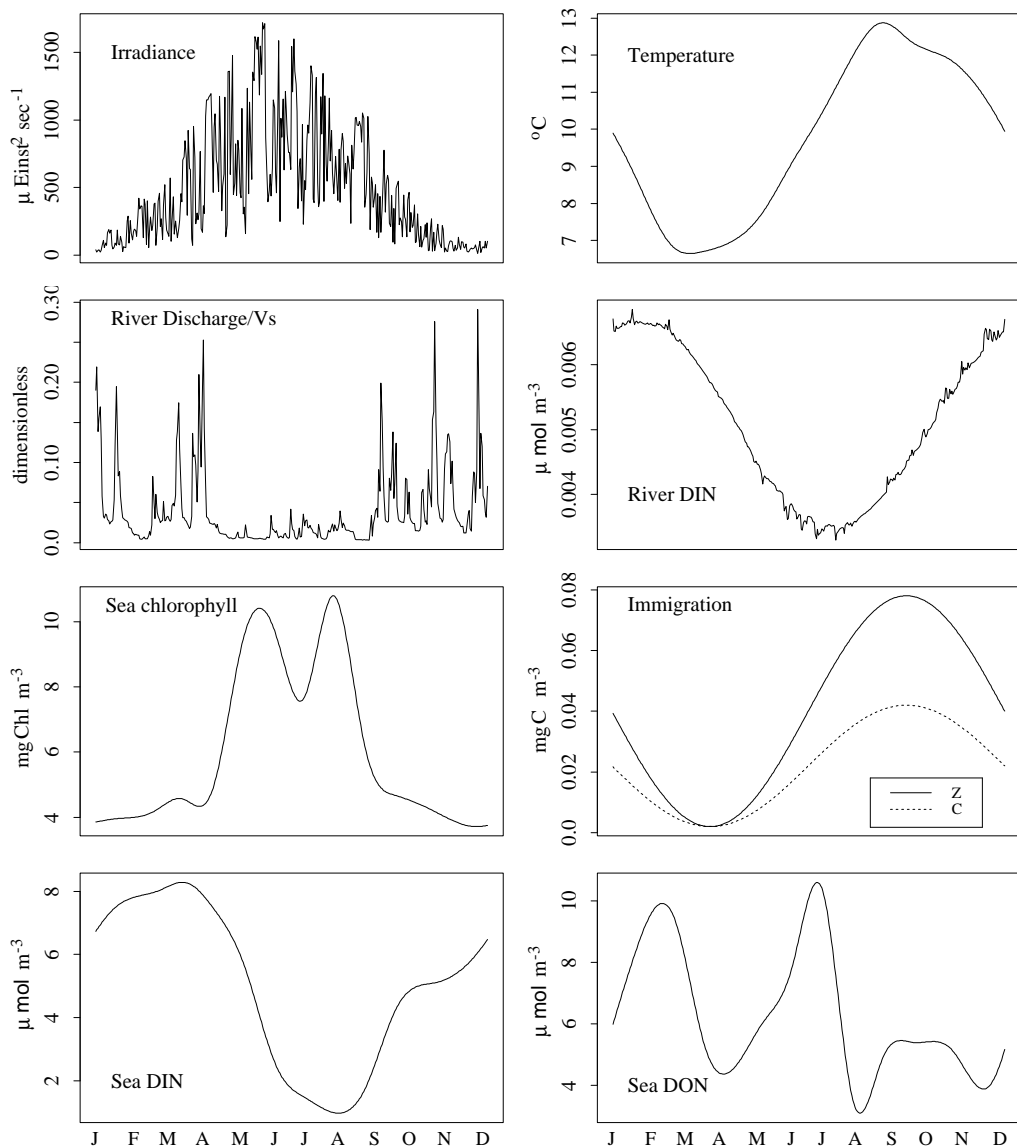


Figure 7.1: Driving Functions for the Inner Basin. Daily values for irradiance, river discharge and nutrient content of the river water. Interpolated values for basin temperature, sea chlorophyll and sea DIN and DON. Sea chlorophyll, sea DIN and DON were all taken from the north of the outer basin. Immigration of zooplankton and carnivores taken to be the same as that used in Ross *et al.* (1994.)

7.3.2 Results

Applying the existing model to the inner basin of Loch Linnhe, with the driving functions as described in fig. 7.1, generates the model output of fig. 7.2 with E_{abs} of 0.80. If the model scores for zooplankton and carnivores are not considered, the E_{abs} falls to 0.34. This error compares well with the results for the other lochs the model has been tested on, but not only is the fit for zooplankton and carnivores extremely poor but the seasonal cycles are clearly wrong.

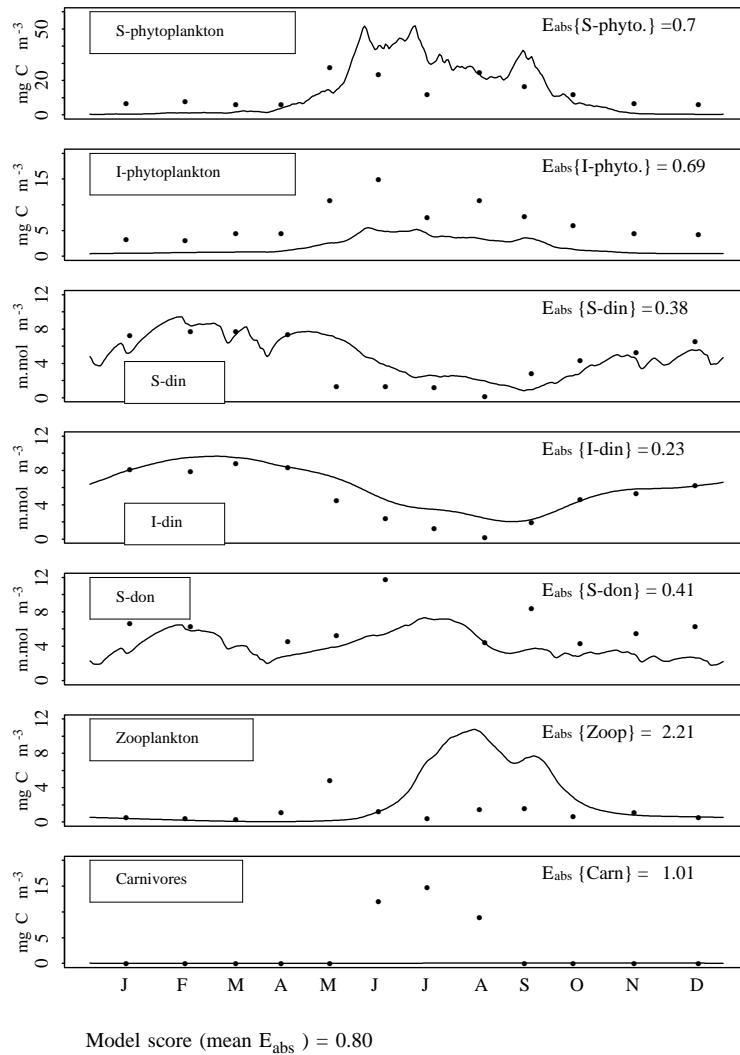


Figure 7.2: Initial model results for the inner basin. Note the different scale for the surface and intermediate layer phytoplankton biomass.

Loch Linnhe is unusual in the low densities of both phytoplankton and zooplankton for 1991. The main problem with the results is that the zooplankton do not appear in the system soon enough and when they do, the population is several magnitudes too large. Immigration from the sea may be an important factor

in starting the zooplankton population and with the bloom being late, the zooplankton may already be there - having been imported into the basin. The other significant problem, is the extremely low model prediction for carnivores, which in turns contributes to the overprediction of zooplankton. The carnivore data available for Loch Linnhe is for large medusae, with the predominant species being *A. aurita* (*M. Heath pers. com.*) but the model was parameterised for ctenophores. From the data, medusae either strobilated or were washed into the Loch Linnhe system between May and June in 1991. Since tidal exchanges between Loch Linnhe and the Firth of Lorne are large, the sea may be an important source of herbivores and carnivores as well as nutrients and phytoplankton. In the inner basin, zooplankton position was influenced strongly by water movements and it is not unusual for zooplankton to be advected into fjord systems (Kaartvedt and Svendsen 1995).

The density of I layer phytoplankton is considerably lower than that of the surface (despite the surface biomass being overpredicted) and is consistently underpredicted throughout the year. Turbulent mixing in deeper water will slow down the sinking rate, prolonging the time cells are suspended in **I**. Overnell and Young (1995) also measured a substantial amount of sediment resuspension by internal waves and deep currents in the inner basin, which may also contribute to the high chlorophyll content of the I-layer. The density of intermediate layer phytoplankton is also affected by advection from the outer basin, as occurred in May.

The model prediction of surface DIN does not fall as rapidly as the observed data, but the observed nutrient values were taken from the sample site data, whereas all the biotic test data were from the axial data and therefore represent an average over the entire basin. Data averaged over the basin typically displays a smoother annual cycle than that from a single point and a basin averaged annual nutrient cycle would be expected to fall more slowly to the summer values. In particular, the sample site, from which the nutrient data was obtained was in a patch of considerably higher density than the rest of the basin in May (fig. 6.19) and would be expected to show a more rapid fall in DIN than the loch as a whole.

7.3.3 Model Sensitivity

An initial stage in assessing the impact of external forcing on the basin, was to consider the sensitivity of the model to changes in the physical parameters. Sensitivity to changes in the hydrodynamic parameters is of particular interest, as some of the values are to a large extent speculative (such as turbulent mixing and entrainment) and vary considerably over the year. The parameters considered were irradiance, the attenuation coefficients and the hydrodynamic parameters. Ross et al (1993) and Ross et al (1994) found irradiance to be the dominant control of primary production in the spring, with predation becoming increasingly influential during the summer. Only for Killary Harbour, however, were the herbivore and carnivore predictions testable. As irradiance varies between years,

the application of a different year's irradiance levels has the potential to affect the accuracy of the model, particularly during times of low predation such as the Spring bloom.

Irradiance

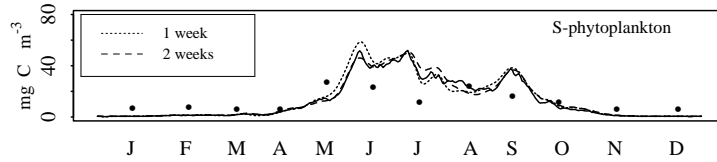


Figure 7.3: Surface phytoplankton with daily irradiance and with irradiance smoothed over 1 and 2 weeks.

Smoothing irradiance over 1 or 2 weeks, as shown in fig. 7.3, not only generates a smoother cycle than the daily values, but also changes the density - particularly in the early summer. This confirms the importance of the irradiance as found by Ross et al (1993) and Ross et al (1994) and shows it to be the primary contributor to the short term fluctuations of the model.

There is a large difference between the self-shading coefficients (κ_o and ρ) derived from Loch Creran by Tyler (1983) and those for Loch Linnhe. The increase in the degree to which light is attenuated reduces the depth at which photosynthesis can take place within Loch Linnhe, generating a significant change in model behaviour. The increase in ρ increases the importance of self-shading in the model - as applied to the inner basin - further decreasing growth.

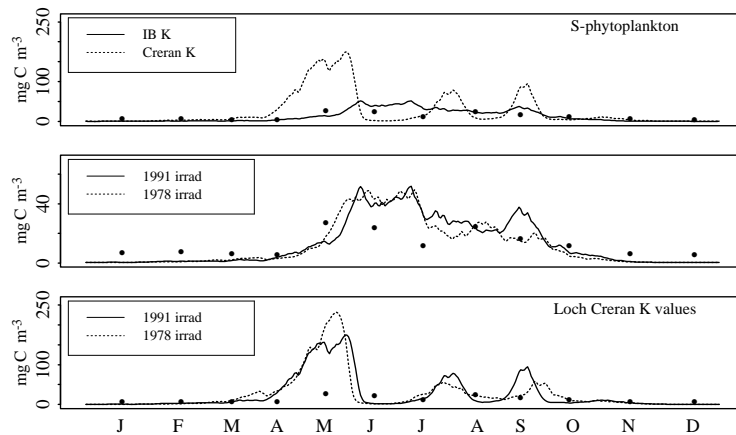


Figure 7.4: Model run with (a) κ_o and ρ as calculated by Tyler (1983), compared to the Inner Basin values for κ_o and ρ , with 1991 irradiance; (b) with 1978 and 1991 irradiance with Loch Linnhe κ_o and ρ and (c) with Loch Creran κ_o and ρ with 1978 and 1991 irradiance.

With the Tyler (1983) values, the bloom is earlier, larger and there are 3 blooms (fig. 7.4a.) With higher light levels and less self-shading, the model output becomes cyclic and less stable. The Loch Etive results published in Ross et al (1994) also display a degree of cyclicity, which may have been caused by background attenuation being too low. The river input into Loch Etive is relatively greater than that into Loch Creran which may generate higher levels of turbidity there than in Loch Creran.

With the 1978 irradiance, as used in Ross et al (1994) (for four sea-lochs, with test data collected in different years) the bloom is slightly earlier and the autumn phytoplankton levels lower. The 1978 data actually provides a better numerical fit for the surface phytoplankton than 1991 irradiance. Applying the Loch Creran κ_o and ρ along with 1978 irradiance, however, increases the magnitude of the spring bloom further (fig. 7.4c.) From this it can be seen that the model is sensitive to the available light and the degree to which it is attenuated - the less turbid the loch, the more sensitive it is to changes in irradiance. Applying either κ_o or ρ as calculated by Tyler (1983) for Loch Creran, in conjunction with a Loch Linnhe value, still increases surface biomass well beyond that measured in Loch Linnhe

Physical Parameters

Smoothing river discharge - as for irradiance above - produces a negligible effect on the model output. Although river discharge is a daily value, as is irradiance, its contribution to the volume of the surface layer is considerably less than that of tidal input - the mean tidal range is 3.25m compared to a typical surface layer depth of 10m or less - and the greatest values and variability of river discharge were during the winter when productivity was low.

Fig. 7.5 illustrates the effect of changes in tidal upwelling, turbulent mixing, tidal input and pycnocline depth of the surface phytoplankton. For all these factors, the influence on productivity is at its greatest during the spring bloom - before predation by zooplankton increased. This level of predation was not however observed in Loch Linnhe. The change in tidal exchange has the least effect on surface phytoplankton biomass of the hydrodynamic parameters with the effect of turbulent mixing and tidal upwelling similar. Surface layer depth produced the most dramatic effect with shallower surface layers generating earlier, higher and shorter blooms with lower summer biomasses.

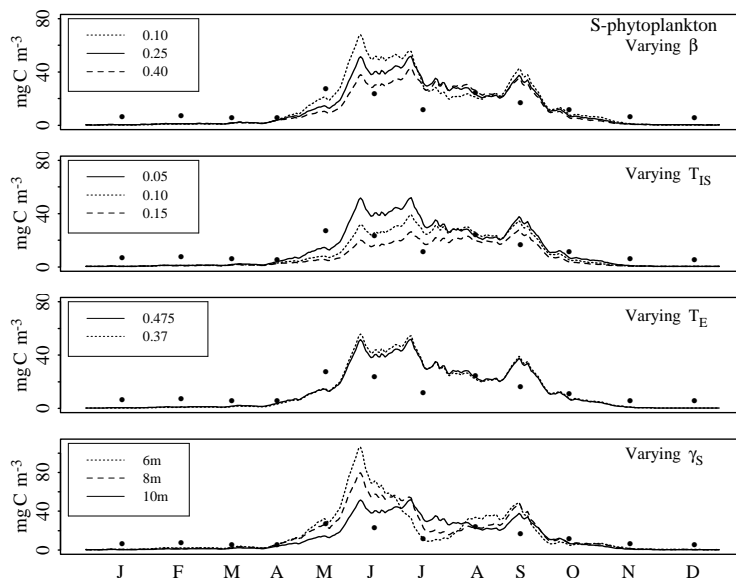


Figure 7.5: Sensitivity of the predicted surface phytoplankton to the hydrodynamic parameters - tidal upwelling (β), turbulent mixing (T_{IS}), tidal inflow (T_E) and surface layer depth (γ_S).

7.4 Changes to Zooplankton and Carnivores

Without a reasonable prediction of the zooplankton and carnivores biomasses the controls of phytoplankton biomass cannot be considered. A representation of the higher trophic levels relevant to Loch Linnhe is required, which involves the reconsideration of immigration and the appropriate carnivore species.

Immigration

In Ross et al (1993) and Ross et al (1994) immigration of zooplankton and carnivores was considered to take place in the autumn (fig. 7.1.) In Loch Linnhe, the biomass of higher trophic levels increased in spring, either from advection, benthic eggs or strobilation. Heath (1995) reported that for Loch Linnhe in 1991, zooplankton were advected into the loch system during the Spring bloom and considered that this exchange with the coastal sea was an important part of the population dynamics. Fig. 3.28 also shows the increase in mesozooplankton moving from the Firth of Lorne up the Loch Linnhe system and the surface zooplankton plots of the inner basin depict the influence of water movements on zooplankton. The data for *A. aurita* (fig. 3.21) would also suggest that they are imported into the basin in the Spring and temperature dependent strobilation of *A. aurita* would produce an import of carnivores into the basin in Spring. The rapid reproduction of *A. aurita* through strobilation provides them with an advantage over zooplankton which need to progress through several stage classes and this along with the late bloom may play a role in the low zooplankton population. *A. aurita* also typically die or are washed from the basin at the end

of the summer and the data shows a rapid fall in all basins, starting from the Firth of Lorne, suggesting that death within the basins rather than outwash is the primary cause of the drop in biomass.

Fig. 7.6 shows the result of applying a simple immigration into the inner basin, of a proportion of the outer basin populations of zooplankton and carnivores - representing advection into the IB. This starts the zooplankton population earlier, though it is still too large from June until October as there is insufficient predation from the carnivores.

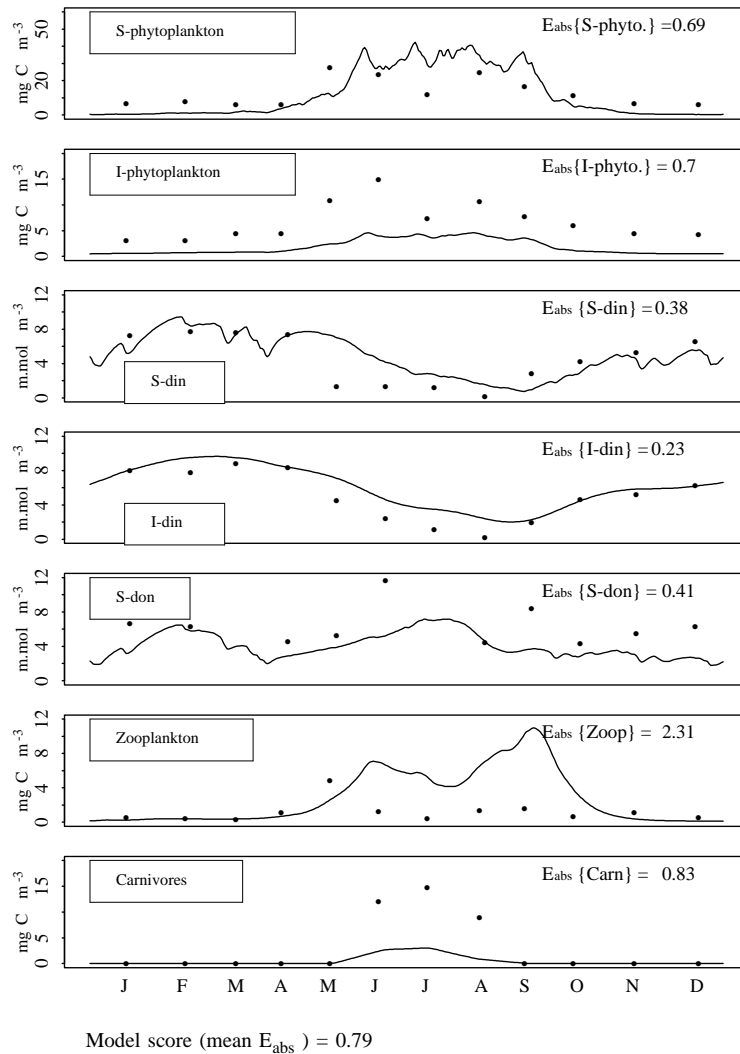


Figure 7.6: Model results with immigration for zooplankton and carnivores based on the outer basin density.

Carnivore Reparameterisation

In Ross et al (1993) the model was parameterised for ctenophores and in Ross et al (1994) the only carnivore data it was tested against was from Killary Harbour - a very shallow Irish sea-loch. Rodhouse and Roden (1987) report that ctenophores constituted 37%, by dry weight, of the gelatinous zooplankton population in Killary Harbour, whereas in Loch Linnhe the data represents medusae. The carnivores were reparameterised to represent medusae - with *A. aurita* or scyphomedusae data preferably used - and are listed in table 7.3.

Schneider (1989) found that excretion (e_{bC}) by *A. aurita* is not heavily dependent on size and measured values of biomass excretion to lie in the range of 15-50% day⁻¹. Purcell (1983) measured assimilation of copepods by siphonophores to be of 87-94% and 93-96% efficiency for carbon and nitrogen respectively. Purcell (1983) suggested that approximately 10% may not be assimilated as copepod exoskeletons comprise $\sim 10\%$ of copepod carbon and are not digested by the jellyfish. I found no data on assimilation by *A. aurita* or other scyphomedusae, but Matsakis and Conover (1991) measured *A. aurita* digestion rates and found them to be low and gelatinous zooplankton often have slow digestion rates coupled with high assimilation efficiencies - Reeve et al. (1978) reported assimilation by the ctenophore *Mnemiopsis mccradyi* to be 74%. In the model, assimilation (a_C) is represented as in eqn. 7.2.

$$a_C = 1 - d_C - e_{UC} \quad (7.2)$$

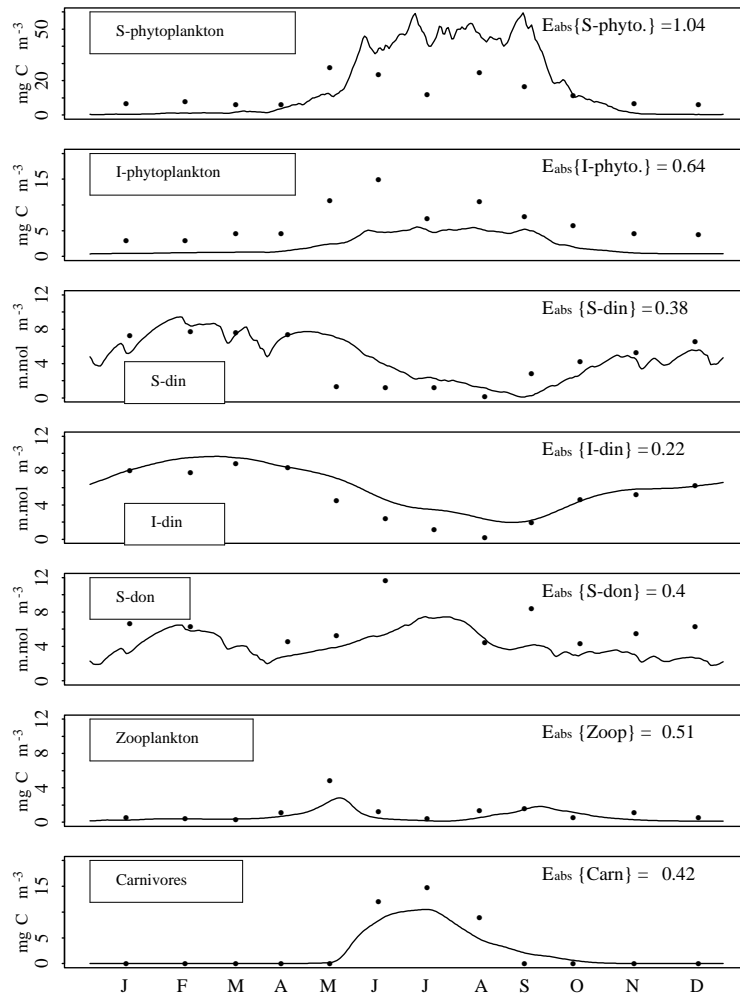
with d_C representing the fraction of carnivore uptake defecated and e_{UC} , the fraction of carnivore uptake excreted.

From Purcell (1992), for *Chrysaora quinquecirrha* medusae > 45mm, 4% of body N is from prey, if they excrete 16% of biomass/day, then they excrete 15.36% of carnivore N/day and 0.024% of ingested N. For medusae < 45mm, and e_{bC} of 16%, 14.56% of carnivore N is excreted/day. For assimilation of 90%, with e_{UC} of 0.024, d_C is 0.076. In water of 10–12 °C Båmstedt et al. (1994) found the daily carbon ration of *A. aurita* to range from 0 to > 600% and in 4°C Matsakis and Conover (1991) measured the daily C ration to be from 400–750% for *A. aurita*, with small medusae consuming proportionally more.

There is little information on growth rates and the required prey densities of scyphomedusae. Olesen et al. (1994) measured growth rates of 0.2 day⁻¹ and with high assimilation efficiency, the half saturation zooplankton concentration (H_Z) is low. Despite being known to be an important predator of zooplankton, zooplankton are not their only food with hydromedusae, barnacle nauplii and fish larvae also forming an important part of their diet (Sullivan et al. 1994). They have also been found to be capable of killing prey too large for them to eat (Hay et al. 1990). The final three parameters in table 7.3 δ_C , λ_C and μ_C were fitted and remain unchanged.

Table 7.3: Carnivore Parameters for *Aurelia aurita*.

	Description		Units
d_C	fraction of carnivore uptake defecated	0.076	d'less
e_{bC}	fraction of carnivore biomass excreted each day	0.16	day ⁻¹
e_{UC}	fraction of carnivore uptake excreted	0.024	d'less
H_Z	half-saturation zooplankton C conc	60	mg C m ⁻³
Γ_{max}	maximum carnivore predation rate	7.5	day ⁻¹
δ_C	carnivore death rate	0.05	day ⁻¹
λ_C	coefficient in carnivore temperature equation	1.0	d'less
μ_C	fraction of carnivore time spent in surface layer	0.5	d'less



Model score (mean E_{abs}) = 0.52

Figure 7.7: Model results with *A. aurita* parameters and modified immigration of zooplankton and carnivores.

The reparameterisation (fig. 7.7) generates a substantial improvement in the model results - both statistically and in the seasonal cycles. The model score at $E_{abs}=0.52$ is considerably better than for the original run where $E_{abs}=0.80$ and with changed immigration at $E_{abs}=0.79$. The increase in carnivore density reduced zooplankton biomass to a more representative level and the seasonal patterns for gelatinous zooplankton and mesozooplankton are also more realistic. The carnivore biomass for Killary Harbour displayed two peaks - as for phytoplankton and zooplankton - which is not an appropriate response for the medusae of Loch Linnhe.

The high carnivore density of Loch Linnhe, keeps the zooplankton biomass low which in turn means that there is low predation of phytoplankton and phytoplankton are overpredicted. The similarity of the predicted and observed zooplankton densities indicates that factors other than predation must maintain the low phytoplankton biomass. Phytoplankton succession may contribute, with a species such as the dinoflagellate *Gonyaulax polyedra* which is common in Loch Creran during the summer (Lewis 1988) and requires more light for growth than *S. costatum*. Physical conditions within the loch have the potential to affect growth and these will be considered in the following sections.

7.5 The Role of the Physical Regime

Changing the timing of zooplankton and carnivore immigration and the parameterisation of the carnivores to *A. aurita* brought about a substantial improvement to the model results as a whole. The prediction of phytoplankton did however deteriorate with the decline in the zooplankton population to a more representative density. This provides an opportunity to evaluate the importance in controlling primary productivity of the physical features identified in Part 2. Physical conditions have already been shown to be of importance in the effect of background attenuation, which in combination with irradiance determines the timing of the bloom. With less predation by zooplankton, irradiance increases in importance as a control of the phytoplankton density - all the predicted peaks in fig. 7.7 coincide with periods of high irradiance. In the basins considered by Ross et al (1994) irradiance was important before the herbivore population was established but less influential thereafter.

The model was originally developed to use average rates of background attenuation, tidal upwelling and turbulent mixing over the year. These factors, however, vary considerably and their variability and importance will be greater in Loch Linnhe than for many other basins. Even without the physical environment being considered more variable, with low herbivory the physical conditions and their variability will become more influential. With more typical levels of herbivores the Spring bloom will tend to be the only time without substantial predation by zooplankton. The physical features I shall concentrate on are the lunar tidal cycle and estuarine circulation. Both these features have the potential to decrease the

productivity of Loch Linnhe and more detailed inclusion of them in the model enables their importance to be assessed. The aim of model simplicity is maintained, with constants only being changed to varying driving functions.

7.5.1 Model Sensitivity

With the reparameterisation of the carnivores to medusae, changes to the hydrodynamic parameters are found to influence phytoplankton biomass throughout the productive season (fig. 7.8.) In the equivalent earlier plot (fig. 7.5) predation by zooplankton controlled phytoplankton density to the extent that changes to the physical conditions had little effect post bloom. As would be expected, with less predation by zooplankton, the physical regime becomes more influential. The low zooplankton population of 1991 may not be typical, *A. aurita* has been found to vary considerably between years and in years of lower jellyfish density, there will be more herbivores as can be seen by comparing figs. 7.2 and 7.7.

If tidal upwelling and turbulent mixing are varied in the Loch Creran model, the effects on phytoplankton biomass are less significant than in Loch Linnhe as predation is the dominant control of primary production there. The low level of biota in Loch Linnhe increases the sensitivity of the model to the hydrodynamic inputs and accentuates the need for their realism. Physical variability in other basins may be as great as in Loch Linnhe, but if the zooplankton population is sufficiently large, the effect of the hydrodynamics will be less - in particular the broad seasonal pattern will be determined by predation as it is in Loch Creran.

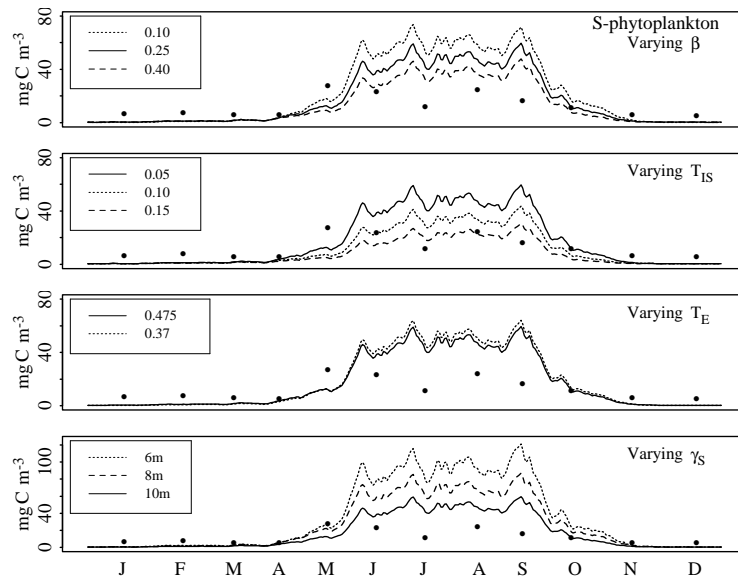


Figure 7.8: Sensitivity of the predicted surface phytoplankton to the hydrodynamic parameters, with the *A. aurita* parameters and spring immigration of zooplankton and jellyfish.

7.5.2 Lunar Tidal Cycle

In Chapter 5 the lunar tidal cycle was shown to dramatically increase vertical mixing, causing the breakdown of stratification in the inner basin - its effect being weaker in the outer basin. While the continual transition from stratification to well mixed may affect the productivity of the basin, it is not clear to what extent. Along with the mixing however, spring tides were linked to resuspension - increasing turbidity, deep water renewal and sedimentation of surface layer phytoplankton. Resuspension is significant and Overnell and Young (1995) found resuspended sediment in traps set at 20m with the seabed at 120m. The tidal influences considered are tidal volume, tidally induced turbidity, sedimentation and variability in entrainment. In section 7.6.1 the influence of tidal mixing is considered in more detail.

Tidal Volume

As the lunar tidal cycle is physically important, I first considered inputting the volume exchange rate of the tide into the intermediate layer as a daily variable. With the large tidal range in this area the tidal input ranges from less than 1/7th to more than 4/5ths of the surface volume. This effects the amount of exchange with the coastal sea (in this case the outer basin) in both influx of biota and nutrients and the subsequent outflow of the surface layer.

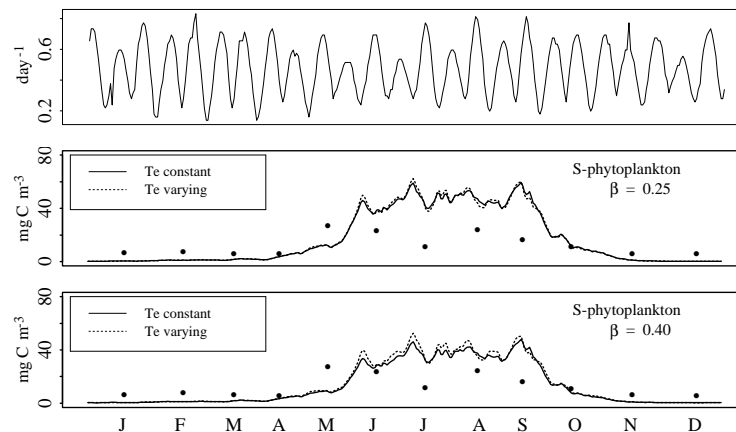


Figure 7.9: Model run with the volume exchange rate T_E/V_S varying as in the top figure, first for $\beta = 0.25$ and then with $\beta = 0.40$. $E_{abs} = 0.51$ for $\beta = 0.25$ with tidal input varying. $E_{abs} = 0.48$ with $\beta = 0.40$ with tidal input both constant and varying but the varying fit is slightly better.

Despite the widely varying volume exchange rate the resulting changes to the model output are slight, the smaller tidal range in May leads to a slightly greater peak and the wider range at the end of the summer leads to lower troughs but the overall effect is small. If tidal upwelling is greater, the effect of varying the volume exchange rate increases, primarily by increasing the role of exchange with the sea. As more tidal input is entrained into the surface, fewer phytoplankton

sediment immediately from the intermediate layer. Similarly more nutrients are input directly into the surface layer.

Tidally Induced Turbidity

Current speed, which is strongly related to tidal flow has been linked to resuspension and turbidity throughout the water column. In Loch Eil, suspended sediment (including resuspended phytoplankton) was measured by Edwards et al. (1980) to increase tenfold from neaps to springs and Overnell and Young (1995) found resuspension to be closely linked to tidal current speed and the freshwater content of the basin. In fig. 7.10 background attenuation (κ_o) varies with $\sqrt{\text{tidal range}}$, with the mean value (of 0.3525) being equivalent to the constant used previously. The model is far more sensitive to cyclicity in the background attenuation than in the volume exchange rate and turbulent mixing as it affects growth directly.

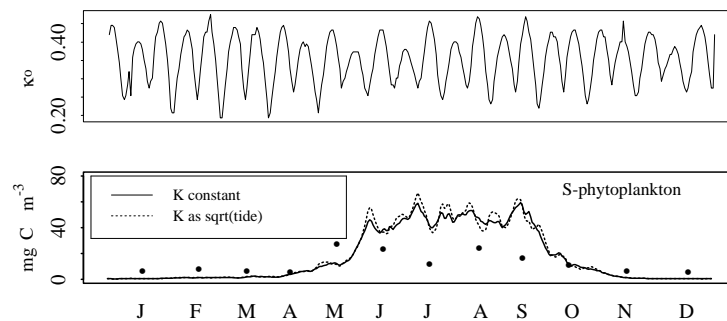


Figure 7.10: Model run with background κ_o varying as in top figure. $E_{abs} = 0.49$

Tidally Induced Sedimentation

Along with resuspension of the sediment, sedimentation of phytoplankton in the inner basin was also found to be linked to spring tides by Overnell and Young (1995). Sinking in the model is represented by the death rate δ_P which if varied in accordance with the tidal range produces fluctuations in surface phytoplankton.

Entrainment

In the Fraser River estuary, Yin et al. (1995) found entrainment increased on Spring tides. This was linked to very low tides allowing more outflow, which in turn generated more entrainment. In fjords however the interaction between tidal height and entrainment is less simple and tidal flow is not typically considered to be a significant source of gravitational circulation (Syvitski et al. 1987). In the inner basin of Loch Linnhe the Hansen-Rattray parameter, ν - as calculated by the method described in Officer and Kester (1991), is very low and thus tidal influence does not play a significant role in gravitational circulation.

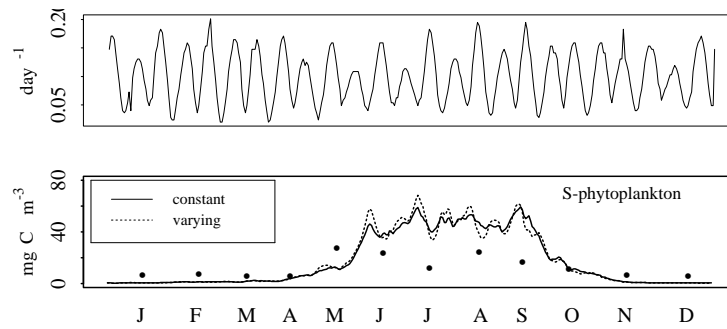


Figure 7.11: Model run with sedimentation rate, δ_P , varying as in the top figure. $E_{abs} = 0.50$

7.5.3 River Discharge

Freshwater inflow into a sea-loch affects estuarine circulation, stratification and turbidity. The greater the freshwater inflow, the faster the seaward flow and the more entrainment. Turbidity is affected by river discharge both by the input of organic matter and the increase in resuspension - which is again related to estuarine circulation.

Entrainment

The amount of entrainment is partially determined by the speed of the seaward flowing surface layer, which in turn is partly controlled by the volume of river discharge and the freshwater content of the surface layer. Wood et al. (1973) considered freshwater river input to determine much of the hydrology of Loch Etive, which receives proportionally more freshwater input than Loch Linnhe. Unlike Loch Linnhe, both basins of Loch Etive also receive direct river input.

If tidal upwelling is taken to always be at least 0.15 and supplemented by $\sqrt{\text{river discharge}}$, then the spring prediction is similar to that from the standard model but the higher discharge levels in July and August reduce the phytoplankton density then (fig. 7.12.)

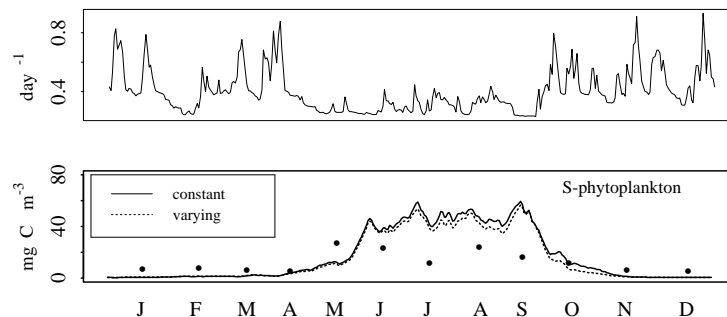


Figure 7.12: Model run with entrainment varying as in the top figure. $E_{abs} = 0.50$

Gravitational Circulation

As the flushing rate in the inner basin depends strongly on river discharge, the Hansen-Rattray parameter, ν is very low. From this it can be taken that river discharge, through its effect on entrainment, is a significant cause of gravitational circulation. Tidal input therefore varies with river discharge. In fig. 7.13, β of 0.25 is taken to be the benchmark value with any variation from that affecting the amount of gravitational circulation.

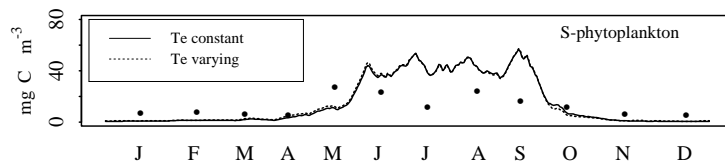


Figure 7.13: With freshwater inflow affecting gravitational circulation and thus exchange with the outer basin. $E_{abs} = 0.51$

The change in model results from entrainment alone is slight, with a slight increase between April and June (when tidal variation was low) and a decrease in October. Residence time in the basin was also low except for September and May when river discharge was at its lowest. As the surface layer of the basin is continually flowing seaward, the residence time in the surface layer of chlorophyll is short, not permitting time for substantial growth.

Turbidity

As the period of the year in which primary production takes place is the period of low river discharge, the large volume of turbid water flowing into the IB may be a factor in the late bloom and low productivity generally. The dominant effect of varying turbidity with the river input is to end the productive season earlier and faster as is shown in fig. 7.14.

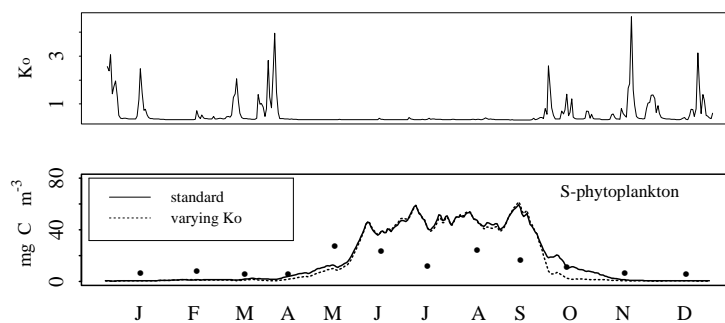


Figure 7.14: Model run with background attenuation varying with river discharge, as in the top figure. $E_{abs} = 0.51$

7.6 Strategic Modelling of Wind and Tidal Forcing

When considered in isolation, variability in the factors considered in the previous section has very little influence on the phytoplankton. In this section the effects of tidal mixing and wind forcing - the predominant features identified in Chapters 5 and 6 are considered more closely.

7.6.1 Tidal Mixing

In Chapter 5 it was shown that the lunar tidal cycle plays a strong role in determining the amount of turbulent mixing in the inner basin, with the large tidal ranges during spring tides leading to a breakdown in stratification and homogenisation of the water column. With stratification and the vertical structure then reestablished as the tidal range falls. Much of this mixing will be due to the interaction between tidal flow and the sill generating internal waves. There is no information available however to ascertain the effect of this on the phytoplankton.

Reduced Model

In order to consider the effect of turbulent mixing in isolation, a simpler model can be used with only phytoplankton C considered and with surface and intermediate layer phytoplankton as the only dependent variables. Horizontal transport is ignored and vertical transport is from sedimentation and turbulent mixing, the turbulent mixing being considered a function of the lunar tidal cycle. Phytoplankton growth is light limited, with surface irradiance and water temperature constant and phytoplankton loss is from constant predation by zooplankton and sedimentation. The full loch model is thereby reduced to the following equations.

C_{PS} and C_{PI} are the surface and intermediate phytoplankton C concentrations in mg C m^{-3} .

$$\frac{dC_{PS}}{dt} = (U_{CS} - m_p C_{PS} V_S - G_S + m_{CIS}) / V_S \quad (7.3)$$

$$\frac{dC_{PI}}{dt} = (U_{CI} - m_p C_{PI} V_I - G_I + \delta_P C_{PS} V_S - m_{CIS}) / V_S \quad (7.4)$$

where U_{CS} and U_{CI} are the phytoplankton growth rates for S and I; m_p the fractional daily loss of biomass from respiration and sinking; $G_{S,I}$ fractional daily loss to predation; m_{CIS} turbulent exchange between the S and I and δ_P sinking.

The surface layer phytoplankton growth rate U_{CS} is defined as :

$$U_{CS} = C_{PS} V_S S_P \left(\Psi_Q \frac{\gamma_{SL}}{\gamma_S} + \frac{R_{ML}}{\gamma_S \kappa_S} \ln \left\{ \frac{L_S \exp(-\gamma_{SL} \kappa_S) + H_L}{L_S \exp(-\gamma_S \kappa_S) + H_L} \right\} \right) \quad (7.5)$$

where κ_S is the attenuation coefficients of the surface irradiance in the S layer with

$$\kappa_S = \kappa_o + \rho C_{PS} \quad (7.6)$$

where κ_o and ρ are as in **7.3.1**; γ_{SL} defines the depth of the productive zone within the surface layers. As turbidity is sufficiently high to prevent growth in the intermediate layer, the intermediate growth rate $U_{CI} = 0$.

$$\gamma_{SL} = \min \left(\gamma_S, \ln \left(\frac{L_S R_{ML}}{H_L \Psi_{SQ}} - 1 \right) / \kappa_S \right) \quad (7.7)$$

The remaining parameters in eqn. 7.5: S_P , Ψ_Q , R_{ML} , L , γ_S , γ_I and H_L are constants, with values and units defined in tables 7.1 and 7.4.

Loss by predation (G_S and G_I) is described by a constant which represents the level of predation predicted by the model to coincide with the irradiance and water temperature. The fractional daily loss of biomass from sedimentation and respiration is described by

$$m_P = \delta_P + e_{bP} S_P \quad (7.8)$$

where e_{bP} represents loss by respiration and transport of phytoplankton by turbulent mixing between the surface and intermediate layer is described by

$$m_{CIS} = T_{IS} (C_{PI} - C_{PS}) \quad (7.9)$$

Table 7.4: Constants for the Reduced Model. VER - volume exchange rate.

	Description		Units
G_S	S-layer zooplankton grazing rate	0.325	day ⁻¹
G_I	I-layer zooplankton grazing rate	0.0	day ⁻¹
δ_P	phytoplankton sinking	0.1	day ⁻¹
Ψ_Q	growth limitation of phyto by N	0.8	day ⁻¹
R_{ML}	max. phyto. growth rate, light limited	1.2	day ⁻¹
L_S	Incident solar radiation	1055.56	Einst m ⁻² s ⁻¹
H_L	half saturation irradiance	60	Einst m ⁻² s ⁻¹
θ	water temperature	8.64	m ⁻¹

Mixing and Phytoplankton

If turbulent mixing is derived entirely from the tidal cycle then it depends on the current velocity across the sill. The kinetic energy input into the basin is a

function of the (current velocity at the sill)³. The maximum mean spring current velocity at Corran is 4.9 m s^{-1} with the corresponding neap value being 1.6 m s^{-1} , the mean variation in energy input therefore is of the order of 28.73 over the lunar tidal cycle.

The variability in turbulent mixing and exchange, over the lunar tidal cycle, does affect the phytoplankton biomass and the greater the variability the greater the effect will be. With constant slow vertical mixing, say 1% of the surface layer the surface density increases. With constant rapid vertical mixing of 28.73% of V_S the density falls. In fig. 7.15a turbulent mixing varies between 1% and 28.73% of V_S over a 14 day period. This generates a cyclic biomass with the surface minima following the mixing maxima. Density within the intermediate layer is determined by constant sedimentation from the surface - creating an intermediate maxima following the surface maxima - and the amount of exchange - greater turbulent exchange also increases the intermediate density.

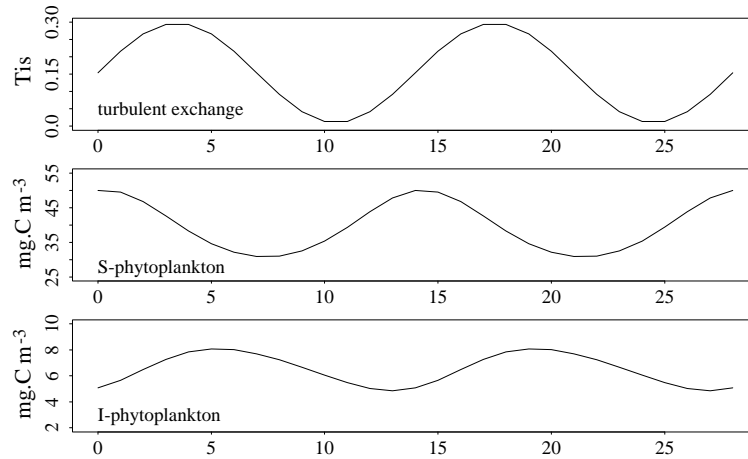


Figure 7.15: Over the lunar tidal cycle, variation in turbulent exchange affects productivity. The turbulent mixing in the top figure, generates a cyclic surface biomass (centre) with the biomass minima following the mixing maxima.

7.6.2 Wind Forcing

Wind has been found to be an important source of turbulent mixing in marine environments and changes in the strength of stratification, brought about by wind mixing, may also play an important role in mass sedimentation of the spring bloom. Sharples and Tett (1994) in modelling the subsurface chlorophyll maximum in a stratified shelf sea, found wind stress and its effect on stratification to be an important factor. In open water such as coastal seas and oceans, however, the role of the wind in turbulent mixing will be more important than in enclosed, small fjords. Sea-lochs may largely be protected from cross-axial winds and axial winds will be funneled along the basin.

In Chapters 5 and 6, the wind was shown to affect entrainment. In the inner basin, upinlet winds generate ponding which by constraining the seaward flow of the surface layer, reduces entrainment and increases stratification - generating a more stable and potentially more productive environment. Downinlet winds increase the flow of the seaward layer, increasing entrainment. In Loch Linnhe less than a day is sufficient for axial wind stress to affect the basin. In April, there was a clear sign of a build up at the head of the basin after one day and in September a substantial amount of entrainment had occurred after only 1 day of downinlet wind. The effect on the biota is however less evident. Ponding is more typically found in strongly stratified fjords but the influence of downinlet winds on surface outflow has been found to be greater in conditions of low stratification (Reigstad and Wassman 1996). There is evidence that ponding did enhance productivity in both the inner and outer basins but outflow after ponding may lead to a substantial part of the new growth being removed from the basin.

Ponding

In fig. 7.16 the effect of upinlet wind on entrainment is considered for 1 day and for continuous periods of 5 and 10 days with ponding represented by no entrainment.

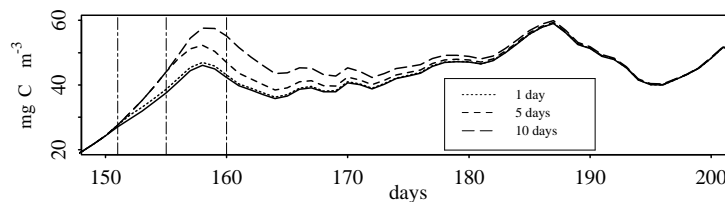


Figure 7.16: Model run with ponding over 1, 5 and 10 days. The solid line of model output represents the prediction with no ponding. Ponding commenced on day 151 (1 June.) The first vertical line indicates the start of ponding, with the other two representing the end of the 5 and 10 day periods respectively.

In fig. 7.16, it is shown that the increase in surface biomass from one day of reduced tidal upwelling (and consequently surface layer outflow) is very small. Longer periods of ponding further increases the surface biomass and the longer the upinlet wind stress is present for, the stronger and more long lasting the effect is. There are however no long term effects and even ponding of ten days, has no influence on the density after 30 days.

An important consideration with ponding not considered above, is the outflow of the surface layer on the cessation or weakening of the upinlet wind stress. The velocity of the seaward flow depends on the extent of the ponding, but entrainment will be high and at least part of the gain in density from ponding will be advected from the basin. In fig. 7.17, after ten days of negligible entrainment two examples of outflow are considered. In the first, there is enhanced entrainment

for 1 day, the other case being of two days of outflow with the second day less than the first.

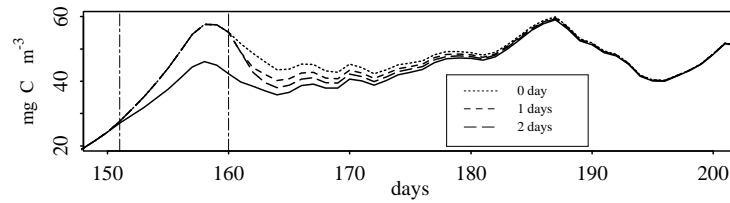


Figure 7.17: Model run with ponding 10 days, followed by 1 and 2 days outflow. The period of ponding (with no entrainment) is between the vertical lines. The solid line of model output represents the prediction with no ponding and those above ponding with no outflow and outflow of 1 and 2 days.

Even with one day of outflow, the surface phytoplankton density rapidly falls and it can be seen that the potential for ponding to have any lasting effect on productivity in the basin is limited. It should also be noted that in these examples ponding prevented entrainment entirely which is an unlikely situation in Loch Linnhe. In particular, the period of most interest - the summer - is the least stratified and stratification aids ponding.

Enhanced Estuarine Circulation

The opposite situation of ponding is that of enhanced surface outflow. In fig. 7.18 the effect of downinlet wind on entrainment is considered, as ponding was above, for 1 day and continuous periods of 5 and 10 days. Tidal upwelling was taken to treble with downinlet winds.

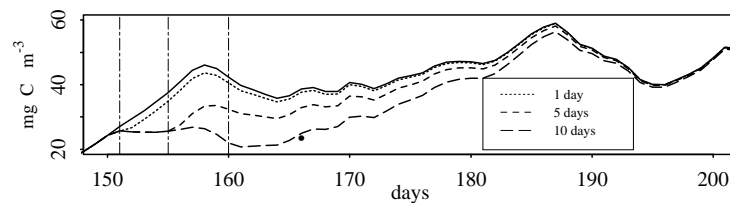


Figure 7.18: Model run with downinlet wind over 1, 5 and 10 days. Increased tidal upwelling commenced on day 151 (1 June) and the vertical lines indicate the end of outflow for the 1, 5 and 10 day periods respectively.

Unlike ponding where the effect of one day is slight, the effect on surface biomass of increasing outflow is instantaneous. Despite the start of June being a period of rapid growth (for the inner basin) throughout the period of high outflow the surface density remains relatively constant and the potential for downinlet wind stress to reduce the surface biomass is apparent.

In the consideration of the relative effects of ponding and enhanced entrainment, entrainment clearly has more potential to be effective in Loch Linnhe, although

upinlet winds are more frequent. Ponding is required to exist for a period of time in order to increase productivity but surface layer outflow instantaneously removes surface phytoplankton, which the advection of I-layer phytoplankton to the surface does not compensate for. In a nutrient depleted surface layer the entrainment of deep water to the surface would be expected to increase entrainment. This is not so for Loch Linnhe where the surface data indicated a high correlation between temperature and chlorophyll with phytoplankton being largely absent in upwelled water.

7.7 Hydrodynamic Events

From the hypothetical consideration of axial winds and tidal mixing in the previous section, it can be seen that they have the potential to influence the productivity of the basin. Key hydrodynamic events, identified in Chapters 5 and 6, include ponding, enhanced estuarine circulation and deep water renewal. Wind will also affect sedimentation and turbidity but these effects shall be ignored as the tidal cycle is a more important factor in their generation. By including the actual axial wind patterns of 1991 in the model, further understanding of their importance and role may be understood. The effect of deep water renewal in May will also be considered as at that time there was an influx of chlorophyll into the basin which coincided with ponding.

7.7.1 Wind Forcing

The relationships between wind, turbulent mixing and entrainment are complex. For a true interpretation of the influence of wind on the inner basin a mechanistic representation is necessary, the formulation of which requires considerably more information than available for Loch Linnhe. In the aim of simplicity and understanding the wind patterns of 1991 are applied to the model as simply as possible and applied where their effects are most obvious in the data.

Downinlet Wind Stress

Downinlet wind in the inner basin enhanced estuarine circulation and increased tidal upwelling. This generated surface patterns with higher salinity in the northern end of the basin (such as shown in fig. 6.8), low phytoplankton densities as the entrained water was low in phytoplankton (fig. 6.21) and caused zooplankton to be advected to the surface (figs. A.11 and A.12.)

From hourly wind speed and direction data, downinlet winds were considered to be effectual within a 90° angle of the loch axis with their importance weighted (those closest to axial being most important.) The wind factor was then multiplied by wind speed and daily mean values taken.

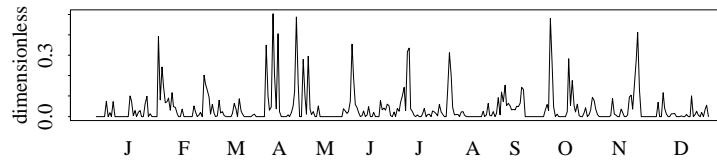


Figure 7.19: A representation of downinlet wind stress on the inner basin in 1991.

A prominent feature of the pattern of wind stress in fig. 7.19 is the dominance of downinlet winds in April and early May - typical months for the start of the Spring bloom. In the Lynn of Lorne, adjacent to the outer basin, the Spring bloom did commence in April. The Lynn of Lorne is more sheltered from downinlet winds than Loch Linnhe, particularly in the north where the phytoplankton density was highest. The strong estuarine circulation and turbulence caused by the downinlet winds may have been a contributing factor in the late bloom in Loch Linnhe. The Lynn of Lorne is more stratified than Loch Linnhe as it experiences less tidal mixing and this may also have protected it from downinlet wind stress - Reigstad and Wassman (1996) found downinlet winds to be more effective with low stratification - contributing to the earlier bloom there.

The wind stress indicated in fig. 7.19, was applied as entrainment to the model in addition to a constant rate of 0.25 (the value used throughout this chapter.) As expected this produces an overall fall in surface phytoplankton density. Downinlet wind stress was then taken to affect turbulent mixing by increasing exchange from 0.05 by a fifth of the value of wind stress in fig. 7.19 the density falls further. In particular there is a fall in the predicted July density. In July residence time in the basin was low (the lowest measured residence time of the year was on 13 July) as was phytoplankton biomass.

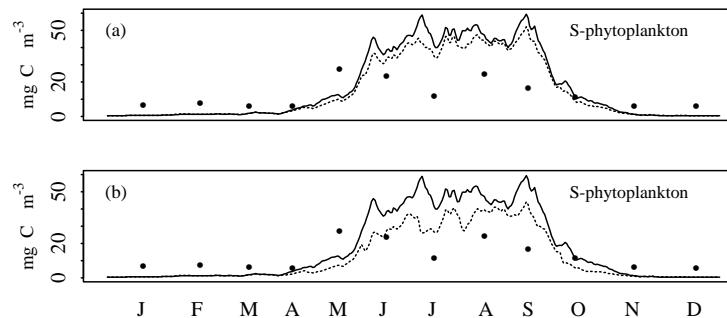


Figure 7.20: Model run with downinlet wind stress compared to the original results from (fig, 7.7) which are represented by the solid line. In (a) enhanced estuarine circulation affects only entrainment and in (b) entrainment, turbulent mixing and phytoplankton retention.

Upinlet Wind Stress

Upinlet wind stress was derived from the data in a similar fashion to that of downinlet. The prevention of estuarine circulation during ponding was partially compensated for on the cessation of the upinlet wind stress. This was only partial as there may have been subsurface seaward flow during the ponding. With the prevailing wind being upinlet, upinlet wind stress was present throughout the year, in comparison with downinlet wind stress which was only present for isolated periods.

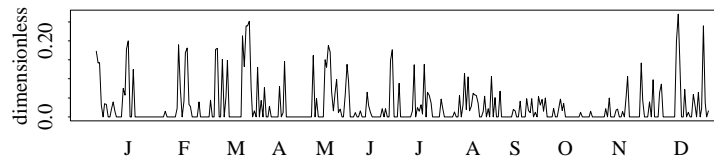


Figure 7.21: A representation of upinlet wind stress on the inner basin in 1991.

As identified in Chapter 5 and 6, the most effective periods of upinlet winds and ponding were in May and August - with that in August weaker. Prolonged periods of upinlet wind stress are visible in May and August in fig. 7.21. Ponding requires a longer period to establish itself than downinlet winds and as greater force is required to prevent the seaward flow than to augment it, the upinlet force is taken to be weaker than that of the downinlet. The wind stress in fig. 7.21 was applied to the model by subtracting it from the constant level of tidal upwelling of 0.25.

Ponding decreases entrainment as estuarine circulation is constrained and stratification increased. Although the increase in stratification associated with ponding decreases turbulent mixing within the ponded region, as ponding does not effect the entire basin, elsewhere the axial wind will generate turbulent mixing. For this reason, turbulent mixing is considered to remain unchanged by ponding. Upon the cessation of the upinlet wind stress, the ponded water flows from the basin and entrainment is slightly higher than the base rate. The effect of the curtailment of river discharge flowing seaward during the duration of the upinlet wind stress is negligible as the freshwater content of the surface layer was very low over the summer.

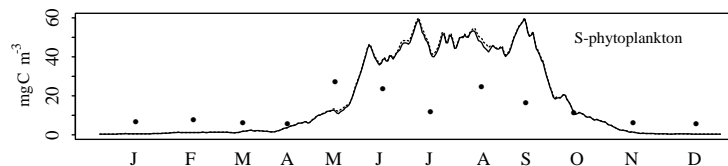


Figure 7.22: Model run with upinlet wind stress compared to the original results from (fig. 7.7) which are represented by the solid line. Restricted estuarine circulation from the upinlet wind stress affects tidal upwelling.

The effect of ponding on the surface biomass is negligible throughout the year. Only in May and August was there any effect. Upinlet wind stress was a frequent event throughout 1991, but the build up of a stable area is determined by the duration of the wind stress, stratification at the time, depth of the surface layer and the amount of river discharge. As river discharge is relatively low through the late spring and summer the effects of ponding are least during the period when they would have the greatest impact on production. The effectiveness of ponding on productivity in the inner basin cannot be quantified by the data as no surface chlorophyll data exists for August and the high density patch in May was outwith the ponded area. A further important consideration with ponding is that it is restricted to part of the basin - its extent governed by the same factors determining the existence of ponding. In the rest of the basin, the increase in wind driven turbulence may reduce phytoplankton density overall.

As was shown in section 7.6.2 and can be seen from figs. 7.20 & 7.22, downinlet wind stress has the potential to be considerably more effectual than upinlet. Overall the effect on the year of the wind stress is to decrease production. Ponding is only temporarily effective in increasing productivity, only affects part of the basin, is required to persist for several days and long term the subsequent outflow at least partly diminishes the population.

7.7.2 Tidal Mixing

In section 7.6.1 it was shown that with all other factors constant, tidally driven turbulent exchange affects phytoplankton biomass. If tidal range is used to estimate the variation in turbulent mixing over the year a pattern such as fig. 7.23a is generated. The energy generated by current flow is proportional to (current velocity)³ and I shall for simplicity assume current velocity to be proportional to the tidal range.

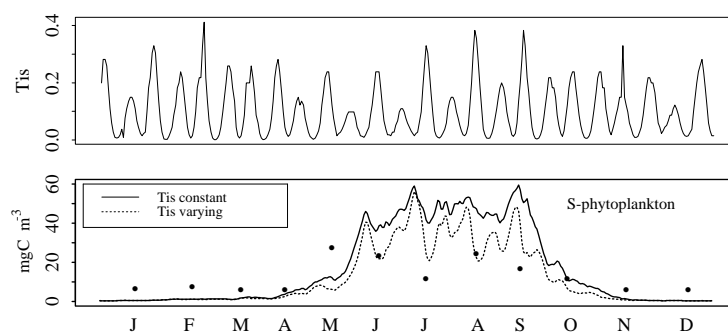


Figure 7.23: Turbulent mixing from the lunar tidal cycle. $E_{abs} = 0.45$

The low tidal ranges in May and June generate lower rates of mixing than at other times of the year and the resulting peaks in biomass are higher.

7.7.3 Deep Water Renewal

The deep water renewal event in May advected chlorophyll into the inner basin. This produced high rates of phytoplankton sedimentation in deep water before the spring bloom was established on the surface (Overnell and Young 1995). Not all cells however, sedimented directly out of the water column and there was a high density patch on the surface in an area of upwelling in the south of the basin (fig. 6.19.) According to Overnell and Young (1995) the bloom peaked more than 3 weeks after this and this increase in surface density appears to have been short lived. By advecting a high density of phytoplankton into the intermediate layer, the effect of this event on the loch may be considered. In fig. 7.24 the model was run with a large short term influx of chlorophyll into the intermediate layer, with a shorter period of upwelling. As expected, most of these cells sediment immediately from the I-layer, but the proportion advected to the surface - through entrainment and tidal upwelling - generate a short burst of higher surface biomass.

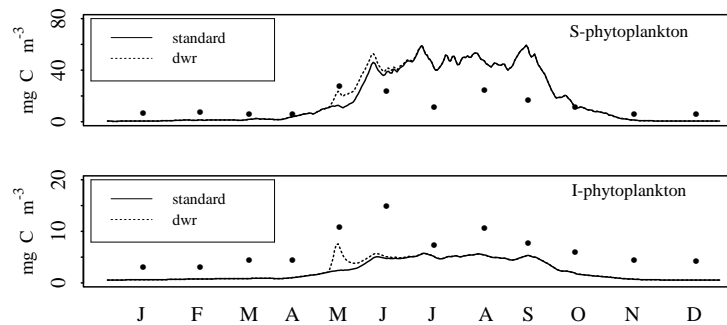


Figure 7.24: Model run with deep water renewal advecting cells into the intermediate layer. $E_{abs} = 0.48$

Renewal in May took place immediately before the upinlet wind stress commenced. If subsequent to the renewal surface layer outflow decreases, the renewal generated bloom persists for longer (fig. 7.25.)

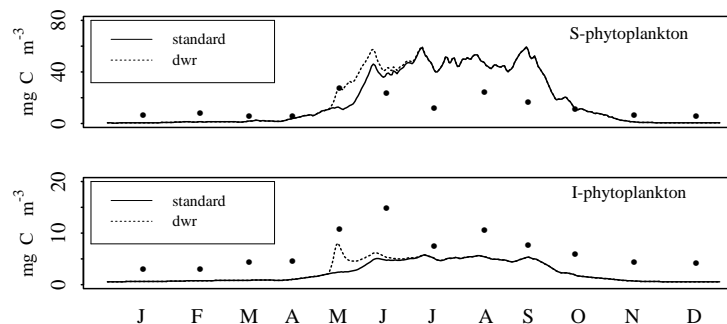


Figure 7.25: Model run deep water renewal advecting cells into the intermediate layer (as above,) followed by ponding of the surface layer. $E_{abs} = 0.48$.

7.8 Further Developments

7.8.1 Physical

In section 7.7 wind and tidal forcing were considered in isolation as was the deep water renewal event in May. Combining surface forcing by axial winds and tidally driven turbulent mixing decreases the surface density further (fig. 7.26.) Although the fit of the surface phytoplankton improves from all the previous plots, by decreasing the surface biomass, the intermediate biomass also falls, as does the early zooplankton as the May surface phytoplankton is underpredicted.

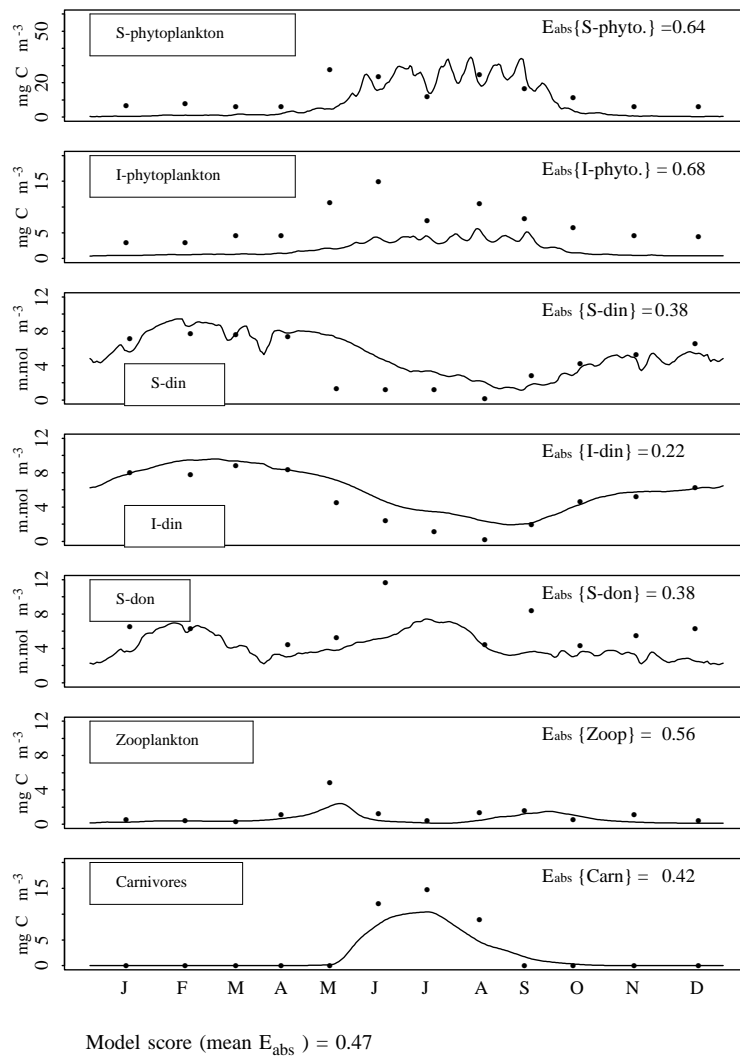


Figure 7.26: Model results with axial wind stress and tidally driven vertical exchange. $E_{abs} = 0.47$.

The model prediction of the spring bloom still appears to be too late - as it has been throughout the application of the model to Loch Linnhe. The more frequent

sampling of Overnell and Young (1995) measured the bloom occurring in early to middle June - which is when the model predicts the first bloom. Comparing the inner basin axial plots of May and June, there was a marked change in the distribution of chlorophyll. In May (fig. 5.8d) chlorophyll was confined to a shallow surface layer ($\sim 5\text{m}$ deep) except where cells had been advected into the basin, whereas by June (fig. 5.21d) it was distributed throughout the surface 20m of the basin.

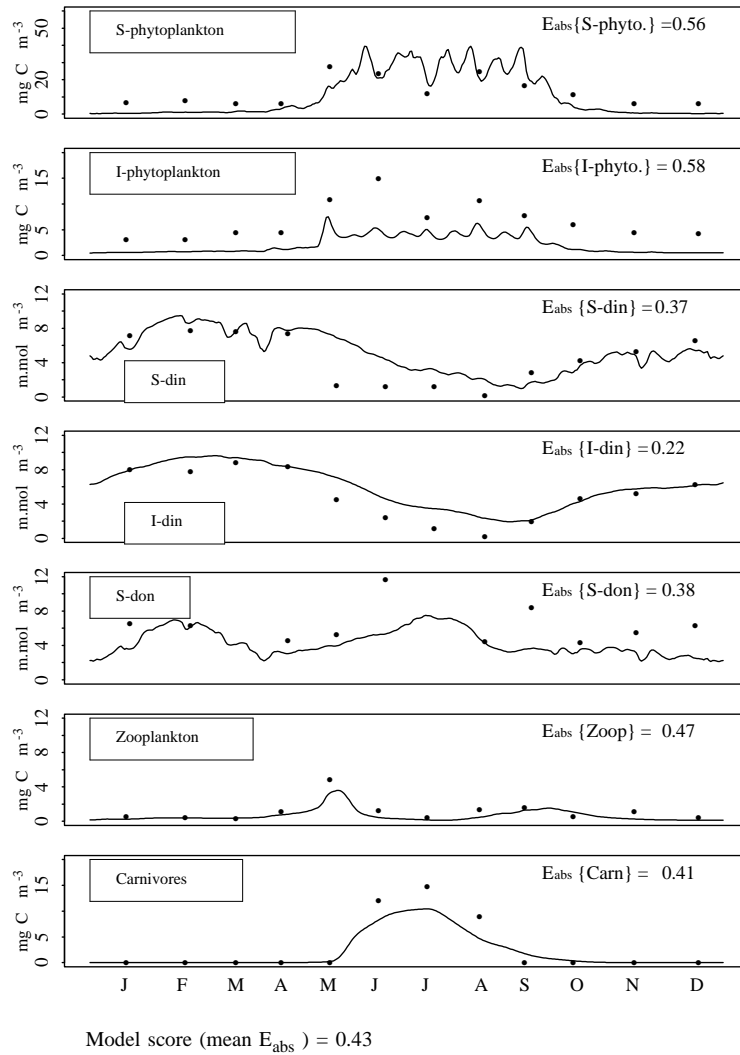


Figure 7.27: Model results with deep water renewal, axial wind stress and tidally driven vertical exchange. $E_{abs} = 0.43$.

The deep water renewal in May, by advecting chlorophyll into the basin and advecting a small proportion of it up into a stable surface layer may have been sufficient to create the transitory increase in biomass then. This highlights the importance of the temporal resolution of the data collection - especially in identifying the timing of short lived events. Without external information, the monthly sampling suggests that the bloom may have occurred in early May - from the

amount of sedimentation in mid-May and that the peak in biomass later was missed. The single sample site in the inner basin also - by being centred in the patch in May - depicts a rapid fall in nutrient content which would not have been typical of the entire basin and also points to an earlier bloom than actually occurred.

By including deep water renewal in the model (fig. 7.27) the May density increases slightly which further increases the June bloom and increases the spring zooplankton biomass. The prediction of the timing of the spring bloom also agrees with that measured by Overnell and Young (1995).

7.8.2 Biological

The principal remaining problem with the model prediction is the low intermediate layer phytoplankton density. A natural effect of decreasing the surface phytoplankton density, has been for the intermediate layer density to decrease further. Turbulence from tidal mixing, internal waves and currents will reduce the phytoplankton sinking rate in deep water. The high exchange with the outer basin will also increase the deep water chlorophyll biomass if the chlorophyll biomass in the inflowing water is greater than that of the resident water. If cells are taking a long time to sink out of the water column, then if they are advected back into the surface layer they will not necessarily grow as they will no longer be viable. The extensive resuspension and high turbidity reported by Overnell and Young (1995) in the intermediate layer may also account for the observed density being higher, cells which have sedimented from the water column may still be resuspended into the water column and their fluorescence measured.

If the intermediate layer sinking rate in the model is reduced to a fortieth of that of the surface layer, then the intermediate layer density increases and while the surface density increases slightly the change is small (fig. 7.28.) The more exchange there is between the surface and intermediate layers, the more effect the higher intermediate layer density has at the surface, though some of this will not occur in a natural system.

The predicted surface DIN, always falls too slowly as the nutrient test data was derived from the sample site, where there was a large bloom in May, whereas all the other test data was based on the entire basin. Even with the extremely large intermediate layer phytoplankton densities (more than twice the observed) with the Loch Creran background attenuation and self-shading applied to the model, the predicted intermediate layer DIN was still too high and varied little in response to changes in phytoplankton density.

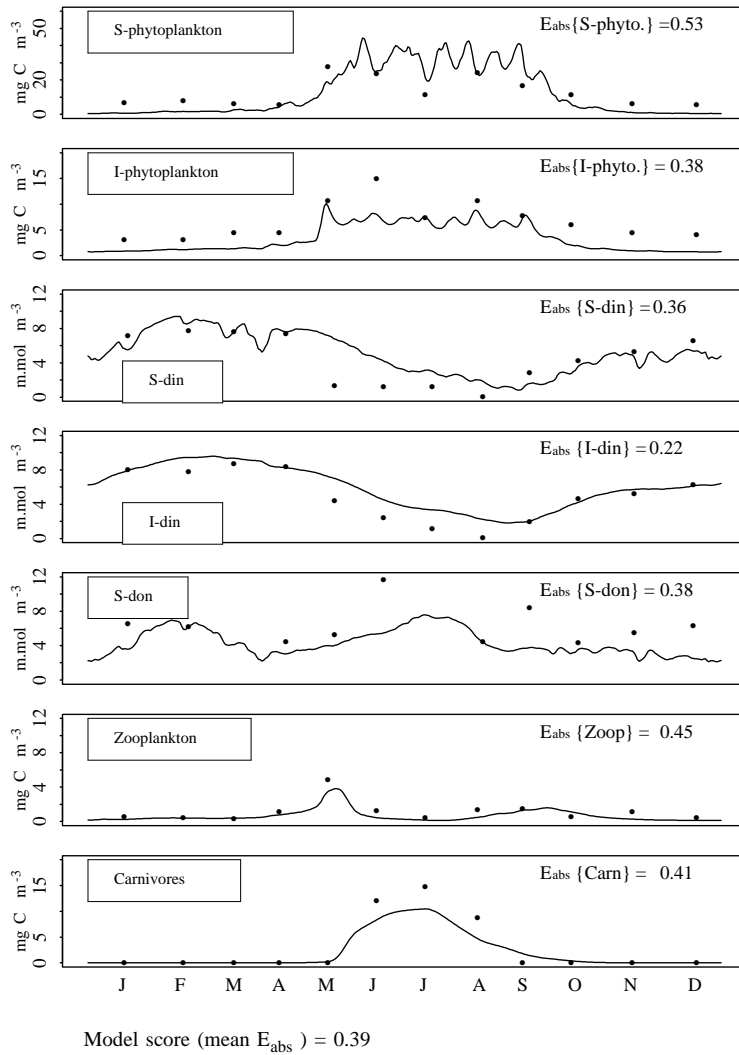


Figure 7.28: Model results with wind stress, tidally driven vertical exchange, deep water renewal and a turbulent intermediate layer. $E_{abs} = 0.39$.

7.9 Discussion

In Chapters 5 and 6, the most important features identified in the data were caused by the lunar tidal cycle and wind forcing. The application of the sea-loch model, to the inner basin of Loch Linnhe, has enabled the consideration of the biological response to some of these features.

7.9.1 Physical Forcing

In section 7.5 many sources of physical forcing were shown to be of little or no consequence in isolation to the model performance. The most important physical determinants of the model behaviour were turbidity, axial wind forcing and tidally driven vertical exchange. Although deep water renewal - when accompanied by an influx of chlorophyll - does increase the surface biomass, its effects are transient.

At a basic level, the high turbidity of Loch Linnhe - along with the strong self-shading component - plays a strong role in the low phytoplankton biomass. Turbidity in Loch Linnhe is generated predominantly by tidal forces. The tidal ranges within Loch Linnhe are high, and current speeds particularly fast at Corran due to the channel being very shallow and narrow. The interaction of tidal flow with the topography generates internal waves, turbulent mixing and considerable re-suspension of the sediment - increasing turbidity. As the high degree of turbidity in Loch Linnhe is clearly a factor in the low productivity there, without a system specific measure of turbidity a representation of the observed data would not have been possible.

The importance of the tidally induced turbulence is also demonstrated by the variation in phytoplankton density with tidally varying vertical exchange. In the period following neap tides, the phytoplankton density increases before falling again after spring tides. High levels of tidally induced turbulence increase exchange between the surface and deep water increasing the advection of cells and within the intermediate layer, the sinking of cells will be slower with more re-suspension, turbulence and internal waves. Low tidal variation in May and June may have contributed to the maximum surface phytoplankton biomass occurring then.

From the application of axial wind stress to the model, it can be seen that down-inlet winds play a role in the low productivity of Loch Linnhe, while the influence of ponding is limited. The importance of downinlet wind agrees with the findings of Chapter 6, where enhanced estuarine circulation was shown to advect cold low chlorophyll water to the surface. Periods of downinlet winds were also associated with the shortest residence times and rapid turnover of the surface layer - particularly in such turbid water - reduces the ability of phytoplankton to grow. A period of predominantly downinlet winds in April and early May (fig. 7.19) will have contributed to the late bloom, along with high turbidity, by setting up a pattern of strong estuarine circulation. In 1992, the spring bloom commenced

at the start of May (Overnell et al. 1995) in comparison with the beginning of June in 1991. With the surface layer flowing rapidly out of the basin and strong entrainment, the surface layer may have been insufficiently stable to allow growth.

From applying ponding to the model, it can be seen that the low growth rate of phytoplankton in Loch Linnhe, along with the transient nature of the stability derived from ponding makes it ineffectual in increasing production. On the cessation of upinlet wind stress there will also be an outflow of the ponded water which may advect a substantial proportion of the new phytoplankton growth with it. Even with no or low levels of subsequent outflow, the effects of ponding are low and short lived. As ponding only effects part of the basin, wind driven turbulent mixing in the rest of the basin may even decrease growth overall.

The principal difference between the influence of downinlet and upinlet wind stress is the time taken for them to have an effect. The response time of the water to the wind stress is less than the growth of phytoplankton to stability. A brief period of ponding will lessen the loss of cells through turbulence and advection but will have little effect on growth.

7.9.2 Other Factors

If axial wind forcing of the surface layer and tidally driven vertical exchange are considered to be key elements in controlling productivity in Loch Linnhe, then stratification and surface layer depth will also be of importance.

The model still underpredicts the May phytoplankton biomass, if this increased so would the spring zooplankton biomass and the carnivore biomass - which would then remain higher through the summer. In fig. 5.8 it can be seen that the surface layer in May was very shallow. With a shallower stratified surface layer, the basin would be more susceptible to ponding and growth faster (figs. 7.4 & 7.8.) The principal problems with varying pycnocline depth are the accurate depiction of the depth changes and the testing of the data. If the surface layer is 6m deep from 9 May until 22 May then the predictions are as for fig. 7.29.

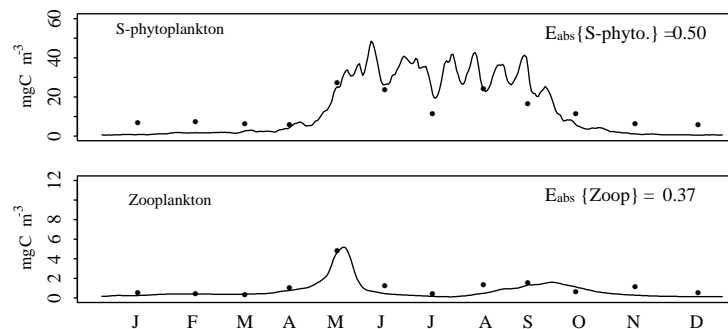


Figure 7.29: Surface phytoplankton and zooplankton with a shallower pycnocline depth in May. $E_{abs} = 0.37$

With different pycnocline depths and varying stratification the impact of wind forcing on the surface will vary. Stratification increases the susceptibility to ponding and surface layer outflow has been found to be more effective with low stratification. Throughout most of the summer stratification in Loch Linnhe was low (fig. 5.1) increasing its susceptibility to enhanced estuarine entrainment. Vertical exchange is also affected by the strength of stratification, as may the extent of tidal mixing.

Despite a period of downinlet winds in September - which generated surface features in both basins (sections 6.2.5 and 6.3.3) - the calculated wind stress for September (fig. 7.19) was relatively weak as wind speed was low. The very low stratification in September at all moorings (figs. 5.1, 5.25 and 5.26) will have increased the impact of the downinlet wind on the loch, enabling the extensive entrainment and cross-basin upwelling. With a greater effectiveness of the downinlet wind in September, the surface phytoplankton biomass would fall further. To estimate the relative importance of wind forcing on the loch on different occasions, more information would be required, is not feasible with the existing dataset and would extend beyond the aim of simplicity.

7.9.3 Carnivores

One of the initial hypotheses in the formulation of the model was that differences in primary production between sea-lochs are determined by the hydrodynamics and physical conditions, enabling the biological parameters to remain constant. Despite this condition holding for the sea-lochs modelled previously, the dominance of large gelatinous zooplankton in Loch Linnhe required reparameterisation of the carnivore parameters from ctenophores to *A. aurita*. The original parameters were appropriate for Killary Harbour as small gelatinous zooplankton constituted a substantial part of the population there, whereas in Loch Linnhe large jellyfish dominated - carnivore data was not available for the other lochs. Whether the *A. aurita* density in 1991 was typical is not known, but the extent of transport between Loch Linnhe and the Firth of Lorne may contribute to the high density of jellyfish there. Loch Linnhe may be unusual in the density of *A. aurita* but other sea-lochs connected directly to the coastal sea may share this feature and *A. aurita* is considered to be common on the west coast of Scotland. The identification of the predominant predator of herbivorous zooplankton in a sea-loch may play an important role in the accuracy of the model predictions. An important effect of the reparameterisation, along with the substantial increase in density, was that the predicted carnivore density has one peak (typical of medusae) rather than the multiple peaks observed in Killary Harbour.

Apart from low phytoplankton density, the high density of *A. aurita* contributes to the low presence of herbivorous zooplankton. Although intense predation of herbivorous zooplankton by medusae has been blamed for red blooms, subsequent high phytoplankton densities are not necessarily obtained. In Kertinge Nor, a shallow eutrophic cove, Riisgård et al. (1995) measured low zooplankton biomass

(< 5mg C m⁻³ for most of the season) due to intensive predation from *A. aurita* but the phytoplankton density never exceeded 120 mg Chl m⁻³.

The reparameterisation of the model indicated that there must be a control over phytoplankton apart from grazing by zooplankton. Apart from the physical factors considered, biotic factors may contribute to this. Grazing may be from fish larvae, macrozooplankton in early stages and gelatinous zooplankton. Hay et al. (1990) and Stoecker et al. (1987) both mention the consumption of diatoms by *A. aurita*. Species succession, which has often been observed in Scottish sea-lochs (Tett 1973; Gamble et al. 1977; Tett et al. 1986a; Lewis 1988; Dodge 1995), with dinoflagellates predominant during the summer, may decrease production after the spring bloom. Chan (1978) measured the growth rates of dinoflagellates to be between a fourth to a sixth of those of diatoms over a range of irradiance.

The application of the model to Loch Linnhe has shown that the biological differences between sea-lochs can be an important factor along with the hydrodynamic regime. In particular the low phytoplankton and zooplankton biomasses in Loch Linnhe highlighted the importance of meteorological and tidal forcing as with lower predation of phytoplankton by zooplankton, the sensitivity of the phytoplankton biomass to the physical conditions is increased.

7.9.4 Sea-lochs and Fjords

The model applied in its original form worked for Lochs Creran and Etive which are both closely situated to Loch Linnhe. Both lochs experience less tidal mixing, less tidal exchange, more river discharge and are more stratified. They are more stable, less turbid environments which enable faster growth of phytoplankton. The small variations in the hydrodynamic parameters, which are so effective when the model is applied to Loch Linnhe, produce negligible changes to the seasonal cycles of Loch Creran. The dominance of zooplankton as a control of phytoplankton growth lessens the importance of hydrodynamics within the model and the sensitivity of the model to changes in the hydrodynamics.

The orientation and alignment of Loch Linnhe makes it particularly vulnerable to wind forcing. In common with many other Scottish sea-lochs, the basins lie in the same direction as the prevailing wind which increases susceptibility to ponding. Unlike many other Scottish sea-lochs however, Loch Linnhe is straight as it lies in a geological fault (the Great Glen,) which by increasing the fetch, increases the effectiveness of wind forcing. In particular, the head of the basin is exposed to downinlet winds funneled down the Great Glen. The glacial formation of fjords means that high ground is often found at the head of lochs, providing some protection from downinlet wind stress. The turbulent mixing and low stratification of Loch Linnhe will also increase the importance of downinlet winds. The season of phytoplankton growth in Loch Linnhe is also the time of low river discharge and low stratification, conditions which will reduce the likelihood of ponding being established.

In Howe Sound, Buckley and Pond (1976) found estuarine circulation and upwelling increased productivity by advecting nutrient rich water into the nutrient depleted surface. This situation occurs in fjords with strong stratification and low turbulent exchange which allows differing nutrient regimes to be generated - a nutrient depleted productive surface and nutrient producing deep water. The advection of parcels of nutrient rich water into the depleted surface therefore prompts growth. With the higher degree of turbulent mixing and lower stratification in Loch Linnhe, the nutrient content of deep water during the summer was not significantly greater than that of the surface and nutrient depletion did not hinder productivity. The entrainment of cold low chlorophyll deep water therefore only led to the advection of phytoplankton out of the basin, with the increased seaward flow. The extent of estuarine circulation combined with high turbidity, kept phytoplankton growth low. In conditions of more light, faster phytoplankton growth would have enabled more growth before cells were advected out of the basin.

Similarly, the forcing of the surface layer out of a fjord (with a corresponding advection of the surface phytoplankton) has been associated with an accompanying compensating inflow and entrainment of nutrient rich water generating another bloom. In the inner basin of Loch Linnhe, the intruding water is not of sufficiently greater nutrient content to generate a bloom and in any case nutrient availability does not constrain productivity.

Part IV

Overview and Discussion

Chapter 8

Overview and Discussion

8.1 Summary

The aim of this work was to assess the role of meteorological and tidal forcing in Loch Linnhe. This was achieved through data visualisation of the extensive dataset collected in 1991 and the application and modification of an existing ecosystem model. The modelling work then permitted the evaluation of the effect of the physical regime on the biota.

Initial assessment of the data revealed Loch Linnhe to have low phytoplankton and zooplankton biomasses, high turbidity and a high concentration of gelatinous zooplankton. Neither basin was nutrient depleted and so a nutrient deficit was not the cause of low productivity.

Analysis of the data - including visualisation - revealed the lunar tidal cycle to be a source of extensive turbulent mixing, with internal waves probably being generated at the sill and substantial vertical mixing occurring, particularly in the inner basin. The fast deep water currents during spring tides were a source of resuspension with turbidity throughout the water column being related to the tidal range. Deep water renewal in both basins was frequent and tidally driven - occurring on spring tides - and the position of the front between the Lynn of Morvern and the Firth of Lorne was also determined by the lunar tidal cycle. The strength of the tidal mixing is due to the large tidal ranges in the area along with the shallow, narrow sills.

Wind forcing is also influential in Loch Linnhe with wind speed and direction strong components in determining the depth and structure of the surface layer. In both basins upinlet winds caused ponding - with a faster response time in the more stratified inner basin. In the inner basin, downinlet winds enhanced estuarine circulation forcing the surface layer seaward. In the wider, less stratified outer basin, downinlet wind stress was able to generate cross basin flow and upwelling within the basin. Along with the different response to downinlet wind the surface structure of the outer basin was also affected by cross-axial winds.

River discharge affects pycnocline depth and stratification, but is not the dominant cause in either during the summer. Vertically, river discharge has more effect on the gradient over the entire basin, within the surface 20m the tidal range is more influential. During periods of extreme river flow in winter, turbidity and estuarine circulation are affected by the river discharge but otherwise the tidal cycle is more influential. In terms of affecting the biota, river discharge is at its minimum during the summer and the effect on the structure of the loch lesser than that of tidal mixing. River discharge and wind direction were found to affect the extent and timing of renewal and the position of the front but only in a role subsidiary to that of the lunar tidal cycle.

Initial runs of the Ross et al (1994) model to Loch Linnhe suggested that straightforward application of the basic model was insufficient to reproduce the seasonal cycle of the sea-loch. The modelling showed that high turbidity and self-shading alone did not account for the low phytoplankton biomass. With the large gelatinous carnivore presence, the zooplankton population remained low and cannot be considered to control the phytoplankton population, thus hydrodynamic factors must be considered. Although many physical factors affecting the loch were shown to be relatively ineffectual, tidally driven vertical exchange and axial wind stress do have the ability to affect phytoplankton biomass. Downinlet winds are of particular importance, increasing the speed of the seaward flowing surface layer and thereby the volume of water entrained. The period of downinlet winds in April and early May, may have contributed to the late bloom and the short residence time in July have contributed to the rapid fall in density at the end of the bloom. The high turbulence in the deep water also appears to have slowed down the sinking of the phytoplankton in deep water.

As for Ross et al (1994) exchange was found to be an important control of the environment within the basin. The frequency of deep water renewal illustrates the connectivity between the basins as do the large tidal ranges. The high presence of jellyfish in Loch Linnhe may be related to its close relationship with the Firth of Lorne - many other sea-lochs do not flow into the coastal sea and experience less tidal exchange. Transport between the Lynn of Lorne and the outer basin is also important as the more productive Lynn of Lorne appears to be a source of phytoplankton for the outer basin.

8.2 Discussion

8.2.1 Data Analysis and Comparison with Other Fjords

The shallow sills and high tidal ranges of Loch Linnhe involve large volumes of water flowing across narrow, shallow sills into the basins. This increases the importance of the lunar tidal cycle in the dynamics of the loch and many of the features of the inner basin of Loch Linnhe can be attributed to the lunar tidal cycle. The interaction of tides with the bathymetry generates internal waves causing resuspension and turbulent mixing, and the frequent renewal events occur on spring tides. The rapid deep water currents and turbulence caused by them also prevent the formation of a lower pycnocline. In comparison with Loch Linnhe where tidal flow does not slow down further into the loch, the speed of tidal inflow into Loch Etive is attenuated by the extremely shallow sill at Connel. With less tidally driven mixing, Loch Etive - like many other Scottish sea-lochs - is able to form a lower pycnocline (Edwards and Edelsten 1977).

Deep water renewal in Loch Linnhe is frequent and driven by spring tides. There is some evidence that exchange is also aided by low freshwater content of the surface layer and increased estuarine circulation from downinlet winds. These conditions for renewal are typical for Scottish sea-lochs. Of Scottish sea-lochs, Loch Ailort (Gillibrand et al. 1996) and Loch Eil (Edwards and Sharples 1986) have been found to renew frequently on spring tides - Loch Ailort on average every 8 weeks and Loch Eil more often. As Loch Eil was found by Edwards and Sharples (1986) to renew so frequently, the regular renewal on spring tides of Loch Linnhe (seaward of Loch Eil) is expected. The innermost of the six Loch Sunart basins was found by Gillibrand and Turrell (1995) to renew in response to estuarine circulation enhanced by downinlet wind stress. All these lochs along with Loch Linnhe experience considerably less river discharge than Loch Etive which Edwards and Edelsten (1977) found renews infrequently - at intervals of approximately 16 months - though still on spring tides. Apart from exceptionally high freshwater input, the tidal range in Loch Etive is also low. Gillibrand and Turrell (1995) found that low river discharge contributed to the timing of renewal events in Loch Sunart.

Comparing Loch Etive and the inner basin of Loch Linnhe, the tidal influence relative to that of river input is considerably greater in Loch Linnhe - reducing the influence of river discharge on renewal. Loch Etive and Loch Kanaird are the only Scottish sea-lochs where O_2 saturation been measured to fall below 50% (Syvitski et al. 1987) and Edwards and Edelsten (1977) considered that as the ratio of buoyant input to turbulent mixing in Loch Etive is exceptionally high for a Scottish sea-loch, the infrequency of renewal and extended periods of stagnation will be uncommon elsewhere in Scotland. The source of freshwater is also a factor. If a sea-loch receives a substantial part of its freshwater input from a loch (as Loch Etive does from Loch Awe) then river discharge will remain higher over the summer than it would if only from a river and periods of very low river input will

be less common. Many Scottish sea-lochs have shallow sills and experience high tidal ranges - especially if compared with fjords in Norway, Washington State or British Columbia - and renewal on spring tides (affected to some degree by river discharge and wind) would be expected to be the typical pattern for other Scottish sea-lochs. High freshwater content of sea-lochs will tend to weaken and prevent renewal. In sufficiently stratified conditions, with low mixing at the sill, high freshwater inflow can aid renewal by increasing estuarine circulation but these conditions which rely on deep sills and small tidal ranges are unlikely in Scotland.

The regular occurrence of deep water renewal in a sea-loch does not imply that fast deep water currents are typical, nor does renewal on high tides mean that the basin is typically well mixed. Despite deep water renewal occurring regularly in Loch Ailort, deep water flow was measured by Gillibrand et al. (1996) to be weak, nutrient levels in deep water high and a lower pycnocline was able to form. With strong stratification the surface layer also covered a wide salinity range - falling to lower values than Loch Linnhe (Gillibrand et al. 1996). These conditions are the opposite to those of Loch Linnhe which does not conform to typical fjord-type stratification. I do not believe that the turbulent, low nutrient conditions in the deep water of Loch Linnhe, with no lower boundary, and relatively weak surface stratification can be considered typical of Scottish sea-lochs.

Although there is evidence of the importance of the lunar tidal cycle - in conjunction with river inflow - on the strength of stratification in Loch Linnhe, there is no evidence of the effect of this on the biota. The lower stratification of the summer - with low river discharge - enabling more extensive vertical exchange may have contributed to the vertical homogeneity of the nutrients. Changes in stratification and mixing elsewhere have often been associated with changes in productivity. The increased stability of stratification can increase productivity, as can its breakdown or the intrusion of deep water into a stratified surface layer. Lochs Striven and Fyne are Scottish sea-lochs with very different conditions and levels of productivity than Loch Linnhe. They are both connected to the northern Firth of Clyde by deep sills and Tett et al. (1986a) described them as having low freshwater input, low tidal exchange, and experiencing periods of deep water stagnation. Typical phytoplankton biomasses in both lochs are greater than in Loch Linnhe and the stability of these lochs enables large blooms of phytoplankton to occur - sufficient to kill fish in fish farms. Estuarine circulation in both lochs is weak, as typically is stratification and Tett et al. (1986a) considered that production was often driven by stratification events.

Wind forcing was shown to contribute strongly to the surface structure of both Loch Linnhe basins. Axial wind stress has been found to be influential in both weakly and strongly stratified fjords. Most fjords where the surface layer has been shown to be forced by the wind are more stratified and experience less tidal mixing than Loch Linnhe, such as in Howe Sound by Buckley and Pond (1976) and Albern Inlet by Farmer and Osborn (1976), where the surface layer is shallow, of very low salinity and the tidal range small. Ponding is a typical feature

of such fjords. As upinlet wind stress in Loch Linnhe, which has a relatively deep surface layer, strong tidal mixing and weak stratification, is able to cause ponding, it would be expected to form in other Scottish sea-lochs. Conversely, in northern Norwegian fjords, Reigstad and Wassman (1996) found the influence of down-fjord wind stress to be at its greatest during periods of weak stratification and the downinlet wind driven coastal upwelling, identified in Porsangerfjord by Cushman-Roisin et al. (1994), was enabled by weak stratification along with the width of the fjord. The degree of stratification in Loch Linnhe suggests that downinlet wind stress will be more influential than upinlet and as the outer basin is less stratified, the impact of downinlet wind will be greater than in the inner.

The influence of the wind on Loch Linnhe is increased by its axis lying in the same direction as the prevailing wind but many other Scottish sea-lochs share this alignment. More important, in comparison with other lochs, is its length and position in a geological fault. The length and straightness increase the wind fetch and other long sea-lochs tend to be more sinuous - such as Loch Fyne - which reduces the power of the wind. The other important result of its position in the Great Glen is that the wind can also be funneled to the end and down the basin - many Scottish sea-lochs are relatively enclosed at the head. The powerful water movements in Loch Linnhe (driven by wind and tide) not only influenced the distribution of phytoplankton, but also zooplankton. The difference in the importance of wind forcing between the two basins can be seen in the zooplankton distribution. In the more active inner basin, the position of zooplankton appears to have been determined by the water movement but in the outer basin there is more spatial correspondence between the position of zooplankton and phytoplankton suggesting greater autonomy by the zooplankton.

In Loch Linnhe there is some evidence of the increased stability with ponding increasing phytoplankton biomass. As ponding events may be short lived and do not extend over the entire basin they cannot be expected to affect productivity long term. Downinlet wind stress in Loch Linnhe enhances estuarine circulation, increasing the advection of the surface layer out of the basin and increasing upwelling. The data for Loch Linnhe indicates that entrainment of deep water and upwelling do not increase productivity. In many other basins, renewal and other events involving upwelling and entrainment are associated with increases in productivity. Reigstad and Wassman (1996) considered meteorological forcing in northern Norwegian fjords to be a significant process in determining the fate of the spring bloom as the advection of the surface layer out of the fjord led to the inflow and entrainment of more productive coastal water. The productivity level of the water seaward of the Loch Linnhe basins is however similar. Increased growth following upwelling is also associated with strongly stratified basins where the surface becomes depleted of nutrients, growth nutrient limited and the intrusion of nutrient rich water increases growth. Such fjords often have deep sills and experience little tidally induced turbulent mixing. In comparison, Loch Linnhe does not become depleted of nutrients and the extensive turbulent mixing means that nutrient concentrations throughout the basin are similar. The advection of deep water to the surface therefore only inputs colder water (in the summer) low

in phytoplankton and increases the surface outflow. The advection of the surface phytoplankton out of the basin would be expected to reduce sedimentation within the basin. The increased advection of water from the outer basin into the deep water of the inner basin may however compensate for this, or even increase the density of deep water.

The width of the outer basin enabled cross-basin upwelling (also aided by low stratification) and increased its exposure to cross-axial winds. Cross-axial winds are not generally considered to be of much influence in fjords and sea-lochs as the steep sides protect them. The influence of winds on Loch Linnhe is enhanced by the relative openness of it in comparison with fjords in more mountainous regions such as Norway and British Columbia. The influence of cross-axial winds may be a common feature of the broader sea-lochs of Scotland and Ireland as the terrain is less mountainous, providing less protection. The number of sea-lochs affected will however be determined by their width and size.

In comparison with nearby lochs, Loch Etive and Loch Creran - which support higher phytoplankton biomass - flow into the Lynn of Lorne which is more productive than the Firth of Lorne. As tidal exchange rates are high, conditions in the coastal sea will affect the productivity within the loch. Tidal flow into both lochs is also lower than into Loch Linnhe and river discharge, especially that into Loch Etive, greater which will generate more stable conditions. The outer basin of Loch Linnhe does experience some exchange with the Lynn of Lorne which appears to locally increase its productivity. Exchange with the Firth of Lorne may also influence the high density of gelatinous carnivores throughout Loch Linnhe, with jellyfish advected into the basin from the coastal sea. Although high predation of herbivores by *A. aurita* has been linked with large phytoplankton densities (including red tides,) phytoplankton density may still remain low despite the low presence of herbivores (Riisgård et al. 1995) as it did in Loch Linnhe.

A crucial difference in the comparison of fjords in temperate climates with those in glaciated regions, is the seasonal pattern of river discharge. A substantial amount of the work carried out on fjords has been in glaciated regions such as northern Norway and mainland Canada. Apart from these fjords tending to be larger, with deeper sills and less tidal mixing, the seasonal pattern of river discharge is also different. They experience little freshwater input in winter, with most freshwater input in summer, whereas in Scottish sea-lochs the opposite is true. If meltwater from glaciers flows into a fjord - as it does for many mainland British Columbian fjords - then the freshwater content of the fjord in summer will be high, generating very strong stratification. The period of strongest stratification therefore coincides with the period when stability augments the potential for phytoplankton growth. It also allows the low salinity surface layer to be nutrient deficient, with intrusions of deeper water being advantageous for growth - the opposite of the situation in Loch Linnhe. Northern Norwegian fjords tend to be less directly influenced by glaciers and as such are less stratified (Reigstad and Wassman 1996) but they receive lower levels of irradiance.

8.2.2 Ecosystem Modelling

Ross et al (1994) found nutrient flux in sea-lochs to be largely from external exchange and the application of the model to Loch Linnhe reconfirms this finding. The main difference between the model findings as applied to Loch Linnhe and to those of Ross et al (1994) is the relative importance of the zooplankton and carnivores. In the other basins, Ross et al (1994) did not find predation by carnivores to account for much of the model behaviour, whereas in Loch Linnhe their predation of zooplankton encompassed a substantial proportion of the resulting biotic structure. The importance of carnivores in 1991 may not be typical. The late spring bloom in 1991 may have contributed to the low zooplankton density as the zooplankton were not established by the time of *A. aurita* strobilation. The high assimilation and low excretion of medusae make them very efficient, despite low prey densities.

The model had previously been applied with the movement of zooplankton and carnivores independent of water movements. In the application of the model to the inner basin of Loch Linnhe, I considered that transport of zooplankton and carnivores is water driven. This decision was based on evidence from Heath (1995) and the surface zooplankton plots which showed their distribution to be determined by upwelling and entrainment. The water movements in Loch Linnhe are particularly strong and in other sea-lochs zooplankton may be able to determine their position most of the time. Even in the outer basin they had more autonomy than in the inner.

With the greater importance of medusae to Loch Linnhe, than the sea-lochs previously considered, more information on densities of *A. aurita* in sea-lochs would be useful. The density in Loch Linnhe may be experienced in other sea-lochs, which would cause problems in the general applicability of the standard loch model with the type of carnivore needing to be considered. Year to year the density may also vary considerably - or the density may remain relatively stable with size varying between years. Data for more accurate parameterisation is of interest as would the relative importance of ctenophores and medusae. In terms of the suitability of individual sea-lochs for aquaculture, gelatinous carnivores can be important. High densities of medusae can kill and damage fish stock and if large blooms of dinoflagellates are generated by low herbivore densities then the fish stock may be damaged.

The application of the model to a loch where zooplankton were not the dominant control of phytoplankton biomass also increased the need for information on the hydrodynamic parameters. This ties in with the aim of the modelling which was to consider the effects of the physical features identified in Part 2 on the biota. In Ross et al (1994), as zooplankton controlled the phytoplankton biomass post spring bloom, the physical parameters were less important and the main differences between Lochs Etive and Creran were tidal exchange and layer volumes - the more easily estimated inputs. Small changes to the physical parameters which altered the model output for Loch Linnhe have little effect in Loch Creran as zoo-

plankton largely control the biota. Without extensive predation of zooplankton the physical behaviour of the loch is less important but if there is a high biomass of gelatinous carnivores in a sea-loch then more information is required on the hydrodynamics.

One of the most obvious biotic features of Loch Linnhe was the low biomass of both phytoplankton and zooplankton. The large carnivore and low phytoplankton biomasses account for the low zooplankton biomass. The causes of the low phytoplankton biomass are more complicated. Although the high beam attenuation and self shading by phytoplankton contributed to the low productivity, they did not account for it. Physical factors were shown by the modelling to be effective in reducing biomass - predominantly from tidally induced turbulence and downinlet winds enhancing estuarine circulation. The effects of both of these in the model are in general similar, increasing exchange between the surface and intermediate layers, which makes the individual importance of each difficult to quantify. The modelling did not attribute ponding with a significant impact on the basin. The most important factors in the model - turbidity, turbulent mixing, exchange with an unproductive coastal sea and enhanced estuarine circulation - are all linked to meteorological (predominantly wind) and tidal effects. The generation of turbidity is predominantly tidal, as is turbulent mixing and the high exchange rate contributes to the short residence in the basin. Wind forcing influences the surface structure, enhances estuarine circulation and also generates turbulent mixing.

Despite the appearance of ponding as a significant effect in increasing productivity from Part 2, the model does not reflect this and ponding may have very little impact on the basin biomass, with increases in biomass localised and short lived and the biomass elsewhere possibly even falling with increased vertical exchange. The advection of cells by the wind into the region of ponding will give an appearance of greater growth there and this effect may have contributed in Linnhe to the greater biomass in ponded regions.

The influence of downinlet wind was greater, which may be linked to the low stratification in the summer of the inner basin. Despite the simplicity of the application of wind stress in the model, it was effective. With more information its reliability, realism and accuracy would be improved. The degree of stratification and surface layer depth will affect the influence of the wind on the surface. The surface will be more susceptible to ponding with strong stratification and a shallow surface layer and downinlet winds more effective with weak stratification. The effectiveness of axial winds will therefore be seasonal with ponding more common in the wetter winter and enhanced estuarine circulation stronger in the drier summer - the pattern most likely to maintain a low phytoplankton biomass.

The thermistor chain data showed the vertical difference in temperature to be determined by the lunar tidal cycle and from the application of tidally varying turbulent mixing to the model, phytoplankton biomass is depicted as behaving, after a time lag, inversely with tidal mixing. Despite this indicating the importance of tidally driven vertical exchange, a more accurate representation of the

role of vertical exchange would be informative. The influence of tidal mixing on vertical exchange will also be affected by the strength of stratification, with greater tidal energy required when the basin is more stratified.

The data analysis in Part 2 suggested that wind forcing and the lunar tidal cycle are important factors in determining the conditions in Loch Linnhe and the modelling largely supported this though it also highlighted the importance of the high medusa biomass. The frequency of deep water renewal does not appear to be influential at the surface, although substantial advection of chlorophyll with the intruding water may have a temporary impact at the surface. As the supply of nutrients is largely controlled by exchange and from remineralisation in the water column, the conditions of the deep water are not of importance.

The physical conditions in the Firth of Clyde in some ways resemble that of Loch Linnhe as it is connected to the shelf sea by a relatively shallow sill of $\sim 45\text{m}$ (though still much deeper than for Loch Linnhe) and experiences strong tidally driven mixing. In the development of a box model of stratification and mixing in the Firth of Clyde, Simpson and Rippeth (1993) found the inclusion of deep water renewal and in particular internal waves, essential in modelling the entire water column. Application of the model with wind-stress and barotropic tides alone gave a reasonable representation of surface temperature but was incapable of predicting changes in deep water temperature. In the loch model the deep water conditions are not particularly important but in Loch Linnhe the turbidity generated by the tidally driven deep water currents and internal waves is.

The model results indicate that the phytoplankton biomass in Loch Linnhe is largely controlled from below - by the hydrodynamic features, with zooplankton controlled at least partly from above, by intensive predation by medusae. In comparison with the model results of Ross et al (1994), this work confirms the overall importance of the physical features of a sea-loch but it also shows that the type of carnivore is important and that the carnivore biomass is influential. The main other point is that with low herbivory, therefore low control of phytoplankton from above a more accurate representation of the hydrodynamic features is required than in a loch where the phytoplankton biomass is controlled from above. Just as when control is by herbivory, which varies throughout the year, hydrodynamic factors are also required to vary throughout the year.

8.2.3 Data Collection

The extent of the Loch Linnhe dataset has enabled the abstraction of many types of information. The daily thermistor chain data revealed the importance of the lunar tidal cycle in driving vertical exchange and more daily mooring data would enable to timing and effectiveness of the renewal events to be estimated more accurately. Spatial data collection enabled the regions of most importance to be identified and the extent of spatial heterogeneity at different times. From the surface data the strength of the upwelling and entrainment in the inner basin was

disclosed, as was the relationship between the surface structure in both basins and wind forcing. The tidal cycle was shown to control frontal position, along with some wind and tidal influence. The importance of exchange with the Lynn of Lorne was also revealed by the surface data and the months with replicate plots showed the rapid structural changes over a short time period. The most important information disclosed by the axial data was the frequency and extent of renewal events. This type of data collection is particularly useful as an exploratory tool as it identifies the more interesting regions of the basin and enables many aspects of fjord behaviour to be considered. In hindsight however, other information would have been useful.

The intensity of the data collection over short periods provided a large volume of data for very limited periods of the year, with large gaps between them. Much of the vertical data was replicated, being available from the sample sites and the axial cruises. Although the axial cruises provided a more representative basin average with which to test the model, a larger number of sample sites and moorings, providing a more frequent record may have been more useful. Apart from the relative vertical consistency along the axis of the loch, which does not require such detailed sampling, the time taken to sample the entire outer basin removes any ability to consider it a snapshot of the structure. From the surface cruises a number of key areas can be chosen and a mooring or sample site in each one would enable most (if not all) of the processes identified in the loch to be assessed more fully than has been possible with the 1991 dataset. The appropriate sites are more obvious for the inner basin as the surface structure was simpler. In comparison the surface data provides information which could not have been gained otherwise.

The low temporal resolution of the data collection is more problematic in interpreting the biological processes than the physical. The timing of data collection encompassed a variety of positions in the lunar tidal cycle - providing information on its control of the front and influence on deep water renewal - and a variety of wind directions, enabling an interpretation of the surface structure. The information on the effect of the physical structure on phytoplankton however, is scarce, particularly with the short season of growth. Although the strong water movements may be considered to largely control the structure and growth of phytoplankton within Loch Linnhe, there is little information on what those effects are.

The size of the outer basin created problems in collecting spatial data - the surface data collection took more than a tidal cycle and the axial cruises took place over more than one day. Semi-diurnal effects may have been small but they cannot be considered.

8.3 Future Work

In continuing the application of a simple model to sea-lochs, more information on the representation of zooplankton and carnivores is of interest. There is scope for a more detailed representation of transport, life cycles and vertical distribution of the higher trophic levels, though for Loch Linnhe there is currently insufficient zooplankton data available for this.

This work has revealed the considerable impact of meteorological and tidal forcing on Loch Linnhe and moving away from the simple sea-loch model, there is potential for the dynamic inclusion of wind and tidal effects. An accurate depiction of turbulence and advection depends on the stability of the basin at the time and should be considered as a relationship between buoyancy and energy. This would enable further understanding of the importance of hydrodynamic features such as internal waves, deep water renewal, estuarine entrainment and wind forcing. At present, the low temporal resolution provides an incomplete picture of the year but analysis of the current meter data, collected as part of the sampling programme in 1991 (but not presently available,) will also increase understanding of the seemingly extensive deep water mixing and circulation.

Part V

Bibliography

Bibliography

- Allredge, A. L. and C. C. Gotschalk (1989). Direct observations of mass flocculation of diatom blooms: characteristics, settling velocities and the formation of diatom aggregates. *Deep-Sea Res.*, **36**, 159–171.
- Allredge, A. L. and W. M. Hamner (1980). Recurring aggregation of zooplankton by a tidal current. *Estuar. Coast. Shelf Sci.*, **10**, 31–37.
- Andersen, V., P. Nival and R. P. Harris (1987). Modelling of a planktonic ecosystem in an enclosed water column. *J. mar. biol. Ass. U.K.*, **67**, 407–430.
- Andersen, V. and P. Nival (1989). Modelling of phytoplankton population dynamics in an enclosed water column. *J. mar. biol. Ass. U.K.*, **69**, 625–646.
- Aksnes, D. L. and U. Lie (1990). A coupled physical-biological pelagic model of a shallow sill fjord. *Estuar. Coast. Shelf Sci.*, **31**, 459–486.
- Balch, W. M. (1981). An apparent lunar tidal cycle of phytoplankton blooming and community succession in the Gulf of Maine. *J. exp. mar. Biol. Ecol.*, **55**, 65–77.
- Baker, E. T., R. A. Feely, M. R. Landry and M. L. Lamb (1985). Temporal variations in the concentration and settling flux of carbon and phytoplankton pigments in a deep fjordlike estuary. *Estuar. Coast. Shelf Sci.*, **21**, 859–877.
- Båmstedt, U. (1990). Trophodynamics of the scyphomedusae *Aurelia aurita*. Predation rate in relation to abundance, size and type of prey organism. *J. Plank. Res.*, **12**, 215–229.
- Båmstedt, U., M. B. Martinnussen and S. Matsakis (1994). Trophodynamics of the two scyphozoan jellyfishes, *Aurelia aurita* and *Cyanea capillata*, in western Norway. *ICES J. mar. Sci.*, **51**, 369–382.
- Bell, W. H. (1973). The exchange of deep water in Howe Sound Basin. *Pacific Marine Science Report*, **73-13**.
- Bienfang, P. K., P. J. Harrison and L. M. Quarmby (1982). Sinking rate response to depletion of nitrate, phosphate and silicate in four marine diatoms. *Mar. Biol.*, **67**, 295–302.
- Bienfang, P. K., J. Syper and E. Laws (1983). Sinking rate and pigment responses to light-limitation of a marine diatom: implications to dynamics of chlorophyll maximum layers. *Oceanol. Acta*, **6**, 55–62.

- Braarud, T. (1974). The natural history of the Hardangerfjord. 11. *Sarsia*, **55**, 90–114.
- Braarud, T. (1976). The natural history of the Hardangerfjord. 13. *Sarsia*, **60**, 41–62.
- Buch, E. (1981). On entrainment and vertical mixing in stably stratified fjords. *Estuar. Coast. Shelf Sci.*, **12**, 461–469.
- Buckley, J. R. and S. Pond (1976). Wind and the Surface Circulation of a Fjord. *J. Fish. Res. Bd. Can.*, **33**, 2265–2271.
- Cannon, G. A. and N. P. Laird (1978). Variability of currents and water properties from year-long observations in a fjord estuary. In Nihoul, J. C. J. (ed). *Hydrodynamics of Estuaries and Fjords*, pp. 515–535. Elsevier.
- Chan, A. T. (1978). Comparative physiological study of marine diatoms and dinoflagellates in relation to irradiance and cell size. I. Growth rates under continuous light. *J. Phycol.*, **14**, 396–402.
- Cloern, J. E. (1991). Tidal stirring and phytoplankton bloom dynamics in an estuary. *J. Mar. Res.*, **49**, 203–221.
- Cokelet, E. D. (1992). Axial and Cross-axial Winter Winds Over Puget Sound. *Monthly Weather Review*, **120**, 826–324.
- Colebrook, J. M. (1960). Some observations on zooplankton swarms in Windermere. *J. Anim. Ecol.*, **29**, 241–242.
- Connor, D. W. (1990). *Marine Nature Conservation Review: a survey of Lochs Linnhe, Eil, Creran and Aline*. NCC.
- Cushman-Roisin, B, V. Tverberg and E. G. Pavia (1989). Resonance of internal waves in fjords: a finite-difference model. *J. Mar. Res.*, **47**, 547–567.
- Cushman-Roisin, B, L. Asplin and H. Svendsen (1994). Upwelling in broad fjords. *Continental Shelf Research*, **14**, 1701–1721.
- Denman, K. L. and T. Platt (1975). Coherences in the horizontal distributions of phytoplankton and temperature in the upper ocean. *Mémoires Société Royale des Sciences de Liège*, 6^e série, tome VII. 19–30.
- Dodge, J. D. (1995). A seasonal analysis of the armoured dinoflagellates of Loch Eriboll, North Scotland. *Mar. Ecol. Prog. Ser.*, **95**, 219–233.
- Dortch, Q. (1990). The interaction between ammonium and nitrate uptake in phytoplankton. *Mar. Ecol. Prog. Ser.*, **61**, 183–201.
- Drinkwater, K. F. (1994). The response of an open stratified bay to wind forcing. *Atmosphere-Ocean*, **32**, 757–781.
- Dugdale, R. C. and J. J. Goering (1967). Uptake of new and regenerated forms of nitrogen in primary productivity. *Limnol. Oceanogr.*, **12**, 196–206.
- Dunn, J., C. D. Hall, M. R. Heath, R. B. Mitchell and B. J. Ritchie (1993). ARIES – a system for concurrent physical, biological and chemical sampling at sea. *Deep-Sea Res. I.*, **40**, 867–878.

- Edwards A and D. J. Edelsten (1977). Deep water renewal of Loch Etive: A three basin Scottish fjord. *Estuar. Coast. Shelf Sci.*, **5**, 575–595.
- Edwards, A., D. J. Edelsten, M. A. Saunders and S. O. Stanley (1980). Renewal and entrainment in Loch Eil; a periodically ventilated Scottish fjord. In Freeland, H. J., D. M. Farmer and C. D. Levings (eds). *Fjord Oceanography*, pp. 453–489. Plenum Press.
- Edwards, A., K. Jones, J. M. Graham, C. R. Griffiths, N. MacDougall, J. Patching, J. M. Richard and R. Raine (1996). Transient coastal upwelling and water circulation in Bantry Bay, a ria on the south-west coast of Ireland. *Estuar. Coast. Shelf Sci.*, **42**, 213–230.
- Edwards, A. and F. Sharples (1986). Scottish Sea Lochs: A Catalogue Nature Conservancy Council Report
- Ellett, D. J. and A. Edwards (1983). Oceanography and inshore hydrography of the Inner Hebrides. *Proceedings of the Royal Society of Edinburgh*, **83B**, 143–160.
- Erga, S. R. and B. R. Heimdal (1984). Ecological studies on the phytoplankton of Korsfjorden, western Norway. The dynamics of a spring bloom seen in relation to hydrodynamical conditions and light regime. *J. Plankton Res.*, **6**, 67–90.
- Eppley, R. W., J. N. Rodgers and J. J. McCarthy (1969). Half-saturation constants for uptake of nitrate and ammonium by marine phytoplankton. *Limnol. Oceanogr.*, **14**, 912–920.
- Farmer, D. M. and H. J. Freeland (1983). The physical oceanography of fjords. *Progress in Oceanography*, **12**, 147–220.
- Farmer, D. M. and T. R. Osborn (1976). The Influence of Wind on the Surface Layer of a Stratified Inlet: Part 1. Observations. *J. Phys. Oceanogr.*, **6**, 931–940.
- Fasham, M. J. R., H. W. Ducklow and S. M. McKelvie (1990). A nitrogen-based model of plankton dynamics in the oceanic mixed layer. *J. Mar. Res.*, **6**, 931–940.
- Folt, C. L. and P. C. Schulze (1993). Spatial Patchiness, Individual Performance and Predator Impacts. *Oikos*, , 560–566.
- Gade, H. G. (1970). Hydrographic investigations in the Oslofjord, a study of water circulation and exchange processes. *Rep. 24*, Geophys. Inst., University of Bergen, Norway.
- Gade, H. G. (1973). Deep water exchanges in a sill fjord. *J. phys. Oceanogr.*, **3**, 213–219.
- Gade, H. G. and A. Edwards (1980). Deep water renewal in fjords. In Freeland, H. J., D. M. Farmer and C. D. Levings (eds). *Fjord Oceanography*, pp. 453–489. Plenum Press.

- Gade, H. G. and H. Svendsen (1978). Properties of the Robert R. Long model of estuarine circulation in fjords. In Nihoul, J. C. J. (ed). *Hydrodynamics of Estuaries and Fjords*, pp. 423–437. Elsevier.
- Gamble, J. K., J. M. Davies and J. H. Steele (1977). Loch Ewe bag experiment, 1974. *Bull. Mar. Sci.*, **27**, 146–175.
- Geyer, W. R. and G. A. Cannon (1982). Sill processes related to deep water renewal in a fjord. *J. Geophys. Res.*, **87**, 7985–7996.
- Gillibrand, P. A. and W. R. Turrell (1995). Deep-water renewal in the upper basin of Loch Sunart, a Scottish Fjord. *J. Phys. Oceanogr.*, **25**, 1488–1503.
- Gillibrand, P. A., W. R. Turrell, D. C. Moore and R. D. Adams (1996). Bottom water stagnation and oxygen depletion in a Scottish sea loch. *Estuar. Coast. Shelf Sci.*, **43**, 217–236.
- Glenne, B. and T. Simensen (1963). Tidal current choking in the land-locked fjord of Nordasvatnet. *Sarsia*, **11**, 43–73.
- Goodrich, D. M. (1988). On Meteorologically Induced Flushing in Three U. S. East Coast Estuaries. *Estuar. Coast. Shelf Sci.*, **26**, 111–121.
- Gowen, R. J. and N. B. Bradbury (1987). The ecological impact of salmonid farming in coastal waters: a review. *Oceanogr. Mar. Biol. Ann. Rev.*, **25**, 563–575.
- Gowen, R. J., P. Tett and K. J. Jones (1992). Predicting marine eutrophication: the yield of chlorophyll from nitrogen in Scottish coastal waters. *Mar. Ecol. Prog. Ser.*, **85**, 153–161.
- Gowen, R. J. and B. M. Stewart (1995). Regional differences in stratification and its effect on phytoplankton production and biomass in the northwestern Irish Sea. *J. Plank. Res.*, **17**, 753–769.
- Griffin, D. A. and P. H. LeBlond (1990). Estuary/ocean exchange controlled by spring-neap tidal mixing. *Estuar. Coast. Shelf Sci.*, **30**, 275–297.
- Haas, L. W. (1977). The effect of the spring-neap tidal cycle on the vertical salinity structure of the James, York and Rappahannock Rivers, Virginia, U.S.A. . *Estuar. Coast. Mar. Sci.*, **5**, 485–496.
- Hansen, D. V. and M. Rattray (1966). New dimensions in estuary classification. *Limnol. Oceanogr.*, **11**, 319–326.
- Haigh, R., F. J. R. Taylor and T. F. Sutherland (1992). Phytoplankton ecology of Sechlet Inlet, a fjord system on the British Columbian coast. 1. *Mar. Ecol. Prog. Ser.*, **89**, 117–134.
- Hamner, W. M., P. P. Hamner and S. W. Strand (1994). Sun compass migration by *Aurelia Aurita* (scyphozoa) - population retention and reproduction in Sannich Inlet, British-Columbia. *Mar. Biol.*, **119**, 347–356.
- Haury, L. R., J. A. McGowan and P. H. Wiebe (1978). Patterns and processes in the time-space scales of plankton distribution. In J. H. Steele (Ed.), *Spatial Patterns in Plankton Communities*, NATO Conference Series IV Marine Sciences Vol. 3, pp. 277–327. Plenum Press.

- Hay, S. J., J. R. G. Hislop and A. M. Shanks (1990). North Sea scyphomedusae: summer distribution, estimated biomass and significance particularly for O-group gadoid fish. *Netherlands Journal of Sea Research*, **25**, 113–130.
- Heath, M. R. (1995). Size spectrum dynamics and the planktonic ecosystem of Loch Linnhe. *ICES J. mar. Sci.*, **52**, 627–642.
- Henderson, E. W. and J. H. Steele (1993). Problems in the meso-scale interpretation of satellite chlorophyll data. *Continental Shelf Research*, **13**, 845–861.
- Hibiya, T. and P. H. LeBlond (1993). The control of fortnightly modulation of tidal mixing processes. *J. Phys. Oceanogr.*, **23**, 2042–2052.
- Hodgins, D. O. (1979). A time dependent two-layer model of fjord circulation and its applicaion to Alberni Inlet, British Columbia. *Estuar. Coast. Mar. Sci.*, **8**, 361–378.
- Holbrook, J. R., R. D. Muench and G. A. Cannon (1980). Seasonal observations of low-frequency atmospheric forcing in the Strait of Juan de Fuca. In Freeland, H. J., D. M. Farmer and C. D. Levings (eds). *Fjord Oceanography*, pp. 305–317. Plenum Press.
- Holligan, P. M. (1981). Biological implications of fronts on the northwest European continental shelf. *Phil. Trans. R. Soc. Lond. A.*, **302**, 547–562.
- Huppert, H. E. (1980). Topographic effects in stratified fluids. In Freeland, H. J., D. M. Farmer and C. D. Levings (eds). *Fjord Oceanography*, pp. 117–141. Plenum Press.
- Hydrographic Department (1977). *Loch Linnhe: Northern Part*. British Admiralty Chart No. 2380. Taunton.
- Hydrographic Department (1977). *Loch Linnhe: Southern Part*. British Admiralty Chart No. 2378. Taunton.
- Hydrographic Department (1977). *Firth of Lorn: Northern Part*. British Admiralty Chart No. 2387. Taunton.
- Jamart, B. M. and D. F. Winter (1978). A new approach to the computation of tidal motions in estuaries. In Nihoul, J. C. J. (ed). *Hydrodynamics of Estuaries and Fjords*, pp. 261–281. Elsevier.
- Jamart, B. M. and D. F. Winter (1980). Finite element computation of the barotropic tides in Knight Inlet, B.C.. In Freeland, H. J., D. M. Farmer and C. D. Levings (eds). *Fjord Oceanography*, pp. 283–289. Plenum Press.
- Jones, K. J. and R. J. Gowen (1990). Influence of stratifiaction and irradiance regime on summer phytoplankton composition in coastal and shelf seas of the British Isles. *Estuar. Coast. Shelf Sci.*, **30**, 557–567.
- Kaartvedt, S. and H. Svendsen (1995). Effect of freshwater discharge, intrusions of coastal water, and bathymetry on zooplankton distribution in a Norwegian fjord system. *J. Plankton Res.*, **17**, 493–511.
- Klinck, J. M., J. J. O'Brien and H. Svendsen (1981). A simple model of fjord and coastal circulation interaction. *J. Phys. Oceanogr.*, **11**, 1612–1626.

- Kolasa, J. and C. D. Rollo (1991). Introduction: The heterogeneity of heterogeneity: A glossary. In Kolasa, J. and S. T. A. Pickett (eds). *Ecological Heterogeneity*, Chap 1, pp. 1–23. Springer-Verlag. New York.
- Lavelle, J. W., E. D. Cokelet and G. A. Cannon (1991). A model of density intrusions into and circulation within a deep, silled estuary: Puget Sound. *J. Geophys. Res. C.*, **96**, 16779–16800.
- LeBlond, P. H., H. Ma, F. Doherty and S. Pond (1991). Deep and intermediate water exchange in the Strait of Georgia. *Atmosphere Ocean*, **29**, 288–312.
- LeBlond, P. H., D. A. Griffin and R. E. Thomson (1994). Surface salinity variations in the Juan de Fuca Strait: test of a predictive model. *Continental Shelf Research*, **14**, 37–56.
- Levings, C. D., A. Ervik, P. Johannessen and J. Aure (1995). Ecological criteria used to help site fish farms in fjords. *Estuaries*, **18**, 81–90.
- Lewis, J. (1988). Cysts and sediments: *Gonyaulax polyedra* (*Lingulodinium machaerophorum*) in Loch Creran. *J. mar. biol. Ass. U.K.*, **68**, 701–714.
- Long, R. R. (1975). Circulations and density distributions in a deep strongly stratified, two-layer estuary. *J. Fluid Mech.*, **71**, 529–540.
- Lucas, C. H. (1994). Biochemical composition of *Aurelia aurita* in relation to age and sexual maturity. *J. Exp. Mar. Biol Ecol.*, **183**, 179–192.
- Lucas, C. H. and J. A. Williams (1994). Population dynamics of the scyphomedusa *Aurelia aurita* in Southampton Water. *J. Plank. Res.*, **16**, 879–895.
- McClimans, T. A. (1978). On the energetics of tidal inlets to land locked fjords. *Marine Science Communications*, **4**, 121–137.
- McGowan, J. A. (1971). Oceanic biogeography of the Pacific. . In Funnell, B. M. and W. R. Riedel (eds). *The Micropalaeontology of the Oceans*, pp. 3–74. Cambridge University Press.
- MacKay, D. W. (1986). Sludge dumping in the Firth of Clyde - a containment site. *Marine Pollution Bulletin*, **17**, 91–95.
- Mann, K. H. and J. R. N. Lazier (1991). *Dynamics of Marine Ecosystems: Biological-Physical Interactions in the Oceans*, Blackwell Scientific Publications.
- Margalef, R. (1978). Life forms of phytoplankton as survival alternatives in an unstable environment. *Oceanologica Acta*, **1**, 493–509.
- Marinone, S. G., S. Pond and J. Fyfe (1996). A three-dimensional model of tide and wind-induced residual currents in the Central Strait of Georgia, Canada. *Estuar. Coast. Shelf Sci.*, **43**, 157–182.
- Marinone, S. G. and S. Pond (1996). A three-dimensional model of deep water renewal and its influence on residual currents in the Central Strait of Georgia, Canada. *Estuar. Coast. Shelf Sci.*, **43**, 183–204.
- Matsakis, S. and R. S. Conover (1991). Abundance and feeding of medusae and their potential impact as predators on other zooplankton in Bedford Basin

- (Nova Scotia, Canada) during Spring. *Can. J. Fish. aquat. Sciences*, **48**, 1419–1430.
- Milne, P. H. (1972). Hydrography of Scottish West Coast Sea Lochs Department of Agriculture and Fisheries for Scotland, Marine Research Report, 3
- Möller, H. (1980). Population dynamics of *Aurelia aurita* medusae in Kiel Bight, Germany (FRG). *Mar Biol.*, **60**, 123–128.
- Napier, I. R. (1995). Growth and collapse of a spring phytoplankton bloom in the Firth of Clyde, Scotland. *Mar Biol.*, **123**, 189–195.
- Nisbet, R. M. and W.S.C. Gurney (1998). *Ecological Modelling*, OUP.
- Nixon, S. W. and J. N. Kremer (1977). Narragansett Bay - The development of a composite simulation model for a New England estuary. In Hall, C. A. S. Hall and J. W. Day (eds). *Ecosystem Modeling in Theory and Practice: An introduction with case histories*, pp. 621–673. Wiley-Interscience.
- Officer, C. B. and D. R. Kester (1991). On estimating the non-advective tidal exchanges and advective gravitational circulation exchanges in an estuary. *Estuar. Coast. Shelf Sci.*, **32**, 99–103.
- Olesen, N. J., K. Frandsen and H. U. Riisgard (1994). Population dynamics, growth and energetics of jellyfish *Aurelia aurita* in a shallow fjord. *Mar. Ecol. Prog. Ser.*, **105**, 9–18.
- Omori, M. and W. M. Hamner (1982). Patchy distribution of zooplankton: behavior, population assessment and sampling problems. *Mar. Biol.*, **72**, 193–200.
- Open University (1989). *Seawater: Its Composition, Properties and Behaviour*. Pergamon Press.
- Overnell, J., A. Edwards, B. E. Grantham, S. M. Harvey, K. J. Jones, J. W. Leftley and D. J. Smallman (1995). Sediment-water column coupling and the fate of the spring phytoplankton bloom in Loch Linnhe, a Scottish fjordic sea-loch. Sediment processes and sediment-water fluxes. *Estuar. Coast. Shelf Sci.*, **41**, 1–19.
- Overnell, J. and S. Young (1995). Sedimentation and Carbon Flux in a Scottish Sea Loch, Loch Linnhe. *Estuar. Coast. Shelf Sci.*, **41**, 361–376.
- Parsons, T. R., R. I. Perry, E. D. Nutbrown, W. Hsieh and C. M. Lalli (1983). Frontal zone analysis at the mouth of Saanich Inlet, British Columbia, Canada. *Mar. Biol.*, **73**, 1–5.
- Parsons, T. R., H. M. Dovey, W. P. Cochlan, R. I. Perry and P. B. Crean (1984). Frontal zone analysis at the mouth of a fjord - Jervis Inlet, British Columbia. *Sarsia*, **69**, 133–137.
- Patalas, K. and A. Salki (1993). Spatial Variation of Crustacean Plankton in Lakes of Different Sizes *Can. J. Fish. Aquat. Sci.*, **50**, 2626–2640.

- Pearson, T. R. (1970). The benthic ecology of Loch Linnhe and Loch Eil, a sea loch system on the west coast of Scotland. I. The physical environment and distribution of the macrobenthic fauna. *J. exp. mar. Biol. Ecol.*, **5**, 1–34.
- Pedersen, Fl. Bo (1978). A brief review of present theories of fjord dynamics. In Nihoul, J. C. J. (ed). *Hydrodynamics of Estuaries and Fjords*, pp. 407–422. Elsevier.
- Pickard, G. L. (1961). Oceanographic features of inlets in the British Columbian mainland coast. *J. Fish. Res. Bd. Canada*, **20**, 1109–1144.
- Pickard, G. L. and K. Rodgers (1959). Current measurements in Knight Inlet, British Columbia. *J. Fish. Res. Bd. Canada*, **16**, 635–678.
- Pinel-Alloul, B. (1995). Spatial Heterogeneity as a Multiscale Characteristic of Zooplankton Community. *Hydrobiologia*, **300/301**, 17–42.
- Pinel-Alloul, B and D. Pont (1991). Spatial distribution patterns in freshwater macrozooplankton: variation with scale. *Can. J. Zool.*, **69**, 1557–1570.
- Purcell, J. E. (1983). Digestion rates and assimilation efficiencies of siphonophores fed zooplankton prey. *Mar. Biol.*, **73**, 257–261.
- Purcell, J. E. (1992). Effects of predation by the scyphomedusan *Chrysaora quinquecirrha* on zooplankton populations in Chesapeake Bay, USA. *Mar. Ecol. Prog. Ser.*, **87**, 65–76.
- Rattray, M. (1960). On the coastal generation of internal tides.. *Tellus*, **12**, 54–62.
- Rees, A. P., N. J. P. Owens, M. R. Heath, D. H. Plummer and R. S. Bellerby (1991). Seasonal nitrogen assimilation and carbon fixation in a fjordic sea loch. *J. Plankton Res.*, **17**, 1307–1324.
- Reeve, M. R., M. A. Walter and T. Ikeda (1978). Laboratory studies of ingestion and food utilization in lobate and tentaculate ctenophores. *Limnol. Oceanogr.*, **23**, 740–751.
- Reigstad, M. and P. Wassman (1996). Importance of advection for pelagic-benthic coupling in north Norwegian fjords. *Sarsia*, **80**, 245–257.
- Riebesell, U. (1991). Particle aggregation during a diatom bloom. II. Biological aspects. *Mar. Ecol. Prog. Ser.*, **69**, 281–291.
- Riisgård, H. U., P. B. Christensen, N. J. Olesen, J. K. Petersen, M. M. Møller and P. Andersen (1995). Biological structure in a shallow cove (Kertinge Nor, Denmark) - control by benthic nutrient fluxes and suspension-feeding ascidians and jellyfish. *Ophelia*, **41**, 329–344.
- La Roche, J. (1983). Ammonium regeneration: its contribution to phytoplankton nitrogen requirements in a eutrophic environment. *Mar. Biol.*, **75**, 231–240.
- Roden, C. M. and R. Raine (1994). Phytoplankton blooms and a coastal thermocline boundary along the west coast of Ireland. *Estuar. Coast. Shelf Sci.*, **39**, 511–526.

- Rodhouse, P. G., and C. M. Roden (1987). Carbon budget for a coastal inlet in relation to intensive cultivation of suspension-feeding bivalve molluscs. *Mar. Ecol. Prog. Ser.*, **36**, 225–236.
- Ross, A. H., W. S. C. Gurney, M. R. Heath, S. J. Hay and E. W. Henderson (1993). A strategic simulation model of a fjord ecosystem. *Limnol. Oceanogr.*, **38**, 128–153.
- Ross, A. H., W. S. C. Gurney and M. R. Heath (1993). A comparative study of the ecosystem dynamics of four fjords. *Limnol. Oceanogr.*, **39**, 318–343.
- Sakshaug, E. and S. Mykkestad (1973). Studies on the phytoplankton ecology of the Trondheimsfjord. 3. *J. exp. mar. Biol. Ecol.*, **11**, 157–188.
- Schneider, D. C. (1989). The common jellyfish *Aurelia aurita*: standing stock, excretion and nutrient regeneration in the Kiel Bight, Western Baltic. *J. Plankton Res.*, **14**, 531–543.
- Schneider, D. C. and C. D. Bajdik (1992). Decay of zooplankton patchiness generated at the sea surface. *J. Plankton Res.*, **14**, 531–543.
- Schneider, G. and G. Behrends (1994). Population dynamics and the trophic role of *Aurelia aurita* medusae in the Kiel Bight and western Baltic. *ICES J. mar. Sci.*, **51**, 359–367.
- Sharples, J., J. H. Simpson and J. M. Brubaker (1994). Observations and Modelling of Periodic Stratification in the Upper York River Estuary, Virginia. *Estuar. Coast. Shelf Sci.*, **38**, 301–312.
- Sharples, J., and P. Tett (1994). Modelling the effect of physical variability on the midwater chlorophyll maximum. *J. Mar. Res.*, **52**, 219–238.
- Simpson, J. H. and D. Bowers (1981). Models of stratification and frontal movement in shelf seas. *Deep-Sea Res.*, **28**, 727–738.
- Simpson, J. H. and T. P. Rippeth (1993). The Clyde Sea: a model of the seasonal cycle of stratification and mixing. *Estuar. Coast. Shelf Sci.*, **37**, 129–144.
- Simpson, J. H., P. B. Tett, M. L. Argote-Espinoza, A. Edwards, K. J. Jones and G. Savidge (1982). Mixing and Phytoplankton Growth Around an Island in a Stratified Sea. *Continental Shelf Research*, **1**, 15–31.
- Skogen, M. D., E. Svendsen, J. Berntsen, D. Aksnes and K. B. Ulvestad (1995). Modelling the primary production in the North Sea using a coupled three-dimensional physical-chemical-biological ocean model. *Estuar. Coast. Shelf Sci.*, **41**, 545–565.
- Smetacek, V., K. von Bröckel, B. Zeitzschel and W. Zenk (1978). Sedimentation of particulate matter during a phytoplankton spring bloom in relation to the hydrographical regime. *Mar. Biol.*, **47**, 211–226.
- Solórzano, L. and B. Grantham (1975). Surface nutrients, chlorophyll *a* and phaeopigment in some Scottish sea lochs. *J. exp. mar. Biol. Ecol.*, **20**, 63–76.

- Solow, A. R. and J. H. Steele (1995). Scales of Plankton Patchiness: Biomass versus Demography. *J. Plankton Res.*, **17**, 1669–1677.
- St John, M. A. and S. Pond (1992). Tidal plume generation around a promontory: effects on nutrient concentrations and primary productivity. *Continental Shelf Research* **12**, 339–354.
- Stanley, S. O., J. W. Leftley, A. Lightfoot, N. Robertson, I. M. Stanley and I. Vance (1981). The Loch Eil project: sediment chemistry, sedimentation and the chemistry of the overlying water in Loch Eil. *J. exp. mar. Biol. Ecol.*, **55**, 299–313.
- Steele, J. H. (1978). Some Comments on Plankton Patches. In J. H. Steele (Ed.), *Spatial Patterns in Plankton Communities*, NATO Conference Series IV Marine Sciences Vol. 3, pp. 1–20. Plenum Press.
- Steele, J. H., S. R. Carpenter, J. H. Cohen, P. K. Dayton and R. E. Ricklefs (1993). Comparing Terrestrial and Marine Ecological Systems. In S. A. Levin, T. M. Powell and J. H. Steele (Eds.), *Lecture Notes in Biomathematics 96: Patch Dynamics*, Part 1, pp. 1–12. Springer Verlag.
- Steele, J. H., and B. W. Frost (1977). The structure of plankton communities. *Phil. Trans, R. Soc. Lond.* **B**, **280**, 485–534.
- Steele, J. H. and C. S. Yentsch (1960). The vertical distribution of chlorophyll. *J. Mar. Biol. Ass. U.K.*, **39**, 217–226.
- Stigebrandt, A. (1977). On the effect of barotropic current fluctuations on the two-layer transport capacity of a constriction. *J. Phys. Oceanogr.*, **7**, 118–122.
- Stigebrandt, A. (1980). Some aspects of tidal interaction with fjord constrictions. *Estuar. Coast. Mar. Sci.*, **11**, 151–166.
- Stigebrandt, A. (1981). A mechanism governing the estuarine circulation in deep strongly stratified fjords. *Estuar. Coast. Shelf. Sci.*, **13**, 197–211.
- Stoecker, D. K., A. E. Michaels and L. H. Davis (1987). Grazing by the jellyfish, *Aurelia aurita*, on microplankton. *J. Mar. Res.*, **9**, 901–915.
- Sullivan, B. K., J. R. Garcia and G. Klein-MacPhee (1994). Prey selection by the scyphomedusan predator *Aurelia aurita*. *Mar. Biol.*, **121**, 335–341.
- Svendsen, H. (1977). A study of the circulation in a sill fjord on the west coast of Norway. *Marine Science Communications*, **3**, 151–209.
- Svendsen, H. and R. O. R. Y. Thompson (1978). Wind-Driven Circulation in A Fjord. *J. Phys. Oceanogr.*, **8**, 703–712.
- Svendsen, H. (1980). Exchange processes above sill level between fjords and coastal water. In Freeland, H. J., D. M. Farmer and C. D. Levings (eds). *Fjord Oceanography*, pp. 355–361. Plenum Press.
- Syvitski, J. P. M., D. C. Burrell and J. M. Skea (1987). *Fjords: Processes and Products*, Springer-Verlag.

- Tamsalu, R. and K. Myrberg (1995). Ecosystem modelling in the Gulf of Finland. I. General features and the hydrodynamic prognostic model FINEST. *Estuar. Coast. Shelf Sci.* **41**, 249–273.
- Tamsalu, R. and P. Ennet (1995). Ecosystem modelling in the Gulf of Finland. II. The aquatic ecosystem model FINEST. *Estuar. Coast. Shelf Sci.* **41**, 429–458.
- Taylor, A. H. and J. A. Stephens (1993). Diurnal variations of convective mixing and the spring bloom of phytoplankton. *Deep-Sea Res. II* **40**, 389–408.
- Tessier, A. J. (1983). Coherence and horizontal movements of patches of *Holopedium gibberum* (Cladocera). *Oecologia*, **60**, 71–75.
- Tett, P. (1973). The use of log-normal statistics to describe phytoplankton populations from the Firth of Lorne area. *J. exp. mar. Biol. Ecol.*, **73**, 121–136.
- Tett, P. (1987). Modelling the growth and distribution of marine microplankton. *Society of General Microbiology, Symposium 41 - Ecology of Microbial Communities*, 387–425.
- Tett, P. and A. Edwards (1984). Mixing and phytoplankton: an interdisciplinary theme in oceanography. *Oceanography and Marine Biology Annual Review* **22**, 99–123.
- Tett, P., A. Edwards and K. Jones (1986). A model for the growth of shelf-sea phytoplankton in summer. *Estuar. Coast. Shelf Sci.* **23**, 641–672.
- Tett, P., R. Gowen, B. Grantham, K. Jones and B. S. Miller (1986). The phytoplankton ecology of the Firth of Clyde sea-lochs Striven and Fyne. *Proc. R. Soc. Edinburgh B.* **90**, 223–238.
- Tiselius, P (1992). Behaviour of *Acartia tonsa* in patchy food environments. *Limnol. Oceanogr.*, **37**, 1640–1651.
- Tiselius, P. and M. Kuylenstierna (1996). Growth and decline of a diatom spring bloom: phytoplankton species composition, formation of marine snow and the role of heterotrophic dinoflagellates. *Journal of Plankton Research*, **18**, 133–155.
- Townsend, D. W., L. M. Cammen, P. M. Holligan, D. E. Campbell and N. R. Pettigrew (1994). Causes and consequences of variability in the timing of spring phytoplankton blooms. *Deep-Sea Res. I*, **5/6**, 747–765.
- Tully, J. P. (1949). Oceanography and prediction of pulp mill pollution in Alberni Inlet. *Bull. Fish. Res. Bd., Canada*, **83**, 169pp.
- Tverberg, V., B. Cushman-Roisin and H. Svendsen (1991). Modeling of internal tides in fjords. *J. Mar. Res.*, **49**, 635–658.
- Tyler, I. D. (1983). *A carbon budget for Creran a Scottish sea loch*. Ph. D. thesis, University of Strathclyde, Glasgow, Scotland.
- Ward, B. B., M. C. Talbot and M. J. Perry (1984). Contributions of phytoplankton and nitrifying bacteria to ammonium and nitrite dynamics in coastal waters. *Continental Shelf Research I*, **3**, 383–398.

- Wassman, P. and A. Aadnesen (1984). Hydrography, nutrients, suspended organic matter and primary production in a shallow fjord system on the west coast of Norway. *Sarsia*, **69**, 139–153.
- Watts, L. J. (1994). *The roles of hydrographic and biogeochemical processes in the distribution of dissolved inorganic nutrients in a Scottish sea-loch system*. Ph. D. thesis, University of Southampton, Southampton, UK.
- Welander, P. (1974). Theory of a two-layer fjord type estuary, with special reference to the Baltic Sea. *J. phys. Oceanogr.*, **4**, 542–556.
- Winter, D. F., K. Banse and G. C. Anderson (1975). The dynamics of phytoplankton blooms in Puget Sound a fjord in the Northwestern United States. *Mar. Biol.*, **29**, 139–176.
- Wood, B. J.B., P. B. Tett and A. Edwards (1973). An introduction to the phytoplankton, primary production and relevant hydrography of Loch Etive. *J. Ecol.*, **61**, 569–585.
- Woods, J., and W. Barkman (1994). Simulating plankton ecosystems by the Lagrangian Ensemble method. *Phil. Trans. R. Soc. Lond.* **B**, **343**, 27–31.
- Woods, J. D., and R. Onken (1982). Diurnal variation and primary production in the ocean - preliminary results of a Lagrangian ensemble model. *J. Plank. Res.*, **4**, 735–756.
- Wu, R. S. S. (1995). The environmental impact of marine fish culture - towards a sustainable future. *Marine Pollution Bulletin*, **31**, 159–166.
- Yin, K., P. J. Harrison, S. Pond and R. J. Beamish (1995). Entrainment of nitrate in the Fraser River estuary and its biological implications. I. Effects of the salt wedge. *Est. Coast. and Shelf Sci.*, **40**, 505–528.
- Yin, K., P. J. Harrison, S. Pond and R. J. Beamish (1995). ENtrainment of nitrate in the Fraser River estuary and its biological implications. I. Effects of spring *vs.* neap tides and river discharge. *Estuar. Coast. Shelf Sci.*, **40**, 529–544.
- de Young, B and S. Pond (1988). The deepwater exchange cycle in the Indian Arm, British Columbia. *Estuar. Coast. Shelf Sci.*, **26**, 285–308.

Part VI

Appendices

Appendix A

Surface data

A.1 Introduction

This appendix contains the entire set of gridded surface cruise data. The scale for each surface map is optimal for that month as the yearly range provides little information of the surface structure.

Table A.1: Daily mean meteorological conditions for the surface cruises. Wind data was measured at Oban (supplied by the Met. Office) and river discharge is the combined flow of the Rivers Lochy and Nevis (collected by the Highland River Board and supplied by MLA.)

date and direction	wind speed (ms^{-1}) and direction	river discharge m^3s^{-1}
23 Jan. → South	4.83 @ 192°	140.349
27 Feb. → S	8.92 @ 117°	59.753
26 Mar. → S	10.42 @ 132°	41.928
23 Apr. → S	8.37 @ 197°	28.584
25 Apr. → North	7.29 @ 142°	23.339
21 May → N	11.54 @ 255°	22.536
18 June → N	8.67 @ 286°	23.927
16 July → N	7.17 @ 249°	44.973
18 July → S	5.75 @ 170°	28.678
14 Aug. → S	6.62 @ 204°	26.107
11 Sept → S	4.12 @ 150°	5.386
9 Oct. → S	4.12 @ 89°	47.705
10 Oct. → N	4.79 @ 112°	43.496
14 Nov. → S	11.67 @ 178°	164.531

Table A.2: Tidal conditions for the surface cruises. The semi-diurnal tidal cycle indicates the time since high water Corpach (HW Oban for the FoL) of the central point of the cruise.

date	lunar tidal cycle	semi-diurnal tidal cycle		
		IB	OB	FoL
23 Jan.	1st quarter	+ 04 22	+ 07 54	- 01 28
27 Feb.	full moon - 1 day	+ 08 17	- 00 16	+ 02 35
26 Mar.	1st quarter + 3 days	- 00 28	+ 03 25	+ 06 39
23 Apr.	1st quarter + 2 days	+ 05 48	+ 01 43	- 01 52
25 Apr.	1st quarter + 4 days	+ 04 58	- 03 36	- 00 34
21 May	1st quarter + 1 day	- 05 17	+ 03 46	+ 01 24
18 June	1st quarter - 1 day	- 05 51	+ 02 31	+00 24
16 July	1st quarter - 2 days	- 03 42	+ 05 18	+ 02 54
18 July	1st quarter	- 01 39	+ 03 45	+ 04 18
14 Aug.	new moon + 4 days	- 05 25	+ 02 47	+ 00 41
11 Sept	new moon + 3 days	+ 02 42	+ 06 53	- 02 46
9 Oct.	new moon + 2 days	+ 05 30	- 03 36	- 00 44
10 Oct.	new moon + 3 days	- 06 12	+ 03 40	NA
14 Nov.	1st quarter	- 01 35	+ 01 32	+ 04 18

A.2 Inner Basin

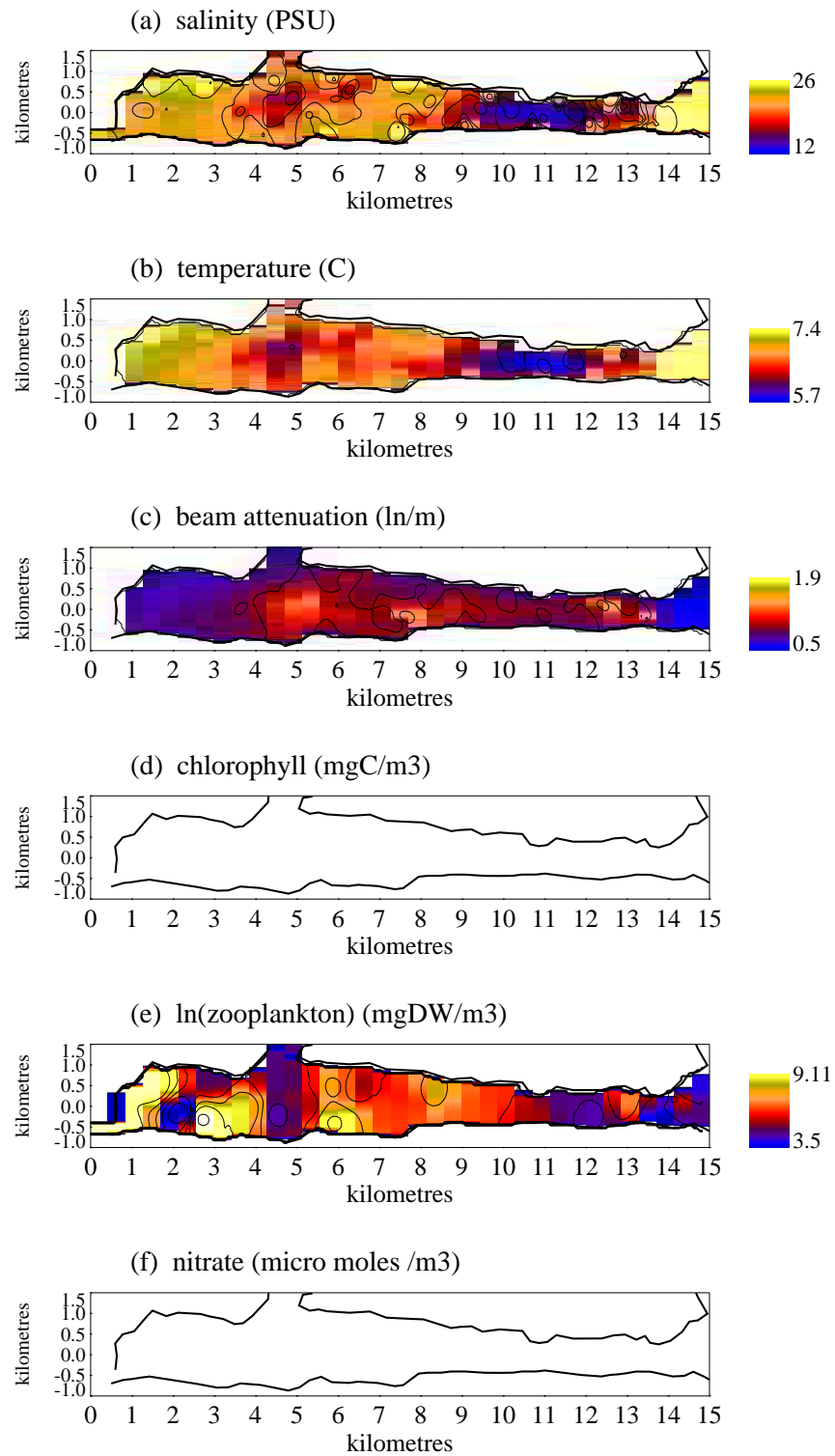


Figure A.1: 23 January 1991

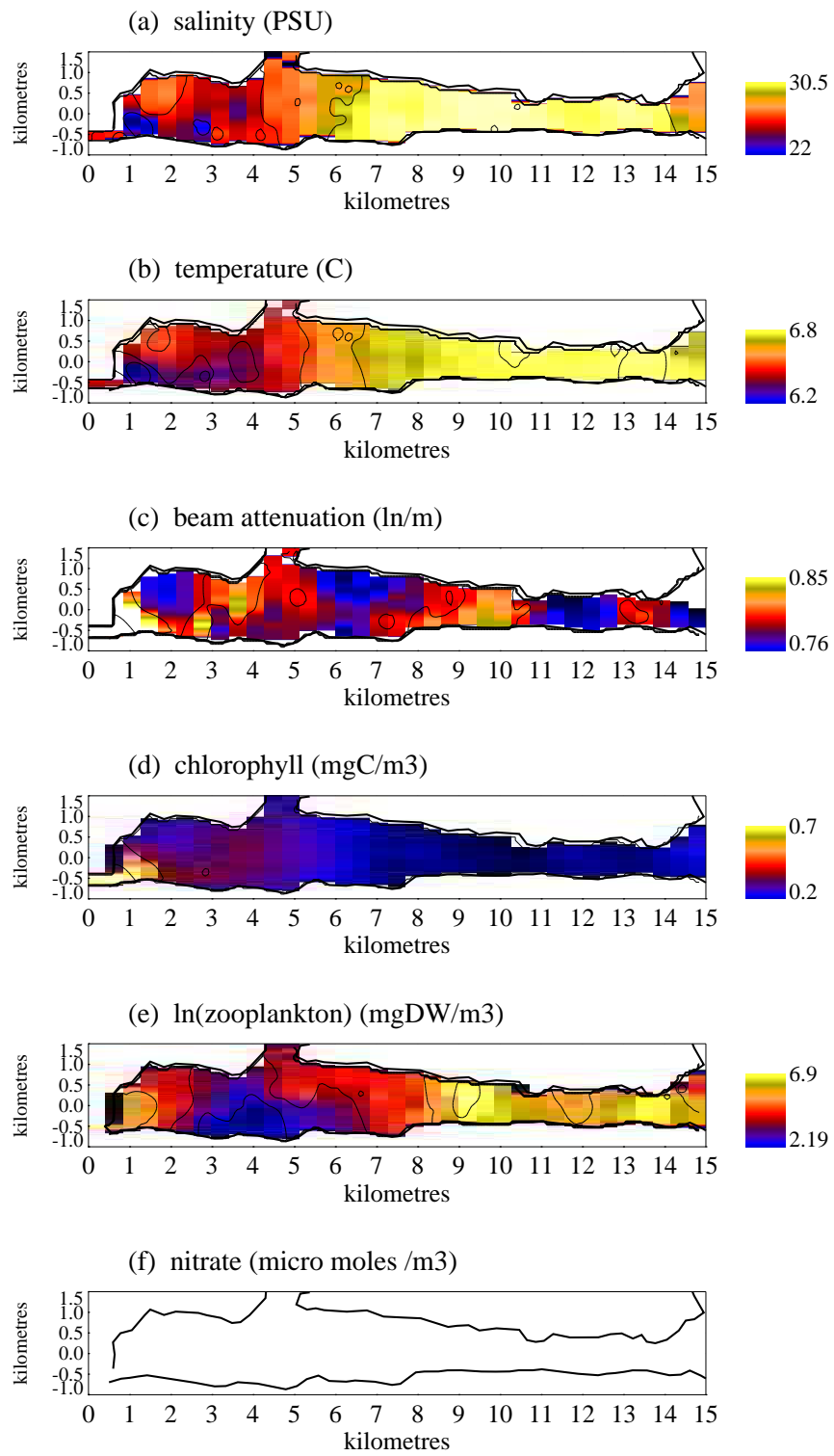


Figure A.2: 27 February 1991

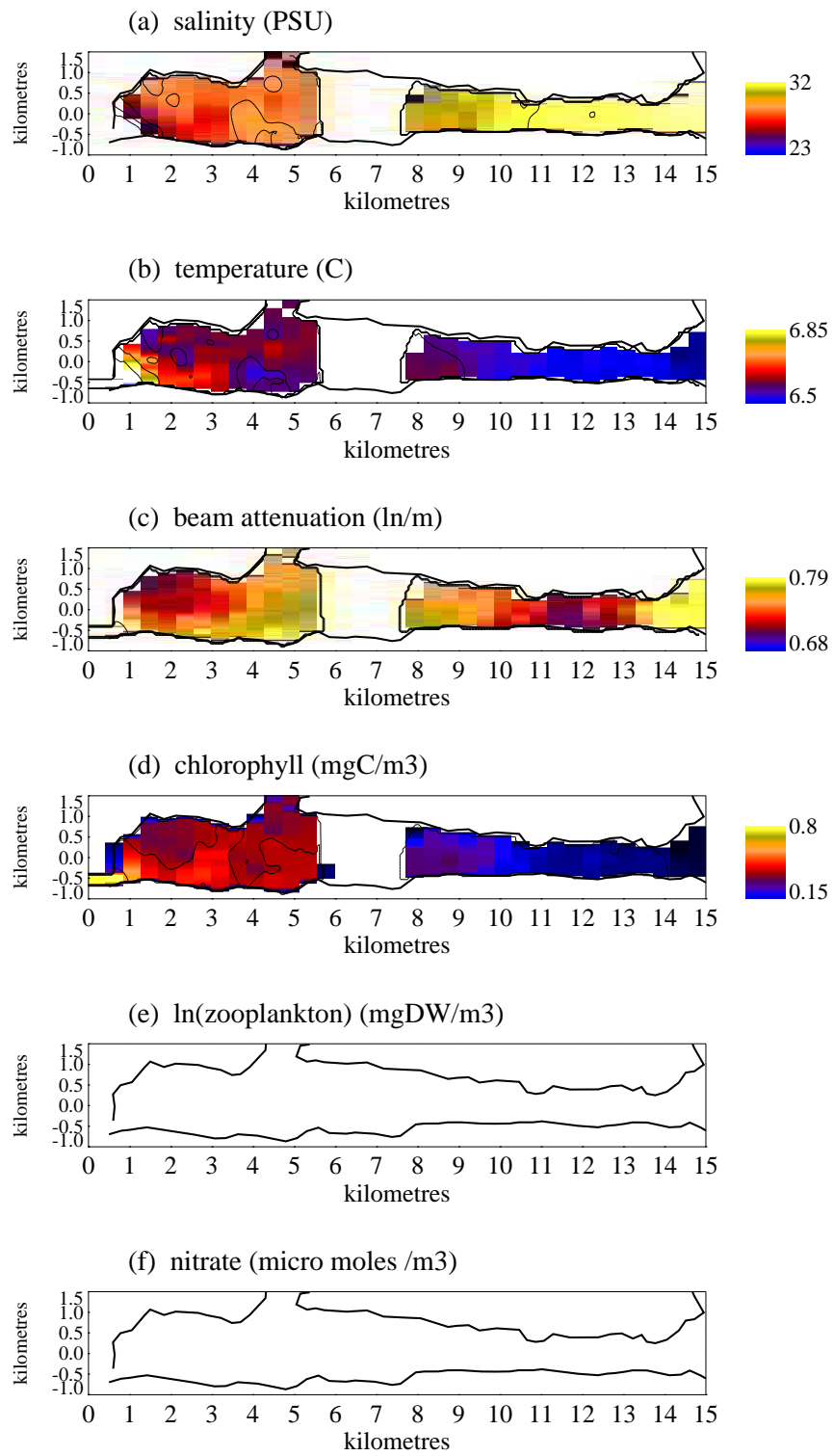


Figure A.3: 26 March 1991

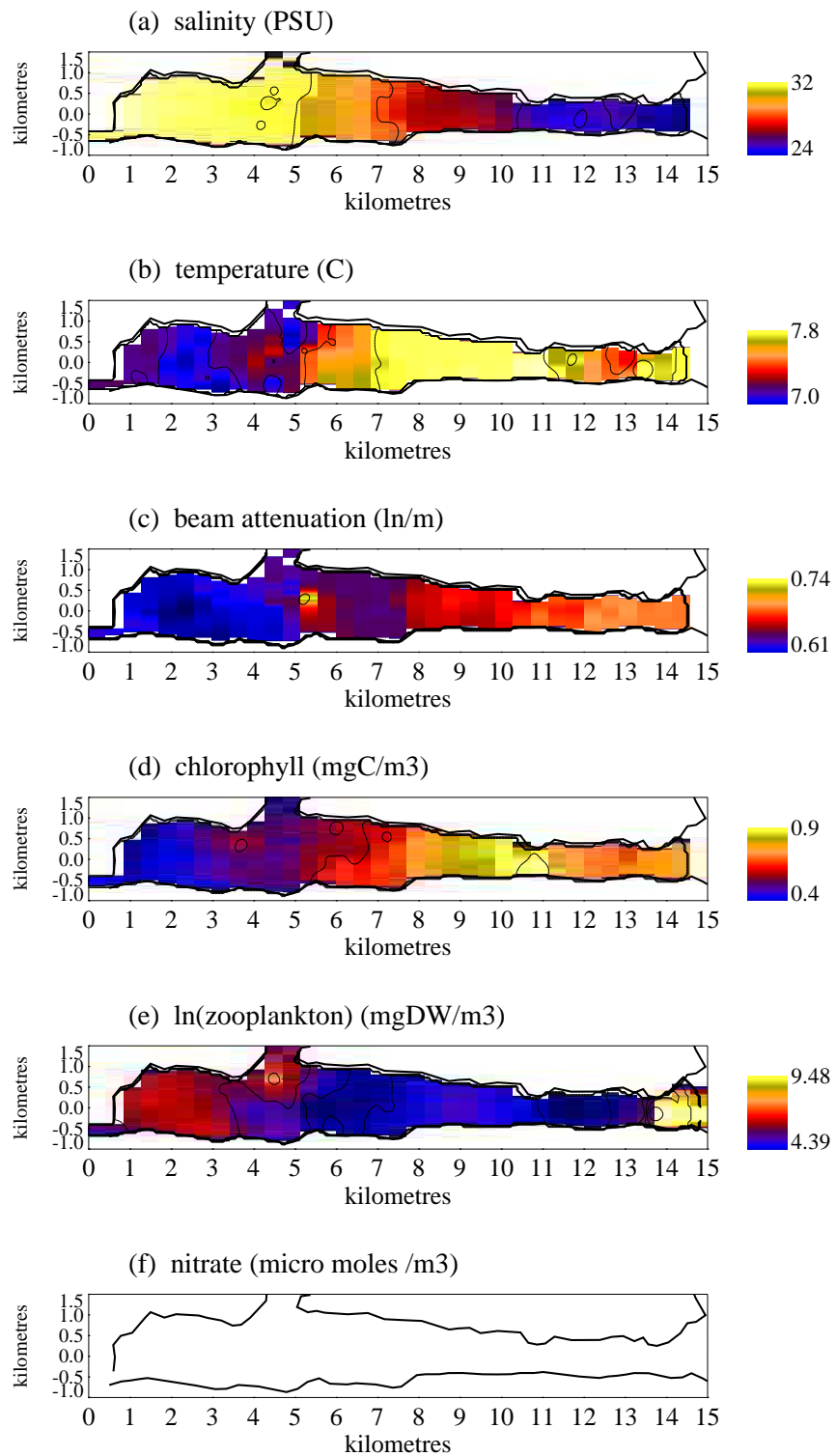


Figure A.4: 23 April 1991

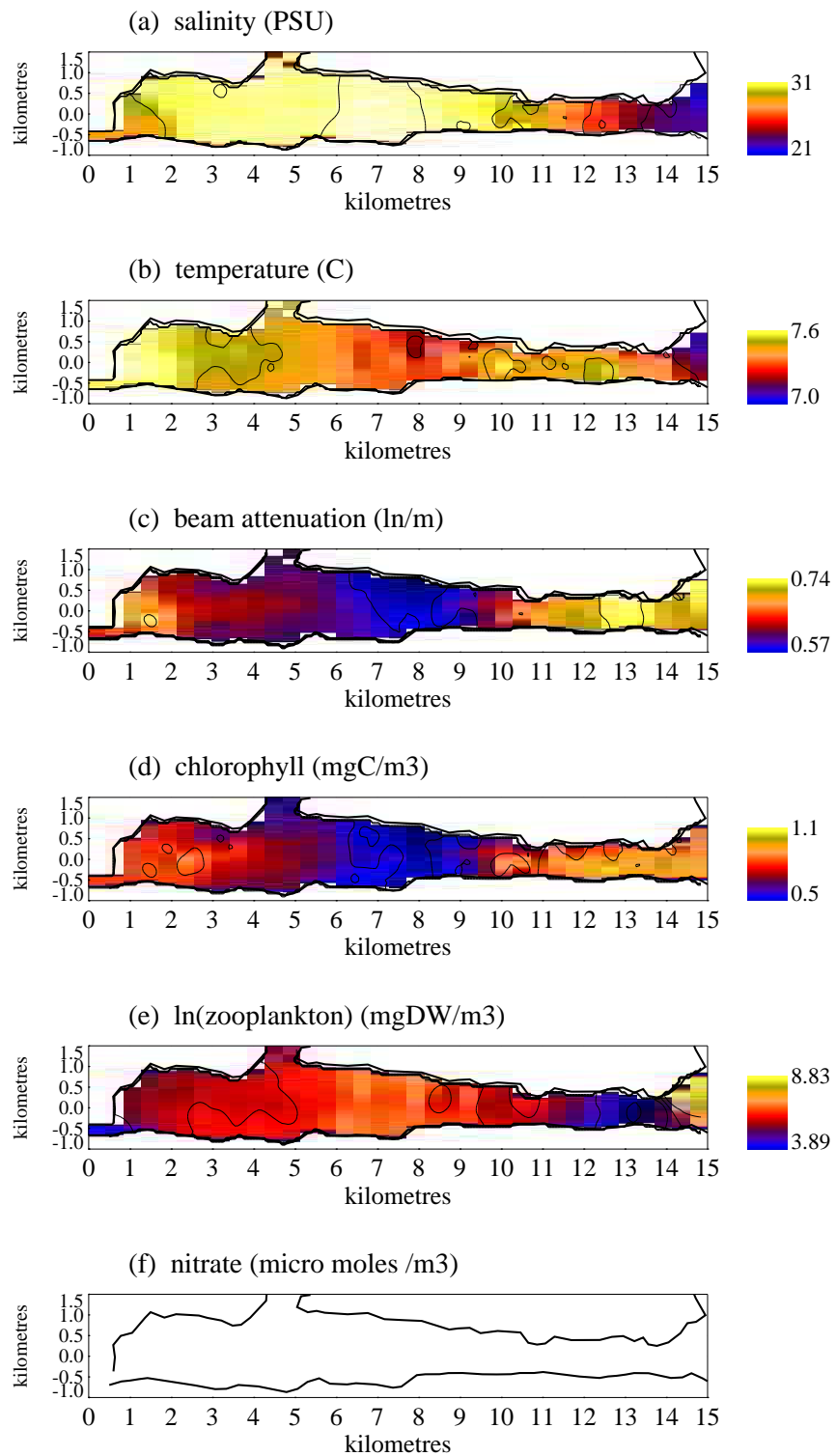


Figure A.5: 25 April 1991

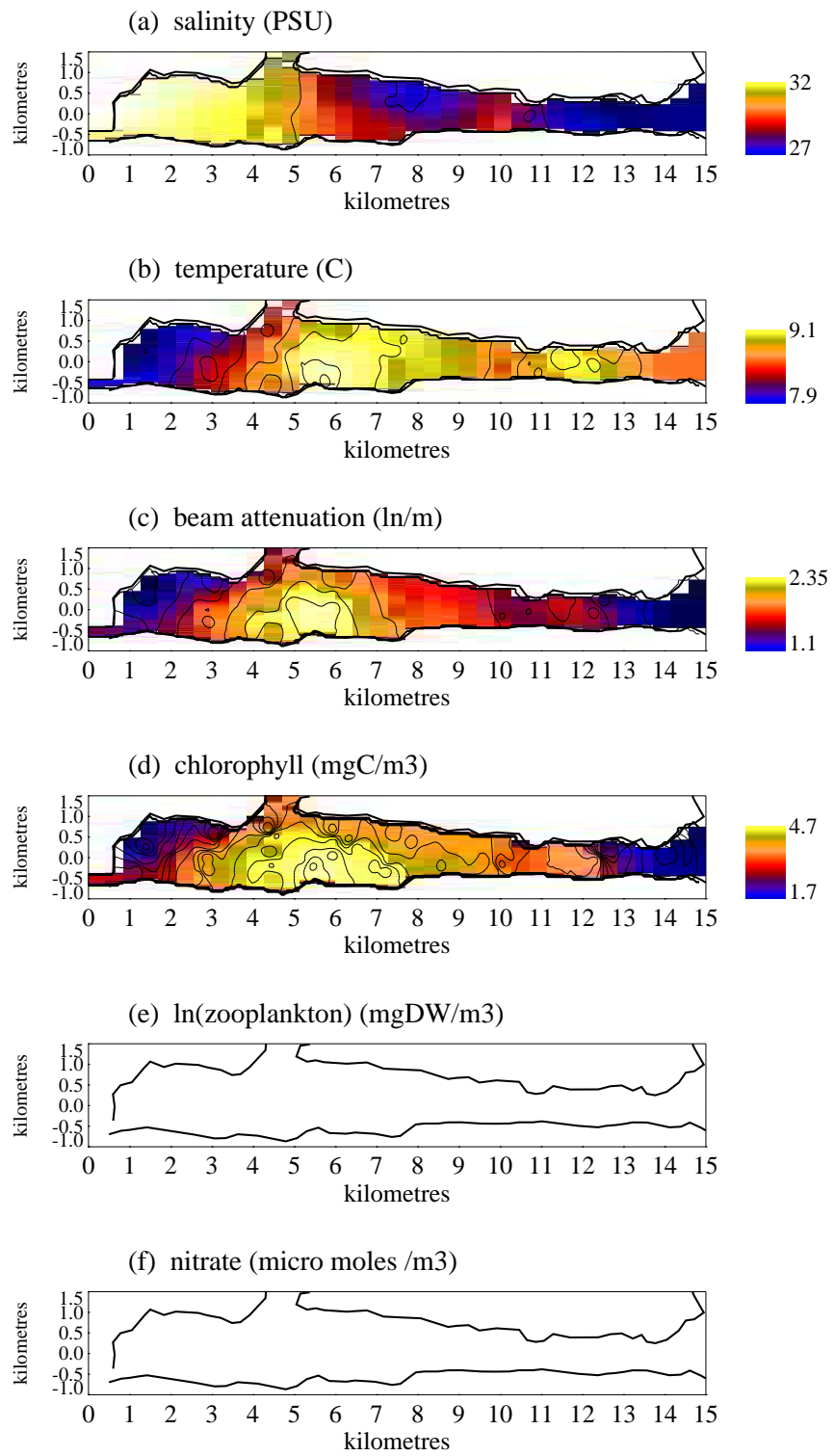


Figure A.6: 21 May 1991

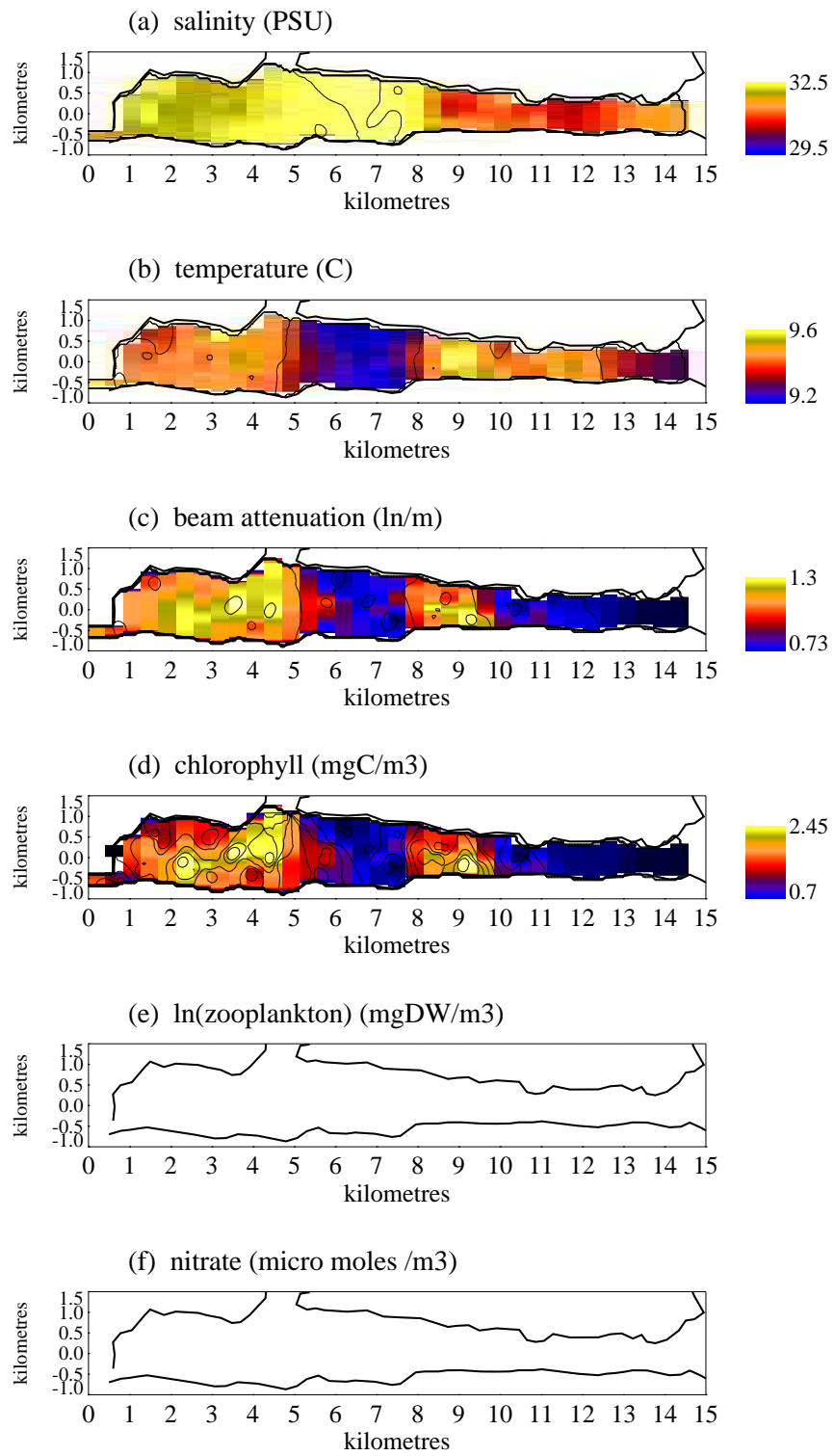


Figure A.7: 18 June 1991

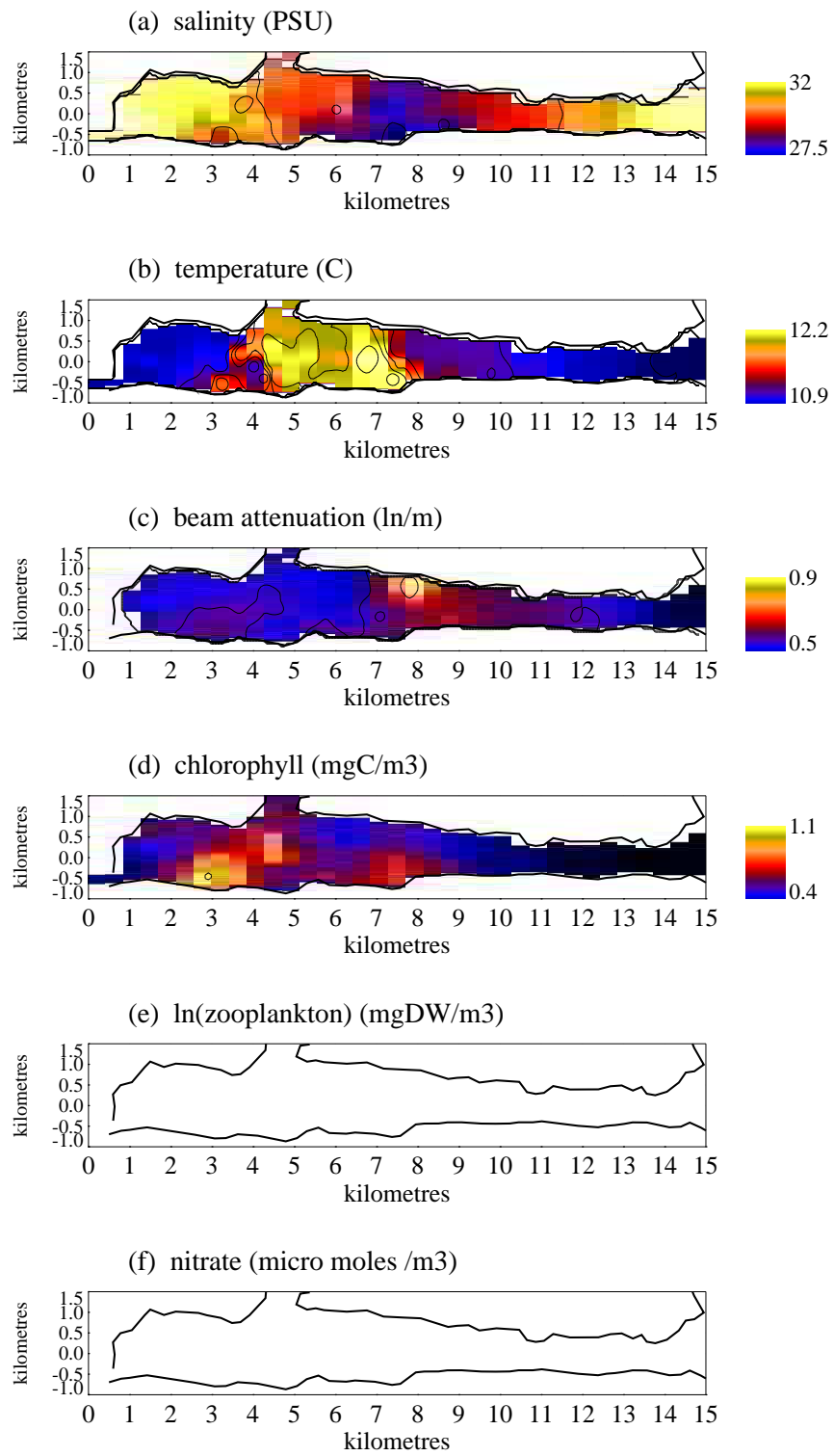


Figure A.8: 16 July 1991

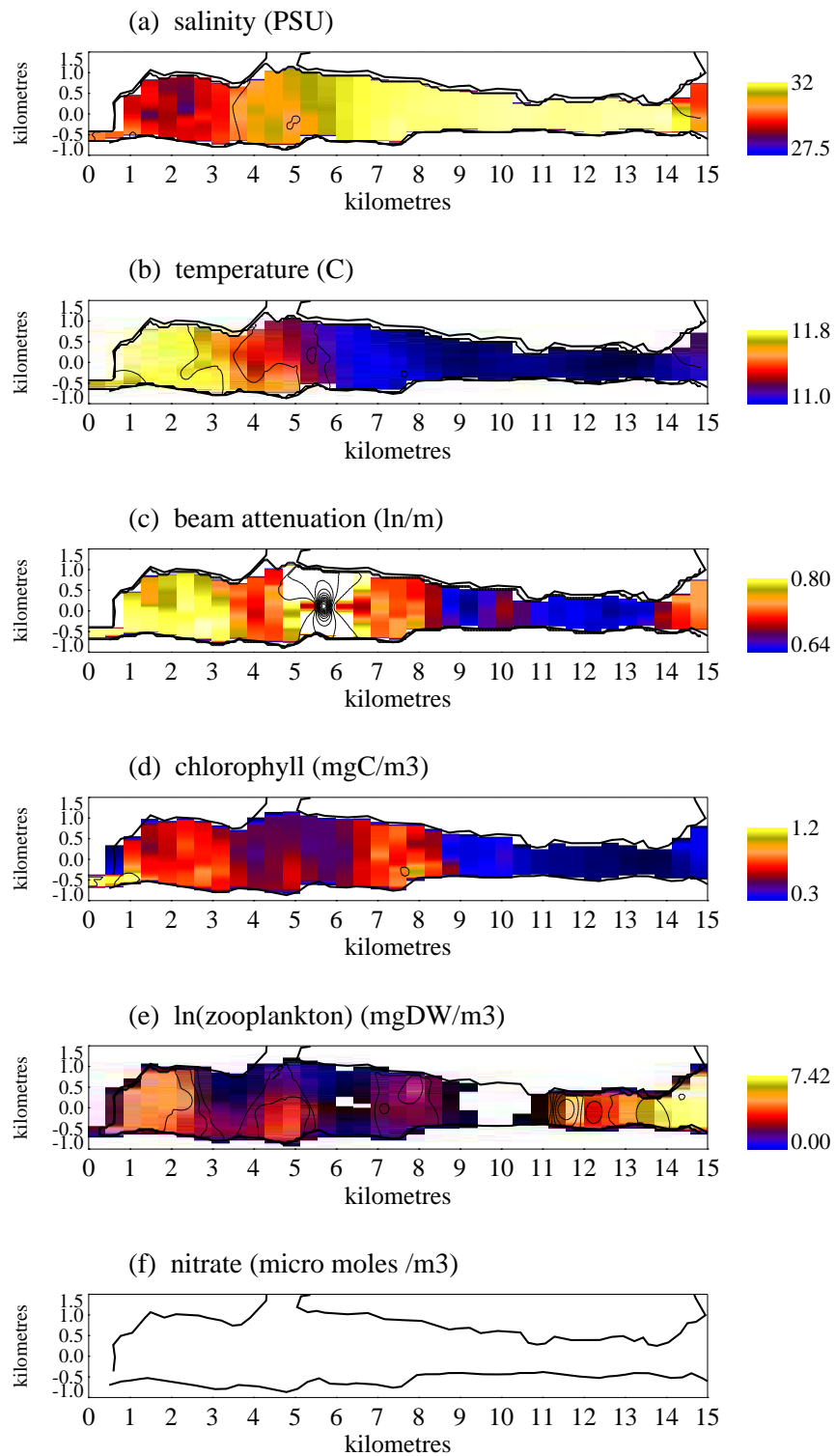


Figure A.9: 18 July 1991

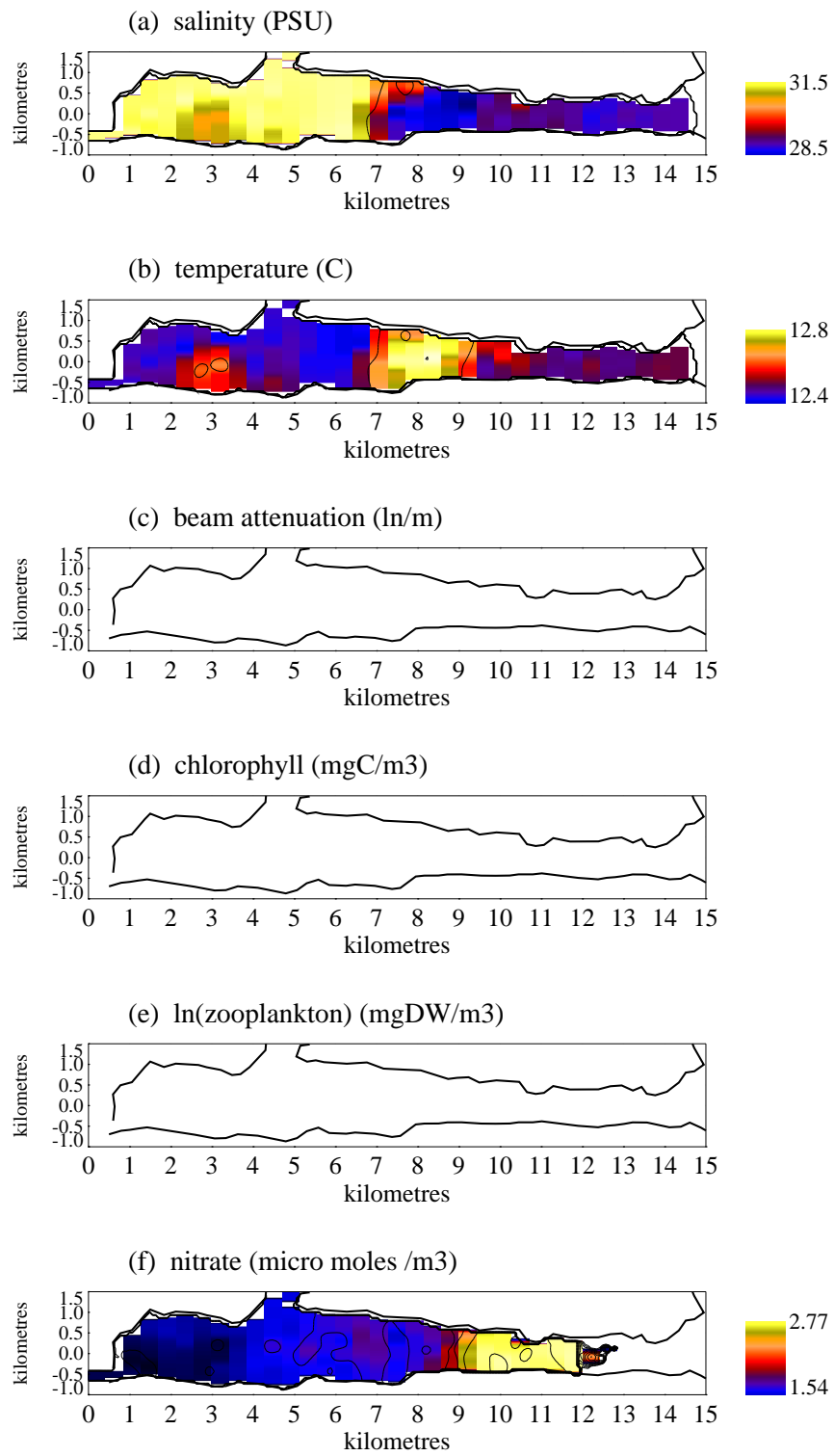


Figure A.10: 14 August 1991

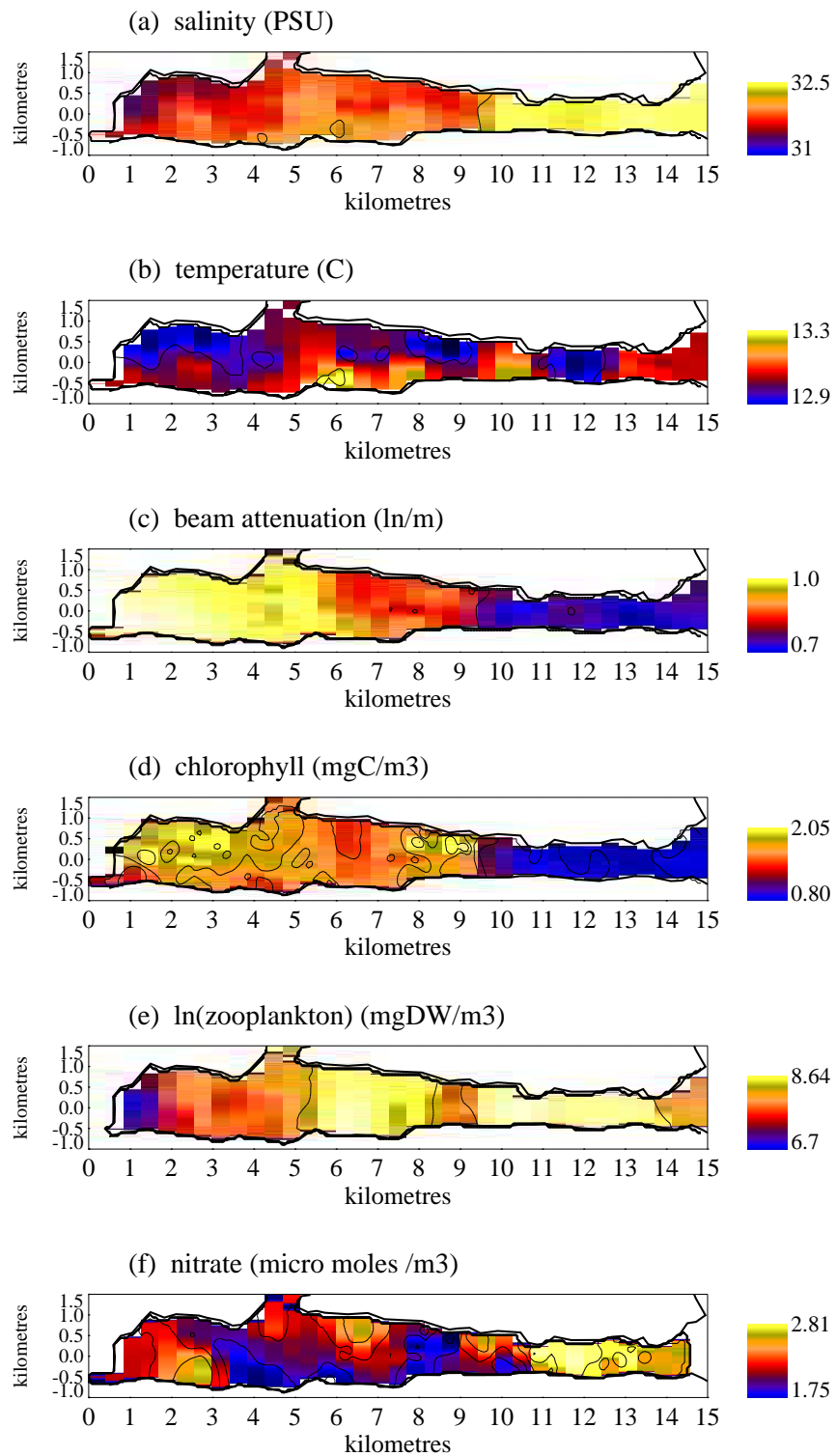


Figure A.11: 11 September 1991

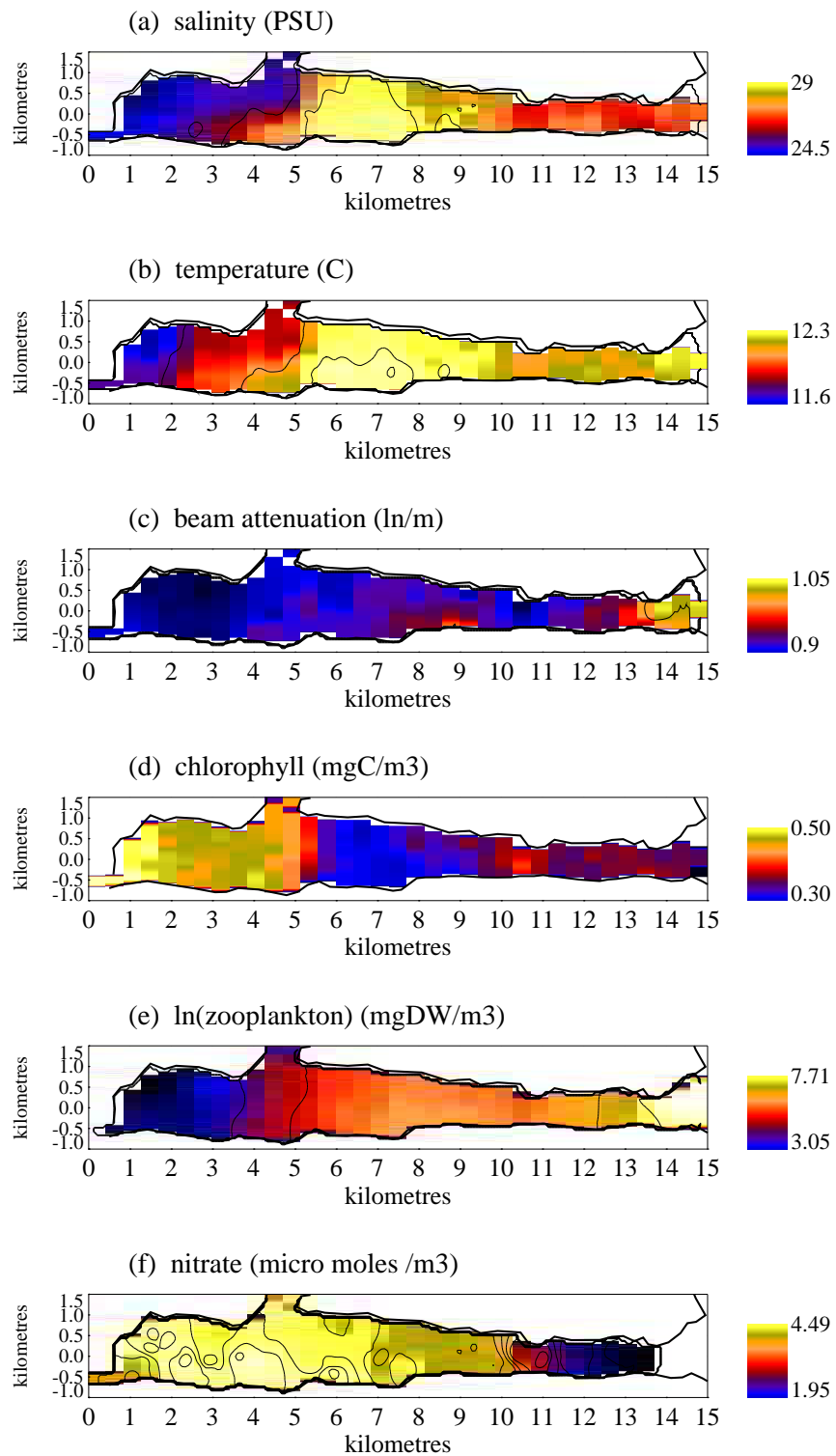


Figure A.12: 9 October 1991

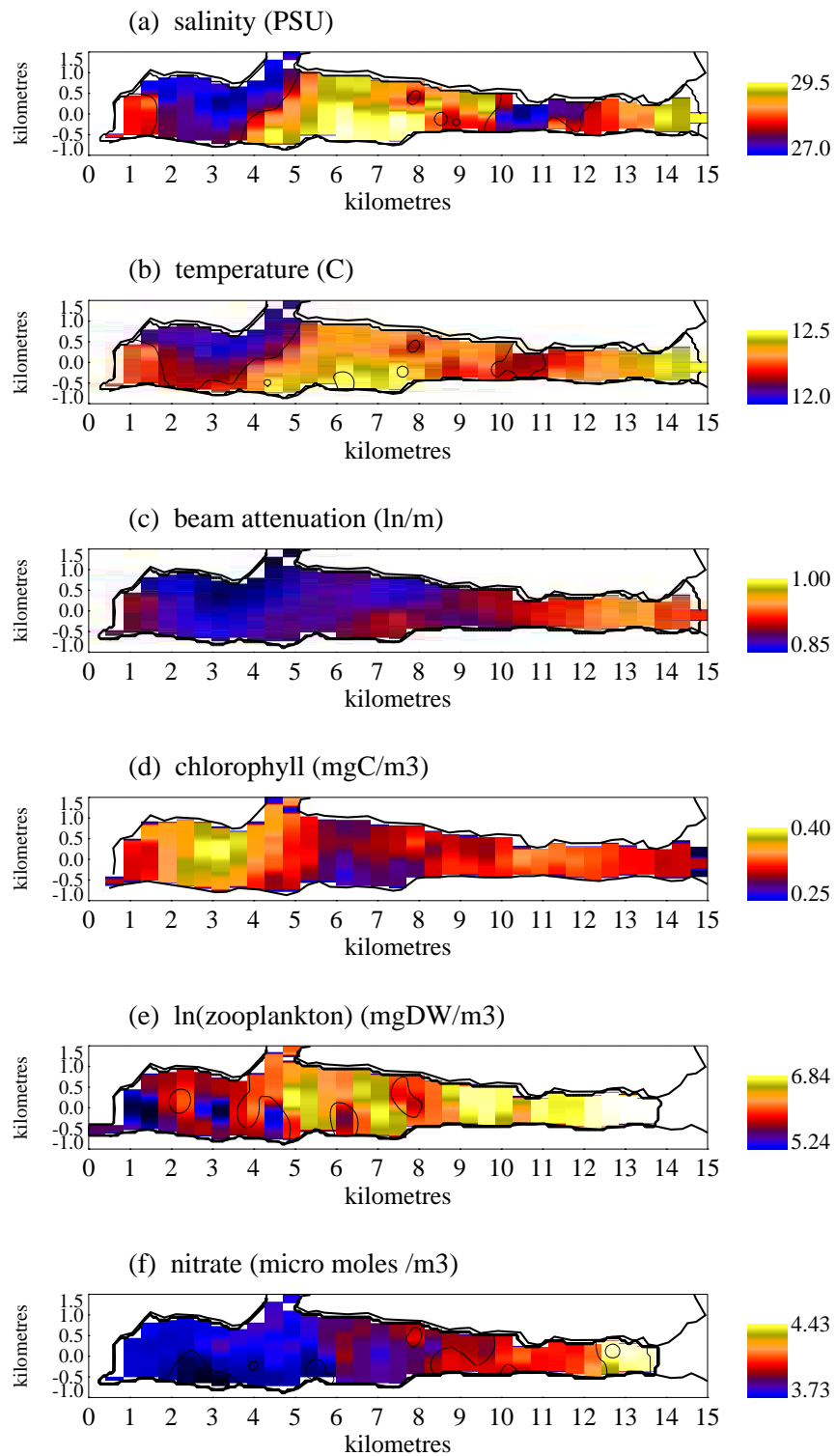


Figure A.13: 10 October 1991

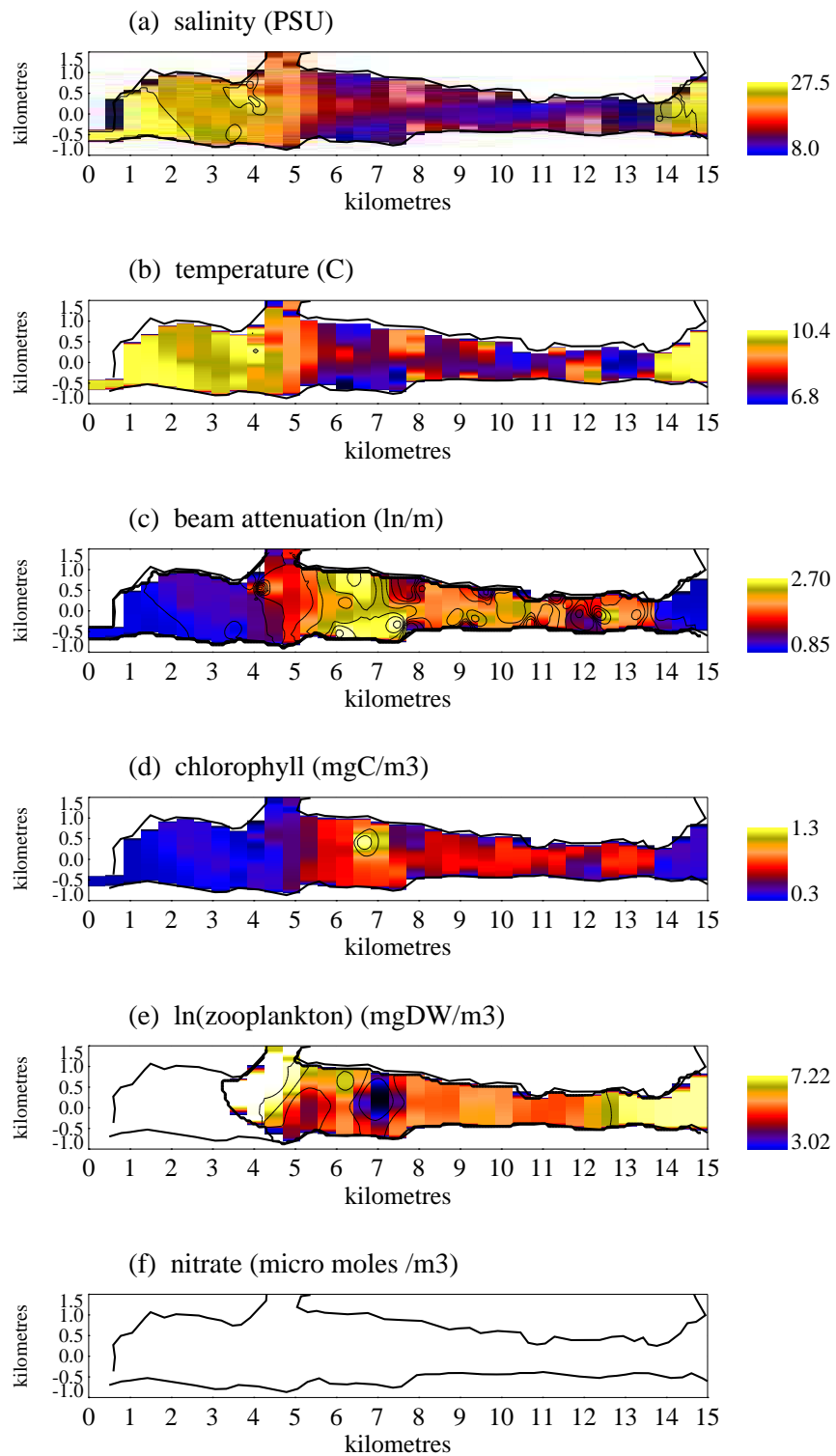


Figure A.14: 14 November 1991

A.3 Outer Basin

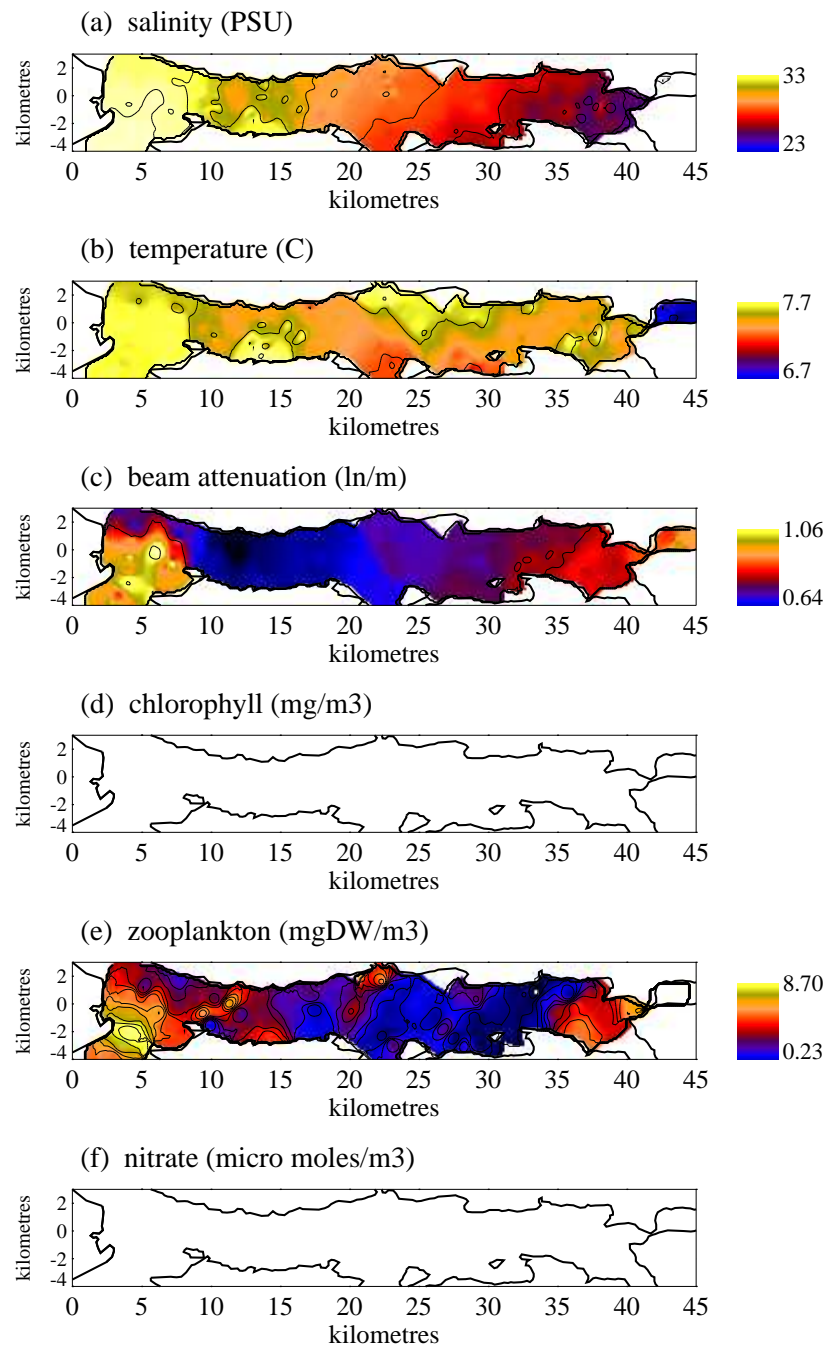


Figure A.15: 23 January 1991

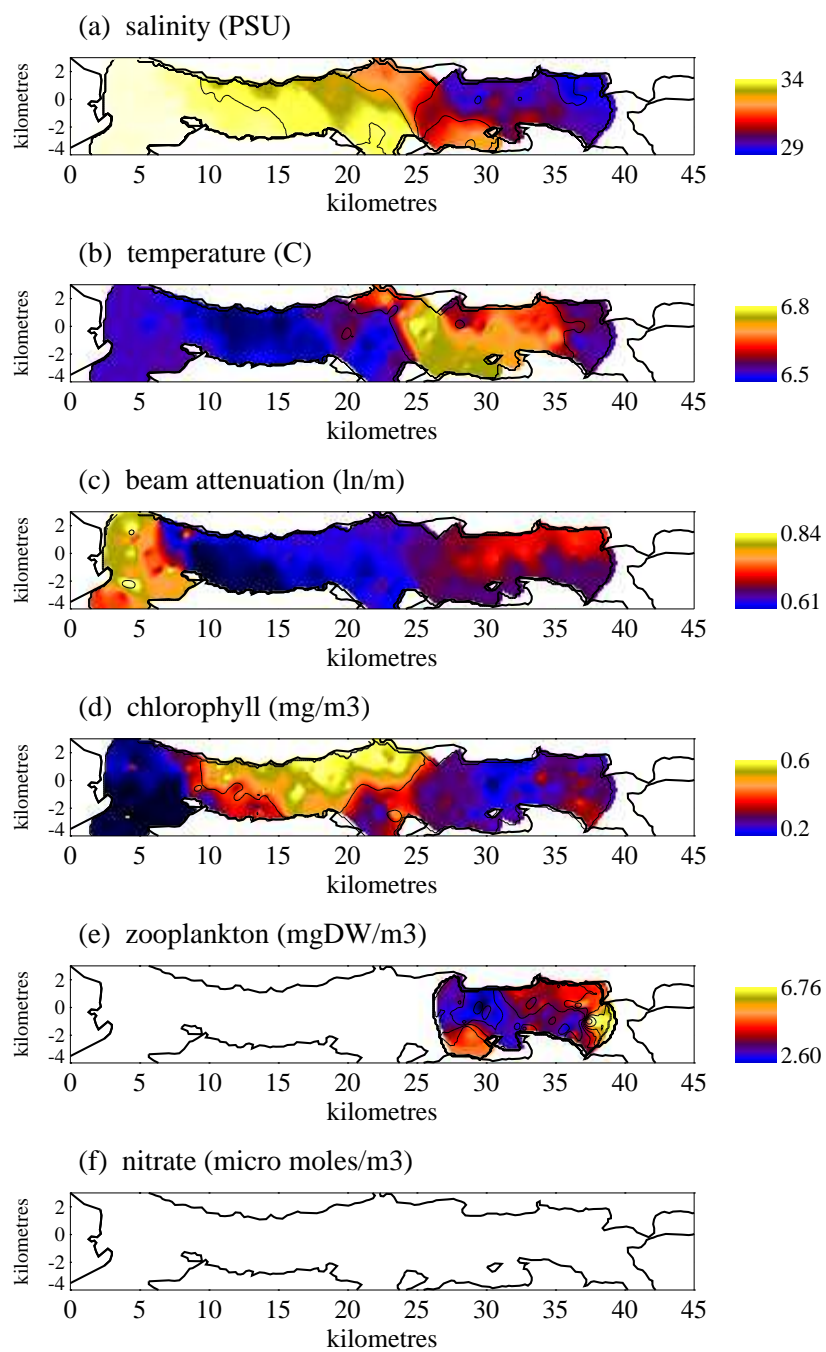


Figure A.16: 27 February 1991

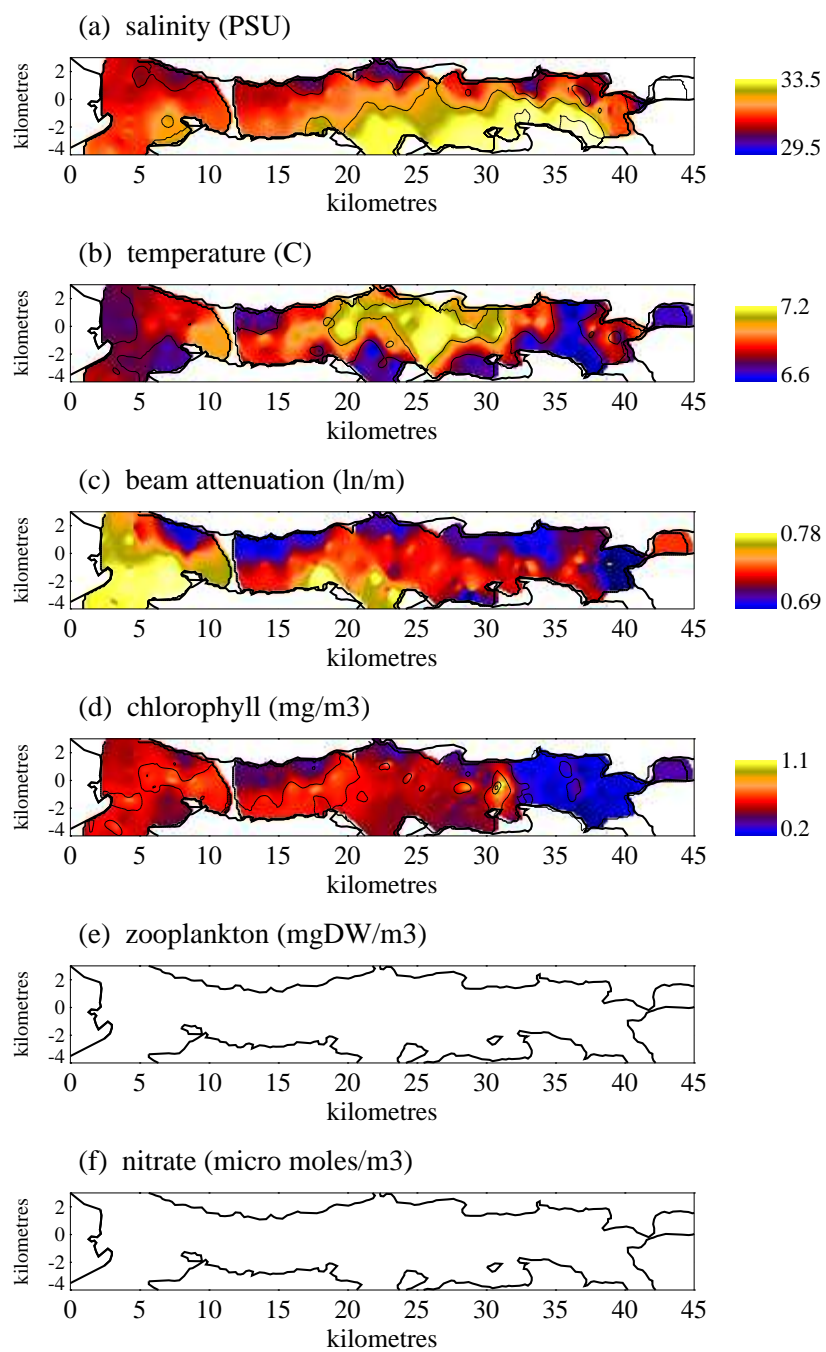


Figure A.17: 26 March 1991

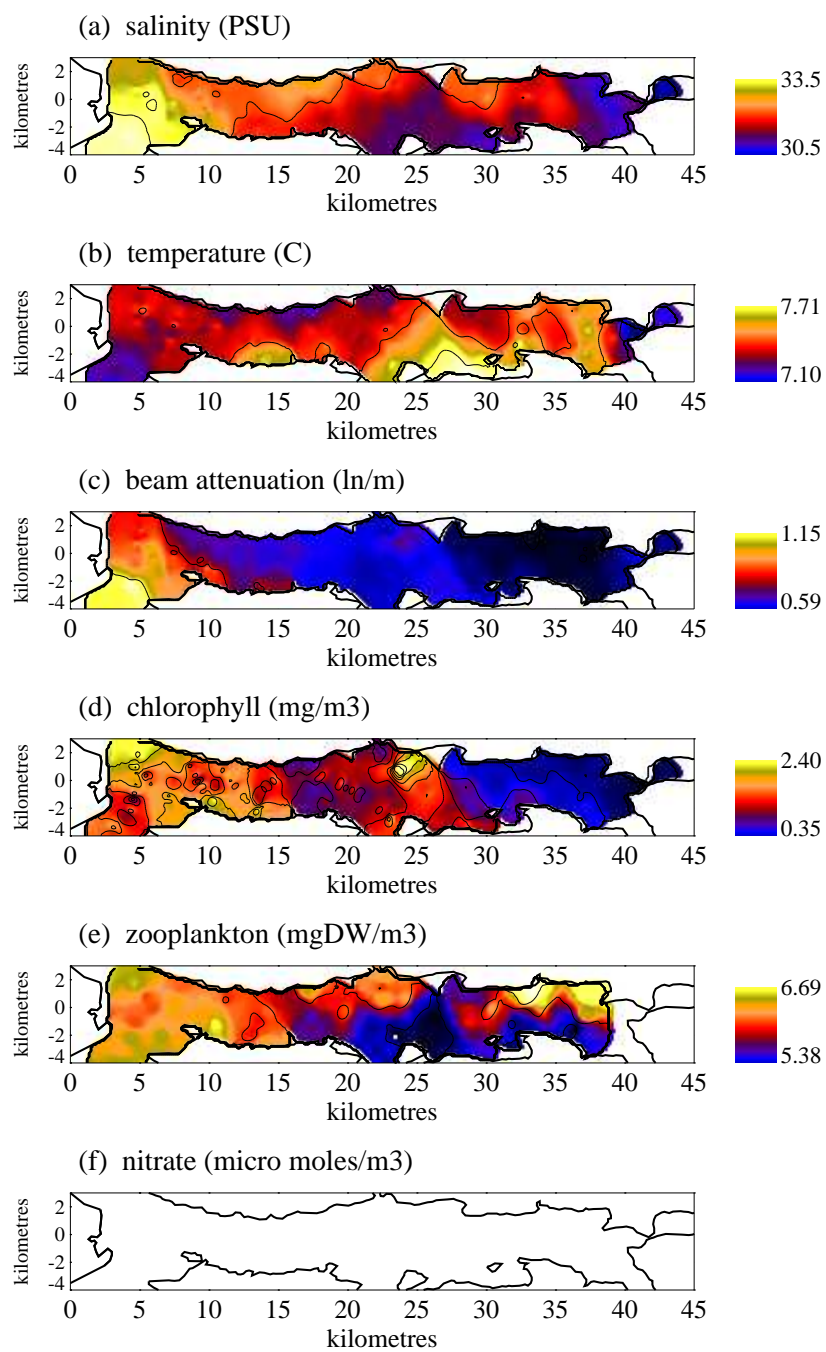


Figure A.18: 23 April 1991

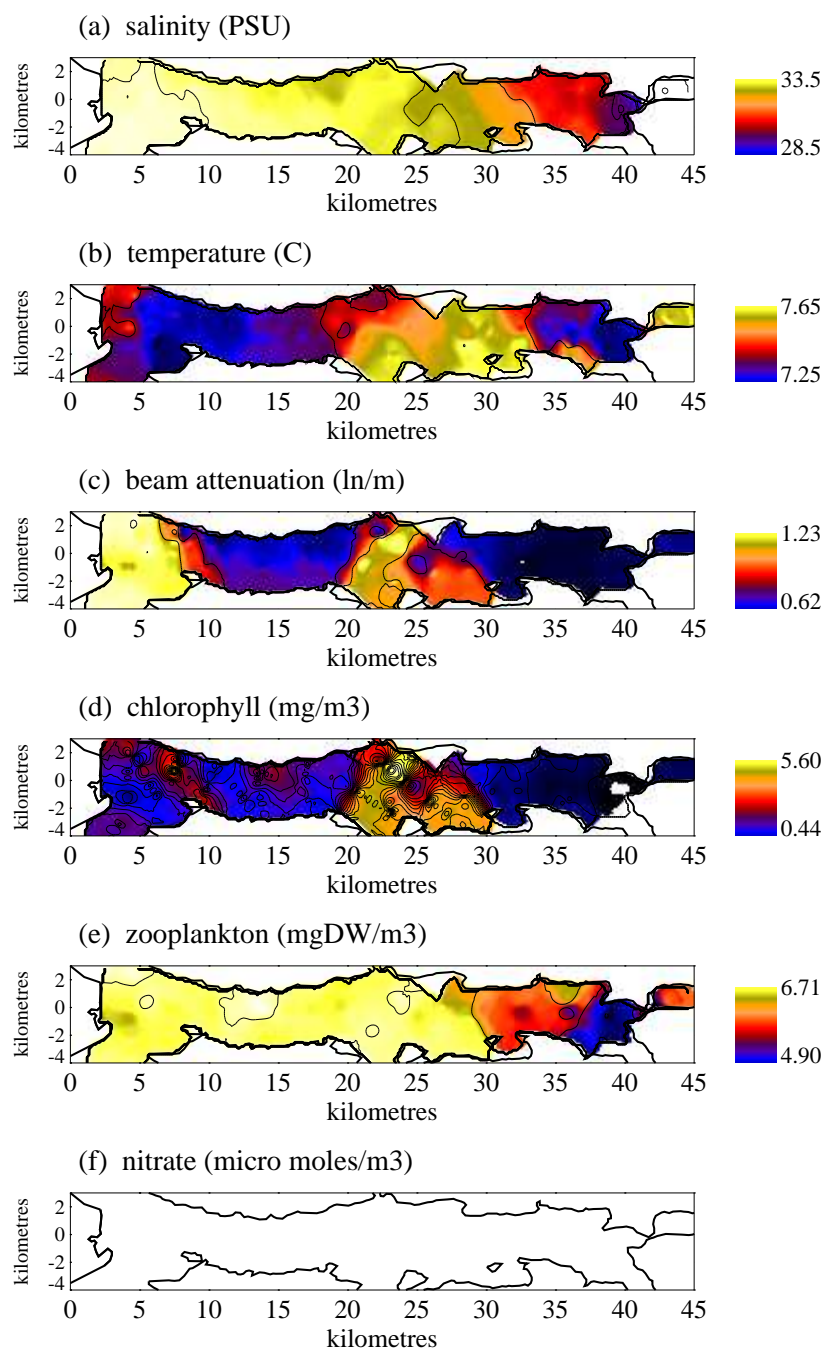


Figure A.19: 25 April 1991

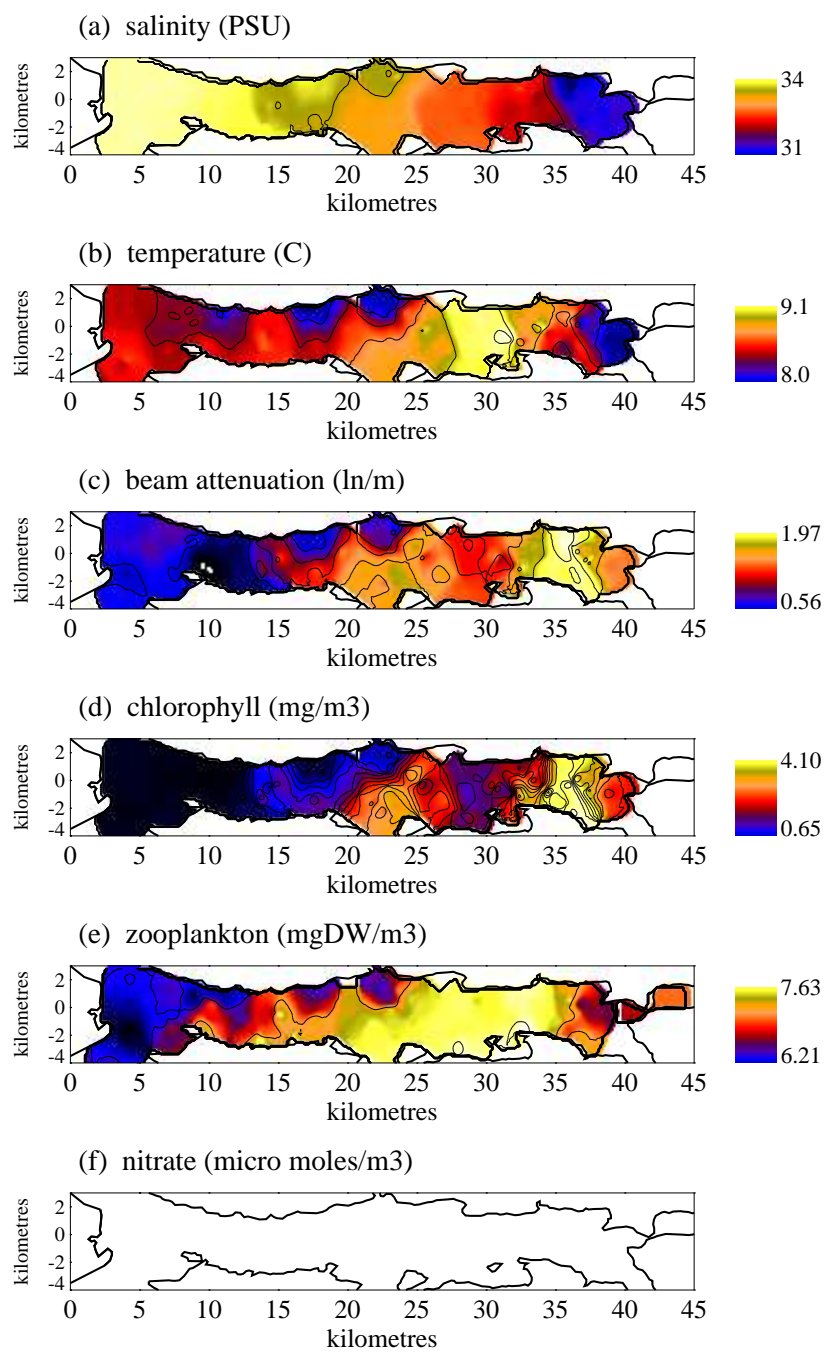


Figure A.20: 21 May 1991

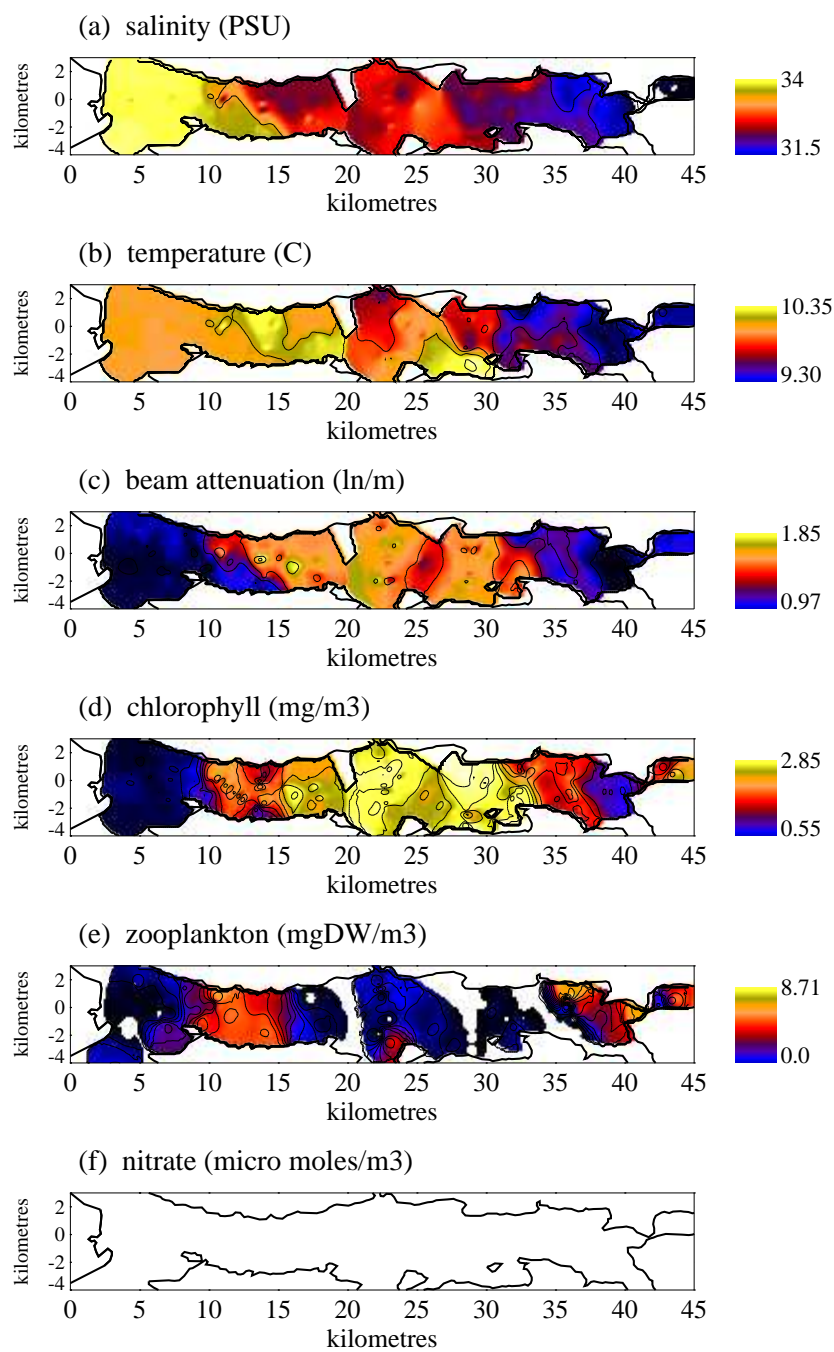


Figure A.21: 18 June 1991

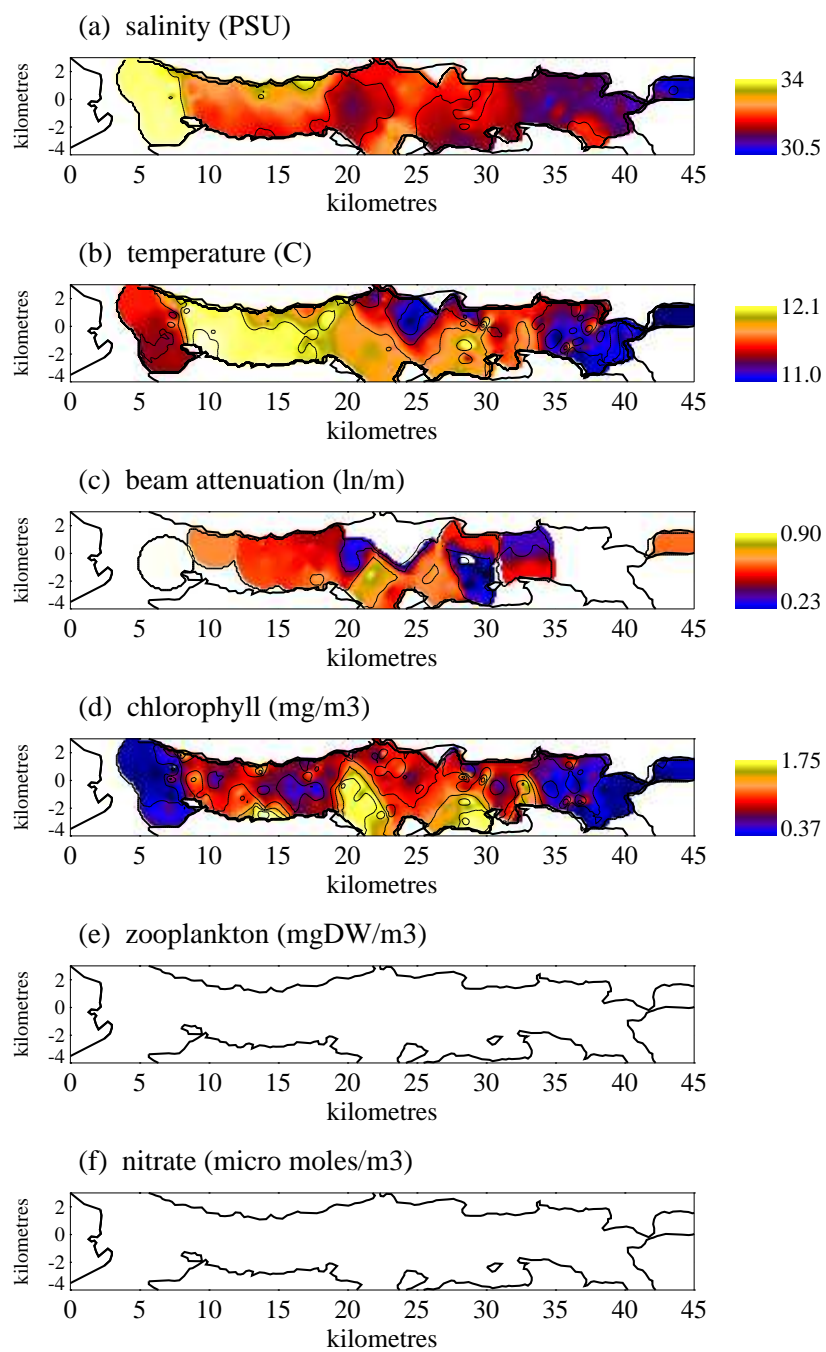


Figure A.22: 16 July 1991

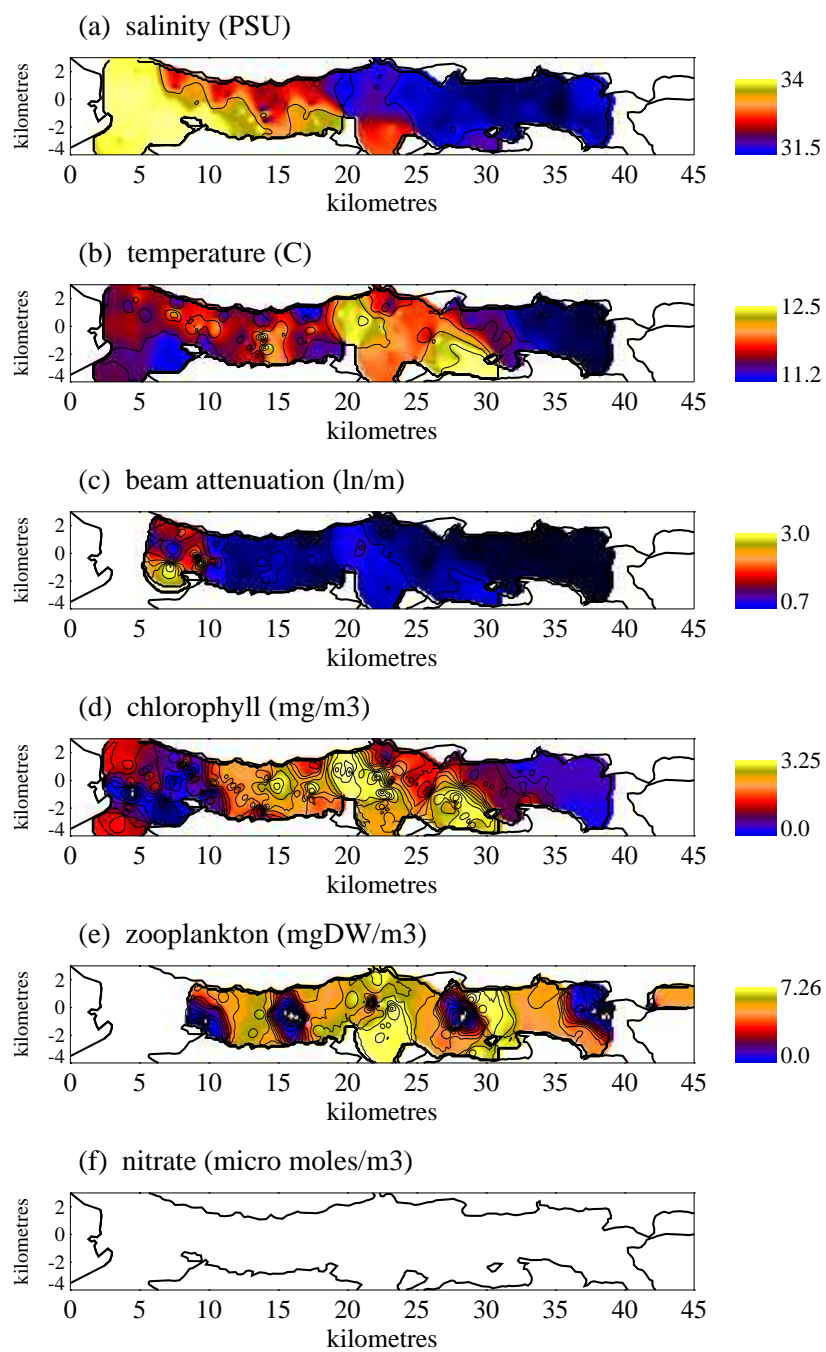


Figure A.23: 18 July 1991

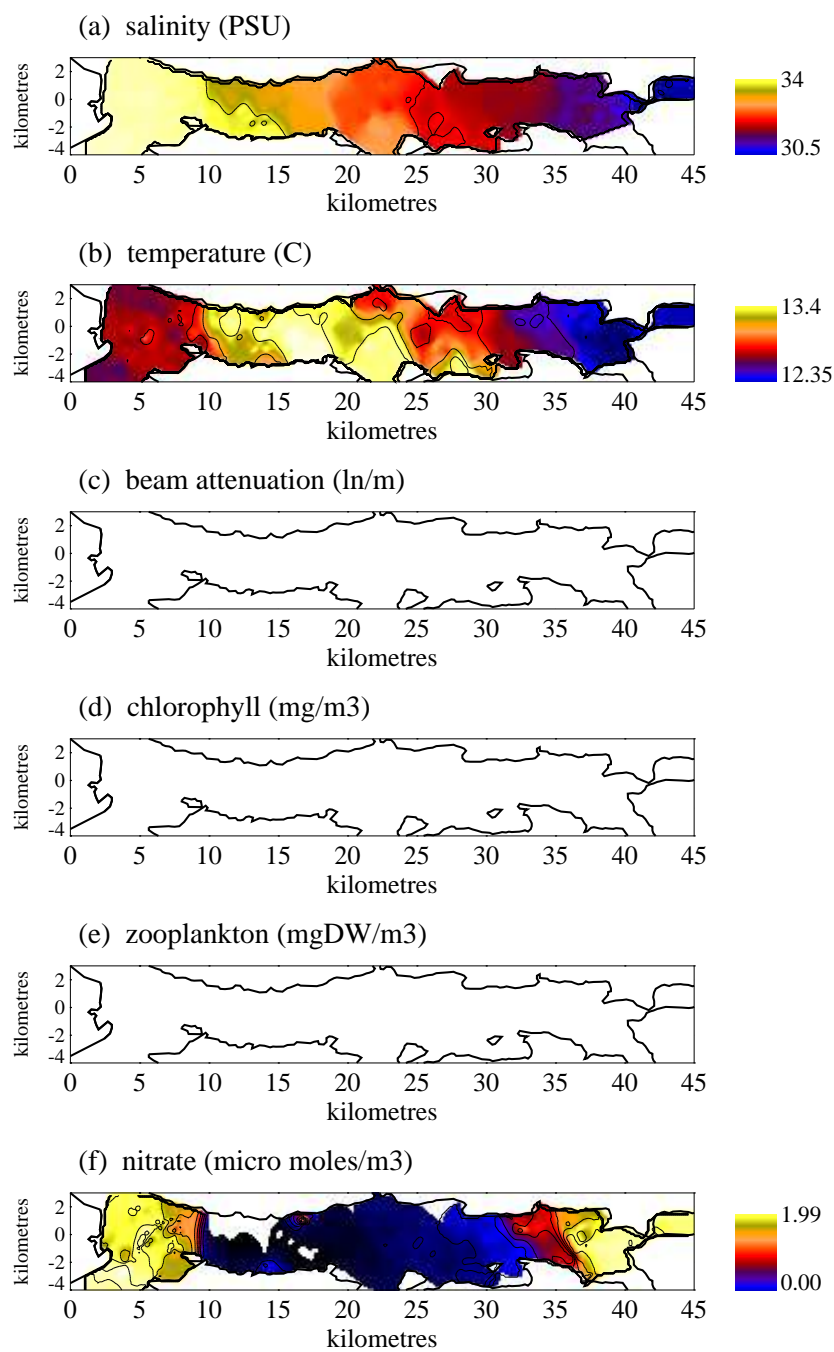


Figure A.24: 14 August 1991

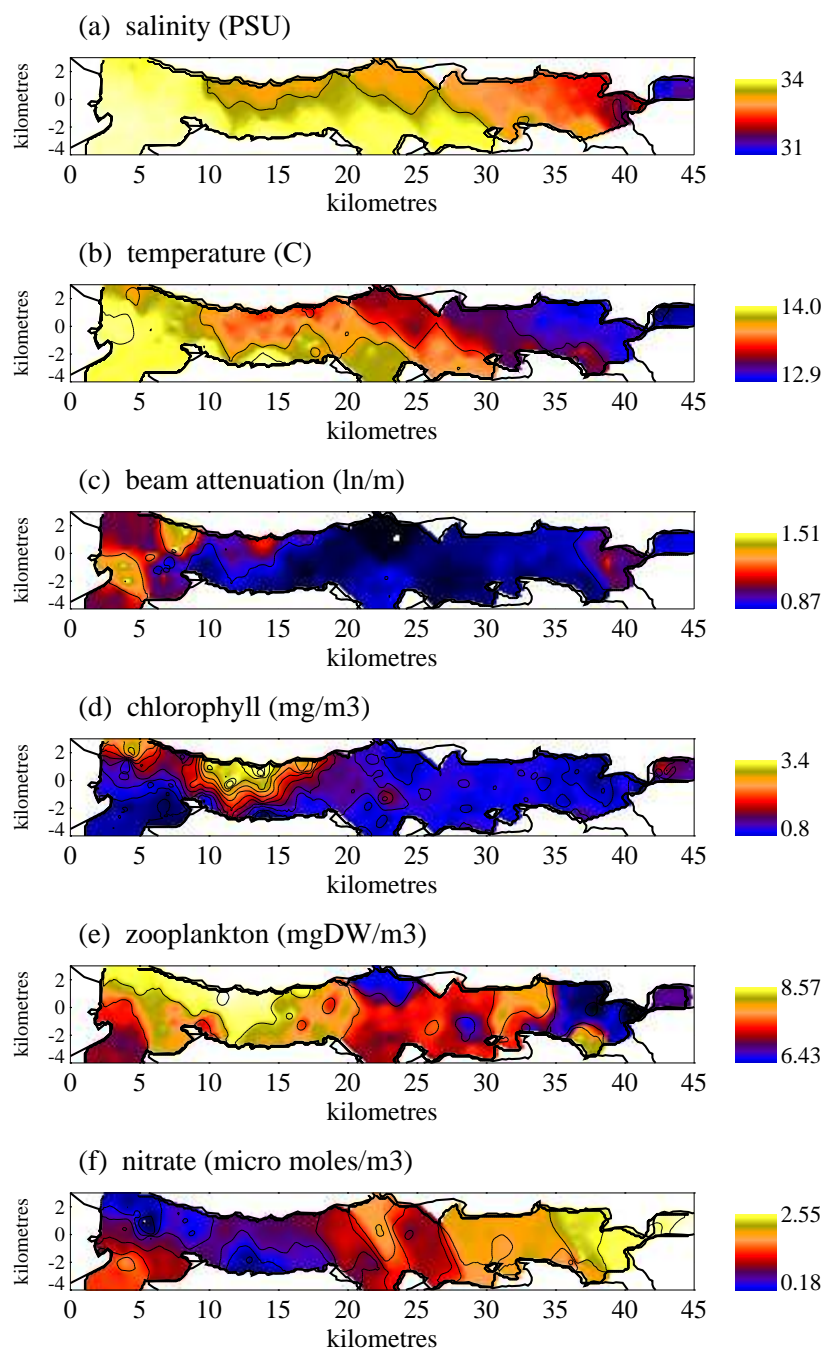


Figure A.25: 11 September 1991

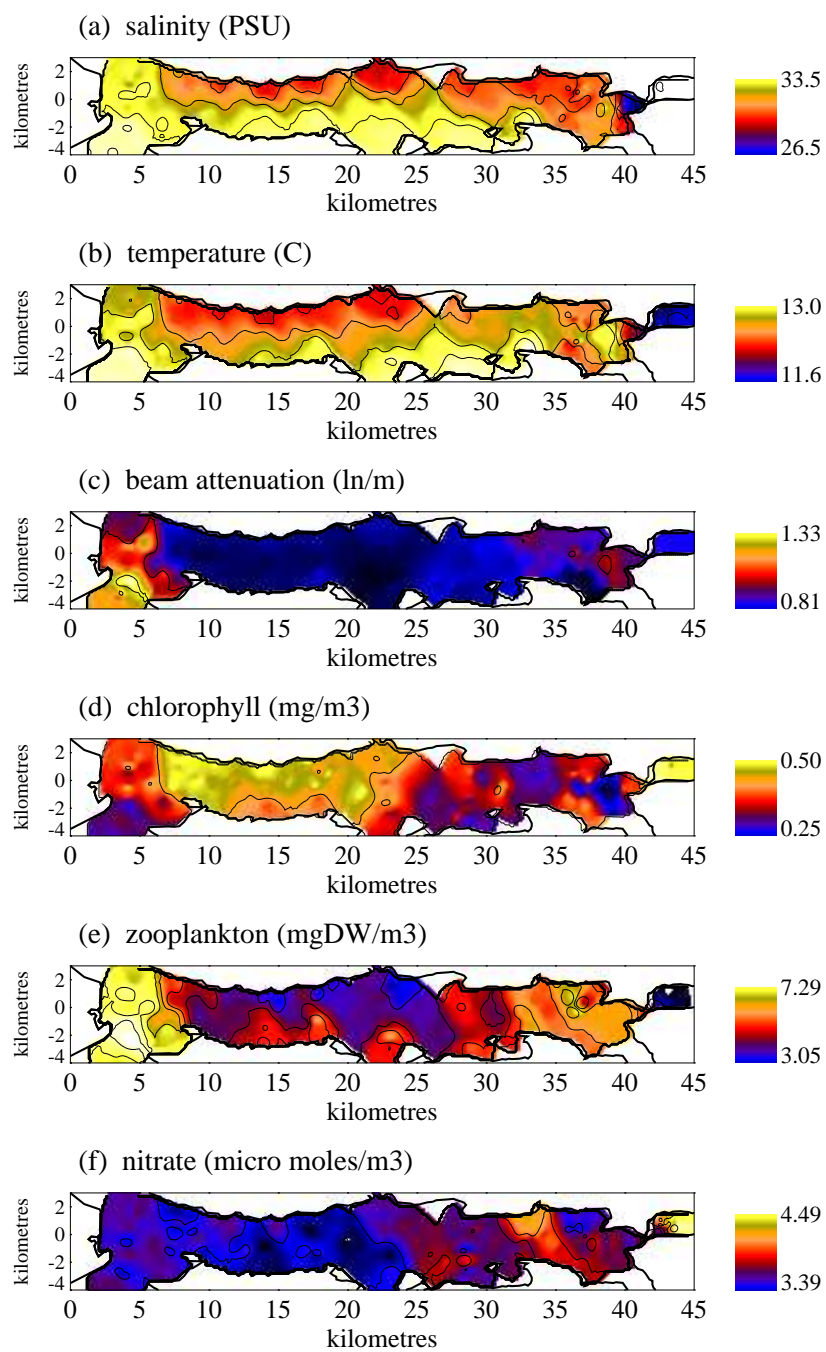


Figure A.26: 9 October 1991

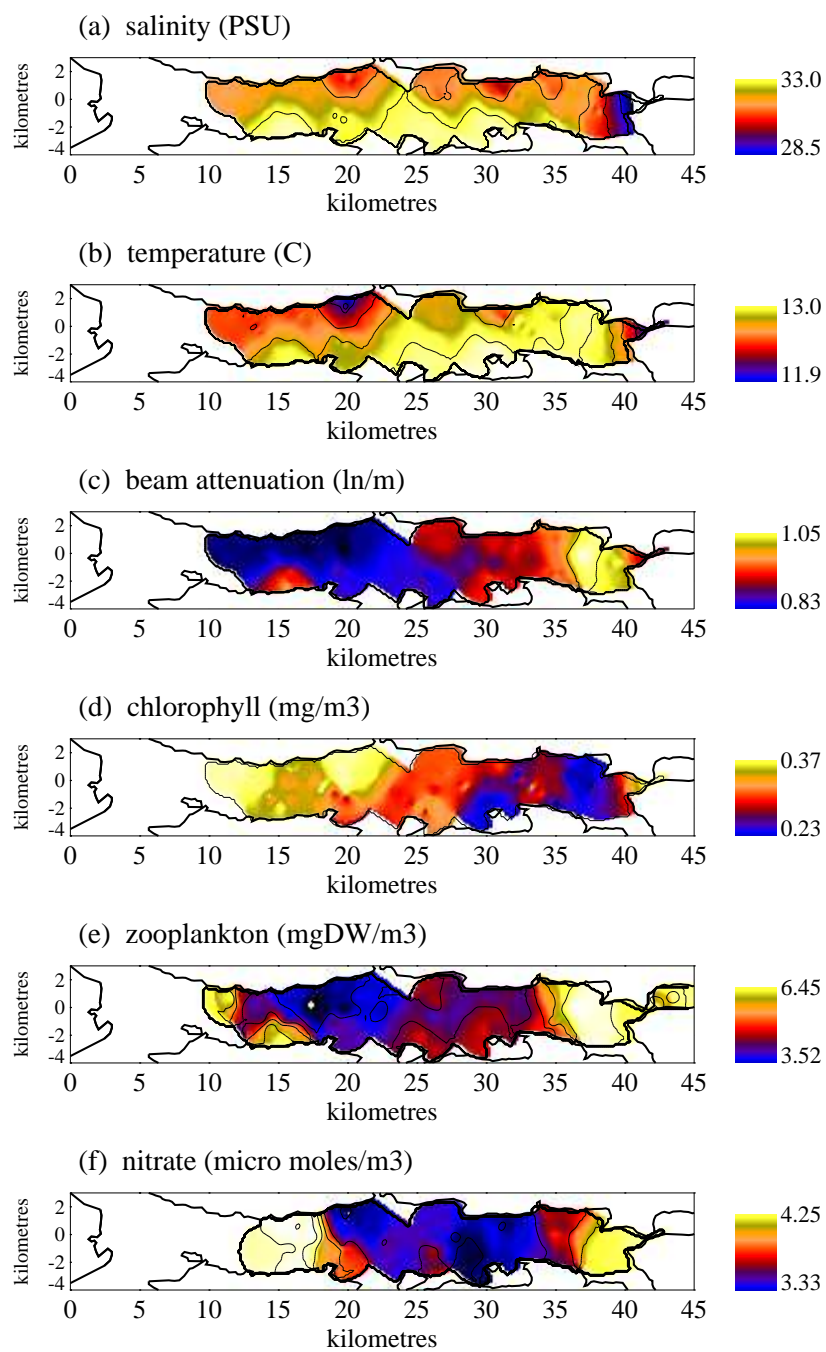


Figure A.27: 10 October 1991

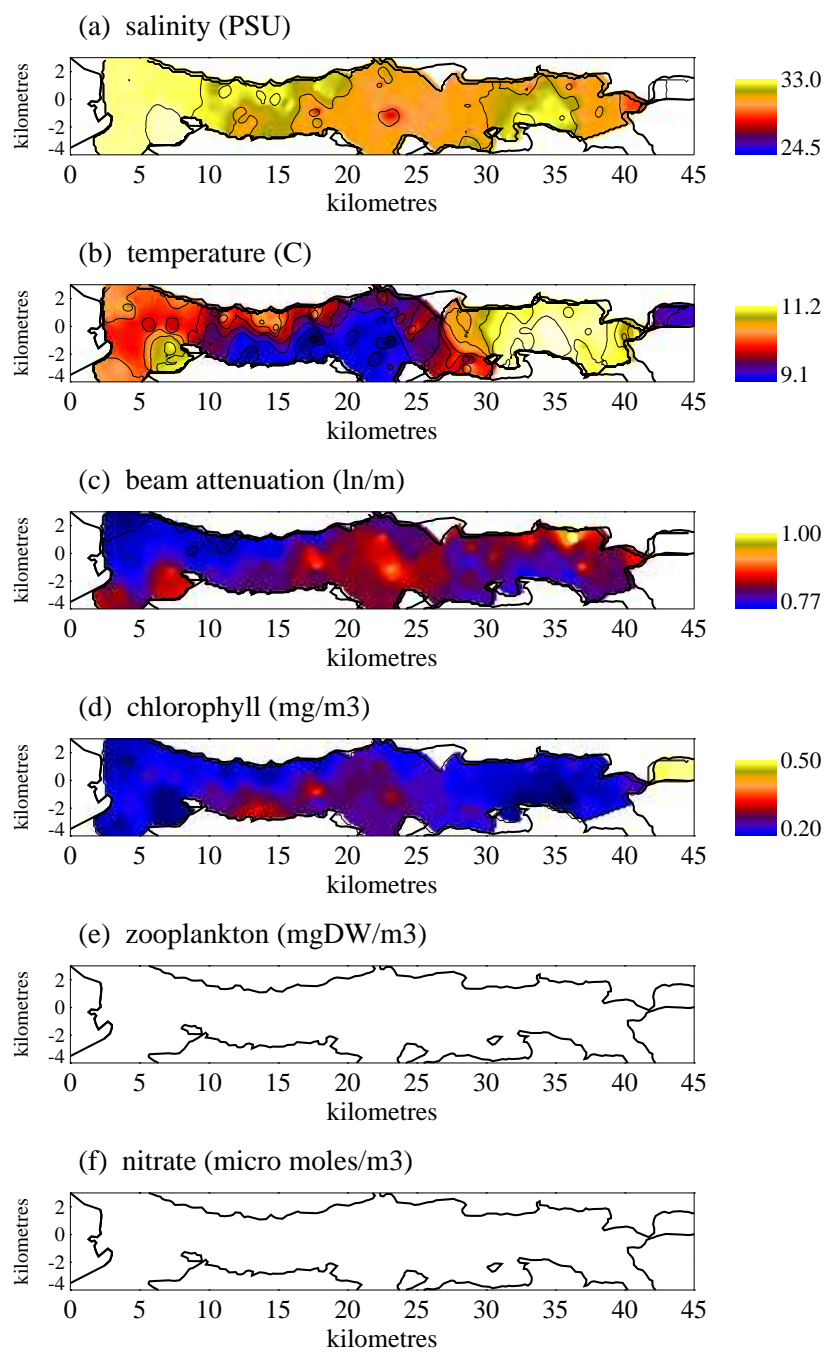


Figure A.28: 14 November 1991

A.4 Firth of Lorne

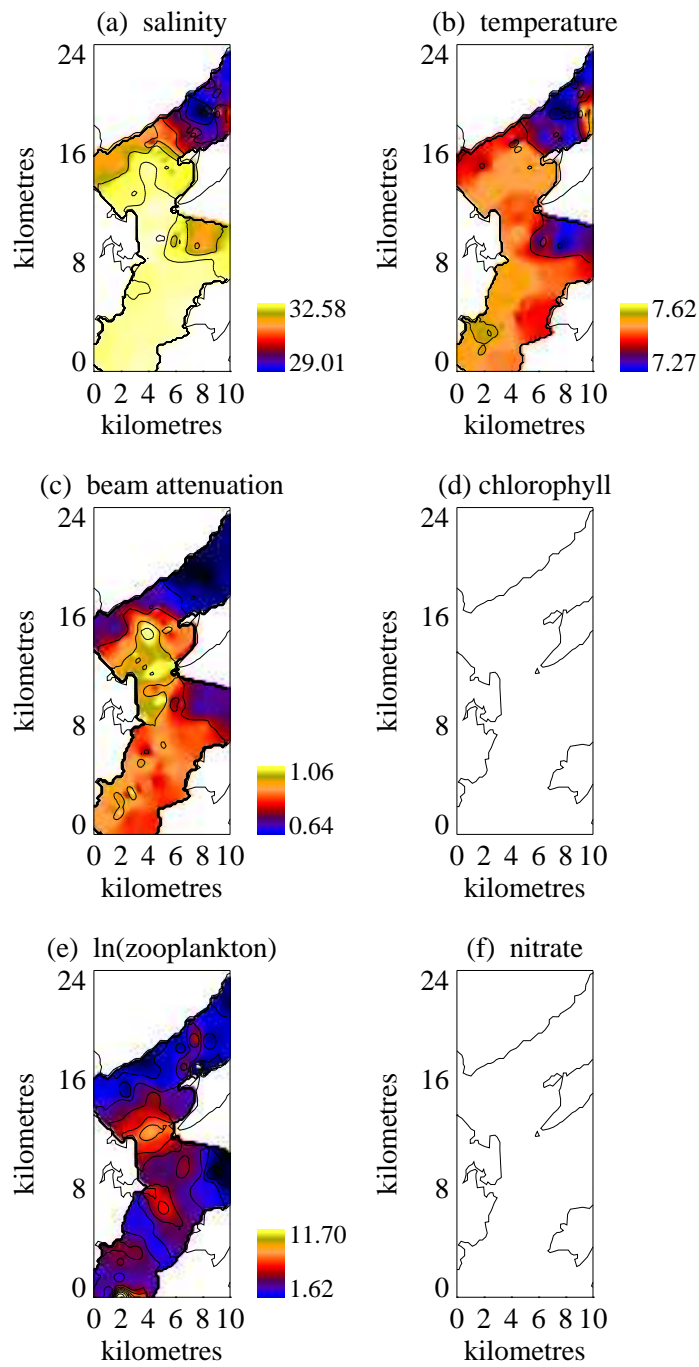


Figure A.29: 23 January 1991

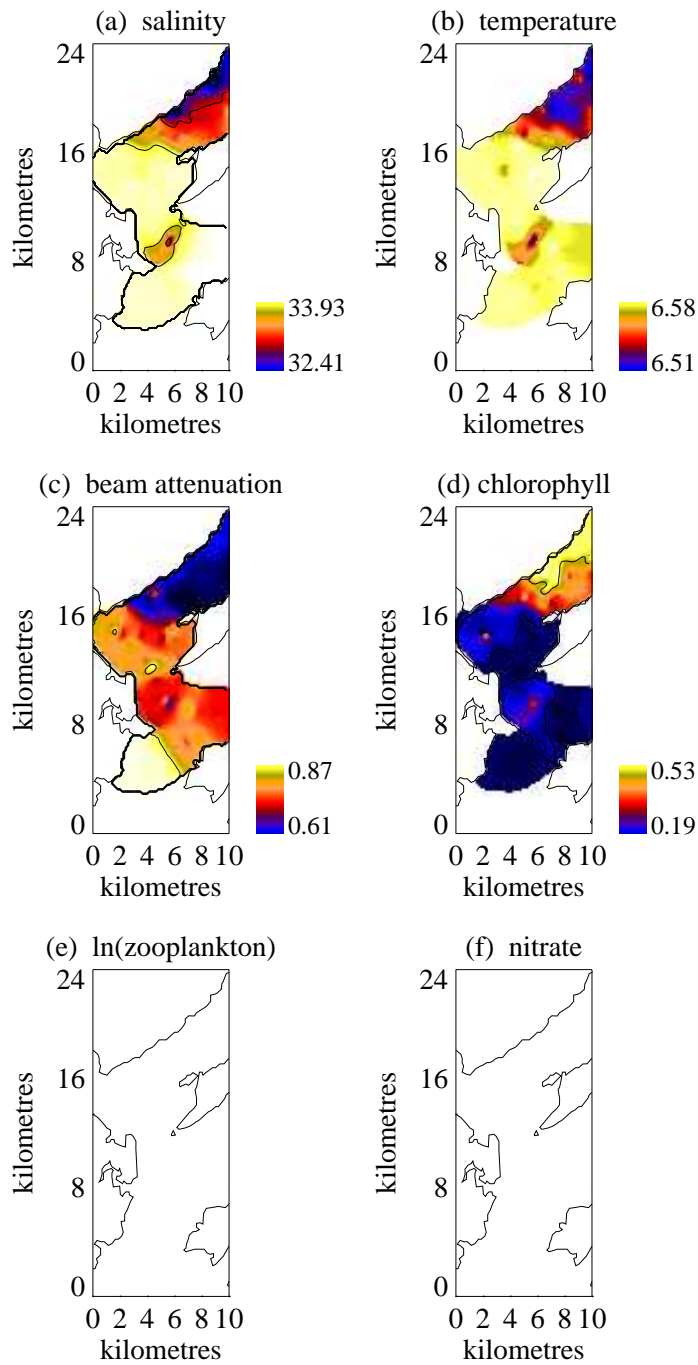


Figure A.30: 27 February 1991

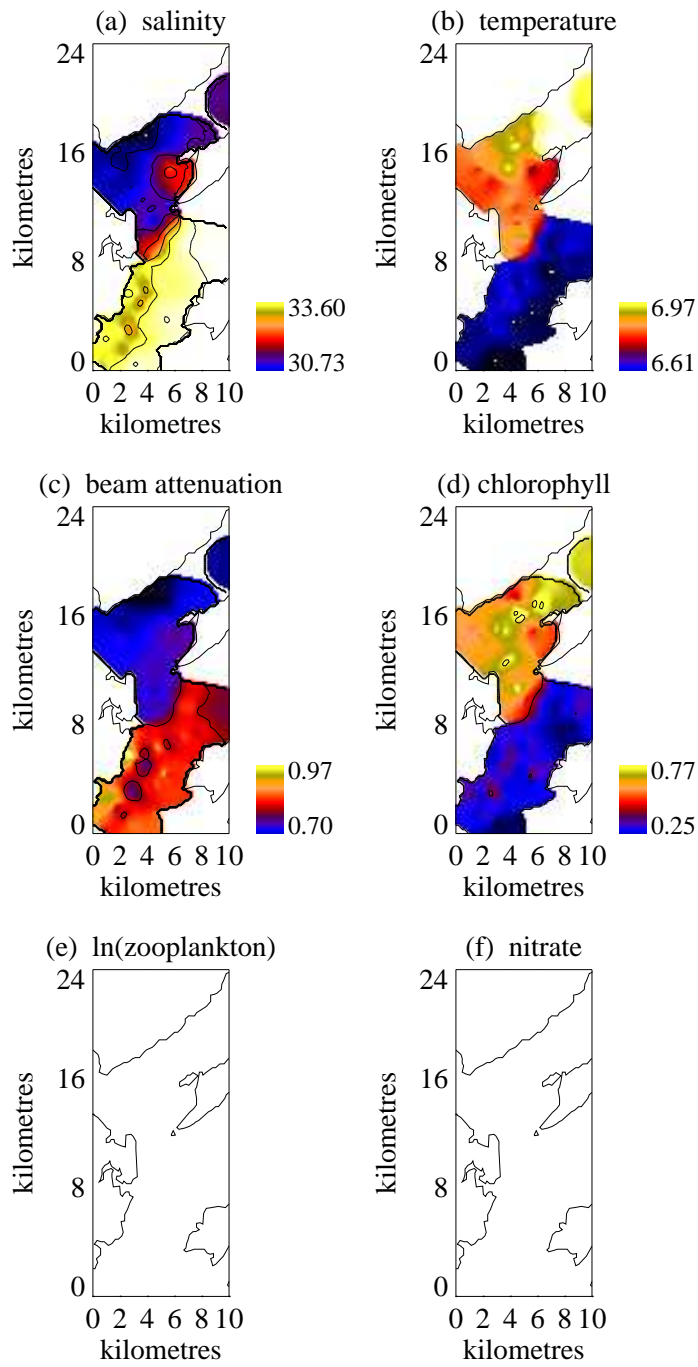


Figure A.31: 26 March 1991

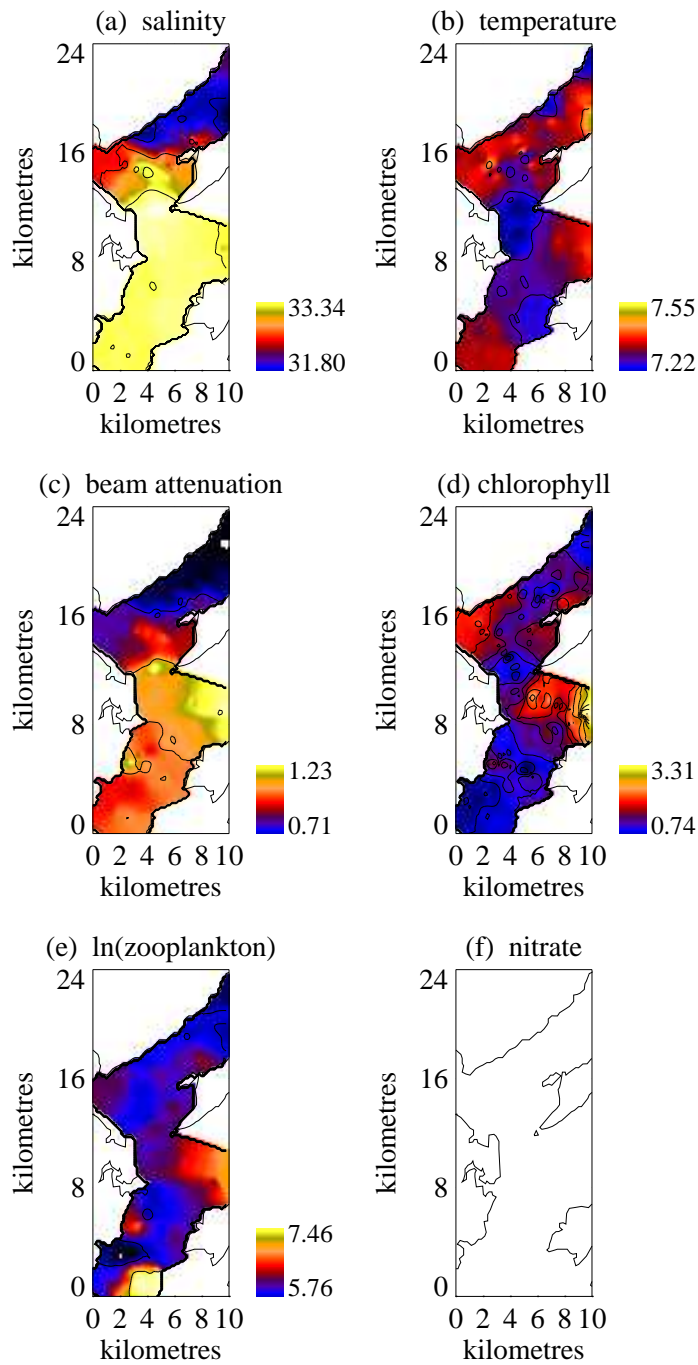


Figure A.32: 23 April 1991

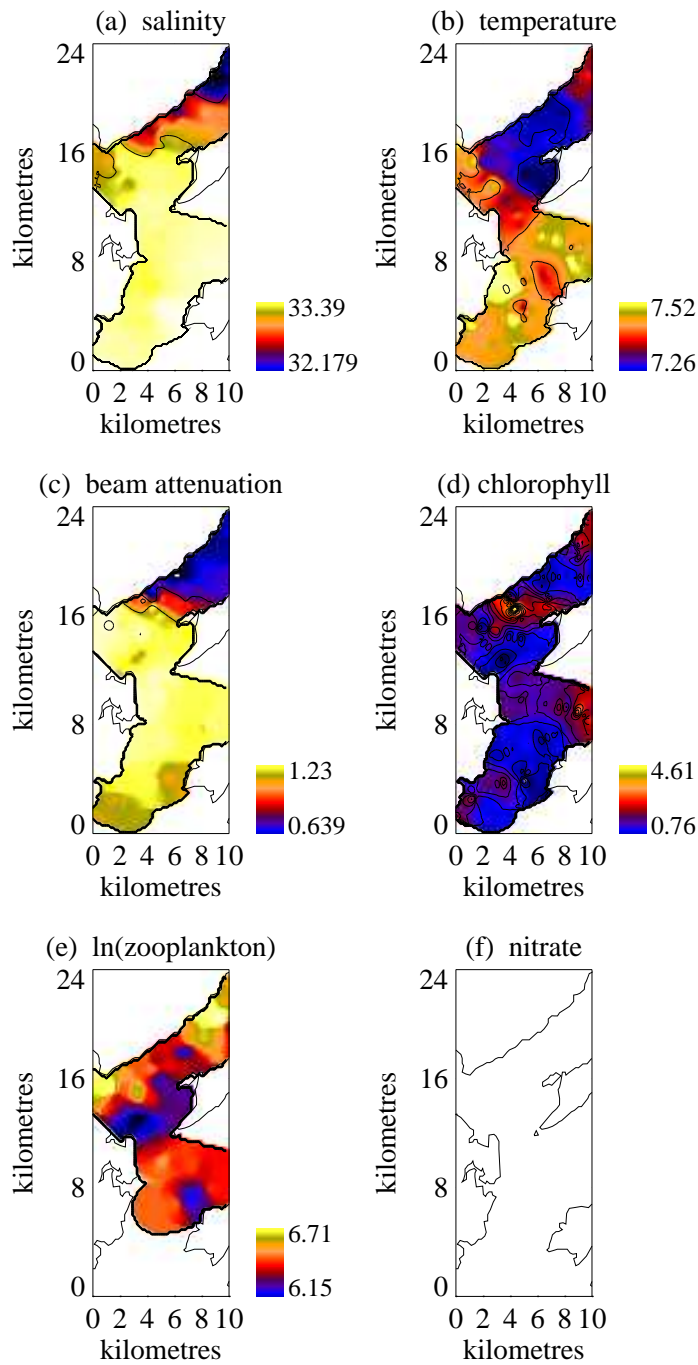


Figure A.33: 25 April 1991

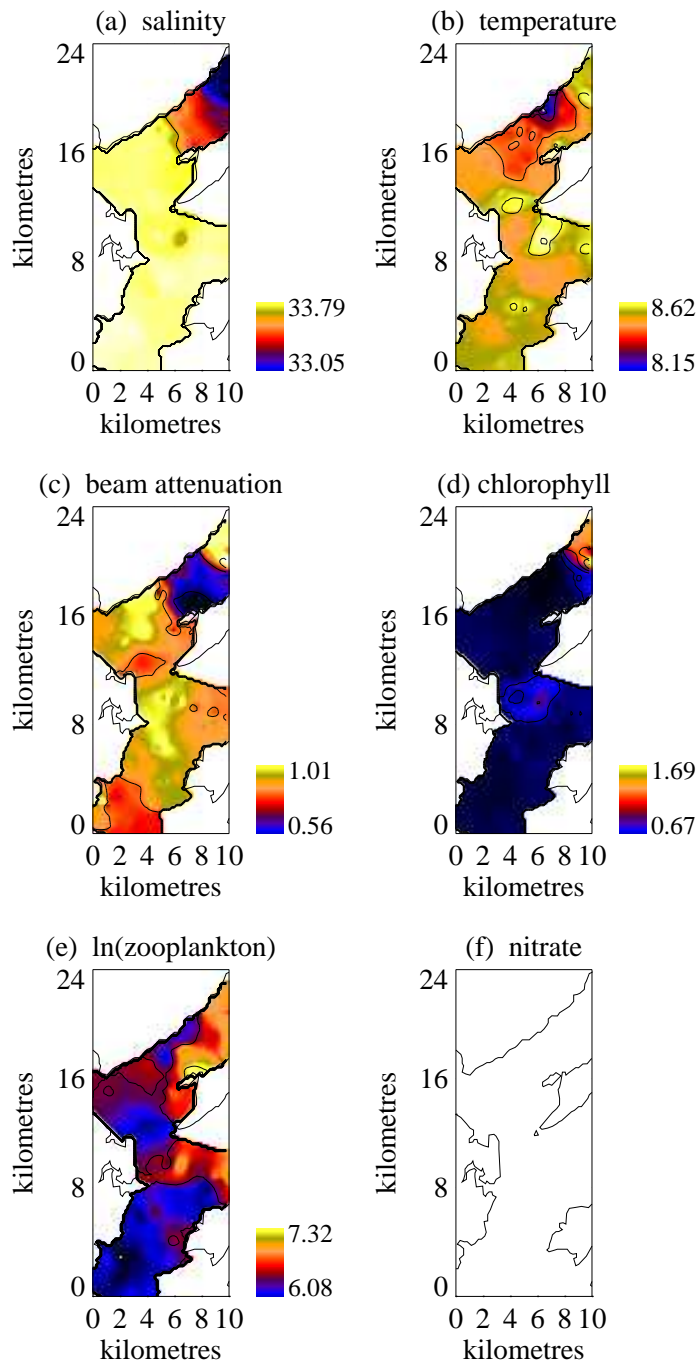


Figure A.34: 21 May 1991

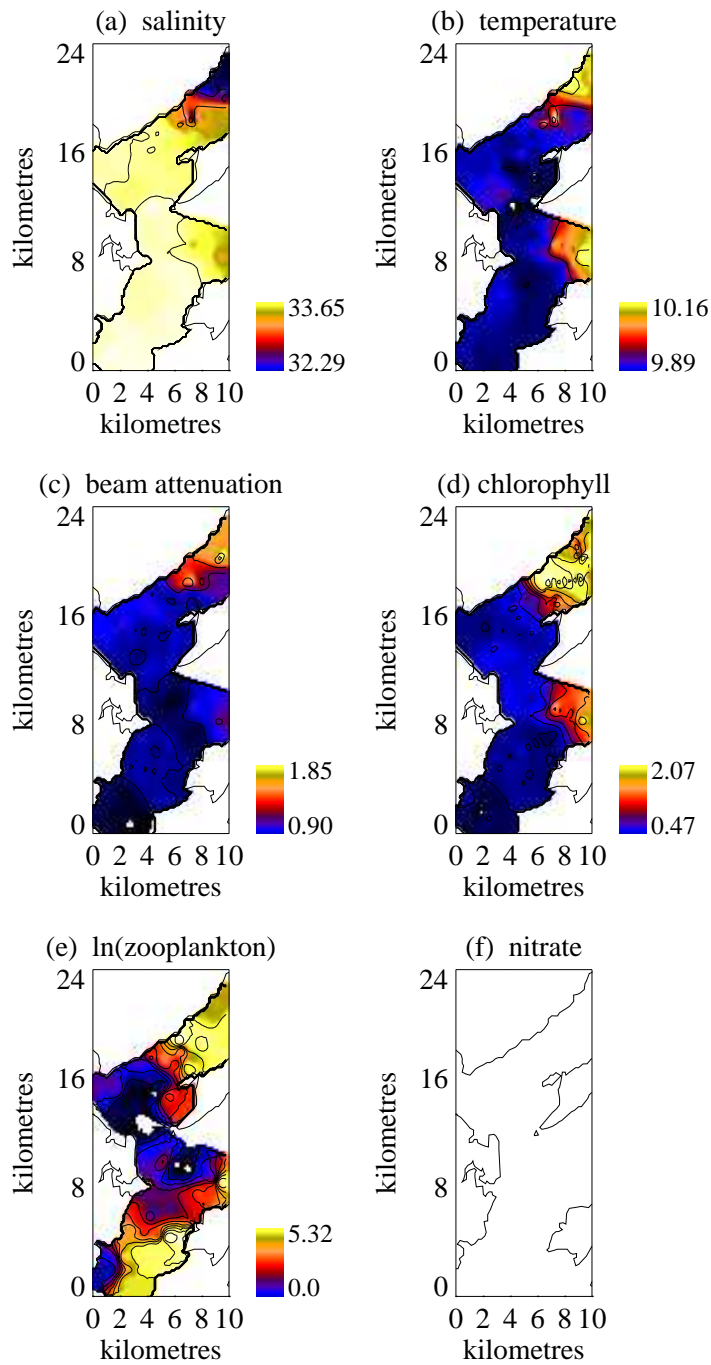


Figure A.35: 18 June 1991

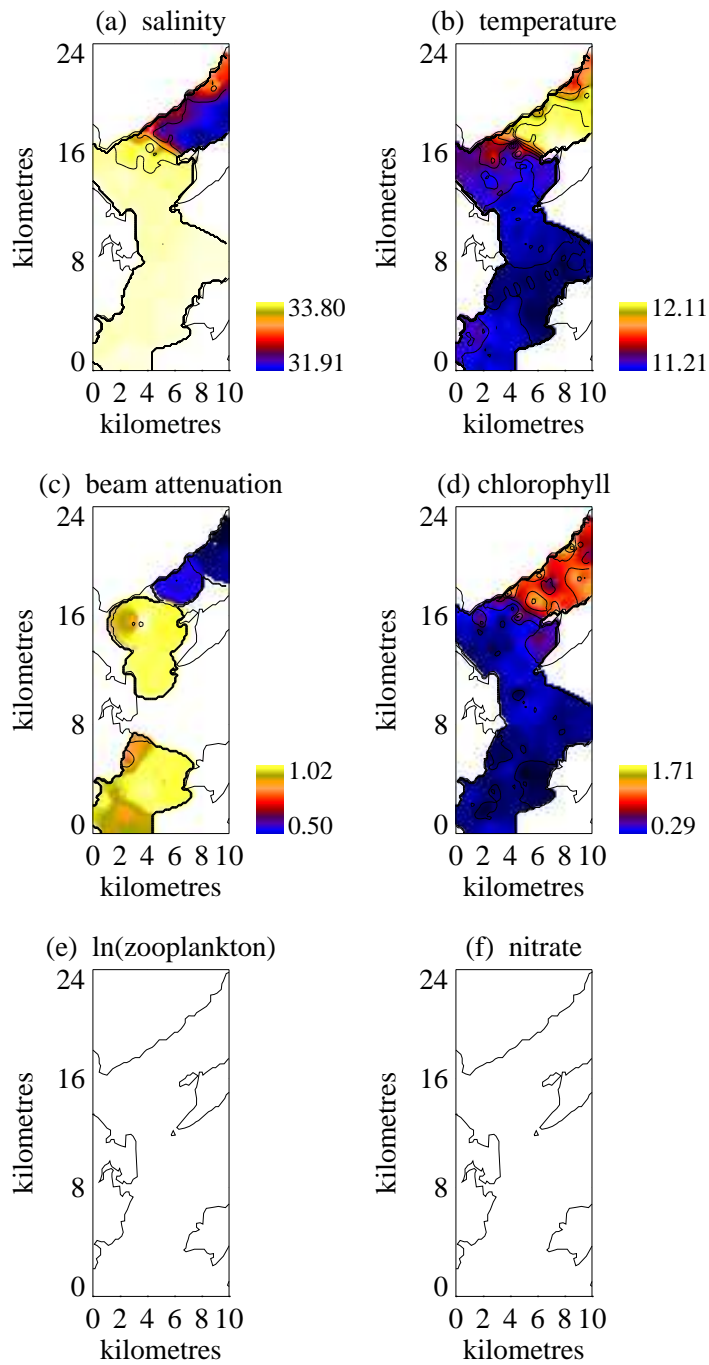


Figure A.36: 16 July 1991

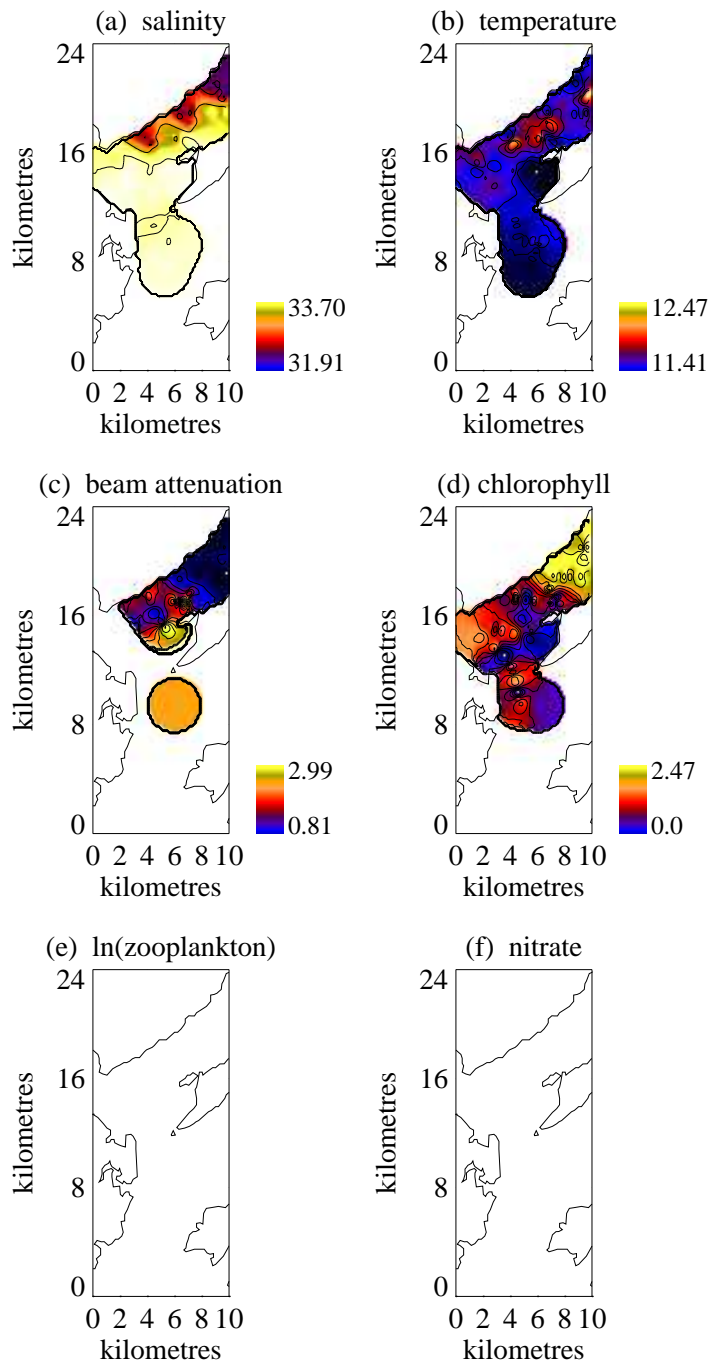


Figure A.37: 18 July 1991

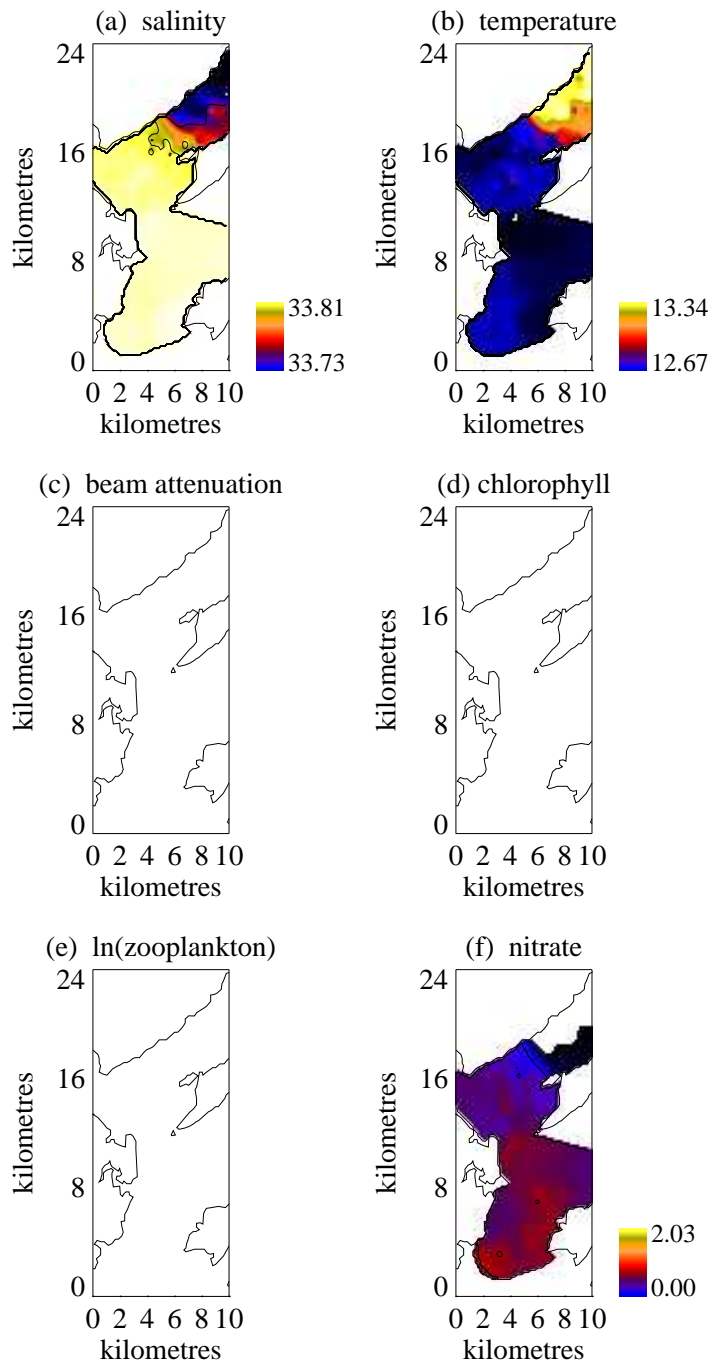


Figure A.38: 14 August 1991

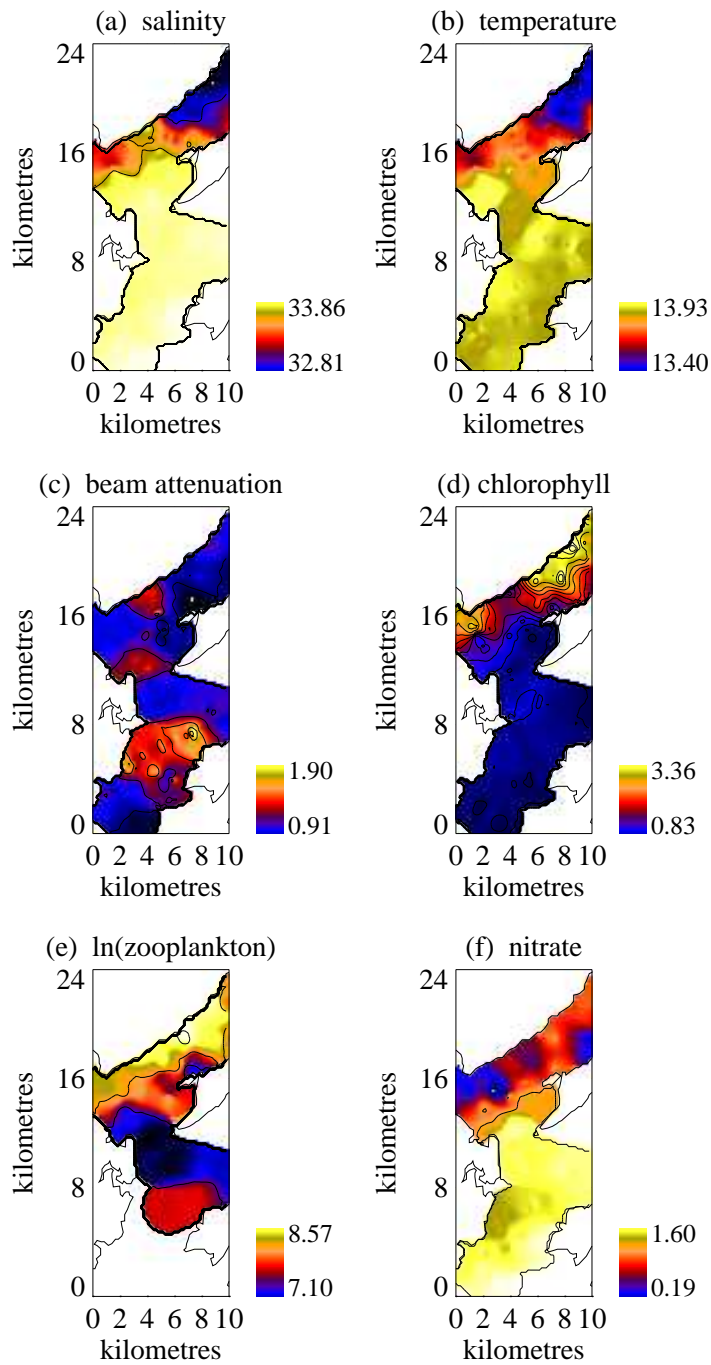


Figure A.39: 11 September 1991

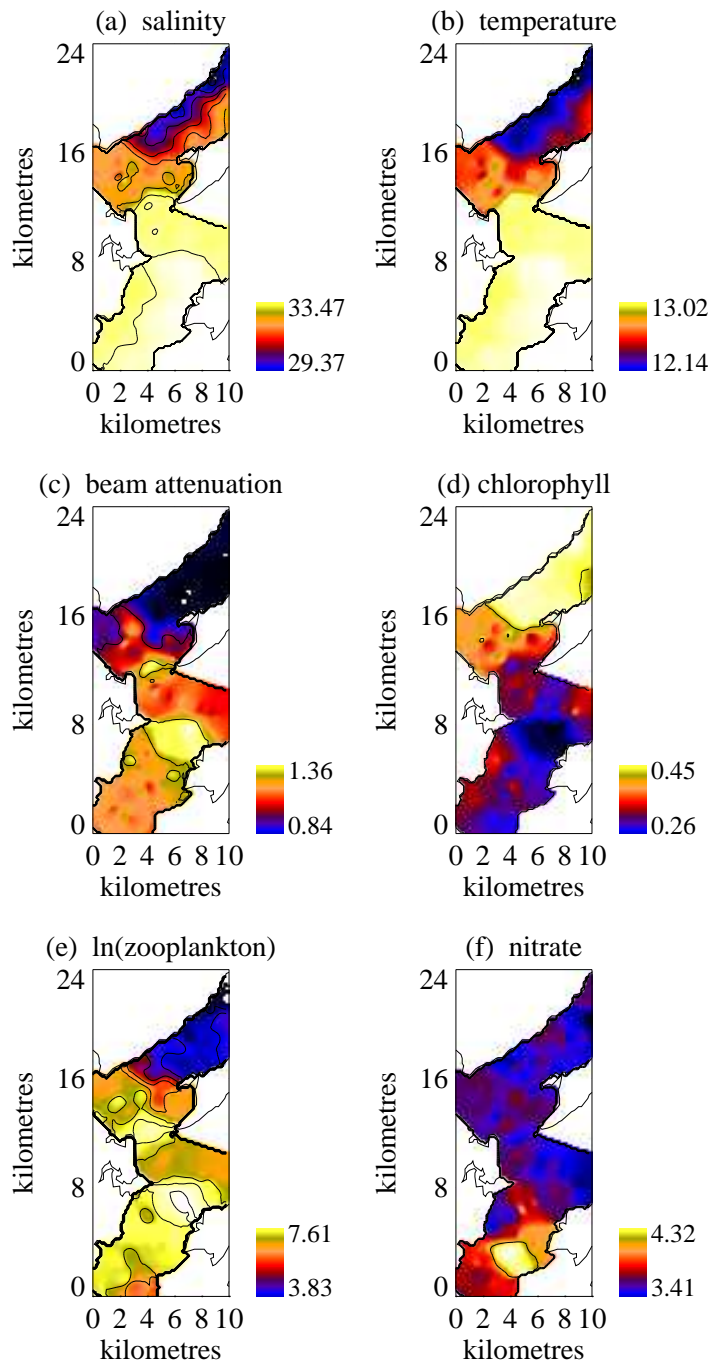


Figure A.40: 9 October 1991

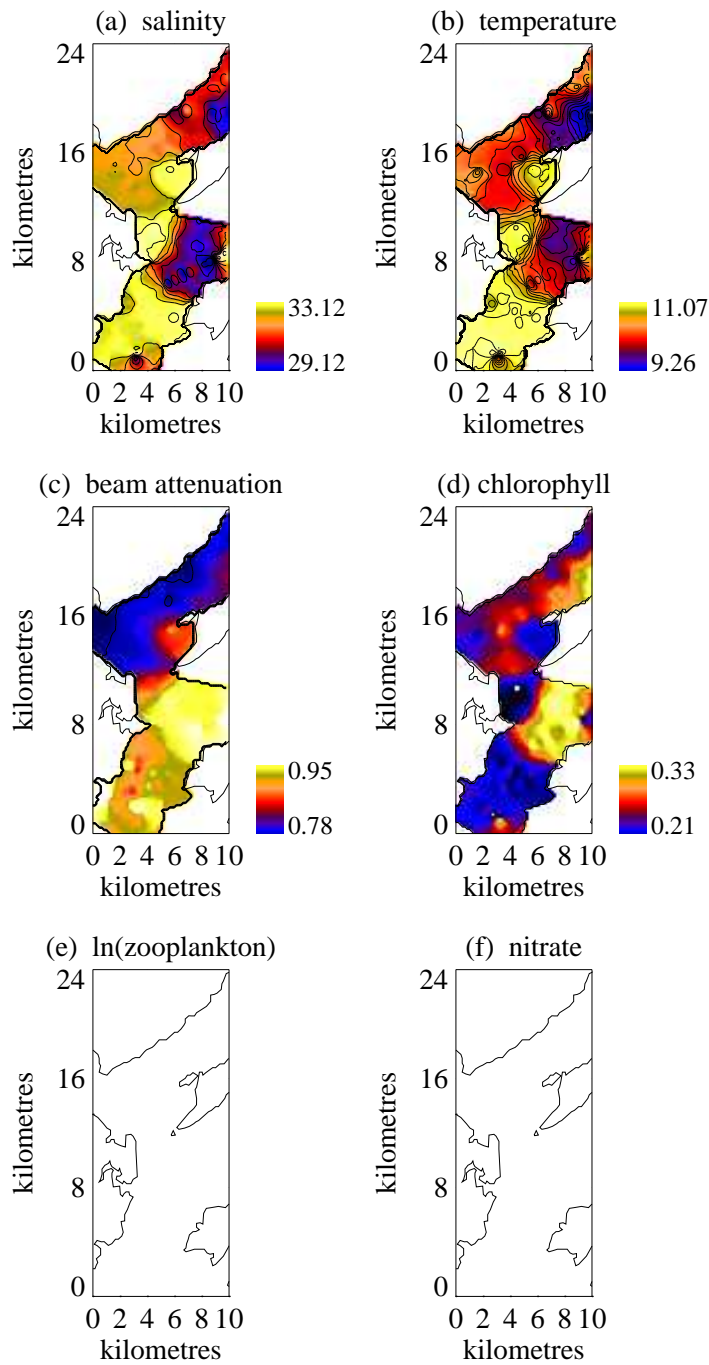


Figure A.41: 14 November 1991

Appendix B

Axial Data

B.1 Inner Basin

Table B.1: Daily mean meteorological conditions for the inner basin axial cruises.

date	wind speed (ms^{-1}) and direction	river discharge (m^3s^{-1})
25 Mar.	5.62 @ 122°	45.215
20 Apr.	4.33 @ 185°	36.454
18 May	5.79 @ 213°	9.281
15 June	5.87 @ 270°	26.703
13 July	10.8 @ 242°	56.094
10 Aug.	5.33 @ 228°	23.157
15 Aug.	11.25 @ 220°	38.835
7 Sept	4.21 @ 202°	5.566
8 Sept	2.33 @ 175°	5.48
10 Nov.	13.67 @ 196°	242.721

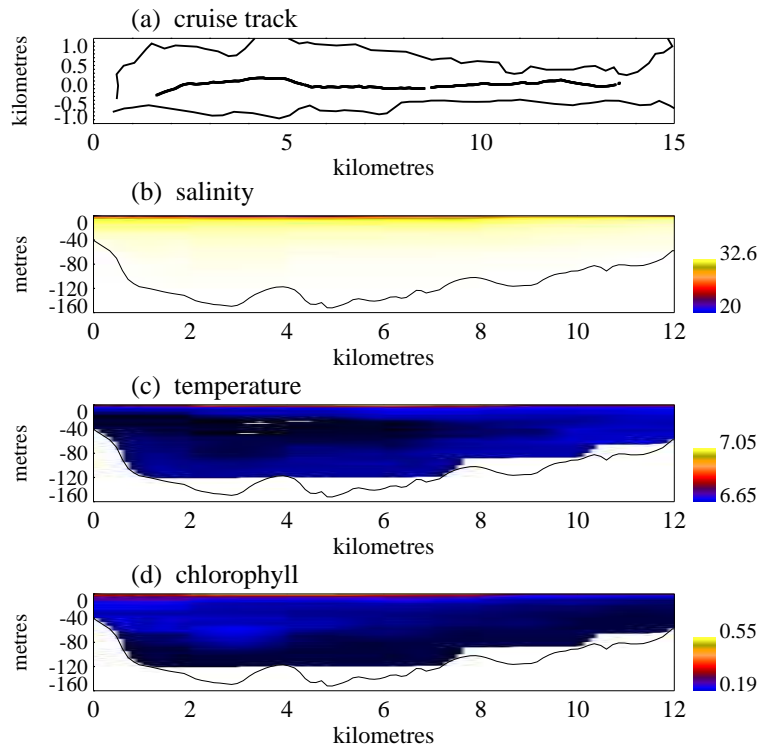


Figure B.1: 25 March 1991

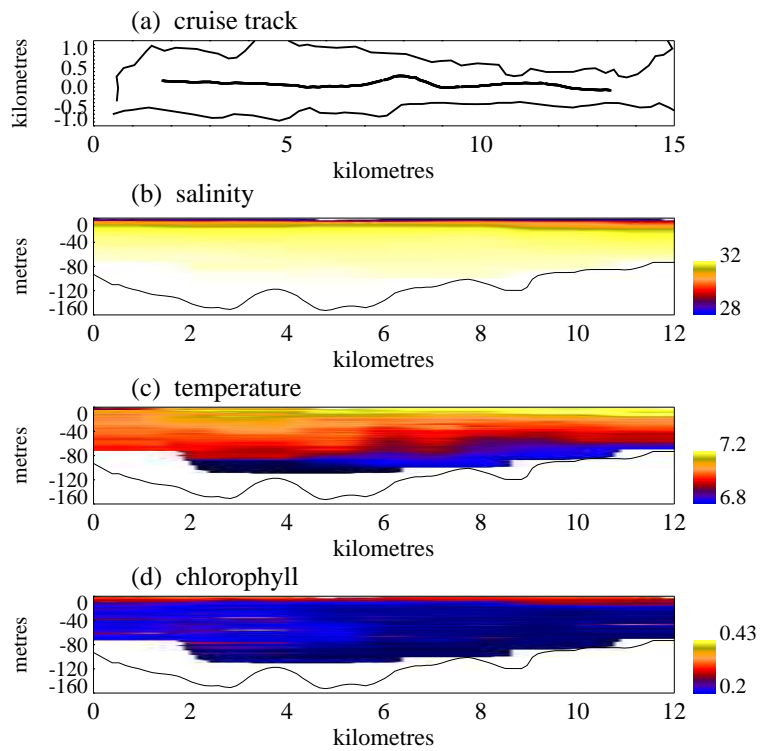


Figure B.2: 20 April 1991

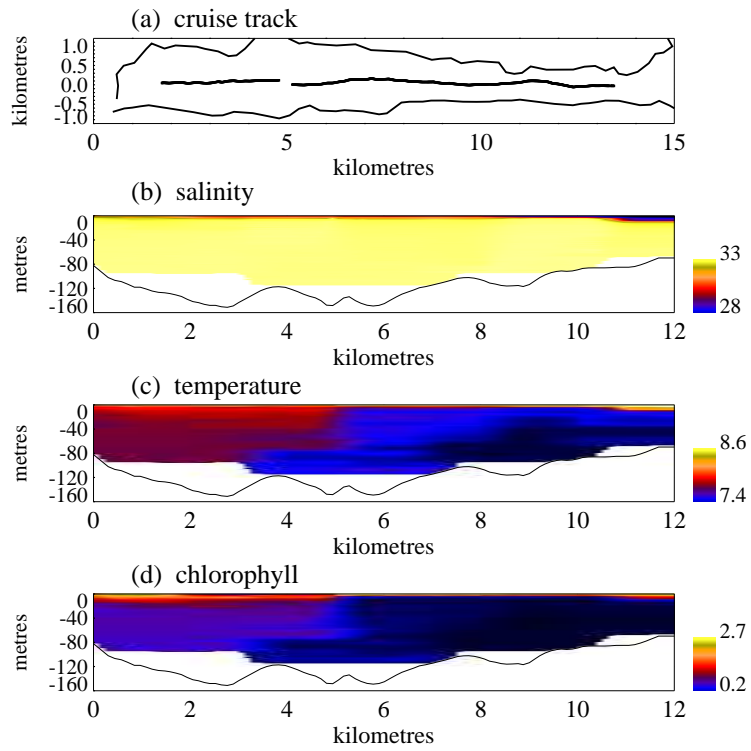


Figure B.3: 18 May 1991

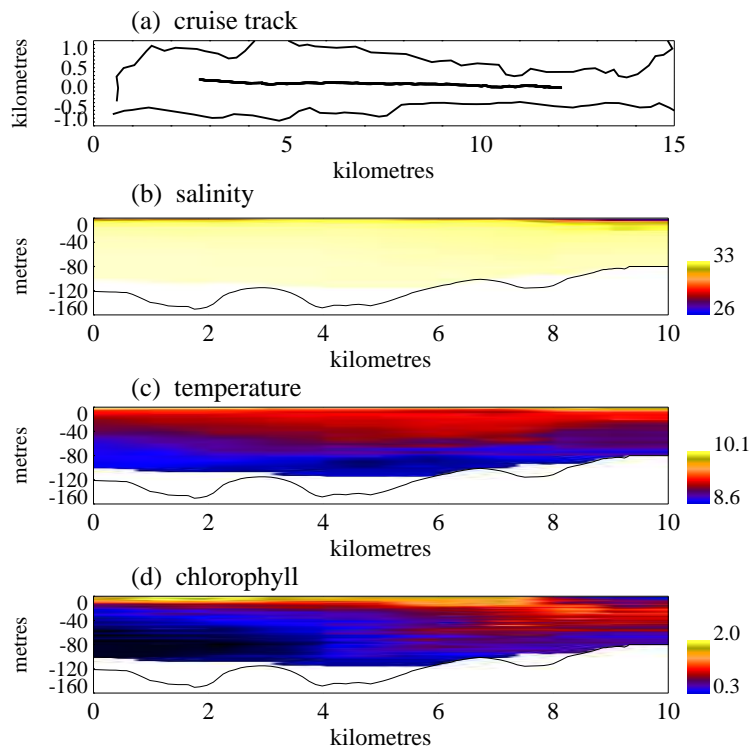


Figure B.4: 15 June 1991

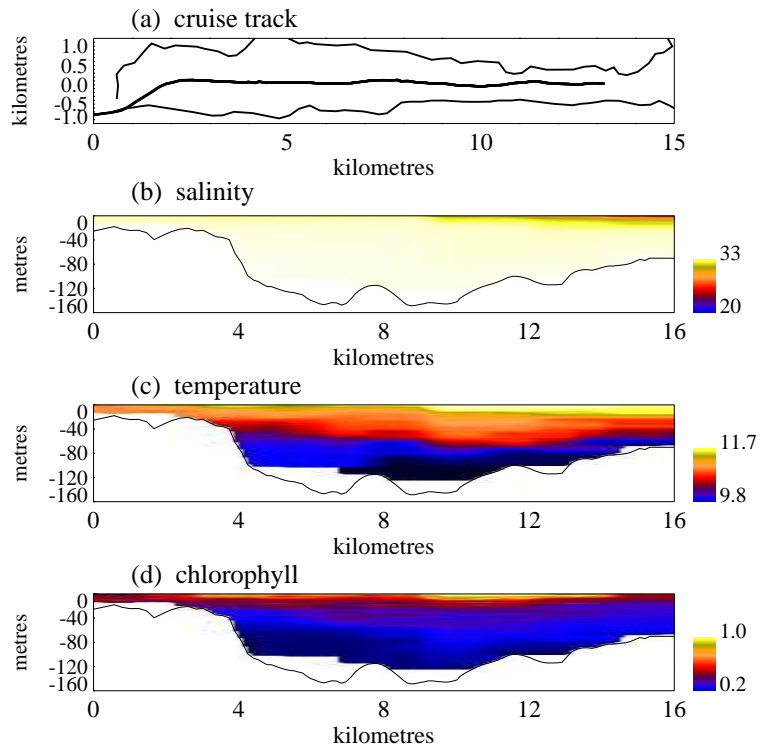


Figure B.5: 13 July 1991

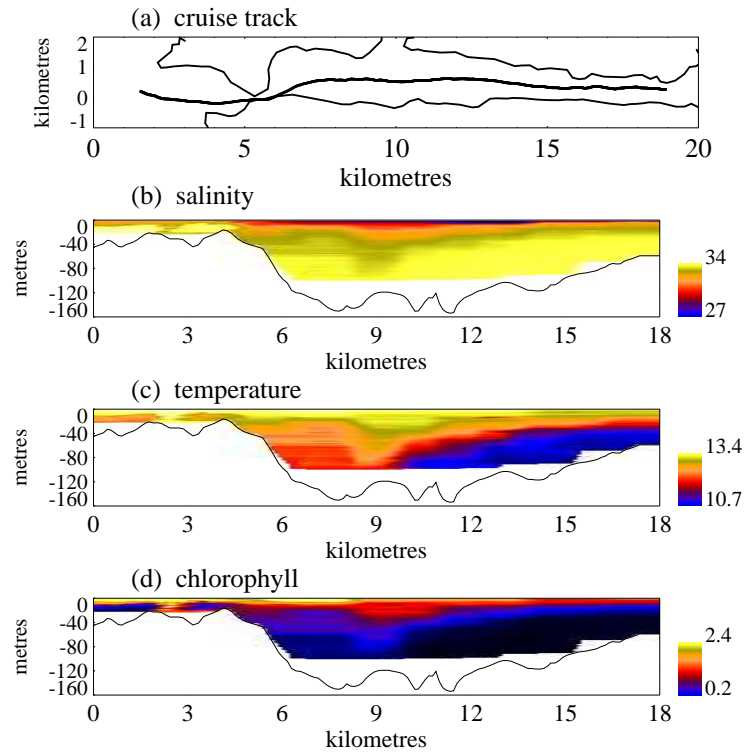


Figure B.6: 10 August 1991

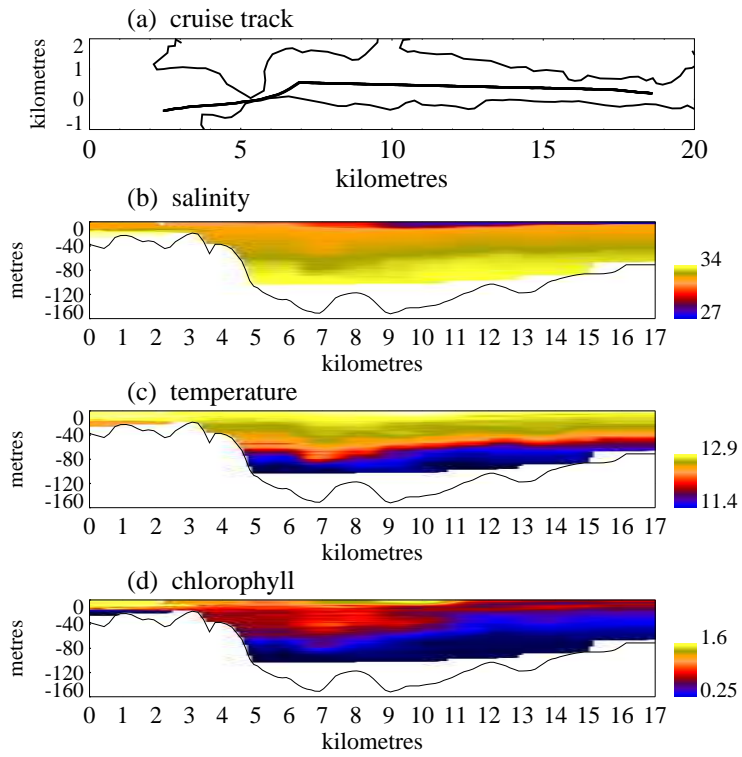


Figure B.7: 15 August 1991

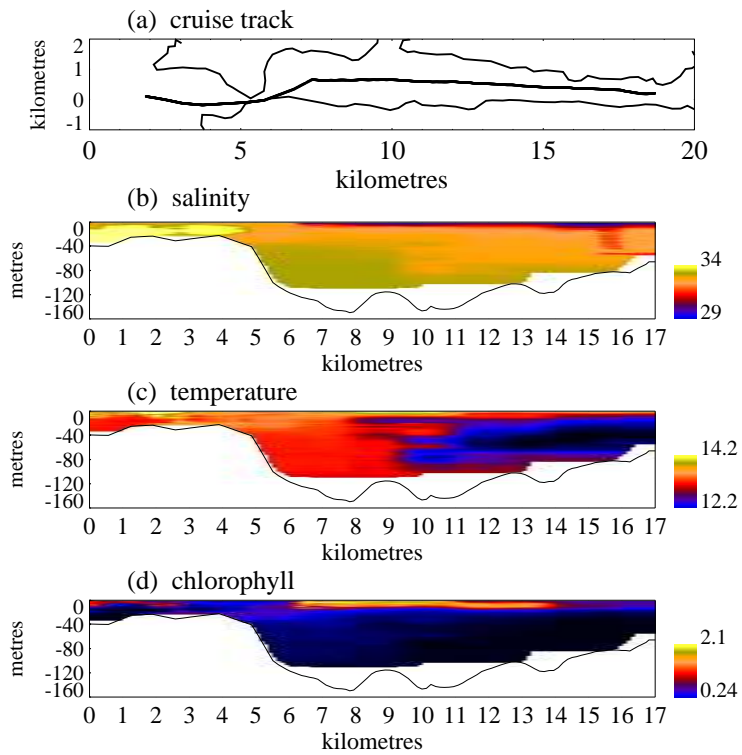


Figure B.8: 7 September 1991

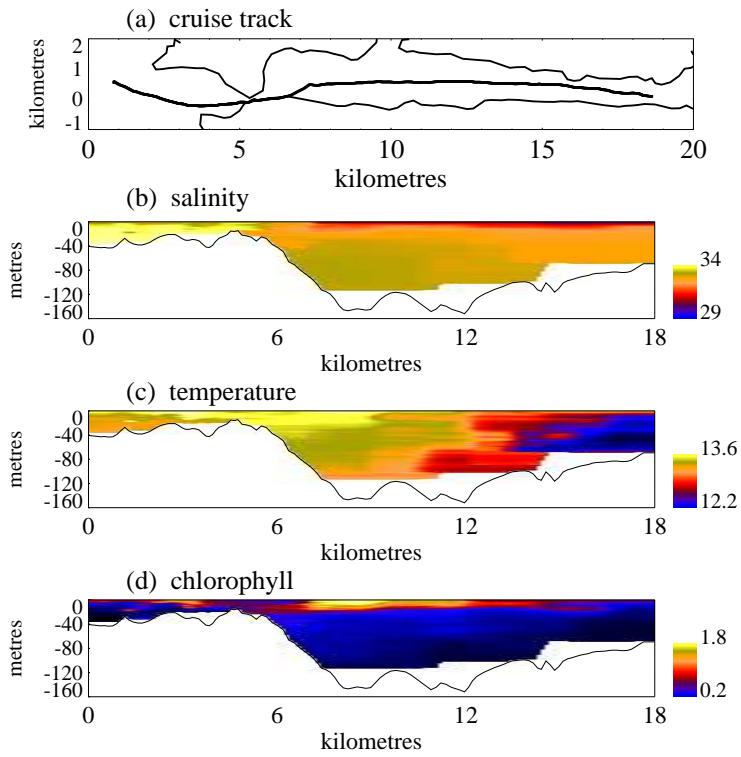


Figure B.9: 8 September 1991

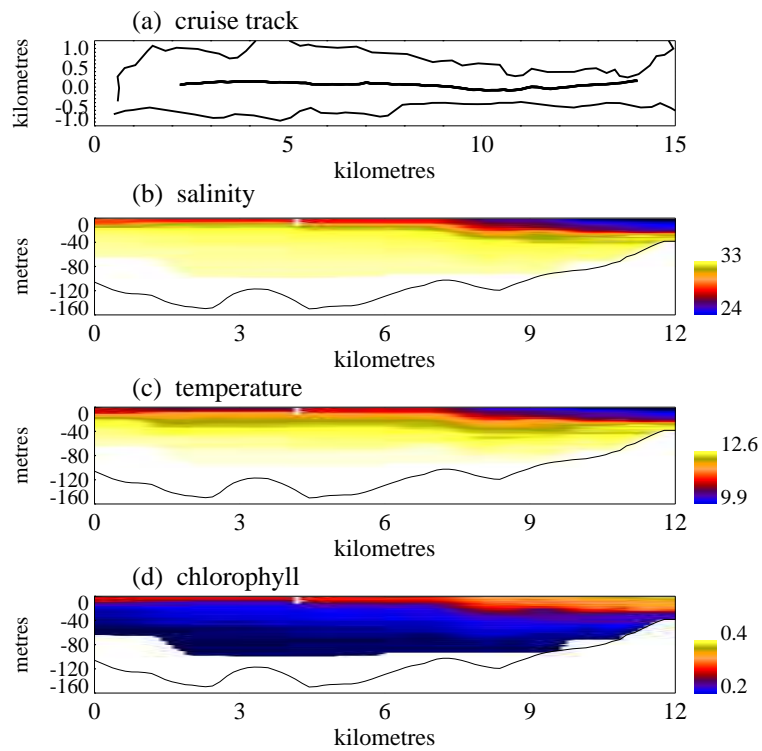


Figure B.10: 10 November 1991

B.2 Outer Basin

Table B.2: Daily mean meteorological conditions for the outer basin and Firth of Lorne axial cruises.

date	wind speed (ms^{-1}) and direction	river discharge (m^3s^{-1})
19 Jan.	13.17 @ 202°	192.881
20 Jan.	13.79 @ 239°	307.825
24 Jan.	2.21 @ 105°	93.039
24 Feb.	8.12 @ 226°	79.804
26 Feb.	10.00 @ 152°	95.298
24 Mar.	3.08 @ 158°	49.261
25 Mar.	5.62 @ 122°	45.215
27 Mar.	3.29 @ 133°	49.261
20 Apr.	4.33 @ 185°	36.454
22 Apr.	7.96 @ 280°	36.058
18 May	5.79 @ 213°	9.281
19 May	6.46 @ 221°	10.08
15 June	5.87 @ 270°	26.703
16 June	9.62 @ 295°	21.79
17 June	9.42 @ 290°	20.277
13 July	10.79 @ 242°	56.094
14 July	6.00 @ 231°	33.229
15 July	5.54 @ 205°	43.123
11 Aug.	11.50 @ 249°	34.922
12 Aug.	7.71 @ 245°	29.877
7 Sept	4.21 @ 202°	5.566
8 Sept	2.33 @ 175°	5.48
9 Sept	3.62 @ 169°	5.38
5 Oct.	9.00 @ 253°	87.608
6 Oct.	11.38 @ 181°	117.594
11 Nov.	14.96 @ 258°	258.591
13 Nov.	8.54 @ 187°	234.919

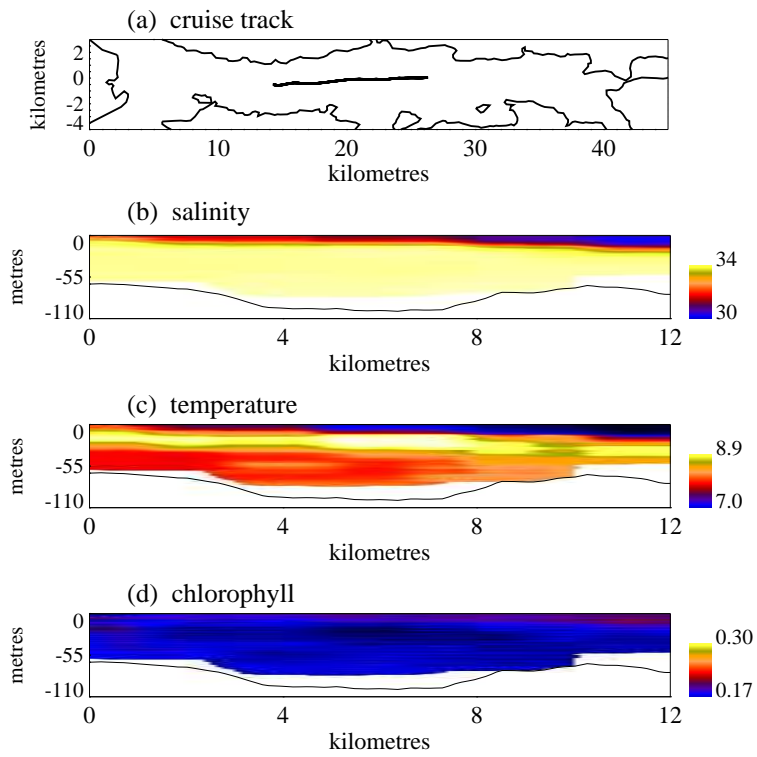


Figure B.11: 19 January 1991

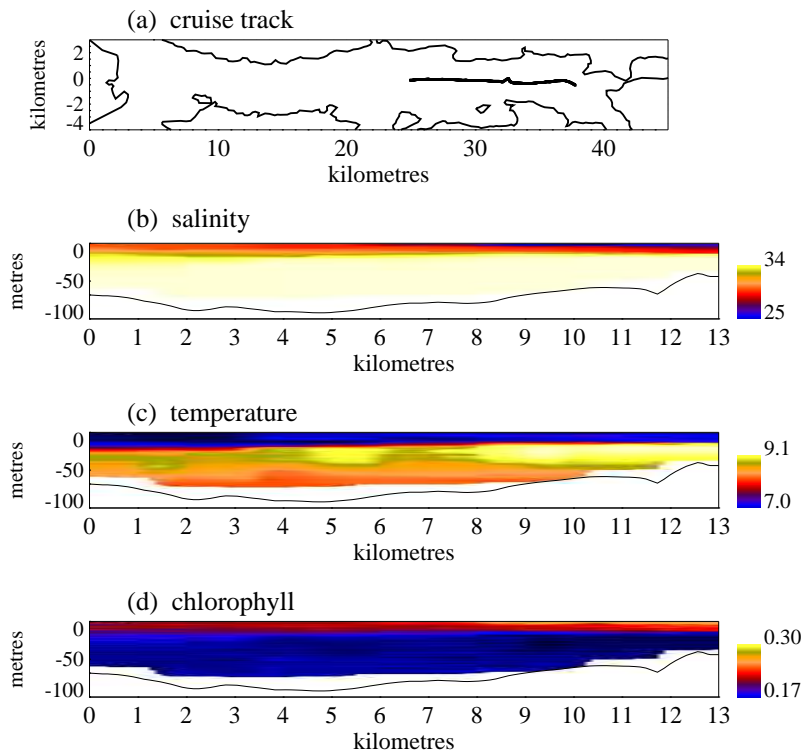


Figure B.12: 20 January 1991

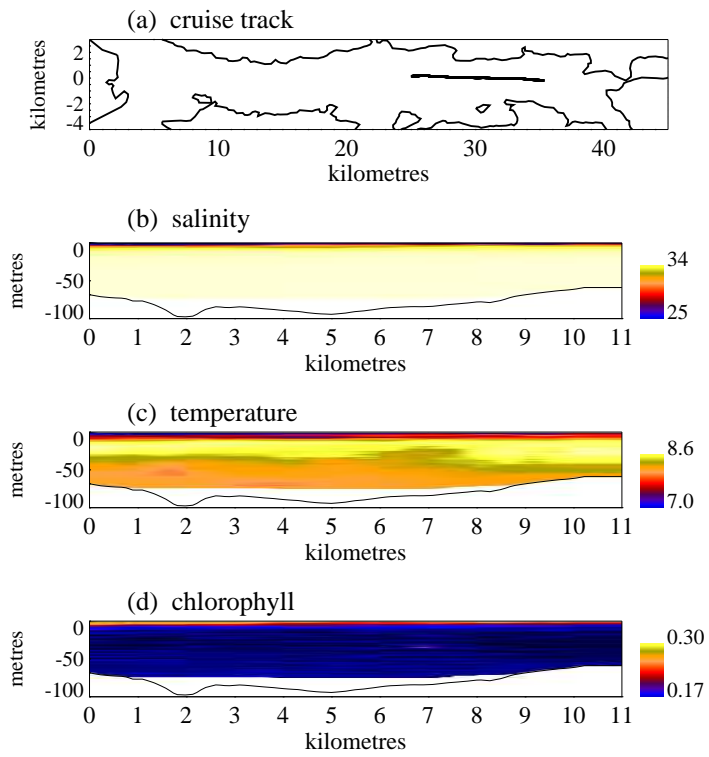


Figure B.13: 24 January 1991

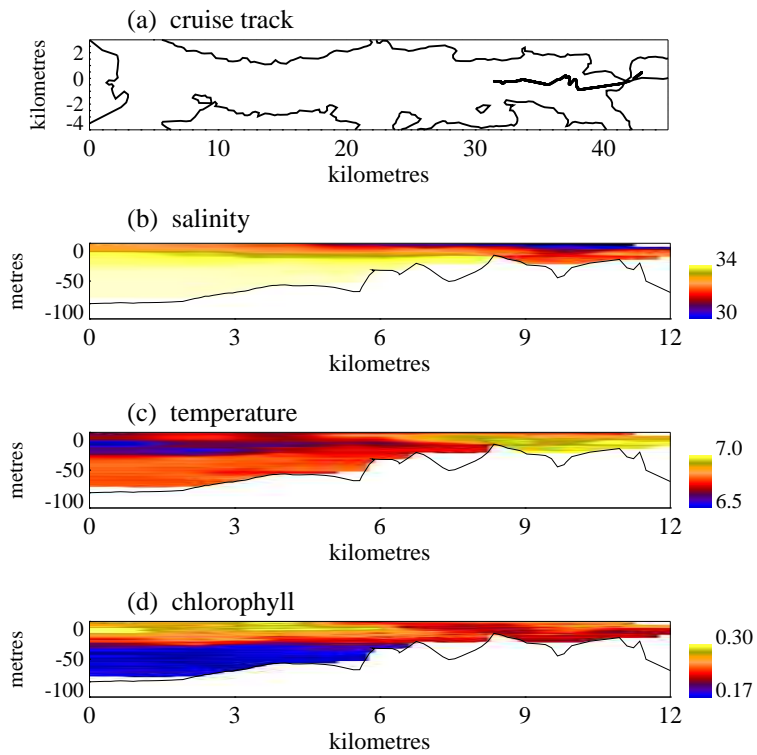


Figure B.14: 24 February 1991

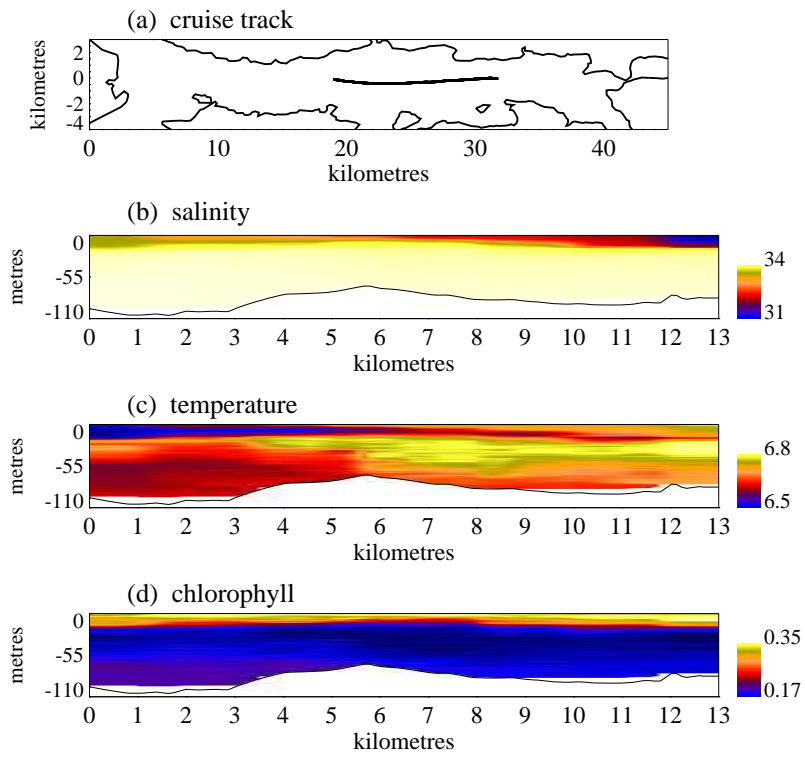


Figure B.15: 26 February 1991

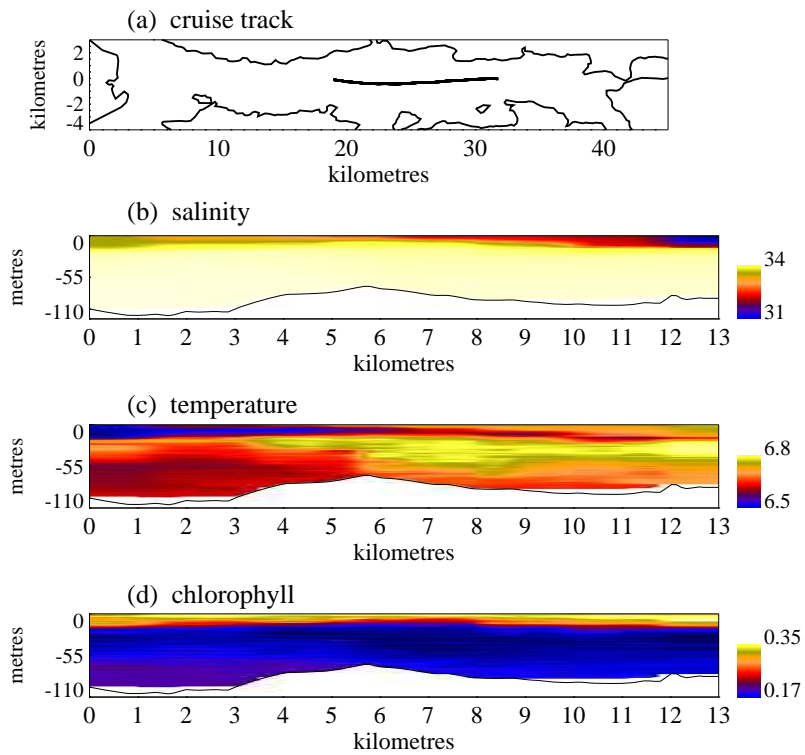


Figure B.16: 26 February 1991

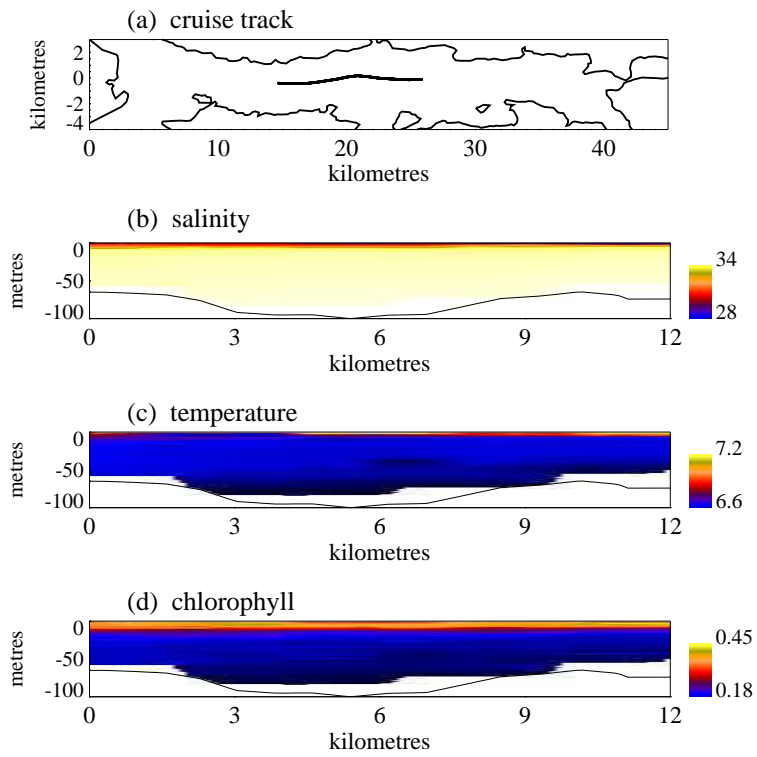


Figure B.17: 24 March 1991

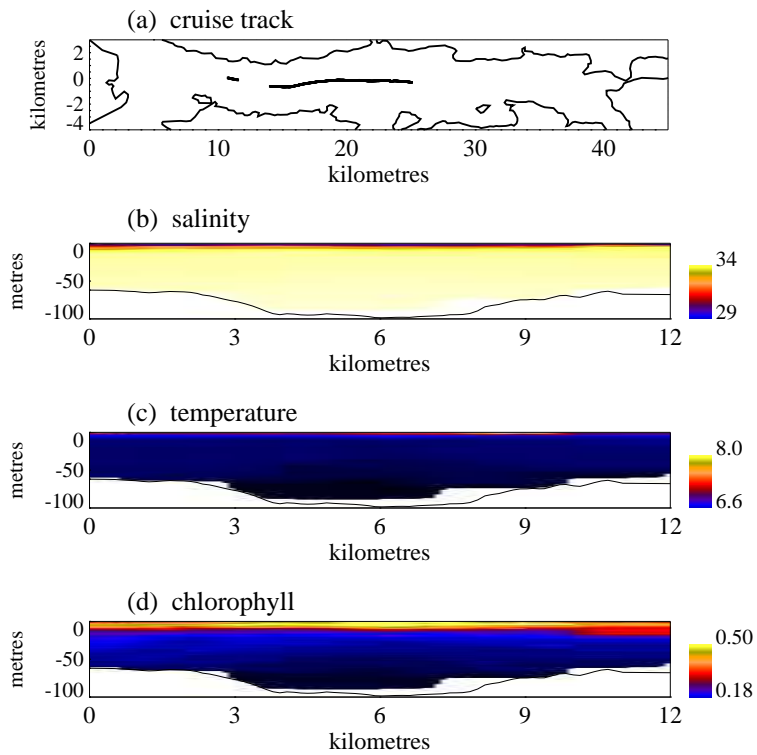


Figure B.18: 25 March 1991

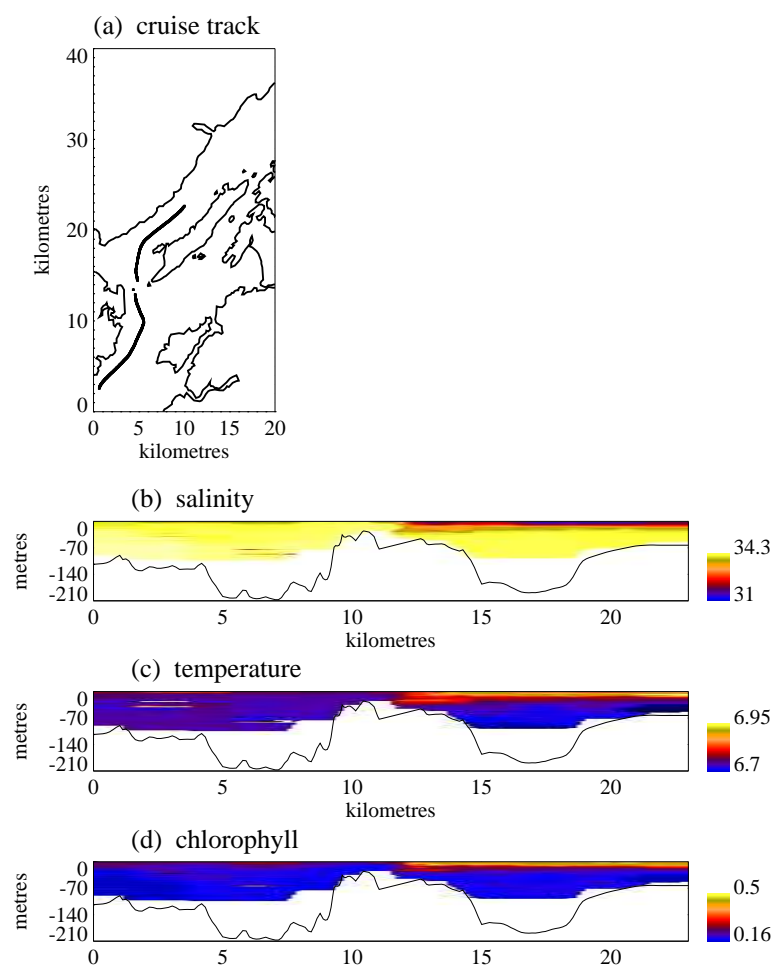


Figure B.19: 27 March 1991

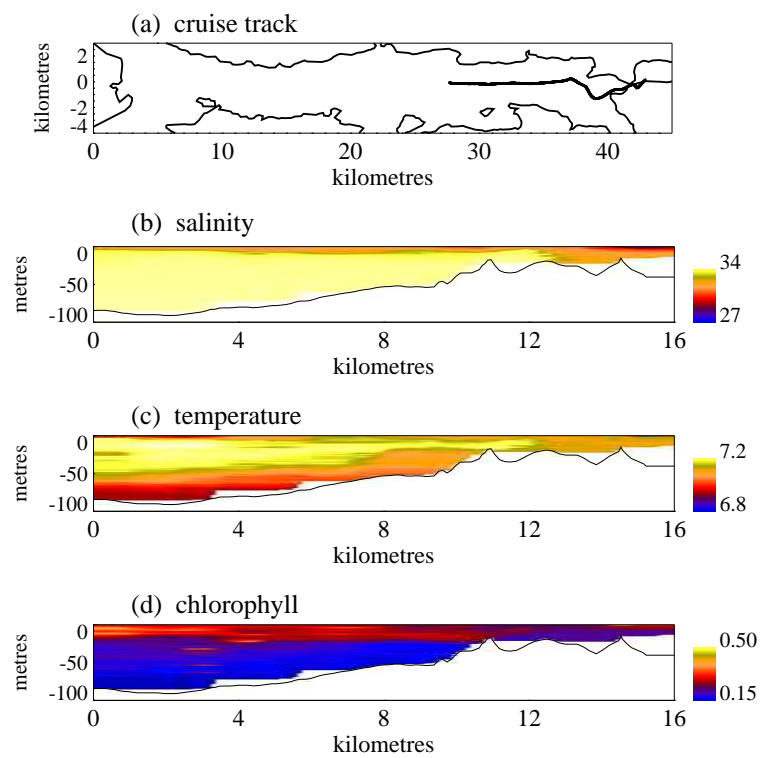


Figure B.20: 20 April 1991

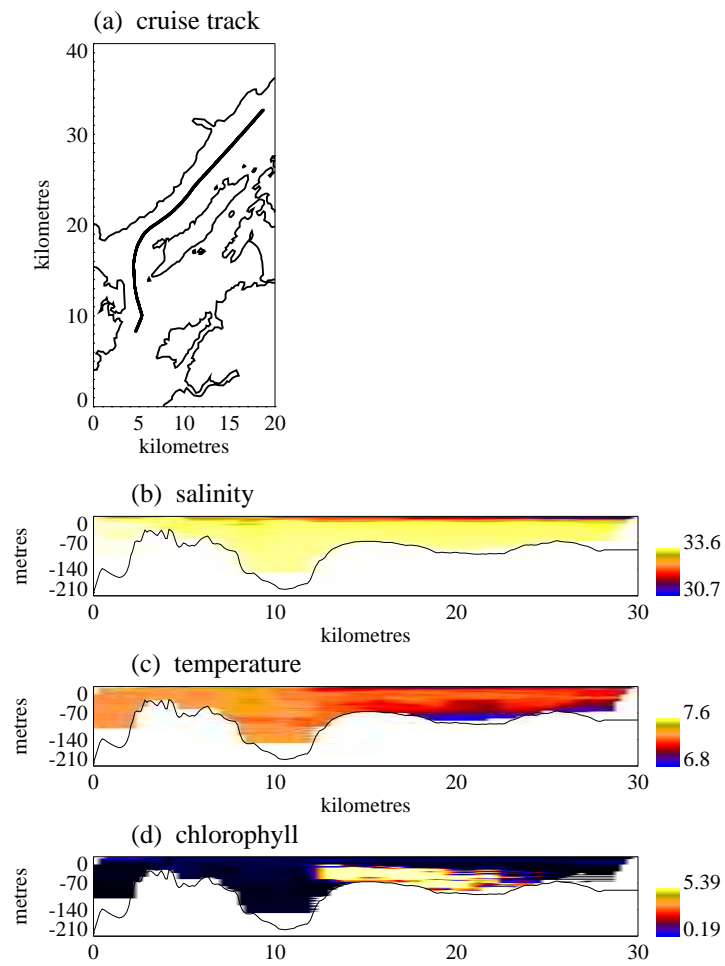


Figure B.21: 22 April 1991

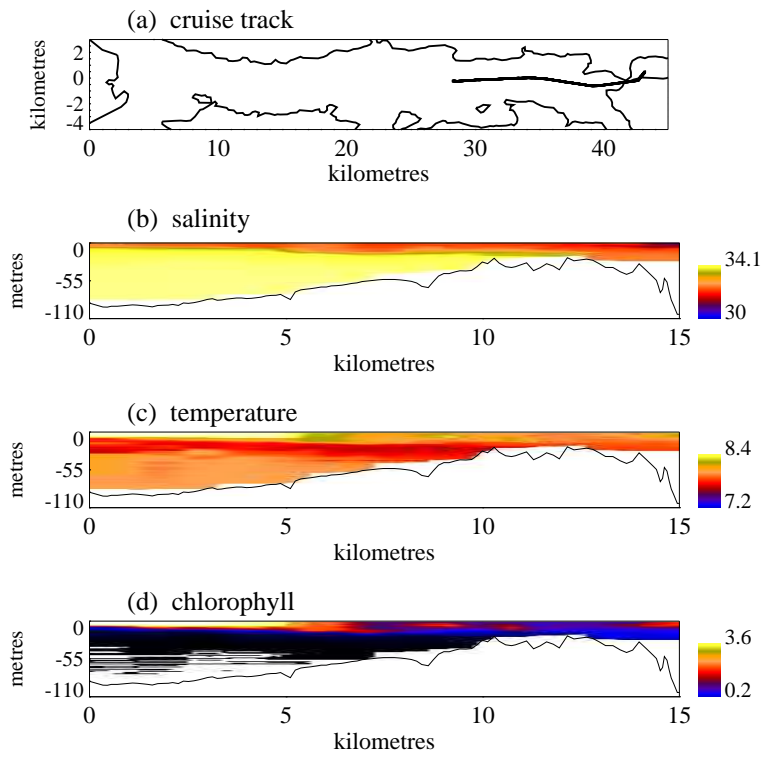


Figure B.22: 18 May 1991

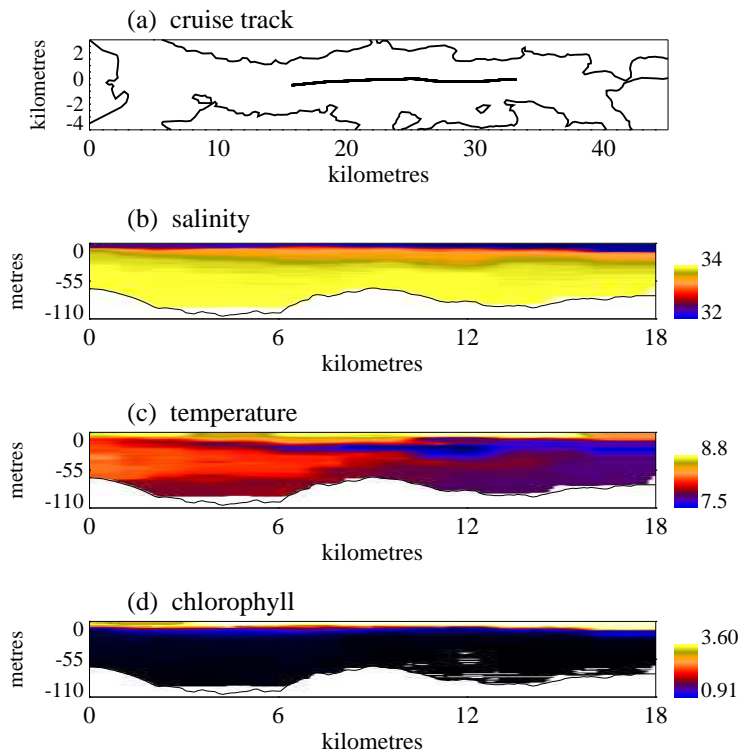


Figure B.23: 19 May 1991

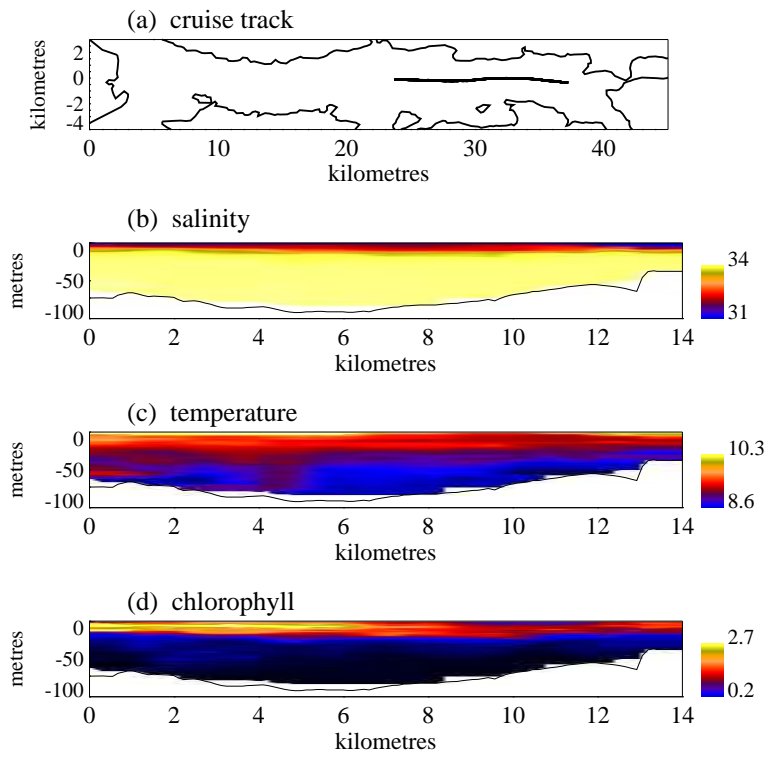


Figure B.24: 15 June 1991

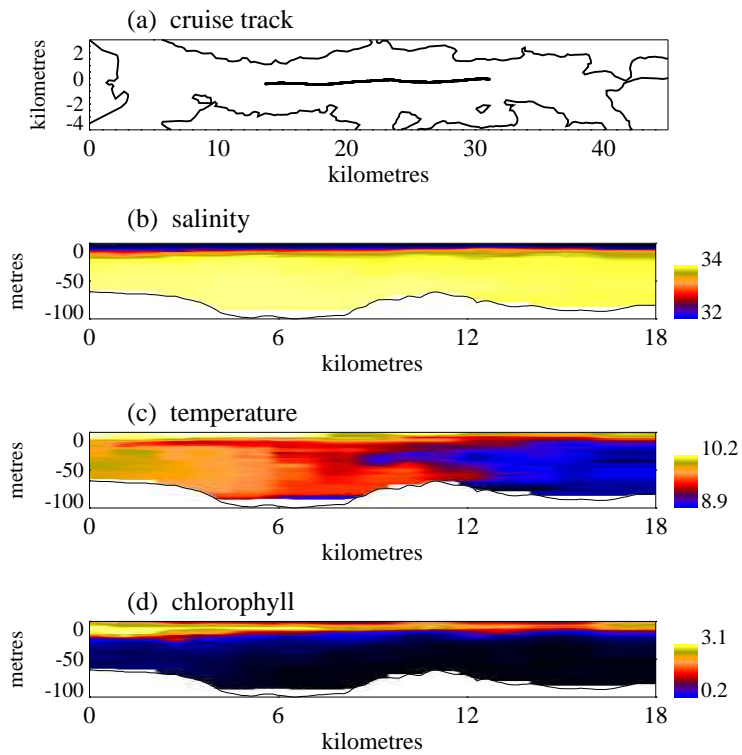


Figure B.25: 16 June 1991

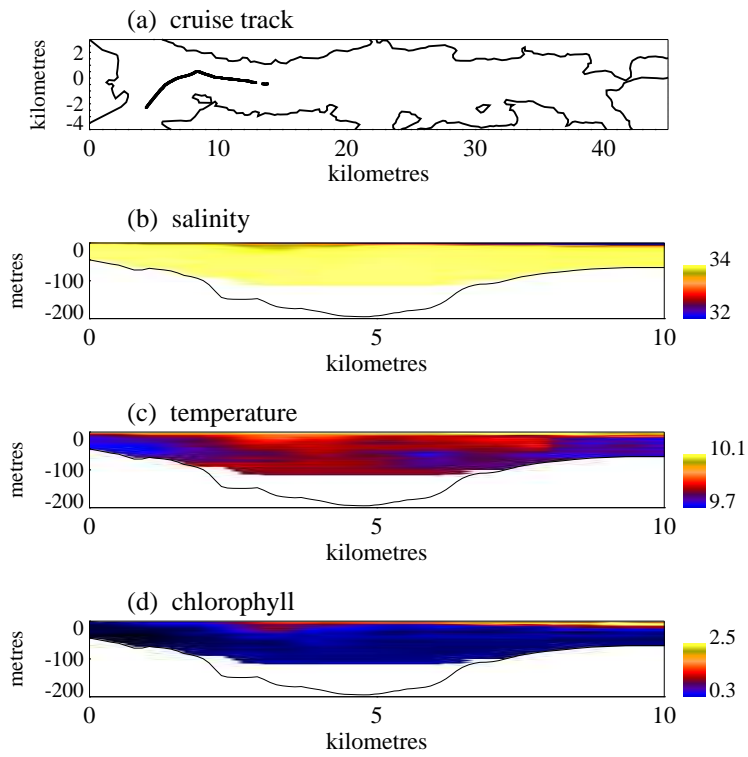


Figure B.26: 17 June 1991

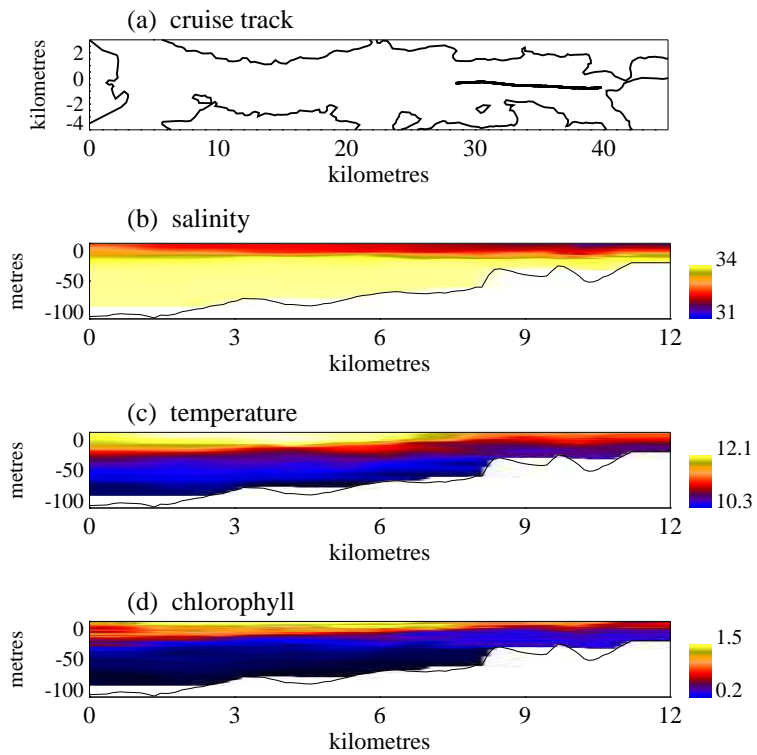


Figure B.27: 13 July 1991

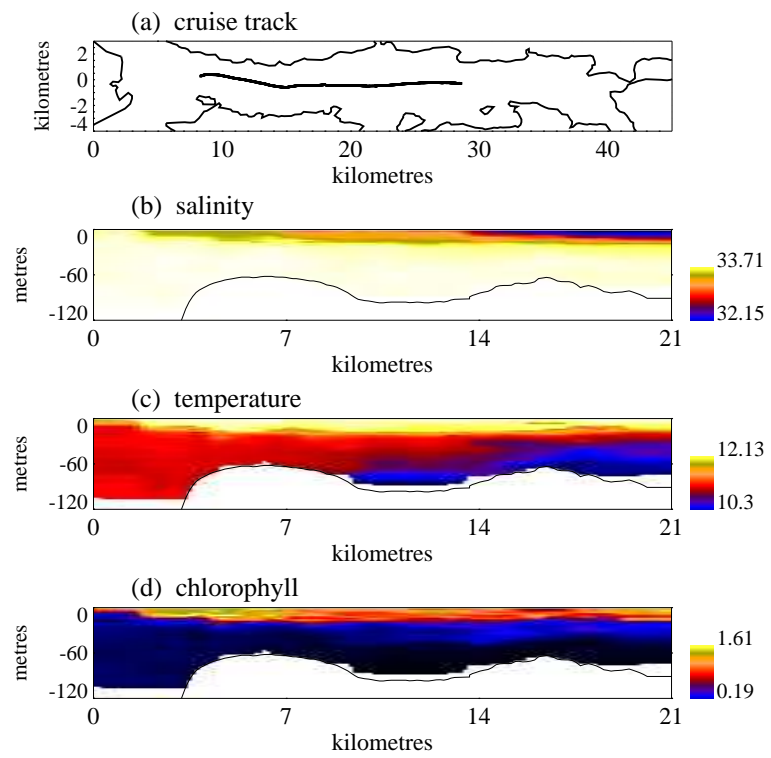


Figure B.28: 14 July 1991

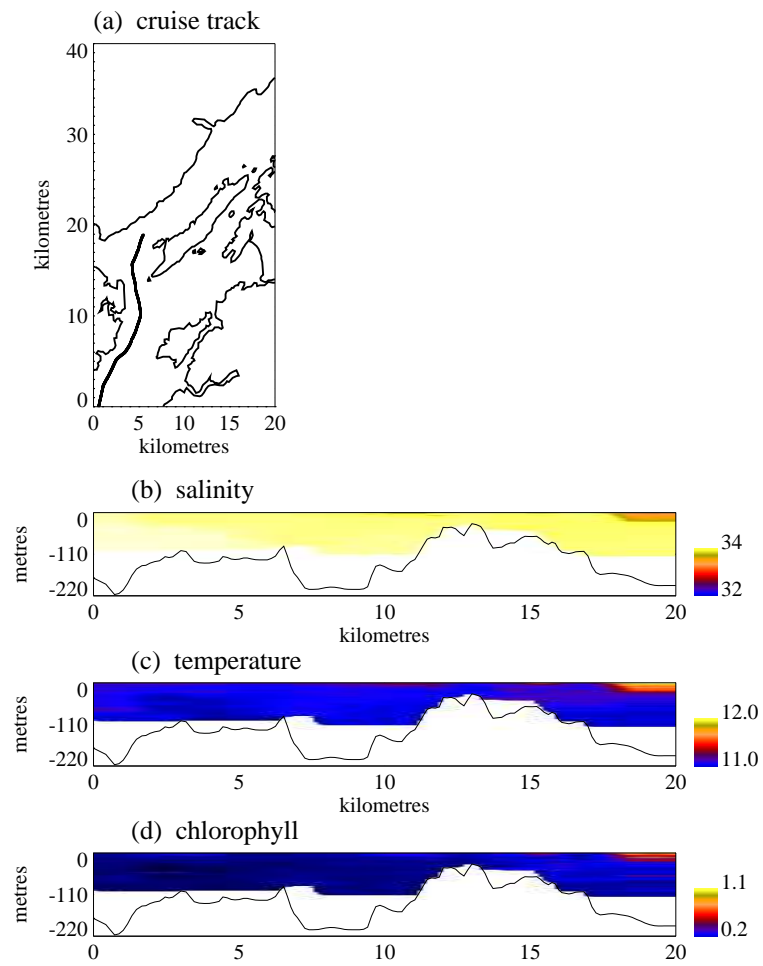


Figure B.29: 15 July 1991

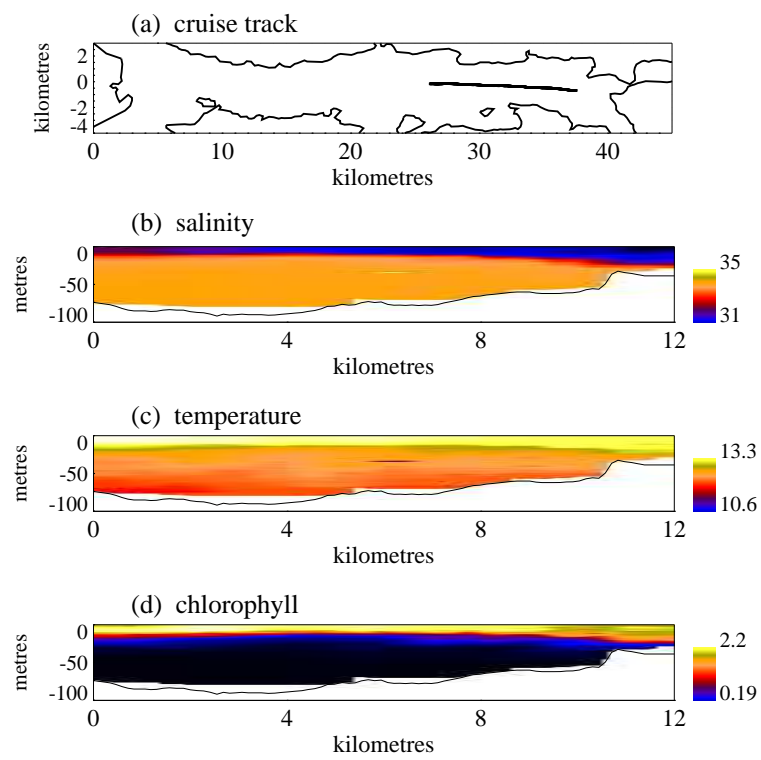


Figure B.30: 11 August 1991

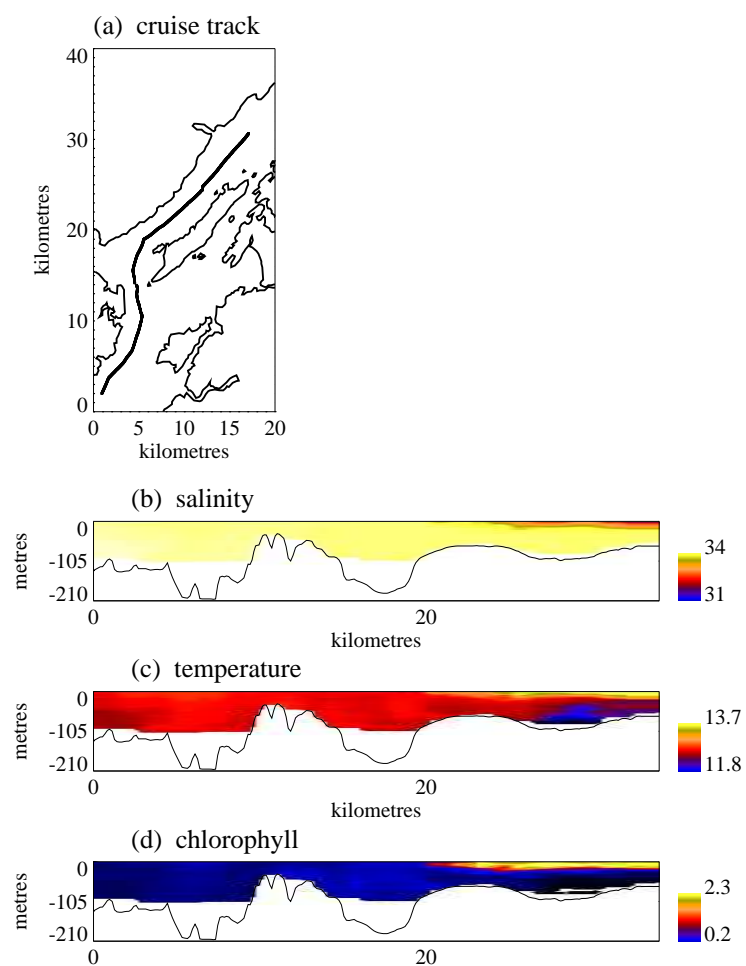


Figure B.31: 12 August 1991

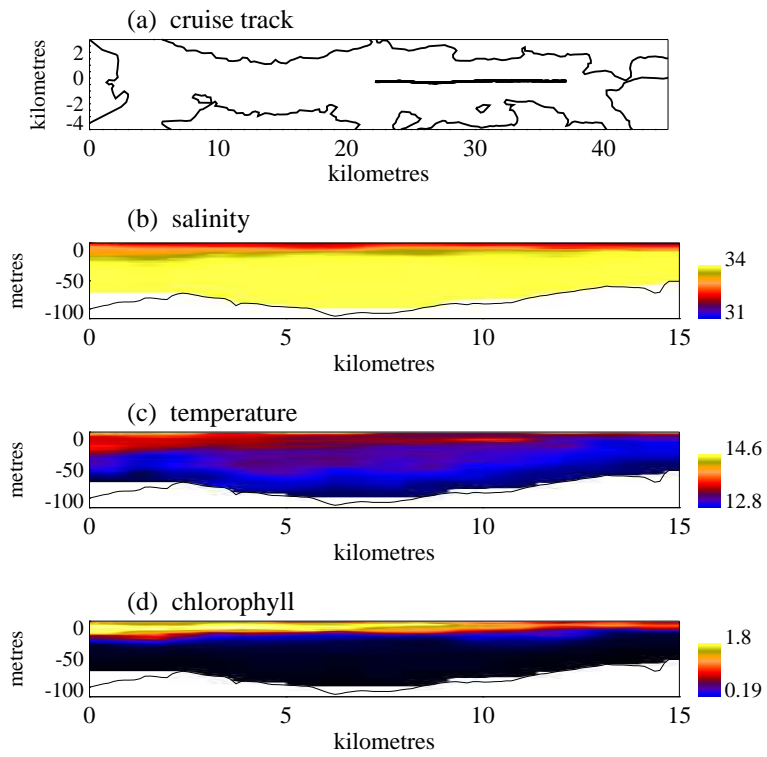


Figure B.32: 7 September 1991

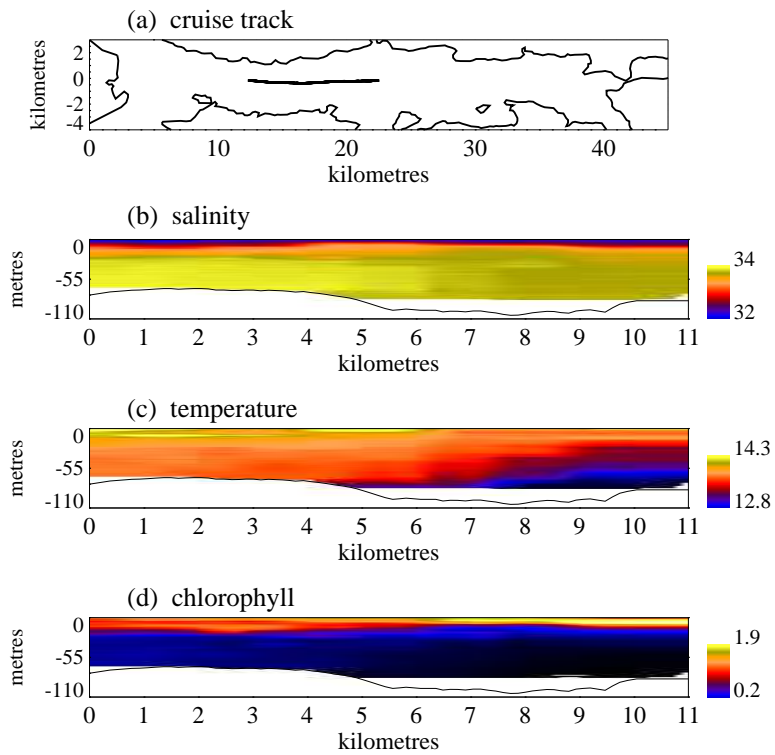


Figure B.33: 8 September 1991

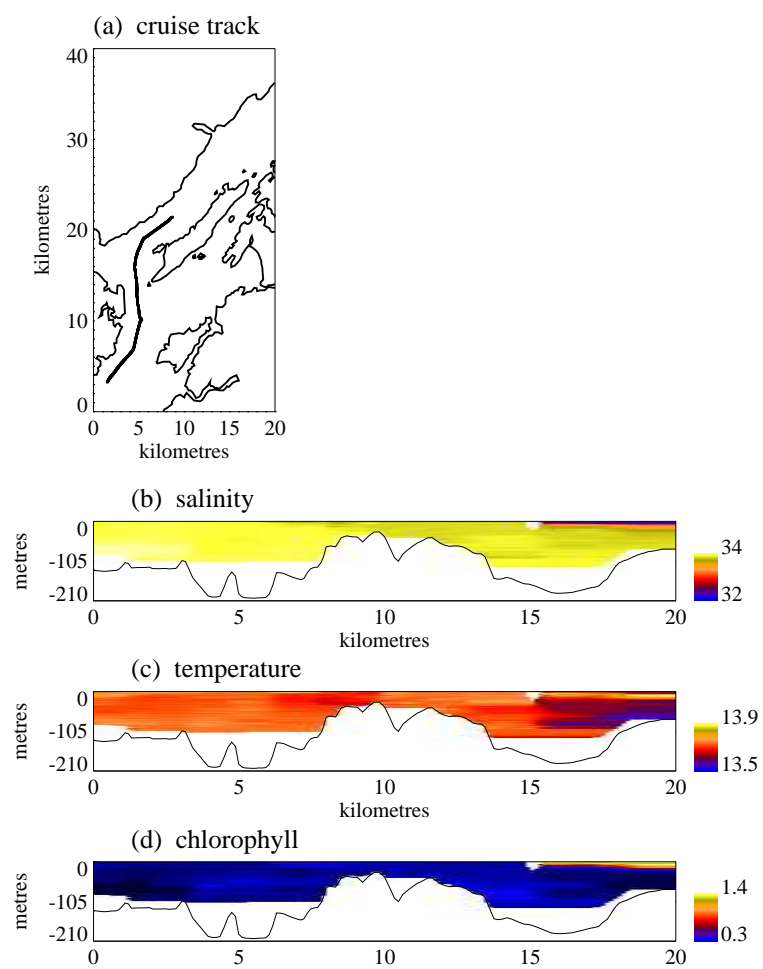


Figure B.34: 9 September 1991

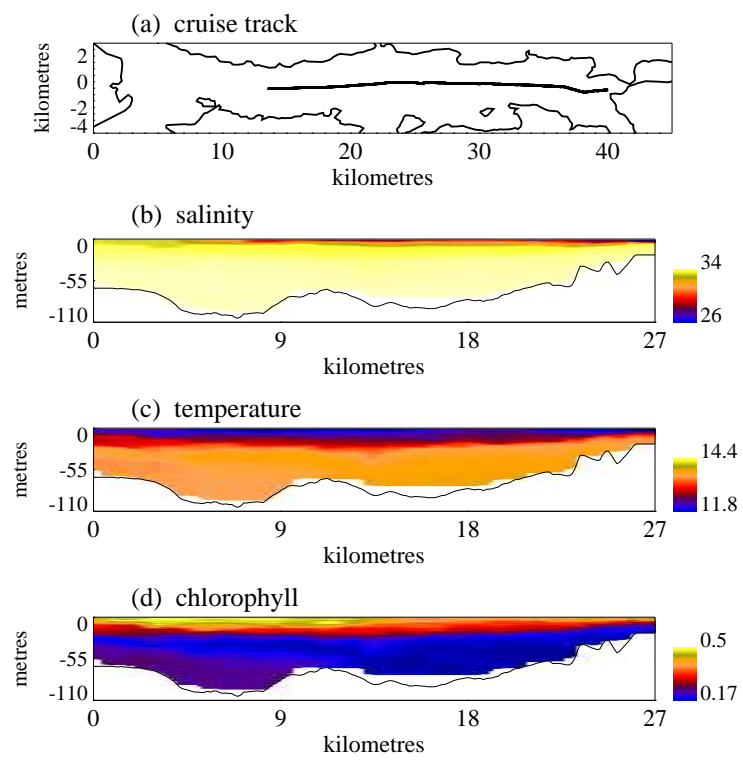


Figure B.35: 5 October 1991

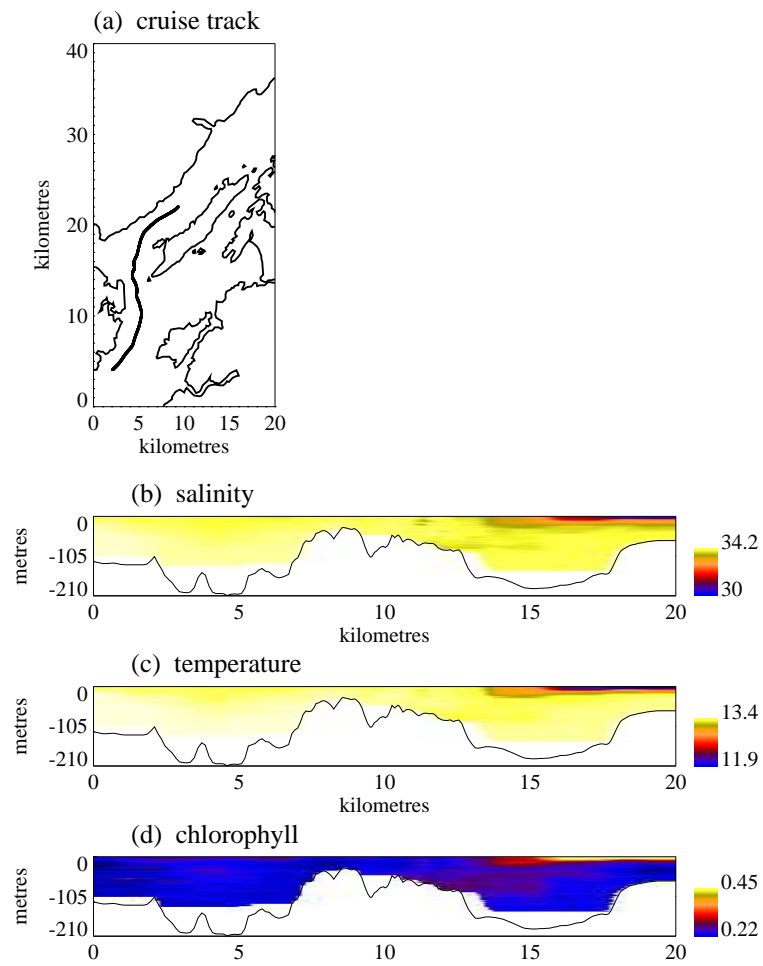


Figure B.36: 6 October 1991

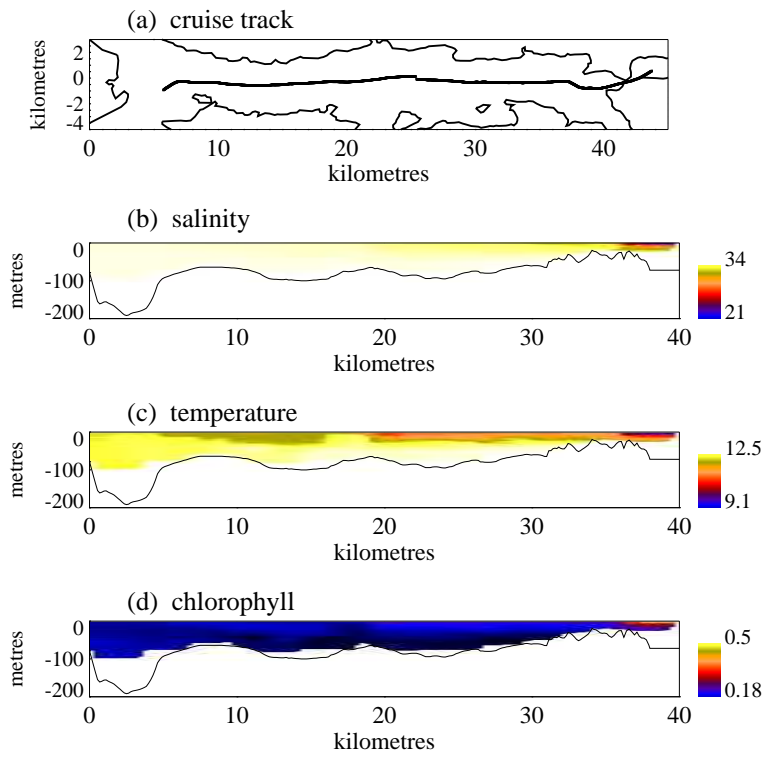


Figure B.37: 11 November 1991

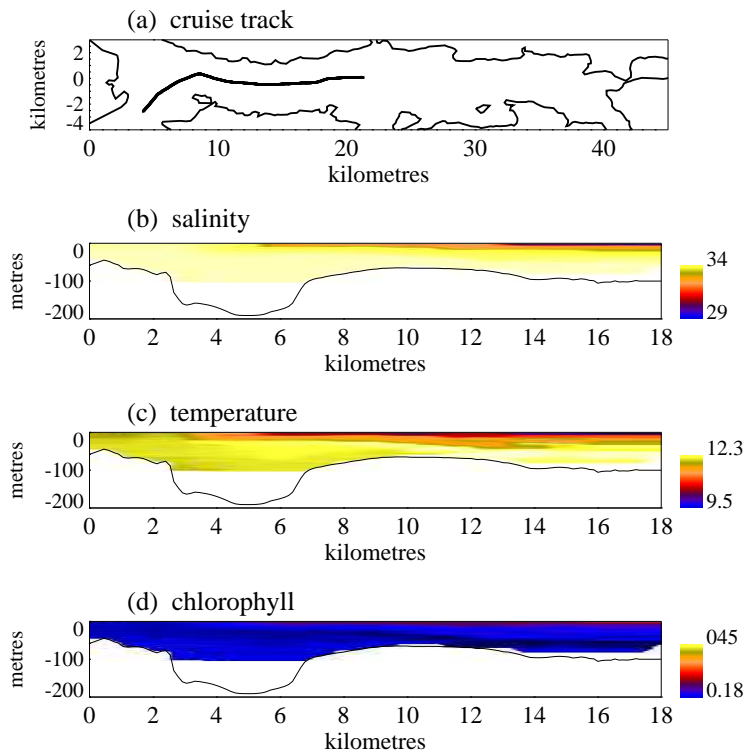


Figure B.38: 13 November 1991

Appendix C

Loch Model

A full description of the loch model and its development are contained in Ross et al (1993) and Ross et al (1994). The following description and tables are based on those in Nisbet and Gurney (1998) of a simplified model.

C.1 The Loch Model

To simplify the model all biological activity, except decomposition, is confined to the surface layer **S** and the nitrogen biomass of phytoplankton, zooplankton and carnivores in **S** are defined as P , Z and C respectively.

Phytoplankton take up dissolved inorganic nitrogen (DIN) (N) from the surface layer and excrete dissolved organic nitrogen (DON) (O). If they sink below the pycnocline they are taken to be unsuitable for primary or secondary production and are described as “detritus” (D) but will eventually be remineralised by bacterial action in the sediment.

Zooplankton and carnivores excrete ammonium which is counted as part of the available nitrogen. Faecal pellets and dead individuals from both these functional groups enter the detritus, and the nutrient they contain is eventually recycled to the surface layer via the bottom waters (B).

Fjords are not closed systems as the water exchanged with the sea carries with it dissolved nitrogen (in both organic and inorganic forms) as well as phytoplankton, zooplankton and carnivores. These exchanges play a vital role in the system dynamics and the model must take explicit account of them.

The fluxes in the system are described in the balance equations below. U_p , U_z and U_c denote the nitrogen uptake rates of the phytoplankton, zooplankton and carnivores respectively. Similarly E_p , E_z and E_c denote excretion rates and L_p , L_z and L_c are loss rates by defecation or mortality. Net tidal exchange rates are defined by T , immigration rates by J , remineralisation rates by R , terrestrial wash-out rates by W and the mixing flux from bottom to top waters by M . The

resulting balance equations are

$$\frac{dO}{dt} = E_p - R_o + T_o - W_o, \quad (\text{C.1})$$

$$\frac{dN}{dt} = E_c + E_z - U_p + R_o + T_n - W_n + M, \quad (\text{C.2})$$

$$\frac{dP}{dt} = U_p - L_p - U_z + T_p - W_p - E_p, \quad (\text{C.3})$$

$$\frac{dZ}{dt} = U_z + J_z - U_c - L_z - E_z, \quad (\text{C.4})$$

$$\frac{dC}{dt} = U_c + J_c - L_c - E_c, \quad (\text{C.5})$$

$$\frac{dB}{dt} = R_d - M, \quad (\text{C.6})$$

$$\frac{dD}{dt} = L_p + L_z + L_c - R_d. \quad (\text{C.7})$$

Tidal action causes the surface layer to exchange a volume F of water with the outside sea daily. The inflowing water carries DON, DIN and phytoplankton at concentrations S_o , S_n and S_p respectively. V represents the volume of the surface layer and the corresponding outflow carries DON and DIN at concentrations O/V and N/V respectively. As phytoplankton often accumulate near the pycnocline the concentration in the outflow water is reduced by a “retention factor” Ω . The net exchange rates for DON, DIN and phytoplankton nitrogen are given, in mgN/day by

$$T_o = F \left[S_o - \frac{O}{V} \right], \quad T_n = F \left[S_n - \frac{N}{V} \right], \quad T_p = F \left[S_p - \frac{\Omega P}{V} \right]. \quad (\text{C.8})$$

Similarly, a volume f of terrestrial run-off enters the system each day, carrying DON and DIN at concentrations ρ_o and ρ_n respectively. This flow displaces an equal volume of surface-layer water, which carries with it DON, DIN and phytoplankton. The net wash-out rates for these quantities are

$$W_o = f \left[\frac{O}{V} - \rho_o \right], \quad W_n = f \left[\frac{N}{V} - \rho_n \right], \quad W_p = f \left[\frac{\Omega P}{V} \right]. \quad (\text{C.9})$$

The bottom to surface nitrogen flux, M , is defined as follows. If water is effectively exchanged between the two locations at $\phi \text{ m}^3/\text{day}$, and the volume of the bottom water is V_b then the rate of nitrogen exchange is

$$M = \phi \left[\frac{B}{V_b} - \frac{N}{V} \right]. \quad (\text{C.10})$$

The only effect of remineralisation in the model is to limit the rate at which nutrient is returned to a form available to the biological system. This effect is

generated by assuming that nutrient stored as detritus or DON is returned to its inorganic form by a first order rate process, so that

$$R_d = k_d D, \quad R_o = k_o O. \quad (\text{C.11})$$

Losses from a functional group to the detritus pool occur because of background mortality (i.e. mortality other than by predation) or rejection of part of the ingested food as faeces. All members of a functional group are assumed to have the same per-capita mortality rate (δ_p , δ_z or δ_c as appropriate) and zooplankton and carnivores reject a proportion d_z or d_c of their consumption as faeces. Losses are therefore defined as

$$L_p = \delta_p P, \quad L_z = \delta_z Z + d_z U_z, \quad L_c = \delta_c C + d_c U_c. \quad (\text{C.12})$$

A proportion of ingested prey (ϵ_p , ϵ_z or ϵ_c as appropriate) is assumed to be excreted and the metabolic activity needed to meet basal costs results in the excretion of a fraction (e_p , e_z or e_c as appropriate) of nitrogen biomass each day. The excretion rates for the three functional groups are therefore

$$E_p = \epsilon_p U_p + e_p P, \quad E_z = \epsilon_z U_z + e_z Z, \quad E_c = \epsilon_c U_c + e_c C. \quad (\text{C.13})$$

The population uptake rates are U_p , U_z and U_c for phytoplankton, zooplankton and carnivores respectively. For the zooplankton and carnivores this is straightforward. An individual zooplankter is assumed to have a type II functional response with a maximum uptake rate I_z (per unit biomass) and half-saturation phytoplankton concentration H_p . An individual carnivore has a type II response with maximum uptake rate I_c and half-saturation zooplankton concentration H_z . Uptake by zooplankton and carnivores is therefore defined by

$$U_z = \frac{I_z P Z}{P + V H_p}, \quad U_c = \frac{I_c Z C}{Z + V H_z}. \quad (\text{C.14})$$

The rate at which an individual phytoplankton cell fixes nitrogen depends both on the local concentration of inorganic nitrogen and on the local irradiance. The response to each factor is assumed to take a type II form, so that in the presence of a local DIN concentration n and light intensity L the nitrogen fixation rate per unit phytoplankton (nitrogen) biomass, $u(n, L)$, is

$$u(n, L) = I_p \left[\frac{n}{n + H_n} \right] \left[\frac{L}{L + H_L} \right]. \quad (\text{C.15})$$

The assumption that the surface layer is well-mixed implies that the DIN concentration $n = N/V$ everywhere. If the surface irradiance is L_s , the local irradiance

at depth x varies according to the Lambert-Beer law, $L(x) = L_s e^{-\kappa x}$. To determine the total fixation rate this expression must be substituted into equation (C.15) multiplied by the local phytoplankton concentration (P/V) and then integrated over the total surface layer volume. If the depth of the surface layer is d , then the result is

$$U_p = \frac{PI_p}{\kappa d} \left(\frac{N}{N + VH_n} \right) \ln \left(\frac{L_s + H_L}{L_s e^{-\kappa d} + H_L} \right). \quad (\text{C.16})$$

The attenuation coefficient, κ , represents the characteristic distance over which a light beam is attenuated as it propagates down the water column. Phytoplankton density contributes to this (self-shading,) generating the following definition of attenuation

$$\kappa = \kappa_b + \kappa_p P/V. \quad (\text{C.17})$$

Changes in water temperature, θ , affects both activity levels and basal metabolic rates and needs to be taken into account. To this end, a seasonality function is defined

$$S(\theta) = 1 - \exp(-\theta/\theta_0), \quad (\text{C.18})$$

which multiplies the maximum ingestion rates and the basal excretion rates

$$I_p = I_p^m S(\theta), \quad e_p = e_p^m S(\theta), \quad I_z = I_z^m S(\theta) \quad \text{and so on.} \quad (\text{C.19})$$

The initial application of the the model led to the introduction of overwintering of zooplankton eggs into the model. In the late summer and autumn, female zooplankton divert much of their resource uptake to the production of “resting eggs” which do not hatch immediately, but instead fall to the bed of the fjord to over-winter and hatch the following spring. This implies that at this season of the year the total zooplankton biomass will remain static, or even shrink, despite an abundance of food. This happens when water temperatures are at their highest, so an additional “mortality” is incorporated which only switches on at high water temperatures. Total zooplankton mortality is therefore

$$\delta_z = \delta_z^b + \Delta_z \exp(-\theta_z/\theta). \quad (\text{C.20})$$

C.2 Parameters and driving functions

The model is simplified by only representing one species in each functional group - in many sea-loch systems one species or a group of similar species tend to dominate. Phytoplankton are represented by the diatom *Skeletonema costatum*, zooplankton by the copepod *Acartia clausi* and gelatinous carnivores by the ctenophore *Pleurobrachia pileus*.

A complete description of the sources of the biological parameters is contained in Ross et al (1993). The only biological parameters not evaluated from the literature were those describing the zooplankton resting egg production (Δ_z and θ_z). Table C.1 is derived from Ross et al (1993).

Table C.1: Sea-loch model – biological parameters

<i>Phytoplankton</i>			
I_p^m	Maximum fixation rate	1.6	day ⁻¹
H_n	Half-saturation nitrogen concentration	4.2	mgN/m ³
H_L	Half-saturation irradiance	60	μ Einst/m ² /sec
δ_p	Background mortality	0.1	day ⁻¹
ϵ_p	Fraction of uptake excreted	0.05	–
e_p^m	Maximum fraction of biomass excreted per day	0.25	day ⁻¹
κ_p	Self-shading coefficient	0.008	m ² /mgN
Ω	Washout retention factor	0.5	–
<i>Zooplankton</i>			
I_z^m	Maximum grazing rate	2	day ⁻¹
H_p	Half-saturation phytoplankton concentration	37.5	mgN/m ³
d_z	Fraction of uptake defecated	0.36	–
δ_z^b	Background mortality	0.05	day ⁻¹
Δ_z	Egg “mortality” coefficient	100	day ⁻¹
θ_z	Egg “mortality” characteristic temp.	100	°C
ϵ_z	Fraction of uptake excreted	0.15	–
e_z^m	Maximum fraction of biomass excreted per day	0.05	day ⁻¹
<i>Carnivores</i>			
I_c^m	Maximum carnivory rate	15	day ⁻¹
H_z	Half-saturation zooplankton concentration	60	mgN/m ³
d_c	Fraction of uptake defecated	0.5	–
δ_c	Background mortality	0.05	day ⁻¹
ϵ_c	Fraction of uptake excreted	0.2	–
e_c^m	Maximum fraction of biomass excreted per day	0.75	day ⁻¹
<i>General</i>			
k_d	Detritus remineralisation rate	0.01	day ⁻¹
k_o	DON remineralisation rate	0.02	day ⁻¹
θ_o	Seasonal characteristic temperature	10	°C

The model also contains a group of parameters and driving functions describing physical processes. Water-temperature, surface irradiance and fresh-water run-in rate are all dynamically important and vary on time-scales relevant to the model, so are treated as driving functions. In comparison, variability in the tidal exchange rate, vertical mixing rate and background turbidity were considered to be averaged out by the model dynamics and taken to be constants. Surface layer depth, though dynamically important and known to vary with changes in hydrodynamic conditions was taken to be a constant as insufficient data were available to determine a time series. Physical parameters and driving functions were determined for each sea-loch system and Table C.2 gives the physical parameters for the four sea-lochs the model was applied to in Ross et al (1994).

Table C.2: Sea-loch model – physical parameters

		<i>Loch Creran</i>	<i>Loch Etive</i>	<i>Killary Harb.</i>	<i>Loch Aird- -bhair</i>	
d	Surface layer depth	8	10	7.5	8	m
F/V	Tidal exchange	0.37	0.6	0.8	1.0	day ⁻¹
V_b/V	Bottom layer vol.	1.0	1.0	1.0	1.0	–
ϕ/V	Vertical mixing	0.05	0.05	0.05	0.05	day ⁻¹
κ_b	Light attenuation	0.22	0.22	0.48	0.22	m ⁻¹